Electronic properties of two-dimensional systems

Tsuneya Ando

Institute of Applied P'ysics, University of Tsukuba, Sakura, Ibaraki 305, Japan and IBM Thomas J Watson Research Center, Yorktown Heights, New York 10598*

Alan B. Fowler and Frank Stern

IBM Thomas J. Watson Research Center, Yorktown Heights, New York 10598

The electronic properties of inversion and accumulation layers at semiconductor-insulator interfaces and of other systems that exhibit two-dimensional or quasi-two-dimensional behavior, such as electrons in semiconductor heterojunctions and superlattices and on liquid helium, are reviewed. Energy levels, transport properties, and optical properties are considered in some detail, especially for electrons at the (100) silicon-silicon dioxide interface. Other systems are discussed more briefly.

CONTENTS

*Permanent address.

LIST OF SYMBOLS

Two-dimensional vectors are usually indicated by boldface letters. When three-dimensional vectors appear at the same time as two-dimensional vectors, the latter are denoted by lower-case characters and the former by upper-case characters. For example, $\mathbf{K}=(\mathbf{k},k_z)$ with $\mathbf{k}=(k_x,k_y)$. Some of the symbols which frequently appear in the text are summarized as follows.

Symbol	Meaning
C_{ins}	insulator capacitance per unit area
d_{ins}	insulator thickness
$D(E)$	density of states
e	magnitude of electronic charge
E	energy; electric field
E_F	Fermi energy
E_n	energy of bottom of nth subband
E_N	energy of Nth Landau level given by $(N+\frac{1}{2})\hbar\omega_c$
E_{nm}	E_n-E_m
F	field; envelope wave function
$f(E)$	Fermi distribution function
g	Landé g factor
g_s	spin degeneracy factor
g_v	valley degeneracy factor
H	magnetic field
$\mathbf{J}$	current density per unit width
k_B	Boltzmann's constant
k_F	Fermi wave vector
l	mean free path; radius of the ground cyclotron orbit [radius of the Nth cyclotron orbit is given by $(2N+1)^{1/2}l$]
m	effective mass
m_0	free-electron mass
m_l	longitudinal effective mass in the bulk
m_t	transverse effective mass in the bulk
m_z	effective mass perpendicular to the interface
m^*	dressed mass (modified by many-body interacions)
N	Landau-level index (starting with 0)
N_A	concentration of acceptor impurities in the bulk
N_D	concentration of donor impurities in the bulk
N_{depl}	concentration of fixed space charges in the depletion layer
N_{ox}	density of charges per unit area in the oxide that does not change with V_G; assumed to be at the $Si-SiO_2$ interface
N_s	concentration of electrons in inversion or accumulation layers
N_{ss}	density of fast surface states per unit area
Q	charge per unit area
Q_{ox}	eN_{ox}
$q_s,\bar{q}_s$	effective screening parameter
Q_{ss}	eN_{ss}
R	resistance
R_H	Hall coefficient
T	temperature
V_G	gate voltage
V_{sub}	substrate bias voltage
V_T	threshold gate voltage
X	x coordinate of center of cyclotron orbit
z	distance from interface
z_{av}	average position of electrons from interface
z_d	thickness of the depletion layer
z_n or $z_{n\bar{n}}$	average position of electrons in nth subband from interface
Δ	root-mean-square height of interface roughness; spin-orbit splitting; gap parameter
ε	energy; dielectric function normalized by $\bar{\kappa}$
$\zeta_n(z)$	envelope wave function of nth subband for motion normal to the interface
Λ	lateral decay length of interface roughness
κ_{ins}	static dielectric constant of insulator
κ_{sc}	static dielectric constant of semiconductor
$\bar{\kappa}$	arithmetic average of κ_{sc} and κ_{ins}
μ	mobility; chemical potential
μ_B	Bohr magneton
μ_{eff}	effective mobility
μ_{FE}	field-effect mobility
μ_H	Hall mobility
ρ	resistivity; mass density; charge density
σ	conductivity; spin index
σ_{min}	minimum metallic conductivity
τ	relaxation time
ϕ	electrostatic potential; phonon field; azimuthal angle
ϕ_s	surface potential
ϕ_{sub}	substrate bias voltage
ω	angular frequency
ω_c	cyclotron angular frequency
ω_p	plasma angular frequency

I. INTRODUCTION

In this article we review the properties of electrons in semiconductor space-charge layers and touch briefly on other systems which have dynamically two-dimensional

character. By dynamically two-dimensional we mean that the electrons or holes have quantized energy levels for one spatial dimension, but are free to move in two spatial dimensions. Thus the wave vector is a good quantum number for two dimensions, but not for the third. These systems are not two-dimensional in a strict sense, both because wave functions have a finite spatial extent in the third dimension and because electromagnetic fields are not confined to a plane but spill out into the third dimension. Theoretical predictions for idealized two-dimensional systems must therefore be modified before they can be compared with experiment.

We shall generally confine our discussion to systems for which parameters can be varied in a given sample, usually by application of an electrical stress. Systems of this sort generally occur in what may broadly be called heterostructures. The best known examples are carriers confined to the vicinity of junctions between insulators and semiconductors, between layers of different semiconductors, and between vacuum and liquid helium. For most of these systems the carrier concentration can be varied, so that a wealth of information can be obtained from one sample. They all have at least one well-defined interface which is usually sharp to a nanometer or less. Several of these systems will be described in Sec. VIII.

Many other experimental systems show two-dimensional character, including layer compounds, intercalated graphite, and thin films. These systems, which have been widely studied, are discussed very briefly in Sec. VIII.

In this chapter we describe some of the basic terms and concepts as an introduction to the more detailed discussion of the following chapters.

A. Field effect

The effects of changes in surface conditions on the conductance of a semiconductor sample have been studied for many years. Such measurements are usually called field-effect measurements because a major physical variable is the electric field normal to the semiconductor surface. One important way to change the surface conditions, and therefore the surface electric field, is through the control of gaseous ambients. A famous example is the Brattain-Bardeen (1953) cycle, in which the surface potential of germanium (the difference of potential between the surface and the interior) was varied by exposing the sample to dry oxygen, wet oxygen or nitrogen, and dry oxygen again. Gaseous ambients are still used to control the surface charge of ZnO (see, for example, Many, 1974), and are one basis of a growing class of ambient sensing devices (see, for instance, Zemel, 1979, and Volume 1 of the new journal *Sensors and Actuators*). A disadvantage of the early measurements was that the conductance of the entire sample was measured, and the surface effects were extracted by taking differences or derivatives as the ambient was changed.

In conjunction with field-effect measurements, theories for the dependence of the mobility of carriers near the surface on the surface conditions were developed and refined. Most of the early work was based on the phenomenological notion of diffuse and specular reflection at the surface, as first used by Fuchs (1938) in studying transport in metal films.

The early work on semiconductor surfaces is reviewed in the books by Many, Goldstein, and Grover (1965) and by Frankl (1967), and provides the classical framework on which the quantum models described below have been built. The classical theory of surface transport has been reviewed by Greene (1969a, 1969b, 1974).

B. Devices

Most of the discussion in this article will be about a particular insulator-semiconductor heterojunction system—the metal-insulator-semiconductor (MIS) and more particularly the metal-oxide-semiconductor (MOS) structure. Most of the work on two-dimensional MIS systems has been done on a technologically well developed example, the metal-silicon dioxide-silicon structure, although work on other materials, especially on compound semiconductors, has been increasing. The silicon MOS field-effect transistor was developed in the 1960s and 1970s as an amplifying and switching device used in integrated circuits (for reviews see, for example, Grove, 1967; Sze, 1969; Nicollian and Brews, 1982). It is the most successful example of a device in which the charge on the plates of a capacitor is changed by the application of a voltage in order to modulate the conductance of one of the plates, and is now one of the major electronic components of memory and logic circuits used in computers. The first proposals date from the 1930s (Lilienfeld's and Heil's patents). Shockley and Pearson (1948) studied an MIS structure which was the archetype of the long series of devices made usually with a slightly oxidized semiconductor, an organic insulating film, and a metallic counter electrode. These structures were used in most of the numerous studies of interface states and surface transport through the 1950s and 1960s.

A related structure, the thin-film transistor (Weimer, 1962), used ohmic contacts to a thin film of highly resistive polycrystalline semiconductor such as CdSe, CdTe, CdS, Se, or Te. Because the properties of these systems were not as favorable as those of the silicon-silicon dioxide system, they have not led to widely used devices and have not proven as amenable to scientific investigation.

The metal-oxide-semiconductor field-effect transistor (MOSFET) or insulated-gate field-effect transistor (IGFET) shown in Fig. 1 uses rectifying contacts to the semiconductor, usually silicon. For the n-channel device shown, no current can flow between the contacts—usually called the source and the drain—unless an n-type inversion layer is established near the silicon-silicon dioxide interface by imposing a positive voltage on the metal electrode, called the gate. For the analogous p-channel devices, voltages and majority carriers are reversed in

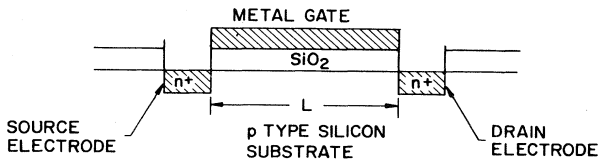

FIG. 1. A cross section of a silicon n-channel metal-oxide-semiconductor field-effect transistor (MOSFET). The n-type contacts known as the source and drain are made by diffusion or by ion implantation into the p-type substrate. The current I_D between them is controlled by the voltage V_G on the metal electrode or gate. When a positive voltage is applied to the gate, it can charge the channel region and control the current between source and drain. An ohmic contact can also be made to the substrate whereby a substrate bias V_{sub} can be applied between the substrate and the normally grounded source.

sign. The MOSFET is a four-terminal device. The electrons are drawn from the source, which is usually at ground potential. They pass along the surface to the drain through the n-type channel induced by a positive voltage on the gate. The fourth terminal, attached to the p-type bulk silicon, is called the substrate contact. The gate, drain, and substrate voltages (with respect to the grounded source) are labeled, respectively, V_G, V_D, and V_{sub}.

Few carriers enter and fewer are trapped in the thermally grown SiO_2 because it is a relatively trap-free insulator with a high barrier to injection of both electrons and holes. In addition, SiO_2 has a high electric breakdown field ($\sim 10^7$ V cm^{-1}), which allows a large charge density to be induced at the surface of the silicon. The interface between silicon and the thermally grown oxide also has a relatively low density of interface states if appropriately treated, which allows most of the induced charge to appear in the semiconductor space-charge layer rather than as charge in interface states. Furthermore, the oxide is quite stable if fast-diffusing species, particularly sodium, are avoided during device preparation. The massive effort in the technology of the silicon-silicon dioxide interface that has been carried out during development of MOSFET devices has made this system particularly well suited to and available for scientific investigation.

Work on materials other than Si has been carried out for many years, even though the interface properties are usually not as desirable as those of the Si-SiO_2 interface. For reports on recent work see, for example, Roberts and Morant (1980), Schulz and Pensl (1981), or the Proceedings of the Conferences on the Physics of Compound Semiconductor Interfaces published annually in the *Journal of Vacuum Science and Technology.*

C. Space-charge layers

The physics of MOS structures begins with a classical solution of Poisson's equation in the direction perpendicular to the surface or interface. The energy-band diagram in the semiconductor is shown in Fig. 2. Here the

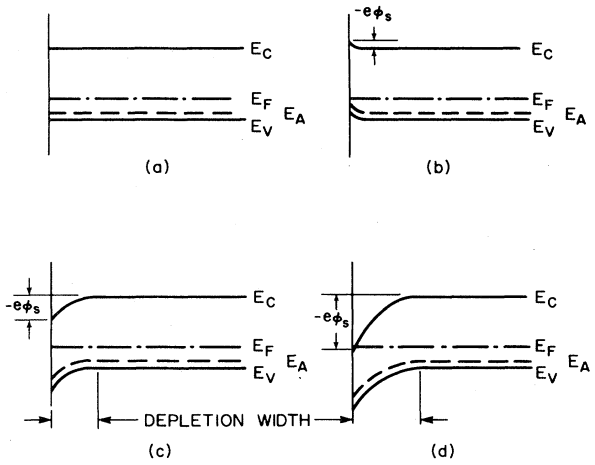

FIG. 2. The energy bands at the surface of a p-type semiconductor for (a) the flat-band case with no surface fields; (b) accumulation of holes at the surface to form an accumulation layer; (c) depletion of the holes or ionization of neutral acceptors near the surface to form a depletion layer; and (d) band bending strong enough to form an inversion layer of electrons at the surface. E_c and E_v are the conduction- and valence-band edges, respectively, E_F is the Fermi energy, and E_A is the acceptor energy. The surface potential ϕ_s measures the band bending.

sample is p type. Figure 2(a) shows the case for zero electric field, called the flat-band voltage condition. Application of a negative bias to the gate [Fig. 2(b)] induces a positive charge in the semiconductor surface, which in the absence of donor interface states can only occur by the induction of excess holes in what is called an accumulation layer. If instead a positive bias is placed on the gate, the energy bands bend down at the surface [Fig. 2(c)]. Negative charge thus induced in the semiconductor is first formed by removing holes from the valence band (or from neutral acceptors near the interface when they are deionized), forming what is called a depletion layer. As the positive gate bias is increased, the fixed negative charge of the acceptor ions and the associated downward band bending increase until the conduction-band edge at the interface approaches the Fermi level and electrons are induced near the interface. When the surface electron density equals or exceeds the hole density in the bulk [Fig. 2(d)], the surface is said to be inverted. The layer of electrons at the surface is called the inversion layer, and the region of fixed negative charge separating this layer from the p-type bulk is called the depletion layer. Another example, with straightforward changes of sign, could also be given for a p-type inversion layer on an n-type substrate.

A quantitative description of the space-charge layer is easy to give, following Kingston and Neustadter (1955), if we assume Boltzmann statistics, assume uniform bulk doping, neglect interface states, and assume all impurities to be ionized. Then the charge density ρ in the one-

dimensional Poisson equation[1]

$$\frac{d^2\phi}{dz^2} = -\frac{4\pi\rho(z)}{\kappa_{sc}} \tag{1.1}$$

for the electrostatic potential $\phi(z)$, which is assumed to vanish in the bulk, i.e., for large values of z, is given by

$$\rho(z) = e(N_D - N_A) + ep_0 e^{-e\phi(z)/k_BT} - en_0 e^{e\phi(z)/k_BT} . \tag{1.2}$$

The first term is the net charge density of bulk donors and acceptors, the second term is the density of holes, with $p_0 \simeq N_A - N_D$ for a p-type bulk, and the last term is the density of electrons, with $n_0 = n_i^2/p_0$, where n_i is the intrinsic carrier concentration appropriate to the semiconductor and the temperature T. Because ρ depends explicitly only on ϕ and not on z one can multiply both sides of Eq. (1.1) by $d\phi/dz$ and integrate to obtain Q, the space-charge density per unit area as follows:

$$Q = \frac{\kappa_{sc}}{4\pi}\left[\frac{d\phi}{dz}\right]_{z=0} = \mp\left[\frac{\kappa_{sc}}{2\pi}[(N_A - N_D)e\phi_s + p_0 k_B T(e^{-e\phi_s/k_BT} - 1) + n_0 k_B T(e^{e\phi_s/k_BT} - 1)]\right]^{1/2} . \tag{1.3}$$

The sign of Q is opposite to the sign of the surface potential $\phi_s = \phi(0)$. For positive ϕ_s the bands bend down [remember that energy-band pictures are for electron energy, whose electrostatic component $-e\phi(z)$ has the opposite sign from that of the potential ϕ] and negative charges are drawn to the surface, while for negative ϕ_s the bands bend up and positive charges are drawn to the surface.

The first term in the square bracket in Eq. (1.3) arises from the fixed charges, while the second and third terms are the contributions of holes and electrons, respectively. For flat bands, with $\phi_s = 0$, the first term is exactly balanced by the second and third. For negative gate bias, with $\phi_s < 0$, the second term dominates and we have surface accumulation. For positive gate bias, with $\phi_s > 0$, the exponential in the second term is reduced. Then the space charge is dominated by the fixed charge and varies as $\phi_s^{1/2}$. When ϕ_s is large enough, the third term, which arises from electrons, will dominate, and at this extreme the surface is inverted. Figure 3 shows the dependence of Q on ϕ_s for an n-type, an intrinsic, and a p-type sample. The curves have been displaced by the difference of the Fermi energies in the bulk.

In extreme inversion or at very low temperatures, Boltzmann statistics are not accurate, and corrections must be made to Eq. (1.3). For accumulation layers at low temperatures, neglect of the impurity ionization energy is not valid.

D. Capacitance

One of the best measures of the response of an MOS system to an applied voltage is its capacitance, or more specifically its differential capacitance per unit area

$$C = \frac{dQ}{dV} , \tag{1.4}$$

where Q is the semiconductor charge density per unit area and V is the applied gate voltage. The voltage drop occurs in the insulator and in the space-charge layer, or, said in another way, the capacitor can be considered to be the insulator capacitance and the semiconductor capacitance in series. Thus the total capacitance per unit area is given by

$$\frac{1}{C} = \frac{1}{C_{ins}} + \frac{1}{C_{sc}} . \tag{1.5}$$

Here

$$C_{ins} = \frac{\kappa_{ins}}{4\pi d_{ins}} \tag{1.6}$$

is the capacitance per unit area of the insulator, whose thickness is d_{ins}, and

$$C_{sc} = \frac{dQ}{d\phi_s} \tag{1.7}$$

is the capacitance per unit area of the semiconductor. If interface charge can be neglected and if the other approximations mentioned above are applicable, then C_{sc} can be obtained directly from Eq. (1.3).

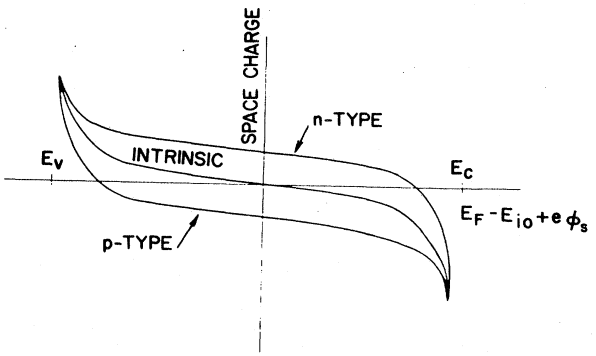

FIG. 3. Charge density versus surface potential. Space-charge density as a function of $E_F - E_{i0} + e\phi_s$ where $E_F - E_{i0}$ is the energy difference of the Fermi level and the intrinsic Fermi level in the bulk and ϕ_s is the surface potential. Curves are shown for n-type, intrinsic, and p-type semiconductors. The charge increases rapidly when the abscissa is close to either band edge. The parabolic regime is dominated by the depletion charge. The derivative of these curves gives the space-charge capacitance.

[1]We use cgs units in most of this article, because most of the existing literature, especially the theory, is written in cgs units. Some representative results are given in both cgs and *Système International* (SI) units in the Appendix.

Figure 4 shows the capacitance as a function of gate voltage for an MOS capacitor on p-type silicon. There are three important regimes to note in such a plot. They are strong accumulation, strong depletion, and flat bands. The strong-accumulation capacitance and the strong-inversion capacitance both correspond to very thin space-charge layers, for which the space-charge capacitance is usually much larger than the insulator capacitance and can either be ignored or corrected for. Thus in these two limits the measured capacitance is approximately equal to the insulator capacitance. The space-charge capacitance per unit area at flat band is found from Eqs. (1.3) and (1.7) to be

$$C_{sc}(\text{flat band})=\left[\frac{(n_0+p_0)e^2\kappa_{sc}}{4\pi k_B T}\right]^{1/2}. \tag{1.8}$$

More generally, the flat-band capacitance of the space-charge layer is the capacitance of a layer of the semiconductor whose thickness is the bulk screening length.

For a real device, the flat-band point is found by combining the insulator capacitance, found as described above, with the calculated space-charge capacitance. This requires knowing the area of the capacitor, because our expressions are all for unit area, as well as any parasitic capacitances that may be present.

In strong inversion, where the capacitance approaches the insulator capacitance, the charge induced by a further increase of the gate voltage goes almost entirely into the inversion layer. This is especially true at low temperatures, where the depletion charge is essentially fixed once the inversion layer is populated. This leads to the very useful approximate relation

$$\delta N_s=\frac{C_{ins}}{e}\delta V_G\ , \tag{1.9}$$

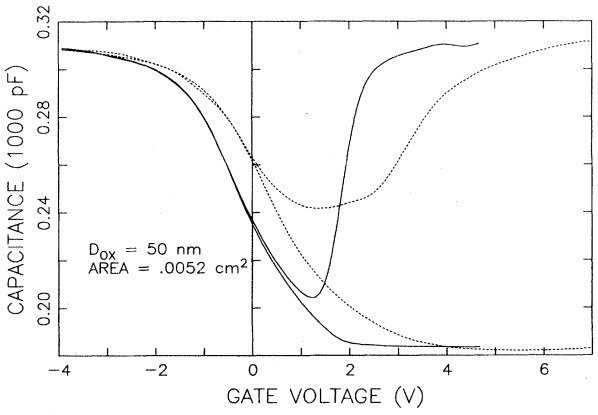

FIG. 4. Capacitance of a metal-insulator-semiconductor (MIS) structure as a function of voltage on the metal. The example shown is for p-type silicon. Curves are shown for samples without (——) and with (· · · ·) surface states. The curves with minima are measured at low frequency. At high frequency the electrons cannot be generated fast enough to respond, and therefore only the depletion capacitance is measured. Figure courtesy of S. Lai.

where N_s is the density of inversion layer electrons per unit area and V_G is the gate voltage. A similiar equation applies to p-type channels.

Capacitance measurements are made by applying a small ac voltage on the gate electrode in addition to the dc gate bias, or by slowly ramping the gate voltage and measuring the current into the capacitor. The minority carriers (the electrons in this discussion) must be thermally generated and therefore cannot follow the ac voltage at high frequencies. Then the measured capacitance does not show a minimum, as illustrated by two of the curves in Fig. 4. The steady-state capacitance is obtained by using low frequencies, a slow ramp, or an FET structure in which the minority carriers can be supplied from the source and drain contacts. Frequency-dependent effects associated with the finite time required to vary the charge in the inversion layer may complicate capacitance measurements for high-resistance surface channels, even if source and drain contacts are present, as found, for example, in capacitance measurements in a strong magnetic field (Kaplit and Zemel, 1968; Voshchenkov and Zemel, 1974). At low temperatures long times may also be required to develop accumulation and depletion layers to equilibrium values (Fowler, 1975).

If interface states are present, the previous discussion must be amended to allow for the charge in those states, which will appear as an additional term in the relation between the semiconductor charge Q and the surface potential ϕ_s. If the interface states can fill and empty at the measurement frequency, the capacitance will be altered as shown by the dotted curves in Fig. 4. If the interface charge does not follow the ac voltage, the states are said to be "slow" as opposed to "fast" states. This can lead to hysteresis if the capacitance curve is traced by sweeping the dc component of the gate voltage up and down through the values at which the interface state charge changes.

The fast states may arise from various sources. Imperfect matching of the SiO_2 to the silicon can result in dangling bonds which may be saturated by hydrogen annealing. Ionic charges or dipoles in the oxide near the interface can give rise to localized states [see, for example, Goetzberger, Klausmann, and Schulz (1976) and Secs. II.E and V.C below] which appear as bound surface states near the band edges in a capacitance measurement. Other interface states may be derived from impurities in the silicon (Snel, 1981). Probably any microscopic defect will appear as a surface state within or without the energy gap; macroscopic fluctuations in charge may appear as inhomogeneities. It is not always easy to sort out these effects, as the large literature bears witness.

One of the reasons that MOSFETs are useful technologically is the same reason that they are useful for scientific studies. That is the possibility, with appropriate treatment, of reducing the number of fast interface states to values ($<10^{10}$ cm^{-2}) that are small compared to the realizable free-carrier concentration ($\sim 10^{10}$ to $\sim 10^{13}$ cm^{-2}). The carriers in these structures have high mobilities at low temperatures. This is because the induced

electrons are separated by a large distance from compensating positive charge in the gate. The barrier between the silicon conduction band and the silicon-dioxide conduction band is large ($\simeq$3.15 eV) so that instabilities due to electrons tunneling into trap states are inhibited and the samples are stable. They share with other insulated-gate structures the major advantage that it is easily possible by application of a voltage to the gate to change the number of induced carriers. Further, in MOSFET structures it is possible to change the electric field seen by a given density N_s of inversion-layer electrons by applying a substrate bias V_{sub} between the substrate and the source. Reverse substrate bias ($V_{\text{sub}}<0$ for our example with a p-type bulk) has the effect of increasing the depletion-layer charge. Gauss's law requires that the total space charge be proportional to the field at the surface, F_s, which in an MOS configuration is approximately proportional to the gate voltage V_G. If the depletion charge is increased by applying reverse substrate bias, the gate voltage must also be increased if the same number of electrons is to be maintained. Thus the electron density N_s and the normal surface field F_s can be varied independently.

E. Quantum effects

The interest in MOS structures is enhanced because they show the electronic properties expected of a two-dimensional electron gas. It was postulated by Schrieffer (1957) that the electrons confined in the narrow potential well of an inversion layer would not behave classically. It is clear that if the carrier wavelength is comparable to the distance from the interface to the classical turning point ($\sim k_BT/eF_s$ in the simplest approximation) then the carrier motion in the direction perpendicular to the interface cannot be treated classically. Quantization of the motion in this direction into discrete levels is expected. When the free-electron behavior along the interface is included, the energy levels take the form

$$E=E_n+\frac{\hbar^2}{2m}(k_x^2+k_y^2)\,, \tag{1.10}$$

where k_x and k_y are the wave-vector components for motion parallel to the surface and the E_n are the electric quantum levels arising from confinement in the narrow potential well. Each value of E_n is the bottom of a two-dimensional continuum called a subband.

Schrieffer felt that interface scattering would broaden the energy levels and that discrete quantum levels would not be observed. Nevertheless, many authors, including Handler and Eisenhour (1964), Murphy (1964), Fang and Triebwasser (1964a, 1964b), Greene (1964), Howard and Fang (1965), Kawaji, Huff, and Gatos (1965), Kawaji and Kawaguchi (1966), and Fang and Howard (1966), searched for these effects, which were invoked to explain anomalous results of field-effect experiments. In the last cited paper, Fang and Howard had observed a pronounced decrease in the electron mobility at high surface fields on a (100) silicon surface at 4.2 K. They postulated that on a (100) surface the degeneracy of the six silicon conduction-band energy minima located along the [100] axes in the Brillouin zone (see Fig. 5) is removed by quantization in the surface potential well. The four valleys for which the effective mass for motion perpendicular to the surface is the light mass m_t are expected to have higher values of the quantum levels E_n of Eq. (1.10) than the two valleys whose long axis, corresponding to the heavy effective mass m_l, is perpendicular to the surface. They assumed that the decrease in mobility appeared when the increasing carrier concentration carried the Fermi level into the subband associated with the higher energy levels, making scattering between the two sets of valleys energetically possible. This explanation was not a correct one for the decrease in mobility but it gave the basis for models of quantization in these surfaces and its predictions as to the lifting of the degeneracy of the valleys and of the two-dimensional nature of the electrons were soon borne out by magnetoconductance measurements of Fowler, Fang, Howard, and Stiles (1966a, 1966b) and then by many other experiments. Piezoresistance measurements (Dorda, 1973) have also been valuable in demonstrating the quantum effects.

The experiments stimulated theoretical work on energy levels in a surface electric field. Self-consistent one-electron Hartree calculations were carried out for n-type surface channels in Si by Duke (1967a), Stern and Howard (1967), and Stern (1972b), among others. Calculations for InAs electron accumulation layers by Appelbaum and Baraff (1971b) and Baraff and Appelbaum (1972) were stimulated by the tunneling measurements of Tsui (1970b, 1971b). Pals (1972a, 1972b, 1972c, 1973) carried out self-consistent calculations in connection with his own capacitance measurements.

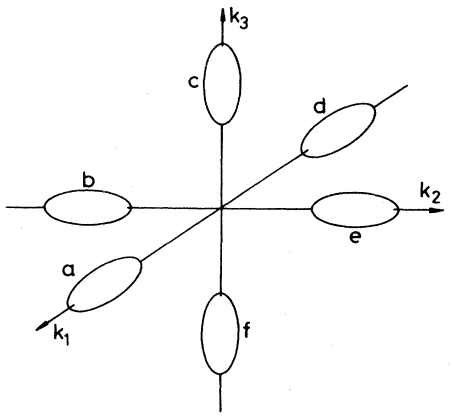

FIG. 5. Schematic constant-energy surfaces for the conduction band of silicon, showing six conduction-band valleys in the ⟨100⟩ direction of momentum space. The band minima, corresponding to the centers of the ellipsoids, are 85% of the way to the Brillouin-zone boundaries. The long axis of an ellipsoid corresponds to the longitudinal effective mass of electrons in silicon, $m_l=0.916m_0$, while the short axes correspond to the transverse effective mass, $m_t=0.190m_0$.

F. Magnetoconductance

A two-dimensional conduction band without spin or valley degeneracy has a constant density of states equal to $m/2\pi\hbar^2$, where m is the effective mass, assumed to be isotropic. If a magnetic field H is perpendicular to the surface, the two-dimensional free-electron motion is converted to a set of quantized Landau levels with spacing $eH\hbar/mc$. The number of electrons per magnetic quantum level is equal to the density of states times the Landau-level splitting, or eH/hc, which equals 2.4×10^{11} cm^{-2} when H equals 10 T. For a Si(100) inversion layer in the lowest subband (if spin and valley splitting are not resolved) this value must be multiplied by a spin degeneracy factor 2 and by a valley degeneracy factor 2.

Magnetoconductance oscillations in inversion layers are unique in that the number of electrons can be varied and counted, as described above, by changing the gate voltage. In the usual Shubnikov—de Haas experiments, oscillatory magnetoconductance is measured by varying the magnetic field with a fixed carrier concentration. In the inversion layer case, variation of the gate voltage and of the carrier concentration at fixed magnetic field leads to periodic changes in conductance, as shown in Fig. 6. The constant period was *prima facie* evidence of two-dimensionality, and the measured number of electrons per oscillation (Fowler *et al.*, 1966a, 1966b) gave a valley degeneracy which agreed within ~5% with the value 2 predicted by Fang and Howard (1966). Furthermore, the prediction that the mass parallel to the surface should be $0.19m_0$, the transverse mass of electrons in silicon, was roughly confirmed by analyzing the temperature dependence of the oscillation amplitudes to find a value of $0.21m_0$.

The magnetoconductance experiment made a two-dimensional model a necessity, at least at low temperatures. Many of the screening and scattering properties for such a model were investigated by Stern and Howard (1967). In 1968, Fang and Fowler published an extensive experimental study of the transport properties of surface space-charge layers, for the first time couched entirely in terms of a physical model that recognized the quantum effects. Some aspects of the large body of work carried out to understand mobilities and scattering mechanisms both experimentally and theoretically are discussed in Sec. IV.

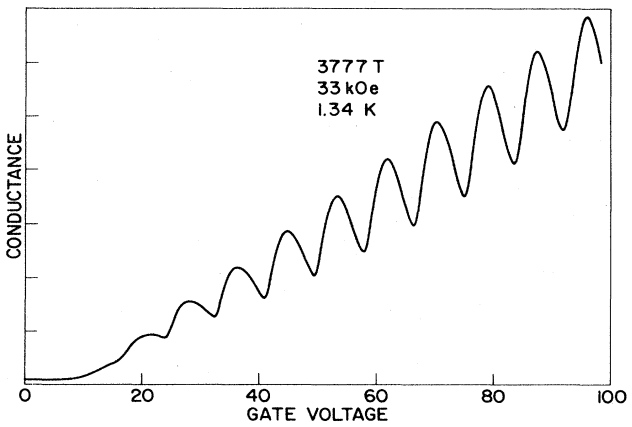

FIG. 6. Conduction on a (100) surface of an n-channel MOSFET with a circular plan or Corbino-disk geometry in the presence of a magnetic field perpendicular to the interface. The oscillations are seen to be uniformly spaced as a function of gate voltage. In this case the spin and valley splittings are not resolved. After Fowler *et al.* (1966a).

An important next step was the recognition that tilting the magnetic field would cause the spin magnetic moment to tilt, while the orbital moment of the Landau levels is fixed in relation to the surface and would follow only the normal component of the field. This difference was used in experiments by Fang and Stiles (1968) to measure the Landé g factor of the electrons, which was found to vary with electron concentration, reaching values larger than 3 for low electron concentrations. This was a puzzle because the spin-orbit interaction, the usual cause of deviations of the g factor from its free-electron value 2.0023, is very weak in silicon. Janak (1969) first recognized that many-body effects, i.e., electron-electron interactions, could account for a large deviation of the g factor from its free-electron value. Careful measurements of the amplitude of the magnetoconductance oscillations by Smith and Stiles (1972, 1974) showed that the effective mass also increases with decreasing carrier concentration, in qualitative agreement with the theory developed by Lee, Ting, and Quinn (1975a, 1975b, 1976), Vinter (1975a, 1976), Ando (1976a, 1976b), Ohkawa (1976a), and Quinn (1976). This subject is discussed more fully in Secs. II.F and VI.B.

The conductance peaks in strong magnetic fields were found by Ando, Matsumoto, Uemura, Kobayashi, and Komatsubara (1972b) to be approximately given by half-integer multiples of $e^2/\pi^2\hbar$, as discussed by Ando and Uemura (1974a).

The Hall conductance measured at the resistance peak between adjacent Landau levels was found by von Klitzing, Dorda, and Pepper (1980) to be an integer multiple of e^2/h, independent of sample geometry, to such precision that it may help to improve the values of the fundamental constants and provide a precise, portable secondary resistance standard. This rapidly developing field has been reviewed by von Klitzing (1981) and is briefly discussed in Sec. VI.B.1.

Reviews of magnetotransport properties have been given by Sugano, Hoh, Sakaki, Iizuka, Hirai, Kuroiwa, and Kakemoto (1973) for low magnetic fields and by Landwehr (1975) and Uemura (1974a, 1974b, 1976) for higher fields.

G. Localization and impurity bands

Early transport measurements (Fang and Fowler, 1968) showed that the inversion layer conductivity had an activated temperature dependence at low carrier densities. This was orginally attributed to freeze-out on im-

purity levels, but is now attributed to localization of the states in band tails. Localized states are also seen in the density-of-states minima between magnetic quantum levels at large magnetic fields. Localization effects take on special interest in inversion layers because the electron concentration can be easily varied, making possible a wider range of experiments than in bulk semiconductors.

Although Coulomb centers can never be completely excluded from the vicinity of an electron or hole layer (electrons on liquid helium are a notable exception), the study of impurity levels in MOS structures is facilitated if fixed charges are purposely introduced. Hartstein and Fowler (1975b; see also Fowler and Hartstein, 1980b) did this by diffusing sodium through the oxide to the silicon-silicon dioxide interface. They showed that a distinct impurity band could be seen in conduction near threshold, and studied the activation energy for motion within the band and for activation to the conduction band. Here also, the ability to change the electron density separately from the impurity density makes possible a new class of experiments.

If samples with activated conductivity are taken to lower temperatures, the dependence of conductivity on $1/T$ often appears curved on a semilogarithmic plot, an effect which is attributed to variable-range hopping, as first proposed for two-dimensional systems by Mott (1973). Other early evidence bearing on localization effects is described by Stern (1974b).

More recently, a new effect has been noted in the conductance of inversion layers at low temperatures. Samples with seemingly metallic behavior, i.e., a weak increase of resistance with increasing temperature at low temperatures, show a weak increase of resistance with *decreasing* temperature at very low temperatures, as first demonstrated for inversion layers by Bishop, Tsui, and Dynes (1980) and Uren, Davies, and Pepper (1980). Such a weak increase, logarithmic in T, has been predicted for two-dimensional electron systems on the basis of localization arguments by Abrahams, Anderson, Licciardello, and Ramakrishnan (1979), who are dubbed the "gang of four," and on the basis of electron-electron interactions by Altshuler, Aronov, and Lee (1980a). Negative magnetoresistance has been found by Kawaguchi and Kawaji (1980b, 1980c) and Wheeler (1981), in good agreement with predictions by Hikami, Larkin, and Nagaoka (1980), Altshuler, Khmel'nitzkii, Larkin, and Lee (1980b), and others. These effects are to be distinguished from the strong localization effects mentioned above, which lead to an activated temperature dependence. Work on weak localization and related effects is progressing very rapidly.

Localization and impurity-band effects are considered in detail in Sec. V.

H. Optical measurements

The early work on semiconductor inversion and accumulation layers was limited to transport measurements and was generally consistent with theoretical predictions of quantum levels. Direct optical measurements of energy-level splitting were first made by Kamgar, Kneschaurek, Koch, Dorda, and Beinvogl (Kamgar *et al.*, 1974a, 1974b). It quickly became clear that energy-level splittings could not be explained on the basis of one-electron models but could be understood if many-body effects were included in the theory, as had already been found in connection with the effective mass and the g factor. Because many-body effects in two-dimensional electron systems are relatively large and because carrier concentrations can be easily varied, inversion and accumulation layers have served as model systems for testing predictions of many-body theory.

Optical measurements have been reviewed by Koch (1975, 1976a). The many-body theory has been described by Ando (1976a, 1976b; 1977a, 1977c), Das Sarma and Vinter (1981a), Jonson (1976), Kalia, Das Sarma, Nakayama, and Quinn (1978, 1979), Nakamura, Ezawa, and Watanabe (1980a), Ohkawa (1976a, 1976b), and Vinter (1976, 1977), among others. Experimental and theoretical results for energy levels and optical transitions are considered in Sec. III.

Because of the energy-level broadening produced by scattering, cyclotron resonance measurements in inversion and accumulation layers must be carried out at magnetic fields high enough so that the Landau-level splitting is comparable to or greater than the level broadening. This pushes the energy range for cyclotron resonance into the far infrared, where it was first detected by Abstreiter, Kneschaurek, Kotthaus, and Koch (1974) and by Allen, Tsui, and Dalton (1974). Many-body effects enter in this experiment in a rather subtle way, as described by Ando (1976a) and Ting, Ying, and Quinn (1976, 1977) and discussed in more detail in Sec. VI.C.

Plasmons in a two-dimensional electron gas were first seen for electrons on liquid helium by Grimes and Adams (1976a, 1976b) and then in inversion layers by Allen, Tsui, and Logan (1977). The plasma-shifted cyclotron resonance (magnetoplasmon effect) was considered theoretically by Horing and Yildiz (1973) and Lee and Quinn (1975) and was observed by Theis, Kotthaus, and Stiles (1977, 1978a, 1978b). This subject was reviewed by Theis (1980) and is discussed in Secs. II.D and VI.C.

I. Prospectus

In the remaining sections the properties of semiconductor space-charge layers and of related two-dimensional and quasi-two-dimensional electron systems are considered in more detail. Section II discusses some properties of ideal or nearly ideal two-dimensional electron systems. In Sec. III, the energy-level structure is considered for realistic models. Section IV discusses transport properties associated with extended states and Sec. V discusses transport properties associated with localized states and impurity bands. Section VI deals mainly with energy levels and transport properties in

strong magnetic fields. Section VII considers some of the more specialized aspects of two-dimensional electron systems. The consequences of the multivalley conduction-band structure of silicon, including valley splitting and the effects of stress and of surfaces tilted from (100), are considered in some detail. The two-dimensional electron crystal is treated in general—both with and without a magnetic field—and with reference to electrons on liquid helium, for which the electron crystal was first observed.

Inversion and accumulation layers at the Si-SiO_2 interface are the most widely studied two-dimensional electron systems for reasons already discussed above. Most of the work has been on *n*-type rather than on *p*-type channels, both because electrons have higher mobility and because the conduction-band structure of silicon makes electrons easier to treat theoretically than holes. The discussion in Secs. I—VII, therefore, deals primarily with electrons in silicon, particularly inversion layers on the (100) surface. In Sec. VIII we consider more briefly a variety of other systems, including holes in silicon and electrons and holes in other semiconductors. Heterojunctions, quantum wells, and superlattices, which have been receiving increasing attention in the last few years, are also covered briefly. Some related systems with large literatures of their own, sometimes predating the work on silicon surface channels, are discussed very briefly. These include thin films, magnetic-field-induced surface states in metals, layer compounds, and intercalated graphite. Section VIII briefly discusses two-dimensional electron-hole systems, which have been treated more often as theoretical constructs than in the laboratory. Section VIII also describes some of the basic properties of electrons on liquid helium and related substrates. This system shares some common features with the other two-dimensional electron systems we consider but has special features of its own. The low densities make the electrons on liquid helium classical (i.e, the kinetic energy exceeds the interelectron potential energy), and the absence of some scattering mechanisms leads to very high mobilities at low temperatures and to sharper spectra than for inversion and accumulation layers. This system was the first in which an electron lattice was realized (Grimes and Adams, 1979).

The Appendix gives algebraic expressions and numerical values for some commonly used quantities. The Bibliography lists papers dealing with the subjects covered herein. An attempt has been made to cover the literature of semiconductor inversion and accumulation layers fairly completely, and to list representative papers from the other fields discussed in this article. Not all papers in the bibliography are cited explicitly. We apologize to authors whose work we have slighted either inadvertently or because time and space did not allow coverage of their work.

This article was submitted before the Fourth International Conference on Electronic Properties of Two-Dimensional Systems, held in New London, New Hampshire in August, 1981. Readers are encouraged to consult the Proceedings of that conference (published in *Surface Science,* Vol. 113, 1982; not included in the bibliography) for recent developments.

II. PROPERTIES OF A TWO-DIMENSIONAL ELECTRON GAS

A. Introduction

The two-dimensional electron systems we consider in this article constitute only a part of the large class of dynamically two-dimensional systems that have been widely studied in recent years. By dynamically two-dimensional we mean that the components of the system are free to move in two spatial dimensions but have their motion constrained in the third dimension. Our principal subject is the system of electrons in semiconductor inversion and accumulation layers. We also consider briefly the electrons in semiconductor heterojunctions, quantum wells, and superlattices and electrons on the surface of liquid helium. Related electron systems mentioned in Sec. VIII include thin films and layer compounds. In addition to these electron systems a number of other two-dimensional systems have received wide attention, including atoms and molecules on graphite and other substrates (Dash, 1975; McTague *et al.,* 1980) and two-dimensional magnetic systems (de Jongh and Miedema, 1974; Pomerantz, 1978, 1980).

Among the properties of two-dimensional systems that have attracted active theoretical and experimental interest are phase transitions (see, for example, Barber, 1980) and long-range order (Imry, 1979). The Proceedings of the Conference on Ordering in Two Dimensions (Sinha, 1980) give a useful entry point to the very extensive literature of this subject.

Transport and percolation properties of disordered two-dimensional systems have been extensively studied (see, for example, Last and Thouless, 1971; Kirkpatrick, 1973, 1979; Stauffer, 1979; Essam, 1980), but percolation theories as such are not covered in this article. Percolation concepts enter briefly in Sec. V.A.3. Transport properties are covered in Sec. V, and recent work on weak localization and electron-electron interactions in two-dimensional systems which leads to the prediction that such systems have vanishing conductivity at absolute zero is discussed in Sec. V.B.

The two-dimensional Coulomb gas, a system of electrons interacting in a strictly two-dimensional universe in which electromagnetic fields are confined to a plane, has been widely studied theoretically (see, for example, Baus and Hansen, 1980). The electrons interact with a logarithmic rather than a $1/r$ potential. While this system does not have an exact physical analog [but see, for example, Doniach and Huberman (1979), Fisher (1980a), and Hebard and Fiory (1980) in connection with vortex-pair interactions in thin-film superconductors] it is an important model system for theoretical investigation.

A good overview of many aspects of the physics of

two-dimensional systems is given by Kosterlitz and Thouless (1978). Many of these aspects are not covered in the present article. This chapter covers some formal aspects of the physics of ideal two-dimensional systems.

B. Density of States

Before going on to a detailed discussion of the two-dimensional electron gas let us recall a basic result for two-dimensional systems, namely the density of states. Because the density of states in n-dimensional wave-vector space is $(2\pi)^{-n}$, the two-dimensional density of electron states per unit area and unit energy is

$$D(E)=2g_v\frac{1}{(2\pi)^2}2\pi k\frac{dk}{dE}\ , \tag{2.1}$$

where g_v is a valley degeneracy factor which gives the number of equivalent energy bands and where we have included a factor 2 for spin degeneracy. If the electron excitation spectrum is given by

$$E=E_0+\frac{\hbar^2k^2}{2m}\ , \tag{2.2}$$

where m is the effective mass,[2] here assumed to be isotropic, we obtain

$$\begin{aligned} D(E)&=\frac{g_v m}{\pi\hbar^2}\ ,\quad E>E_0\\ &=0\ ,\quad E<E_0\ . \end{aligned} \tag{2.3}$$

Note that the density of states rises abruptly at the energy E_0 (in the absence of disorder or level broadening) and is constant for higher energies. There will be additional step increases in the density of states if there are two-dimensional bands at higher energies. When only the lowest band is occupied, the number of electrons per unit area at absolute zero is

$$N_s=\frac{g_v m}{\pi\hbar^2}(E_F-E_0)\ , \tag{2.4}$$

where E_F is the Fermi energy. The Fermi surface for the two-dimensional electron system is a curve, also called the Fermi line. In the simplest case of isotropic effective mass it is a circle whose radius is the Fermi wave vector

$$k_F=(2\pi N_s/g_v)^{1/2}\ . \tag{2.5}$$

For elliptical Fermi surfaces with a quadratic dependence of E on k the effective mass in Eqs. (2.3) and (2.4) must be replaced by density-of-states effective mass m_d whose value is given in Eq. (3.6). For more complex energy spectra, such as those that obtain for electrons in nonparabolic conduction bands or for holes in warped, nonparabolic valence bands, the density of states must generally be found numerically.

[2]The free-electron mass is called m_0 throughout this article.

C. Polarizability and screening

The most important property of a two-dimensional electron gas to be considered in this chapter is its response to electromagnetic fields. The simplest example of this kind is the response of the system to a weak, static potential that is slowly varying in space. In addition, we first assume that the electron gas is in a sheet of zero thickness at $z=0$ surrounded by homogeneous media with dielectric constants $\kappa_{\rm ins}$ for $z<0$ and $\kappa_{\rm sc}$ for $z>0$.

The additional electrostatic potential ϕ produced by an external source is related to the charge density ρ by Poisson's equation

$$\nabla\cdot(\kappa\nabla\phi)=-4\pi\rho\ , \tag{2.6}$$

where $\rho=\rho_{\rm ext}+\rho_{\rm ind}$ is the sum of the external charge density and the induced charge density, and κ is the dielectric constant, which can be a function of position. In the long-wavelength limit used here, the induced charge density at a point $\mathbf{r}$ in the plane $z=0$ is a function only of the local potential seen by the electrons, as in the three-dimensional Thomas-Fermi model, and we have

$$\rho_{\rm ind}(\mathbf{r})=-e[N_s(\bar\phi)-N_s(0)]\delta(z)\ , \tag{2.7}$$

where $\bar\phi=\phi(\mathbf{r},0)$ is the value of the electrostatic potential at $\mathbf{r}$ averaged over the electron distribution in z, which is a delta function in the present simplified case. Equation (2.7) is the two-dimensional analog of the Thomas-Fermi approximation.

A potential $\bar\phi$ changes the energy levels by $-e\bar\phi$ and the separation of the Fermi energy E_F from the bottom of the conduction band by $e\bar\phi$. Because we are assuming a weak potential, we can linearize Eq. (2.7) and find

$$\begin{aligned} \rho_{\rm ind}(\mathbf{r})&=-e\bar\phi(\mathbf{r})\frac{dN_s}{d\phi}\delta(z)\\ &=-e^2\bar\phi(\mathbf{r})\frac{dN_s}{dE_F}\delta(z)\ . \end{aligned} \tag{2.8}$$

Then Eq. (2.6) becomes

$$\nabla\cdot(\kappa\nabla\phi)-2\bar\kappa\bar q_s\bar\phi(\mathbf{r})\delta(z)=-4\pi\rho_{\rm ext}\ , \tag{2.9}$$

where $\bar q_s$ is a screening parameter with dimensions of reciprocal length, defined by

$$\bar q_s=\frac{2\pi e^2}{\bar\kappa}\frac{dN_s}{dE_F}\ , \tag{2.10}$$

with

$$\bar\kappa=\frac{\kappa_{\rm sc}+\kappa_{\rm ins}}{2}\ . \tag{2.11}$$

Contrast Eq. (2.9) with the corresponding equation for linear screening in a homogeneous three-dimensional system:

$$\nabla^2\phi-Q_s^2\phi=-4\pi\rho_{\rm ext}/\kappa\ , \tag{2.12}$$

where Q_s is the three-dimensional screening parameter,

often called q_{TF}. When the external charge is a point charge Ze at the origin, the solution of Eq. (2.12) is the familiar exponentially screened Coulomb potential $\phi=(Ze/\kappa R)\exp(-Q_s R)$.

To find the screened Coulomb potential for our two-dimensional example, we use a Fourier-Bessel expansion for the potential:

$$\phi(\mathbf{r},z)=\int_0^\infty qA_q(z)J_0(qr)dq \ , \tag{2.13}$$

where J_0 is the Bessel function of order zero and $A_q(z)$ is a function of q and z, whose value averaged over the delta-function electron distribution is $\bar{A}_q=A_q(0)$.

The solution of Eq. (2.9) when the external charge is a point charge is a point at $r=0$, $z=z_0\leq 0$ is easily obtained. We give here only the value of the Fourier coefficient of the potential in the electron plane as follows:

$$\bar{A}_q=\frac{Ze}{\bar{\kappa}}\frac{e^{qz_0}}{q+\bar{q}_s} \ . \tag{2.14}$$

For large values of r, where $\bar{q}_s r>>0$, the asymptotic form of the average potential seen by the electrons is (Stern, 1967):

$$\bar{\phi}(r)\sim\frac{Ze(1+\bar{q}_s z_0)}{\bar{\kappa}\bar{q}_s^2 r^3} \ . \tag{2.15}$$

This inverse-cube dependence of the potential on distance is much slower than the exponential decay found in the three-dimensional case, and is one of the principal qualitative differences between two-dimensional and three-dimensional screening.

The foregoing example assumed that all the electronic charge was in a plane. Let us now consider the more realistic case of nonzero thickness for the electron layer. The simplest approximation for the charge distribution of electrons is the one first made for inversion layers by Fang and Howard (1966):

$$g(z)=\frac{b^3}{2}z^2e^{-bz} \ . \tag{2.16}$$

This is also the appropriate charge density for electrons in the lowest subband for the image potential outside liquid helium (Cole, 1974) if the thickness of the helium-vacuum interface is taken to be zero. Expressions for the parameter b and a discussion of the validity of this approximate charge distribution are given in the following chapter. With this charge distribution, the previous considerations are slightly modified: $g(z)$ replaces $\delta(z)$ in Eq. (2.9), and the average potential felt by the electrons is

$$\bar{\phi}(\mathbf{r})=\int_0^\infty g(z)\phi(\mathbf{r},z)dz \ , \tag{2.17}$$

whose Fourier-Bessel transform is again called $\bar{A}_q$.

Because of the form of Eq. (2.16), it is easy to solve Eq. (2.9) to find the explicit results for the Fourier-Bessel coefficients of the average potential seen by the electrons in the inversion layer (Stern and Howard, 1967):

$$\bar{A}_q=\frac{Ze}{\bar{\kappa}}\frac{P_0e^{qz_0}}{q+q_sP_{\rm av}+q_s\delta_\kappa P_0^2} \ , \quad z_0\leq 0 \tag{2.18a}$$

$$\bar{A}_q=\frac{Ze}{\kappa_{\rm sc}}\frac{P(z_0)+\delta_\kappa P_0e^{-qz_0}}{q+q_sP_{\rm av}+q_s\delta_\kappa P_0^2} \ , \quad z_0>0 \tag{2.18b}$$

where

$$\delta_\kappa=\frac{\kappa_{\rm sc}-\kappa_{\rm ins}}{\kappa_{\rm sc}+\kappa_{\rm ins}}=\frac{\kappa_{\rm sc}-\kappa_{\rm ins}}{2\bar{\kappa}} \ , \tag{2.19}$$

$$q_s=\frac{2\pi e^2}{\kappa_{\rm sc}}\frac{dN_s}{dE_F} \ , \tag{2.20}$$

$$P_0=\frac{b^3}{(b+q)^3} \tag{2.21}$$

$$P_{\rm av}=\frac{8b^3+9b^2q+3bq^2}{8(b+q)^3} \tag{2.22}$$

$$P(z)=\frac{b^3}{(b-q)^3}[e^{-qz}-(a_0+a_1z+a_2z^2)e^{-bz}] \ , \quad q\neq b$$

$$a_0=\frac{2q(3b^2+q^2)}{(b+q)^3} \ ,$$

$$a_1=\frac{4bq(b-q)}{(b+q)^2} \ ,$$

$$a_2=\frac{q(b-q)^2}{b+q} \ , \tag{2.23a}$$

$$P(z)=\tfrac{1}{8}[1+2bz+2b^2z^2+\tfrac{4}{3}b^3z^3]e^{-bz} \ , \quad q=b \ . \tag{2.23b}$$

Note that in the limit of large b the results in Eq. (2.18a) reduce to those for the extreme two-dimensional limit given in Eq. (2.14).

Equations (2.18) can be used to calculate the Born-approximation cross section for scattering of electrons in the lowest subband by charged centers in the oxide and in the semiconductor, as discussed in Sec. II.G and Sec. IV. Recently there have been calculations which treat the scattering centers in a more sophisticated way by taking into account the occupation of the bound state in the presence of a screening charge distribution (Vinter, 1978; Takada, 1979). These results will be discussed in the next section in relation to bound states and in Sec. IV.C in relation to scattering. The results given above are the two-dimensional analog of the conventional Brooks-Herring treatment of ionized impurity scattering in semiconductors (see, for example, Smith, 1978).

Let us now look more closely at the screening parameter q_s, defined in Eq. (2.20), which gives the screening effects in the long-wavelength, static approximation, and on the related parameter $\bar{q}_s$, defined in Eq. (2.10), which enters in the extreme two-dimensional limit. We have

$$\kappa_{\rm sc}q_s=\bar{\kappa}\bar{q}_s=\frac{2\pi e^2N_s}{E_d} \ , \tag{2.24}$$

where

$$E_d=\frac{N_s}{(dN_s/dE_F)} \tag{2.25}$$

is called the diffusion energy because it enters in the generalized Einstein relation (see, for example, Spenke, 1955)

$$D=\frac{E_d}{e}\mu \tag{2.26}$$

connecting the diffusion coefficient D and the mobility μ.

For the simple two-dimensional density of states given by Eq. (2.3), we have (Stern and Howard, 1967)

$$\frac{E_d}{k_BT}=\left[1+\exp\left[\frac{E_0-E_F}{k_BT}\right]\right]\ln\left[1+\exp\left[\frac{E_F-E_0}{k_BT}\right]\right]. \tag{2.27}$$

At low temperatures, when $E_F-E_0>>k_BT$, the diffusion energy is $E_d\sim E_F-E_0$ and

$$q_s=2g_v/a^*\ ,\quad a^*=\frac{\kappa_{sc}\hbar^2}{me^2} \tag{2.28a}$$

$$\bar{q}_s=2g_v/\bar{a}^*\ ,\quad \bar{a}^*=\frac{\bar{\kappa}\hbar^2}{me^2} \tag{2.28b}$$

where a^* and $\bar{a}^*$ are the effective Bohr radii using the semiconductor dielectric constant and the average of the semiconductor and insulator dielectric constants, respectively. At high temperatures the diffusion energy is $E_d\sim k_BT$ and

$$\kappa q_s=\bar{\kappa}\bar{q}_s=\frac{2\pi e^2N_s}{k_BT}\ . \tag{2.29}$$

Note, however, that at high temperatures more than one subband will be populated with carriers, and the expressions given here must be generalized. Such generalizations have been given by Stern and Howard (1967) and more fully by Siggia and Kwok (1970), and have been applied to mobility calculations by Stern (1978a) and by Mori and Ando (1979). The mobility calculations are discussed in Sec. IV.

The results given so far in this section have assumed that the potentials being screened are very slowly varying in space and static in time. In several kinds of problems, including the calculation of bound states and the scattering of carriers at elevated temperatures or in more than one subband, this approximation no longer suffices. The simplest approximation that gives the response of the system to shorter wavelengths and to time-varying potentials is the self-consistent or random-phase approximation, in which each electron is assumed to move in the external field plus the induced field of all electrons. This is the model which leads to the famous Lindhard (1954) dielectric function for a three-dimensional electron gas. It ignores dynamical correlation effects and is known to lead to errors in various quantities such as the pair correlation function (see, for example, Jonson, 1976), but it is nevertheless widely used because it gives the simplest nontrivial result for the linear response of the system to an external field.

The polarization induced by one component $\mathbf{F}(\mathbf{q},\omega)=\mathbf{F}_0\exp(i\mathbf{q}\cdot\mathbf{r}-i\omega t)$ of the total (external plus induced) electric field acting on the sheet of electrons at $z=0$ can be written

$$\mathbf{P}(\mathbf{q},\omega)=\chi(\mathbf{q},\omega)\mathbf{F}(\mathbf{q},\omega)\delta(z)\ , \tag{2.30}$$

where χ is the polarizability of the layer, given by Ehrenreich and Cohen (1959):

$$\chi(\mathbf{q},\omega)=\frac{e^2}{q^2L^2}\lim_{\alpha\to0}\sum\frac{f_0(E_\mathbf{k})-f_0(E_{\mathbf{k}+\mathbf{q}})}{E_{\mathbf{k}+\mathbf{q}}-E_\mathbf{k}-\hbar\omega-i\hbar\alpha}\ , \tag{2.31}$$

f_0 is the Fermi-Dirac occupation probability, L^2 is the normalization area, and the sum is over all one-electron states of wave vector $\mathbf{k}$ and energy $E_\mathbf{k}$.

For an isotropic two-dimensional electron gas with energy levels $E_\mathbf{k}=\hbar^2k^2/2m$ and Fermi wave vector k_F, Eq. (2.31) evaluated at absolute zero gives $\chi=\chi_1+i\chi_2$, where (Stern, 1967)

$$\chi_1=\frac{2me^2N_s}{\hbar^2k_Fq^3}\left\{\frac{q}{k_F}-C_-\left[\left[\frac{q}{2k_F}-\frac{mk_F\omega q}{\hbar}\right]^2-1\right]^{1/2}-C_+\left[\left[\frac{q}{2k_F}+\frac{mk_F\omega q}{\hbar}\right]^2-1\right]^{1/2}\right\}, \tag{2.32a}$$

$$\chi_2=\frac{2me^2N_s}{\hbar^2k_Fq^3}\left\{D_-\left[1-\left[\frac{q}{2k_F}-\frac{mk_F\omega q}{\hbar}\right]^2\right]^{1/2}-D_+\left[1-\left[\frac{q}{2k_F}+\frac{mk_F\omega q}{\hbar}\right]^2\right]^{1/2}\right\}, \tag{2.32b}$$

$$C_\pm=\mathrm{sgn}\left[\frac{q}{2k_F}\pm\frac{mk_F\omega q}{\hbar}\right], \tag{2.32c}$$

$$D_\pm=0\ ,\quad \left|\frac{q}{2k_F}\pm\frac{mk_F\omega q}{\hbar}\right|>1\ , \tag{2.32c}$$

$$C_\pm=0\ ,\quad D_\pm=1\ ,\quad \left|\frac{q}{2k_F}\pm\frac{mk_F\omega q}{\hbar}\right|<1\ . \tag{2.32d}$$

These results are best understood by looking at a number of special cases. The simplest is the static, long-wavelength limit considered above. Then we find, for $\omega=0$, $q\sim0$, that

$$\rho_{\mathrm{ind}}=-i\mathbf{q}\cdot\mathbf{P}=-q^2\chi(q)\bar{\phi}(r)\delta(z)=-\frac{N_se^2}{E_F}\bar{\phi}(r)\delta(z)\ , \tag{2.33}$$

in agreement with Eq. (2.8). More generally, $\delta(z)$ is replaced by $g(z)$.

The dielectric constant for the physical system we are dealing with will be a nonlocal function in general (Dahl and Sham, 1977; Eguiluz and Maradudin, 1978a, 1978b), but can be expressed in a simple form when the inversion layer is a sheet of charge in the plane $z=0$ embedded in a homogeneous medium with dielectric constant κ. Then

one can define a dielectric constant for longitudinal excitation within the plane of electrons to be (Stern, 1967)

$$\kappa(\mathbf{q},\omega)=\kappa+2\pi\beta\chi(\mathbf{q},\omega)\ , \tag{2.34}$$

where $\beta^2=q^2-\kappa\omega^2/c^2$. For the corresponding results in a more general case, see Dahl and Sham (1977).

For static fields Eqs. (2.32) and (2.34) give

$$\kappa(\mathbf{q},0)=\kappa\left[1+\frac{q_s}{q}\right]\ ,\quad q\le 2k_F\ ,$$
$$=\kappa\left[1+\frac{q_s}{q}\left\{1-\left[1-\left[\frac{2k_F}{q}\right]^2\right]^{1/2}\right\}\right]\ ,\quad q>2k_F\ . \tag{2.35}$$

For small q, this dielectric constant leads to the same results that we obtained in a different way above. For $q>2k_F$, the screening effects fall off much more rapidly. This removes a conceptual difficulty that arises when the long-wavelength dielectric constant at absolute zero is considered for an ideal two-dimensional electron gas of very low density. The screening parameter, given by Eq. (2.28), is independent of carrier concentration, and we would have the unphysical result that a very low density of carriers continues to screen as effectively as a higher density. This difficulty is removed by Eq. (2.35), because k_F goes to zero as the density goes to zero, so that the screening affects a smaller and smaller range of q. In a real system, finite temperature and band tailing effects will also limit the screening at low electron densities.

A more important effect of the cutoff of screening for large wave vectors is the change of slope of the dielectric function at $q=2k_F$. This change leads to Friedel oscillations in the response of the system to a localized disturbance, just as in three dimensions. The leading term in the potential at large distances for a screened Coulomb potential induced by a point charge Ze in the same plane as the sheet of electrons is (Stern, 1967):

$$\bar{\phi}(\mathbf{r})\sim-\frac{Zeq_s}{\kappa}\frac{4k_F^2}{(2k_F+q_s)^2}\frac{\sin(2k_Fr)}{(2k_Fr)^2}\ . \tag{2.36}$$

Similar results have been found for three-dimensional semiconductors with cylindrical energy bands by Roth, Zeiger, and Kaplan (1966; see also Gabovitch *et al.*, 1978, for metals); for carrier-induced magnetic interactions in two-dimensional systems by Fischer and Klein (1975); and, apart from a phase difference, for the interaction between adsorbed atoms induced by the response of a partially filled band of surface states, by Lau and Kohn (1978).

Maldague (1978a) showed how the temperature-dependent static polarizability can be obtained from the values at absolute zero. His results can be written

$$\chi(\mathbf{q},\omega;T,\mu)=\int_0^\infty\frac{\chi(\mathbf{q},\omega;0,\mu')}{4k_BT\cosh^2\dfrac{\mu-\mu'}{2k_BT}}d\mu'\ , \tag{2.37}$$

where T is the absolute temperate and μ is the chemical potential. The high-temperature limit of the static dielectric function was found by Fetter (1974b) to be

$$\kappa(q,0)=\bar{\kappa}\left[1+\frac{q_s(q)}{q}\right]\ ,$$
$$q_s(q)=\frac{2\pi N_se^2}{\bar{\kappa}k_BT}g_1(q\lambda)\ ,$$
$$\lambda=\left[\frac{2\pi\hbar^2}{mk_BT}\right]^{1/2}\ ,$$
$$g_1(x)=\frac{2\pi^{1/2}}{x}\Phi\left[\frac{x}{4\pi^{1/2}}\right]\ . \tag{2.38}$$

Here

$$\Phi(y)=\pi^{-1/2}\mathscr{P}\int_{-\infty}^{\infty}dz\frac{e^{-z^2}}{y-z}\ , \tag{2.39}$$

where $\mathscr{P}$ denotes principal value, is the real part of the plasma dispersion function as defined by Fetter and Walecka (1971, p. 305), whose definition differs by a factor -1 from that of Fried and Conte (1961). Note that $g_1(0)=1$, and that Eq. (2.38) therefore reduces to (2.29) for small q. At high temperatures for which more than one subband is occupied Eq. (2.38) can give misleading results unless the occupations and spatial extents of the higher-lying subbands are taken into account. The wave-vector dependence of the effective screening parameter in a single subband at absolute zero and at higher temperatures as calculated by Stern (1980b) is illustrated in Fig. 7.

The screening properties of electrons in coupled layers, as in layer compounds or intercalated graphite, have been discussed by Visscher and Falicov (1971), Fetter (1974a), and Pietronero, Strässler, and Zeller (1979).

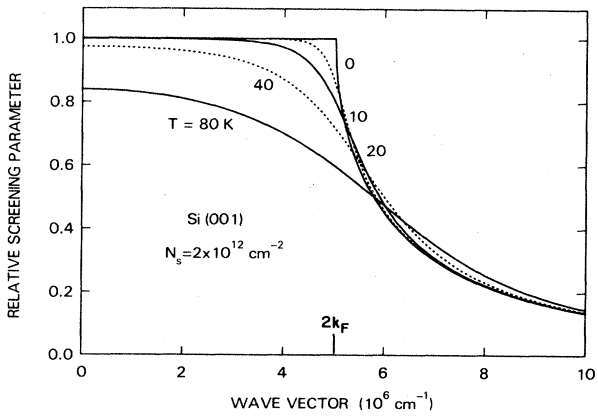

FIG. 7. Wave-vector dependence of the effective screening parameter $q_s(q,T)$ normalized to its value $q_s(0,0)$ at long wavelengths and absolute zero, for $T=0$, 10, 20, 40, and 80 K. The curves are calculated for a Si(001) inversion layer with 2×10^{12} electrons per cm^2, for which the Fermi circle diameter is $2k_F=5.01\times10^6$ cm^{-1}. After Stern (1980b).

D. Plasmons

We next consider some dynamical consequences of the dielectric constant Eq. (2.32). The simplest of these are the longitudinal modes of the system, or plasmons, which are solutions of

$$\kappa(\mathbf{q},\omega)=0 . \tag{2.40}$$

For long wavelengths, for which $m\omega >> \hbar q k_F$, the polarizability reduces to the free-electron value $\chi=-N_s e^2/m\omega^2$, and the solution of Eq. (2.40) with the dielectric constant (2.34) is

$$q^2-\frac{\kappa\omega^2}{c^2}=\left[\frac{m\kappa\omega^2}{2\pi N_s e^2}\right]^2 . \tag{2.41}$$

For very long wavelengths, for which $q<2\pi N_s e^2/mc^2$, the right side of Eq. (2.41) becomes negligible and $q\sim\kappa^{1/2}\omega/c$. A similar result obtains for bulk and surface plasmons (Ferrell, 1958). Effects due to the finite insulator thickness, discussed in the next paragraph, generally modify the effective dielectric constant and the plasmon dispersion before these so-called retardation effects become operative.

The effective dielectric constant given in Eq. (2.34) is valid when the sheet of carriers is embedded in a homogeneous medium. In the case of inversion layers, the insulating layer is generally bounded by a metallic gate electrode and the semiconductor space-charge layer is bounded by the bulk. In the case of electrons on liquid helium there are usually metal electrodes present. The presence of conducting boundaries modifies the plasmon dispersion relation. If retardation effects are neglected, the plasma frequency is given by (Dahl and Sham, 1977)

$$\omega_p^2=\frac{4\pi N_s e^2 q}{m(\kappa_{sc}\coth qd_{sc}+\kappa_{ins}\coth qd_{ins})} , \tag{2.42}$$

where d_{ins} and d_{sc} are the insulator thickness and the effective thickness of the semiconductor, respectively. If the semiconductor bulk can be considered to be metallic for $\omega\sim\omega_p$, as is likely to be the case if there is a substantial density of free carriers in the bulk, then d_{sc} is equal to the depletion layer thickness z_d. If the semiconductor bulk is effectively a dielectric near ω_p, as is likely to be the case at low temperatures if the free carriers are frozen out, then d_{sc} becomes the sample thickness if there is a metallic substrate electrode or it becomes effectively infinite if there is not.

If $qz_d \gtrsim 1$, $\coth qz_d \sim 1$, Eq. (2.42) reduces to one given by Chaplik (1972a), Eguiluz, Lee, Quinn, and Chiu (1975), and implicitly by Nakayama (1974a). If $qd_{sc}<1$, $qd_{ins}<1$, so that the hyperbolic cotangents can be replaced by the reciprocals of their arguments, we have

$$\omega_p\sim q\left[\frac{4\pi N_s e^2/m}{\frac{\kappa_{sc}}{d_{sc}}+\frac{\kappa_{ins}}{d_{ins}}}\right]^{1/2} . \tag{2.43}$$

At shorter wavelengths the corrections associated with finite insulator thickness become less important. If these effects are neglected and the polarizability is expanded to the next order in q/ω, we find that the plasmon dispersion deduced from Eqs. (2.32), (2.34), and (2.40) is

$$\omega_p^2\sim\frac{2\pi N_s e^2 q}{m\kappa}+\frac{3}{4}q^2 v_F^2 . \tag{2.44}$$

The leading term in Eq. (2.44) leads to a square-root dependence of plasmon energy on wave vector, a result first given for two-dimensional systems by Ritchie (1957) and by Ferrell (1958). Fetter (1973) used the hydrodynamic approximation, and found a result similar to Eq. (2.44) but with the coefficient of the second term replaced by $\frac{1}{2}$. Beck and Kumar (1976) calculated the plasmon dispersion taking correlation effects and the finite spatial extent of the inversion layer into account. They found that the leading term of Eq. (2.44) was not affected but that the second term was significantly changed both for degenerate and nondegenerate electron gases. Rajagopal (1977a), in his paper on the longitudinal and transverse dielectric functions of the degenerate two-dimensional electron gas, pointed out a correction to one term in the original result given by Beck and Kumar. The effect of several different model dielectric functions on plasmon dispersion has been considered by Jonson (1976).

The predicted plasmon dispersion at long wavelengths was first verified by Grimes and Adams (1976a, 1976b), who measured radio-frequency standing-wave resonances of electrons on liquid helium in a rectangular cell. It was subsequently seen in inversion layers by Allen, Tsui, and Logan (1977) and by Theis, Kotthaus, and Stiles (1978a, 1978b), who measured far-infrared transmission. Plasmon emission has been observed by Tsui, Gornik, and Logan (1980) from inversion layers excited by passing an electric current through the source-drain contacts. In all these experiments the wave vector is selected by placing a grating of period a close to the electron layer, so that plasmons with wave-vector components $q_n=2\pi n/a$ along the surface can be coupled in or out of the system. It has not been possible yet to achieve large enough values of q to test higher-order terms in the plasmon dispersion relation, because this requires rather small values of the grating period. Such experiments would be of considerable interest, however, because the higher-order terms are sensitive to details of the physical interactions in the system and because at large wave vectors one will reach the regime where plasmon modes and single-particle modes overlap.

Another interesting feature of the plasmon dispersion arises if the insulator is bounded by another semiconductor layer or by a semimetal. Opposite charges will be induced on opposite sides of the insulator and there will be two coupled plasmon branches. This problem was considered by Eguiluz *et al.* (1975) and by Caillé and Banville (1976). The dispersion relation simplifies if the bounding materials are semiconductors with the same dielectric constant κ_{sc}, if the effects of finite depletion layer thickness are ignored, and if $qd_{ins}<<1$. Then the

two branches are given at long wavelengths by

$$\omega_-^2=\frac{4\pi N_s e^2 q^2 d_{\rm ins}}{(m_e+m_h)\kappa_{\rm ins}}\ ,\quad \omega_+^2=\frac{2\pi N_s e^2(m_e+m_h)q}{m_e m_h \kappa_{\rm sc}}\ , \tag{2.45}$$

where m_e and m_h are the electron and hole masses of the induced carriers on opposite sides of the insulator. The two branches can be called the acoustic and optical coupled plasmon modes. They have not yet been observed. Acoustic plasmons can arise within a single space-charge layer with one type of carrier if more than one subband is occupied (Takada, 1977). Coupled plasmon modes have also been considered by Das Sarma and Madhukar (1980a, 1981a). Englert, Tsui, and Logan (1981) measured the plasmon resonance in (001) Si under stress, and determined the conditions under which carriers transfer to the $E_{0'}$ subband, which has a different optical effective mass from that of the lowest subband for motion parallel to the surface. Plasmon-phonon coupling has been treated by Caillé, Banville, and Zuckerman (1977), Gersten (1980), Chaplik and Krasheninnikov (1980), and Tannous and Caillé (1980).

Plasma oscillations in layered electron gases have been considered by many authors, including Grecu (1973), Fetter (1974a), Apostol (1975), Roberts (1975), and Shmelev *et al.* (1977), and, for layers in a magnetic field, by Kobayashi, Mizuno, and Yokota (1975). For a recent experimental on intercalated graphite, see Mele and Ritsko (1980). Systems in which layers of electrons and holes are present have been widely studied theoretically. They are discussed in Sec. VIII.G.

The effects of magnetic fields on the dielectric properties of a two-dimensional electron gas have been considered theoretically by Chiu and Quinn (1974), Horing, Orman, and Yildiz (1974), Horing and Yildiz (1976), Nakayama (1974b), Lee and Quinn (1975, 1976), Horing, Kamen, and Orman (1981), and Horing, Orman, Kamen, and Glasser (1981), and have been studied experimentally by Theis, Kotthaus, and Stiles (1977).

Plasmons have been considered as a possible source of superconductivity in inversion layers by Takada and Uemura (1976) and Takada (1977, 1978, 1980b). A brief discussion of superconductivity in inversion layers is given at the end of Sec. II.F.1 in connection with silicon and in Sec. VIII.B.3 in connection with InAs.

A good review of experimental and theoretical work on plasmons and magnetoplasmons in inversion layers has been given by Theis (1980); see also Litovchenko (1978). Additional discussion of plasmon and magnetoplasmon properties appears in Sec. VI.C.3.

E. Bound states

Bound states associated with impurities and defects strongly affect the electrical and optical properties of bulk semiconductors. We shall here explore some of the effects associated with bound states in two-dimensional systems, particularly inversion layer bound states induced by charged impurities.

The simplest bound states in bulk semiconductors are those associated with singly charged attractive Coulomb centers in a medium with dielectric constant $\kappa_{\rm sc}$ and an isotropic effective mass m. For a simple, parabolic band these states have a hydrogenic spectrum with energy levels

$$E_n=-\frac{me^4}{2\kappa_{\rm sc}^2\hbar^2 n^2}\ ,\quad n=1,2,\ldots \tag{2.46}$$

relative to the adjacent band edge.

If an impurity with charge e is placed at the semiconductor surface, or at the boundary between the semiconductor and an insulator, then the Coulomb potential energy of an electron is $-e^2/\bar{\kappa}R$. If there is a large potential barrier which keeps electrons out of the insulator, then as a first approximation we can require that the envelope wave function of the electron goes to zero at the interface. If we ignore the image potential and band bending near the interface, the energy-level spectrum is again hydrogenic:

$$E_n=-\frac{me^4}{2\bar{\kappa}^2\hbar^2 n^2}\equiv-\frac{\overline{Ry}^*}{n^2}\ ,\quad n=2,3,\ldots \tag{2.47}$$

where $\overline{Ry}^*$ is the effective rydberg calculated with the average dielectric constant. The boundary condition excludes s states, so the level index n begins with $n=2$. This problem was first considered by Levine (1965). Subsequent authors added polarization effects (Prokop'ev, 1966), mass anisotropy (Bell *et al.*, 1967), the image potential (Petukhov *et al.*, 1967; Karpushin, 1969), and a weak electric field (Karpushin, 1968). A qualitative discussion of binding to a surface dipole was given by Karpushin and Chaplik (1967).

If we include the presence of a surface electric field which induces electric subbands, and suppose that only the lowest subband plays a role, we convert the problem to a two-dimensional one. In the extreme two-dimensional limit, in which the Coulomb center is located in a sheet of electrons at $z=0$, the energy-level spectrum is (Flügge and Marschall, 1952)

$$E_n=-\frac{me^4}{2\bar{\kappa}^2\hbar^2(n-\frac{1}{2})^2}\ ,\quad n=1,2,\ldots . \tag{2.48}$$

This strict two-dimensional limit was considered further by Stern and Howard (1967), who calculated the bound states as the charge moved away from the sheet of electrons, and who included screening effects of mobile electrons. We do not consider their results here because the strict two-dimensional limit is too unrealistic, as shown by Martin and Wallis (1978). Also unrealistic is the treatment by Goetzberger, Heine, and Nicollian (1968), who did not include the requirement that the envelope wave function go to zero in the oxide and therefore took the ground state as $n=1$ in Eq. (2.47).

A more realistic treatment of bound states in the presence of an interface and an electric field is that of Martin and Wallis (1976, 1978), who used a variational approximation to calculate binding energies associated with a

single subband in a Si-SiO_2 inversion layer as a function of electric field in the Si. They included the image potential and calculated the binding energy of the ground state and of the first excited state as well as the magnitude of the matrix element for optical transitions between them. These states become the $n=2$ and $n=3$ states, respectively, in Eq. (2.47) when the electric field vanishes and the image potential and mass anisotropy are ignored, and become the $n=1$ and $n=2$ states, respectively, in the two-dimensional limit given in Eq. (2.48) as the electric field becomes infinite. The binding energy increases by an order of magnitude as the electric field increases from very small to very large values.

Lipari (1978) extended these calculations by using a more complete basis set, and by allowing the Coulomb center to lie in the insulator or in the semiconductor as well as at the interface. He expanded the wave function in spherical harmonics—taking full advantage of the symmetry—each of which was multiplied by a radial function taken to be a sum of exponentials. Enough terms were taken in the sums to assure convergence. Lipari studied the influence of the image potential and of the mass anisotropy of the lowest conduction-band valley on the calculated binding energy of the lowest bound state. His results for silicon give binding energies somewhat larger than those of Martin and Wallis. Figure 8 gives the binding energy as a function of the distance of the Coulomb center from the interface as calculated by Lipari for the case of flat bands. Vinter (1978) expanded the wave function of the bound states in a sum of products of functions z times functions of r and θ. The functions of z were taken from the solution of the Schrödinger equation with no impurity present, and the radial functions were determined numerically. His calculated binding energies are also slightly larger than those of Martin and Wallis.

Effects of screening by charges in the inversion layer were included in the crude calculation by Stern and Howard and in more realistic but still somewhat empirical calculations by Hipólito and Campos (1979), who found that screening effects do lower the binding energy.

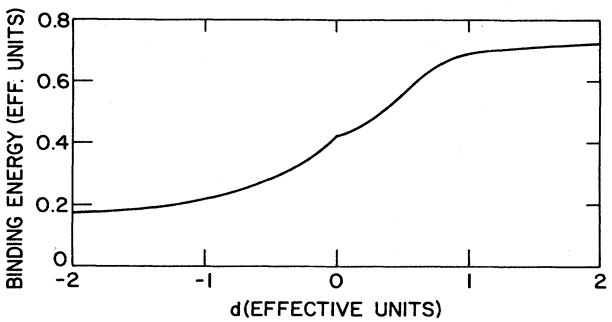

FIG. 8. Binding energy of an electron in silicon bound to a positive charge e located a distance d from the Si-SiO_2 interface, for the case of flat bands. The energy unit is the effective rydberg, $\overline{Ry}^* \sim 43$ meV, and the distance unit is the effective Bohr radius, $\bar{a}^* \sim 2.2$ nm. Note the change of slope as the charge crosses the interface, which arises from the different dielectric constants of the Si and the SiO_2. After Lipari (1978).

The experimental system with which these calculations can be compared is the Si-SiO_2 system with sodium ions at or near the interface, as studied by Hartstein, Fowler, Ning, and Albert, which is described in detail in Sec. V.C. The calculated binding energy is related—but probably not equal—to the measured activation energy E_1, attributed to activation of electrons from the impurity band to the mobility edge. To minimize the complications of level broadening and of screening, which are not included in the calculations, the experimental results should be extrapolated to zero sodium concentration and zero carrier concentration. Experimental and theoretical results are compared in Fig. 100.

A more sophisticated calculation of states associated with a Coulomb center in the presence of free carriers was carried out by Vinter (1978), who treated the occupation of the bound state and the screening of inversion layer electrons in a self-consistent way using the Kohn-Sham local density scheme, but without spin or valley polarization. The levels are quite weakly bound, as found in previous calculations that included screening effects (Stern and Howard, 1967; Martin and Wallis, 1976), and are found to have fourfold degeneracy even when a valley density formalism is used (Vinter, 1980) to try to remove the degeneracy. The calculations for bound states in the presence of free carriers have so far ignored level broadening effects and effects of overlap of wave functions of electrons from adjacent ions, and should therefore be treated with considerable caution, as pointed out by Vinter (1980). Calculations of bound states in the presence of free carriers were also carried out by Takada (1979), who estimated the effect of the occupied bound states on the mobility. This is discussed in more detail in Sec. IV.C.

Kramer and Wallis (1979) made the first calculations of bound states associated with higher subbands. They used rather simple variational wave functions and calculated bound states attached to the lowest and the first two excited subbands of the lowest valleys. They found that the transitions between the bound states attached to the two lowest subbands lie at higher energies than the transitions between the subbands in the absence of impurities. This is in qualitative agreement with experimental results of McCombe and Cole (1980), who found that the presence of sodium ions broadens the intersubband transitions and shifts them to higher energies. However, the experiments are done in the presence of significant concentrations of free carriers, while the calculation of Kramer and Wallis does not include screening effects. For additional details on the optical measurements, see Sec. V.C.

We conclude this section with some general results about bound states in two-dimensional systems. First we note that an arbitrarily weak attractive potential can support a bound state although the binding energy for a very weak potential ϕ is likely to be unobservably small (Landau and Lifshitz, 1977, p. 163). In three dimensions, on

the other hand, a potential must have a minimum strength before it will bind a state (see, for example, Bargmann, 1952). There are conditions on the strength of the potential needed to bind states with angular momentum quantum numbers l greater than 0 in two-dimensional systems. Stern and Howard (1967) adapted a result of Bargmann (1952) to show that the number n_l of bound states with $l>0$ obeys the inequality

$$n_l l < \frac{me}{\hbar^2}\int_0^\infty R\,|\phi(R)|\,dR\ . \tag{2.49}$$

Stern and Howard (1967) showed that the model potential for which the Fourier-Bessel coefficients are given in Eq. (2.18) is not strong enough to bind states with $l>0$ in an inversion layer if the long-wavelength, low-temperature screening approximation is used for all values of q. That conclusion would have to be reexamined for the more accurate screening given by Eq. (2.35), or for the weaker screening present at high temperatures, or in the presence of band tailing.

F. Many-body effects

1. Quantum electron fluid

In a two-dimensional system in which electrons are confined to move within a plane placed in vacuum, the Fourier transform $V(q)$ of the electron-electron interaction is given by $2\pi e^2/q$ in contrast to $4\pi e^2/q^2$ in three dimensions. The extension to a more realistic system is straightforward. Let us consider the model in which a semiconductor with dielectric constant κ_{sc} fills the half space $z>0$ and the other $z<0$ is filled with an insulating medium of dielectric constant κ_{ins}. The electron layer is placed on the semiconductor side near the semiconductor-insulator interface. The Coulomb interaction between a pair of electrons located at $(\mathbf{r},z)$ and $(\mathbf{r}',z')$ is given by

$$\begin{aligned}V(\mathbf{r}-\mathbf{r}';z,z') &= \frac{e^2}{\kappa_{sc}}[(\mathbf{r}-\mathbf{r}')^2+(z-z')^2]^{-1/2}+\frac{(\kappa_{sc}-\kappa_{ins})e^2}{\kappa_{sc}(\kappa_{sc}+\kappa_{ins})}[(\mathbf{r}-\mathbf{r}')^2+(z+z')^2]^{-1/2}\\ &= \sum_q \frac{2\pi e^2}{\kappa_{sc} q}e^{i\mathbf{q}\cdot(\mathbf{r}-\mathbf{r}')}\left[e^{-q|z-z'|}+\frac{\kappa_{sc}-\kappa_{ins}}{\kappa_{sc}+\kappa_{ins}}e^{-q|z+z'|}\right].\end{aligned} \tag{2.50}$$

This result is obtained from classical electrostatics by solving Poisson's equation. The first term of (2.50) describes the direct interaction, and the second arises from the interaction with an image of the other electron. The image term is further modified when the thickness of the insulator is finite and a metallic plate is placed at $z=-d_{ins}$. However, the condition $qd_{ins}>>1$ is usually satisfied, and the presence of the metallic electrode is neglected. Therefore, if the nonzero thickness of the electron layer is included, the effective potential becomes $V(q)=(2\pi e^2/\bar{\kappa}q)F(q)$ with $\bar{\kappa}=(\kappa_{sc}+\kappa_{ins})/2$, and

$$F(q)=\tfrac{1}{2}\int_0^\infty dz\int_0^\infty dz' g(z)g(z')\left[\left[1+\frac{\kappa_{ins}}{\kappa_{sc}}\right]e^{-q|z-z'|}+\left[1-\frac{\kappa_{ins}}{\kappa_{sc}}\right]e^{-q|z+z'|}\right]. \tag{2.51}$$

For the density distribution $g(z)$ given by Eq. (2.16) the form factor $F(q)$ is given by the following analytic expression:

$$F(q)=\frac{1}{16}\left[1+\frac{\kappa_{ins}}{\kappa_{sc}}\right]\left[1+\frac{q}{b}\right]^{-3}\left[8+9\frac{q}{b}+3\left[\frac{q}{b}\right]^2\right]+\frac{1}{2}\left[1-\frac{\kappa_{ins}}{\kappa_{sc}}\right]\left[1+\frac{q}{b}\right]^{-6}. \tag{2.52}$$

In the limit of vanishing thickness ($b\to\infty$) the form factor $F(q)$ becomes unity and the Coulomb potential in the strict two-dimensional limit is recovered in case of $\bar{\kappa}=1$.

The electron-electron interaction can affect various properties of the two-dimensional electron gas. Among them the quasiparticle properties such as the effective mass and the g factor first attracted much attention because they are directly observable experimentally. The g factor was first obtained by Fang and Stiles (1968) in an n-channel inversion layer on the Si(100) surface and found to be enhanced from the bulk value close to two. Smith and Stiles (1972) determined the effective mass in the same system and showed that it was again enhanced and decreased with the electron concentration. See Sec. VI.B for more detailed discussion on various problems related to these experiments.

The most popular way to discuss such quasiparticle properties is to use Landau's Fermi liquid theory (Landau, 1956), in which the so-called f function plays a central role. The object of a microscopic theory is to determine from first principles the values of the f function as a function of the electron concentration. The random-phase approximation is most common and has been fully discussed by Rice (1965) in three dimensions. In this approximation the quasiparticle energy $E_{\sigma v}(\mathbf{k})$ of an electron with a spin $\sigma(\pm1)$ and a valley index v is obtained from the total energy by taking a functional derivative with respect to the Fermi distribution function $n_{\sigma v}(\mathbf{k})$. We have

$$E_{\sigma v}(\mathbf{k})=\varepsilon(\mathbf{k})-\int\frac{d\omega}{2\pi i}\sum_q\frac{V(q)}{\varepsilon(q,\omega)}G^0_{\sigma v}(\mathbf{k}-\mathbf{q},\varepsilon(k)-\omega)\ , \tag{2.53}$$

where $\varepsilon(k)=\hbar^2k^2/2m$,

$$G^{(0)}_{\sigma v}(k,E)=\frac{n_{\sigma v}(k)}{E-\varepsilon(k)-i0}+\frac{1-n_{\sigma v}(k)}{E-\varepsilon(k)+i0}\ , \tag{2.54}$$

and $\varepsilon(q,\omega)$ is the dielectric function, given by

$$\varepsilon(q,\omega)=1+V(q)\Pi(q,\omega)\ , \tag{2.55}$$

with

$$\Pi(q,\omega)=-\sum_{\sigma v}\int\frac{dE}{2\pi i}\sum_{k}G^{(0)}_{\sigma v}(k,E)G^{(0)}_{\sigma v}(\mathbf{k}+\mathbf{q},E+\omega)\ . \tag{2.56}$$

This polarization part is related to the polarizability $\chi(q,\omega)$ given by Eq. (2.31) through $\Pi(q,\omega)=(q^2/e^2)\chi(q,\omega)$. The f function is obtained by further taking the functional derivative of Eq. (2.53) with respect to $n_{\sigma' v'}(\mathbf{k}')$. The result can be split into two parts:

$$f_{\sigma v;\sigma' v'}(\mathbf{k},\mathbf{k}')=f_0(\mathbf{k},\mathbf{k}')+\delta_{\sigma\sigma'}\delta_{vv'}f_e(\mathbf{k},\mathbf{k}')\ . \tag{2.57}$$

Then we get

$$\frac{m}{m^*}=1-\frac{m}{(2\pi\hbar)^2}\sum_{\sigma\sigma'}\sum_{vv'}\int d\theta f_{\sigma v;\sigma' v'}(\theta)\cos\theta \tag{2.58}$$

and

$$\frac{g}{g^*}=1+\frac{m^*}{(2\pi\hbar)^2}\int d\theta f_e(\theta)\ , \tag{2.59}$$

where $f(\theta)=f(\mathbf{k},\mathbf{k}')$ with $k=k'=k_F$ and $\mathbf{k}\cdot\mathbf{k}'=k_F^2\cos\theta$. The effective mass m^* and the effective g factor g^* are defined as usual by

$$\frac{1}{m^*}=\frac{1}{\hbar^2k_F}\frac{\partial}{\partial k}E_{\sigma v}(k)\,|_{\,k=k_F} \tag{2.60}$$

and

$$E_{\sigma v}(k_F)=E(k_F)-\tfrac{1}{2}g^*\sigma\mu_B H \tag{2.61}$$

in a weak magnetic field H, where μ_B is the Bohr magneton. Such a scheme was first introduced in the two-dimensional system by Suzuki and Kawamoto (1973) and later by Ting, Lee and Quinn (1975).

Historically, various people calculated g^* and m^* in different approximation schemes. Janak (1969) is the one who first noted that the extraordinarily large g factor observed experimentally in the n-channel inversion layer on the Si(100) surface could be due to an exchange enhancement. He treated the self-energy shift to the lowest order in the statically screened Coulomb interaction and calculated g^*. His result is similar to Eq. (2.59) except that m^* is replaced by the bare mass m. As he erroneously multiplied the second term of (2.59) by a factor of 2, however, the resulting g value became extremely large. The error in the calculation of Janak was first pointed out by Suzuki and Kawamoto (1973), who showed that the g factor was drastically reduced from the result of Janak. However, there is a problem in their treatment of the image effect in the electron-electron interaction. They also calculated the effective mass, neglecting the dynamical screening and replacing $\varepsilon(q,\omega)$ by $\varepsilon(q,0)$ in Eq. (2.53). This static approximation is appropriate for the g factor, but inappropriate for the effective mass. The g factor is essentially determined by the difference of the exchange interactions of up- and down-spin electrons in the vicinity of the Fermi line, whereas the effective mass is determined by virtual excitations of electron-hole pairs and plasmons with a wide range of energy. Ando and Uemura (1974b, 1974c) corrected Janak's calculation and also investigated effects of the nonvanishing thickness of the inversion layer. The thickness effect was shown to reduce the $\Delta g=g^*-g$ by about 20% around $N_s\sim5\times10^{12}$ cm^{-2}. It is Ting, Lee, and Quinn (1975) who really followed the approximation scheme mentioned above. The effective-mass enhancement was shown to make the N_s dependence of the g factor steeper than that obtained by Ando and Uemura, who neglected the mass shift. Ting *et al.* considered also the Hubbard approximation (Hubbard, 1957, 1958), which approximately includes effects of short-range correlation, and found that the g factor increased with the concentration in contrast to the behavior predicted in the random-phase approximation. A similar behavior was also found in a three-dimensional system at low concentrations (Ando, 1976b). This strange behavior is thought to be a result of insufficiencies of the Hubbard approximation. A corresponding calculation for the quasi-two-dimensional system was done by Lee, Ting, and Quinn (1975a). Ohkawa (1976a) employed a similar approximation but included effects of the existence of several subbands as well as the nonzero thickness. The effective mass seems to become slightly larger if one includes intersubband mixings.

Equation (2.53) is written as

$$E(k)=\varepsilon(k)+\Sigma(k,\varepsilon(k))\ , \tag{2.62}$$

instead of the exact Dyson equation

$$E(k)=\varepsilon(k)+\Sigma(k,E(k))\ , \tag{2.63}$$

where the self-energy $\Sigma(k,E)$ is evaluated to the lowest order in the dynamically screened interaction. The Green's functions appearing in the self-energy and in the dielectric function are taken to be free-particle Green's functions. Vinter (1975a, 1976) used a somewhat different approximation scheme. In this approach one uses the exact Dyson equation (2.63) instead of (2.62). He introduced a simplification in evaluating the self-energy. The screened interaction can be separated as

$$V(q)\varepsilon(q,\omega)^{-1}=V(q)+V(q)[\varepsilon(q,\omega)^{-1}-1]\ . \tag{2.64}$$

Instead of the numerical integration of (2.53) over q and ω, the second term of (2.64) is replaced by coupling to one effective plasmon as follows:

$$\mathrm{Im}[\varepsilon(q,\omega)^{-1}-1]=\alpha\delta(\omega-\omega_q)\ . \tag{2.65}$$

The energy of the plasmon ω_q and the coupling constant α are determined by the requirement that the f sum rule

$$\int_0^\infty d\omega\,\omega\,\mathrm{Im}[\varepsilon(q,\omega)^{-1}-1]=-\tfrac{1}{2}\pi\omega_p^2 \tag{2.66}$$

and the zero-frequency Kramers-Kronig relation

$$\int_0^\infty \frac{d\omega}{\omega}\mathrm{Im}[\varepsilon(q,\omega)^{-1}-1]=\frac{\pi}{2}[\varepsilon(q,0)^{-1}-1] \quad (2.67)$$

should be fulfilled, where ω_p is the plasma frequency, defined by $\omega_p^2=2\pi N_s e^2 q/\bar{\kappa}m$. The validity of this plasmon pole approximation for the dielectric function was discussed by Lundqvist (1967a, 1967b) and Overhauser (1971) in three dimensions. Vinter calculated the effective mass using this scheme. The calculated mass enhancement showed an N_s dependence qualitatively the same as that calculated by Lee, Ting, and Quinn (1975a) and by others. However, the absolute value turned out to be smaller than those of others.

There has been discussion whether one should use Eq. (2.62) or (2.63) to evaluate the effective mass (Lee *et al.*, 1975b, 1976; Quinn, 1976). By differentiating (2.62) and (2.63) with respect to k and evaluating on the Fermi line one obtains

$$1-\frac{m}{m_D^*}=Z\left[1-\frac{m}{m_R^*}\right], \quad (2.68)$$

where the renormalization constant Z is the value of $[1-\partial\Sigma(k,E)/\partial E]^{-1}$ on the energy shell at the Fermi line. The subscripts D and R refer to results obtained by the Dyson equation (2.63) and Rice's approximation (2.62), respectively. Since Z varies from 0.3 to 0.8 in the density range $10^{11}-10^{13}$ cm^{-2} in an n-channel inversion layer on the Si(100) surface, the difference between m_D^* and m_R^* is an important one. Lee, Ting, and Quinn (1975b, 1976) argued, following Rice (1965), that Rice's approach gives a more accurate result if the self-energy is evaluated only to the lowest order in the effective screened interaction. The reason for this is the partial cancellation of higher terms in the self-energy with the correction to the approximate equation (2.62) incorporated in the Dyson equation. As a matter of fact Eq. (2.63) does not give a correct high-density expansion, whereas (2.62) does in three dimensions (Rice, 1965). For actual electron concentrations, however, this cancellation is not complete, and it is not easy to tell which procedure gives more accurate results.

A density-functional formulation has also been used to calculate the effective mass and the g factor (Ando, 1976a, 1976b). Details will be discussed in Sec. III.B. Some of the theoretical results for the effective mass are plotted together with the experimental results of Smith and Stiles (1972) in Fig. 9.

Various properties of a two-dimensional electron gas other than those mentioned above have been studied. Zia (1973) calculated a high-density expansion of the correlation energy, evaluating the ring diagrams and the second-order exchange diagram. Errors in his result were pointed out and corrected by Rajagopal and Kimball (1977) and by Isihara and Toyoda (1977a, 1977b). The total energy per electron in rydberg units was expressed as

$$\varepsilon(r_s)\sim\frac{1}{r_s^2}-\frac{1.2}{r_s}-0.38-0.172r_s\ln r_s+O(r_s), \quad (2.69)$$

where r_s is defined by $N_s^{-1}=\pi a_B^2 r_s^2$ and $a_B=\hbar^2/m_0e^2$ is the Bohr radius for free space, because we are here treating an ideal two-dimensional electron gas, without considering the effects of the medium via its dielectric constant and effective mass. Jonson (1976) compared the correlation energies and the pair correlation functions calculated in the random-phase approximation, the Hubbard approximation, and the approximation proposed by Singwi, Tosi, Land, and Sjölander (1968). He found that both the random-phase and the Hubbard approximations are less satisfactory in two dimensions than in three dimensions, suggesting the importance of short-range correlations not properly accounted for in these approximations. A similar conclusion was reached by Bose (1976). The comparison was extended to the n-channel inversion layer on Si(100). The finite thickness effect was shown to improve the validity of the approximations greatly, since the finite thickness makes the short-range interaction weaker. There have been more investigations on related properties (Isihara and Toyoda, 1976, 1980; Glasser, 1977; Freedman, 1978; Toyoda *et al.*, 1978; Isihara and Ioriatti, 1980). A similar consideration was extended to the case in the presence of a magnetic field (Isihara and Toyoda, 1979; Isihara and Kojima, 1979; see also Isihara, 1980; Glasser, 1980). The diamagnetic and paramagnetic susceptibilities were calculated within the random-phase approximation in weak and intermediate fields. The weak-field orbital susceptibility was discussed also by Rajagopal (1977a).

All the theoretical considerations mentioned above assume that the ground state is a paramagnetic uniform occupation of different spin (and also valley, if necessary) states. It is well known that such a uniform distribution becomes unstable against the formation of the Wigner crystal at sufficiently low electron concentrations. This

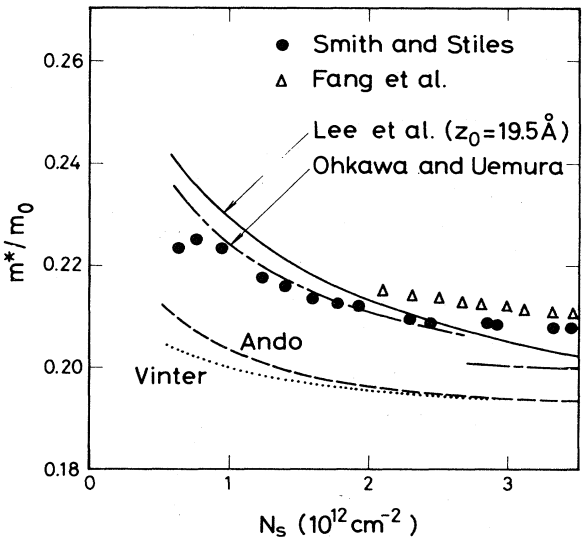

FIG. 9. Calculated effective masses (Vinter, 1975a, 1976; Lee *et al.*, 1975a; Ohkawa, 1976a; Ando, 1976a, 1976b) and experimental results of Smith and Stiles (1972) and of Fang *et al.* (1977) in an n-channel inversion layer on a Si(100) surface.

problem will be discussed in Sec. VII.C. Various kinds of instabilities have been proposed in addition to the Wigner crystallization. Rajagopal and coworkers (Rajagopal, 1977b; Rajagopal *et al.*, 1978a, 1978b) investigated ferromagnetic properties of the two-dimensional system. They calculated the total energy as a function of the spin polarization $\zeta=(n_\uparrow-n_\downarrow)/(n_\uparrow+n_\downarrow)$ in the random-phase approximation, where $n_\uparrow$ and $n_\downarrow$ specify the density of up- and down-spin electrons, respectively. The result shows an abrupt transition to the saturated ferromagnetic state at $r_s=5.4$ in the strict two-dimensional system. In a quasi-two-dimensional system the finite layer thickness was found to cause the transition to be gradual and reduce the critical electron concentration greatly. For $N_{\rm depl}>7.6\times10^{10}$ cm^{-2} the paramagnetic state is stable above $N_s\sim5\times10^{10}$ cm^{-2}.

In addition to the spin degeneracy, the valley degeneracy—equal to two for the Si(100) surface—must also be considered. As long as a weak valley coupling, which will be discussed in Sec. VII.A, is neglected, there is theoretically no difference between the ferromagnetic ground state and a single-valley occupancy state in which only one valley is occupied by up-spin and down-spin electrons. Other more complicated configurations are also possible. The possibility of the single-valley occupancy state was studied in a density-functional formulation by Bloss, Sham, and Vinter (1979), who predicted an abrupt transition at much larger electron concentration ($N_s\sim2.3\times10^{11}$ cm^{-2} for $N_{\rm depl}=1\times10^{11}$ cm^{-2}). Effects of the different occupation multiplicity on energy separations between electric subbands were studied (Bloss *et al.*, 1980). Ceperly (1978) calculated the ground-state energy of a strict two-dimensional system using a Monte Carlo variational method and suggested that the spin-polarized state is stable at densities below $r_s>13$. The possibility of a spin-density wave or valley-density wave was examined by Bergman and Rice (1977). In these states, as originally suggested by Overhauser (1962) in three dimensions, the occupation of the two spin states or of the different valleys oscillates in space with a characteristic wave vector $\mathbf{Q}$ with $|\mathbf{Q}|\sim2k_F$, while the total electronic charge density remains uniform. They suggested that these states could be lower in energy than the usual uniform state below $N_s\sim8\times10^{11}$ cm^{-2} in the n-channel layer on the Si(100). Kalia and Quinn (1978) used a density-functional approach for a similar discussion. Maldague (1978a, 1978b) calculated the first-order exchange correction to the static polarizability and found a sharp peak at $q=2k_F$. This behavior differs drastically from that in three dimensions, where the exchange correction does not give a peak structure although it enhances the polarizability near $q=2k_F$. Although this sharp peak becomes smaller if higher-order effects are included, it suggests a pronounced tendency of the two-dimensional system to instabilities toward a charge-density or spin-density-wave ground state. A density-functional approach has been used also to discuss the onset of charge-density-wave instability and has given $r_s\sim17$ as the critical electron concentration in exact two dimensions (Sander *et al.*, 1980). Sato and Nagaoka (1978) calculated the static polarizability in the direction normal to the layer in a two-subband system and suggested the possibility of an instability against a polarization-wave state when the Fermi energy is close to the bottom of the upper subband. In this state a polarization wave with wave vector k_F is spontaneously formed.

The possibility of superconductivity was recently examined in inversion layers. Takada and Uemura (1976) studied various possible mechanisms which can give rise to superconductivity in inversion layers on InAs and suggested acoustic plasmons as a candidate for systems in which several subbands with different effective masses were occupied (see also Sec. VIII.B.3). Takada (1978) later showed that the plasmon itself can cause superconductivity in both two- and three-dimensional electron gases. The theory was applied to the n-channel inversion layer on the Si(100) surface under a uniaxial stress (Takada, 1980b). Hanke and Kelly (1980a, 1980b; Kelly and Hanke, 1981a) included electron-phonon interactions and intersubband excitations in addition to the plasmon mechanism and estimated the transition temperature on the (111) Si-SiO_2 surface. In their theory the transition temperature rises to a value of order 10 mK as N_s increases to $\sim10^{13}$ cm^{-2}.

2. Classical electron fluid

So far we have considered two-dimensional electron gases at low temperatures. There have been a number of theoretical investigations of classical two-dimensional systems in connection with the image-potential-induced surface state on liquid helium. In the classical regime the dimensionless coupling constant which characterizes the importance of the Coulomb interaction is given by $\Gamma=\pi^{1/2}N_s^{1/2}e^2/k_BT$. The plasma parameter Γ is defined as the ratio of the mean potential energy $e^2(\pi N_s)^{1/2}$ to the mean kinetic energy k_BT. For a dilute system at high temperatures Γ is small ($\Gamma<1$) and the Coulomb interaction is less important. At intermediate densities ($1<\Gamma<100$) the motion of electrons becomes highly correlated or liquidlike. At high densities and low temperatures ($\Gamma>100$), the Coulomb potential energy predominates and the electrons are expected to undergo a phase transition to form a periodic crystalline array. This electron solid will be discussed in detail in Sec. VII.C. Here we confine ourselves to the case of relatively small Γ. In the electron system outside liquid helium Γ varies from 1 to 95 for 10^5 cm$^{-2}<N_s<10^9$ cm^{-2} at 1 K.

We first study some properties of a two-dimensional classical plasma in the random-phase approximation, which is equivalent to the Debye-Hückel approximation and is known to be valid for a dilute plasma at high temperatures ($\Gamma<1$) in three dimensions. The dielectric function in the classical regime becomes

$$\varepsilon(q,\omega)=1+\frac{q_s}{q}W\left[\frac{\omega}{q}\left[\frac{m}{k_BT}\right]^{1/2}\right], \tag{2.70}$$

where q_s is the two-dimensional Debye screening constant defined by $q_s=2\pi e^2N_s/k_BT$, and $W(z)$, the derivative of the plasma dispersion function, is given by

$$W(z)=\frac{1}{(2\pi)^{1/2}}\int_{-\infty}^{+\infty}\frac{x\exp(-x^2/2)}{x-z-i0}dx\ . \tag{2.71}$$

The real part of $W(z)$ is equal to $\Phi'(z/\sqrt{2})/2$, where Φ is given by Eq. (2.39). With the use of the fluctuation-dissipation theorem the static form factor becomes

$$S(q)=-\frac{2}{N_s}\int_0^\infty d\omega\frac{k_BTq}{2\pi^2\omega e^2}\mathrm{Im}[\varepsilon(q,\omega)^{-1}-1]$$
$$=\frac{q}{q+q_s}\ . \tag{2.72}$$

The pair correlation function is related to $S(q)$ through

$$g(r)-1=\frac{1}{N_s}\sum_q[S(q)-1]\exp(i\mathbf{q}\cdot\mathbf{r})$$
$$=-\frac{1}{k_BT}\frac{e^2}{r}\int_0^\infty dx\frac{x}{x+q_sr}J_0(x)\ . \tag{2.73}$$

The pair correlation function $g(r)$ diverges as $g(r)\sim-(1/k_BT)(e^2/r)$ near the origin. The correlation energy per electron, ε_c, and the equation of state are given with the aid of the virial theorem by

$$\frac{\varepsilon_c}{k_BT}=2\left[\frac{p}{N_sk_BT}-1\right]$$
$$=\frac{N_s}{2k_BT}\int d\mathbf{r}\frac{e^2}{r}[g(r)-1]\ , \tag{2.74}$$

where p is the pressure. Because of the divergence of $g(r)$ near the origin, the correlation energy diverges logarithmically, which is a direct manifestation of the inadequacy of the random-phase approximation. In three dimensions, however, the integral of the right-hand side of (2.74) does not diverge, fortunately, and gives a well-known result of Debye and Hückel. This strongly suggests again the importance of short-range correlations in the two-dimensional system. From the dielectric function (2.70) one can obtain the plasma frequency ω_p and the Landau damping γ_L as

$$\omega_p=\left[\frac{2\pi N_se^2q}{m}\right]^{1/2}\left[1+\frac{3}{2}\frac{q}{q_s}\right], \tag{2.75}$$

and

$$\gamma_L=\left[\frac{\pi}{8}\right]^{1/2}\left[\frac{q_s}{q}\right]^{3/2}\exp\left[-\frac{q_s}{2q}-\frac{3}{2}\right]\omega_p\ , \tag{2.76}$$

for $q<<q_s$.

Physically the divergence in Eq. (2.74) appears because the linear screening approximation in the Debye-Hückel treatment is invalid in the vicinity of an electron where induced charges exceed the background density and one must introduce a cutoff distance r_c. The result of Fetter (1974b) corresponds to putting $r_c=\lambda_{\mathrm{th}}$ with the thermal wavelength $\lambda_{\mathrm{th}}=(2\pi\hbar^2/mk_BT)^{1/2}$. Actually r_c is given by e^2/k_BT, which is roughly the classical distance of closest approach of two electrons of energy k_BT. We then have

$$\frac{\varepsilon_c}{k_BT}=2\left[\frac{p}{N_sk_BT}-1\right]=\Gamma^2\ln 2\Gamma^2\ , \tag{2.77}$$

in the limit of small Γ. This expression is correct in the dilute limit. An expansion of the equation of state with respect to Γ was obtained by Chalupa (1975) and Totsuji (1975, 1976, 1979a). Effects of electron-electron collisions on the damping of the plasma oscillation were studied and the collisional damping was shown to be more important than the Landau damping in the domain where the plasma oscillation was a well-defined collective mode (Totsuji, 1976; Onuki, 1977).

Recently various attempts have been made to extend the study to the domain $\Gamma>1$ (Totsuji, 1979b, 1979c; Totsuji and Kakeya, 1979; Nagano *et al.*, 1980). Numerical experiments have also been used to determine thermodynamic quantities like the equation of state and the pair correlation function (Hockney and Brown, 1975; Totsuji, 1978; Gann *et al.*, 1979; Itoh *et al.*, 1978; Itoh and Ichimaru, 1980) and to give dynamic properties such as the dynamic structure factor and the plasmon dispersion (Totsuji, 1980; Totsuji and Kakeya, 1980). The domain $\Gamma>100$ will be discussed in detail in Sec. VII.C.

G. General aspects of transport in two-dimensional systems

The basic machinery for discussing the transport properties of electrons in two dimensions, as considered for silicon inversion and accumulation layers in Sec. IV, is quite similar to that used for three dimensions, but some of the details are different. Thus, for example, the cross section for elastic scattering can be described by phase shifts η_l for partial waves of angular momentum quantum number l, and is given by (Stern and Howard, 1967)

$$\sigma(\theta)=\frac{2}{\pi k}\left|\sum_{l=-\infty}^{\infty}e^{i(l\theta+\eta_l)}\sin\eta_l\right|^2, \tag{2.78}$$

where θ is the scattering angle, the angle between the wave vectors $\mathbf{k}$ and $\mathbf{k}'$ of the incident and scattered beams, given by

$$S=|\mathbf{k}-\mathbf{k}'|=2k\sin\frac{\theta}{2}\ . \tag{2.79}$$

The phase shifts must satisfy a two-dimensional analog of the Friedel phase-shift sum rule, given at absolute zero for only one occupied band by (Stern and Howard, 1967)

$$2g_v\sum_{l=-\infty}^{\infty}\eta_l(E_F)=\pi Z\ , \tag{2.80}$$

to insure that a scattering center of charge Z is fully screened at large distances.

The phase-shift analysis can be used to study the accuracy of the Born approximation

$$\sigma(\theta)=\frac{\pi}{2k}\left[\frac{2m}{\hbar^2}\right]^2\left[\int_0^\infty V(r)J_0(Sr)r\,dr\right]^2 \tag{2.81}$$

applied to two-dimensional elastic scattering by a screened Coulomb potential. Stern and Howard (1967) found, for a simple screening model, that the Born approximation underestimates the scattering for an attractive potential and overestimates it for a repulsive potential. When the scattering center is far enough from the electron plane the error made by the Born approximation is small. That generally applies for scattering in semiconductor inversion and accumulation layers because of the thickness of the electron layer.

A very instructive example of scattering in two dimensions that can be solved exactly is the scattering of electrons by an unscreened Coulomb potential energy $V(r)=-Ze^2/\bar{\kappa}r$ produced by a charge Ze located in the electron plane. The nonrelativistic Schrödinger equation for this case can be solved (Stern and Howard, 1967) and gives a scattering cross section

$$\sigma(\theta)=\frac{G\tanh\pi G}{2k\sin^2\frac{\theta}{2}}\,, \tag{2.82}$$

where $G=mZe^2/\bar{\kappa}k\hbar^2=Z/\bar{a}^*k$. The Born-approximation result is obtained from Eq. (2.81) using (2.14) with $z_0=0$ and $\bar{q}_s=0$, and gives

$$\sigma(\theta)=\frac{\pi(Ze^2/\bar{\kappa}\hbar v)^2}{2k\sin^2\frac{\theta}{2}}\,, \tag{2.83}$$

where $v=\hbar k/m$, for the unscreened Coulomb potential. The corresponding classical cross section is (Kawaji and Kawaguchi, 1966)

$$\sigma(\theta)=\frac{|Z|e^2}{2\bar{\kappa}mv^2\sin^2\frac{\theta}{2}}\,. \tag{2.84}$$

The Born approximation is valid for a Coulomb potential when the scattering contribution to the wave function is small, which occurs when $Ze^2/\bar{\kappa}r \ll \hbar v/r$ (Landau and Lifshitz, 1977, p. 161), i.e., $G \ll 1$, and the classical approximation is valid when the electron wavelength (divided by 2π) corresponding to energy E is small compared to the radius corresponding to potential energy of magnitude E, which occurs when $\hbar/(2mE)^{1/2} \ll Ze^2/\bar{\kappa}E$ (Schiff, 1955, p. 120), i.e., $G \gg \frac{1}{2}$. The exact result (2.82) goes over to the Born-approximation result (2.83) and to the classical result (2.84) in the appropriate limits.

This example is especially instructive because the corresponding comparison cannot be made for three-dimensional Coulomb scattering. The Born-approximation, classical, and exact cross sections all agree in that case.

III. ENERGY LEVELS AND WAVE FUNCTIONS

A. Subband structure

1. Hartree approximation for electrons in silicon space-charge layers

In this section we describe the methods used to calculate energy levels and wave functions of electrons in semiconductor inversion and accumulation layers. The simple Hartree approximation is described first, to give the form of the self-consistent one-electron potential and the Schrödinger equation in the presence of the semiconductor-insulator interface. Later in the section more realistic approximations are presented and their effect on energy levels and wave functions are described.

Electrons near semiconductor-insulator interfaces move in a rather complex potential. On one side of the interface they see the periodic potential of the semiconductor, on which is superposed the relatively slowly varying electric field induced by the applied voltage, by the work-function difference of the gate and the substrate, and by any fixed charges which may be present. On the other side they see the potential of the insulator, which is usually amorphous. There is usually a large potential barrier which tends to keep electrons out of the insulator. In addition, there may be a transition layer whose properties are different from those of the semiconductor or the insulator.

A complete treatment of this system is beyond the scope of present theories, although there has been progress on some aspects of the electronic structure of the semiconductor-insulator interface [see, for example, Laughlin, Joannopoulos, and Chadi (1978, 1980) and Herman, Batra, and Kasowski (1978)]. There is also improved understanding of the microscopic structure of the interface, which will be discussed below.

We shall treat the energy levels in semiconductor space-charge layers first by making all possible approximations that do not do violence to the underlying physical system and then by examining the effects of these approximations. In particular, we start with the Hartree approximation that each electron moves in the average potential produced by all electrons, neglecting many-body interactions. We use the effective-mass approximation to smooth out the microscopic structure of the semiconductor. We also assume that the barrier which keeps electrons out of the insulator is so large that the electron envelope wave function can be assumed to vanish at the semiconductor-insulator interface, taken at $z=0$. This approximation has been made in most calculations, although it was not made in Duke's (1967a) original calculation. It is reasonably good for the silicon-silicon dioxide interface, but is not valid for other interfaces, such as the GaAs-(Ga,Al)As interface or the sur-

face of liquid helium. See Sec. III.E for additional discussion of the boundary condition.

Our treatment is at first limited to electrons because of the simpler structure of the conduction band and because of the experimental importance of n-channel inversion and accumulation layers in silicon.

One may well question the use of effective-mass approximation for electronic states whose spatial extent is, in cases of confinement by strong surface electric fields, limited to a few atomic layers. This problem has been addressed by Schulte (1979, 1980a), and also arises in connection with valley splitting, discussed in Sec. VII.A, and with heterojunctions and superlattices, discussed in Sec. VIII.D. A test with high precision cannot be made without more detailed knowledge of the structure of the interface. We expect, however, that in most cases it is the lack of knowledge of physical parameters and uncertainties in the many-body aspects of the problem, rather than the effective-mass approximation itself, that limits the accuracy of the calculations of interest here.

The simplest version of the effective-mass approximation treats the electrons as though they had masses characteristic of a conduction-band minimum, neglecting nonparabolicity and coupling to other band extrema. The kinetic energy operator can be written

$$T=-\frac{\hbar^2}{2}\sum_{i,j} w_{ij}\frac{\partial^2}{\partial x_i \partial x_j} , \tag{3.1}$$

where the w_{ij} are the elements of the reciprocal effective-mass tensor for the particular conduction-band minimum being considered. Since the potential energy is taken to be a function of z only, the wave function can be written as the product of a Bloch function, a z-dependent factor, and a plane-wave factor representing free motion in the xy plane. A simple transformation to remove the first derivative in the Schrödinger equation leaves the wave function in the form (Stern and Howard, 1967)

$$\psi(x,y,z)=\zeta_i(z)e^{ik_1x+ik_2y} \times\exp\left[-i\left[\frac{w_{13}}{w_{33}}k_1+\frac{w_{23}}{w_{33}}k_2\right]z\right]u_\alpha(\mathbf{R}) , \tag{3.2}$$

where $u_\alpha(\mathbf{R})$ is the Bloch function for the bottom of the conduction-band valley being considered, including both the periodic part and the factor $\exp(i\mathbf{k}_\alpha\cdot\mathbf{r})$, where $\mathbf{k}_\alpha$ is the wave vector at the energy minimum of the αth valley and k_1 and k_2 are wave vectors in the k_x-k_y plane measured relative to the projection of $\mathbf{k}_\alpha$ on this plane. The envelope function $\zeta_i(z)$ satisfies

$$\frac{\hbar^2}{2m_z}\frac{d^2\zeta_i}{dz^2}+[E_i-V(z)]\zeta_i(z)=0 , \tag{3.3}$$

where $m_z=w_{33}^{-1}$, subject to the boundary conditions that ζ_i go to zero for $z=0$ and $z\to\infty$. [This separation of variables in the Schrödinger equation is not generally valid if the boundary condition $\zeta_i(0)=0$ is relaxed.] The ζ_i are assumed to be normalized:

$$\int_0^\infty \zeta_i^2(z)dz=1 . \tag{3.4}$$

The energy levels are given by

$$E(k_1,k_2)=E_i+\frac{\hbar^2}{2}\left[\left[w_{11}-\frac{w_{13}^2}{w_{33}}\right]k_1^2 +2\left[w_{12}-\frac{w_{13}w_{23}}{w_{33}}\right]k_1k_2 +\left[w_{22}-\frac{w_{23}^2}{w_{33}}\right]k_2^2\right] , \tag{3.5}$$

and lead to constant-energy parabolas above the level E_i which is the bottom of the ith subband. The principal effective masses, m_x and m_y, of these parabolas depend on the orientation of the constant-energy ellipsoids in the bulk with respect to the surface. They are given in Table I for the high-symmetry surfaces of semiconductors with conduction-band minima along the ⟨001⟩ directions, like those of silicon, and along the ⟨111⟩ directions, like those of germanium, in terms of the transverse and longitudinal effective masses of electrons in the bulk. If the values $m_t=0.19m_0$ and $m_l=0.916m_0$ are used for silicon (Hensel *et al.*, 1965), we obtain the principal effective masses given in Table II.

By analogy with three-dimensional ellipsoidal energy bands, we can also introduce two other important mass parameters. One is the density-of-states effective mass

$$m_d=(m_xm_y)^{1/2} , \tag{3.6}$$

the other is the conductivity or optical mass

$$m_{\rm op}=\frac{2}{\frac{1}{m_x}+\frac{1}{m_y}} , \tag{3.7}$$

which enters in transport properties (Smith, 1978). Values of these masses for high-symmetry surfaces of silicon are given in Table II.

The energy levels E_i for a given value of m_z constitute a series of subband minima called a subband ladder. For different orientations of the bulk constant-energy surfaces with respect to the surface, there may be different values of m_z, and therefore different ladders. One way to name these levels is to number the levels of the lowest ladder 0,1,2, . . . , those of the second ladder 0′,1′,2′, . . . , the third ladder 0″,1″,2″, . . . , and so on. If all conduction-band valleys have the same orientation with respect to the surface there will be only one ladder. Because of the kinetic energy term in the Schrödinger equation the valleys giving the largest effective mass m_z for motion perpendicular to the surface will have the lowest energy. Corrections to the simple effective-mass approximation which take interactions between conduction-band minima into account lead to changes in this simple picture, as will be discussed below.

The potential energy $V(z)$ which enters in Eq. (3.3) can be written as the sum of three terms as

TABLE I. Effective masses for three surface orientations, for semiconductors having band structures like those of the conduction band of Si (six { 100 } ellipsoids of revolution) or of Ge (four { 111 } ellipsoids of revolution). The principal effective masses in the ellipsoids are m_t, m_t, and m_l. The derived values are m_z, the effective mass perpendicular to the surface, and m_x and m_y, the principal effective masses of the constant-energy ellipse in the surface. The degeneracy of each set of ellipses is g_v. After Stern and Howard (1967).

	Si				Ge			
Surface Orientation	m_x	m_y	m_z	g_v	m_x	m_y	m_z	g_v
{ 100 }	m_t	m_t	m_l	2	m_t	$(m_t+2m_l)/3$	$3m_tm_l/(m_t+2m_l)$	4
	m_t	m_l	m_t	4				
{ 110 }	m_t	$(m_t+m_l)/2$	$2m_tm_l/(m_t+m_l)$	4	m_t	$(m_l+2m_t)/3$	$3m_tm_l/(m_l+2m_t)$	2
	m_t	m_l	m_t	2	m_t	m_l	m_t	2
{ 111 }	m_t	$(m_t+2m_l)/3$	$3m_tm_l/(m_t+2m_l)$	6	m_t	m_t	m_l	1
					m_t	$(m_t+8m_l)/9$	$9m_tm_l/(m_t+8m_l)$	3

$$V(z)=V_d(z)+V_s(z)+V_I(z)\ , \tag{3.8}$$

which represent, respectively, the contributions from fixed space charges, from induced charges in the space-charge layer, and from image charges at the semiconductor-insulator interface. In this section we assume that the interface is sharp and that there is an infinite barrier which keeps electrons out of the insulator.

If the band bending ϕ_d associated with the depletion layer is not too small, if the bulk is p type, and if the acceptor density N_A is constant throughout the depletion layer, then a good approximation for the potential energy in the depletion layer is

$$V_d(z)=\frac{4\pi e^2N_{\rm depl}}{\kappa_{\rm sc}}z\left[1-\frac{z}{2z_d}\right]\ ,\quad 0<z<z_d\ , \tag{3.9}$$

$$N_{\rm depl}=N_Az_d\ , \tag{3.10}$$

$$z_d=\left[\frac{\phi_d\kappa_{\rm sc}}{2\pi eN_A}\right]^{1/2}\ . \tag{3.11}$$

$N_{\rm depl}$ is the number of charges per unit area in the depletion layer, whose thickness is z_d. If compensating donors are present, N_A should be replaced by N_A-N_D. As ϕ_d increases, z_d and $N_{\rm depl}$ both increase until the inversion layer begins to form, at which point all three quantities tend to saturate, especially at low temperatures.

When an inversion layer has formed, the band bending ϕ_d in (3.11) is given approximately at low temperatures by

$$e\phi_d\simeq E_c-E_F\ , \tag{3.12}$$

the energy difference between bottom of the conduction band in the bulk and the Fermi level. There are several

TABLE II. Numerical values of effective masses for silicon inversion layers. After Stern (1972b).

Surface		(001)		(110)		(111)
Valleys		Lower	Higher	Lower	Higher	All
Degeneracy	g_v	2	4	4	2	6
Normal mass[a]	m_z	0.916	0.190	0.315	0.190	0.258
Principal masses	m_x	0.190	0.190	0.190	0.190	0.190
	m_y	0.190	0.916	0.553	0.916	0.674
Conductivity mass[b]	$m_{\rm op}$	0.190	0.315	0.283	0.315	0.296
Density-of-states mass per valley[b]	m_d	0.190	0.417	0.324	0.417	0.358

[a]All effective masses are in units of the free-electron mass; they are based on the conduction-band masses $m_t=0.190m_0$ and $m_l=0.916m_0$ given by Hensel *et al.* (1965).
[b]$m_{\rm op}=m_xm_y/(m_x+m_y)$; $m_d=(m_xm_y)^{1/2}$.

corrections to this value. The first and most important of these applies if there is a substrate bias ϕ_{sub} applied between the source or drain contacts at the semiconductor surface and the bulk of the semiconductor. This extra potential generally drops across the high-resistance depletion layer. If the bulk is at a negative potential with respect to the surface, corresponding to negative ϕ_{sub}, the depletion layer width increases.

The second correction to ϕ_d takes more careful account of the position of the band edge at the surface in relation to the Fermi level, which lies at the same energy in the bulk as at the surface in the absence of substrate bias. The energies which enter in this correction are illustrated in Fig. 10.

The third correction to ϕ_d, which takes into account the gradual falloff of the potential at the interface between the depletion layer and the bulk, is $-k_BT/e$ [see, for example, Eq. (1.3)] except at very low temperatures, where it is determined by the acceptor level broadening (Stern, 1972b).

When these three corrections are included, the band bending $e\phi_d$ which enters in Eq. (3.11) is given by

$$e\phi_d=(E_c-E_F)+(E_F-E_0)+E_0 - \frac{4\pi e^2 N_s z_{av}}{\kappa_{sc}}+e\phi_{sub}-k_BT\,, \tag{3.13}$$

where the second term on the right is the separation of the Fermi level from the bottom of the lowest subband at the surface, E_0 is the energy of the bottom of the lowest subband relative to the nominal conduction band edge at the surface, as found from Eq. (3.3), N_s is the total concentration of inversion layer electrons, and z_{av} is their average distance from the semiconductor-insulator interface. The fourth term on the right in Eq. (3.13) is the potential drop associated with the inversion-layer charge. Note that ϕ_d, which is the quantity that enters in (3.11), is not the same as the surface potential ϕ_s, as illustrated in Fig. 10.

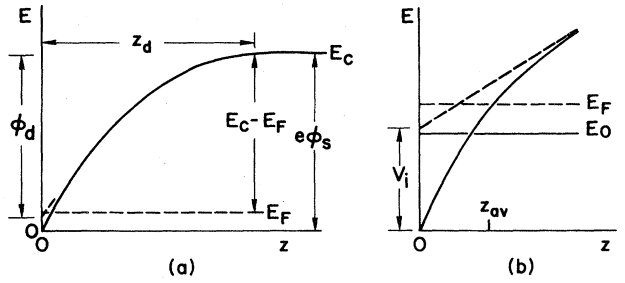

FIG. 10. Schematic band bending near a semiconductor-insulator interface, showing the nominal conduction-band edge (solid) and the corresponding band bending associated with the fixed depletion layer charges only (dashed). The depletion layer is shown in (b) for a case in which no substrate bias voltage is applied. A negative substrate bias ϕ_{sub} would raise the Fermi level and the conduction-band edge in the bulk relative to the values at the surface. An expanded view of the surface region that contains the inversion layer is shown in (b), and illustrates some of the terms that enter in Eq. (3.13) for the band bending ϕ_d in the depletion layer. In particular, $V_i=4\pi N_s e^2 z_{av}/\kappa_{sc}$ is the contribution of inversion layer electrons to the potential energy at $z=0$.

Finally, the depletion potential would have to be corrected for any deviation of the acceptor doping from homogeneity. Such deviations arise in some cases as the impurities redistribute themselves during oxidation (see, for example, Margalit *et al.*, 1972, and references cited therein) but have not usually been taken into account in inversion layer calculations. The effect of nonuniform bulk doping in the depletion layer can generally be neglected provided that the value of N_A used in Eqs. (3.10) and (3.11) gives the depletion charge obtained from a solution of Poisson's equation for the actual doping distribution.

In most cases of interest for silicon, the depletion layer is much wider than the inversion layer, and it is usually a good approximation to neglect the term quadratic in z in Eq. (3.9). However, for heavily doped substrates, for positive substrate bias voltages, or for semiconductors with a small effective mass m_z and a correspondingly wide inversion layer, the term quadratic in z can be significant. In numerical calculations there is no difficulty in keeping both terms, but in some analytic or variational treatments it is easier to keep only the linear term. This is the frequently used triangular potential or triangular well approximation, so called because the potential well is bounded on one side by the vertical barrier that keeps electrons out of the insulator and on the other side by the linearly rising potential given by the first term in Eq. (3.9). The triangular approximation is discussed in more detail in Sec. III.A.3.

The preceding discussion applies to the depletion layer potential when a positive gate voltage is applied to a structure with a p-type substrate. Under a limited range of conditions, the same treatment applies also to accumulation layers which result when a positive gate voltage is applied to a structure with an n-type substrate. If the sample is at a low enough temperature so that the electron concentration in the bulk is negligible, then the fixed charges are those of the minority acceptor impurities (Stern, 1974e) and the potential due to fixed charges is again given by Eqs. (3.9)—(3.11), but $e\phi_d$ is now of order 45 meV, the donor binding energy, rather than of order 1.1 eV, the silicon band gap.

At higher temperatures, or at high bulk impurity concentrations for which the impurity binding energy goes to zero, the model used here does not apply to accumulation layers. A treatment that includes the contribution of electrons in the bulk has been given by Appelbaum and Baraff (1971b; see also Baraff and Appelbaum, 1972) for n-type accumulation layers on InAs, and will not be considered in detail here.

$V_s(z)$, the second term in Eq. (3.8), is the contribution to the potential energy from the charge distribution of the electrons in the space-charge layer, and is given by the solution of Poisson's equation with the charge density in all subbands as the source term. The result is

$$V_s(z)=\frac{4\pi e^2}{\kappa_{sc}}\sum_i N_i\left[z+\int_0^z(z'-z)\zeta_i^2(z')dz'\right], \tag{3.14}$$

where N_i is the electron concentration in the ith subband and $\zeta_i(z)$ is the corresponding normalized envelope wave function. The arbitrary constant of integration has been chosen to make $V_s(0)=0$. When $z\to\infty$,

$$V_s(z)\to\frac{4\pi e^2}{\kappa_{sc}}\sum_i N_i z_i=\frac{4\pi e^2}{\kappa_{sc}}N_s z_{av}, \tag{3.15}$$

where

$$z_i=\int_0^\infty z\zeta_i^2(z)dz \tag{3.16}$$

is the average distance from the semiconductor-insulator interface of the electrons in the ith subband and z_{av} is the corresponding value for all surface electrons.

The last term in the potential energy (3.8) is the image term

$$V_I(z)=\frac{\kappa_{sc}-\kappa_{ins}}{\kappa_{sc}+\kappa_{ins}}\frac{e^2}{4\kappa_{sc}z}\equiv\frac{\delta_\kappa e^2}{4\kappa_{sc}z} \tag{3.17}$$

which arises because of the different dielectric constants of the semiconductor and the insulator. The semiconductor has the higher dielectric constant in all cases of interest here, so that this term is repulsive on the semiconductor side of the interface, where the electrons are. (Note, however, that the sign is different for electrons on liquid helium, considered in Secs. III.E and VIII.H.)

We need to consider whether the appropriate dielectric constant to be used in Eq. (3.17) is the optical or the static dielectric constant. For Si these two values are the same, but for SiO_2 they are different, and electrons couple to the electric fields of optical phonons. Such polaron effects were studied by Sak (1972; see also Mahan, 1974) for electrons bound to polar crystals by an image potential, and by Pollmann and Büttner (1975, 1977; see also Kane, 1978) for exciton binding in three dimensions. Interface phonons are discussed in connection with transport properties of inversion layers by Hess and Vogl (1979).

There are two characteristic energies in the surface polaron problem. One is the surface binding energy E_i. The other is the surface optical-phonon energy $\hbar\omega_s$, where ω_s is the solution of $\kappa_{sc}(\omega)+\kappa_{ins}(\omega)=0$, and is given by

$$\omega_s^2=\omega_T^2\frac{\kappa_0+\kappa_{sc}}{\kappa_\infty+\kappa_{sc}}, \tag{3.18}$$

where κ_0 and κ_∞ are the static and optical dielectric constants of the insulator and $\hbar\omega_T$ is the transverse optical-phonon energy at long wavelengths. For materials like SiO_2 that have more than one transverse mode, there will be a corresponding number of surface modes. It is mainly the surface optical phonons whose fields couple to the electrons in the silicon inversion layer.

There are also two characteristic lengths, a polaron length

$$r_{pol}=\left[\frac{\hbar}{m_z\omega_s}\right]^{1/2}, \tag{3.19}$$

and z_i, the average distance of the electrons in the ith subband from the interface. If we take $\hbar\omega_s\sim 60$ meV for SiO_2, we find $r_{pol}\sim 1$ nm. For weakly bound electronic states, with $E_i<\hbar\omega_s$ and $z_i>r_{pol}$, we expect that Eq. (3.17) will be a good approximation if the static dielectric constant is used. For more strongly bound states, neither of these inequalities is expected to hold, and more detailed calculations are needed to find the polaron effects. No simple local image potential expression is likely to be applicable in that case. There has not been any quantitative consideration of these questions for inversion layers. Fortunately, the image potential generally has a rather small effect on the electronic structure, as will be discussed below.

2. Self-consistent calculations and results

It is the $V_s(z)$ term in the effective one-electron potential of Eq. (3.8) that makes the Schrödinger equation a nonlinear eigenvalue problem, because the potential depends on the wave functions. Such equations are generally solved iteratively, with an assumed input potential leading to output wave functions from which a potential can again be derived using Eq. (3.14). The simplest method is to use as the input potential for solving the Schrödinger equation in the $(n+1)$st iteration a linear combination of the input and output potentials of the previous iteration:

$$V_{in}^{(n+1)}(z)=V_{in}^{(n)}(z)+f\times[V_{out}^{(n)}(z)-V_{in}^{(n)}(z)]. \tag{3.20}$$

The output potential from the nth iteration cannot be taken as the input for the $(n+1)$st iteration, which corresponds to $f=1$ in Eq. (3.20), because that process can diverge. There are many methods, both empirical and systematic, for dealing with this problem. A safe but slow method is to use a small value of f and many iterations. Methods to achieve faster convergence are discussed in the context of semiconductor space-charge layers by Stern (1970a) and in the context of the surface of the jellium model of metals by Lang and Kohn (1970). The interested reader is referred to those papers and the papers cited therein for additional information on this problem, which will not be discussed further here.

The first self-consistent solutions of Eq. (3.3) were those of Howard (1966, unpublished), Stern and Howard (1967), Duke (1967a), and Pals (1972b), and there have been many others subsequently. We give here some results of numerical self-consistent calculations for specific examples of inversion layers in (001) silicon, taken from Stern (1972b). His calculations included neither the image potential nor many-body effects and therefore have only qualitative validity.

Figure 11 shows the energy levels of a Si(100) inversion layer at absolute zero as the electron concentration is increased. Several features should be noted because

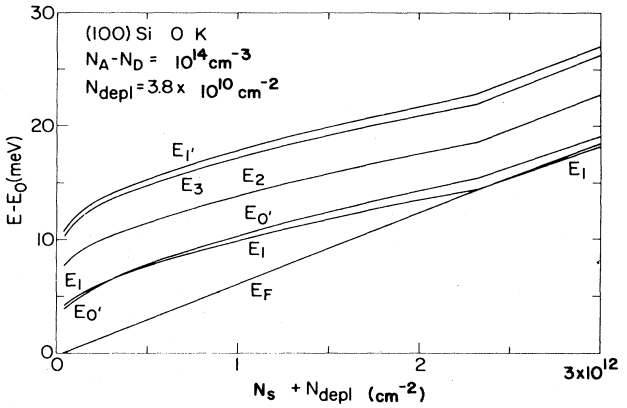

FIG. 11. Energy-level splittings and Fermi energy at 0 K for a (100) inversion layer on p-type silicon with 10^{14} acceptors per cm^3 in the bulk. All energies are measured from the bottom of the lowest subband. After Stern (1972b).

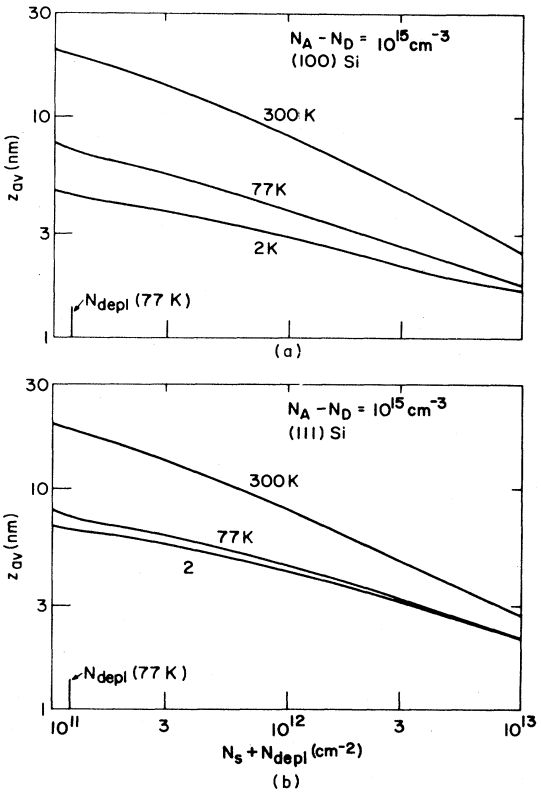

FIG. 12. Average spatial extent of the inversion layer electrons from the surface, z_{av}, as a function of the total density of inversion and depletion charges for (a) (100) and (b) (111) surfaces on p-type silicon with 10^{15} acceptors per cm^3 in the bulk at 2, 77, and 300 K. After Stern (1972b).

they enter in the interpretation of many experimental results. First, note that the $E_{0'}$ and E_1 levels are very close in energy and cross when $N_s/N_{\rm depl}=5.3$. This closeness in energy is a consequence of the ratio of transverse and longitudinal electron effective masses in silicon and the way in which they enter in the energy-level spectrum, and is therefore specific to (100) silicon. The actual ordering of these two levels has not been definitively determined. Optical measurements (Kneschaurek and Koch, 1977) suggest that $E_{0'}$ is lower, and analysis (Mori and Ando, 1979) of mobility results when two bands are occupied would suggest that E_1 is lower than, or at least very close to, $E_{0'}$. See Sec. III.C and Sec. IV.C for additional discussion.

The energy-level increase with increasing N_s shown in Fig. 11 occurs because the average electric field in the inversion layer increases as the total space charge increases. Note that $N_{\rm depl}$ is essentially constant at low temperatures once the inversion layer is occupied. At higher temperature, say 300 K, $N_{\rm depl}$ will continue to increase as N_s increases until the Fermi level has risen above the bottom of the lowest subband.

Another important feature of Fig. 11 is the pinning of the Fermi level to the bottom of the first excited subband after they cross, accompanied by a discontinuity in their variation with N_s. The pinning is simply a consequence of the increased density of states after the second subband is occupied. The increase in the rate of change of the energy of the excited subbands is a consequence of their much more extended wave functions. The average field seen by the electrons in the excited subband is much more strongly affected by an increase in population of that subband than by the same increase in population of the lowest subband, and therefore changes slope when the excited subband begins to be occupied. Because of the increased density of states the Fermi level also changes slope and increases less rapidly above the crossing than below with increasing N_s. All these changes in slope will be more gradual when broadening of energy levels is considered. They are also more gradual at elevated temperatures.

Figure 12 shows the average spatial extent of the charge distribution from the interface at 2, 77, and 300 K for (100) and (111) Si. The decrease of $z_{\rm av}$ with increasing space charge is a reflection of the increasing average field seen by the electrons, which pushes them closer to the surface and overpowers the increase that might have been expected when the higher subband is occupied.

Figure 13 shows the temperature dependence of the energy levels and of $z_{\rm av}$ at a fixed value of inversion-layer charge. The increase in $z_{\rm av}$ and in the energy levels occurs because electrons are transferred from the lowest subband to higher subbands as the temperature increases and N_s is held constant. The more extended wave functions of the higher subbands lead to the increase in $z_{\rm av}$, and that in turn increases the effective electric field seen by electrons in the higher subbands, increasing their energy.

Quantum effects play an important role in the properties of the space-charge layer, especially at low temperatures and high carrier concentrations. The charge density, illustrated in Fig. 14, found quantum mechanically goes essentially to zero in the oxide because of the high barrier there, and has its peak well inside the silicon.

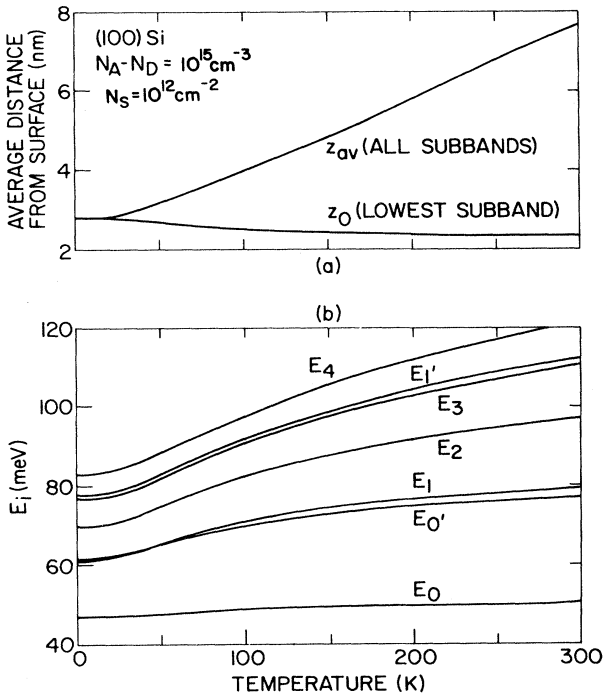

FIG. 13. Temperature dependence of (a) z_0 and z_{av}, the average distance of inversion layer electrons in the lowest subband and in all subbands, respectively, from the interface, and (b) the energies of the seven lowest subbands, for a (100) surface with 10^{12} electrons per cm^2. The bulk acceptor concentration is 10^{15} cm^{-3}. After Stern (1972b).

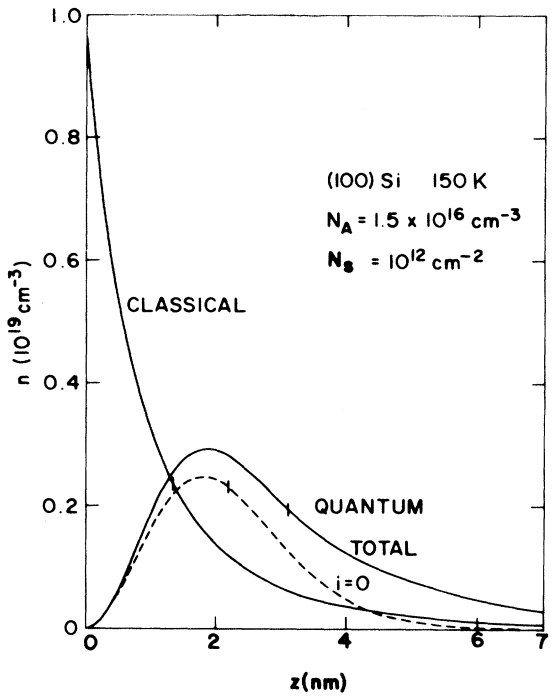

FIG. 14. Classical and quantum-mechanical charge density for a (100)Si inversion layer at 150 K with 10^{12} electrons per cm^2 and a bulk acceptor doping of 1.5×10^{16} cm^{-3}. The dashed curve shows the contribution of the lowest subband to the quantum-mechanical charge density. After Stern (1974a).

The classical Thomas-Fermi solution, in which the charge density depends only on the local separation of the band edge and the Fermi level, has a peak at the interface. In addition, the average spatial extent of the charge from the interface is greater when calculated quantum mechanically than when calculated classically. Another example of quantum effects is the difference in z_{av} for different surface orientations shown in Fig. 12, especially at low temperatures, which arises because of the different effective masses for the two surfaces. The classical solution is independent of surface orientation.

Another measure of the importance of quantum effects is the population of subbands associated with the conduction-band valleys. Classically, all six valleys are equally occupied. The quantum model, on the other hand, predicts that at low temperatures all the electrons are in the subbands associated with the two valleys whose heavy mass is perpendicular to the (100) surface, provided N_s is not too large. Figure 15 shows that the fractional occupation of the subbands associated with these two valleys is one at low temperatures but approaches the classical value $\frac{1}{3}$ at 300 K for low electron concentrations, for which the energy-level splittings are smallest.

The specific numerical examples shown here are subject to error because they were calculated without including many-body effects. These effects, as discussed in Sec. III.B, increase the splitting between the lowest subband and the higher subbands, and therefore enhance the importance of quantum effects.

Determination of subband splittings by far-infared spectroscopy is discussed in Sec. III.C. Another test of the splittings is to look for a change in the period of Shubnikov–de Haas oscillations at low temperatures as the carrier concentration increases and the Fermi level passes into a higher subband, as discussed in Sec. III.C.

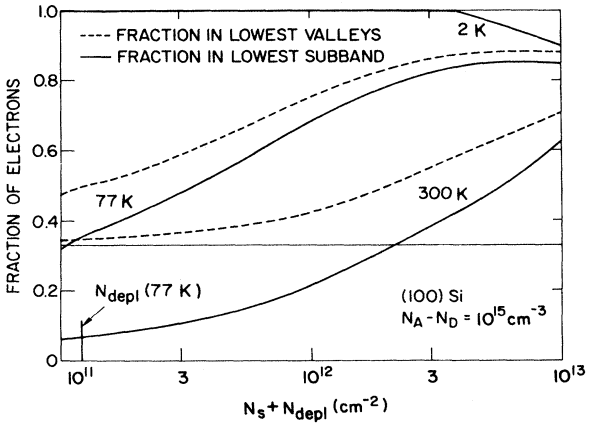

FIG. 15. Fraction of electrons in the lowest subband and in all the subbands associated with the lowest valleys—those that have the heavy mass perpendicular to the interface—for a (100)Si inversion layer. The fraction in the lowest valleys is $\frac{1}{3}$ when quantum effects are negligible. After Stern (1972b).

3. Approximate energies and wave functions

In this section we describe a number of approximate solutions that are helpful when full self-consistent solutions cannot be conveniently obtained, or when estimates of properties of inversion layers need to be made. We first describe the triangular potential approximation, for which an exact solution can be found. Then we describe simple variational solutions.

a. Triangular potential approximation

If the image potential is excluded, the remaining terms of the potential (3.8) increase linearly at the semiconductor-insulator interface and then bend over to approach a constant value. The inversion layer contribution becomes constant after a small multiple of the average inversion-layer penetration $z_{\rm av}$, and the depletion-layer contribution becomes constant at z_d, the edge of the depletion layer. Because z_d is generally much larger than $z_{\rm av}$, the curvature of the depletion potential $V_d(z)$, given in Eq. (3.9), can be neglected without substantial error in many cases, especially when the depletion charge is small compared to the inversion charge. However the inversion-layer contribution $V_s(z)$ to the potential varies significantly in the inversion layer and can only be neglected if N_s is small compared to $N_{\rm depl}$ or if the advantages of an exact solution outweigh the error made in the potential.

In the triangular well approximation, the potential energy is given by an infinite barrier for $z<0$ and by

$$V(z)=eFz \tag{3.21}$$

for $z>0$, where

$$F=\frac{4\pi(N_{\rm depl}+fN_s)e}{\kappa_{\rm sc}} \tag{3.22}$$

is the effective field and f is a numerical coefficient which is unrelated to the coefficient in (3.20). Choosing $f=1$ gives the field at the interface, $f=0$ gives the depletion layer contribution alone, and $f=\frac{1}{2}$ gives the average field in the inversion layer. The Schrödinger equation is solved with the condition that the envelope wave function go to zero at $z=0$ and at infinity. The solutions are Airy functions (Abramowitz and Stegun, 1964),

$$\zeta_i(z)=\mathrm{Ai}\left[\frac{2m_zeF}{\hbar^2}\left[z-\frac{E_i}{eF}\right]\right], \tag{3.23}$$

where the eigenvalues E_i are given asymptotically for large i by

$$E_i\sim\left[\frac{\hbar^2}{2m_z}\right]^{1/3}\left[\frac{3\pi eF}{2}\left[i+\frac{3}{4}\right]\right]^{2/3},\quad i=0,1,2,\ldots. \tag{3.24}$$

The exact eigenvalues have $i+\frac{3}{4}$ in Eq. (3.24) replaced by 0.7587, 1.7540, and 2.7575, respectively, for the three lowest solutions. The normalization and some other properties of the Airy functions are given in Appendix B of Stern (1972b). We note here only that the average value of z is $z_i=2E_i/3eF$, and that the average value of z^2 is $\frac{6}{5}z_i^2$ for the ith subband.

b. Variational wave function for the lowest subband

Simple analytic wave functions make calculations of properties of inversion layers much more convenient than they would be if numerical self-consistent solutions or cumbersome analytic solutions like the Airy functions had to be used. For that reason approximate solutions have been widely used in inversion layer calculations. The simplest of these, first proposed for inversion layers by Fang and Howard (1966), is

$$\zeta_0(z)=\left[\frac{b^3}{2}\right]^{1/2}ze^{-(1/2)bz}. \tag{3.25}$$

The average penetration of the charge into the semiconductor for this wave function is

$$z_0=\frac{3}{b}. \tag{3.26}$$

The same wave function also applies to the lowest subband of electrons on liquid helium if the barrier for entering the helium is infinite and the solid-vapor interface is sharp (Cole, 1974).

The parameter b in Eq. (3.25) is determined by minimizing the total energy of the system for given values of the inversion- and depletion-layer charges. Because of the simplicity of the wave function, it is easy to evaluate the expectation values of all the terms in the Hamiltonian. We find

$$\begin{aligned}
\langle T\rangle&=\frac{\hbar^2b^2}{8m_z},\\
\langle V_d\rangle&=\frac{12\pi e^2N_{\rm depl}}{\kappa_{\rm sc}b}-\frac{24\pi e^2N_A}{\kappa_{\rm sc}b^2},\\
\langle V_s\rangle&=\frac{33\pi e^2N_s}{4\kappa_{\rm sc}b},\\
\langle V_I\rangle&=\frac{\kappa_{\rm sc}-\kappa_{\rm ins}}{\kappa_{\rm sc}+\kappa_{\rm ins}}\frac{e^2b}{8\kappa_{\rm sc}}\equiv\frac{\delta_\kappa e^2b}{8\kappa_{\rm sc}},
\end{aligned} \tag{3.27}$$

where the terms are the expectation values of the kinetic energy, the potential energy of an electron interacting with the depletion-layer charges, the potential energy of an electron interacting with the other electrons in the inversion layer, and the image potential, respectively. The energy of the lowest subband is

$$E_0=\langle T\rangle+\langle V_d\rangle+\langle V_s\rangle+\langle V_I\rangle. \tag{3.28}$$

However the total energy per electron, which is the quantity to be minimized, is

$$E/N=\langle T\rangle+\langle V_d\rangle+\tfrac{1}{2}\langle V_s\rangle+\langle V_I\rangle\ , \tag{3.29}$$

where the factor $\frac{1}{2}$ prevents double counting of electron-electron interactions.

If the image potential and the second term in $\langle V_d\rangle$ are neglected the value of b that minimizes the total energy per electron is

$$b=\left[\frac{48\pi m_z e^2 N^*}{\kappa_{sc}\hbar^2}\right]^{1/3}, \tag{3.30}$$

where

$$N^*=N_{depl}+\tfrac{11}{32}N_s\ , \tag{3.31}$$

a result first given by Stern and Howard (1967). Figure 16 shows that the values of E_0 and z_0 calculated for the lowest subband from the variational wave function (3.25) exceed the values found from a self-consistent Hartree solution by less than 7% in the absence of the image potential (Stern, 1972b).

If all the terms in Eq. (3.29) are to be retained, the minimization must be done numerically, but is still very easy. It is also possible to add the exchange energy (Chaplik, 1971a), whose average value per electron when the variational function (3.25) is used is

$$E_x=-\frac{4e^2k_F}{3\pi\kappa_{sc}}\left[G'\left[\frac{b}{k_F}\right]+\delta_\kappa G''\left[\frac{b}{k_F}\right]\right], \tag{3.32}$$

where k_F is the Fermi wave vector, δ_κ is the coefficient which appears in the image potential Eq. (3.17), and G' and G'' are functions whose values have been calculated and plotted by Stern (1974d). The expressions for the exchange contribution to the one-electron energy of the lowest subband have also been given there.

Figure 17 shows how the values of E_0 and z_0 change as the image and exchange contributions to the energy are included or omitted. The image term, which is repulsive, tends to expand the wave function, while the exchange term tends to contract it. At high densities it is often better to omit both terms than to include either term alone. This is an *a posteriori* justification of the omission of the image term in the Hartree calculations by Stern and Howard (1967). For low carrier densities, on the other hand, the exchange term is negligible, and the image term must be included.

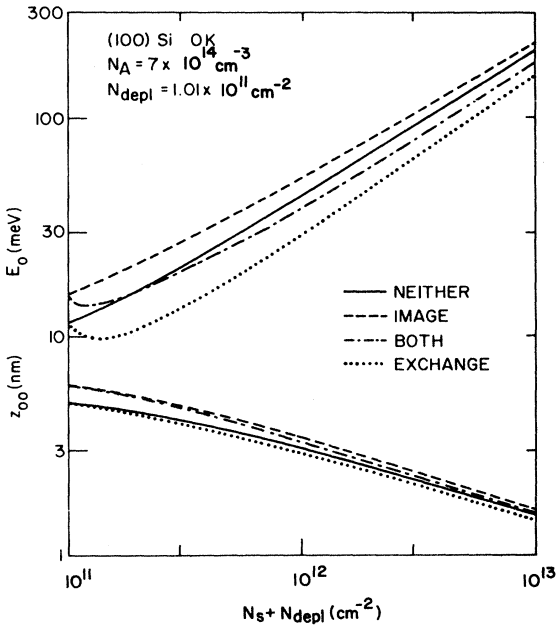

FIG. 17. Effect of exchange and image potential on the variationally calculated energy and spatial extent of the lowest subband. The dashed curve is calculated including the image contribution to the energy, the dotted curve included the exchange contribution, the full curve includes neither, and the chain curve includes both. After Stern (unpublished).

The exchange energy is only the simplest term in the many-body energy. A more detailed consideration of many-body effects is given in Sec. III.B.

Figure 18 compares the variational wave function without image or exchange contributions to the corresponding self-consistent Hartree wave function and com-

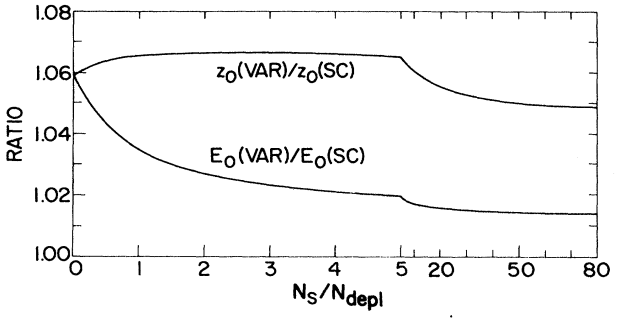

FIG. 16. Ratios of variational to self-consistent values of the energy E_0 and the average spatial extent from the interface z_0 of the lowest subband vs the ratio of the density of inversion layer charges to the density of depletion layer charges. The values are calculated without image or many-body effects. Note the change of scale at $N_s/N_{depl}=5$. After Stern (1972b).

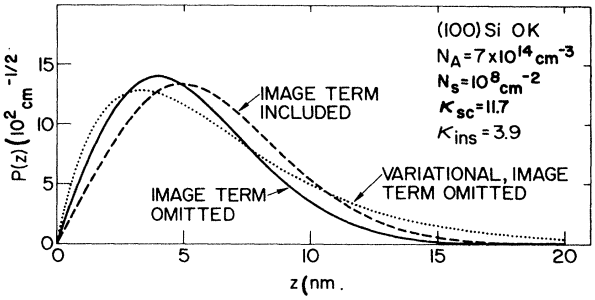

FIG. 18. Envelope wave functions calculated self-consistently with (dashed curve) and without (full curve) including the image potential, and the Fang-Howard variational wave function (3.25) in which the parameter b is determined by minimizing the total energy without including the image potential. Exchange and correlation effects are not included in any of the curves. After Stern (unpublished).

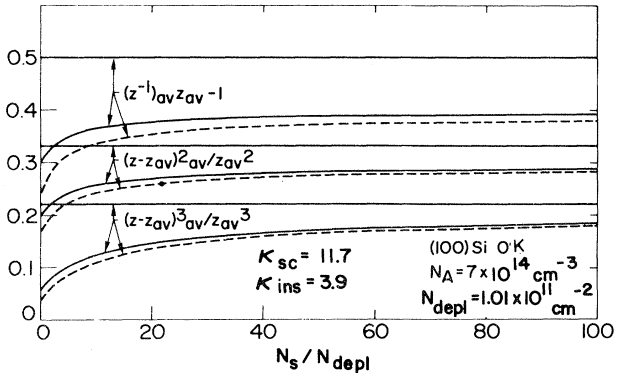

FIG. 19. Normalized average of various powers of z, the distance from the surface, evaluated using self-consistent Hartree wave functions calculated with (dashed curves) and without (full curves) including the image potential, are plotted against the ratio of the densities of inversion-layer and depletion-layer charges. The horizontal lines are calculated using the variational wave function (3.25), and show that it is a poor representation of the shape of the more accurate wave functions, especially at small values of $N_s/N_{\rm depl}$. After Stern (unpublished).

pares self-consistent wave functions with and without the image contribution to the potential. The differences are seen to be substantial.

It is useful to have measures of the accuracy of the wave function other than the energy itself, because rather poor wave functions can give rather good energies. Figure 19 shows the normalized expectation values of some powers of z for the variational wave function (3.25), and for self-consistent Hartree solutions with and without the image potential as functions of the ratio of inversion-layer charge to depletion-layer charge. Note that the Airy-function solution corresponds to the Hartree solution without an image term when that ratio equals zero. The variational solution is seen to be very inaccurate at small values of $N_s/N_{\rm depl}$, but to be somewhat better as N_s increases.

An even more dramatic example of the errors that can result from use of the variational wave function (3.25) was pointed out by Matsumoto and Uemura (1974) in their paper on surface roughness scattering, which is discussed in more detail in Sec. IV.C.2. Prange and Nee (1968) gave the relevant matrix element in terms of the derivative of the wave function at the surface. Matsumoto and Uemura showed that it can also be written in terms of the expectation value of the potential gradient. The two formulations are equivalent, since for the exact wave function one finds, by multiplying the Schrödinger equation (3.3) by $d\zeta_i/dz$ and integrating over all z, that

$$\left[\frac{d\zeta_i}{dz}\right]^2_{z=0} = \frac{2m_z}{\hbar^2}\int_0^\infty \zeta_i^2(z)\frac{dV}{dz}dz \ . \tag{3.33}$$

Matsumoto and Uemura showed that for a triangular potential their formulation gives results independent of the wave function used, while the formation in terms of the derivative of the wave function gives surface roughness scattering too big by a factor of 9 when the variational function (3.25) is used, because the left side of Eq. (3.33) is three times as large as the right side. For larger values of $N_s/N_{\rm depl}$ the resulting error will be smaller, but this example is a dramatic warning that the variational wave function can lead to serious errors in some cases.

The variational wave function of Eq. (3.25) is by no means the only one possible. It has been widely used because of its simplicity, but can lead to substantial errors, as we have seen. Another one-parameter wave function which is considerably closer to the self-consistent solution is

$$\zeta_0(z) = (\tfrac{3}{2}b^3)^{1/2} z e^{-(1/2)(bz)^{3/2}} , \tag{3.34}$$

which has been proposed by Takada and Uemura (1977). Many-parameter expansions can also be used (Ohkawa and Uemura, 1976, 1977b).

c. Higher subbands

Variational functions have been used to give approximate wave functions and energy levels for higher-lying subbands (Takada and Uemura, 1977; Kalia *et al.*, 1978; Das Sarma *et al.*, 1979; Kramer and Wallis, 1979; Mori and Ando, 1979). They provide an alternative to numerical self-consistent calculations. The energy levels can also be estimated by starting from the values in the depletion potential alone, given approximately by Eq. (3.24), and adding the effect of the additional inversion-layer potential as a perturbation (Stern, 1972b). This approximation is reasonably good if the higher-lying levels have wave functions which extend far beyond the region where the inversion layer potential is strongest. These methods are adequate if great accuracy is not essential.

B. Many-body effects

In the preceding section the subband structure was discussed within the Hartree approximation. This approximation is valid when the electron concentration is sufficiently high, i.e., when the average kinetic energy of electrons is much larger than the average interaction energy. This condition is usually written as $r_s << 1$, where the parameter r_s is defined in three dimensions as the radius of a sphere containing one electron, in units of the effective Bohr radius a^* given by Eq. (2.28a). A corresponding result is expected to hold for two-dimensional systems. Therefore, the Hartree approximation is expected to work quite well for two-dimensional systems in semiconductors with a small energy gap, like InSb and InAs, because they have a small effective mass and a large dielectric constant. For these materials, typical charge densities like 10^{12} cm^{-2} correspond to $r_s << 1$. In the case of inversion layers on silicon surfaces, however, the effective mass is larger, and r_s then become comparable to or larger than unity for typical values of N_s. Many-

body effects such as exchange and correlation can then play an important role.

The exchange energy was briefly discussed by Chaplik (1971a) and calculated explicitly by Stern (1973, 1974d). Stern has shown that the exchange energy is comparable to or even larger than the energy separations between subbands calculated in the Hartree approximation, suggesting the importance of the many-body effects. Insufficiencies of the Hartree results were pointed out also by comparison with various experimental results, especially infrared intersubband absorption. In this section we consider such many-body effects on the subband structure in the n-channel layer on the Si(100) surface. We confine ourselves to the model of the abrupt interface and to the case in which only the ground subband is occupied by electrons, and treat the problem in the effective-mass approximation.

One way to study the many-body effects theoretically is to treat the exchange and correlation perturbationally using the subband structure calculated in the Hartree approximation as the unperturbed states. The Hamiltonian is given by

$$\mathscr{H}=\sum_{ik\sigma v}[E_i+\varepsilon(k)]a^+_{ik\sigma v}a_{ik\sigma v}+\frac{1}{2}\sum_{ijlm}\sum_{kk'q}\sum_{\sigma\sigma' vv'}V_{(ij)(lm)}(q)\times a^+_{ik\sigma v}a^+_{lk'\sigma' v'}a_{mk'-q\sigma' v'}a_{jk+q\sigma v}\ , \tag{3.35}$$

where $a^+_{ik\sigma v}$ and $a_{ik\sigma v}$ are the creation and annihilation operators, respectively, of an electron of the ith subband with the wave vector $\mathbf{k}$, the spin σ, and the valley v. The electron-electron interaction is given by

$$V_{(ij)(lm)}(q)=\frac{2\pi e^2}{\bar{\kappa}q}F_{(ij)(lm)}(q)\ , \tag{3.36}$$

with

$$F_{(ij)(lm)}(q)=\frac{1}{2}\int_0^\infty dz\int_0^\infty dz'\left[\left[1+\frac{\kappa_{\rm ins}}{\kappa_{\rm sc}}\right]e^{-q|z-z'|}+\left[1-\frac{\kappa_{\rm ins}}{\kappa_{\rm sc}}\right]e^{-q|z+z'|}\right]\times\zeta_i^*(z)\zeta_l^*(z')\zeta_j(z)\zeta_m(z')\ . \tag{3.37}$$

The form factor $F(q)$ of Eq. (2.51) corresponds to $F_{(00)(00)}(q)$. The existence of the other sets of valleys is neglected in the Hamiltonian for simplicity. The Hartree treatment of Eq. (3.35) recovers the Hartree result as is expected. The Green's function becomes a matrix with respect to the subband indices and satisfies the Dyson equation

$$G_{ij}(k,E)=G^{(0)}_{ij}(k,E)+\sum_l G^{(0)}_{ii}\Sigma_{il}(k,E)G_{lj}(k,E)\ , \tag{3.38}$$

where $\Sigma_{ij}(k,E)$ is the self-energy matrix, and the unperturbed Green's function is given by

$$G^{(0)}_{00}(k,E)=\frac{\theta(k-k_F)}{E-\varepsilon(k)-E_0+i0}+\frac{\theta(k_F-k)}{E-\varepsilon(k)-E_0-i0}\ ,$$

$$G^{(0)}_{ij}(k,E)=\frac{\delta_{ij}}{E-\varepsilon(k)-E_i+i0}\quad(i,j\neq 0) \tag{3.39}$$

with $\theta(x)$ being the step function defined by $\theta(x)=1$ for $x>0$ and $\theta(x)=0$ for $x<0$. The subband energy is determined by

$$\det[G^{(0)}_{ii}(k,E)^{-1}\delta_{ij}-\Sigma_{ij}(k,E)]=0\ . \tag{3.40}$$

One has to introduce some approximations to evaluate the self-energy explicitly. Vinter (1975b, 1977) neglected contributions from scattering processes in which an electron changes subband. The self-energy becomes diagonal in this approximation. He then calculated the self-energy to the lowest order in the dynamically screened Coulomb interaction and employed the plasmon pole approximation discussed in Sec. II.F. The self-energy is given by

$$\Sigma_{00}(k,E)=-\int\frac{d\omega}{2\pi i}\sum_q\frac{V(q)}{\varepsilon(q,\omega)}G^{(0)}_{00}(\mathbf{k}+\mathbf{q},E+\omega)\ , \tag{3.41}$$

and

$$\Sigma_{11}(k,E)=-\int\frac{d\omega}{2\pi i}\sum_q\left[V_{(11)(11)}(q)-V_{(11)(00)}\frac{\Pi(q,\omega)}{\varepsilon(q,\omega)}V_{(00)(11)}(q)\right]\times G^{(0)}_{11}(\mathbf{k}+\mathbf{q},E+\omega)\ , \tag{3.42}$$

where $V(q)=V_{(00)(00)}(q)$, and $\varepsilon(q,\omega)$ and $\Pi(q,\omega)$ are given in Eqs. (2.55) and (2.56), respectively. Hedin (1965) proposed an approximate procedure to include higher-order effects which appear when one uses dressed Green's functions instead of unperturbed ones in the expression for the self-energy. In this scheme one assumes a constant-energy shift in the Green's functions appearing in Eq. (3.41). The Dyson equation becomes

$$E_0(k)=E_0+\varepsilon(k)+\Sigma_{00}(k,E_0(k)-\mu_{xc})\ , \tag{3.43}$$

where the constant shift is taken to be the exchange-correlation part of the chemical potential μ_{xc} and is chosen to be

$$\mu_{xc}=\Sigma_{00}(k_F,E_0+\varepsilon(k_F))\ . \tag{3.44}$$

Vinter proposed similarly

$$E_1(k)=E_1+\varepsilon(k)+\Sigma_{11}(k,E_1(k)-\mu_{xc}) \tag{3.45}$$

for the excited subband. Equations (3.43) and (3.45) were solved numerically. He showed that $E_1(k)$ obtained from (3.45) was quite different from the result of the approximation in which $E_1(k)-\mu_{xc}$ was replaced by $E_1+\varepsilon(k)$ in the self-energy of Eq. (3.45). The $\mathbf{k}$ depen-

dence of the self-energy shift was small and similar for the two subbands. An example of the calculated energy shift at $k=k_F$ is shown in Fig. 20 as a function of the electron concentration for $N_{\rm depl}=1\times10^{11}$ cm^{-2}. The shift of the ground subband is comparable to the unperturbed E_0 in the Hartree approximation. The same is applicable to the excited subband. Figure 21 compares the calculated subband energy separations averaged over **k** with the corresponding Hartree result of Stern as a function of N_s for the same $N_{\rm depl}$ as in Fig. 20. One sees that the many-body effects are considerable and extremely important in the n-channel inversion layer on the Si(100) surface.

Ohkawa (1976a) extended Rice's method discussed in Sec. II.F to the many-subband case. The self-energy is diagonal in this method and the subband energy shift is given by

$$E_i(k)=E_i+\varepsilon(k)+\Sigma_{ii}(k,E_i+\varepsilon(k))\ , \tag{3.46}$$

where $\Sigma_{ii}(k,E)$ is calculated to the lowest order in the dynamically screened Coulomb interaction. Taking into account subband mixings among the lowest three subbands ($i=0$, 1, and 2), he calculated the self-energy shift. The calculated shift turned out to be very close to that of Vinter for the lowest subband, but 25% smaller than that of Vinter for the first excited subband. A similar approach was used later by Kalia, Das Sarma, Nakayama, and Quinn (Kalia *et al.*, 1978, 1979; Das Sarma *et al.*, 1979) for the study of temperature and stress effects.

Since the **k** dependence of the energy shift is small and unimportant, the energy shift of the ground subband is given in Vinter's scheme by $\Sigma_{00}(k_F,\varepsilon(k_F)+E_0)$, which is the same as Eq. (3.46). Therefore the agreement between the results of Vinter and Ohkawa is expected for the ground subband. The discrepancy between the energy shifts for the first excited subband mainly originates from the difference between Eqs. (3.45) and (3.46). Equation

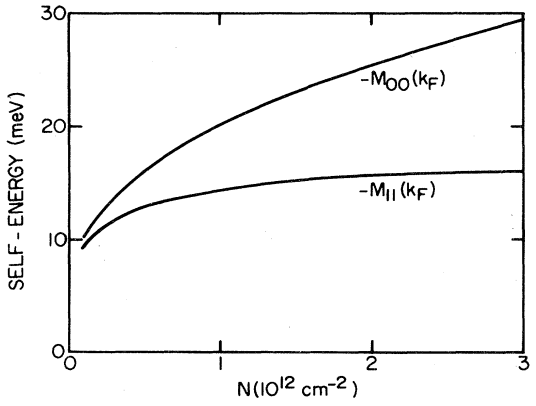

FIG. 20. Self energies at the Fermi wave vector in the ground and the first excited subbands in the n-channel inversion layer on a Si(100) surface. The electron concentration is denoted by N and the self-energies are written as M_{00} and M_{11} instead of Σ_{00} and Σ_{11} in the text. $N_{\rm depl}=1\times10^{11}$ cm^{-2}. After Vinter (1977).

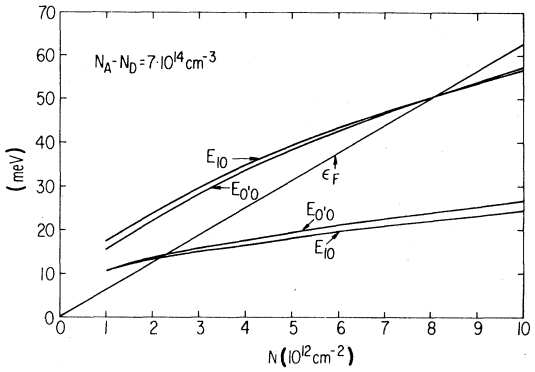

FIG. 21. An example of calculated energy separations from the ground subband to the first excited subband for the doubly degenerate set of valleys (E_{10}) and to the lowest subband of the fourfold-degenerate set ($E_{0'0}$), calculated by Vinter (1977). The lower curves show the results in the Hartree approximation, and in the upper curves exchange and correlation are included. The Fermi energy (ε_F) is measured from the bottom of the ground subband. N represents the electron concentration. $N_{\rm depl}=1\times10^{11}$ cm^{-2}. After Vinter (1977).

(3.45) seems rather inconsistent and its meaning is not clear. One has introduced μ_{xc} in the energy variable of the self-energy because one expects that the self-energy which appears in $G_{00}(\mathbf{k}+\mathbf{q},E+\omega)$ in place of $G_{00}^{(0)}(\mathbf{k}+\mathbf{q},E+\omega)$ is roughly given by μ_{xc} independent of the momentum and the energy. If one follows the same approximation scheme, one has to introduce some constant-energy shift of the first excited subband in Σ_{11} instead of μ_{xc}, since the energy shift is expected to be smaller for the excited subband. Vinter assumed it to be μ_{xc}, which seems to be the main origin of the larger energy shift of the first excited subband than that of Ohkawa.

A disadvantage of the perturbation method is that it is not applicable when the change in the subband structure caused by the exchange and correlation is considerable, since it is based on the Hartree result. The result is, therefore, expected to be good in the inversion layer with values of $N_{\rm depl}$ that give large subband energy separations in the Hartree approximation. It is especially not applicable to accumulation or inversion layers with extremely small $N_{\rm depl}$ for which subband separations are very small. As a result of intersubband mixings the electron density distribution becomes narrower than that calculated in the Hartree approximation. This is because the Hartree approximation overestimates the Coulomb repulsive force of other electrons. As will be shown in the following, this change in the density distribution is not negligible even in the inversion layer and can affect the Hartree energy separation through the change in the self-consistent potential. Vinter tried to take into account this effect using the wave function calculated by neglecting the image potential, under the assumption that the change of the density distribution caused by the exchange and correlation cancels that caused by the image potential. This cancellation had been demonstrated

by Stern (1974d) with the use of a variational wave function in the Hartree-Fock approximation, as has been discussed in Sec. III.A. The cancellation is not complete, however, if one takes into account the correlation effect, as will be shown later. In any case, the fact that the density-distribution change due to the many-body effects is not negligible suggests that the off-diagonal part of the self-energy should give a sizable energy shift. Although each off-diagonal matrix element is small (Stern, 1974d), the total contribution from many subbands possibly becomes appreciable. Takada and Ando (1978) proposed a method in which the change in the density distribution can be included within a single-subband approximation. See Sec. VII.B for a more detailed discussion on this method.

An alternative way to study the exchange-correlation effect on the subband structure is to use the density-functional method. Hohenberg, Kohn, and Sham (Hohenberg and Kohn, 1964; Kohn and Sham, 1965) have shown that the density distribution of an interacting electron gas under an external field can be obtained by a one-body Schrödinger-type equation containing an exchange correlation potential v_{xc} in addition to the usual Hartree potential and the external potential. The exchange-correlation potential is given by a functional derivative of the exchange-correlation part of the ground-state energy $E_{xc}[n(\mathbf{R})]$ with respect to the number density $n(\mathbf{R})$ of electrons. The functional $E_{xc}[n(\mathbf{R})]$ is not known and is replaced by a product $n(\mathbf{R})\varepsilon_{xc}(n(\mathbf{R}))$ in the usual local approximation, where $\varepsilon_{xc}(n)$ is the exchange-correlation energy per electron of a uniform electron gas with the density n. In this approximation $v_{xc}(\mathbf{R})$ becomes the exchange-correlation part of the chemical potential μ_{xc} of the uniform electron gas. This theory has been used and known to be successful in a number of different problems, although the reason for the success has not been fully elucidated yet. The density-functional formulation was first applied to the space-charge layer by Ando (1976a, 1976b).

There are some problems in the choice of v_{xc} in our system. The conduction band of Si is anisotropic, and one needs μ_{xc} of anisotropic electron gas. Ando used μ_{xc} of an electron gas characterized by isotropic mass $m_{\rm op}$ defined by $m_{\rm op}^{-1}=(2m_t^{-1}+m_l^{-1})/3$. The neglect of the anisotropy seems to be justified (Combescot and Nozieres, 1972; Brinkman and Rice, 1973). Another problem arises because of the image effect caused by the insulating layer. Considering the nature of the local approximation, Ando used $\mu_{xc}(n(z);z)$ of an electron gas where the mutual interaction between electrons at $(\mathbf{r}_1,z_1)$ and $(\mathbf{r}_2,z_2)$ is given by

$$V(\mathbf{r},z_1-z_2;z)=\frac{e^2}{\kappa_{\rm sc}}[\mathbf{r}^2+(z_1-z_2)^2]^{1/2} + \frac{e^2(\kappa_{\rm sc}-\kappa_{\rm ins})}{\kappa_{\rm sc}(\kappa_{\rm sc}+\kappa_{\rm ins})}[\mathbf{r}^2+(z_1-z_2)^2+4z^2]^{-1/2}, \tag{3.47}$$

where $\mathbf{r}=\mathbf{r}_1-\mathbf{r}_2$.

Strictly speaking, the energy eigenvalue $E_i(k)$ obtained from the Schrödinger-type equation does not necessarily represent the quasiparticle energy. Sham and Kohn (1966) proposed a local energy-dependent exchange-correlation potential for calculating quasiparticle energies. The proposed $v_{xc}(E)$ is given by $\Delta\varepsilon(K)$, which is the quasiparticle energy shift in the uniform electron gas, defined by

$$\Delta\varepsilon(K)+\frac{\hbar^2K^2}{2m_{\rm op}}=E-\mu+\frac{\hbar^2K_F^2}{2m_{\rm op}}+\mu_{xc}, \tag{3.48}$$

where K_F is the Fermi wave vector of a uniform three-dimensional electron gas. The potential coincides with $v_{xc}(n(z);z)$ for $E=\mu$, with μ being the chemical potential. Using such a potential, one can calculate various two-dimensional quasiparticle properties. For example, the quasiparticle effective mass m^* is given by

$$\frac{m^*}{m_t}=\int_0^\infty dz\frac{m^*(n(z);z)}{m_{\rm op}}n(z)\left[\int_0^\infty dz n(z)\right]^{-1}, \tag{3.49}$$

where $m^*(n(z);z)$ is the effective mass of the homogeneous three-dimensional electron gas. The quasiparticle g factor is also calculated if one extends the theory to include effects of spin interaction with an external magnetic field (Kohn and Sham, 1965). It is given by

$$\frac{g^*}{2}=\frac{m_{\rm op}}{m^*}\int_0^\infty dz\frac{m^*(n(z);z)g^*(n(z);z)}{2m_{\rm op}} \times\left[\int_0^\infty dz\, n(z)\right]^{-1}, \tag{3.50}$$

where $g^*(n(z);z)$ is the effective g factor in three dimensions. An example of the results calculated in this way is given in Fig. 9. Actual evaluation of the energy-dependent potential shows, however, that the energy dependence is small, and one can regard the eigenvalues of the Schrödinger-like equation as the subband energies in a good accuracy. Finally, one has to use a different exchange-correlation potential for an electron in subbands associated with other sets of valleys. These exchange-correlation potentials were calculated in the Hubbard-like approximation in the case where the valley degeneracy is two.

Figure 22 compares the electron density distribution and the self-consistent potential with those calculated in the Hartree approximation for the inversion layer ($N_s=1\times10^{12}$ cm^{-2} and $N_{\rm depl}=1.55\times10^{11}$ cm^{-2}). Energies of the subbands are strongly lowered by the exchange-correlation effect. The change in the density distribution is also appreciable and responsible for the shift of the Hartree part of the potential at large z. The subband energies and the Fermi energy measured from the bottom of the ground subband are shown in Fig. 23. An example for an accumulation layer ($N_A=1\times10^{14}$ cm^{-3}, which corresponds to an inversion layer with $N_{\rm depl}=7.7\times10^9$ cm^{-2}) is given in Figs. 24 and 25. The exchange-correlation effect modifies the subband struc-

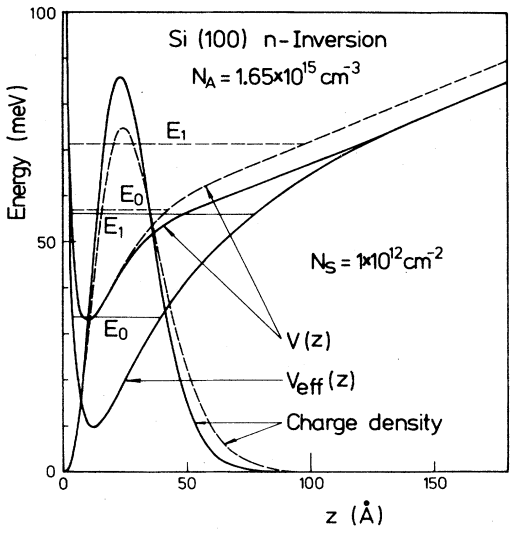

FIG. 22. An example of electron density distribution, self-consistent potential, and bottoms of the subbands in the n-channel inversion layer, calculated in the density-functional formulation. Corresponding Hartree results are given by broken lines. The difference between $V_{eff}(z)$ and $V(z)$ gives the exchange-correlation potential. The electrostatic potential is also modified if the exchange-correlation effect is included. After Ando (1976a, 1976b).

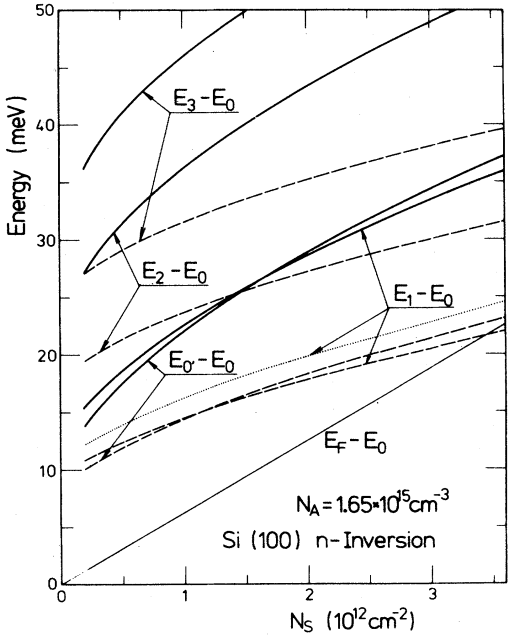

FIG. 23. Subband energies and the Fermi energy measured from the bottom of the ground subband in the n-channel inversion layer on a Si(100) surface. $N_{depl} = 1.55\times10^{11}$ cm^{-2}. The corresponding results in the Hartree approximation are given by broken lines. The dotted curve represents the Hartree result obtained by neglecting the image effect. After Ando (1975b).

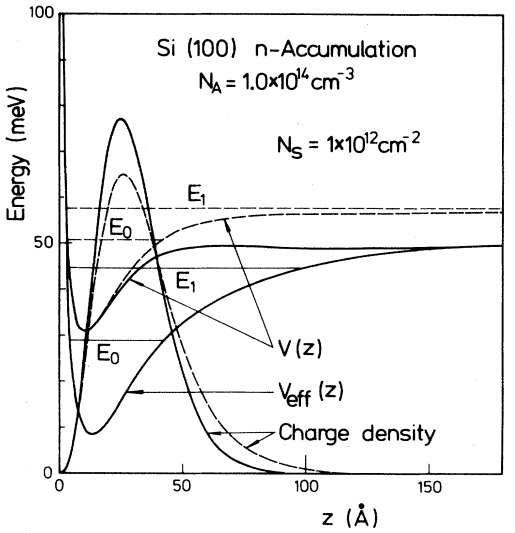

FIG. 24. An example of electron density distribution, self-consistent potential, and bottoms of the subbands for the n-channel accumulation layer on a Si(100) surface, as in Fig. 22. After Ando (1976b).

ture even qualitatively in an accumulation layer. In the Hartree approximation, only the ground subband is strongly localized in the interface region, and all the other subbands are much more extended, quasicontinuum states. When the exchange-correlation effect is taken into account, the first excited subband becomes localized in the surface region. This is consistent with experimental results of intersubband optical absorption by Kamgar and co-workers (Kamgar *et al.*, 1974a, 1974b; Kneschaurek *et al.*, 1976), who observed a narrow lineshape similar to that observed in the inversion layer. The narrow lineshape cannot be explained by the Hartree result.

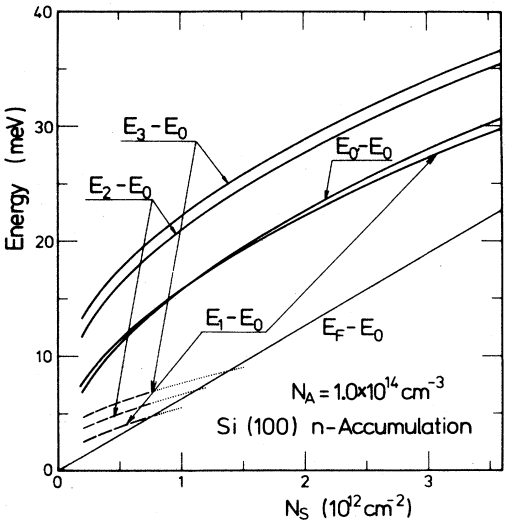

FIG. 25. An example of subband energies and the Fermi energy measured from the bottom of the ground subband for the n-channel accumulation layer on a Si(100) surface, as in Fig. 23. After Ando (1976b).

Kalia, Kawamoto, Quinn, and Ying (1980) have proposed a simplified approach for calculating the subband structure which in a way gives a connection between the perturbation method and the density-functional approach. They introduce an effective one-body potential, $V'_{xc}(z)$, similar to the exchange-correlation potential appearing in the density-functional theory, and calculate the subband structure in the Hartree approximation including $V'_{xc}(z)$ as an external potential. Basing their method on the calculated energy levels and wave functions, they treat exchange-correlation effects and also $-V'_{xc}(z)$ perturbationally and calculate the self-energy shifts. The effective potential $V'_{xc}(z)$ is determined so as to minimize the self-energy shift of the ground subband. The resulting $V'_{xc}(z)$ has turned out to be close to the exchange-correlation potential of the density-functional theory. Further, the calculated subband energies are in rather good agreement with those of the simple-minded perturbation theory (Das Sarma *et al.*, 1979) discussed above.

The temperature dependence of many-body effects has been studied by two groups. Nakamura and co-workers (Nakamura *et al.*, 1978, 1980a) extended the perturbation scheme to the case of high temperatures, where the electron distribution is described by a classical Maxwell-Boltzmann distribution. They considered the seven subbands (E_0 to E_3 and $E_{0'}$ to $E_{2'}$) obtained by Stern in the Hartree approximation and tried to determine the self-energy shift to the subbands at $T=200$ and 300 K. It has been shown that the imaginary part of the self-energy is very large, even larger than subband energy separations. The real part seems to depend strongly on how the imaginary part is treated. Further, this short electron lifetime caused by electron-electron collisions makes the validity of the quasiparticle picture doubtful at high temperatures. However, there seem to be no observable phenomena in which the large imaginary part of the self-energy plays a vital role. Especially it should be noticed that it has no direct effect on the two-dimensional conductivity and the broadening of intersubband optical transitions. On the other hand, Kalia, Das Sarma, Nakayama, and Quinn (Kalia *et al.*, 1978, 1979; Das Sarma *et al.*, 1979) considered the three subbands (E_0, E_1, and $E_{0'}$) variationally in the Hartree approximation and calculated the real part of the self-energy obtained to the lowest order in the dynamically screened Coulomb interaction for $0<T<200$ K. Changes in the Hartree potential caused by exchange and correlation effects were completely neglected. The shift of the E_0 subband shows a monotonic decrease with temperature, whereas those of other subbands exhibit a complicated behavior depending on N_s and the separation between the different sets of valleys in the bulk, which can be controlled by stress. A general feature found by them is that the subband separation is rather insensitive to the temperature up to $T\sim200$ K, in contrast to the prediction in the Hartree approximation. In the Hartree approximation the occupation of higher subbands having larger spatial extent makes the density distribution wider. Consequently the effective potential becomes steeper, which increases the subband energy separations. These authors claimed that the imaginary part of the self-energy is not important, in contrast to the conclusion of Nakamura *et al.* (1978, 1980a). A more elaborate calculation was reported quite recently by Das Sarma and Vinter (1981), who showed that the subband energy separation increased with temperature.

C. Intersubband optical transitions

In addition to spectroscopic measurements of intersubband optical transitions, there is another way to get some information on the subband energy separations. Attempts have been made to measure the electron concentration at which a higher subband starts to be occupied by electrons (Tsui and Kaminsky, 1975b; Howard and Fang, 1976). In principle one can detect this threshold concentration by careful examination of the period of the Shubnikov–de Haas oscillation in magnetic fields perpendicular to the interface. Each period corresponds to the filling of one Landau level in the ground subband. When a higher subband starts to be populated, this period is expected to change. Such a period change has been observed experimentally, but results do not agree with each other. Howard and Fang (1976) obtained threshold concentrations for several samples with different $N_{\rm depl}$. They obtained, for example, $N_s\sim7.6\times10^{12}$ cm^{-2} for $N_{\rm depl}\sim3\times10^{11}$ cm^{-2}. The threshold N_s was found to decrease with decreasing $N_{\rm depl}$ consistent with the theoretical expectation. These concentrations are, however, substantially larger than the Hartree results but substantially smaller than the results obtained by including the exchange-correlation effect. On the other hand, Tsui and Kaminsky (1975b) measured the threshold to be 7.4×10^{12} cm^{-2} for $N_{\rm depl}\sim1\times10^{11}$ cm^{-2}. This result is closer to the theoretical results but disagrees with that of Howard and Fang, who estimated it to be 4.7×10^{12} cm^{-2} by interpolation for the same $N_{\rm depl}$. Tsui and Kaminsky (1975b) found also that the threshold is lowered when stress is applied, and suggested that $E_{0'}$ is lower than E_1 at the threshold concentration. Since $E_{0'}$ and E_1 are very close to each other, it is difficult to tell which is actually lower in energy from a purely theoretical point of view. As a matter of fact, both the Hartree and the density-functional calculation predict $E_{0'}>E_1$ near the threshold concentration, whereas Vinter's results show $E_{0'}<E_1$. Various mechanisms that could give values of $E_{0'0}\equiv E_{0'}-E_0$ different from the results calculated in the ideal model have been suggested. Stern (1977) considered effects of a thin transition layer at the interface and showed that $E_{0'0}$ could become smaller, as will be discussed in Sec. III.E. Sham and Nakayama (1978, 1979; see also Nakayama, 1980) suggested a possibility of different effective boundary positions for $E_{0'}$ and E_1 which can modify their relative energies. This will be discussed in Sec. VII.A. The possible presence of internal stresses of various origins also affects the relative

values of $E_{0'}$ and E_1. See Secs. IV.B.3 and VII.B.2 for more discussion of related problems. Some of the experiments on the stress effect suggest that $E_{0'0}$ can be different from the theoretical result, as will be discussed in Sec. VII.B. The relative position of $E_{0'}$ and E_1 also affects the behavior of the mobility limited by interface roughness, which will be discussed in Sec. IV.C.2. The situation is further complicated because local strain effects at the Si-SiO_2 interface are difficult to measure and control in real structures. More elaborate and systematic experimental investigations are needed in order to clarify these problems.

The best way to study the subband structure is to observe intersubband optical transitions. As a matter of fact, there has been considerable progress in our understanding through such spectroscopic measurements. However, various additional effects must be considered in optical transitions and these can shift the resonance energy from the corresponding subband separation. These additional effects are called the depolarization effect and its local field correction. In the early stages of spectroscopic study, the importance of these effects was not realized, and one assumed implicitly that resonance occurred when the energy of infrared light was equal to the subband separation.

To illustrate the depolarization effect let us consider a slab model introduced by Chen, Chen, and Burstein (1976). In this model we replace the inversion layer by an electron gas confined within a narrow slab of thickness $d_{\rm eff}$ and having a conductivity $\sigma_{zz}(\omega)$ in a unit area, given by

$$\sigma_{zz}(\omega)=\frac{N_s e^2 f_{10}}{m}\frac{-i\omega}{\omega_{10}^2-\omega^2-2i\omega/\tau}\ , \tag{3.51}$$

where $\hbar\omega_{10}=E_1-E_0$, f_{10} is the oscillator strength and τ is a phenomenological relaxation time. The intersubband transition is induced by an external field $E_{\rm ext}e^{-i\omega t}$ applied normal to the slab. The induced current in a unit area is written as

$$J_z=\sigma_{zz}(\omega)E\ , \tag{3.52}$$

where the electric field inside the slab E is related to $E_{\rm ext}$ through

$$E_{\rm ext}=\varepsilon_{zz}(\omega)E\ , \tag{3.53}$$

with

$$\varepsilon_{zz}(\omega)=1+\frac{4\pi i}{\kappa_{\rm sc}\omega}\frac{1}{d_{\rm eff}}\sigma_{zz}(\omega)\ . \tag{3.54}$$

Therefore, we have

$$J_z=\tilde{\sigma}_{zz}(\omega)E_{\rm ext}\ , \tag{3.55}$$

with

$$\tilde{\sigma}_{zz}(\omega)=\sigma_{zz}(\omega)\varepsilon_{zz}(\omega)^{-1}\ . \tag{3.56}$$

The absorption in a unit area is

$$\tfrac{1}{2}\,{\rm Re}J_z E^*=\tfrac{1}{2}\,{\rm Re}\tilde{\sigma}_{zz}(\omega)E_{\rm ext}^2\ . \tag{3.57}$$

The resonance occurs at a pole of $\tilde{\sigma}_{zz}(\omega)$ which describes the response of current to the external field. If we substitute Eq. (3.51) into (3.54) and (3.56), we have

$$\tilde{\sigma}_{zz}(\omega)=\frac{N_s e^2 f_{10}}{m}\frac{-i\omega}{\tilde{\omega}_{10}^2-\omega^2-2i\omega/\tau}\ , \tag{3.58}$$

with

$$\tilde{\omega}_{10}^2=\omega_{10}^2+\tilde{\omega}_p^2\ , \tag{3.59}$$

where

$$\tilde{\omega}_p^2=\frac{4\pi N_s e^2 f_{10}}{\kappa_{\rm sc} m d_{\rm eff}}\ . \tag{3.60}$$

The resonance energy is shifted from the subband energy separation by an amount related to the effective plasma frequency $\tilde{\omega}_p$. For $d_{\rm eff}\sim 50$ Å and $f_{10}\sim 0.5$ the plasma frequency is usually not small, and the depolarization effect is appreciable. In actual systems one can calculate $\tilde{\sigma}_{zz}(\omega)$ from the following two equations (Nakayama, 1977a, 1977b; Dahl and Sham, 1977):

$$j(z)=\int dz'\sigma_{zz}(z,z';\omega)E(z') \tag{3.61}$$

and

$$E_{\rm ext}=E(z)-\frac{4\pi i}{\kappa_{\rm sc}\omega}j(z)\ , \tag{3.62}$$

where $\sigma_{zz}(z,z';\omega)$ can be constructed from the known subband structure in the Hartree approximation. An alternative way will be discussed below.

Strictly speaking, one has to derive dispersion relations of waves propagating near the interface in various external configurations used experimentally. Chen, Chen, and Burstein (1976) have shown that poles of $\tilde{\sigma}_{zz}(\omega)$ can be observed in an attenuated total reflection experiment in which the Si is used as its own attenuated total reflection prism. Nakayama (1977a) has calculated the dispersion of a wave propagating along a strip transmission line used in absorption experiments and has shown that the change in the transmission is essentially given by ${\rm Re}\tilde{\sigma}_{zz}(\omega)$ under usual experimental conditions.

Physically the depolarization effect arises because each electron feels a field which is different from the external field by the mean Hartree field of other electrons polarized by the external field. As has frequently been mentioned, however, the Hartree approximation overestimates the Coulomb repulsive force of other electrons, and the exchange-correlation effect greatly reduces the effective repulsive potential. Therefore we expect that the exchange-correlation effect on the depolarization effect greatly reduces the shift of the resonance energy. Diagrams for $\tilde{\sigma}_{zz}(\omega)$ are shown in Fig. 26. In the random-phase approximation $\tilde{\sigma}_{zz}(\omega)$ is given by the sum of an infinite series of bubbles, each of which corresponds to $\sigma_{zz}(\omega)$ calculated in the Hartree approximation. When one inserts the dressed Green's functions in the bubbles one must take into account corresponding vertex corrections, as is also shown in Fig. 26. In this sense the local field correction to the depolarization effect is often called

the excitonlike effect or the final-state interaction.

The proper inclusion of the exchange-correlation effect on the optical transition is not a simple matter. Great care must be taken in going beyond the random-phase approximation (equivalent to the Hartree approximation) in including the self-energy and the vertex correction. Ando (1977a, 1977c) made a rather drastic assumption that the same exchange-correlation potential $v_{xc}(n(z);z)$ introduced in Sec. III.B can be used in the presence of a dynamical external field. This cannot be justified on a rigorous theoretical basis as in the case of a static field (Hohenberg and Kohn, 1964), but has been expected to give a reasonable magnitude for the local field effect. In terms of diagrams this approximation corresponds to using the same proper vertex part, denoted by γ in Fig. 26, for the dynamical response as that for the static response. The neglect of the frequency dependence is consistent with the small energy dependence of the exchange-correlation potential, as has been mentioned in Sec. III.B.

Let $\Delta n(z)e^{-i\omega t}$ be the change in the density distribution in the presence of an external electric field $E_{\rm ext}e^{-i\omega t}$. The effective perturbation becomes

$$\mathscr{H}'e^{-i\omega t}=[eE_{\rm ext}z+\Delta V_s(z)+\Delta V_{xc}(z)]e^{-i\omega t}\ , \quad (3.63)$$

where the change in the Hartree potential is

$$\Delta V_s(z)=-\frac{4\pi e^2}{\kappa_{\rm sc}}\int_0^z dz'\int_0^{z'} dz''\Delta n(z'')\ , \quad (3.64)$$

and the change in the exchange-correlation potential is

$$\Delta V_{xc}(z)=\frac{\partial v_{xc}(n(z);z)}{\partial n(z)}\Delta n(z)\ . \quad (3.65)$$

In Eq. (3.63), $\Delta V_s(z)$ describes the depolarization effect and $\Delta V_{xc}(z)$ its local field correction. By the use of perturbation theory one gets

$$\Delta n(z)=-2\sum_{n\neq 0}\zeta_n(z)\zeta_0(z)\times\frac{\hbar\omega_{n0}}{(\hbar\omega_{n0})^2-(\hbar\omega)^2}(n\mid\mathscr{H}'\mid 0)\ , \quad (3.66)$$

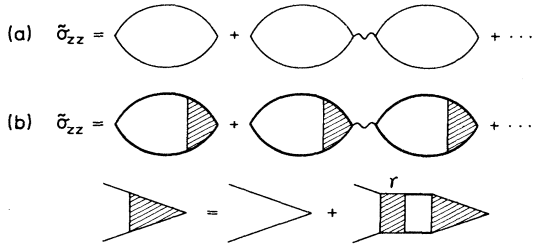

FIG. 26. Diagrammatic representation of the dynamical conductivity $\tilde{\sigma}_{zz}(\omega)$ which gives the intersubband optical absorption. (a) The Hartree approximation. (b) Exchange and correlation are included. The shaded part represents an appropriate vertex correction which should be consistent with an approximation for the dressed Green's function.

where $\zeta_n(z)$ is chosen to be real, $\hbar\omega_{n0}=E_{n0}=E_n-E_0$, and only the ground subband is assumed to be occupied by electrons initially. The induced current can be obtained from Eq. (3.66) by the equation of continuity as

$$j(z)=-\int_0^z dz'(-e)(-i\omega)\Delta n(z')\ , \quad (3.67)$$

and the desired conductivity becomes

$$\tilde{\sigma}_{zz}(\omega)=E_{\rm ext}^{-1}\int_0^\infty dz\, j(z)\ . \quad (3.68)$$

From Eqs. (3.63) and (3.66) one gets the self-consistency equation,

$$\sum_m[A_{nm}-(\hbar\omega)^2\delta_{nm}]u_m=\left[\frac{2m_l}{\hbar^2}\hbar\omega_{n0}\right]^{1/2}z_{n0}\ , \quad (3.69)$$

with

$$z_{nm}=\int_0^\infty dz\,\zeta_n(z)z\zeta_m(z)\ , \quad (3.70)$$

$$A_{nm}=(\hbar\omega_{n0})^2\delta_{nm}-\hbar\omega_{n0}(\alpha_{nm}-\beta_{nm})\hbar\omega_{m0}\ , \quad (3.71)$$

and

$$u_n=(eE_{\rm ext})^{-1}\left[\frac{2m_l}{\hbar^2}\hbar\omega_{n0}\right]^{1/2}\times\frac{1}{(\hbar\omega_{n0})^2-(\hbar\omega)^2}(n\mid\mathscr{H}'\mid 0)\ . \quad (3.72)$$

We have defined

$$\alpha_{nm}=2\frac{4\pi e^2}{\kappa_{\rm sc}}N_sS_{nm}\left[\frac{1}{\hbar\omega_{n0}}\frac{1}{\hbar\omega_{m0}}\right]^{1/2}\ , \quad (3.73)$$

and

$$\beta_{nm}=-2N_s\left[\frac{1}{\hbar\omega_{n0}}\frac{1}{\hbar\omega_{m0}}\right]^{1/2}\times\int_0^\infty dz\,\zeta_n(z)\zeta_m(z)\zeta_0(z)^2\frac{\partial v_{xc}(n(z);z)}{\partial n(z)}\ , \quad (3.74)$$

where the length tensor S_{nm} introduced by Allen, Tsui, and Vinter (1976) is defined by

$$S_{nm}=\int_0^\infty dz\,\zeta_n(z)\zeta_0(z)\int_0^z dz'\int_0^{z'} dz''\zeta_m(z'')\zeta_0(z'')$$
$$=\frac{1}{\hbar\omega_{n0}}\frac{1}{\hbar\omega_{m0}}\left[\frac{\hbar^2}{2m_l}\right]^2\times\int_0^\infty dz[\zeta_n'(z)\zeta_0(z)-\zeta_n(z)\zeta_0'(z)]\times[\zeta_m'(z)\zeta_0(z)-\zeta_m(z)\zeta_0'(z)]\ . \quad (3.75)$$

When we introduce a matrix U in such a way that $\tilde{A}=U^{-1}AU$ is diagonal, we get

$$\tilde{\sigma}_{zz}(\omega)=\frac{N_se^2(-i\omega)}{m_l}\sum_{n\neq 0}\frac{\tilde{f}_{n0}}{\tilde{\omega}_{n0}^2-\omega^2-2i\omega/\tau}\ , \quad (3.76)$$

with $\hbar\tilde{\omega}_{n0}=(\tilde{A}_{nn})^{1/2}$ and

$$\tilde{f}_{n0}=\left[\sum_m\left[\frac{2m_l}{\hbar^2}\hbar\omega_{m0}\right]^{1/2}z_{m0}U_{mn}\right]^2 . \tag{3.77}$$

A phenomenological relaxation time τ has been introduced in Eq. (3.76). The resonance occurs at $\omega=\tilde{\omega}_{n0}$ with its strength $\tilde{f}_{n0}$.

If ω is close to ω_{n0} and contributions of other subbands can be neglected one gets

$$\tilde{\sigma}_{zz}(\omega)=\frac{N_s e^2 f_{n0}}{m_l}\frac{-i\omega}{\tilde{\omega}_{n0}^2-\omega^2-2i\omega/\tau} , \tag{3.78}$$

where

$$\tilde{\omega}_{n0}^2=\omega_{n0}^2(1+\alpha_{nn}-\beta_{nn}) , \tag{3.79}$$

and

$$f_{n0}=\frac{2m_l}{\hbar^2}\hbar\omega_{n0}z_{n0}^2 . \tag{3.80}$$

In the Hartree approximation ($\beta_{nn}=0$) the depolarization effect raises the resonance energy by an amount α_{nn}. Comparison with Eq. (3.60) gives

$$d_{\text{eff}}=f_{10}\frac{\hbar^2}{2m_l S_{11}}\frac{1}{\hbar\omega_{10}} . \tag{3.81}$$

When the exchange-correlation effect is included ($\beta_{nn}>0$), the local field correction tends to decrease the resonance energy, as expected.

Figure 27 shows an example of calculated resonance energies in an n-channel inversion layer on the Si(100) surface with $N_{\text{depl}}=1\times10^{11}$ cm^{-2}. The resonance energies obtained by including the depolarization effect alone, the excitonlike effect alone, and both effects combined are compared with the subband energy for the 0→1 transition. At low electron concentrations the excitonlike effect is more important than the depolarization effect, and the resonance energy becomes slightly smaller than the subband separation. With increasing electron concentration the depolarization effect becomes stronger and the resonance energy becomes larger than the subband separation. Figure 28 compares the resonance lineshapes calculated in the Hartree and density-functional approximations for an inversion layer ($N_s=1\times10^{12}$ cm^{-2}, $N_{\text{depl}}=1\times10^{11}$ cm^{-2}, and $\hbar/\tau=1$ meV). In the Hartree approximation couplings between different subbands are important. They modify the intensity of transitions in such a way that transitions with higher energies tend to have large oscillator strengths. This is analogous to the behavior in the usual uniform electron gas in which the plasma oscillation has larger intensity than single-particle excitations in the dynamical structure factor for large wavelengths. Allen, Tsui, and Vinter (1976) calculated the lineshape including only the three lowest subbands, E_0, E_1, and E_2, and showed that the transition 0→2 has much higher intensity than 0→1. When the exchange-correlation effect is included, couplings become weak. A corresponding lineshape for extremely small N_{depl} (corresponding to the accumulation layer) is given in Fig. 29 for $N_s=1\times10^{12}$ cm^{-2}. As has been discussed in Sec. III.B, only the ground subband is closely localized near the interface, and all the excited subbands are nearly continuum states in the Hartree approximation. Consequently the lineshape is so broad that one can hardly identify its peaks. The sharp peak in Fig. 29 corresponds to the transition between the ground and the first

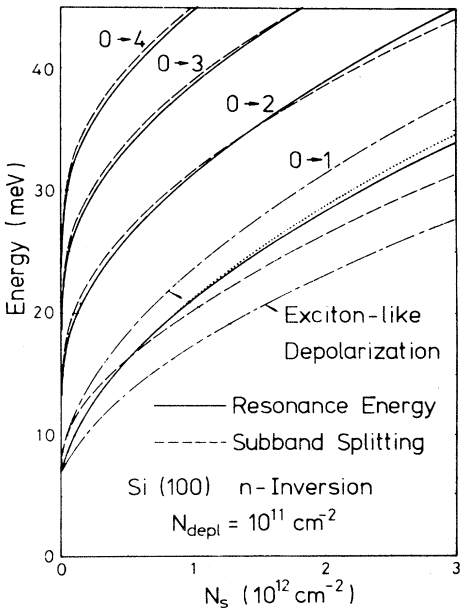

FIG. 27. Calculated resonance energies (solid lines) as a function of the electron concentration N_s in an n-channel inversion layer on a Si(100) surface. $N_{\text{depl}}=1\times10^{11}$ cm^{-2}. The broken lines represent corresponding subband energy separations. The resonance energies calculated by including only the depolarization effect or the excitonlike effect are also shown for the transition 0→1. The dotted curve represents the resonance energy for 0→1 obtained by neglecting mixing effects of different subbands. After Ando (1977c).

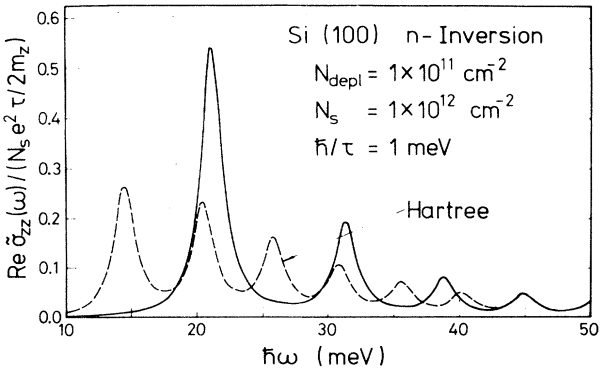

FIG. 28. Calculated real part of the dynamical conductivity $\tilde{\sigma}_{zz}(\omega)$ in an n-channel inversion layer on a Si(100) surface. $N_s=1\times10^{12}$ cm^{-2}, $N_{\text{depl}}=1\times10^{11}$ cm^{-2}, $\hbar/\tau=1$ meV. The solid line represents the result calculated in the density-functional formulation and the broken line the result in the Hartree approximation. After Ando (1977c).

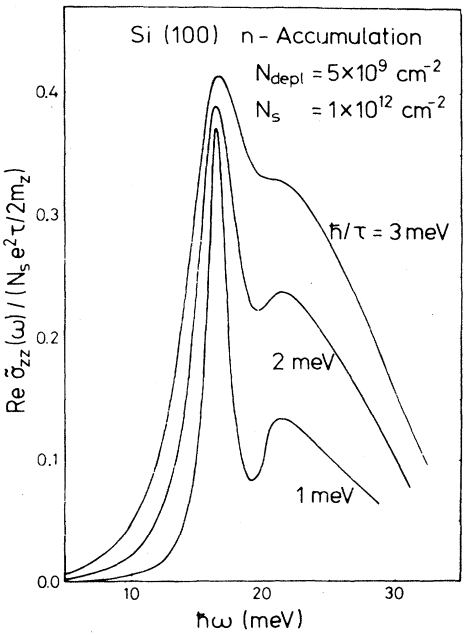

FIG. 29. Calculated real part of the dynamical conductivity $\tilde{\sigma}_{zz}(\omega)$ in an n-channel accumulation layer on a Si(100) surface for $\hbar/\tau=1$, 2, and 3 meV. $N_s=1\times10^{12}$ cm^{-2}. After Ando (1977c).

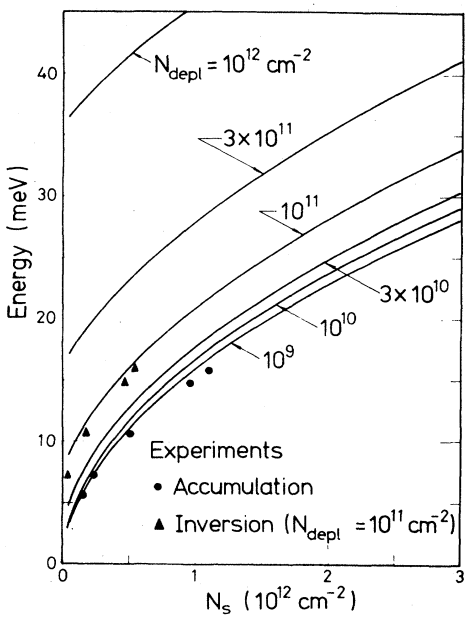

FIG. 30. Calculated resonance energy for the transition 0→1 as a function of the electron concentration N_s in n-channel layers on a Si(100) surface. The curve for the smallest N_{depl} corresponds to the accumulation case. Experimental results (Kamgar *et al.*, 1974a, 1974b; Kneschaurek *et al.*, 1976) are also shown. After Ando (1977c).

excited subband which becomes a "bound state" due to the exchange-correlation effect. The broad absorption at the higher energy side corresponds to transitions to higher quasicontinuum states. Figure 30 shows the resonance energy for the 0→1 transition for different values of N_{depl}. The curve for the smallest N_{depl} actually corresponds to the accumulation layer. Results of infrared absorption measurements (Kamgar *et al.*, 1974a, 1974b; Kneschaurek *et al.*, 1976) are also shown. The agreement between theory and experiment is excellent. The experimental results and also the theoretical results show that the effect of N_{depl} is relatively small at low concentrations and becomes more important with increasing concentration. This is one of the direct manifestations of the importance of the additional corrections in optical transitions. The effect of N_{depl} on the subband energy separation is more important at low electron concentrations and becomes less important at high concentrations where the self-consistent potential is mainly determined by the potential of electrons themselves.

Vinter (1977; see also Vinter and Stern, 1976) calculated the resonance energy for the transition 0→1 neglecting the vertex correction. His result is essentially given by Eq. (3.59), with $\hbar\omega_{10}$ being the energy separation calculated by including the exchange-correlation effect in his approximation as discussed in Sec. III.B. This approximation is, however, inconsistent with the importance of the exchange-correlation effect in the subband structure. He then tried to calculate the excitonlike effect to the lowest order in the statically screened Coulomb interaction. The binding energy is found to vary from 0.9 to 1.8 meV for the electron concentration between 10^{12} and 3×10^{12} cm^{-2}. Without calculating the intensity of the transitions, he speculated that the transitions to both the "bound exciton" state and the free state were allowed and gave rise to the two-peak structure observed by the early photoconductivity experiments of Wheeler and Goldberg (1975). However, the above discussion shows that the transition to the exciton "bound state" is allowed and others are essentially forbidden (see also Ando, 1977c; Bloss and Sham, 1979). As will be discussed below, the two-peak structure has turned out to result from completely different origins.

Broadening of intersubband optical transitions caused by elastic scatterers has been studied theoretically (Ando, 1976c, 1978c). The dynamical conductivity for $\omega\sim\omega_{10}$ is written as

$$\mathrm{Re}\sigma_{zz}(\omega)=\frac{e^2 f_{10}}{2m_l}\int\frac{m_t}{2\pi\hbar^2}f(E)dE\frac{\hbar\Gamma_{\mathrm{op}}(E)}{(\hbar\omega-\hbar\omega_{10})^2+\Gamma_{\mathrm{op}}(E)^2}\,, \tag{3.82}$$

with

$$\Gamma_{\rm op}(E)=\frac{1}{2}\left[\frac{\hbar}{\tau_0(E)}+\frac{\hbar}{\tau_1(E)}\right]-\frac{\hbar}{\tau_{10}(E)} \tag{3.83}$$

$$=\pi\sum_{\mathbf{k}'}\langle\,|(0\mathbf{k}'\,|\,\mathscr{H}_1\,|\,0\mathbf{k})-(1\mathbf{k}'\,|\,\mathscr{H}_1\,|\,1\mathbf{k})\,|^2\rangle\delta(\varepsilon(k)-\varepsilon(k'))\,|_{E=\varepsilon(k)+E_0}$$

$$+\pi\sum_{\mathbf{k}'}\langle\,|(0\mathbf{k}'\,|\,\mathscr{H}_1\,|\,1\mathbf{k})\,|^2\rangle\delta(\varepsilon(k)-\varepsilon(k')+E_{10})\,|_{E=\varepsilon(k)+E_0}\,, \tag{3.84}$$

where $\mathscr{H}_1$ represents potentials of scatterers and $\langle\cdots\rangle$ means an average over all configurations of scatterers. The broadening is not determined by the simple arithmetic average of the broadenings $\hbar/\tau_0$ and $\hbar/\tau_1$ of the two subbands, but contains a correction term $-\hbar/\tau_{10}$. The broadening vanishes when the effective potentials of the scatterers are the same for both subbands and there is no intersubband mixing. In the case of a model with short-range surface roughness scattering (see Sec. IV.C), for example, Ando (1976c) obtained

$$\frac{3}{8}\frac{\hbar}{\tau_0}\le\Gamma_{\rm op}\le\frac{1}{2}\frac{\hbar}{\tau_0}\,, \tag{3.85}$$

which shows that the broadening is less than that determined by the mobility. However, Eq. (3.84) shows that the relation between the mobility and the broadening of the intersubband transitions is not simple for realistic scatterers. Effects of Na^+ ions near the interface on the broadening have been studied experimentally. McCombe and Cole (1980) have demonstrated clearly that broadening increases with increasing Na^+ ion concentration but is less than the width estimated from the corresponding effective electron mobility. This is in qualitative agreement with the theoretical prediction of the simple model discussed above. On the other hand, Chang *et al.* (1980) obtained a peculiar result for low concentrations of Na^+ ions: The subband linewidth was independent of the ion concentration, while the mobility changed substantially.

Effects of electron-electron collisions on the broadening of optical transitions have been investigated by Ting and Ganguly (1979). They included the imaginary part of the self-energy of the first excited subband in addition to the real part, and calculated the resonance lineshape. The imaginary part was shown to have little effect on the position of the resonance except at low electron concentrations, but to contribute to broadening. Broadening of intersubband transitions caused by electron-electron interactions seems to be a difficult problem, however. If one employs the same approximation as for the calculation of the cyclotron resonance lineshape one gets the wrong result that electron-electron interactions cause broadening, contrary to Kohn's theorem that they do not affect the cyclotron resonance lineshape in translationally invariant systems (Kohn, 1961). Further, if a similar approximation is applied to subband transitions in an electron system outside of liquid He, one has an extremely large broadening of the resonance which has never been observed (Ando, unpublished). Experimental results in the inversion layer seem to show that the broadening comes from the same mechanisms as those limiting the usual mobility (Neppl *et al.*, 1977; McCombe and Cole, 1980), and electron-electron collisions seem to have little influence.

Three different methods have been employed to observe intersubband optical transitions: infrared absorption, emission, and photoconductivity. Figure 31 gives a schematic drawing of the experimental arrangement used in absorption experiments (Kamgar *et al.*, 1974a, 1974b; Kamgar and Kneschaurek, 1976; Kneschaurek *et al.*, 1976; Koch, 1975, 1976a, 1976b). A molecular gas laser is used as the source of far-infrared radiation. The separation of the transmission-line plates is the sample thickness, which ranges between 0.2 and 0.35 mm. Since the effective spacing is of the order of 10 wavelengths, many modes propagate in the sample instead of a pure TEM mode. However, the presence of the thick conducting plate close to the space-charge layer causes the rf electric field to be predominantly perpendicular to the Si-SiO_2 interface. The samples lack the source-drain contacts of a regular MOSFET, and visible radiation from a light-emitting diode is used to generate electrons near the interface. In the course of such experiments it has been found that at low temperatures the inversion layer and the bulk behave as two nearly isolated electrical systems because of the thick depletion layer, and their quasi-Fermi levels are not necessarily the same. Consequently the thickness of the depletion layer and the value of $N_{\rm depl}$ can be smaller than the equilibrium values. These values have been determined from observed capacitance versus gate voltage curves. The absorption of the laser radiation at fixed energy $\hbar\omega$ is measured as a function of the gate voltage V_G. An example is shown in Fig. 32. Positive and negative gate voltages correspond to electron inversion and hole accumulation, respectively.

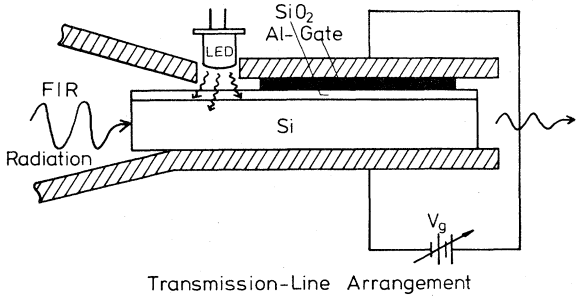

FIG. 31. Sample and transmission-line assembly used for absorption experiments. After Kneschaurek *et al.* (1976).

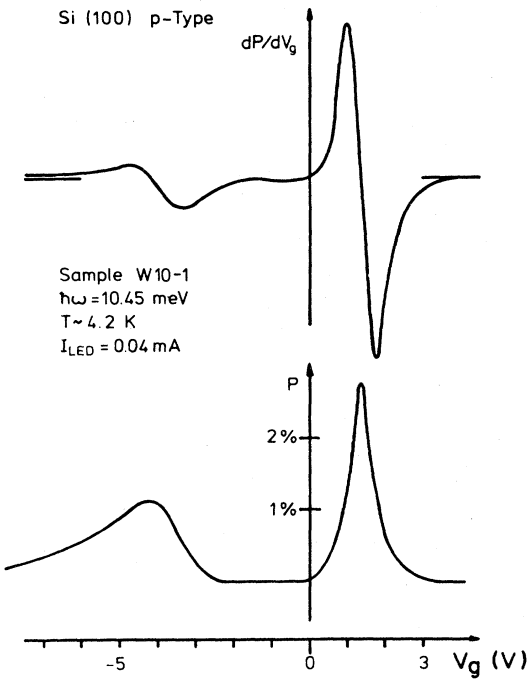

FIG. 32. Intersubband resonance signals observed as a power absorption derivative dP/dV_G and in differential absorption with on-off modulation of V_G. P is given in terms of percent of transmitted power at $N_s=0$ and for dimensions of the sample and transmission line as shown in Fig. 31. Positive and negative gate voltages correspond to electron inversion and hole accumulation, respectively. After Kneschaurek *et al.* (1976).

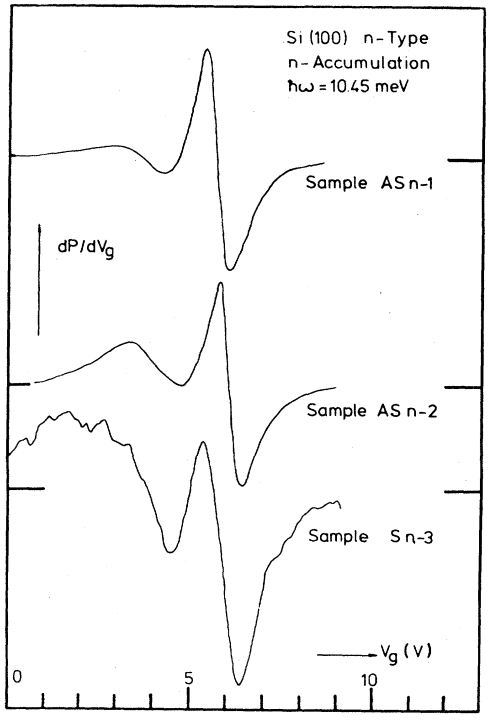

FIG. 33. Electron accumulation signals observed in samples from different batches. After Kneschaurek *et al.* (1976).

A sharp single resonance is observed for the inversion layer. Figure 33 gives examples for the accumulation layer. The sharp peak at higher gate voltages is the transition $0\rightarrow 1$, and a weak and broad absorption at lower gate voltages is considered to be due to transitions to higher excited subbands which are extremely close to each other in energy. The observed resonance energies for the $0\rightarrow 1$ transition are summarized in Fig. 30. Effects of negative substrate bias, i.e., the depletion field proportional to N_{depl}, have also been studied. Kneschaurek, Kamgar, and Koch (1976) find a linear dependence of the resonance energy on N_{depl} for N_s values between 4.6×10^{11} and 6×10^{11} cm^{-2}.

Resonant photoconductivity has also been used to observe intersubband transitions (Wheeler and Ralston, 1971; Wheeler and Goldberg, 1975). Wheeler and Goldberg (1975) observed negative photoconductivities in the presence of far-infrared laser radiation. An example of an observed change in the conductivity is given in Fig. 34. Both the sharp peak and the broad structure at lower gate voltage move to higher N_s with increase of the laser energy and are identified as intersubband optical transitions. However, the resonance energies obtained are in disagreement with those of the absorption experiments discussed above. The electron densities N_s at which the resonances occur are about 30% higher than the corresponding N_s values of Kneschaurek, Kamgar, and Koch (1976), although the depletion charge N_{depl}, if estimated from the doping of the samples, is almost the same. The position of the sharp peak is rather close to that of the absorption in the accumulation layer. Furthermore, the photoconductive effect exhibits a completely different lineshape. On the other hand, Gornik and Tsui (1976) detected hot-electron-induced infrared emission caused by intersubband transitions. They populated the excited subbands by heating up the electron distribution with an electric field along the surface. The energy separations obtained were in agreement with the photoconductivity data of Wheeler and Goldberg (1975) and in disagreement with the absorption results. The three ex-

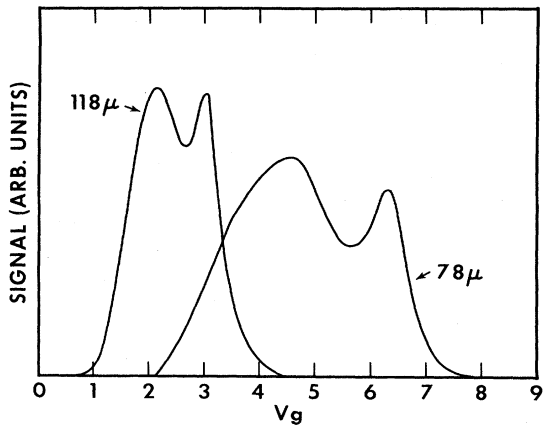

FIG. 34. Photo-induced response as a function of the gate voltage V_G for the two wavelengths 118 μm ($\hbar\omega=10.45$ meV) and 78 μm (15.81 meV). After Wheeler and Goldberg (1975).

periments were performed on different types of samples fabricated in different laboratories. The discrepancy was at first believed to arise from real effects such as inhomogeneity of the doping or the structure of the Si-SiO_2 transition layer. However, more recent observation of absorption and photoconductivity on the same samples has revealed that both experiments give identical resonance positions and similar lineshape (Neppl *et al.*, 1977; Kamgar *et al.*, 1977, 1978; Hu *et al.*, 1978). Kamgar, Tsui, and Sturge (1977; see also Kamgar *et al.*, 1978) performed time-resolved experiments and demonstrated that the resonance position depends on the degree to which electrostatic equilibrium is established in the Si substrate. Actually, difficulties in achieving real electrostatic equilibrium had long been anticipated (see, for example, Fowler, 1975 and references therein). The absence of a depletion layer in the experiments of Wheeler and Goldberg (1975) and of Gornik and Tsui (1976) was found to be the main cause of the discrepancy, and all the later experiments have confirmed the results of the absorption experiments.

The mechanism of the intersubband resonant photoresponse is not yet understood. Wheeler and Goldberg (1975) and Hu, Pearse, Cham, and Wheeler (1978) reported that the response time of the photoconductivity is very long (of the order of 10^{-3} s) and that the signal amplitude is almost independent of temperature between 4.2 and 1.6 K. Neppl, Kotthaus, Koch, and Shiraki (1977), on the other hand, observed a strong temperature dependence. As the mechanism of the negative photoresponse, Wheeler and Goldberg (1975) proposed that electrons photoexcited to an upper level have lower mobilities, which cause the decrease in surface conductivity. This is the same as the model suggested earlier by Katayama, Kotera, and Komatsubara (1970, 1971) for explaining a negative photoconductivity observed on InSb surfaces. Döhler (1976a, 1976b) suggested a model in which the existence of the $E_{0'}$ subband plays an important role. Electrons excited into E_1 are scattered into $E_{0'}$ by intervalley impurity scattering and stay there for a while. Although this model seems to explain the long response time, it cannot explain a strong temperature dependence. Existence of a long-lived surface trap level has also been proposed. Neppl, Kotthaus, and Koch (1979) proposed that the increase of electron temperature relative to lattice temperature caused by absorption is the main origin of the photoresponse. They could not substantiate the long response time observed previously, and showed that the response time is shorter than 10^{-5} s. By applying a magnetic field perpendicular to the surface they convincingly demonstrated that the photoresponse and $\partial\sigma/\partial T$ depend in the same way on magnetic field. However, they have shown also that the heating mechanism cannot explain all the different experimental results observed in different kinds of samples.

Kneschaurek and Koch (1977) studied the temperature dependence of intersubband optical transitions between 4.2 and 130 K. An example of the observed lineshapes is given in Fig. 35. With rising temperature, the lines originating from the E_0 subband shift and diminish in amplitude, as is shown in the inset of the figure. At the same time a small extra peak appears at a low electron concentration and grows in amplitude. The new peak is considered to represent transitions from the thermally occupied lowest subband level of the fourfold-degenerate valleys with light mass normal to the surface. The resonance position seems to be consistent with $E_{1'}-E_{0'}$ estimated theoretically. One has to assume, however, a value of $E_{0'}-E_0$, which is much smaller than the theoretical prediction, to explain the observed temperature dependence of the relative amplitudes of the absorptions. This problem will be discussed also in Sec. VII.B in connection with stress effects. Temperature dependence was also studied on the (111) and (110) surfaces of Si (Kamgar, 1979). The width of the resonance line at high temperatures presents a problem. The experiments show that the increase in width is not appreciable, while the mobility decreases and the broadening of the cylotron resonance increases considerably with rising temperature (see Secs. IV.C and VI.B). Therefore, the experiments

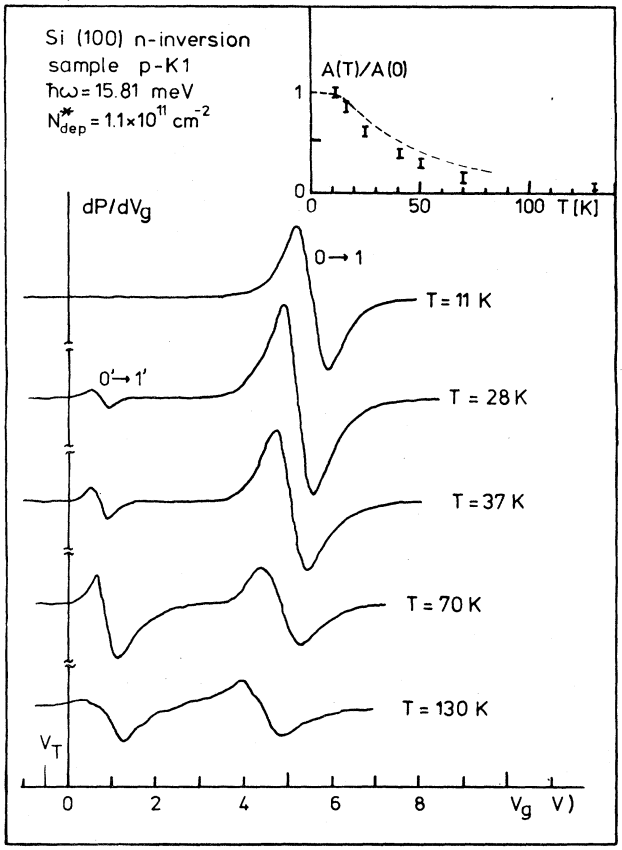

FIG. 35. Intersubband resonance at different temperatures for $\hbar\omega = 15.81$ meV. The inset shows the variation of the resonance amplitude for the $0\rightarrow 1$ transition with temperature. Along with the decay of the $0\rightarrow 1$ amplitude a new resonance associated with the thermally populated 0′ level is observed. After Kneschaurek and Koch (1977).

show, somewhat surprisingly, that neither phonon scattering nor electron collisions are effective in determining the broadening of intersubband optical transitions. Quite recently experiments were extended even to room temperature (Schäffler and Koch, 1981; Chang *et al.*, 1980). The resonance energy was found to increase considerably, rather in agreement with a prediction given in the Hartree approximation discussed in Sec. III.A.

All the experiments mentioned above have been carried out at discrete frequencies while sweeping the gate voltage to tune the subband transitions into coincidence. This approach possesses some inherent disadvantages. Since N_s and the self-consistent potential both change during the gate voltage sweep, it is difficult to determine the lineshape and the relative intensities of the various transitions. Only in the last few years has Fourier transform spectroscopy been applied to this system (McCombe and Schafer, 1979; McCombe *et al.*, 1979; McCombe and Cole, 1980). McCombe, Holm, and Schafer (1979) showed that the observed relative intensities of $0\rightarrow1$, $0\rightarrow2$, and $0\rightarrow3$ transitions cannot be explained by the Hartree result and are fully consistent with the result of the density-functional calculation. As has been discussed above, the Hartree calculation predicts a large depolarization effect, which drastically modifies the relative strengths of resonance intensities in such a way that transitions to higher excited subbands have larger intensities. On the other hand, the reduction of the depolarization effect due to exchange and correlation makes the $0\rightarrow1$ transition the strongest, in agreement with the experiments. McCombe, and co-workers have carried out quite extensive and detailed subband spectroscopy and have shown that there is excellent agreement with calculations over a much wider range of $N_{\rm depl}$ and frequency than is shown in Fig. 30. The study has been extended to (110) and (111) surfaces (McCombe and Cole, 1980; Cole and McCombe, 1980), where intersubband spectroscopy can provide information on valley degeneracy and on the nature of the ground state. This will be discussed in Sec. VII.B. Effects of Na^+ ions near the interface have also been studied using this technique, as has already been mentioned above. They have also observed transitions associated with bound states of Na^+ ions. This was already mentioned in Sec. II.E and will be more fully discussed in Sec. V.C.

Different methods have been employed to observe intersubband transitions in space-charge layers on semiconductors other than Si. A simple transmission configuration in which light is incident normal to the surface can excite subband transitions in narrow-gap semiconductors because of the nonparabolic dispersion of the bulk band structure (see Sec. VIII.B). Resonant light scattering can also be used in III-V semiconductors. For example, quite recent observations of spin-flip and non-spin-flip excitations in GaAs-AlGaAs heterostructures have determined the subband energy separation and corresponding resonance energy independently, as will be discussed briefly in Sec. VIII.D.

D. Subbands and optical transitions in magnetic fields

Additional details of the subband structure and of the depolarization effect and its local field correction appearing in optical transitions can be obtained by studying effects of magnetic fields. When a magnetic field is applied in the y direction parallel to the surface, electrons moving in the positive and negative x directions are affected by different Lorentz forces and the subband structure is modified. Usually in the inversion layer the radius of the cyclotron motion (typically, 81 Å in 100 kOe) is much larger than the thickness of the inversion layer, and the magnetic field is treated as a small perturbation. When the magnetic field is tilted, the perpendicular component of the field quantizes the electron motion parallel to the surface into discrete Landau levels. Although a parallel magnetic field usually has little effect on two-dimensional properties, it can strongly affect the spectrum of intersubband optical transitions.

Let us assume that a magnetic field $(0,H_y,H_z)$ is applied along the yz plane in the n-channel inversion layer on the Si(001) surface. In the Hartree approximation the subband dispersion is determined by the Hamiltonian

$$\mathscr{H}=\frac{1}{2m_t}\left[p_x+\frac{e}{c}H_y z\right]^2+\frac{1}{2m_t}\left[p_y+\frac{e}{c}H_z x\right]^2+\frac{1}{2m_l}p_z^2+V(z)\ , \quad (3.86)$$

where we have chosen the gauge $\mathbf{A}=(H_y z,H_z x,0)$. To lowest order in H_y one immediately gets an effective Hamiltonian for the electron motion parallel to the surface in the nth subband (Stern and Howard, 1967),

$$\mathscr{H}_n=\frac{1}{2m_t}\left[p_x+\frac{e}{c}H_y z_{nn}\right]^2+\frac{1}{2m_t}\left[p_y+\frac{e}{c}H_z x\right]^2+E_n+\frac{\hbar^2}{2m_t l_y^4}[(z^2)_{nn}-(z_{nn})^2]\ , \quad (3.87)$$

where $l_y^2=c\hbar/eH_y$. The last term of Eq. (3.87) represents a diamagnetic energy shift. This shift was first observed by a tunneling experiment in an accumulation layer on InAs by Tsui (1971a). In the case of a purely parallel magnetic field ($H_z=0$) the dispersion is given by a parabola with its minimum position shifted by $-z_{nn}/l_y^2$ in the k_x direction. In the case of nonzero H_z, Eq. (3.87) gives the Landau level,

$$E_{nN}=\hbar\omega_c(N+\tfrac{1}{2})+\frac{\hbar^2}{2m_t l_y^4}[(z^2)_{nn}-(z_{nn})^2]+E_n\ , \quad (3.88)$$

with $\omega_c=eH_z/m_t c$ which is determined by the perpendicular component. The corresponding wave function is given by

$$\psi_{nNX}(\mathbf{r},z)=\frac{1}{\sqrt{L}}\exp\left[-\frac{iXy}{l_z^2}-i\frac{z_{nn}(x-X)}{l_y^2}\right]\times\chi_N(x-X)\zeta_n(z)\ , \quad (3.89)$$

where $l_z^2=c\hbar/eH_z$ and $\chi_N(x)$ is the usual Landau-level wave function. The factor $\exp[-iz_{nn}(x-X)/l_y^2]$ arises because of the shift of the center of cyclotron motion in **k** space.

The above results are valid to first order in H_y. To second order in H_y one should add to Eq. (3.87) a term given by (Stern, 1968)

$$\frac{p_x^2}{m_t}\frac{\hbar^2}{m_t l_y^4}\sum_{m\neq n}\frac{|z_{mn}|^2}{E_n-E_m}\,. \tag{3.90}$$

This term gives rise to an increase of the effective mass in the x direction for the ground subband:

$$\frac{m_t}{m_x(H_y)}=1-\frac{2\hbar^2}{m_t l_y^4}\sum_{m\neq 0}\frac{|z_{m0}|^2}{E_m-E_0}\,. \tag{3.91}$$

This amounts to an increase of only a few percent in the effective mass for $N_s=1\times10^{12}$ cm^{-2} and $N_{\rm depl}=1\times10^{11}$ cm^{-2} in $H_y=100$ kOe. One sees, therefore, that the lowest-order expressions (3.88) and (3.89) are usually valid except in extremely strong magnetic fields. The fact that the Landau level structure is determined only by the perpendicular component has been utilized experimentally for many purposes. Uemura and Matsumoto (1971; see also Uemura, 1974b) discussed the effect of H_y using a variational wave function of the form given by Eq. (3.25). They ascribed an anomalous magnetoresistance observed by Tansal, Fowler, and Cotellessa (1969) to the effect of deformed wave functions in a parallel magnetic field. See Sec. IV.B for a more detailed discussion of the experiments. Such a perturbation treatment is not valid for higher subbands, especially in case of accumulation layers, since the spread of the wave functions can be comparable to or larger than the radius of the cyclotron motion. A self-consistent calculation has been performed in the Hartree approximation in strong parallel magnetic fields (Ando, 1975b). The ground subband was shown still to be described by the lowest-order perturbation, but excited subbands become magnetic surface states perturbed by a weak surface potential, since they are quite extended and nearly continuum states in the absence of H_y. The corresponding calculation, including exchange and correlation effects, has also been made in a density-functional formulation (Ando, 1978a, 1978b). An example of the results is given in Fig. 36. The subband structure becomes a mixture of the electric subband and the magnetic surface states.

Since the optical transition occurs vertically (**k** conservation), the relative shift in **k** space of the energy minima and the diamagnetic energy shift cause broadening and shifting of intersubband absorption spectra in a parallel magnetic field. In the simplest case, where one can neglect couplings between different subbands and where the magnetic field is sufficiently weak, one has

$$\tilde{\sigma}_{zz}(\omega)=\frac{N_s e^2 f_{n0}}{m_l}\frac{-i\omega}{\omega_{n0}^2}L_n(\omega)[1+\gamma_{nn}L_n(\omega)]^{-1}\,, \tag{3.92}$$

where γ_{nn} $(=\alpha_{nn}-\beta_{nn})$ represents the strength of the depolarization effects and its local field correction, $\hbar\omega_{n0}=E_n-E_0$, and

$$L_n(\omega)=\frac{g_v g_s}{N_s}\frac{1}{L^2}\sum_{\text{occupied }\mathbf{k}}\frac{\omega_{n0}^2}{\omega_{n0}(k_x)^2-\omega^2}\,, \tag{3.93}$$

with $\hbar\omega_{n0}(k_x)=E_n(\mathbf{k})-E_0(\mathbf{k})$. In the case of $\gamma_{nn}=0$, this gives a semielliptic spectrum around $\hbar\omega_{n0}(k_x=-z_{00}/l_y^2)$ with the width $\hbar^2k_F(z_{nn}-z_{00})m_t l_y^2$ proportional to H_y. It should be noted that the resonance peak is not given by $\hbar\omega_{n0}(k_x=-z_{00}/l_y^2)\times(1+\gamma_{nn})^{1/2}$ in the presence of the depolarization effect, but its shift is enhanced because of the deformed lineshape (Ando, 1977b). The broadening and the shifts of the resonance have been observed experimentally (Kamgar *et al.*, 1974a; Beinvogl *et al.*, 1976). An example of the experimental results for the accumulation layer on the Si(100) surface is plotted in Fig. 37. The signal shifts to lower and lower gate voltages and the linewidth shows an increase with increasing magnetic field. The shift of the resonance peak is found to be larger for high electron concentrations. This fact is a direct consequence of the depolarization effect, and cannot be explained by the diamagnetic shifts alone. If we neglect the depolarization effect, the effect of the magnetic field should be smaller with increasing electron concentration because the electrons become more closely bound near the surface. Actually, however, both the depolarization effect and the deformation of the lineshape become stronger with N_s and consequently the shift of the peak increases with N_s. Experiments have been extended to the inversion layer (Beinvogl *et al.*, 1976), but

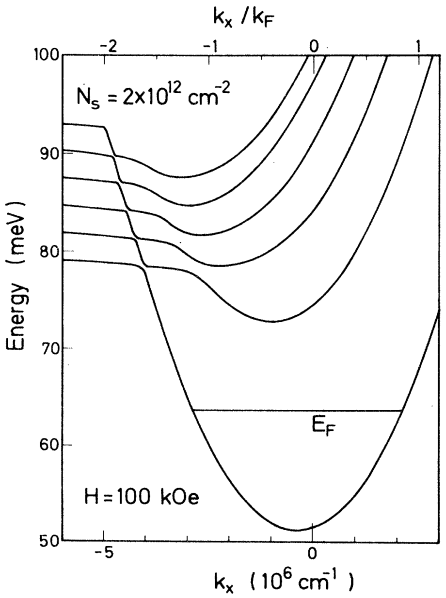

FIG. 36. An example of the calculated subband dispersion relation E vs k_x in an n-channel accumulation layer on a Si(100) surface in a magnetic field applied parallel to the surface (the y direction). $N_s=2\times10^{12}$ cm^{-2}. $H=100$ kOe. After Ando (1978b).

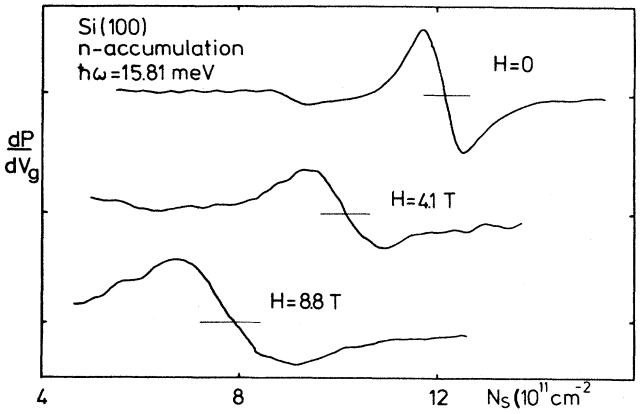

FIG. 37. Influence of a parallel magnetic field on the position and line shape of the intersubband resonance in the accumulation layer. After Beinvogl *et al.* (1976).

the magnetic field effect has turned out to be very small. Figure 38 gives examples of absorption spectra for the accumulation case calculated in a density-functional formulation (Ando, 1978b) and shows the broadening and shifting of the spectra. The overall asymmetry of the lineshape is consistent with the experimental results. Beinvogl *et al.* (1976) obtained the peak shift of $\Delta E \sim 2.8$ meV near $N_s \sim 0.6\times10^{12}$ cm^{-2} and $\Delta E \sim 3.9$ meV near $N_s \sim 1\times10^{12}$ cm^{-2} at $H_y = 100$ kOe. The corresponding theoretical results are given by $\Delta E \sim 2.3$ meV at $N_s = 0.6\times10^{12}$ cm^{-2} and $\Delta E \sim 3.5$ meV at $N_s = 1\times10^{12}$ cm^{-2}. The theoretical shifts are slightly smaller, but can be said to be in good agreement with the experimental results.

Figure 39 gives a schematic illustration of the subband and Landau-level structure in a magnetic field tilted from the z direction. Because of shifts of the center of the Landau orbit in k_x-k_y space, combined intersubband-cyclotron transitions become allowed in addition to the main transition. Such combined resonance

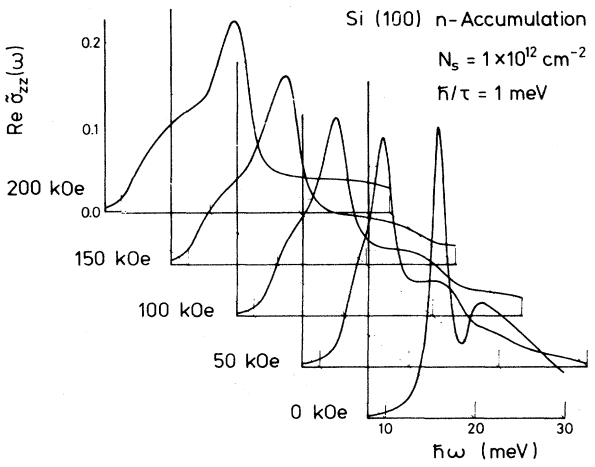

FIG. 38. Calculated real part of the dynamical conductivity $\tilde{\sigma}_{zz}(\omega)$ at $N_s = 1\times10^{12}$ cm^{-2} for $H = 0$, 50, 100, 150, and 200 kOe in an n-channel accumulation layer on Si(100). $\hbar/\tau = 1$ meV. After Ando (1978b).

was first observed in a system of electrons trapped outside of liquid helium by the image potential (Zipfel *et al.*, 1976a). A pair of satellite peaks, displaced symmetrically by about the Landau-level separation from the main intersubband transition, was observed. In inversion and accumulation layers the existence of the depolarization effect makes the spectrum much more complicated, but the observation of the combined resonances has been shown to provide important information on the strength of the depolarization effect (Ando, 1977b).

Let us first consider the simplest case discussed above for the case of a parallel magnetic field. The dynamical conductivity in a tilted magnetic field is given by Eq. (3.92) with

$$L_n(\omega) = \frac{g_v g_s}{2\pi l_z^2 N_s} \sum_N \sum_{N'} f(E_{0N})[1-f(E_{nN'})] \times \frac{\hbar^2\omega_{n0}^2 J_{NN'}(\Delta_{n0})^2}{(E_{nN'}-E_{0N})^2-(\hbar\omega)^2}, \tag{3.94}$$

where

$$\Delta_{nm} = \frac{l_z}{l_y^2}(z_{nn}-z_{mm}), \tag{3.95}$$

and $J_{NN'}(x)$ is the overlap integral of the Landau-level wave functions whose centers are displaced by an amount $(z_{nn}-z_{00})/l_y^2$ in k_x-k_y space, given by

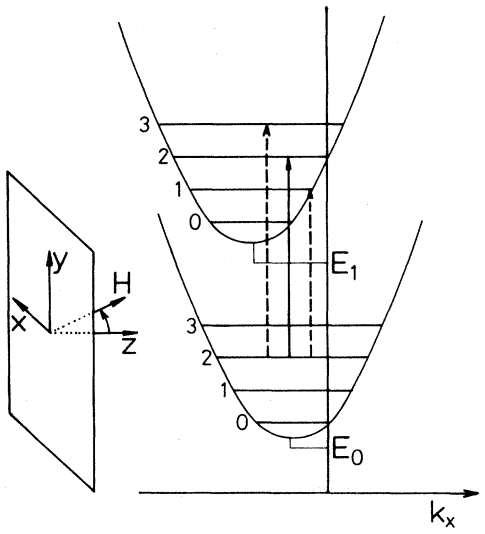

FIG. 39. Schematic illustration of the subband and Landau-level structure in an inversion layer in a tilted magnetic field. The magnetic field is in the y-z plane, and the z direction has been chosen in the direction normal to the surface. The two parabolas represent the dispersion relation in the absence of H_z. Because of shifts of the center of the Landau orbit in k_x-k_y space, combined intersubband-cyclotron transitions become allowed in addition to the main transition. After Ando (1979c).

$$J_{NN'}(x)=J_{N'N}(-x)$$
$$=\left[\frac{N'!}{N!}\right]^{1/2}\left[\frac{x}{\sqrt{2}}\right]^{N-N'}L_{N'}^{N-N'}(\tfrac{1}{2}x^2)\exp(-\tfrac{1}{4}x^2)\,, \tag{3.96}$$

with $L_N^{\alpha}(x)$ being the associated Laguerre polynomial. The intensity of the transition $0N\rightarrow nN'$ is determined by $J_{NN'}(\Delta_{n0})^2$, which is easily understood from Fig. 39. When $\Delta_{n0}<<1$, we get

$$J_{NN}(\Delta_{n0})^2=1-(N+\tfrac{1}{2})\Delta_{n0}^2$$
$$=1-(N+\tfrac{1}{2})\frac{l_z^2(z_{nn}-z_{00})^2}{l_y^4}\,, \tag{3.97}$$

and

$$J_{NN\pm1}(\Delta_{n0})^2=\tfrac{1}{2}(N+\tfrac{1}{2}\pm\tfrac{1}{2})\frac{l_z^2(z_{nn}-z_{00})^2}{l_y^4}\,. \tag{3.98}$$

Since the diamagnetic energy shift is usually not important, the position of the combined resonances $\Delta N\neq0$ is given by $E_{n0}+\Delta N\hbar\omega_c$ when the amplitude is sufficiently small, while the main resonance is determined by $\tilde{E}_{n0}=(1+\gamma_{nn})^{1/2}E_{n0}$, which is the resonance energy in the absence of a magnetic field. Thus we can determine the strength of the depolarization effect from the relative shift of the combined and main resonances in such a case. In the opposite limit $H_y>>H_z$, on the other hand, the lineshape can be shown to approach that in the parallel magnetic field except for the appearance of a quantum structure caused by the nonzero H_z.

The combined resonance was observed in the accumulation layer by Beinvogl and Koch (1978; see also Koch, 1981), although a first attempt failed (Beinvogl *et al.*, 1976). An example of the experimental results is shown in Fig. 40, where the absorption derivative dP/dN_s is plotted as a function of N_s for $\hbar\omega=15.8$ meV. The main transition is at $N_s\sim1.2\times10^{12}$ cm^{-2} in the absence of H_y and is shifted to higher N_s with H_y. We can see at $N_s\sim1.05\times10^{12}$ cm^{-2} a combined resonance for $\Delta N=+1$, which splits into two peaks above $H_y\sim50$ kOe, and at $N_s\sim1.7\times10^{12}$ cm^{-2} a weak combined resonance for $\Delta N=-1$. The relative shift of the main resonance from the center of the combined resonances shows clearly the existence of the depolarization effect (positive γ_{11}). Figure 41 gives experimental positions of the main and combined resonances in $H_z=35$ and 50 kOe for sufficiently small H_y, together with E_{10}, $E_{10}\pm\hbar\omega_c$, and $\tilde{E}_{10}$, where E_{10} and $\tilde{E}_{10}$ are the subband energy separation and the resonance energy calculated in the density-functional formulation. The theoretical results for the resonance energy in the absence of a magnetic field are about 10% higher than the experiments. This slight difference in the absolute values is within the accuracy of the approximations employed in the theoretical calculation. A possible error might also exist on the experimental side because of uncertainties in determining exact values of N_s. The agreement on positions of the com-

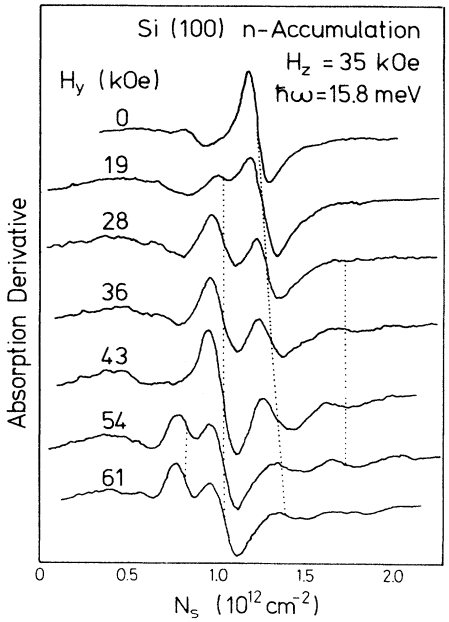

FIG. 40. Experimental results of absorption in an n-channel accumulation layer on Si(100) in tilted magnetic fields observed by Beinvogl and Koch (1978). The absorption derivative dP/dN_s is plotted as a function of N_s for $\hbar\omega=15.81$ meV. The main transition is at $N_s\sim1.2\times10^{12}$ cm^{-2}. We can see at $N_s\sim1.05\times10^{12}$ cm^{-2} a combined resonance for $\Delta N=+1$ which splits into two above $H_y\sim50$ kOe, and at $N_s\sim1.7\times10^{12}$ cm^{-2} a weak combined resonance for $\Delta N=-1$. After Ando (1979c).

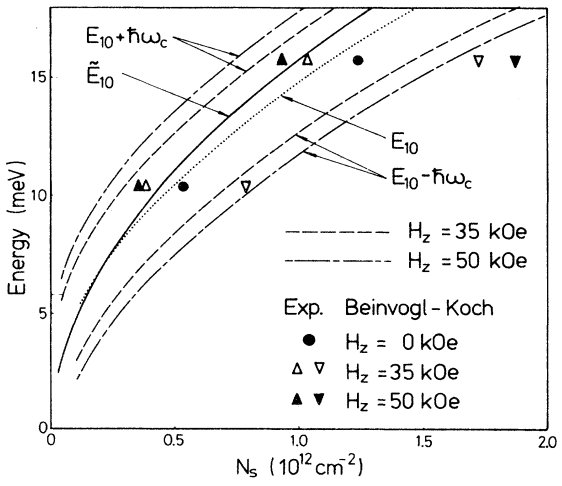

FIG. 41. Comparison of the theoretical and experimental positions of the main and the combined transitions ($\Delta N=\pm1$) in n-channel accumulation layers on Si(100) in tilted magnetic fields. $H_z=35$ and 50 kOe. The solid line represents the calculated resonance energy and the dotted line the subband energy separation for the transition from the ground to the first excited subband in the absence of a magnetic field. Expected positions of combined resonances are given by dashed and dot-dashed lines. After Ando (1979c).

bined resonances relative to the main resonances is sufficient to allow us to conclude that the calculated strength of the depolarization effect agrees with the experiments.

A self-consistent calculation in a density-functional approximation has been carried out by Ando (1979a, 1979c, 1980b) for inversion and accumulation layers in tilted magnetic fields. Figure 42 shows an example of calculated optical spectra in an n-channel accumulation layer on Si(100) for $N_s = 1 \times 10^{12}$ cm^{-2}. A weak but distinct peak at $\hbar\omega \sim 12.7$ meV is the combined resonance $\Delta N = -1$. Around $\hbar\omega \sim 17$ meV combined resonances $\Delta N = +1$ can be seen. For small H_y, the positions of these combined resonances are given by $E_{10} \pm \hbar\omega_c$ and that of the main resonance is at $\tilde{E}_{10}$, as expected. Although the theoretical results explain general features of the experiments, especially the splitting of the combined resonance $\Delta N = +1$ above $H_y \sim 50$ kOe, there are some disagreements, especially concerning the strength of the combined resonances relative to that of the main resonance. Experimentally the combined resonances become stronger at a smaller H_y, which seems to suggest that the actual first excited subband is more loosely bound than theoretically predicted. This seems, however, to be inconsistent with the absence of a diamagnetic energy shift in the experiments. Perhaps one must include a change in the exchange-correlation effect in the presence of a magnetic field to explain such details of the subband structure.

E. Interface effects

In most calculations for inversion and accumulation layers, it has been assumed that the semiconductor-insulator interface is sharp and that there is an infinite barrier which keeps electrons out of the insulator. But the barrier from the bottom of the conduction band in Si to the bottom of the conduction band in SiO_2 is known to be 3.1 to 3.2 eV (Williams, 1977), which will permit a small amount of penetration of the wave function into the insulator. In addition, the notion of a sharp barrier must break down on an atomic scale. The proper way to deal with this problem is to use the correct microscopic structure of the interface to solve the problem without use of the effective-mass approximation. Such an approach is not possible now because the interface structure is not known precisely. It would be difficult in any case because the interface between a crystal (the semiconductor) and an amorphous material (the insulator) can only be dealt with approximately.

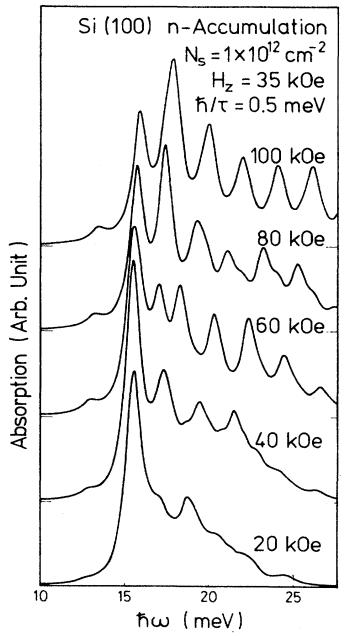

FIG. 42. Calculated optical spectra for different values of H_y in an n-channel accumulation layer on a Si(100) surface. $N_s = 1 \times 10^{12}$ cm^{-2} and $H_z = 35$ kOe. The numbers appearing in the figure represent values of H_y. After Ando (1979c).

Within the spirit of the effective-mass approximation, we can deal with this problem by modeling the interface region in such a way that the atomic structure is smoothed out, and by using appropriate effective masses for the insulator. In this section we describe such an approach for the Si-SiO_2 interface and for the surface of liquid helium. For interfaces with smaller barrier heights, like those that enter in semiconductor heterostructures, the interface becomes a central part of the problem of determining energy levels. That case is discussed briefly in Sec. VIII.D.2.

Once electron penetration into the insulator is allowed, a sharp interface can no longer be used because the singularity in the image potential, Eq. (3.17), cannot be handled where the wave function is nonzero. Fortunately, a smoothly graded interface removes the singularity in the image potential.

Experimental evidence regarding the Si-SiO_2 interface appears to be converging toward a model in which the Si and the SiO_2 are separated by only one or two atomic layers of intermediate stoichiometry. Earlier studies using Auger spectroscopy and argon ion sputtering (see, for example, Johannessen *et al.*, 1976) had indicated a transition region 2 to 3.5 nm wide, but other measurements using photoemission (DiStefano, 1976; Raider and Flitsch, 1976, 1978; Bauer *et al.*, 1978, 1979; Ishizaka *et al.*, 1979; Ishizaka and Iwata, 1980), nuclear backscattering (Sigmon *et al.*, 1974; Feldman *et al.*, 1978a, 1978b; Jackman *et al.*, 1980), and high-resolution electron microscopy (Krivanek *et al.*, 1978a, 1978b; Krivanek and Mazur, 1980) have reduced this value and suggest an interface only one or two atomic layers thick.

There are several possible ways to define the interface thickness, as pointed out by Pantelides and Long (1978) and by Stern (1978b). One of these looks at the atomic structure of the interface, and could lead to a zero nominal interface width for the structure in Fig. 43, in which a plane separates the two materials. A second definition considers the local environment of each atom, and defines the transition layer as the region in which these environments differ from those in the bulk. For the case shown in Fig. 43, the transition layer would be at least two atomic layers wide. Finally, one could consider

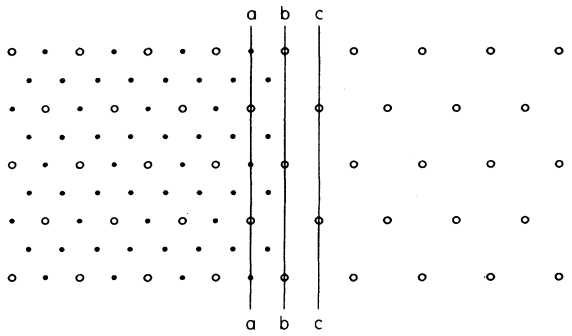

FIG. 43. Schematic picture of a transition from a crystalline element A to a crystalline compound AB_3. The line bb is the nominal interface, but A atoms on this line have different bonding than do A atoms on either side. The transition layer can be considered to be bounded by the lines aa and cc, and therefore has a finite width even though the crystallographic interface is sharp.

properties that depend on excited states of the system, such as energy gaps and dielectric properties. In that case the transition layer could be wider than the one given by the second definition, because the excited states can be expected to spread out beyond the range of the potential that is varying. It is the last of these definitions that enters in our case, because the barrier height, the effective mass, and the dielectric function all involve conduction-band states.

We proceed by constructing a model for the transition layer, calculating the image potential for this model, and solving the Schrödinger equation for the envelope wave function. The parameters that vary across the transition layer are the effective mass m_z, the barrier height E_B, and the dielectric constant. All of these quantities are assumed to change with the same grading function $S(z)$. Thus we assume:

$$\begin{aligned}\kappa(z)&=\kappa_{\rm ins}+(\kappa_{\rm sc}-\kappa_{\rm ins})S(z)\ ,\\ m_z(z)&=m_{z,\rm ins}+(m_{z,\rm sc}-m_{z,\rm ins})S(z)\ ,\\ V_B(z)&=E_B-E_BS(z)\ ,\end{aligned}\tag{3.99}$$

where $S=0$ on the insulator side and $S=1$ on the semiconductor side of the interface.

The simplest grading function is a linear dependence through the transition layer. Such a dependence has been found (Stern, 1978b) to lead to unphysical logarithmic singularities in the image potential. To remove these singularities, Stern used a linear grading with rounded corners. The image potential is found by solving Poisson's equation

$$\nabla\cdot\kappa(z)\nabla\phi=-4\pi Q\delta(\mathbf{r})\delta(z-z')\ ,\tag{3.100}$$

taking the potential at the position of the point charge Q minus the potential

$$\frac{Q}{\kappa(z')[(z-z')^2+r^2]^{1/2}}$$

that the same charge would give in a homogeneous medium whose dielectric constant has the local value $\kappa(z')$, and multiplying by a factor $\frac{1}{2}$ to take into account the fact that the image potential is a self-energy. The image potential energy is obtained by multiplying the potential by Q, and is independent of the sign of Q. It is a continuous function through the interface and becomes the conventional image potential for distances more than a few transition layer widths away. Note that the conventional image potential is attractive on the low-dielectric-constant side of the interface and repulsive on the high-dielectric-constant side.

The potential energy in the Schrödinger equation can be written

$$V(z)=V_d(z)+V_s(z)+V_I(z)+V_B(z)\ ,\tag{3.101}$$

where $V_s(z)$ must be determined from a solution of Poisson's equation with a spatially varying dielectric constant, and can therefore no longer be found from Eq. (3.14).

The spatially varying effective mass changes the form of the Schrödinger equation, which must now be written

$$-\frac{\hbar^2}{2}\frac{d}{dz}\frac{1}{m_z(z)}\frac{d\zeta_i}{dz}+[V(z)-E_i]\zeta_i(z)=0\tag{3.102}$$

to conserve probability current through the transition layer (Harrison, 1961; BenDaniel and Duke, 1966).

For the (001) Si-SiO_2 interface there are two ladders of subbands, the twofold-degenerate lowest ladder with $m_z=0.916m$ in silicon, and the fourfold upper ladder with $m_z=0.19m$ in silicon. The corresponding masses in SiO_2 are not universally agreed upon, even for energies near the bottom of the conduction band, which is thought to lie at $k=0$. Tunneling measurements have given values of $0.42m$ (Lenzlinger and Snow, 1969), $0.48m$ (Weinberg *et al.*, 1976), $0.65m$ (Kovchavtsev, 1979), and $0.85m$ (Maserjian, 1974; see also Lewicki and Maserjian, 1975), among others. The situation is even more difficult for the fourfold valleys, which lie away from $k=0$ and therefore connect to points away from the bottom of the conduction band in the SiO_2. Calculations for the conduction bands of crystalline SiO_2 (Calabrese and Fowler, 1978; Schneider and Fowler, 1978; Batra, 1978) suggest that the barrier height is ~ 5 eV for the energy levels connected with the fourfold valleys, i.e., ~ 2 eV higher than for electrons from the twofold valleys, but tunneling measurements of Weinberg (1977) for the (100), (110), and (111) surfaces do not appear to support such a large difference.

Stern (1977) originally used a graded interface model as a possible alternative to interface roughness scattering. He assumed that the penetration of the wave function into the transition layer reduced the mobility in proportion to the fraction of the total inversion-layer charge density that was in the transition layer. He obtained rough agreement with experimental results. A subsequent attempt (Stern, unpublished) to derive this mobility reduction using the Born approximation led to a reduction proportional to the square of the charge penetration

into the transition layer, with much too small a magnitude. There is now increasing evidence from work of Krivanek and co-workers (Krivanek *et al.*, 1978a, 1978b; Krivanek and Mazur, 1980; Sugano, Chen, and Hamano, 1980; Hahn and Henzler, 1981) and others for interface roughness of approximately the required magnitude, so this alternative mechanism is neither needed nor theoretically well founded. We should add that the values of energy shifts calculated by Stern (1977) used an even more primitive model than the one described here and are therefore unreliable. He found that the presence of a transition layer decreased the splitting $E_{0'0}$, whereas Nakayama (1980) finds an increase using a more detailed model. Experimental evidence relating to this splitting is discussed in Secs. III.C and IV.C.

Because of all the uncertainties in the model, and more particularly because many of the material constants that enter the model are not well known for the Si-SiO_2 interface, we do not show any quantitative results for energy-level shifts attributed to the interface transition layer. Laughlin *et al.* (1978, 1980), Herman *et al.* (1978, 1980), Schulte (1979), and Nakayama (1980) have all undertaken calculations which treat the interface microscopically. Aside from the difficulty of characterizing the amorphous oxide, first-principles calculations like those of Laughlin *et al.* and Herman *et al.* face the difficulty that they must give the subband energies with a precision of order 1 meV if they are to reproduce subband splittings correctly, not an easy task when the subband splittings are compared to energy gaps of order 1 eV or larger.

A guide to the behavior to be expected from a transition layer can be obtained by assuming that the layer leads to a boundary condition on the logarithmic derivative of the envelope function at the interface. If we also assume a simple triangular potential, we can use results for the solution of the Airy equation (see, for example, Stern, 1972b) to learn that for small enough values of $\zeta(0)/\zeta'(0)$ all the subbands of a given ladder will move down in energy by about the same amount with respect to the values obtained with the boundary condition $\zeta(0)=0$, as shown in Fig. 44. Numerical solutions of Eq. (3.102) bear this out. However, different subband ladders shift by different amounts because different values of m_z and E_B obtain for each ladder.

Electrons on liquid helium

For electrons on the surface of liquid helium (see Sec. VIII.H for a brief review of this two-dimensional electron system) there are both theoretical reasons (Lekner and Henderson, 1978; Mackie and Woo, 1978; see also the earlier papers cited in Stern, 1978b) and reasons based on analysis of experiments on reflection of ^{4}He atoms from liquid ^{4}He (Echenique and Pendry, 1976a, 1976b; Edwards and Saam, 1978; Edwards and Fatouros, 1978) to believe that there is a gradually varying density at the surface. Estimated interface widths are of order 0.3 to 0.8 nm. Thus this system should be a good candidate for the kind of analysis described above, without some of the uncertainties that limit its application to the Si-SiO_2 interface. Stern (1978b) used the same approach as above, with one arbitrary parameter in the interface grading function $S(z)$. He used a barrier height $E_B=1$ eV and an effective mass $m_z=1.1m$ (Springett *et al.*, 1967) for electrons in liquid helium, and obtained a good fit to the energy splitting of the first two excited subbands from the lowest subband (Grimes *et al.*, 1976). The interface width (10% to 90%) deduced from the fit is 0.57 nm, which is within the range of previous estimates. The same parameters also give a good fit to the recent results of Lambert and Richards (1981), who extended the measurements to higher electric fields. Calculated and measured results are shown in Sec. VIII.H.

The model Stern used for the helium surface gives a good fit to experiment, but it is by no means unique. For example, the model potential

$$V(z)=-\frac{\kappa-1}{\kappa+1}\frac{e^2}{4(z+\beta)},\quad z\geq 0$$
$$=V_0,\quad z<0 \tag{3.103}$$

also gives a good fit to experiment with $\beta=0.108$ nm (Zipfel and Simons, 1976, unpublished) or 0.101 nm (Hipólito *et al.*, 1978). Sanders and Weinreich (1976) give analytic expressions for the level shifts for a number of cases. Calculations with more realistic microscopic surface models should be carried out for comparison with the spectroscopic data.

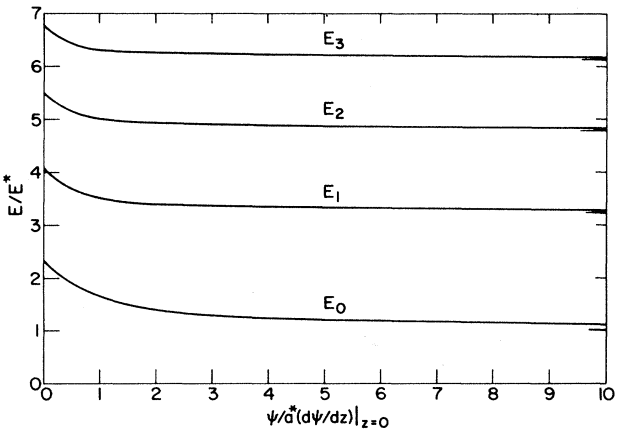

FIG. 44. Effect of boundary condition at the semiconductor-insulator interface on the energies of a ladder of levels in a triangular potential well. The abscissa is the scaled ratio of the envelope wave function at the interface to its derivative there. The scaling distance a is $(\hbar^2/2m_zeF)^{1/3}$, where F is the electric field in the semiconductor, and the scaling energy is $E^*=eFa$. The energies for vanishing derivative of the envelope wave function at the interface are marked at the right. After Stern (1972b).

IV. TRANSPORT: EXTENDED STATES

A. Measurements

The purpose of this section is to give the reader some idea about the nature of the transport measurements cited and some feeling for their accuracy. Low-frequency transport measurements would seem to be amongst the simplest. As in the case of solid semiconductor samples, the accurate extraction of relevant information is more difficult. The problem is to derive the fundamental properties—free-carrier concentration, mobility, trap distributions, densities of states, etc.—from the measured quantities—conductance, Hall effect, field-effect mobility, magnetoresistance, capacitance, etc.

The simplest measurable quantity is the sheet conductivity,

$$\sigma = eN_s\mu = g_D L/W \ , \tag{4.1}$$

where e is the electronic charge, N_s the areal free charge density, μ the mobility, g_D the source-drain conductance, L the length of a MOSFET structure as shown in Fig. 1, and W its width. Even this measurement can be troublesome because of nonohmic effects (source-drain fields must be kept to less than 1 $\mathrm{V\,cm^{-1}}$ and sometimes 10^{-3} $\mathrm{V\,cm^{-1}}$ at low temperatures), contact resistances comparable to the channel resistance, leakage currents, or poorly defined channel lengths. Four-probe measurements can be used to eliminate contact effects. If the conductivity can be unambiguously measured, the problem is then to determine N_s and μ independently. For some three-dimensional semiconductors at low carrier concentration this has been achieved to reasonable accuracy by a combination of conductivity, Hall effect, drift mobility, cyclotron resonance, and other measurements as a function of temperature, which have been carefully matched and iterated with theory (see Smith, 1978, for instance). Probably only for germanium and silicon are the detailed properties accurately known, and then only for the lower carrier densities.

For inversion layers a drift mobility measurement cannot be made, but there is additional information available as compared to solids: the number of carriers can be estimated from the gate voltage dependence of the capacitance and the conductance.

Several mobilities are used to characterize MOSFETs. The effective mobility

$$\mu_{\mathrm{eff}} = \frac{\sigma}{C_{\mathrm{ox}}(V_G - V_T)} \ , \tag{4.2}$$

where σ is the small signal conductivity, C_{ox} is the capacitance per unit area across the oxide, V_G is the gate voltage, and V_T is the threshold gate voltage, depends on the somewhat arbitrary definition of the threshold voltage or the turn-on voltage. V_T is often defined as the voltage where the Fermi level is as close to the conduction (or valence) band at the surface as to the valence (or conduction) band in the bulk. Experimentally it is often determined by the straight-line extrapolation to zero conductance of the turn-on region measured as a function of gate voltage [see Fig. 45(a)]. Both thermal broadening and trapping tend to obscure these definitions. An overestimate of V_T results in low values for N_s and high values for μ_{eff} as compared to μ. The effective mobility can also differ from the mobility μ in the presence of trapping at the interface. A simple model gives

$$\mu_{\mathrm{eff}} = f\mu \ , \tag{4.3}$$

where f is the fraction of the induced electrons that are free (i.e., not trapped or in depletion charge).

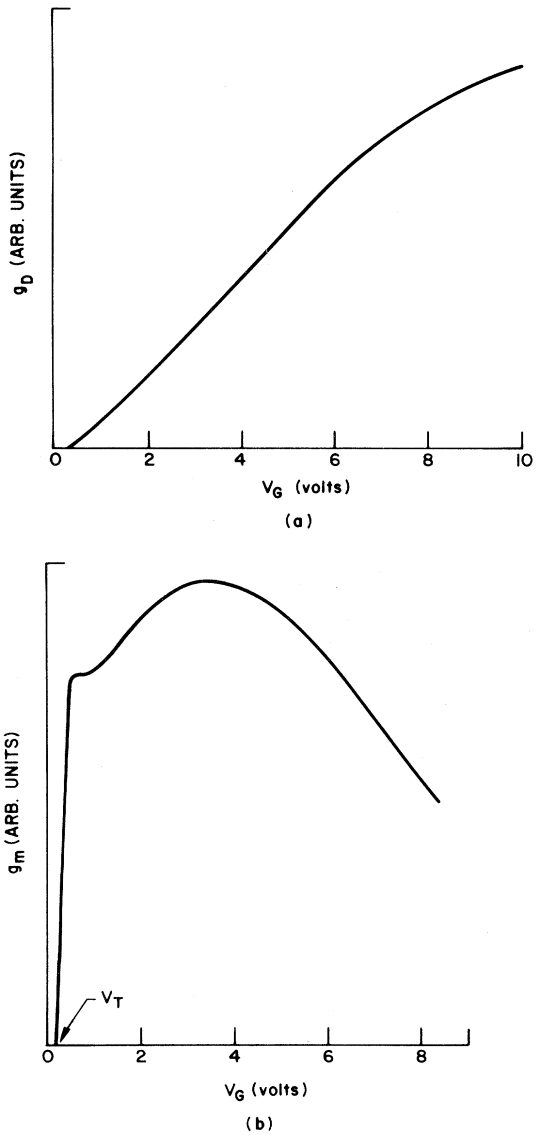

FIG. 45. Typical plot of (a) conductance g_D and (b) transconductance g_m as a function of gate voltage. Because of the tails at low gate voltage, the threshold voltage V_T is taken from a straight-line extrapolation of one or the other curve, but usually from g_m. When looked at carefully even the transconductance curves show a tail near threshold, which is broadened by increasing temperature or by interface states.

The field-effect mobility is derived from the transconductance

$$g_m = dI_D/dV_G \mid_{V_D} , \tag{4.4}$$

where I_D is the drain current and V_D the drain voltage, and g_m is normalized for geometric factors. Then (Fang and Fowler, 1968)

$$\mu_{FE} = \frac{g_m}{C_{ox} V_D} = f\mu + (V_G - V_T)\left[\mu \frac{df}{dV_G} + f\frac{d\mu}{dV_G}\right] , \tag{4.5}$$

which illustrates the hazards of extracting information from the field-effect mobility. All voltages are referred to the source. Because g_m goes to zero at threshold it can be used to define V_T, but again, because of broadening effects, only somewhat better than conductance can [see Fig. 45(b)]. Many of the effective mobility data at low temperatures discussed below were extracted by an extrapolation of the transconductance at 77 K and by use of the V_T thus derived with the conductance data. For conductance and transconductance measurements, closed (typically circular) structures can be made to avoid leakage at the edges. If the drain voltages are kept low in ac transconductance experiments, capacitive feedthrough from the gate can add to the drain current significantly and cause severe errors, particularly for $W \leq L$.

The Hall mobility μ_H also need not equal the mobility μ. We can write

$$\mu_H = r\mu = R_H c\sigma , \tag{4.6}$$

where r is the Hall ratio and R_H is the Hall constant. The Hall ratio is discussed in Smith (1978), for instance, and need not equal unity. It is expected to be unity for circular Fermi surfaces at low temperatures. Hall-effect measurements without an adequate theory of scattering cannot unambiguously give either the mobility or the carrier density. Thus the effects of trapping cannot be separated from the effects of scattering on the Hall ratio without a great deal of circular reasoning (Fowler *et al.*, 1964; Fang and Fowler, 1968; Sakaki *et al.*, 1970). No calculations of the Hall ratio except for some based on rather simple assumptions (Sugano *et al.*, 1973) have been made, even at low temperatures where only one subband is occupied, although Sakaki *et al.* (1970) inferred a value of about 0.85 at 300 K. At higher temperatures (greater than about 40 K) a multiple-band theory is needed. In the absence of trapping the measured carrier concentration,

$$N_H = \frac{1}{eR_H c} = \frac{N_s}{r} , \tag{4.7}$$

can reasonably be used to define a threshold by extrapolation to zero carrier concentration. However Hall-effect measurements are more difficult than conductance measurements, and the samples are more complex and larger, and without special precautions, open at the edges. As is usual with Hall measurements, geometric effects must be accounted for properly. Contact resistance effects which can be a problem in conductance geometry samples are avoided, at least by open-circuit Hall voltage measurements. The larger size increases the chances that the sample may be macroscopically inhomogeneous (Fang and Fowler, 1968; Thompson, 1978b). The open structures increase the chance that leakage currents around the periphery can obscure results at low N_s, although it is possible to make samples with guard electrodes.

At higher temperatures leakage currents through the source diode into the substrate can result in errors which are especially important at low carrier densities and especially when a substrate bias is applied.

The *C-V* curves—capacitance measured as a function of gate voltage—can be used to measure free-carrier, depletion, and surface trapped carrier densities near threshold, at least above the temperature for freeze-out of the bulk. Sze (1969) has presented an excellent overview. Although there are many techniques for interpreting the *C-V* data, they are far from trivial and not uncontroversial. With few exceptions (Sakaki *et al.* 1970) careful capacitance studies have not been combined with transport measurements. Nicollian and Brews (1982) will extensively review these measurements.

The capacitance can be used to characterize the surface because the charge is not induced within a few angstroms of the silicon-insulator interface as it would be in a metal-insulator interface. Fast interface states are usually considered to be at the interface and are fast because they empty and fill faster than the measurement frequency. Inversion-layer electrons are induced from several to several hundred angstrom units away from the surface, depending on field. The depletion charge can be induced many thousands of angstroms from the surface. In general one can write an expression (Kingston and Neustadter, 1955) for the classically induced charge,

$$Q = \pm\left[\frac{\kappa_{sc} e}{2\pi}\left\{N_A\phi_s + p_0\frac{kT}{e}\left[\exp\left[\frac{-e\phi_s}{kT}\right]-1\right] + n_0\frac{kT}{e}\left[\exp\left[\frac{e\phi_s}{kT}\right]-1\right]\right\}\right]^{1/2} + Q_{is}(\phi_s) , \tag{4.8}$$

where Q is the total induced charge and is positive when ϕ_s, the surface potential measured between the bulk and the surface, is negative. N_A is the acceptor density and p_0 and n_0 are the bulk hole and electron densities, respectively. Some of these points have been addressed in Sec. I. $Q_{is}(\phi_s)$ is the interface state charge density and depends on whether the states are acceptors or donors and on the position of the states in the gap. When this expression is combined with

$$V_{appl} = E_{ox} d_{ox} + \phi_s \tag{4.9}$$

and Gauss's law at the interface is applied, an expression relating the induced charge and the applied voltage is obtained which can be differentiated to obtain the capacitance. Many hundreds of papers have been published on

this subject. Much of the literature is reviewed in Sze (1969) and by Goetzberger, Klausmann, and Schulz (1976), Schulz (1980), and Nicollian and Brews (1982). The last especially consider the effects of inhomogeneities.

This classical model results in capacitance curves as shown in Fig. 4, where the effects of interface states are shown. V_{FB}, the voltage for which the space charge is zero, is determined if the substrate doping is known. Work-function differences between the silicon and gate metal and charge in the oxide or interface states can result in displacement of V_{FB} from zero—a built-in voltage. For both accumulation and inversion, charge is induced near the surface, and at least in thick ($\gtrsim$500 Å) oxides the capacitance equals approximately the oxide capacitance. In depletion the capacitance decreases as the charge is induced farther into the silicon. Near the minimum, inversion electrons are just beginning to be induced with increased surface field.

The effect of reducing the temperature is to sharpen the turn-on and also to change V_{FB} because the Fermi level in the bulk moves closer to the valence band, which increases the work-function differences between the gate and the silicon and therefore changes the built-in voltage due to differences in the silicon and gate work functions.

The results must be modified to account for quantum effects, which tend to result in the electrons being extended farther into the silicon and are important when the oxide thickness is small (Pals, 1972b; Stern, 1972b, 1974a). The classical expressions derived in Sze (1969) are not valid for oxide thicknesses less than 300 Å, but no complete set of curves based on a self-consistent quantum theory has been published.

Another technique for counting the number of free electrons as a function of gate voltage is to measure the Shubnikov–de Haas oscillations in the magnetoresistance at moderate fields as a function of V_G and magnetic field. Each oscillation contains the number of electrons in a Landau level which fortunately is independent of the mass (Fowler *et al.*, 1966). Extrapolation of a fan diagram of the location of the levels as a function of field and gate voltage to zero magnetic field gives the effective threshold, at least where band tailing effects are unimportant. This is illustrated in Fig. 46, where the positions of the peaks in the transconductance are shown. Some spread in the extrapolated threshold determination for different Landau levels can occur if there is a strong dependence of mobility on carrier concentration. If the average conductance increases rapidly at low voltages and decreases at high voltages there is a displacement of the peaks which can account for this spread. Usually transconductance rather than conductance is used because the oscillations are more pronounced, so that measurements can be made at the lowest magnetic fields to reduce the extrapolation range. The spacing of the Landau levels gives a very accurate measurement of C_{ox}. For thin oxides the spacing should measure the variation in z_{av}.

If trapping, band tailing, or depletion charge are important (as they are near threshold) no single experiment can unambiguously give the mobility and carrier concentrations. Most techniques are accurate to 5% or better for carrier concentrations above $10^{12}/cm^2$. An exception would be in samples with many interface states when measured near and above room temperature (Sakaki *et al.*, 1970; Fang and Fowler, 1968). The interpretation of the measurements is increasingly unreliable at carrier concentrations below 10^{12} cm^{-2} (Fowler and Hartstein, 1980a). A combination of Hall-effect, conductance, Shubnikov–de Haas, and C-V measurements is really needed (Sakaki *et al.*, 1970). Capacitance, however, is difficult to measure near threshold at 4.2 K and requires large samples which may suffer from inhomogeneity (Thompson, 1978b; Brews, 1972a, 1972b, 1975a, 1975b; Ning and Sah, 1974) and is therefore useful on only relatively ideal samples. Capacitance measurements are difficult to interpret at 4.2 K because the minority charge must flow in along a distributed-resistance-capacitor network from the source and drain (Voschchenkov and Zemel, 1974), and because depletion charge is not readily established when the majority carriers are frozen out. Use of infrared light to supply mobile charge introduces various photovoltages such as the surface photovoltage and Dember effects. However, at higher temperatures a combination of complex conductance measurements has allowed accurate determination of mobility and carrier concentration as low as 10^9 cm^{-2} (Shiue and Sah, 1979; Chen and Muller, 1974).

The measurement of threshold voltage or the flat-band voltage V_{FB} is important to determine oxide charge. It also measures the charge in fast states for flat bands, Q_{ss}

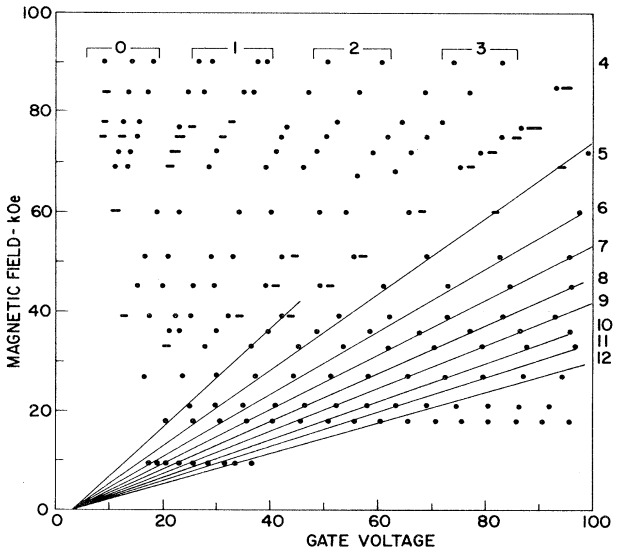

FIG. 46. A fan diagram of the peaks in the transconductance resulting from magnetoconductance oscillations. The threshold voltage V_T is determined by extrapolation of the peaks for the various Landau levels. The oxide capacitance C_{ox} can also be determined to high accuracy from such diagrams because when the nth Landau level is filled, $n\hbar\omega_c D(E)=N_s=C_{ox}(V_G-V_T)$. After Fowler *et al.* (1966b).

(acceptor states below the Fermi level and donor states above). The oxide charge is taken conventionally as an equivalent oxide charge residing at the silicon-silicon dioxide interface,

$$eN_{ox}=Q_{ox}=\frac{1}{d_{ox}}\int_0^{d_{ox}} en_{ox}(z)dz\ , \tag{4.10}$$

where N_{ox} is the equivalent charge density at the interface, d_{ox} is the oxide thickness, z is the distance from the gate to the point in the oxide where the charge concentration is $n_{ox}(z)$ measured away from the interface. Measurement of the distribution of charge, which is needed to calculate scattering, is difficult (DiMaria, 1978).

In general the flat-band voltage depends on the oxide charge, the work function of the metal, and the work function of the silicon (and therefore on the doping of the silicon and the temperature) so that

$$V_{FB}=\frac{[(\chi_{sc}+E_F-E_v)-\chi_m]}{e}-\frac{Q_{ox}}{C_{ox}}-\frac{Q_{ss}}{C_{ox}}\ , \tag{4.11}$$

where χ_{sc} and χ_m are, respectively, the energy differences between the valence band of the silicon and the Fermi level of the metal and the conduction band of the silicon dioxide, and E_F-E_v is the Fermi energy of the silicon measured from the valence band. χ_{sc} is 4.2 ± 0.1 eV for silicon and χ_m is about $3.2-3.5$ eV for an aluminum gate, depending on processing (Solomon and DiMaria, 1981). Hickmott (1980) has summarized his results and those of others and has concluded that $\chi_m-\chi_{sc}$ can vary up to 0.15 V, depending on postmetallization annealing. The values for other metals range from 2.2 to 4.2 eV and have been determined by internal photoemission (see, for instance, Goodman and O'Neill, 1966).

The threshold voltage is approximately given by

$$V_T=V_{FB}+\frac{Q_{depl}}{C_{ox}}+\phi_D\ , \tag{4.12}$$

where $Q_{depl}=(\kappa_{sc}eN_A\phi_d/2\pi)^{1/2}$, ϕ_d is the potential across the depletion layer at the threshold for inversion (see also Sec. III.A.1) and N_A is the acceptor density in the silicon. At low temperatures and for all but pathologically compensated doping, ϕ_d is approximately equal to the energy gap (1.15 V) when the source is grounded to the substrate at low temperature. However, Q_{depl} can be varied by using a substrate bias, V_{sub}.

If there are interface states that are filled as the surface is depleted, their effect Q_{ss}/C_{ox} must be added. If the fast states are normally neutral when filled (donors) then V_{FB} will be shifted but V_T will not be, unless there are states above the Fermi level at the surface at threshold. As can be seen, the extraction of information about the transport properties is easier in the absence of fast states which by proper processing can be reduced below 10^{10} cm^{-2}. In general, the various techniques used for extrapolation of thresholds—Hall measurements, Shubnikov–de Haas fan diagrams, capacitance and extrapolation of nitrogen temperature transconductance—are in good agreement for samples with low fast-interface-state density ($\sim10^{10}$ cm^{-2}) and oxides that are relatively thick (>500 Å). They are not for samples with high fast-interface-state densities, as when sodium is introduced, so that errors can be larger (10^{11} carriers/cm^2) in such cases (Fowler and Hartstein, 1980a).

B. Experimental results

1. Introduction

There is a large and confusing mass of data on transport in inversion layers. Only a few papers have attempted to survey the whole field: Fang and Fowler (1968), Komatsubara, Narita, Katayama, Kotera, and Kobayashi (1974), and a series of papers by Cheng (1971, 1972, 1973a, 1973b, 1974), Cheng and Sullivan (1973a, 1973b, 1973c, 1974), and Sah and associates (Sah *et al.*, 1972b; Shiue and Sah, 1976, 1979, 1980). Most papers have attacked limited ranges of temperature or sample characteristics, with the result that a coherent picture is not obvious. Here we shall attempt to give some coherence to the experimental results by examining primarily conduction of electrons in the unactivated regime mainly on the (100) silicon surface. (We ignore weak localization here; it will be discussed in Sec. V.B) The (100) surface has been studied most because it has the highest mobility and the most nearly perfect oxides of any of the silicon surfaces. It also leads to a simpler theory because it is orthogonal or parallel to all the principal axes of the conduction-band minima. Hole conduction has been studied in far less detail and is discussed briefly in Sec. VIII.A.

In general at room temperature the electron mobility in the surface is less than in the bulk because of increased scattering. However, at low temperatures it is higher, partly because the electrons are in the lowest subband so that the effective mass parallel to the surface is light and partly because they are separated from their compensating positive charge in the gate, so that Coulomb scattering is reduced.

The general characteristics are illustrated in Fig. 47, where Hall-mobility data are shown as a function of $N_s\equiv(ecR_H)^{-1}$ for two samples, both with 2-ohm-cm p-type substrates for $V_{sub}=0$. The high-mobility sample had a 990 Å oxide and was annealed at 1000 °C in N_2 after oxidation; the low-mobility sample had a 500 Å oxide and was not annealed in N_2 at high temperature. The first had an oxide charge of $(6\pm2)\times10^{10}$ cm^{-2} and the latter $(13.4\pm4)\times10^{10}$ cm^{-2}.

The differences between these samples are most striking at 4.2 K, although the samples show the same general variation of mobility with N_s and T. At 4.2 K there is a smooth rise in mobility as N_s increases, followed by a decrease. At low N_s the maximum mobility is 18 000 $cm^2V^{-1}s^{-1}$ for the low-oxide-charge samples. The higher-oxide-charge sample had a maximum mobility of only 4000 occuring at higher N_s. At high values of N_s the mobilities approach the same values and decrease as

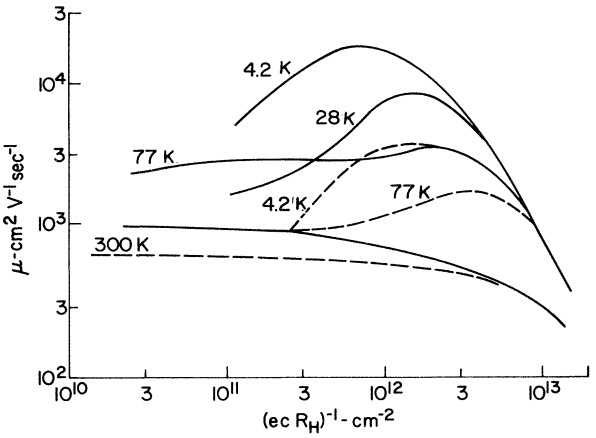

FIG. 47. Hall mobility as a function of $1/ecR_H = N_H$ for two samples. The solid curves are for a sample where $N_{ox} = (6 \pm 2) \times 10^{10}$ cm^{-2}. The dashed curves are for a sample with $N_{ox} = (13.4 \pm 4) \times 10^{10}$ cm^{-2}. Data are shown for 300, 77.3, 28, and 4.2 K. The overlap of the 77.3 K data for low oxide charge and the 4.2 K data for high oxide charge over a large part of the range is coincidental. All low-temperature curves approximately coincide at high values of N_s. After Fowler (unpublished).

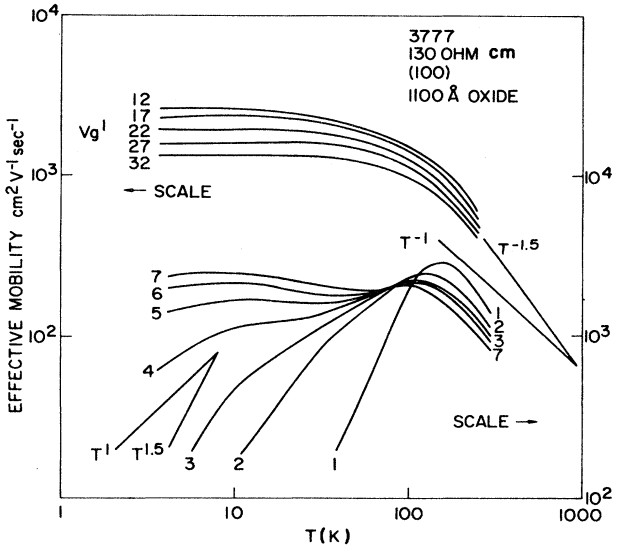

FIG. 48. Typical temperature dependence of the effective mobility μ_{eff} for an n-channel device. The carrier density N_s in units of cm^{-2} is given by $2 \times 10^{11}\ V_g'$, and the value of $V_g' = (V_G - V_T)$ in volts is indicated for each curve. The oxide charge N_{ox} was about 2×10^{11} cm^{-2}. The upper and lower sets of data are displaced. After Fang and Fowler (1968).

about N_s^{-2} to a value of about 1000 at $N_s = 10^{13}$ cm^{-2}. Generally, this behavior can be ascribed to oxide charge scattering, which decreases as N_s increases, and surface roughness scattering, which increases with N_s, although other mechanisms may affect the mobility to a lesser extent, especially near threshold.

The mobility is seen to decrease between 4.2 and 77 K at low N_s but is relatively temperature independent at high N_s. At low carrier concentrations depending on N_{ox} the temperature dependence can reverse sign. The 77 K data also show some structure that will be discussed below.

At 300 K the mobility is lower than at lower temperatures over most of the range of N_s and is much less dependent on N_s or N_{ox}. This is a range where oxide charge scattering should be weak, the conduction-band electrons are not degenerate, many subbands contribute to the conduction, and phonon scattering should be strong.

Representative plots of the temperature dependence as a function of N_s are shown for samples with high N_{ox} ($\sim 2 \times 10^{11}$ cm^{-2}) in Fig. 48, taken from Fang and Fowler (1968). Similar extensive data may be found in that paper—all for low-mobility samples—and in Komatsubara *et al.* (1974). Generally there is a strong increase in μ_{eff} with increasing temperature for $N_s < 2 - 10 \times 10^{11}$ cm^{-2} which can be activated (Fang and Fowler, 1968). Above this N_s range the mobility varies weakly in high N_{ox} samples in complex fashion until it decreases at high temperatures as about $T^{-1.5}$. In high-mobility samples the temperature dependence of resistance can be stronger and has been reported as high as T^{4-5} (Kawaguchi and Kawaji, 1980a) below 10 K.

Below we shall discuss in more detail these and other data, dividing the data generally into the ranges around 300 K, near 4.2 K, and 4.2—90 K for electrons on (100) silicon samples. In Sec. IV.B.5 some other cases will be discussed briefly.

2. 300 K range

As may be seen in Fig. 47, the mobility is nearly constant or decreases slowly over the entire range of N_s at room temperature. This result differs from early results of Fang and Fowler (1968), where an initial increase was observed as shown in Fig. 49. The samples showing a

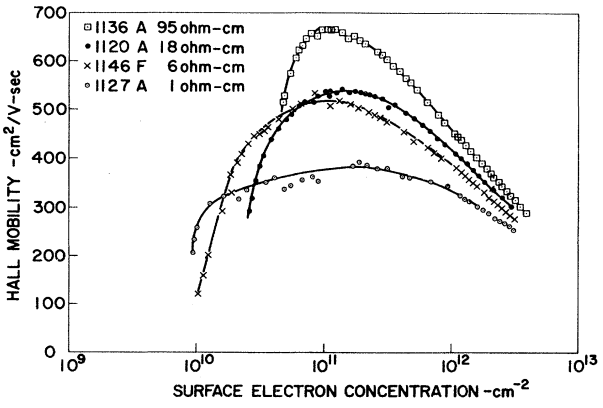

FIG. 49. Hall mobility μ_H for a sample with large oxide charge (2×10^{11} cm^{-2}) as a function of $(ecR_H)^{-1} \approx N_s$ at 300 °C. Note the decrease in μ_H at low N_s. After Fang and Fowler (1968).

decrease of μ_{eff} at low N_s are characterized by oxide changes of 2×10^{11} cm^{-2} or greater.

Brews (1972a, 1972b, 1975a, 1975b) has considered the effect of spatial fluctuations in N_s resulting from fluctuations in N_{ox} and has concluded that $\mu\sim(1-\frac{1}{2}\langle\sigma_s^2\rangle)$, where $\langle\sigma_s^2\rangle$ is the variance of the surface potential. He concludes that for N_{ox} less than 3×10^{10} cm^{-2} no decrease in mobility with decreasing N_s should be seen, at least down to $N_s=3\times10^9$ cm^{-2}, whereas a maximum should occur at $N_s\simeq10^{11}$ cm^{-2} for $N_{\text{ox}}=3\times10^{11}$ cm^{-2}. This is consistent with Fig. 49, where there are about 2×10^{11} cm^{-2} oxide charges, and Fig. 47, where the oxide charge is low. Comparison with data of Chen and Muller (1974) and with Shiue and Sah (1979) also bears out his conclusion, although the latter have a somewhat different explanation. The latter have carried out measurements to values of N_s as low as 10^8 cm^{-2} and do observe a small decrease in mobility below 10^9 cm^{-2} in samples with $N_{\text{ox}}\simeq1.4\times10^{11}$ cm^{-2}. However, their samples with $N_{\text{ox}}=1.17\times10^{12}$ cm^{-2} show only a slightly greater decrease, even though $\mu_{\max}\approx600$ cm^{2}V^{-1}s^{-1} as compared to 1000 for the better samples.

In the now more generally studied samples with $N_{\text{ox}}<10^{11}$ cm^{-2} the mobility is quite flat versus N_s for $10^{10}<N_{\text{ox}}<2\times10^{11}$ cm^{-2} with mobilities over 1000 cm^{2}V^{-1}s^{-1} for the best samples. Figure 47 demonstrates that the oxide charge contributes to the scattering even at 300 K and that an oxide charge difference of about 7.5×10^{10} cm^{-2} has reduced the maximum 300 K mobility by about 30%. This is clearly shown in Fig. 50, taken from Sah *et al.* (1972b), where a mobility dependence on N_{ox} was measured. The mobility did not depend on crystal orientation. As N_s increases, the mobility decrease is initially weak but grows stronger as N_s approaches the range where surface roughness scattering may become important. No simple power law in N_s describes the variation. For $10^{12}<N_s<5\times10^{12}$ cm^{-2} again no power law seems to obtain in N_s, but the dependence is roughly as $(N_s+N_{\text{depl}})^{-1/3}$. Calculation of the scattering in this range is very difficult because many subbands are occupied and because inter- and intrasubband scattering and optical- and acoustic-phonon scattering are involved, as is surface roughness scattering at high N_s. Probably the best comparison with phonon scattering theory could be made at $N_s=2-5\times10^{12}$ cm^{-2} in the cleanest samples.

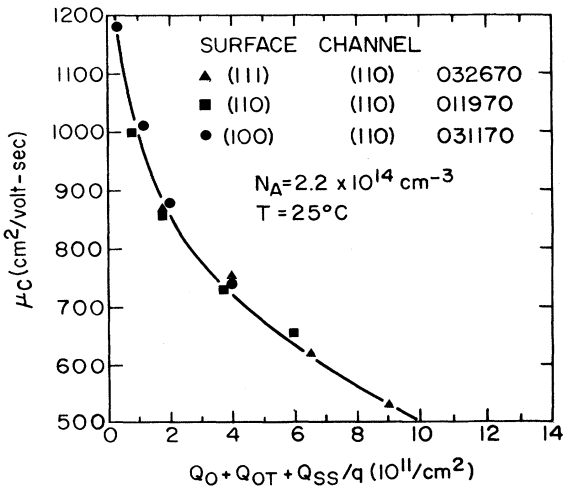

FIG. 50. Effective mobility at 298 K at low carrier density as a function of total oxide charge. Note that the samples made on the (100), (110), and (111) surface lie on the same curve. After Sah *et al.* (1972b).

In the 300 K range the mobility varies as about $T^{-1.5}$ (Leistiko *et al.*, 1965; Fang and Fowler, 1968; Komatsubara *et al.*, 1974) although acoustic-phonon scattering for one subband (which is not realized at high temperature) should follow a T^{-1} law (Kawaji, 1969). Sah *et al.* (1972b) found somewhat weaker temperature dependence. Phonon scattering is discussed theoretically in Sec. IV.D.

It should be noted that in this temperature range the Fermi level is usually below the conduction-band edge, so that interface states can change occupancy with surface field and temperature as discussed by Fang and Fowler (1968), Sakaki, Hoh, and Sugano (1970), and Sah *et al.* (1972b). The surface state contribution to the scattering can vary, depending on temperature and on whether the states are donors or acceptors.

3. 4.2 K range

At 4.2 K the electrons are generally in the quantum limit, in that only the lowest-energy E_0 subbands are occupied in a perfect unstrained sample. On the (100) surface these have spin and twofold valley degeneracy. Furthermore, as is well known, Matthiessen's rule may be applied with confidence at 4.2 K to separate the various scattering mechanisms. As noted above, there is a large body of experimental data for samples with different N_{ox}. However, as noted in Sec. IV.A, the estimate of N_{ox} is difficult for small values and for thin oxides. Furthermore, the location of the charge in the oxide is not usually known. The data are usually compared to theory for the different scattering mechanisms added appropriately. Another approach to the problem of separating the contributions of the different scattering mechanisms is to vary the oxide charge methodically. Even though the absolute value of N_{ox} may not be known, the change may be determined accurately. The oxide charge can be varied by annealing as in Sah *et al.* (1972b) and Tsui and Allen (1975). The position of this oxide charge is not known precisely. Oxides can be grown with known densities of neutral electron and/or hole traps that can be filled by charge injection (DiMaria, 1978). Even though the positions and densities of these charges have been measured, an experiment using trapping in the oxide has not been done. Double-insulator structures such as MNOS (metal-nitride-oxide-silicon) devices may be used (Pepper, 1974a), but the charge distribution again is not accurately known. Another approach is to drift sodium ions from the metal

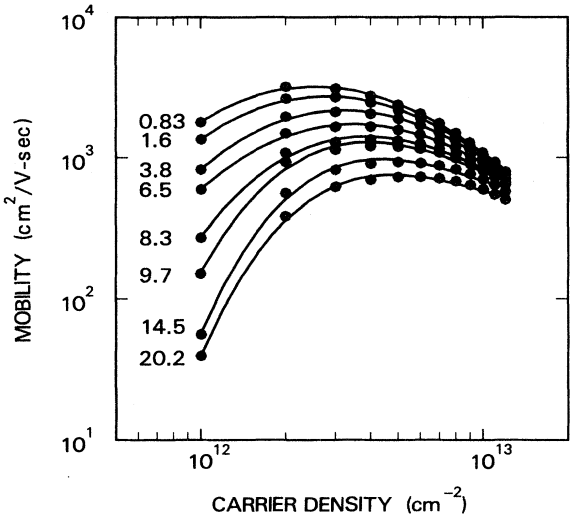

FIG. 51. Some of the extensive measurements on a set of samples in which N_{ox}, the oxide charge density, was varied by drifting Na^+ ions through the SiO_2. The effective mobility μ_{eff} is plotted as a function of the carrier density N_s. The measurements were made at 4.2 K. After Hartstein *et al.* (1980).

to the silicon interface (Harstein and Fowler, 1976, 1978, 1980b). The Na^+ ions have been shown to reside very near one or the other interface (DiMaria, Aitken, and Young, 1976; DiMaria, 1978). Besides introducing fixed oxide charge, the sodium also introduces acceptor surface states (Fowler and Hartstein, 1980a) which are neutralized before the inversion electrons are induced. This approach was used methodically to vary the mobility with N_s, N_{depl}, and N_{ox}. The mobility varied as a function of N_s and N_{ox} at V_{sub} equal to zero, as shown in Fig. 51. At constant N_s the data were fitted to

$$\mu_{eff}^{-1} = c + aN_{ox} + bN_{ox}^2 \ . \tag{4.13}$$

The first term represents scattering that is not a function of N_{ox} and to first order was assumed to be primarily μ_{SR}^{-1}, the reciprocal of the surface roughness scattering. This amounts to an assumption that there is no interaction between surface roughness scattering and oxide charge scattering. Values of the intercept are shown in Fig. 52 plotted versus $(N_{depl}+N_s)^2$ for different substrate biases. This plot most nearly rectified the curve and was far better than a plot versus $(N_{depl}+N_s/2)^2$. Comparison of these data with theory is made in Sec. IV.C. Sugano *et al.* (1980) have reported significantly increased surface roughness scattering on severely roughened surfaces. Earlier, Cheng and Sullivan (1973c) and more recently Kohl *et al.* (1981) observed increased surface roughness scattering as a result of treatments which roughened the surface, although the latter ascribed the effect in their treatment to an increase in neutral defects. It should be noted that the failure of the curve in Fig. 52 to intersect the axis at 0 is an indication of an additional scattering mechanism.

The reciprocal of the linear coefficient a in Eq. (4.13) is shown in Fig. 53. As may be seen, this part of the scattering decreases with N_s. These results are compared with theory in Sec. IV.C. The quadratic term presumably arises from multiple scattering events. It is only strong for low values of N_s where k_F^{-1} is long as compared to the $(N_{ox})^{-1/2}$. It is shown for $N_s = 2\times10^{12}$

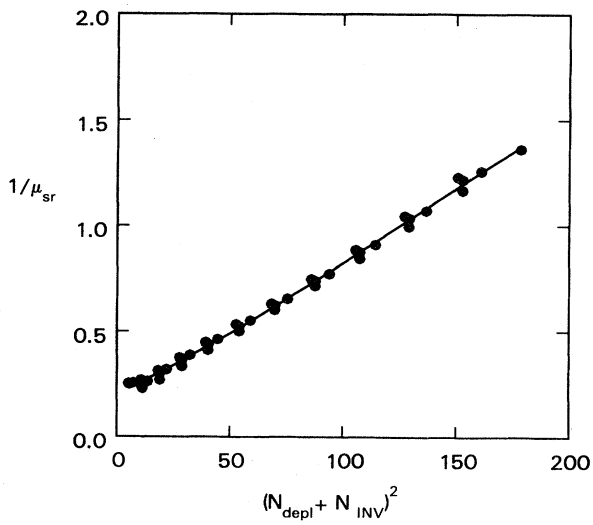

FIG. 52. The intercept of μ_{eff}^{-1}, the reciprocal of mobility, when extrapolated to $N_{ox}=0$ from a plot against N_{ox}, is plotted versus $(N_{depl}+N_s)^2$. The mobility is in units of 10^3 $cm^2V^{-1}s^{-1}$. N_{depl}, the number of charges per unit area in the depletion layer, and N_s (called N_{INV} in the figure), the number of electrons per unit area in the inversion layer, are in units of 10^{12} cm^{-2}. While it is assumed that the scattering for $N_{ox}=0$ is primarily due to surface roughness scattering, the failure of the curve to intercept the origin indicates an additional scattering mechanism. Data are for various values of substrate bias voltage V_{sub}, i.e., for different values of N_{depl} as well as N_s. After Hartstein *et al.* (1980).

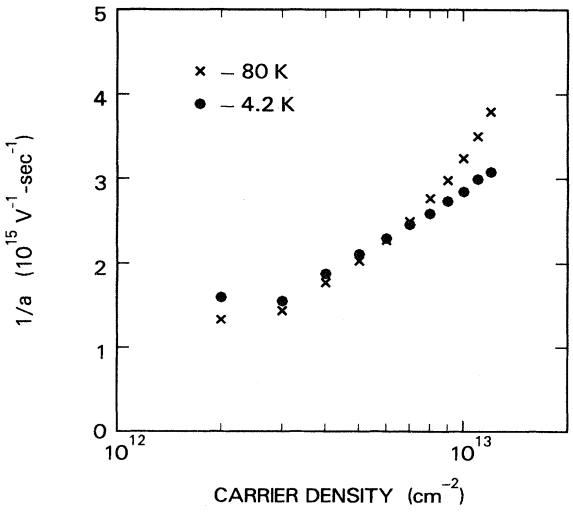

FIG. 53. The reciprocal of the linear coefficient a, taken from fitting $\mu_{eff}^{-1} = c + aN_{ox} + bN_{ox}^2$, as a function of N_s at 4.2 and 80 K. The data were taken from Fig. 51. After Hartstein *et al.* (1980).

cm^{-2} in Fig. 54 as a function of temperature for different substrate biases. As may be seen, it decreases rapidly with increasing temperature. It is only measured at low N_s. On the other hand, the temperature dependence of the linear term a is much weaker and depends on N_s, as may be seen in Fig. 55. At low carrier concentrations, a increases with temperature. Unless this increase is taken into account in analyzing the weak temperature dependence of μ from phonon scattering, for instance, errors will result. Oxide charge scattering is compared to theory in Sec. IV.C.1.

Other scattering may obtain at 4.2 K that may modify the simple picture above. Below 30 K a negative magnetoresistance has been reported (Eisele and Dorda, 1974a; Kawaguchi *et al.*, 1978a, 1978b; Kawaguchi and Kawaji, 1980b, 1980c) that was at first attributed to the decrease of some scattering mechanism in a magnetic field. It varies as N_s^{-1}. It depends only on the normal component of magnetic field, in contrast to an effect in InAs (Kawaji and Kawaguchi, 1966). Similar effects have been seen on n-channel (111) samples and on p-channel devices. The effect is quadratic at low fields and saturates at about 1—1.5 T. The saturation value of the magnetoconductivity change has a maximum value of 4% at 4.2 K, decreases with increasing temperature, and vanishes at about 30 K. The quadratic dependence of the magnetoconductivity on magnetic field follows a Curie-Weiss law. Dorda found that the effect decreased with large surface state density. Attempts to explain these effects on the basis of spin-spin scattering seem futile because of the dependence on the direction of magnetic field. Recently this effect has been related to localization effects (Kawaguchi and Kawaji, 1980b; Hikami *et al.*, 1980) discussed in Sec. V.B.

Inability to fit experimental results, especially at low N_s, with theories of the major scattering processes has led to the postulate of an additional short-range scattering mechanism (Matsumoto and Uemura, 1974; Takada, 1979) sometimes called neutral impurity scattering. Neutral impurities are difficult to detect except possibly by trapping (DiMaria, 1978) or by electron spin resonance; so are charge dipoles (Hess and Sah, 1975). The nature of these scatterers is elusive but Yagi and Kawaji (1978, 1979) associated them with growth parameters, as have Kohl *et al.* (1981). They found that the maximum mobility decreased from 10^4 to 7.5×10^3 $cm^2V^{-1}s^{-1}$ as the oxide thickness was reduced from 2700 to 910 Å. However, samples with different processing can show mobilities of 2×10^4 $cm^2V^{-1}s^{-1}$ for a thickness of 990 Å (Fig. 47). These results may be related to surface roughening results reported by Sugano *et al.* (1980) and to the final oxidation rate and the oxygen defect gradient at the silicon interface.

The temperature dependence of the mobility near 4.2 K has been the subject of extensive study and of some controversy. As may be seen in Fig. 48, there is a significant temperature dependence for high values of gate voltage or carrier density above the activated regime. In high-mobility (or low-oxide-charge) samples the mobility shows a somewhat smaller decrease with increasing T, but as in the low-mobility samples illustrated by Fig. 48 the effect decreases as N_s increases. These effects have been studied by Cham and Wheeler (1980b) as a function of the maximum mobility, which is a measure of the oxide charge scattering in the sample, by Kawaguchi and Kawaji (1980a), and by Kawaguchi, Suzuki, and Kawaji (1980). Earlier papers such as Fang and Fowler (1968) or Komatsubara *et al.* (1974) contain some of the same data, although they have not reduced the data in the same way, nor gathered data with such care when the variations with temperature were small. The more recent papers have presented the data by extrapolating the reciprocal mobility data to $T=0$ and subtracting the extrapolated value of $1/\tau$ from the value at any given temperature. The difference is labeled $1/\tau_T$. It is not clear

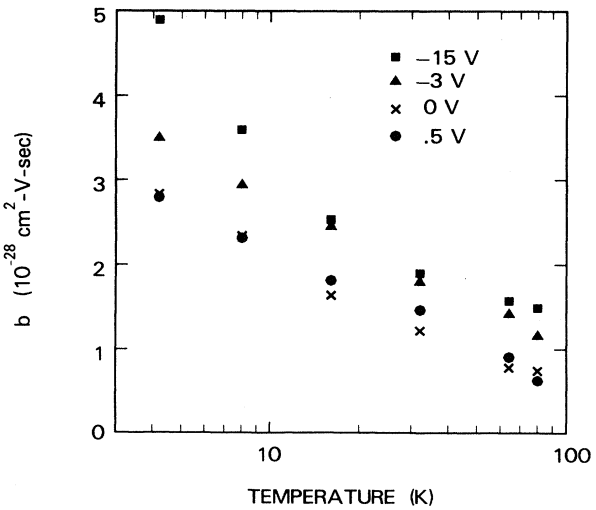

FIG. 54. The coefficient b of the quadratic term, for the same fit described in Fig. 53. These data are for $N_s=2\times10^{12}$ cm^{-2}. After Hartstein *et al.* (1980).

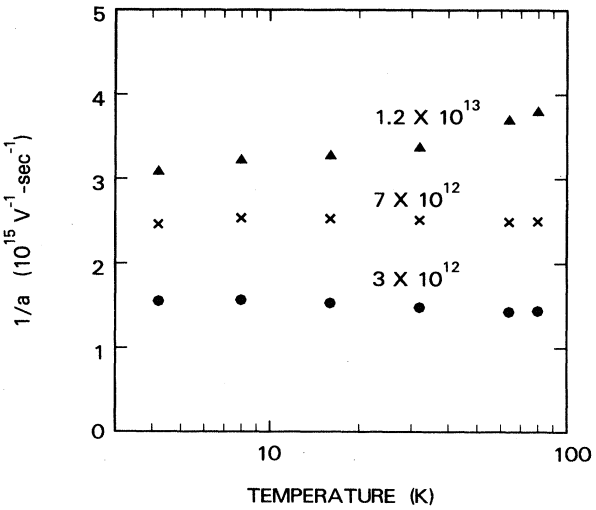

FIG. 55. The temperature dependence of $1/a$, the reciprocal of the linear coefficient, as described in Fig. 53, for three values of N_s. After Hartstein *et al.* (1980).

that this procedure has any simple physical meaning. It may lead to erroneous conclusions if more than one scattering mechanism is involved but, especially when the temperature variations are small, it is convenient. Some of the raw data of Kawaguchi and Kawaji (1980a) are shown in Fig. 56. Kawaguchi and Kawaji (1980a) have, in addition, corrected for the negative magnetoresistance effect, although it is not clear what the justification for so doing is or at least how it should be done properly. The extrapolation to $T=0$ is also dangerous, especially when the logarithmic effects arising from weak localization are important (see Sec. V.B).

Kawaguchi and Kawaji (1980a), using these procedures, found a very strong dependence of $1/\tau_T$ on temperature, which they ascribed to phonon scattering although they remarked that theory predicted a much weaker magnitude of phonon scattering. Cham and Wheeler (1980b) and Kawaguchi *et al.* (1981) found much weaker temperature dependence (about $T^{1.8-2.0}$). The former concluded that the effects arise primarily from the temperature dependence of other mechanisms such as oxide charge scattering and surface roughness scattering. The temperature variation for these processes arises primarily from the temperature dependence of the screening and has been calculated in a simple approximation by Stern (1980b). Stern's calculations for the temperature dependence of impurity scattering have also been compared with the results of Hartstein and Fowler (1980) (see Fig. 55), and good agreement was found for $N_s=3\times10^{11}$ cm^{-2}. All of the experiments discussed above require extreme care in measurement because often the changes with temperature are small. The extraction of the data in terms of $1/\tau_T$ is not straightforward, and the interpretation involves at least oxide charge, surface roughness, and phonon scattering and possibly other scattering mechanisms, so that this problem remains somewhat unresolved. This has a bearing on the weak localization effects discussed in Sec. V.B

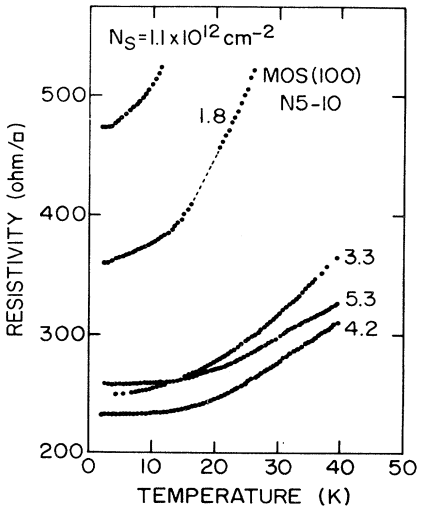

FIG. 56. The temperature dependence of the resistivity of a (100) silicon inversion layer. The parameters are the electron densities N_s. After Kawaguchi and Kawaji (1980a).

Piezoresistance effects have proven a valuable tool for the study of transport at 4.2 K. These have been studied by applying stresses in various ways—most extensively and controllably by bending bar samples (Colman *et al.*, 1968; Dorda, 1971a; Dorda and Eisele, 1973; Dorda *et al.*, 1972a; Eisele *et al.*, 1976a; Eisele, 1978; Gesch *et al.*, 1978), by studying silicon on sapphire (Kawaji *et al.*, 1976), and by using epoxy cements (Fang, 1980). The effects arise primarily because of the displacement of the valleys lying along axes with different orientations to the stress. For the (100) surface a compressive stress along the [010] direction lowers the valleys in that direction relative to the (100) and (001) valleys. Enough stress can lower the (010) and/or (001) valleys which are the subbands with light mass perpendicular to the surface—the primed subbands—below the (100) or unprimed subbands, especially if the surface quantum splittings, $E_0-E_{0'}$, are small (N_s and $N_{\rm depl}$ small). Anisotropy results from such stresses and has been studied by Dorda (1973). Typical results are shown in Fig. 57. The mobility decreases as the electrons transfer to the primed valleys. Dorda and Eisele (1973) have concluded that there may be an intrinsic stress of 80 N mm^{-2}; on the basis of other arguments (Eisele, 1978) they estimate an average stress of 10–50 N mm^{-2}. Nicholas *et al.* (1976) have estimated a stress of 30 N mm^2 using an optical technique. These estimates are for the average macroscopic stress. Local stresses may be higher. The local and macroscopic stresses may vary depending on sample size, oxide thickness, and on whether the sample is free-standing or bonded to a metal or ceramic header. The reader should refer to Sec. VII.B for further relevant comments.

Electron transfer effects are demonstrated if the field-

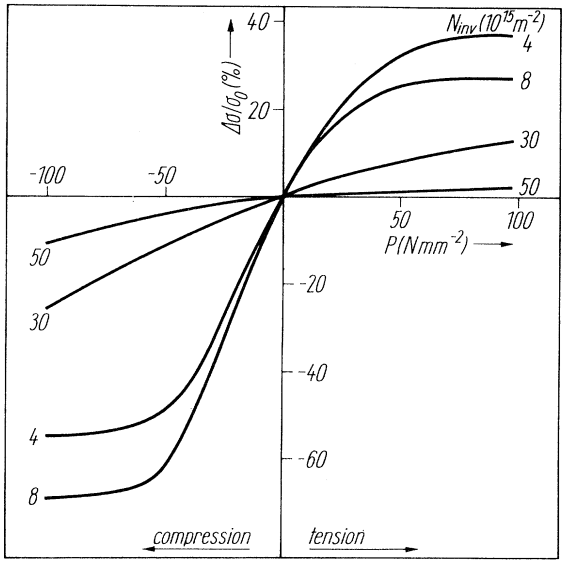

FIG. 57. Relative change of conductivity $\Delta\sigma/\sigma_0$ for a (100) surface with current and strain in the [010] direction at 6.4 K. After Dorda and Eisele (1973).

effect mobility, a derivative, is plotted as a function of N_s at different stresses (Eisele, 1978; Gesch *et al.*, 1978) as shown in Fig. 58 for the case where the current is in the light-mass direction of the (001) subband. The authors interpret the first peak under stress as resulting from transfer of electrons from the (001) to the (100) subbands as the electric field splitting, increasing with N_s, approaches the stress splitting. Presumably the minima occur when all of the electrons are transferred, and the second maxima arise from the usual maxima in mobility as a function of N_s for a single set of subbands. The subband splittings have been estimated from these measurements and are reasonably in agreement with theory (Eisele, 1978). Attempts to fit the transport theory (Takada, 1979), emphasizing the effects of screening, were successful in giving the right shape of the curves, but were badly off in magnitude. Stress effects will be discussed further in Sec. VII.B.

4. 4.2-90 K

Figures 47 and 48 demonstrate some of the complexity of the mobility variation with N_s in the intermediate temperature range. For low N_s ($< 10^{12}$ cm^{-2}, depending on N_{ox} and sample preparation) the conductance may increase rapidly and is probably activated (Fang and Fowler, 1968) (see Sec. V.A). As discussed above, the scattering may increase with temperature in samples with high oxide charge. At the higher temperatures of this range the higher subbands can be occupied (Stern, 1972b). Hartstein, Fowler, and Albert (1980) have attempted to resolve the temperature dependence of the several scattering mechanisms by drifting Na^+ ions to vary the oxide charge scattering and applying Matthiessen's rule, a questionable procedure above 10 K (Stern, 1980b). A slight increase was seen in what they have labeled the surface roughness scattering at high temperatures, which may arise from phonon scattering. The temperature dependence of the impurity scattering coefficient is shown in Fig. 55. The reciprocal of this scattering increases linearly at low N_s and decreases at high N_s.

Figure 47 also shows an interesting feature of the mobility above 4.2 K—an inflection in the mobility versus N_s curve at about 10^{12} cm^{-2} electrons at 77 K. This is most easily observed in the field-effect mobility in samples with low depletion charge, as reported by Fang and Fowler (1968). The dependences on temperature and on substrate bias are shown in Fig. 59 and Fig. 60, respectively. A sharp peak may be seen near threshold at 77 K, which decreases rapidly as the temperature is reduced. This is in a range of N_s where activated conductivity is often ascribed to Anderson localization. This peak is strikingly similar to the peaks observed under pressure by Eisele (1978) in Fig. 58 for samples where stress was used to make $E_{0'} < E_0$ at low N_s. This peak in the data in Fig. 59 may arise from phenomena similar to the stress effects, as suggested by Brews (1975b) and Gesch, Eisele, and Dorda (1978). At 77 K some elec-

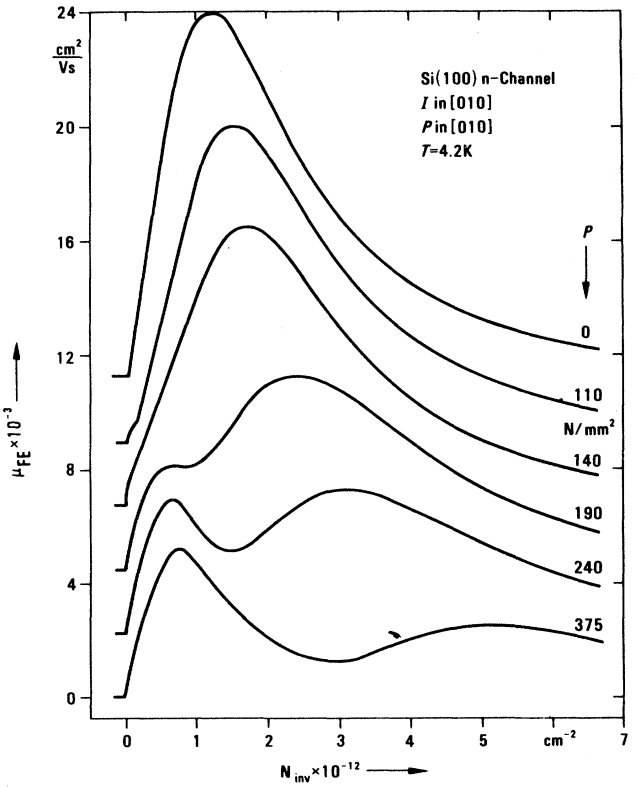

FIG. 58. Field-effect mobility μ_{FE} as a function of N_s under compressive stress at 4.2 K. After Eisele (1978).

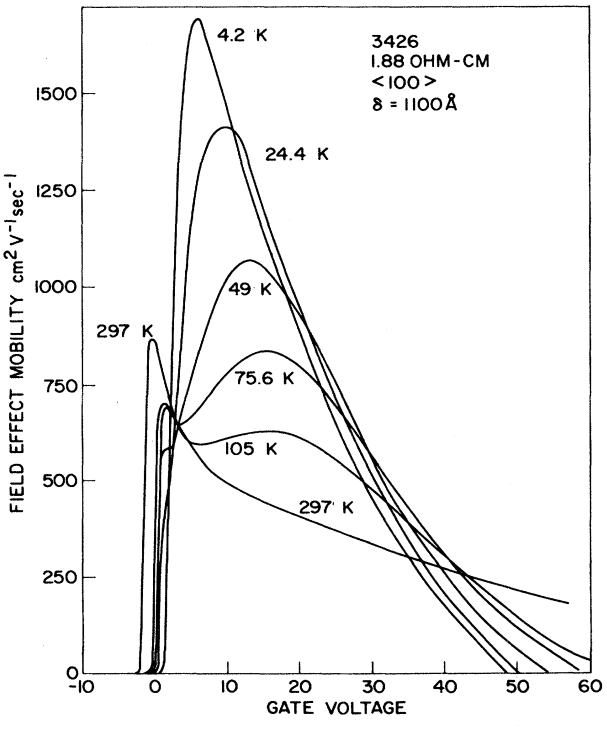

FIG. 59. Field-effect mobility at various temperatures on a (100) surface. After Fang and Fowler (1968).

trons can occupy the fourfold subbands even if they are not lower than the twofold. Gesch *et al.* were able to affect this structure at 77 K under stress. The peaks could be enhanced if there were intrinsic strains in the surface. The common appearance of two and sometimes more peaks might arise from an inhomogeneous strain or from splitting of the (010) and (001) subbands. These peaks are suppressed with substrate bias or as the doping is increased because both increase N_{depl} and therefore $E_{0'}-E_0$. Komatsubara *et al.* (1974) have seen more complex behavior that depends on the samples. They attributed some of the structure to interface bound states. This was later also suggested by Tidey and Stradling (1974). As shown in Fang and Fowler (1968), $d(R_H^{-1})/dV_G$ increases slowly and smoothly through this range in samples where this structure appears, but the Hall mobility shows the same structure as the effective mobility. Trapped electrons would not give the high mobility observed in the first peak. On the other hand, these data could be consistent with a two-band model of the Hall effect.

When these peaks are observed an anomalous magnetoresistance is also seen (Tansal *et al.*, 1969; Sakaki and Sugano, 1969) when the magnetic field lies in the silicon surface. It follows the law $\Delta g/g=\alpha \mathbf{H}\times\mathbf{I}+\beta H^2$. Uemura and Matsumoto (1971) have ascribed the quadratic effect to a diamagnetic shift in the ground-state wave functions, but have not calculated the change in $E_{0'}-E_0$. The direction of the Lorentz-force term is in a direction to increase this splitting and so to transfer electrons to the low-mass valleys.

Clearly the behavior of the transport properties in this range is complex. For a simple comparison with theory it is probably best to work with a maximum subband splitting, which corresponds to large N_{depl}.

5. Other surfaces—*n* channel

We have concentrated on the (100) surface because even with its complexity it is the simplest and the most studied. This does not mean that the other primary surfaces—(110) and (111)—have not received attention and do not have many interesting phenomena associated with them. Indeed, the apparent anomalies in valley degeneracy have been of very great interest. In general, the mobilities on surfaces other than the (100) are lower and, except for the (111), are anisotropic. Sato *et al.* (1972), Sah *et al.* (1972b), and Arnold and Abowitz (1966) have shown that there is a strong correlation with the oxide charge. The field-effect mobility dependence is shown in Fig. 61. Results for planes vicinal to the (100) plane generally show a peak in the field-effect mobility at low N_s at 77 K, but those for the (111) and (110) planes do not. The temperature dependence of μ_{FE} for all planes is similar to that of the (100) surfaces above 77 K. The anisotropies increase as the temperature is reduced (Sato *et al.*, 1971; Sah *et al.*, 1969; Sakaki and Sugano, 1972a).

6. Noise

The subject of noise in metal-insulator-semiconductor devices has a substantial literature that is only partially represented in the bibliography (Abowitz *et al.*, 1967; Aoki *et al.*, 1977; Berz, 1970a, 1975a; Berz and Prior, 1970; Broux *et al.*, 1975; Das and Moore, 1974; Flinn *et al.*, 1967; Fu and Sah, 1972; Jindal and van der Ziel, 1978; Katto *et al.*, 1977; Klaassen, 1971; Nougier *et al.*, 1978; Park *et al.*, 1981; Sato *et al.*, 1969; Vandamme, 1980; Voss, 1977, 1978). Many authors find a correlation between the amount of $1/f$ noise and the density of surface states, but there is no general agreement as to details of mechanisms. Noise is not discussed in any detail

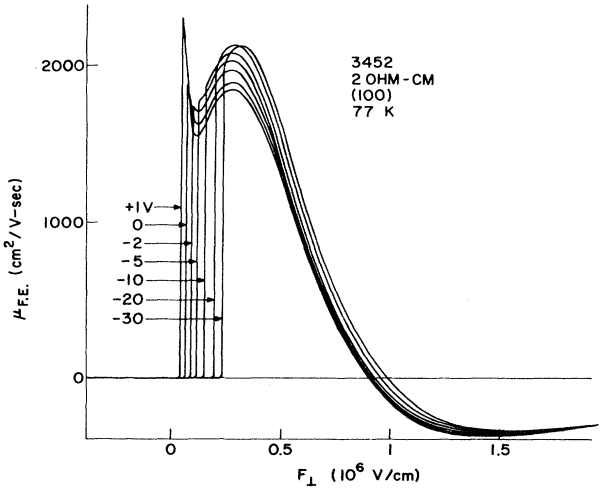

FIG. 60. Field-effect mobility as a function of N_s for varying substrate bias at 77 K for different values of surface electric field F_s (proportional to N_s+N_{depl}). After Fang and Fowler (1968).

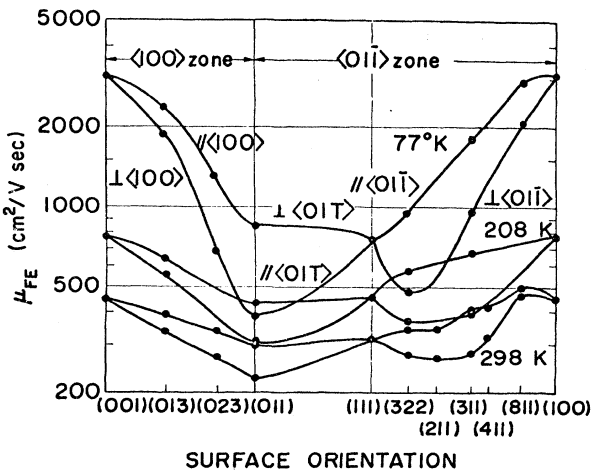

FIG. 61. Dependence of field-effect mobility on surface and current direction at 77, 208, and 298 K for $N_s\cong 3\times 10^{12}$ cm^{-2}. The mobility is highest on the (001) surface, for which the oxide charge is lowest. After Sato *et al.* (1971a).

in this article. For a recent review, see Hooge *et al.* (1981).

C. Scattering mechanisms at low temperatures

1. Coulomb scattering

The scattering from charged centers in the electric quantum limit has been formulated by Stern and Howard (1967). We briefly review the theory in this section. We confine ourselves to the n-channel inversion layer on the Si(100) surface where the Fermi line is isotropic. Let us first calculate the potential of a charged center located at $(\mathbf{r}_i,z_i)$. This problem has been treated in Sec. II.C within the Thomas-Fermi approximation. Here we shall discuss it in a different way which allows the treatment to be readily extended to many-subband cases. Using the usual image method, we have

$$V_i^{(\mu)}(\mathbf{r},z)=\frac{Z^{(\mu)}e^2}{\bar{\kappa}}[(\mathbf{r}-\mathbf{r}_i)^2+(z-z_i)^2]^{-1/2} \tag{4.14}$$

for $z_i<0$, and

$$V_i^{(\mu)}(\mathbf{r})=\frac{Z^{(\mu)}e^2}{\kappa_{sc}}[(\mathbf{r}-\mathbf{r}_i)^2+(z-z_i)^2]^{-1/2} + \frac{(\kappa_{sc}-\kappa_{ins})Z^{(\mu)}e^2}{\kappa_{sc}(\kappa_{sc}+\kappa_{ins})}[(\mathbf{r}-\mathbf{r}_i)^2+(z+z_i)^2]^{-1/2} \tag{4.15}$$

for $z_i>0$. Here, $\bar{\kappa}=(\kappa_{sc}+\kappa_{ins})/2$ and $Z^{(\mu)}$ is the charge of the μth kind of charge center. The effective potential for electrons in the inversion layer in the electric quantum limit is given by

$$v_i^{(\mu)}(\mathbf{r})=\int_0^\infty dz\ |\zeta_0(z)|^2 V_i^{(\mu)}(\mathbf{r},z)\ . \tag{4.16}$$

This can be expressed in a more elegant form in terms of the following two-dimensional Fourier transform. We have

$$v_i^{(\mu)}(\mathbf{r})=\sum_q v_q^{(\mu)}(z_i)\exp[i\mathbf{q}\cdot(\mathbf{r}-\mathbf{r}_i)]\ , \tag{4.17}$$

with

$$v_q^{(\mu)}(z_i)=\frac{2\pi Z^{(\mu)}e^2}{\bar{\kappa}q}F(q,z_i)\ , \tag{4.18}$$

where for $z_i<0$

$$F(q,z_i)=e^{qz_i}\int_0^\infty dz\, e^{-qz}|\zeta_0(z)|^2\ , \tag{4.19}$$

and for $z_i>0$

$$F(q,z_i)=\tfrac{1}{2}\int_0^\infty dz\ |\zeta_0(z)|^2\left[\left[1+\frac{\kappa_{ins}}{\kappa_{sc}}\right]e^{-q|z-z_i|} + \left[1-\frac{\kappa_{ins}}{\kappa_{sc}}\right]e^{-q(z+z_i)}\right]\ . \tag{4.20}$$

The form factor $F(q,z_i)$ becomes unity in the limit of vanishing q. The screening effect can be included within the linear approximation by dividing $v_q^{(\mu)}(z_i)$ by the dielectric constant $\varepsilon(q)$ with

$$\varepsilon(q)=1+\frac{2\pi e^2}{\bar{\kappa}q}F(q)\Pi(q)\ , \tag{4.21}$$

where $\Pi(q)$ is the static polarization part defined by Eq. (2.56) and $F(q)$ is the form factor for electron-electron interactions given by Eq. (2.51).

In the Born approximation the transport relaxation time is given by

$$\frac{1}{\tau(\varepsilon(k))}=\frac{2\pi}{\hbar}\sum_{k'}\sum_{\mu}\int_{-\infty}^{\infty}N_i^{(\mu)}(z)dz\ |v_{\mathbf{k}-\mathbf{k}'}^{(\mu)}(z)|^2 \times(1-\cos\theta_{\mathbf{k}\mathbf{k}'})\delta(\varepsilon(k)-\varepsilon(k'))\ , \tag{4.22}$$

where $N_i^{(\mu)}(z)dx\,dy\,dz$ is the concentration of the μth kind of charged center within the volume $dx\,dy\,dz$, $\theta_{\mathbf{k}\mathbf{k}'}$ is the angle between the vectors $\mathbf{k}$ and $\mathbf{k}'$, and $\varepsilon(k)=\hbar^2k^2/2m_t$. We have assumed that the charged centers are distributed completely at random in the plane parallel to the surface. The mobility is given by

$$\mu=\frac{e}{m_t}\langle\tau\rangle\ , \tag{4.23}$$

with

$$\langle\tau\rangle=\frac{\sum_k\varepsilon(k)\tau(\varepsilon(k))\left[-\frac{\partial f}{\partial\varepsilon(k)}\right]}{\sum_k\varepsilon(k)\left[-\frac{\partial f}{\partial\varepsilon(k)}\right]}\ , \tag{4.24}$$

where $f(\varepsilon(k))$ is the Fermi distribution function. At sufficiently low temperatures we have $\langle\tau\rangle=\tau(E_F)$, with E_F being the Fermi energy.

There are two cases where we can get explicit expressions of the form factors. The simplest case is the two-dimensional limit, defined by

$$|\zeta_0(z)|^2=\delta(z)\ . \tag{4.25}$$

We have

$$F(q,z_i)=e^{-q|z_i|}\ , \tag{4.26}$$

corresponding to

$$v_i^{(\mu)}(\mathbf{r})=\frac{Z^{(\mu)}e^2}{\bar{\kappa}}[(\mathbf{r}-\mathbf{r}_i)^2+z_i^2]^{-1/2}\ . \tag{4.27}$$

If we use the usual variational wave function (3.25), we can express the form factor for $z_i<0$ as

$$F(q,z_i)=P_0e^{qz_i}\ , \tag{4.28}$$

and for $z_i>0$ as

$$F(q,z_i)=\frac{1}{2}\left[1+\frac{\kappa_{ins}}{\kappa_{sc}}\right]P(z_i)+\frac{1}{2}\left[1-\frac{\kappa_{ins}}{\kappa_{sc}}\right]P_0e^{-qz_i}\ , \tag{4.29}$$

where P_0 and $P(z)$ are given by Eqs. (2.21) and (2.23), respectively.

The important length in the scattering is $1/k_F$. As is clear from Eqs. (4.19) and (4.20), charged centers which contribute to scattering are limited by the condition $|z_i| < 1/k_F$. (If $\langle z \rangle > 1/k_F$ for $z_i > 0$, the thickness of the inversion layer $\langle z \rangle$ determines the region of z_i instead of $1/k_F$. Usually, however, $\langle z \rangle < 1/k_F$.) The value of $1/k_F$ is typically 100 Å around $N_s = 10^{12}$ cm^{-2}. Many charged centers can contribute to scattering at low electron concentrations, but only a small number of centers, especially ones which are located near the interface, contribute to it at high electron concentrations. Usually the charged acceptors in the bulk silicon play little role as scatterers except at extremely small electron concentrations. For bulk doping of 10^{16} cm^{-3}, for example, there are only $\sim 10^{10}$ cm^{-2} acceptors within 100 Å from the interface. This density is very small and there are many more oxide charges at or near the interface in most samples.

In the random-phase approximation we have (Stern, 1967)

$$\Pi(q) = \frac{2g_v m_t}{2\pi\hbar^2}\left\{1-\theta(q-2k_F)\left[1-\left[\frac{2k_F}{q}\right]^2\right]^{1/2}\right\}, \tag{4.30}$$

where $\theta(x)$ is the usual step function [$\theta(x)=1$ for $x>0$ and $\theta(x)=0$ for $x<0$] and g_v is the valley degeneracy factor. Thus the effective potential becomes

$$v_q^{(\mu)}(z_i) = \frac{2\pi Z^{(\mu)} e^2}{\bar{\kappa}(q+\bar{q}_s F(q))} F(q,z_i), \tag{4.31}$$

where $\bar{q}_s$ is the Thomas-Fermi screening constant given by $\bar{q}_s = 2\pi e^2 \Pi(0)/\bar{\kappa} = 2g_v m e^2/\bar{\kappa}\hbar^2$. We see that $1/\bar{q}_s$ is of the order of 5 Å and much smaller than $1/k_F$. Therefore the screening dominates the strength of scattering, and the ratio of the form factors $F(q,z_i)/F(q)$ determines the dependence of the mobility limited by the Coulomb scattering on the electron concentration. Since $F(q,z_i)$ decreases much more rapidly than $F(q)$ with increasing q for $z_i < 0$, the net effective mobility increases with the increase of the electron concentration at low temperatures. Further, the actual mobility is sensitive to the distance of the charged centers from the interface and decreases rather rapidly with increasing distances. A possible distribution of charged centers in the z direction causes an additional dependence.

As has been discussed in Sec. IV.B, Hartstein, Ning, and Fowler (1976) and Hartstein, Fowler, and Albert (1980) extensively studied the mobility limited by the Coulomb scattering. They varied oxide charges controllably by drifting sodium ions through the oxide to the interface. The numbers of ions which were believed to be just at the interface (within a few angstroms from the interface) were counted by measuring the shift of the conduction threshold. Hartstein *et al.* determined the mobility which depended on the concentration of the ions. An example of their results is shown in Fig. 62, together with theoretical results for two different values of N_{depl}. The theoretical result has been obtained in the electric quantum limit, i.e., by assuming that only the ground electric subband is occupied by electrons. An example calculated by Stern (1978a) is also shown. He considered graded interface effects, which tend to shift the electrons to the oxide more than in the case of a sharp interface and give larger effects of scattering at high electron concentrations. The agreement is reasonable except for some differences at low and extremely high electron concentrations.

In spite of such good agreement there are several problems with the theory of the mobility mentioned above. We have used the Born approximation for the calculation of the scattering strength. Stern and Howard (1967) studied higher-order effects in the simplest two-dimensional limit, using the phase-shift method. Roughly speaking, higher-order effects tend to increase the scattering in case of attractive scatterers, since the wave function tends to have a large amplitude around the position of charged centers. Effects are opposite for repulsive scatterers. There has been no such investigation for more realistic potentials, but we expect that the Born approximation works quite well actually because the effective scattering potential becomes much smaller in actual inversion layers than that in the two-dimensional limit.

The effects of exchange and correlation on the screening pose a problem. As has been shown in Sec. III.B, the exchange-correlation effect is important in determining the subband structure. The same is expected to hold for the screening effect. Maldague (1978a) studied the exchange effect on the dielectric function and found an

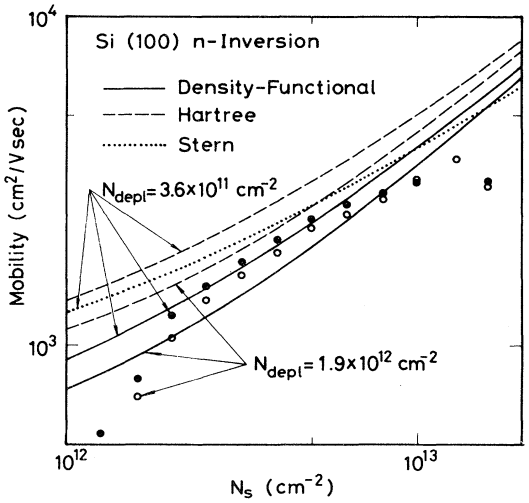

FIG. 62. Mobilities limited by charges at the Si-SiO_2 interface ($N_{ox} = 1\times10^{12}$ cm^{-2}) calculated in the linear screening approximation. The solid lines represent the results calculated with exchange-correlation effects included, the dashed lines those calculated in the random-phase (Hartree) approximation, and the dotted curve that of Stern (1978a), who took into account effects of interface grading. Experimental results of Hartstein, Ning, and Fowler (1976) are also shown.

increase of the polarization part with q, in contrast to the constant value in the random-phase approximation, and sharp structure at $q=2k_F$. Such a sharp structure disappears in actual systems because of the broadening effect and higher-order correlation effects, but the increasing polarization part and consequently the increasing dielectric function remains valid. If we go beyond the random-phase approximation, however, the simple replacement of the impurity potential by a screened potential is not sufficient, and we have to take into account the so-called vertex correction. An example of mobilities calculated in the density-functional formulation (Ando, unpublished) is also shown in Fig. 62. If account is taken of the exchange and the correlation, electrons do not experience so much repulsive force due to other electrons and consequently feel impurity potentials more strongly. Thus the mobility decreases. The agreement seems to become better.

There is a more serious question on the linear screening approximation. It is known that any attractive potential has a bound state in two dimensions, in contrast to three dimensions (see Sec. II.E). Thus the potential of charged centers can have a bound state after being screened by free electrons. In this case the linear screening might no longer be valid, and we have to calculate the total potential self-consistently, although the difference in the effective potential and consequently in the value of the mobility might be expected to be not so large if the binding is weak. Takada (1979) calculated the binding energy and effective potential assuming a variational wave function of a bound electron and taking into account the effect of other free electrons in the linear screening approximation. This method is too crude and tends to overestimate effects of screening, since orthogonalization of the wave functions of extended states to those of the localized states is completely neglected. Therefore, it gives too large values of the mobility. Vinter (1978, 1980) studied this problem in a density-functional formulation. He calculated the energy for cases of different numbers of bound electrons and showed that the case in which four electrons are bound in a single level is the only self-consistent solution. The binding energy he obtained is less than 1 meV and slightly increases with increasing electron concentration. The resulting mobility has turned out to be very close to the corresponding result of the linear screening approximation shown in Fig. 62. A plausible reason for the fourfold occupancy of a single bound state is as follows: Because of the strong screening by free electrons, the potential due to a point charge near the interface has a short-range attractive part and an additional oscillatory part at large distances. The binding energy is small and the wave function of the bound state is much extended. Suppose that a single electron is bound in this bound state. The bound charge gives only a slowly-varying repulsive potential that can easily be screened out by other free electrons. Therefore, the resulting potential has a large short-range attractive part which can bind another electron of different spin or different valley. This continues until the bound state can contain no more electrons because of the Pauli exclusion principle.

At lower electron concentrations like $N_s \sim 10^{12}$ cm^{-2}, the broadening $\hbar/\tau$ is rather comparable to the Fermi energy; the simple Boltzmann transport equation is no longer valid, and multiple-scattering effects become important. The experimental analysis by Hartstein *et al.* (1976) assumed that the change in the inverse of the mobility due to N_{ox} is linear in N_{ox}. Subsequent more careful analysis by Hartstein *et al.* (1980) seems to show that the results deviate from the linear relationship at low electron concentrations, where $1/k_F$ becomes comparable to distances between charged centers. At still lower concentrations the conductivity becomes activated and electronic states are believed to be localized. Therefore the deviation from the above simple theory is not surprising. At extremely high electron concentrations like $N_s > 10^{13}$ cm^{-2}, higher electric subbands are occupied by electrons, and we have to consider the problem of multisubband transport. This problem will be discussed in Sec. IV.C.3.

There have been various investigations of the behavior of the mobility with the increase of temperature. There might be two different regions of temperature, where the mobility shows different temperature dependence. At sufficiently high temperatures, around room temperature, the screening effect is already very small, and the mobility would be expected to increase roughly in proportion to k_BT (in the absence of phonon scattering) because of the q-dependence of the Coulomb scattering matrix element. There might also be additional temperature dependence which arises from the form factor and distribution of charges in the oxide. At lower temperatures, around nitrogen temperature, the screening effect is still appreciable and the dependence becomes complicated. The increase of the kinetic energy of electrons tends to reduce the scattering but at the same time reduces the screening effect. Therefore the actual temperature dependence is determined by the relative importance of these two effects. The original experiments of Fang and Fowler (1968) showed that the mobility, except at low electron concentrations, decreased with increasing temperature. At low concentrations the mobility showed an increase with temperature, but this was considered to be due to thermal excitation of electrons from localized to extended states. Sah, Ning, and Tschopp (1972b) argued that the increase of the mobility observed by them at low electron concentrations could be explained by the decrease in Coulomb scattering with temperature. However, they neglected the screening effect and the possibility of electron localization. Experiments of Komatsubara *et al.* (1974) showed the decrease of the mobility except for a very peculiar temperature dependence at extremely low electron concentrations. More recently the temperature dependence of the mobility at relatively low temperatures has attracted much attention. Kawaguchi and Kawaji (1980a; see also Kawaguchi *et al.*, 1980) ascribed a part of the observed resistivity dependence on temperature to acoustic-phonon scattering (see Sec. IV.D for more discussion). Hartstein *et al.* (1980) separated contributions

from controllable Na^+ ions and showed that the mobility associated with scattering from the ions decreases with increasing temperature at relatively low electron concentrations. Cham and Wheeler (1980a) also reported a decrease of the mobility. Stern (1978a) calculated the mobility limited by the Coulomb scattering at 4.2 and 77 K and demonstrated that the decrease of the screening effect is much more important and reduces the mobility between these temperatures. A later more systematic calculation (Stern, 1980b) showed that the reciprocal of the mobility has a term roughly linear in T below 80 K. This agrees with extensive measurements by Cham and Wheeler (1980b) for samples containing a large number of interface charges. The large change in the mobility with temperature thus obtained roughly accounts for most of the temperature dependence observed by Kawaguchi and Kawaji (1980a) and by Hartstein *et al.* (1980), although there remain disagreements concerning detailed dependence on the temperature. Stern has demonstrated further that a strong energy dependence of the relaxation time makes simple separation of the resistivity into different contributions no longer valid at elevated temperatures (Fig. 63), as in three dimensions.

2. Surface roughness scattering

Surface asperities at the $Si\text{-}SiO_2$ interface are considered to be inherent to space-charge layers and are expected to constitute a major cause of scattering, especially at high electron concentrations. Since their exact nature is not yet known, this surface roughness scattering—also called interface roughness scattering or simply roughness scattering—has been studied theoretically within a simple model. This model assumes an infinite barrier at the interface, whose position $z=\Delta(\mathbf{r})$ may have a small and slowly varying displacement. Classically when quantization of the electron motion in the z direction is not important, scattering due to the surface has customarily been treated by a boundary condition on the electron distribution function, following the initial work of Schrieffer (1957). He assumed diffuse scattering at the surface. More generally, the so-called Fuchs (1938) parameter p phenomenologically describes intermediate cases between diffuse scattering ($p=0$) and specular reflection ($p=1$). This is defined by the boundary condition for the electron distribution function at $z=0$, through

$$f_1(v_z)=pf_1(-v_z)\,, \tag{4.32}$$

where f_1 is the nonequilibrium part of the electron distribution function and v_z is the velocity component perpendicular to the surface (see, for example, review papers by Greene, 1969a, 1969b, 1974, 1975). We do not go into the discussion of this classical case but confine ourselves to the case of the inversion layer at low temperatures, where the electron motion is quantized. The scattering of electrons from such roughness in quantized subbands was first theoretically studied by Prange and Nee (1968) for magnetic surface states in metals, and by many people for thin films. Later many authors tried to apply this model to the inversion layer problem (Cheng, 1971, 1972, 1973b, 1974; Cheng and Sullivan, 1973a–1973c; Matsumoto and Uemura, 1974), but a more complete theory has appeared relatively recently,

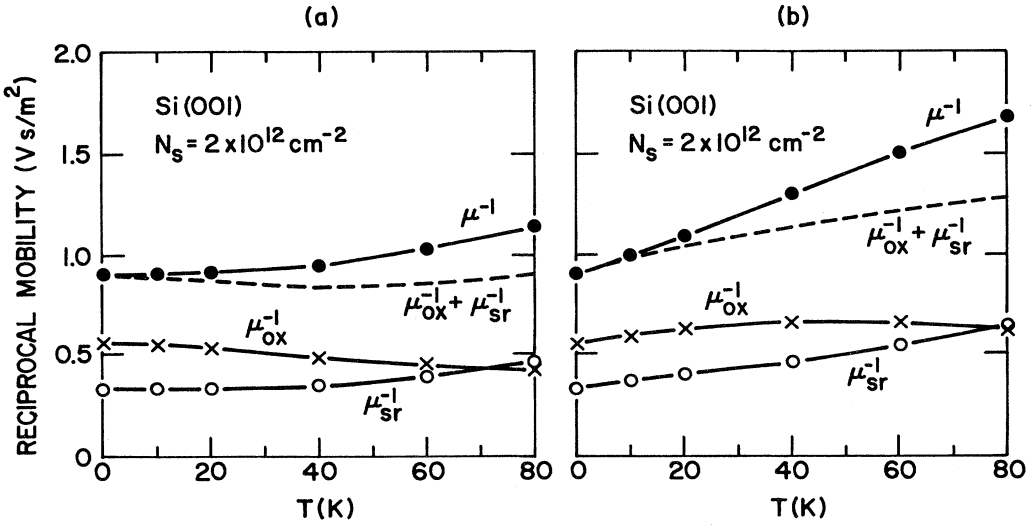

FIG. 63. Temperature dependence of reciprocal mobility for a silicon inversion layer, with all electrons assumed to be in the lowest subband, with (a) the long-wavelength limit for the temperature-dependent screening parameter and (b) the full wave-vector dependence. Results are shown for oxide charge scattering alone (μ_{ox}), surface roughness scattering alone (μ_{sr}), and for the sum of the two mechanisms (μ). The difference between the upper full curve and the dashed curve shows the departure from Matthiessen's rule. The mobility limited by surface roughness has been calculated without $\Delta V(\mathbf{r},z)$ (see Sec. IV.C.2). After Stern (1980b).

even within such a simple model (Ando, 1977d). In the following a brief review of the theory is given. We again restrict ourselves to the n-channel inversion layer on the Si(100) surface.

When energy separations between different subbands are sufficiently large and the change in the form of the wave function can be neglected, the effect of surface roughness is calculated to lowest order from the matrix element as follows:

$$V^{\mathrm{SR}}_{n\mathbf{k}n'\mathbf{k}'}=\int dz\int d\mathbf{r}\,L^{-1/2}e^{-i\mathbf{k}\cdot\mathbf{r}}\{\zeta_n^*(z-\Delta(\mathbf{r}))[\mathscr{H}_0+\Delta V(\mathbf{r},z)]\zeta_{n'}(z-\Delta(\mathbf{r}))-\zeta_n^*(z)\mathscr{H}_0\zeta_{n'}(z)\}L^{-1/2}e^{i\mathbf{k}'\cdot\mathbf{r}}$$
$$=\int dz\int d\mathbf{r}\,L^{-1/2}e^{-i\mathbf{k}\cdot\mathbf{r}}\left[\frac{d\zeta_n^*}{dz}\Delta(\mathbf{r})\frac{\mathbf{p}^2}{2m_t}\zeta_{n'}-\zeta_n^*\frac{\mathbf{p}^2}{2m_t}\Delta(\mathbf{r})\frac{d\zeta_{n'}}{dz}+\Delta(\mathbf{r})\frac{\partial V}{\partial z}\zeta_n^*\zeta_{n'}+\zeta_n^*(z)\Delta V(\mathbf{r},z)\zeta_{n'}(z)\right]L^{-1/2}e^{i\mathbf{k}'\cdot\mathbf{r}}\,, \tag{4.33}$$

where $\mathscr{H}_0$ is the Hamiltonian in the absence of surface roughness and $\Delta V(\mathbf{r},z)$ describes the change in the potential energy due to surface roughness. For a matrix element between states with the same energy, we have

$$V^{\mathrm{SR}}_{n\mathbf{k}n'\mathbf{k}'}=\frac{\hbar^2}{2m_l}\Delta_{\mathbf{k}-\mathbf{k}'}\frac{d\zeta_n^*}{dz}\frac{d\zeta_{n'}}{dz}\bigg|_{z=0}+\int dz\int d\mathbf{r}\,e^{-i(\mathbf{k}-\mathbf{k}')\cdot\mathbf{r}}\zeta_n^*(z)\Delta V(\mathbf{r},z)\zeta_{n'}(z)\,, \tag{4.34}$$

where

$$\Delta(\mathbf{r})=\sum_q\Delta_q e^{i\mathbf{q}\cdot\mathbf{r}}\,, \tag{4.35}$$

and we have used the identity:

$$\frac{\hbar^2}{2m_l}\frac{d\zeta_n^*}{dz}\frac{d\zeta_n'}{dz}\bigg|_{z=0}=\int dz\left[\zeta_n^*\frac{\partial V}{\partial z}\zeta_{n'}-E_{n'}\frac{d\zeta_n^*}{dz}\zeta_{n'}+E_n\zeta_n^*\frac{d\zeta_{n'}}{dz}\right], \tag{4.36}$$

which can easily be proved by taking a matrix element of the commutator:

$$[p_z,\mathscr{H}_0]=\frac{\hbar}{i}\frac{\partial V(z)}{\partial z}\,. \tag{4.37}$$

The first term of Eq. (4.34) is the result of Prange and Nee (1968). In the electric quantum limit we have (Matsumoto, unpublished)

$$V^{\mathrm{SR}(1)}_{\mathbf{k}\mathbf{k}'}=\frac{\hbar^2}{2m_l}\Delta_{\mathbf{k}-\mathbf{k}'}\left|\frac{d\zeta_0}{dz}\right|^2 \tag{4.38}$$

$$=\Delta_{\mathbf{k}-\mathbf{k}'}\int_0^\infty dz\,|\zeta_0(z)|^2\frac{\partial V}{\partial z} \tag{4.39}$$

$$=\Delta_{\mathbf{k}-\mathbf{k}'}\left[\frac{4\pi e^2}{\kappa_{\mathrm{sc}}}\left[\frac{1}{2}N_s+N_{\mathrm{depl}}\right]-\frac{(\kappa_{\mathrm{sc}}-\kappa_{\mathrm{ins}})e^2}{4\kappa_{\mathrm{sc}}(\kappa_{\mathrm{sc}}+\kappa_{\mathrm{ins}})}\left\langle\frac{1}{z^2}\right\rangle\right]. \tag{4.40}$$

Equations (4.38) and (4.39) are completely equivalent if we use an exact self-consistent wave function. In the case of variational wave functions, however, we should use Eq. (4.39) rather than (4.38), since it gives the exact result (4.40), while (4.38) does not. For example, if we use the variational wave function (3.25) in Eq. (4.38), the inadequate value of the derivative at $z=0$ gives a wrong dependence on N_s and N_{depl}, as shown by Matsumoto and Uemura (1974).

Next we consider the potential $\Delta V(\mathbf{r},z)$. We first assume that $\Delta(\mathbf{r}',z)>0$ to calculate $\Delta V(\mathbf{r},z)$. The other case can be treated in a similar manner. The change in the electron density distribution,

$$n[z-\Delta(\mathbf{r})]-n(z)=-\Delta(\mathbf{r})\frac{\partial n(z)}{\partial z}\,, \tag{4.41}$$

gives the potential at $(\mathbf{r},z)$ $(z>0)$,

$$-\frac{e^2}{\kappa_{\mathrm{sc}}}\int d\mathbf{r}'\int dz'[(\mathbf{r}-\mathbf{r}')^2+(z-z')^2]^{-1/2}\Delta(\mathbf{r}')\frac{\partial n(z')}{\partial z'}-\frac{(\kappa_{\mathrm{sc}}-\kappa_{\mathrm{ins}})e^2}{\kappa_{\mathrm{sc}}(\kappa_{\mathrm{sc}}+\kappa_{\mathrm{ins}})}\int d\mathbf{r}\int dz[(\mathbf{r}-\mathbf{r}')^2+(z+z')^2]^{1/2}\Delta(\mathbf{r}')\frac{\partial n(z')}{\partial z'}$$
$$=-\sum_q\frac{2\pi e^2}{\kappa_{\mathrm{sc}}q}\Delta_q e^{i\mathbf{q}\cdot\mathbf{r}}\int dz'e^{-q|z-z'|}\frac{\partial n(z')}{\partial z'}-\sum_q\frac{2\pi(\kappa_{\mathrm{sc}}-\kappa_{\mathrm{ins}})e^2}{\kappa_{\mathrm{sc}}(\kappa_{\mathrm{sc}}+\kappa_{\mathrm{ins}})q}\Delta_q e^{i\mathbf{q}\cdot\mathbf{r}}\int dz'e^{-q(z+z')}\frac{\partial n(z')}{\partial z'}\,. \tag{4.42}$$

The deformed Si-SiO_2 interface gives an effective dipole moment at $z=0$,

$$p_z(\mathbf{r}')=-\frac{\kappa_{\mathrm{sc}}-\kappa_{\mathrm{ins}}}{4\pi}\frac{4\pi e}{\kappa_{\mathrm{ins}}}(N_s+N_{\mathrm{depl}})\Delta(\mathbf{r}')d\mathbf{r}'\,, \tag{4.43}$$

which gives the potential

$$\frac{1}{\kappa_{sc}}\left(1-\frac{\kappa_{sc}-\kappa_{ins}}{\kappa_{sc}+\kappa_{ins}}\right)p_z(\mathbf{r}')z[(\mathbf{r}-\mathbf{r}')^2+z^2]^{-3/2}\,. \tag{4.44}$$

Thus we have the potential modification

$$\sum_q \frac{4\pi e^2(\kappa_{sc}-\kappa_{ins})}{\kappa_{sc}(\kappa_{sc}+\kappa_{ins})}(N_s+N_{depl})\Delta_q e^{i\mathbf{q}\cdot\mathbf{r}}e^{-qz}\,. \tag{4.45}$$

The image potential is also modified. An electron existing at $(\mathbf{r},z)$ $(z>0)$ causes an extra polarization at the deformed interface. The extra dipole moment is given by

$$\mathbf{p}(\mathbf{r}')=-\frac{e}{2\pi}\frac{\kappa_{sc}-\kappa_{ins}}{\kappa_{sc}+\kappa_{ins}}\Delta(\mathbf{r}')d\mathbf{r}'\frac{\mathbf{r}-\mathbf{r}'}{[(\mathbf{r}-\mathbf{r}')^2+z^2]^{3/2}}\,. \tag{4.46}$$

The dipole in the z direction, $p_z(\mathbf{r}')$, is obtained by replacing $\mathbf{r}-\mathbf{r}'$ by z in (4.46). This dipole moment gives rise to the potential at $(\mathbf{r},z)$

$$(-e)\left[\frac{1}{\kappa_{sc}}\frac{\mathbf{p}\cdot(\mathbf{r}-\mathbf{r}')+p_z z}{[(\mathbf{r}-\mathbf{r}')^2+z^2]^{3/2}}+\frac{1}{\kappa_{sc}}\frac{\kappa_{sc}-\kappa_{ins}}{\kappa_{sc}(\kappa_{sc}+\kappa_{ins})}\frac{\mathbf{p}\cdot(\mathbf{r}-\mathbf{r}')-p_z z}{[(\mathbf{r}-\mathbf{r}')^2+z^2]^{3/2}}\right]. \tag{4.47}$$

Thus we have the modification of the potential energy,

$$\frac{(\kappa_{sc}-\kappa_{ins})e^2}{4\kappa_{sc}(\kappa_{sc}+\kappa_{ins})}\sum_q \Delta_q e^{i\mathbf{q}\cdot\mathbf{r}}q^2\left[\frac{K_1(qz)}{qz}-\frac{1}{2}\frac{\kappa_{sc}-\kappa_{ins}}{\kappa_{sc}+\kappa_{ins}}K_0(qz)\right], \tag{4.48}$$

where K_0 and K_1 are the modified Bessel functions and we have multiplied by a factor of $\frac{1}{2}$ in Eq. (4.48) because the image potential is a self-energy. The final $\Delta V(\mathbf{r},z)$ can be obtained by adding all these terms. In the electric quantum limit, we have

$$V^{SR}_{\mathbf{k}\mathbf{k}'}=V^{SR}_{0\mathbf{k}0\mathbf{k}'}=\Delta_{\mathbf{k}-\mathbf{k}'}\Gamma(|\mathbf{k}-\mathbf{k}'|)\,, \tag{4.49}$$

with

$$\Gamma(q)=\gamma(q)+\gamma_{image}(q)\,, \tag{4.50}$$

where

$$\gamma(q)=\frac{4\pi e^2}{\bar{\kappa}}(\tfrac{1}{2}N_s+N_{depl})+\frac{2\pi e^2(\kappa_{sc}-\kappa_{ins})}{\kappa_{sc}(\kappa_{sc}+\kappa_{ins})}N_s\left[1-\left[\int_0^\infty dz\,|\xi_0|^2e^{-qz}\right]^2\right]$$
$$-\frac{4\pi e^2(\kappa_{sc}-\kappa_{ins})}{\kappa_{sc}(\kappa_{sc}+\kappa_{ins})}(N_s+N_{depl})\left[1-\int_0^\infty dz\,|\xi_0|^2e^{-qz}\right], \tag{4.51}$$

and

$$\gamma_{image}(q)=\frac{(\kappa_{sc}-\kappa_{ins})e^2}{\kappa_{sc}(\kappa_{sc}+\kappa_{ins})}q^2\int_0^\infty dz\,|\xi_0(z)|^2\left[\frac{K_1(qz)}{qz}-\frac{1}{(qz)^2}-\frac{1}{2}\frac{\kappa_{sc}-\kappa_{ins}}{\kappa_{sc}+\kappa_{ins}}K_0(qz)\right]. \tag{4.52}$$

We have

$$\gamma(q)=\frac{4\pi e^2}{\bar{\kappa}}(\tfrac{1}{2}N_s+N_{depl}) \tag{4.53}$$

for $q\to 0$ and

$$\gamma(q)=\frac{4\pi e^2}{\kappa_{sc}}(\tfrac{1}{2}N_s+N_{depl}) \tag{4.54}$$

for sufficiently large q. The factor $\frac{1}{2}$ of the term including N_s in Eqs. (4.53) and (4.54), first derived by Matsumoto and Uemura (1974), has a simple physical meaning. This term describes the effective electric field which arises from N_s positive charges at the gate electrode and $-N_s$ negative charges of electrons in the inversion layer. The average value of the field due to electrons themselves vanishes because electron-electron interactions are an internal force. Only the field due to positive charges at the gate electrode contribute to the field, which gives the difference of the factor $\frac{1}{2}$ from the term proportional N_{depl}. The image term vanishes for small q, since a uniform displacement of the interface does not give rise to the change in the image potential which an electron feels.

The relaxation time is given by

$$\frac{1}{\tau_{SR}(\varepsilon(k))}=\frac{2\pi}{\hbar}\sum_{k'}\langle|\Delta_{\mathbf{k}-\mathbf{k}'}|^2\rangle\left[\frac{\Gamma(\mathbf{k}-\mathbf{k}')}{\varepsilon(\mathbf{k}-\mathbf{k}')}\right]^2$$
$$\times(1-\cos\theta_{\mathbf{k}\mathbf{k}'})\delta(\varepsilon(k)-\varepsilon(k'))\,, \tag{4.55}$$

where we have included the screening effect in the linear approximation. The mobility decreases in proportion to N_s^{-2} at high electron concentrations, which explains the usual behavior of experimental mobilities. Although there is no definite physical ground, we usually assume a Gaussian form of the correlation of the surface roughness:

$$\langle \Delta(\mathbf{r})\Delta(\mathbf{r}')\rangle = \Delta^2 \exp\left[\frac{(\mathbf{r}-\mathbf{r}')^2}{\Lambda^2}\right], \tag{4.56}$$

where Δ is the average displacement of the interface and Λ is of the order of the range of its spatial variation in the direction parallel to the surface. Then we have

$$\langle |\Delta_q|^2\rangle = \pi\Delta^2\Lambda^2 \exp\left[-\frac{q^2\Lambda^2}{4}\right]. \tag{4.57}$$

For values of parameters usually used, this Gaussian form of the correlation is not important as long as Λ is not so large, and the product $\Lambda\Delta$ is an important parameter which determines the value of the mobility. Since the image effect is small, the dependence of τ_{SR}^{-1} on N_s and N_{depl} is determined by $(N_s+2N_{depl})^2$ and the form factor $F(q)$ of the screening function $\varepsilon(q)$. Since the form factor becomes larger with increasing N_{depl}, the effect of N_{depl} becomes smaller than that given by $(N_s+2N_{depl})^2$ if we take into account the screening effect. An example of the calculated mobility limited by the surface roughness scattering is shown in Fig. 64 together with experimental results of Hartstein *et al.* (1976). To explain the experimental results we need roughness of the order of $\Delta\sim 4.3$ A and $\Lambda\sim 15$ A. We cannot choose larger values of Λ, because the scattering effect becomes ineffective at high electron concentrations and the calculated N_s dependence of the mobility deviates from experimental N_s dependence if Λ becomes comparable to $1/k_F$. The existence of surface roughness of such magnitude is considered to be reasonable. Hartstein *et al.* (1976) experimentally subtracted the contribution of scattering from charged centers and showed that the dependence of the mobility on N_s and N_{depl} was given by $(N_s+N_{depl})^2$ rather than $(N_s+2N_{depl})^2$. Because of the screening effect the theoretical result shows weaker dependence on N_{depl}, but seems to deviate from the experimental results at very high electron concentrations above $N_s\sim 7\times 10^{12}$ cm^{-2}. At higher electron concentrations, however, higher subbands are occupied by electrons, and the above simple result cannot directly be applicable. This problem will be discussed in Sec. IV.C.3.

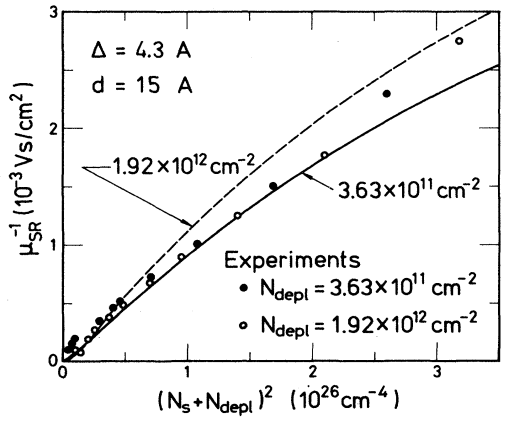

FIG. 64. Calculated mobility limited by surface roughness scattering and examples of experimental results (Hartstein *et al.*, 1976) for two different values of depletion charges. The lateral decay length (Λ in the text) is denoted as d in the figure. After Ando (1977d).

Although the simple theoretical model described above seems to explain the experimental results reasonably well, there are several problems on the theoretical side. The validity of the expansion in terms of Δ is one of them and has not been fully elucidated yet. The first term of Eq. (4.34) can also be obtained more simply by treating modification of the interface barrier as a perturbation (Ando, 1977d). We assume a finite interface barrier $V_0\theta(-z+\Delta(\mathbf{r}))$ and the same effective mass m_l also for $z<0$ for simplicity. The perturbation is given by $V_0\theta(-z+\Delta(\mathbf{r}))-V_0\theta(-z)=V_0\Delta(\mathbf{r})\delta(z)$. For sufficiently large V_0 the wave function near $z=0$ is given by

$$\zeta_n(z)=\left[\frac{\hbar^2}{2m_lV_0}\right]^{1/2}\zeta_n'(0)\exp\left[-\left[\frac{2m_lV_0}{\hbar^2}\right]^{1/2}z\right], \tag{4.58}$$

where $\zeta_n'(0)$ is the derivative of the wave function in the case of infinite V_0. Therefore we get

$$V_{n\mathbf{k}n'\mathbf{k}'}^{SR(1)}=\frac{\hbar^2}{2m_l}\frac{d\zeta_n^*}{dz}\frac{d\zeta_{n'}}{dz}\bigg|_{z=0}\Delta_{\mathbf{k}-\mathbf{k}'}, \tag{4.59}$$

which is the same as the first term of Eq. (4.34). If we calculate higher-order terms we see that the expansion parameter in this formalism is given by $(2m_lV_0/\hbar^2)^{1/2}\Delta$. Therefore Eq. (4.59) is valid only if $(2m_lV_0/\hbar^2)^{1/2}\Delta \ll 1$. Actually, however, Δ is comparable to or larger than $(\hbar^2/2m_lV_0)^{1/2}$. Although this derivation is different from the previous one and the relationship between the two derivations is not yet clear, this fact casts some doubt on the expansion in terms of the surface roughness. The parameters of the surface roughness obtained above might have only a qualitative meaning. More theoretical investigation is necessary to clarify the problem of the surface roughness scattering even within the simple model.

All the above expressions have been obtained under the assumption of slowly varying surface roughness, i.e., $\Delta \ll \Lambda$. Actually, however, there can be roughness with shorter ranges or of atomic scales. These might become more and more important at high electron concentrations. Such short-range roughness might be related to the interface grading studied by Stern (1977). Stern showed that the experimental behavior of the mobility at high electron concentrations could also be explained by assuming that the scattering due to the grading or to scatterers in the oxide was proportional to the part of the

density distribution of electrons within the transition layer and the oxide. Microscopic formulation of this picture has not been successful.

As has been discussed in Sec. III.E., there have been various experimental investigations on the structure of the Si-SiO_2 interface. From these measurements one can now obtain preliminary information on the nature of the interface roughness. For example, Krivanek, Tsui, Sheng, and Kamgar (Krivanek *et al.*, 1978a, 1978b) studied the interface using high-resolution (~ 3 Å) cross-sectional transmission electron microscopy. They found that the interface is quite smooth, although it has a long-range modulation of a height ~ 4 Å with a wavelength of 200–500 Å. This is not inconsistent with the model discussed above, since cross-sectional transmission electron micrographs give the envelope of the asperities projected to the plane normal to the interface, and short-range roughness contributing to the electron mobility is averaged out. Sugano and associates (Sugano *et al.*, 1980; see also Sugano, 1980) used normal transmission microscopy. They obtained values for the correlation length and the root mean square of the interface roughness which are consistent with the model discussed above.

If we include the two scattering mechanisms, charged centers in the oxide and surface roughness, we can explain the overall behavior of experimental mobilities at low temperatures. The mobility increases first, takes a maximum value around $N_s \sim 10^{12}$ cm^{-2}, and then decreases with increase of the electron concentration. Quantitatively, however, the two mechanisms alone cannot reproduce the experimental behavior, as first noted by Matsumoto and Uemura (1974). An example of calculated mobilities and unpublished experimental results of Kawaji is given in Fig. 65. Matsumoto and Uemura

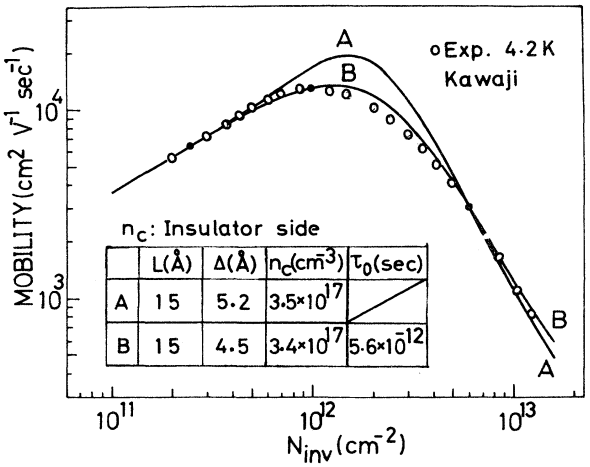

FIG. 65. Calculated mobility vs electron concentration N_{inv}. Curve A is obtained by combining oxide charge scattering and surface roughness scattering. Curve B is obtained by adding a third relaxation process, independent of the electron concentration. The circles show experiments of Kawaji (unpublished). The lateral decay length of the surface roughness is denoted here as L. After Matsumoto and Uemura (1974).

assumed a uniform distribution of charged centers in the oxide and neglecting $\Delta V(\mathbf{r},z)$ for the surface roughness scattering. The two mechanisms explain the behavior at both low and high electron concentrations, but are insufficient near the electron concentration where the mobility has a maximum. If we assume that charged centers are located only at the interface, the agreement becomes worse. The situation does not change even if the correction term $\Delta V(\mathbf{r},z)$ is included. The curve B was obtained by adding a phenomenological relaxation time independent of N_s. The figure shows that there are other scattering mechanisms which are important, especially around $N_s = 10^{12}$ cm^{-2}. These are expected to be of short range (see also the discussion in Sec. VI.B).

Many people have proposed other scattering mechanisms in connection with various experimental results (see also Sec. IV.B). Neumark (1968, 1969, 1970) has proposed that misfit dislocations may form a network along the interface and may contribute to scattering. Sakaki and Sugano (1972a) argued that defects of gigantic cross section (like cavities in Swiss cheese) could be important. This model was originally suggested by Fang and Fowler (1968). Hess and Sah (1975) and Pepper (1977a) argued the existence of dipoles (positive and negative charges located close to each other) in the oxide (see also Karpushin and Chaplik, 1967), which would result in a scattering with short range. Eisele and Dorda (1974b) discussed scattering through surface states above the conduction-band edge. This is in addition to scattering by charges in surface states arising from dangling bonds (Arnold and Abowitz, 1966). Two-electron localized centers were proposed by Ngai and Reinecke (1976; see also Ngai and White, 1978, 1980; White and Ngai, 1978a, 1978b). Takada (1979) argued that neutral centers consisting of a charge near the interface and a bound electron in the inversion layer could be possible scatterers. Yagi and Nakai (1980) tried to explain the strong N_s dependence of observed mobilities below the mobility maximum by assuming a reduced screening of the Coulomb scattering due to smearing of the density of states at low energies. One must assume extremely large values of the level broadening to account for the experimental N_s dependence, however.

3. Multisubband transport

So far we have mainly been concerned with the transport problem in the electric quantum limit, where only the ground electric subband is occupied by electrons. At high electron concentrations or at nonzero temperatures, higher subbands can be populated, and we have to deal with the problem of the multisubband transport even in n-channel inversion layers on the Si surfaces. This is also true in the presence of appropriate uniaxial stresses, where subbands associated with other valleys can have the same or lower energies and electrons are transferred from the usual two valleys to other valleys in the n-channel layers on the Si surfaces. In this section we

briefly review the work on this multisubband transport in the n-channel inversion layer on the Si(100) surface at sufficiently low temperatures. The problem is also related to the subband structure; the results of such investigation are expected to give further information on the subband structure and scattering mechanisms in this system.

Occupation of higher subbands leads to several effects. The transport now includes contributions from several subbands, and we must also take into account intersubband scattering processes. Further, the screening effect becomes larger, since all the subbands contribute to the screening of scattering potentials. The polarization caused by virtual intersubband transitions might also be important.

The formal extension of the previous theory to the case of more than one occupied subband is straightforward and has been done by Siggia and Kwok (1970). However, actual calculations are very tedious and have been performed only relatively recently. In general, the density matrix has off-diagonal elements between different subbands in the presence of intersubband scattering processes. When the broadening of levels due to intersubband scattering is sufficiently small in comparison with subband energy separations, we can neglect such off-diagonal parts and use the usual Boltzmann transport equation, which becomes a set of coupled equations for distribution functions associated with each subband in the presence of intersubband scattering processes. Let us consider the case when the two-dimensional Fermi line is isotropic. Then

$$\frac{-e}{m}\hbar\mathbf{k}\cdot\mathbf{E}\frac{\partial f_i}{\partial\varepsilon(k)}=\sum_j\frac{2\pi}{\hbar}\langle|(i\mathbf{k}|\mathscr{H}_1|j\mathbf{k}')|^2\rangle\delta(E_i+\varepsilon(k)-E_j-\varepsilon(k'))[f_j(\mathbf{k}')-f_i(\mathbf{k})]\,, \tag{4.60}$$

where $\mathbf{E}$ is an electric field, $f_i(\mathbf{k})$ is the distribution function of the ith subband, m is the effective mass for the motion parallel to the surface ($m=m_t$ for the subbands E_0, E_1,...), $\mathscr{H}_1$ describes potentials of scatterers, and $\langle\cdots\rangle$ means average over scatterers. At low temperatures intervalley scattering is expected to be sufficiently weak and can be neglected. In this case electrons in the different valleys can be regarded as independent current carriers, and there is no coupling between their distribution functions. The coupled Boltzmann equations can be solved exactly by introducing energy-dependent relaxation times associated with each subband. We have

$$f_i(\mathbf{k})=f(E_i+\varepsilon(k))-\tau_i(E_i+\varepsilon(k))\frac{(-e)}{m}\hbar\mathbf{k}\cdot\mathbf{E}\frac{\partial f(E_i+\varepsilon(k))}{\partial\varepsilon(k)}\,, \tag{4.61}$$

where $f(E)$ is the Fermi-Dirac distribution function. The Boltzmann equation then leads to a system of linear simultaneous equations for $\tau_i(E)$ as follows:

$$E-E_i=\sum_j K_{ij}(E)\tau_j(E)\,, \tag{4.62}$$

where

$$K_{ij}(E)=\frac{2\pi^2\hbar^3}{m_t^2}\int\frac{d\mathbf{k}}{(2\pi)^2}\int\frac{d\mathbf{k}'}{(2\pi)^2}\left[\delta_{ij}\sum_l\langle|(i\mathbf{k}|\mathscr{H}_1|l\mathbf{k}')|^2\rangle\delta(E_i+\varepsilon(k)-E)\delta(E_l+\varepsilon(k')-E)k^2\right.$$
$$\left.-\langle|(i\mathbf{k}|\mathscr{H}_1|j\mathbf{k}')|^2\rangle\delta(E_i+\varepsilon(k)-E)\delta(E_j+\varepsilon(k')-E)\mathbf{k}\cdot\mathbf{k}'\right]\,. \tag{4.63}$$

The current can be calculated as

$$\mathbf{J}=(-e)2g_v\sum_i\int\frac{d\mathbf{k}}{(2\pi)^2}\frac{\hbar\mathbf{k}}{m}f_i(\mathbf{k})\,, \tag{4.64}$$

where g_v is the valley degeneracy. The mobility of the ith subband at zero temperature is given by

$$\mu_i=(e/m)\tau_i(E_F)\,, \tag{4.65}$$

The effective mobility is given by

$$\bar{\mu}=\sum_i\mu_i\frac{N_i}{N_s}\,, \tag{4.66}$$

where N_i is the electron concentration in the ith subband.

The screening effect can, in the random-phase approximation, be included in terms of a matrix dielectric function,

$$\varepsilon_{(ij)(i'j')}(q)=\delta_{ij}\delta_{i'j'}+\frac{2\pi e^2}{\bar{\kappa}q}\Pi_{ij}(q)F_{(ij)(i'j')}(q)\,, \tag{4.67}$$

where the form factor is defined by Eq. (3.37) and the polarization part is given by

$$\Pi_{ij}(q)=2g_v\sum_k\frac{f(E_i+\varepsilon(k))-f(E_j+\varepsilon(\mathbf{k}+\mathbf{q}))}{E_i+\epsilon(k)-E_j-\varepsilon(\mathbf{k}+\mathbf{q})}\,. \tag{4.68}$$

The effective potential becomes

$$(V_{\mathbf{q}}^{\text{eff}})_{ij}=\sum_{i'j'}(V_{\mathbf{q}}^{\text{bare}})_{i'j'}[\varepsilon(q)^{-1}]_{(i'j')(ij)}\,, \tag{4.69}$$

where $(V_{\mathbf{q}}^{\text{bare}})_{ij}$ is the two-dimensional Fourier transform of the matrix element of the bare scattering potential and $\varepsilon(q)^{-1}$ is the inverse of the matrix dielectric function.

So far we have assumed that there is only a single set

of subbands associated with equivalent valleys. The extension of the above formalism to the case in which different sets of subbands are occupied by electrons is straightforward. In this case the total current is a sum of contributions of subbands of different valleys, since at low temperatures intervalley scattering processes are expected to be sufficiently weak. As for the case of the screening effect, we have a coupling of contributions of different valleys, as has been discussed by Stern (1978a). The polarization part is diagonal with respect to valley indices but can be dependent on them. The same thing applies to the form factor. There do not exist terms which correspond to intervalley scattering, but we have to take into account mutual interactions of electrons in different valleys. Therefore the dielectric function also has a matrix form.

The first actual calculation of the mobility in the multisubband system was done by Nelson and Brown (1974). They assumed short-range scatterers which were distributed near the interface to simulate the surface roughness scattering and also uniformly throughout the bulk Si to simulate bulk phonons. They used the triangular potential for the surface electric field and calculated mobilities at room temperature. In spite of these *ad hoc* assumptions they demonstrated the importance of the intersubband scattering effects. Ezawa (1976) calculated phonon-limited mobilities using Stern's Hartree results.

At low temperatures under usual conditions there are two possible ways the excited subbands can be occupied when the electron concentration increases. The Hartree calculation of Stern predicts that $E_{0'} > E_1$ at sufficiently high electron concentrations, and consequently the first excited subband of the usual two valleys becomes occupied by electrons first. Many-body effects such as exchange and correlation modify the subband structure, as has been discussed in Sec. III.B. A density-functional calculation of Ando (1976a, 1976b) predicts a qualitatively similar result to the Hartree calculation, while a perturbation calculation of Vinter (1977) showed that $E_{0'}$ is lower. Stern (1977) studied effects of the grading of the Si-SiO_2 interface and showed that the grading reduces $E_{0'}$, as has been discussed in Sec. III.E. Sham and Nakayama (Sham and Nakayama, 1978, 1979; Nakayama, 1980) have suggested possible differences of effective interface positions for different sets of valleys, which can also affect the relative positions of $E_{0'}$ and E_1 subbands. This theory will be discussed in Sec. VII.A. Therefore, the occupation of higher subbands includes rather a subtle problem, and we have to consider the two cases separately.

Stern (1978a) studied the case in which the subbands 0 and 0′ were occupied by electrons, neglecting the anisotropy of the Fermi line of the 0′ subband. In this case intersubband scattering is absent and the problem is slightly simpler. He employed a formulation which is an extension of that described in Sec. II.C for the screening effect and took into account the graded interface. As long as the thickness of the graded region is sufficiently small (~ 5 Å), qualitative behavior of the results is the same as for the results obtained by the above formulation. An example of his results for charged centers is shown in Fig. 66. The charged centers were assumed to be located on the semiconductor side of the graded region. This might be unreasonable if we consider the fact that the potential for positive Na^+ ions has a very deep minimum on the insulator side, as has later been shown by Stern (1978b). Roughly speaking, the change in the position of charged centers makes the absolute value of the mobility larger or smaller but does not modify the qualitative behavior. The mobility increases dramatically when the subband 0′ becomes occupied. When the excited subband is occupied, electrons in the subband have very high mobility values because effective potentials for the electrons in the excited subband become very weak. Further, the screening effect itself also becomes stronger, since electrons in both subbands contribute to the screening of scattering potentials. These two effects cause the abrupt increase of the mobility when the subband 0′ becomes occupied. Note that the position of the occupation of the excited subband occurs at higher electron concentrations than predicted in the Hartree approximation because Stern has included an increase of the subband separation due to many-body effects by phenomenologically adding an energy which is proportional to $(N_s + N_{\text{depl}})^{1/3}$. He obtained similar behavior for the mobility limited by the surface roughness scattering, although he did not take into account various corrections discussed in Sec. IV.C.2.

Mori and Ando (1979) studied the case in which subbands 0 and 1 are occupied by electrons. In this case we have to treat the intersubband scattering properly. An example of results for surface roughness scattering is shown in Fig. 67 together with the experimental results

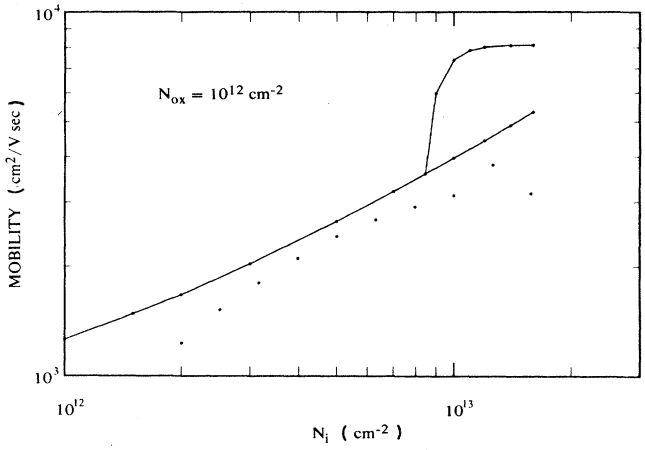

FIG. 66. Measured and calculated mobilities resulting from scattering by 10^{12} charges per cm^2 at the semiconductor edge of the transition layer between Si and SiO_2 vs the concentration of inversion layer electrons (N_i). The measured values are from Harstein *et al.* (1976). The smooth curve is the calculated mobility with only the lowest subband occupied. The upper branch is the calculated mobility with subbands E_0 and $E_{0'}$ occupied. After Stern (1978a).

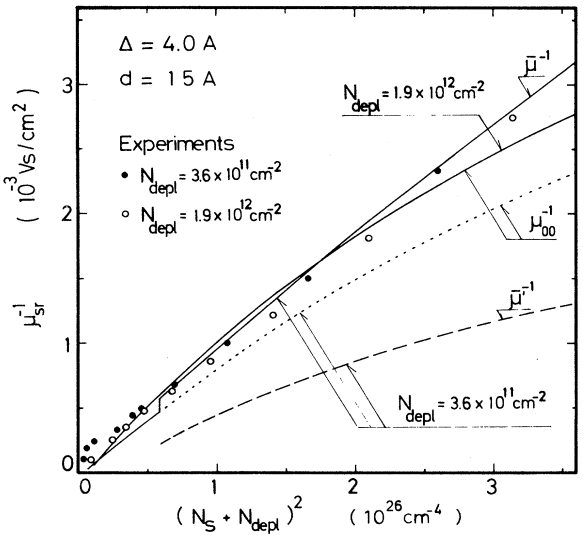

FIG. 67. Calculated and experimental mobilities limited by surface roughness scattering for two different values of N_{depl}. The solid lines are obtained with the two subbands, E_0 and E_1, included. The dotted line is the case in which only the lowest subband is assumed to be occupied for $N_{depl}=3.6\times10^{11}$ cm^{-2}. The dashed line is obtained if intersubband scattering is neglected. Experimental results are from Hartstein *et al.* (1976). The lateral decay length of the surface roughness is denoted as d in the figure. After Mori and Ando (1979).

of Hartstein *et al.* (1976) for $N_{depl}=3.6\times10^{11}$ and 1.9×10^{12} cm^{-2}. For $N_{depl}=3.6\times10^{11}$ cm^{-2} the E_1 subband becomes occupied around $(N_s+N_{depl})^2=0.6\times10^{26}$ cm^{-4}. The mobility decreases discontinuously at this concentration and becomes smaller than that obtained by neglecting the occupation of the excited subband. This is because the intersubband scattering is crucial and reduces the mobility, especially of the excited subband, considerably. The occupation of the excited subband tends to make the mobility a function of $(N_s+N_{depl})^2$. The mobility limited by charged centers shows the same behavior, as is shown in Fig. 67.

As we have seen, the mobility behaves quite differently, depending on which subband is occupied by electrons first. Comparison with experimental results seems to show that subband 1 is usually lower than the 0′ subband at high electron concentrations (in the absence of stresses). This supports the result of the Hartree and the density-functional calculations.

The sharp drop or increase of the effective mobility when higher subbands become occupied by electrons is very sensitive to the level broadening effect, which has not been included in the above formulation. Mori and Ando (1979) studied this effect within a simple model of surface roughness scattering for the case in which subbands 0 and 1 are occupied by electrons. They have shown that the density of states of subband 1 has a relatively large low-energy tail and that the sharp drop of the mobility can easily be smeared out. Therefore, it is not possible to observe such a structure experimentally. The existence of the low-energy tail of the density of states is more serious when the 0′ subband becomes occupied. Electronic states in the tail region are highly likely to be localized, and results might be quite different from the above, even qualitatively, when the Fermi level lies in this tail region. Those problems have not been worked out yet.

By applying an appropriate uniaxial stress we can bring energies of the bottoms of different valleys down and transfer electrons from the usual two valleys to other sets of valleys. There have been a number of experiments on the effects of uniaxial stress on various properties. A humplike structure of the mobility has been observed by Kawaji, Hatanaka, Nakamura, and Onga (1976) in an n-channel inversion layer on (100) surface of Si on sapphire, where a large difference in the thermal expansion coefficient of silicon and sapphire gives a large compressive stress along the interface. Similar structure has also been observed by Gesch, Eisele, and Dorda (1978; see also Fang, 1980) on the Si(100) surface under applied uniaxial stress. Those structures are believed to appear when the Fermi level comes close to the bottom of subband 0, which is higher in energy than the 0′ subband at low electron concentrations under sufficiently large stresses. So far experimental results seem to show that the valley degeneracy remains two in spite of the electron transfer effect. More detailed discussion of this problem will be given in Sec. VII.B.

Takada (1979) calculated the mobility in an n-channel inversion layer on the Si(100) surface under stress. He used the formulation described above and calculated the mobility assuming two scattering mechanisms, charged centers in the oxide, and surface roughness scattering. He showed that the mobility increases by more than one order of magnitude when the subbands of the different valleys are occupied by electrons at the same time. This is completely analogous to the result of Stern (1978a). Experimentally such an anomalous increase of the mobility has not been observed, which seems to suggest the importance of other kinds of scattering mechanisms at relatively low electron concentrations where the mobility has a maximum. Takada showed that neutral impurities, which consist of positive charges near the interface on the insulator side and a bound electron in the inversion layer, could be a candidate for an additional scattering mechanism. Vinter (1978, 1980) studied screening of a positive charge in a density-functional formulation. He investigated various possible configurations of numbers of electrons in bound states and also calculated mobilities. The self-consistent configuration of electrons seems to be different from that assumed by Takada, as has been discussed in Sec. IV.C.1.

D. Phonon scattering at high temperatures

Lattice vibrations are an inevitable source of scattering and can dominate the scattering near room temperature. In the range of electron concentrations $N_s=0.5-5\times10^{12}$ cm^{-2} and around room temperature, the mobility μ is

known to behave like $\mu \propto N_s^{-(1/6-1/3)}T^{-(1-1.5)}$ and to have the magnitude $200-1000$ $\mathrm{cm^2\,V^{-1}\,s^{-1}}$ depending on the crystallographic orientation of the surface. This behavior of the mobility has been discussed in Sec. IV.B and is generally believed to be determined by phonon scattering. In this section we shall review the theory of phonon scattering in the inversion layer.

Scattering by lattice vibrations can be expected to cause three different types of electronic transitions, i.e., transitions between states within a single valley via acoustic phonons (called intravalley acoustic-phonon scattering) and optical phonons (called intravalley optical-phonon scattering), and transitions between different valleys (called intervalley scattering). The intravalley acoustic-phonon scattering involves phonons with low energies and is almost an elastic process. The intravalley optical-phonon scattering is induced by optical phonons of low momentum and high energy and is considered to be negligible in silicon. The intervalley scattering can be induced by the emission and absorption of high-momentum, high-energy phonons, which can be of either acoustic- or optical-mode nature. Intervalley scattering can therefore be important only for temperatures high enough that an appreciable number of suitable phonons is excited or for hot electrons which can emit high-energy phonons. Hot-electron effects are discussed in the following section.

Kawaji (1969) proposed a model of two-dimensional phonons and calculated the electron mobility limited by acoustic phonons. His argument was essentially a dimensional analysis based on the Bardeen-Shockley theory in the bulk (Bardeen and Shockley, 1950), and led to an expression:

$$\frac{1}{\tau_K}=\frac{2\pi}{\hbar}\frac{\Xi_u^2 k_B T}{\rho c_l^2\langle z\rangle}\frac{m_{||}}{2\pi\hbar^2}\propto N_s^{1/3}T\ , \tag{4.70}$$

where ρ is the mass density, c_l is the longitudinal sound velocity, Ξ_u is the deformation potential, $m_{||}$ is an effective mass parallel to the surface, and $\langle z\rangle \sim z_{\mathrm{av}}$ is the effective thickness of the inversion layer. This expression explains the qualitative behavior of the mobility observed experimentally at high temperatures. Acoustic-phonon scattering was later studied extensively by Ezawa, Kawaji, Nakamura, and co-workers (Ezawa *et al.*, 1971a, 1971b; Ezawa, Kuroda, and Nakamura, 1971; Kawaji *et al.*, 1972; Ezawa *et al.*, 1974; Ezawa, 1976). In the following we first derive the above formula based on a more rigorous formulation.

Let us restrict ourselves to the ground subband in an n-channel layer on the Si(100) surface. We usually replace the silicon by an isotropic elastic continuum, which is known to be a good approximation in the bulk in dealing with acoustic-phonon scattering. Define $\mathbf{U}=(\mathbf{u},u_z)$ as the displacement of the elastic medium. We have

$$H_{\text{el-ph}}=\Xi_u\phi(\mathbf{r},z)\ , \tag{4.71}$$

$$\phi(\mathbf{r},z)=D\nabla\cdot(\mathbf{r},z)+\frac{\partial}{\partial z}u_z(\mathbf{r},z)\ , \tag{4.72}$$

where $D=\Xi_d/\Xi_u$ is the ratio between deformation potentials in the two different directions. It is known that $\Xi_u=9$ eV and $D=-0.67$. Silicon is, however, anisotropic, and one must modify these numbers so as to be consistent with the isotropic phonon model. Ezawa *et al.* (1974) chose $\Xi_u=12$ eV and $D=-0.67$. At sufficiently high temperatures, around room temperature, a typical phonon energy, given by $c_l q$ with $q\sim(2m_t k_B T/\hbar^2)^{1/2}$ or $q\sim 1/\langle z\rangle$, is much smaller than a typical electron energy of the order of $k_B T$, and can be neglected. This means that the scattering can be treated as an elastic process. The transport relaxation time becomes

$$\frac{1}{\tau(\varepsilon(k))}=\frac{2\pi}{\hbar}\Xi_u^2\sum_{k'}(1-\cos\theta_{\mathbf{k}\mathbf{k}'})\delta(\varepsilon(k)-\varepsilon(k'))\times\int_0^\infty dz\int_0^\infty dz'\,|\zeta_0(z)|^2|\zeta_0(z')|^2 D(z,z';|\mathbf{k}-\mathbf{k}'|)\ , \tag{4.73}$$

where $D(z,z';q)$ is the phonon correlation function, defined by

$$D(\mathbf{r},z;\mathbf{r}',z')=\sum_q \exp[i\mathbf{q}\cdot(\mathbf{r}-\mathbf{r}')]D(z,z';q)$$
$$=\langle\phi(\mathbf{r},z)\phi(\mathbf{r}',z')\rangle=\frac{\mathrm{Tr}\exp(-\beta\mathscr{H}_{\mathrm{ph}})\phi(\mathbf{r},z)\phi(\mathbf{r}',z')}{\mathrm{Tr}\exp(-\beta\mathscr{H}_{\mathrm{ph}})}\ , \tag{4.74}$$

where $\mathscr{H}_{\mathrm{ph}}$ is the Hamiltonian for phonons and $\beta=1/k_B T$.

For simplicity we neglect the existence of the Si-SiO_2 interface and use the bulk phonon spectrum. We have

$$\mathbf{U}(\mathbf{r},z)=\sum_{\mathbf{q}}\sum_{q_z}\sum_{\lambda}\left[\frac{\hbar}{2\rho\omega_Q^{(\lambda)}}\right]^{1/2}\mathbf{e}_{\mathbf{Q}}^{(\lambda)}[b_{\mathbf{Q}}^{(\lambda)}\exp(i\mathbf{Q}\cdot\mathbf{r}+iq_z z)+\mathrm{H.c.}]\ , \tag{4.75}$$

where λ denotes phonon modes ($\lambda=1,2$ for transverse modes and $\lambda=3$ for the longitudinal mode), $\mathbf{Q}=(\mathbf{q},q_z)$, $\mathbf{e}_{\mathbf{Q}}^{(\lambda)}$ is the polarization vector, $\omega_Q^{(\lambda)}=cQ$ with $c=c_t$ for $\lambda=1$ and 2 and $c=c_l$ for $\lambda=3$, $b_{\mathbf{Q}}^{(\lambda)}$ is the phonon destruction operator, and H.c. denotes Hermitian conjugate. At sufficiently high temperatures we can use

$$\langle b_{\mathbf{Q}}^{(\lambda)+}+b_{\mathbf{Q}'}^{(\lambda')}\rangle=\delta_{\mathbf{Q}\mathbf{Q}'}\delta_{\lambda\lambda'}\langle b_{\mathbf{Q}}^{(\lambda)+}+b_{\mathbf{Q}}^{(\lambda)}\rangle\cong\delta_{\mathbf{Q}\mathbf{Q}'}\delta_{\lambda\lambda'}\frac{k_BT}{\hbar\omega_{\mathbf{Q}}^{(\lambda)}}\ , \tag{4.76}$$

and get

$$D(z,z';q)=\frac{k_BT}{\rho c_l^2}\sum_{q_z}\left[D^2+2\frac{q_z^2}{Q^2}+\frac{q_z^4}{Q^4}+\frac{c_l^2}{c_t^2}\left[\frac{q_z^2}{Q^2}-\frac{q_z^4}{Q^4}\right]\right]e^{iq_z(z-z')}\ . \tag{4.77}$$

Therefore we have

$$\frac{\tau_K}{\tau(\varepsilon(k))}=\int_0^{\pi}\frac{d\theta}{\pi}(1-\cos\theta)\int_{-\infty}^{+\infty}\frac{\langle z\rangle dq_z}{2\pi}\left|\int_0^{\infty}dz\ |\zeta_0(z)|^2e^{iq_zz}\right|^2 \times\left[D^2+2\frac{q_z^2}{Q^2}D+\frac{q_z^4}{Q^4}+\frac{c_l^2}{c_t^2}\left[\frac{q_z^2}{Q^2}-\frac{q_z^4}{Q^4}\right]\right]\Bigg|_{q=2k\sin(\theta/2)}\ . \tag{4.78}$$

If we use the variational expression (3.25), it is easy to perform the integration over q_z. Since the right-hand side of (4.78) is a slowly varying function of $\varepsilon(k)$ and N_s, the main dependence of the mobility on the temperature and the electron concentration is given by that of τ_K, thus confirming Kawaji's simple-minded result. Because of the two-dimensional energy-independent density of states, no additional T dependence appears in the mobility, in contrast to the usual result for three-dimensional systems. As is clear from the above derivation, the T^{-1} behavior of the mobility reflects the number of phonons excited at T. The phonon system is essentailly three-dimensional, while the electron system is two-dimensional. Momentum conservation gives a severe restriction only on the components of the phonon momentum q in the direction parallel to the surface, and phonons which have q_z with $|q_z|\leq 1/\langle z\rangle$ contribute equally to the scattering. This gives the factor $\langle z\rangle\propto N_s^{-1/3}$ in the expression for the mobility.

The existence of the interface affects the phonon modes near the interface. The oxide is softer than silicon and has lower sound velocities.[3] Thus the phonon amplitudes near the interface become larger than in the bulk, and the electron-phonon scattering is expected to be stronger. To investigate this effect, Ezawa, Kawaji, Nakamura, and co-workers (Ezawa *et al* 1971a; Ezawa, Kuroda, and Nakamura, 1971; Ezawa *et al.*, 1974; Kawaji *et al.*, 1972) studied an extreme case by assuming that the oxide was infinitely soft, i.e., the interface could be replaced by a stress-free boundary. Ezawa (1971) obtained a complete orthonormal set of eigenmodes of phonons in an isotropic elastic continuum occupying a half-space. Those modes are called surfons. The Rayleigh wave which is localized near the surface is one of the surfons. We do not go into the problem of finding the surfon modes, and those who are interested should refer to Ezawa's paper. Ezawa *et al.* (1974) calculated the phonon correlation function (4.74) and mobilities in n-channel layers on three major surfaces, (100), (110), and (111). Their work is equivalent to a corresponding one for the bulk by Herring and Vogt (1956). It is clear that the temperature and electron concentration dependence of the mobility is essentially given by that for the bulk phonon scattering, and that only the absolute value can be modified by the interface effect. Their results were rather disappointing, however. The calculated mobility was only 10—20% smaller than that for the bulk phonon scattering, which indicates that the interface effect is not important in determining the strength of scattering. Further, the oxide is actually not infinitely soft, and the situation is rather closer to the bulk phonon case than to the case of the stress-free boundary. We can conclude, therefore, that the existence of the interface does not play an important role in electron-phonon scattering in actual inversion layers, except that the electron motion is two-dimensional.

Ezawa and co-workers calculated the mobility and found that it was quite sensitive to D. Their assumed value $D=-0.67$ roughly corresponded to a maximum value of mobility. In general theoretical results have turned out to be much larger than experimental ones. For example, the calculated mobility on the (100) surface is given by $\mu=3500\ \mathrm{cm^2V^{-1}s^{-1}}$ at $N_s=1\times10^{13}\ \mathrm{cm^{-2}}$ and $T=300$ K, and becomes larger roughly in proportion to $N_s^{-1/3}$ with decreasing electron concentration. In contrast typical experimental values of the mobility at room temperatures are between 300 and 400 $\mathrm{cm^2V^{-1}s^{-1}}$ at $N_s\sim10^{13}\ \mathrm{cm^{-2}}$, one order of magnitude smaller than the calculated values. There is, however, a possibility that some other scattering mechanisms still contribute to the mobility even at room temperatures for such high electron concentrations.

So far we have assumed the electric quantum limit, where only the ground subband is occupied by electrons.

[3]McSkimin (1953) measured the velocity in both Si and SiO_2 at room temperature. According to him, for example, $c_l=9.13\times10^5$ cm/s, $c_{t\langle1\bar10\rangle}=4.67\times10^5$ cm/s, and $c_{t\langle001\rangle}=5.84\times10^5$ cm/s for waves propagating in the $\langle110\rangle$ direction in Si. For amorphous SiO_2 he obtained $c_l=5.97\times10^5$ cm/s and $c_t=4.76\times10^5$ cm/s.

Actually this assumption may not be valid at room temperature. Stern's self-consistent calculation (Stern, 1972b) shows that only 20% of the electrons are in the ground subband on the (100) surface at $N_s = 1 \times 10^{12}$ cm^{-2}. This occupation ratio increases with N_s, but 40% of the electrons are still in excited subbands even at $N_s = 1 \times 10^{13}$ cm^{-2}. The situation becomes slightly better on other surfaces like (110) and (111), but the electric quantum limit does not apply to the room-temperature case. When excited subbands are occupied, intersubband scattering becomes very important and should be taken into account properly. Ezawa (1976) studied this effect on the (100) surface using Stern's self-consistent wave functions. Occupation of excited subbands associated with the two valleys which are located in the [100] and [$\bar{1}$00] directions and which give the ground subband reduces the mobility because of important intersubband scattering. This is completely analogous to the case at low temperatures discussed previously. The mobility of electrons occupying subbands associated with the other four valleys becomes smaller than that of electrons in the two valleys, because the decrease of scattering caused by a larger $\langle z \rangle$ is cancelled by the mass increase in the direction parallel to the surface. Consequently the mobility decreases if we take into account the higher subband occupation. Ezawa showed that the effect was substantial and reduced the mobility to as low as half of the value in the electric quantum limit at $N_s = 1 \times 10^{13}$ cm^{-2}. It is easy to understand that the temperature dependence becomes steeper than the T^{-1} dependence found for the electric quantum limit. However, the agreement becomes worse for the N_s dependence. With decreasing N_s population of electrons in higher subbands, and consequently the reduction of the mobility, becomes more and more substantial. Thus the electron concentration dependence becomes smaller. As a matter of fact Ezawa's numerical calculation gave mobilities which were almost independent of N_s, in contrast to the $N_s^{-1/3}$ dependence in the electric quantum limit.

The theory of phonon scattering is, therefore, at an unsatisfactory stage. The calculated mobility limited by acoustic-phonon scattering is not only much larger than experiments, but does not reproduce $\mu \propto N_s^{-1/3}$ behavior. The discrepancy in the absolute value is easily reduced if we assume a larger value of the deformation potential Ξ_u near the interface. If we consider the fact that electrons are far from the interface on an atomic scale, however, it is highly unlikely that the value is different from that in the bulk. The electron concentration dependence of the mobility might become steeper if many-body effects on the subband structure are included. Exchange and correlation increase energy separations between subbands and population of electrons in the ground subband. Further the effect becomes larger at lower electron concentrations. Calculations have shown that the exchange and correlation are still substantial, even at room temperature (Nakamura *et al.*, 1978, 1980a; Kalia *et al.*, 1978, 1979; Das Sarma and Vinter, 1981). This means that the electric quantum limit might still be a good approximation and reduces the role of intersubband scattering. Therefore the dependence of the mobility on the electron concentration becomes steeper, although its absolute value becomes close to that for the electric quantum limit. The calculation of Nakamura *et al.*, (1978, 1980a) showed that the quasiparticle energy of electrons had a large imaginary part caused by electron-electron scattering at high temperatures. A preliminary investigation of the effects of such short lifetimes by Nakamura *et al.* (1980b) suggested an increase of the mobility of electrons in the ground subband. This is because the large imaginary part of the self-energy gives rise to a low-energy tail of the density of states and consequently reduces the strength of scattering through the reduction of the final-state density of state.

Intervalley phonon scattering is known to be necessary to account for mobilities in the bulk at room temperature. As a matter of fact intervalley scattering reduces the mobility as much as a factor of 3 from the calculated only for acoustic-phonon scattering in the bulk at $T = 300$ K (Long, 1960). This mechanism is also important in the inversion layer and will reduce the discrepancy between the theory and experiments discussed above. There have been some investigations of intervalley phonon scattering effects on the mobility (Sah *et al.*, 1972b; Ezawa *et al.*, 1974; Ferry, 1976a; Roychoudhury and Basu, 1980), but they are still qualitative. This is because of the need to know the subband structure, especially the relative energies of subbands associated with the different valleys.

Electrons in the inversion layer are coupled to polar optical phonons of SiO_2 across the interface by the macroscopic electrostatic fringe fields of these modes, as has been discussed in Sec. III.A. This remote polar phonon has been suggested to be an effective scattering mechanism, especially for energy loss of electrons in the nonohmic (hot-electron) regime (Hess and Vogl, 1979). However, since energies of optimal phonons in SiO_2 are very large (> 670 K), this scattering mechanism is ineffective in determining the mobility at room temperature in the ohmic regime (Moore and Ferry, 1980b, 1980c).

Experiments to study phonon scattering at lower temperatures have also been carried out. Kawaguchi and Kawaji (1980a; see also Kawaguchi *et al.*, 1980) measured the mobility for temperatures between 4.2 and 50 K. The total resistivity ρ was assumed to consist of three terms, $\rho = \rho_{ph} + \rho_r + \rho_a$, where ρ_r is residual resistivity, assumed to be independent of temperature, and ρ_a is an "anomalous" term dependent on the temperature logarithmically. By applying a weak magnetic field Kawaguchi and Kawaji suppressed the anomalous term and determined the temperature-dependent resistivity ρ_{ph}, which was ascribed to acoustic-phonon scattering. Although the resulting temperature dependence of ρ_{ph} seemed to agree with the calculation by Shinba and Nakamura (1981), its absolute value has turned out to be much larger. Hartstein, Fowler, and Albert (1980) made similar but more extensive experiments for varying con-

centrations of Na^+ ions near the $Si\text{-}SiO_2$ interface. A part of the resistivity independent of the concentration of the charges was ascribed to acoustic-phonon scattering and temperature-independent surface roughness scattering. The temperature dependence of the mobility was also studied by Cham and Wheeler (1980a, 1980b), as has been discussed in Secs. IV.B. and IV.C.1. Stern (1980b) took into account the temperature dependence of the screening effect and calculated the mobility limited by charged centers and surface roughness. He demonstrated that the charge and roughness scattering alone can approximately account for most of the observed temperature dependence. Further, Matthiessen's rule is invalid at elevated temperatures, which cast doubt on the separation of various scattering contributions at such high temperatures.

E. Hot-electron effects

It was observed very early (Fowler *et al.*, 1966a; Fang and Fowler, 1968) that especially at low temperatures the conductance of electrons depended on the source-drain field F_D. This result of electron heating can be viewed either as an annoyance or as an opportunity. Experimentally, it adds to the difficulty of making conductivity or mobility measurements. At very low temperatures elaborate techniques are sometimes required to extract the conductivities because fields as low as 10^{-3} V cm^{-1} may be required to avoid significant electron heating (see, for instance, Bishop *et al.*, 1980). Generally, however, fields of the order of 0.1 V cm^{-1} are low enough to avoid heating effects. Hot-electron effects represent an opportunity in that they allow a study of phonon scattering in greater detail, especially at low temperatures where elastic scattering dominates at low F_D. At very high fields, even at 300 K, most of the electron energy is transferred to the lattice through optical phonons; eventually the electron velocity saturates as in the bulk (Fang and Fowler, 1970; Coen and Muller, 1980). This has practical implications for device design (Das, 1969) and also allows further study of intervalley and intersubband scattering. Reviews have been written by Hess (1978a) and by Ferry (1978a).

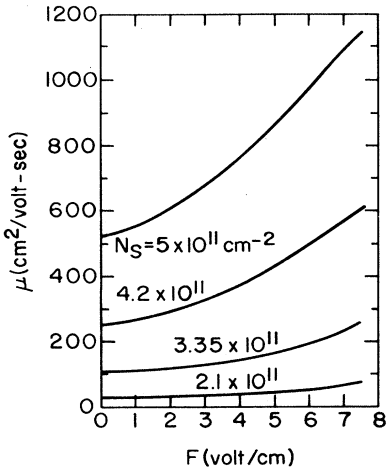

FIG. 68. Field dependence of the electron mobility at 4.2 K for different electron densities. After Fang and Fowler (1970).

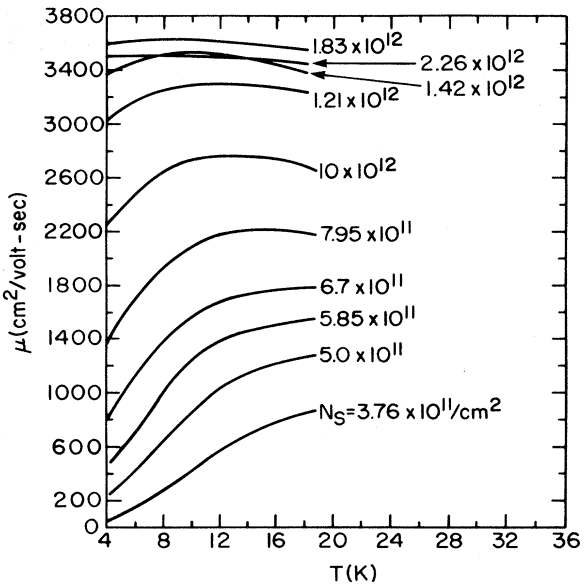

FIG. 69. Temperature dependence of the zero-field mobility for the same samples and electron densities as in Fig. 68. These data can be used with those in Fig. 68 to infer the electron temperatures as a function of drain field. After Fang and Fowler (1970).

Hot-electron studies evolve naturally into two regimes—low and high field. To understand the hot-electron effects it is necessary to understand all of the various scattering mechanisms—oxide charge, surface roughness, and optical and acoustic phonon—for the intrasubband, intersubband-intravalley, and intervalley cases. As discussed in Secs. IV.C and IV.D, the first two cases are reasonably well understood, but the phonon scattering is much less well understood and the fits to data are largely empirical.

There are two primary ways of observing electron heating. If the mobility is temperature dependent, then it is relatively simple to measure a change of conductance with F_D and relate it to a change of electron temperature as illustrated in Figs. 68, 69, and 70. However,

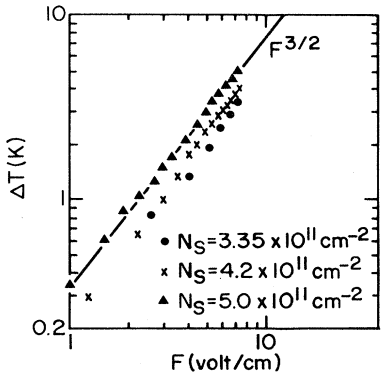

FIG. 70. Electron temperature rise as a function of drain field, deduced from the data in the two previous figures showing $\Delta T \approx 0.3 F_D^{3/2}$. In the range of these measurements, the conductivity is activated. After Fang and Fowler (1970).

if the temperature dependence of the mobility is weak, as it is at 4.2 K for $N_s > 10^{12}$ cm^{-2}, then measurements are difficult. Then it is possible to use the temperature dependence of the magneto-oscillations as a thermometer in measuring the electron temperature as F_D increased. Results of such measurements are shown in Fig. 71 from Fang and Fowler (1970).

When the conductance is measured as a function of V_D at a constant lattice temprature, T, the data can be fitted at low values of F_D with

$$\mu=\mu_0(1+\beta F_D^2) . \tag{4.79}$$

To first order the field dependence can be fitted to an electron temperature by comparison with the temperature dependence of the low field mobility at the same electron concentration. The electron temperature must be a valid concept as F_D approaches zero. Hess and Sah (1974a) have argued that a Maxwellian distribution is more nearly valid for a two-dimensional than for a three-dimensional gas when the electron distribution is perturbed by a field.

While there are different degrees of sophistication possible in discussing hot-electron effects (see Conwell, 1967; Ferry, 1976c, 1978a, 1978b), we shall follow Hess and Sah (1974a) by using a Boltzmann-equation approach. First, the simplest expression for the acoustical- and optical-mode phonon scattering is assumed to hold:

$$\tau_{\rm ac}^{-1}=\Xi_{\rm ac}^2 k_B T(m_e m_r)^{1/3}\hbar^{-3}\rho^{-1}c_l^{-2}\langle z\rangle^{-1} , \tag{4.80}$$

$$\tau_{\rm opt}^{-1}=\sum_R \frac{(m_t m_l)^{1/2}\Xi_R^2\hbar\omega_R}{2\hbar\rho c_R^2}[(N_R+1)\Theta(x-x_R)+N_R] , \tag{4.81}$$

where Ξ is the deformation potential for the appropriate mode, ρ is an areal mass density in a layer of effective thickness $\langle z\rangle$, c is the appropriate sound velocity, $x=E/k_BT$, $x_R=\hbar\omega_R/k_BT$, Θ is a step function, ω_R are the appropriate phonon frequencies, and N_R is the number of phonons per mode. The effective thickness

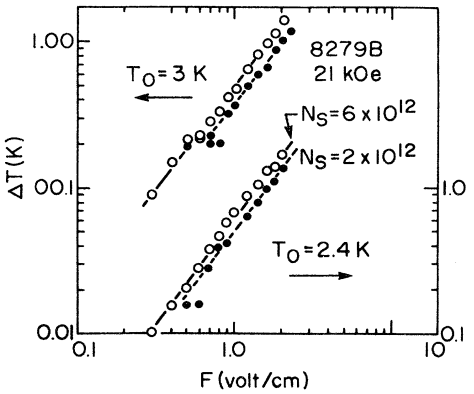

FIG. 71. Electron temperature rise as a function of electric field, deduced from the dependence of magneto-oscillation amplitude on temperature and drain field. The ambient temperatures were 2.4 and 3.0 K. The electron densities were not in an activated range. $\Delta T \sim F_D^{3/2}$. After Fang and Fowler (1970).

$\langle z\rangle$ that enters in the areal density is not very well defined, but is approximately equal to $z_{\rm av}$ (see also Sec. IV.D). For the warm-electron case at low temperature, where only acoustic and elastic scattering are important, Hess and Sah (1974a) show that the distribution is approximately Maxwellian. At higher values of F_D, when the electron temperature is such that many electrons have energies greater than $\hbar\omega_R$, there is a departure from a Maxwellian distribution at $E=\hbar\omega_R$. The mean energy deviation Δ from kT is

$$\Delta=\langle E-k_BT\rangle=\tau_E\left\langle\frac{dE}{dt}\right\rangle , \tag{4.82}$$

where τ_E is the energy relaxation time and

$$\left\langle\frac{dE}{dt}\right\rangle=e\mu F_D^2\approx e\mu_0 F_D^2 . \tag{4.83}$$

The change in mobility is fitted by Eq. (4.79) above. Then approximately

$$\beta=e(d\mu/d\Delta)\tau_E . \tag{4.84}$$

This should hold in the limit as F_D approaches zero. From these arguments Hess and Sah (1974a) find that for acoustic-mode scattering

$$\left\langle\frac{dE}{dt}\right\rangle_{\rm ac}=\frac{2(m_t m_l)^{1/2}\Xi_A^2}{\hbar^3\rho}(k_BT-k_BT_e) . \tag{4.85}$$

Thus T_e-T should be expected to vary as F_D^2 in the limit of small drain fields. For the optical modes

$$\left\langle\frac{dE}{dt}\right\rangle_{\rm opt}=\frac{(m_l m_t)^{1/2}\Xi_R^2\omega_R^2}{2\hbar\rho c_R^2}\times\left[N_R-(N_R+1)\exp\left[-\frac{\hbar\omega_R}{k_BT_e}\right]\right] . \tag{4.86}$$

They find that for the Maxwellian case on the (110) surface β should decrease from a value of about 10^{-8} cm^{2}V^{-2} at 50 K to 10^{-9} at 230 K. When optical-mode scattering is important β is nearly constant at 10^{-7} cm^{2}V^{-2}.

Fang and Fowler (1970) have found results that seem to be in contradiction to the above. At 4.2 K and low values of N_s ($<10^{12}$ cm^{-2}) they found that $\beta\approx10^{-2}$ cm^{-2}V^{-2}. However, these data are in a range where localization phenomena (see Sec. V.A) occur, so that the above arguments are not expected to be relevant. Further, they found at all values of N_s studied that (T_e-T) is proportional to $F_D^{3/2}$ (Figs. 70 and 71). Clearly, more experimental and theoretical work is required.

Assuming β not to be a function of V_g, Hess and Sah (1974a) found experimentally that β on (110) surfaces was proportional to the mobility μ, as expected from Eq. (4.84). They found at 77 K that $\beta_{\langle100\rangle}=(5\pm2)\times10^{-8}$ cm^{2}V^2 and $\beta_{\langle110\rangle}=(2\pm0.6)\times10^{-8}$ cm^{2}V^{-2}, while $\mu_{\langle100\rangle}=4000$ cm^{2}V^{-1}s^{-1} and $\mu_{\langle100\rangle}=2800$ cm^{2}V^{-1}sec^{-1}. This is in reasonable agreement with the predictions above. As they pointed out, repopulation of

the higher subbands was not taken into account. To have done so would have been a nontrival undertaking because it would have had to be done self-consistently and because the energy distribution would have been seriously perturbed. They made a rough estimate of the effects of repopulation and concluded that in this case they were small. Inherent in this approximation is a knowledge of the Debye temperature $\Theta_R \equiv \hbar\omega_R$. For f-type scattering (two valleys not on the same axes) Hess and Sah used $\Theta_1 = 670$ K and $\Theta_2 = 190$ K (Norton *et al.*, 1973). They used $\Xi_1 = 17.6$ eV and $\Xi_2 = 7.4$ eV. There is some uncertainty in these constants.

Fang and Fowler (1970) also measured the electron velocities to very high fields (up to about 5×10^5 V cm^{-1}). They used thick oxide films and relatively small source-drain lengths to minimize the variation of carrier density along the channel. Coen and Muller (1980) used a resistive gate with the voltage drop along it properly adjusted for the same purpose (but could not eliminate the effects of varying N_{depl}). Their results and those of others are quite similar [Sugano *et al.*, 1973; Sato *et al.*, 1971b (for holes)] and show saturation at the highest fields to a velocity v_{sat}. Typical results of Fowler and Fang (1969) are shown in Fig. 72. These experiments averaged the conductance over all directions on the (100) surface. However there are quantitative differences between experiments. Recent results of Cooper and Nelson (1981) give higher values of the saturation velocity. See also Muller and Eisele (1980). The differences have not been resolved.

Hess and Sah (1974a) used the E_0 and $E_{0'}$ subbands, only f phonons, and the arguments above to fit the high-field data of Fang and Fowler (1969) with reasonable success, as shown in Fig. 73. Ferry (1976a) used the E_0, E_0', and E_1 subbands and six phonons. Nakamura (1976) carried out a somewhat more elaborate calculation and compared it to unpublished data of Namiki and Kawaji (Fig. 74). Basu made a Monte Carlo calculation (1978a). Theory and experiment are compared in Fig. 75. Experiment is somewhat lower than theory. Ferry attained the closest fit to the data.

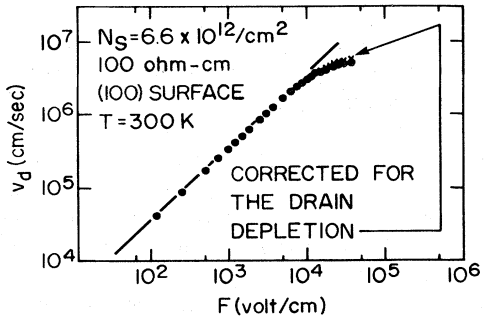

FIG. 72. Typical drift velocity variation as a function of field for electrons in the (100) surface at 300 K. The sample had a channel length of 10 μm and a gate oxide thickness of 1 μm. The two sets of data shown at high drain field are uncorrected and approximately corrected for the slight decrease of carrier concentration near the drain at high drain voltage. After Fang and Fowler (1970).

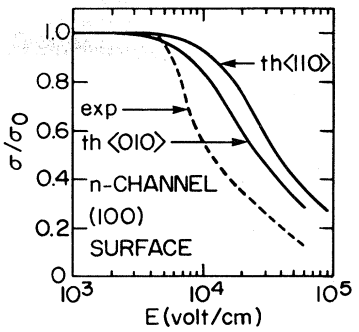

FIG. 73. Comparison of theoretical predictions of Hess and Sah (1974) for electron velocity saturation for two directions in the (001) surface with experiment. The ordinate is σ/σ_0 or μ/μ_0. The data were taken from Fang and Fowler (1970). After Hess and Sah (1974a, 1974b).

The saturation velocity ($\sim 6\times10^6$ cm s^{-1}) for the (100) surface at 300 K is somewhat lower than the bulk value of about 10^7 cm s^{-1} (Canali *et al.*, 1975). At first glance, this may seem surprising because at the high electron temperatures ($\sim$1000 K) near saturation the electrons might be expected to look almost bulklike, and they would be so far from the surface that surface effects

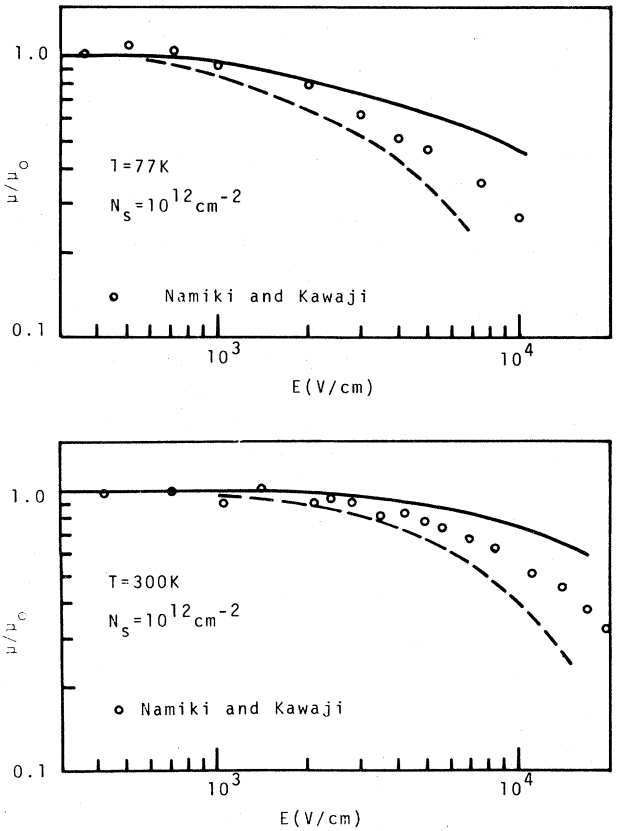

FIG. 74. Comparison of theoretical predictions of Nakamura (1976) with unpublished data of Namiki and Kawaji for electrons in the (100) surface. The dashed lines are for the one-subband approximation; the solid lines take account of higher subbands. After Nakamura (1976).

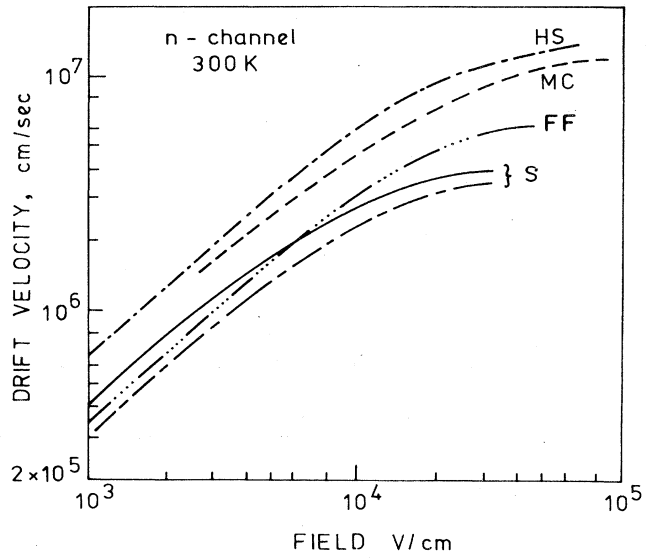

FIG. 75. Drift velocity vs drain field for electrons in n-type inversion layers. The calculated curves are from Hess and Sah (HS) (1974a, 1974b) and the Monte Carlo calculations of Basu (MC) (1978a). Experimental results are from Sato (S) *et al.* (1971b) for two gate voltages, and from Fang and Fowler (FF) (1970). After Basu (1978a).

should be minimal. Nonetheless, because of the varying potential perpendicular to the surface, the electron energy distribution averages perpendicular to the surface might be expected to be different than it would be in a constant potential.

There is a fascinating possibility that negative differential resistance similar to that seen in bulk GaAs could be observed if the heated electrons in the E_0 subband were transferred to the $E_{0'}$ subband, which has greater mass and lower mobility. Observations of such an effect were first reported by Katayama *et al.* (1972) and were further studied by Sugano *et al.* (1973), Hess *et al.* (1975), and Neugebauer *et al.* (1978). Experiments were carried out by pulsing the drain voltage and observing the drain current at a given time for different V_D as shown in Fig. 76, as an example. It is remarkable that for these data and all others reported the relaxation times attributed to

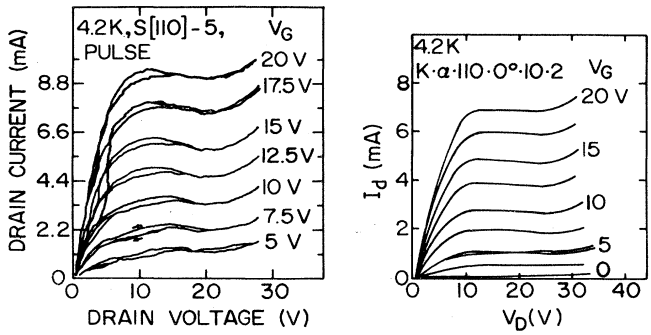

FIG. 76. The drain current I_D vs the drain voltage V_D at 4.2 K on (100) Si sampled at 70 ns from the pulse front. After Sugano *et al.* (1973).

transfer are of the order of 10—50 ns. If the electron transfer mechanism obtained, one would expect these times to be much shorter—of the order 10 ps or less. This intuition is supported by the calculations of Das *et al.* (1978) and Moore and Das (1979). Sugano *et al.* (1973), after an extensive series of measurements, concluded that the relaxation was due to lattice heating. Microwave measurements of hot-electron effects predicted by Ferry and Das (1977) might show the transfer effects, but so far have not.

An interesting application of hot-electron effects has been due to Gornik and Tsui (Gornik and Tsui, 1976, 1978a; Tsui 1978b; Gornik and Müller 1979; Tsui and Gornik, 1978; Gornik *et al.*, 1980a, 1980b). They observed light emission due to transitions of electrons heated to higher subbands or higher Landau levels, or by exciting plasmons. Because the emission is weak, it is difficult to measure the spectra with high resolution, but they correspond roughly to the expected transitions.

Thus hot-electron effects are approximately described by simple theory. They offer the hope of better understanding of phonon scattering.

V. ACTIVATED TRANSPORT

A. Activated conductance near threshold

1. Introduction

In three-dimensional systems, the effects of disorder, band tails, and metal-insulator transitions have long been of interest. See Mott and Davis (1979) and Mott (1974b) for reviews. Here we review evidence of similar effects at the band edges in inversion layers. Again the ability to vary E_F and N_s is used to advantage.

There are known to be charges in the oxide either near to the Si-SiO_2 interface or spread throughout the oxide. Such charges can cause discrete bound states (Stern and Howard, 1967; Fang and Fowler, 1968; Goetzberger *et al.*, 1968) (see Sec. II.E and Sec. V.C below) or random surface potential fluctuations, as shown graphically in Fig. 77. If the potential fluctuations are mainly long range it is possible for $\mathbf{k}$ to be a good quantum number for the electrons within a potential minimum. Then it might be expected that the electron will behave according to a classical percolation theory if the voltage is such that there are isolated "lakes" or networks of electrons. If short-range fluctuations dominate, the lowest-energy electrons can be localized in the potential wells unless the electron density is such that the Ioffe-Regel criterion (see Mott, 1974a) that $k_F l < 1/2\pi$, where l is the mean free path, is exceeded. In the latter case, the electronic wave functions are extended. In either case, the density of states averaged over the surface no longer abruptly increases to its constant value for two dimensions of $g_v m/\pi\hbar^2$, where g_v is the valley degeneracy. Instead, as shown graphically in Fig. 78, there is a band tail. Mott (1966) has proposed that below some energy E_c, called

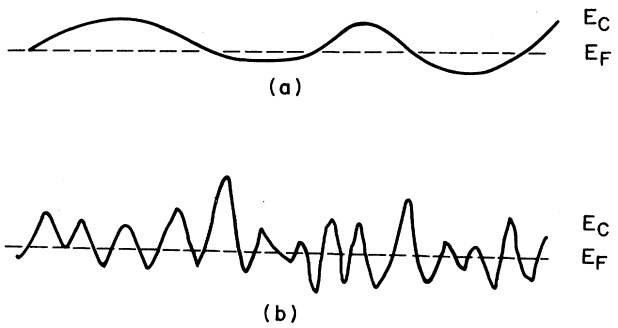

FIG. 77. Fluctuations in the conduction- and valence-band edges. (a) shows long-range fluctuations, whereas (b) shows short-range fluctuations. The Fermi level is shown for a case where the electrons might be expected to be localized.

the mobility edge, the electrons are localized; above they are free or at least in extended states.

In this section, experimental evidence for strong localization will be reviewed. Here the conductivity is thermally activated. The logarithmic regime of weak localization is discussed in Sec. V.B. It should be noted that there are still many open questions both for weak (logarithmic) and strong (activated) localization.

Mott (1973) and Stern (1974b, 1974c) had speculated that the activated conductance reported by Fang and Fowler (1968) was evidence of Anderson localization. Several reviews of this subject have been written (Mott *et al.*, 1975; Pepper *et al.*, 1975; Pepper, 1977a, 1978g; Adkins, 1978a). There remains a lot of experimental work to be done. Samples differ markedly, and no similar set of samples exists for which all of the various experiments have been performed. Therefore it is not always possible to argue about the interrelationship of experimental results with confidence.

The conductance data are generally of two types, both assumed to arise from fluctuations of the oxide charge near the Si-SiO_2 interface. Both show thermally activated currents for N_s less than about 10^{12} cm^{-2} in the temperature range from 2—4 K to 50 K, with the activation energy decreasing as N_s increases. The first case (sometimes referred to as "ideal" below) generally seems to fit the Mott model for transport for an Anderson transition as modified by Pepper (Pepper *et al.*, 1974c, 1975; Mott *et al.*, 1975) for two dimensions in the thermally activated range. They find

$$\sigma=\sigma_{\min}e^{-W/k_BT}, \tag{5.1}$$

where $\sigma_{\min}$ is approximately the minimum metallic conductivity predicted for two dimensions—0.1 $e^2/\hbar$—W decreases with increasing N_s but $\sigma_{\min}$ is constant. In inversion layers $\sigma_{\min}$ appears never to be much smaller than 0.1 $e^2/\hbar$ but is often larger. This idealized behavior is shown in Fig. 79(a). In the second case, shown in Fig. 79(b) (sometimes referred to as the "nonideal" case in that it does not fit the Mott-Pepper model), the prefactor σ_0 increases with N_s and W decreases as in the other case. This behavior has been ascribed to long-range fluctuations in the oxide charge (Arnold, 1974, 1976), in which conductance corresponds to classical percolation either through metallic one- or two-dimensional paths and/or by thermal activation over barriers.

Below we shall discuss the evidence from conductance

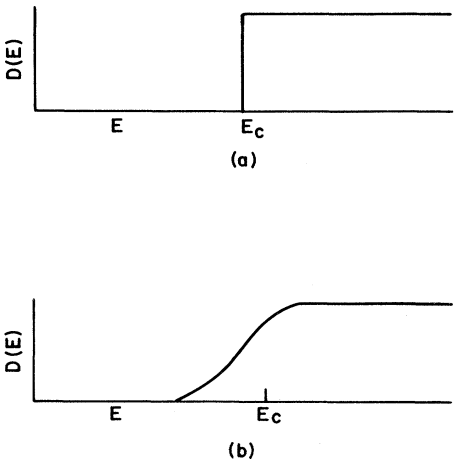

FIG. 78. The density of states $D(E)$ for (a) an unperturbed and (b) a perturbed band in two dimensions. The mobility edge is shown at E_c.

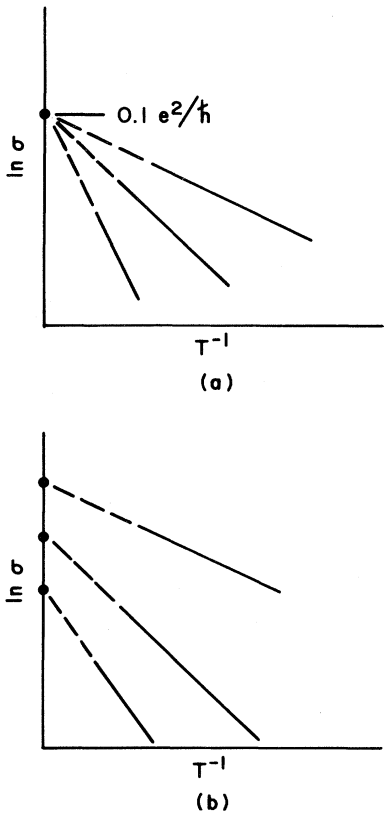

FIG. 79. A graphic illustration of the two types of activated conductivity. (a) demonstrates the "ideal" Anderson localization, with the curves converging at $\sigma_{\min}=0.1e^2/\hbar$. (b) is the "nonideal" case, with σ_0 increasing with N_s. The intercepts are normally at values greater than $0.1e^2/\hbar$.

data for the short- and long-range fluctuation or alternately the "ideal" and "nonideal" models, followed by discussions of the effect of substrate bias, the Hall effect, and miscellany. Very recently, Gold and Götze (1981) have analyzed the effects of long- and short-range fluctuations. In general, their theory supports the idea that the ideality is reduced as the range of the disorder increases.

2. The Anderson transition

In 1958 Anderson argued that if fluctuations of $\pm V_0/2$ were introduced in a tight binding model with bandwidth B, all of the electrons would be localized if V_0/B exceeded some critical value. Mott (1966, 1967) argued that even if all of the electrons in the band were not localized, those near the edges would be. He introduced the idea of the mobility edge at E_c, an energy marking the boundary between localized electrons with wave functions decaying as $\exp(-\alpha r)$ and electrons in extended states with short mean free paths. Just above E_c the electrons diffuse, but below they can only move by thermally activated tunneling to another site (Miller and Abrahams, 1960) or by being thermally excited to states above the mobility edge. Mott has proposed that the conductivity decreases to zero discontinuously as E_F passes through E_c at $T=0$. A so-called metal-insulator transition takes place.

For two dimensions Pepper (Mott *et al.*, 1975) modified Mott's derivation of the minimum metallic conductivity $\sigma_{\min}$, the conductivity at the mobility edge, to find

$$\sigma_{\min}=\frac{\pi e^2}{4z\hbar}\left[1+\frac{V_0^2}{B^2}\right]^{-1}, \tag{5.2}$$

where z is the number of nearest neighbors. Thouless (1974) found that V_0/B at the mobility edge was $\frac{4}{3}$ so that $\sigma_{\min}$ is about $0.07\ e^2/\hbar$ or 1.8×10^{-5} S in this relatively crude model. Computer models of Licciardello and Thouless (1975a, 1975b, 1976a) predict that $\sigma_{\min}=0.12e^2/\hbar$ or 2.9×10^{-5} S.

Mott (1968) predicts that Eq. (5.1) holds at intermediate temperatures below the mobility edge. This isn't obvious if one approaches the problem by assuming that the electrons have some fixed mobility at and near the mobility edge and a density of states $N(E_c)$. Then

$$\sigma=e\mu_{\min}k_BTN(E_c)\exp[(E_F-E_c)/k_BT]\ . \tag{5.3}$$

The derivation of $\sigma_{\min}$ assumes a diffusive process at the mobility edge, and it is then argued that the diffusion constant $k_BT\mu$ is constant in analogy with metals, so that $\sigma_{\min}$ is not temperature dependent. This implies that when $(E_F-E_c)<0$ the number of carriers above the mobility edge is activated and that the mobility decreases as T^{-1}. We shall return to this in a discussion of the Hall effect. Experiments are not accurate enough to determine any temperature dependence in $\sigma_{\min}$.

Figure 80 (Pollitt, 1976) shows one of the many examples of such behavior in the literature. Similar results have been reported in n- and p-type inversion layers and in simple MOS structures and MNOS memory devices. The values of $\sigma_{\min}$ measured range from 1.5 to 5×10^{-5} S. This is certainly close to the expected value, although $\sigma_{\min}$ does not appear to be quite a universal constant.

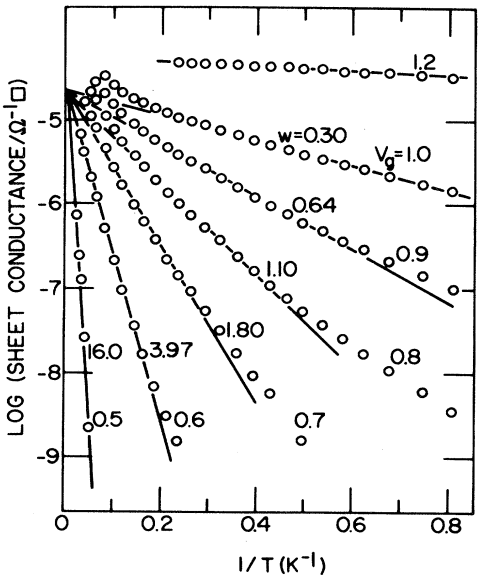

FIG. 80. Logarithm of the conductance vs $1/T$. The carrier concentration N_s (proportional to V_G-V_T) ranges from about 10^{10} to 10^{11} cm^{-2}. The activation energies $W(=E_c-E_F)$ in meV are indicated. After Pollitt (1976).

Because the MOS structure is a capacitor, the number of electrons is directly related to the gate voltage, so that N_s can be measured approximately and the change in N_s can be determined quite accurately. Therefore, if the density of states and E_c do not change as N_s changes, the density of states $D(E_c)$ in the tail of the conduction band can be inferred from a measurement of the activation energy (E_c-E_F) as a function of N_s. This was first reported by Adkins, Pollitt, and Pepper (1976) and has been applied by Pollitt (1976) to data for a device with 1.8×10^{11} cm^{-2} localized electrons and $\sigma_{\min}=2\times10^{-5}$ S.

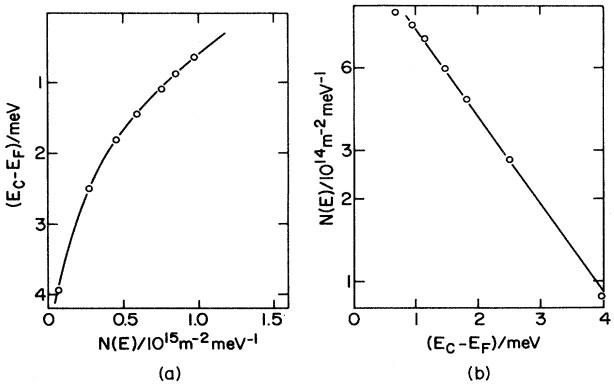

FIG. 81. (a) Density of localized states $N(E)$ plotted against E_c-E_F calculated from Fig. 80. (b) Logarithm of $N(E)$ vs E_c-E_F, the difference of energy between the mobility edge and the Fermi level. After Pollitt (1976).

The results are shown in Fig. 81. The density of states decreases exponentially in the band tail as expected (Zittartz and Langer, 1966; Thouless and Elzain, 1978). $D(E_F)$ does not exceed the density of states in the unperturbed conduction band (1.6×10^{11} cm^{-2}meV^{-1}). This analysis may be too simple. $D(E)$ may vary either because of correlation effects (Tsui and Allen, 1974) or in samples with low N_{depl} because increasing N_s decreases z_{av} and could change the potential fluctuations. In some cases $D(E)$ varies significantly over k_BT, although the experiments discussed were carried out below 10 K. The maximum measured value of $D(E)$ seems to lie between 0.5 and 0.75 of 1.6×10^{11} cm^{-2}meV^{-1} so long as the number of apparent localized states is less than about 3×10^{11} cm^{-2} (Pepper *et al.*, 1976; Adkins *et al.*, 1976). In samples with a higher number of localized states, however, the deduced $D(E)$ can rise to values well above 1.6×10^{11} cm^{-2}meV^{-1} (Tsui and Allen, 1975; Adkins *et al.*, 1976) by as much as a factor of 20. Correlation effects have been invoked by Tsui and Allen (1975) but no model exists. Mott *et al.* (1975) have suggested that electrons trapped on sites increase disorder—that is, the increase in random potential due to the localized electrons must dominate over the screening of the potential fluctuations. It is not clear why this should happen. If N_{depl} is small, increasing N_s should increase the depth of the localized states just as reverse substrate bias does (Pepper, 1977a and discussion below in Sec. V.A.4) because, for low N_{depl}, changes in N_s strongly affect z_{av}. No correlation of this effect to N_{depl} has been made.

There are several arguments about the density of states $D(E_c)$ where the transition occurs. Early arguments (Mott *et al.*, 1975) suggested that $D(E_c)$ was about $\frac{1}{5}$ the unperturbed band value. Thouless and Elzain (1978), using a white-noise model, have estimated that the ratio is nearer $\frac{4}{5}$, which is certainly more nearly consistent with the measurements where the maximum ratio observed in well behaved samples with a small number of localized electrons was 0.7 (Adkins *et al.*, 1976).

At both higher and lower temperatures there is a departure from a simply activated dependence. At higher temperatures other subbands may be involved (see Sec. IV.B.4). At low temperatures, conduction is believed to proceed by variable-range hopping (Pepper *et al.*, 1974c; Tsui and Allen, 1974). The theory (Mott, 1968; Ambegaokar *et al.*, 1971) for this process is developed from the theory of Miller and Abrahams (1960) for nearest-neighbor hopping within a band. Miller and Abrahams found that nearest-neighbor hopping is a simple activated process with an activation energy comparable to the bandwidth. In the band tail, the bandwidth has to be of the order of (E_c-E_F) so that activation to the mobility edge would always be expected to dominate nearest-neighbor hopping. However, at low enough temperatures, longer hops with lower activation energy become favored and the expected dependence is a modification of Mott's theory for three dimensions (Mott, 1968), as made by Pollack (1972) and Hamilton (1972). They found

$$\ln(\sigma/\sigma_0)=-3\alpha^{2/3}[\pi D(E_F)k_BT]^{-1/3}\,, \tag{5.4}$$

where $\sigma_0=\frac{1}{4}D(E_F)[\pi\alpha D(E_F)k_BT]^{-2/3}\nu_p$ and $D(E_F)$ is assumed to be constant over a few k_BT, α is the localization factor in $\psi\sim\exp(-\alpha r)$, and ν_p is a frequency factor that depends on the electron-phonon interaction. The condition that $D(E)$ varies slowly as compared to k_BT does not appear unreasonably violated in Fig. 81 (Mott *et al.*, 1975). Pollitt (1976; see also, Mott *et al.*, 1975) tested this relationship carefully for several samples and found that $\ln\sigma$ was proportional to $-(1/T)^{0.32\pm0.02}$. Typical data are shown in Fig. 82. No account was apparently taken in these fits of any temperature dependence in the prefactor.

From these data α can be calculated using the values of $D(E)$ as derived above from the activated regime. It has been predicted that

$$\alpha\propto(E_c-E_F)^s\,. \tag{5.5}$$

Early experiments on (111) surfaces well below the mobility edge, where an overshoot of $D(E)$ was seen, showed $s=0.73\pm0.07$ (Pepper *et al.*, 1974b). This was close to a prediction of Abram (1973) that $s\sim0.75$ for a two-dimensional system. However, more extensive measurements on better behaved samples with fewer localized electrons (Pollitt, 1976) showed that s was not constant with (E_c-E_F) and increased from values of 0.6 deep in the band tail to about one near the mobility edge. This of course means that α is not described by a power-law dependence in the energy difference. Mott (1976) has argued that $s=1$ for two dimensions as E_F approaches E_c because values of s less than one are inconsistent with a discontinuous change in σ at $T=0$—a metal-insulator transition. Licciardello and Thouless (1975b) found even higher values. At least some of Mott's arguments have been disputed by Licciardello and Thouless (1977). At large values of (E_c-E_F) one might expect that $s\to0.5$ (Adkins *et al.*, 1976).

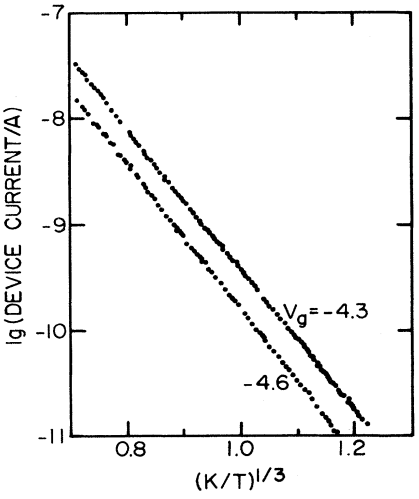

FIG. 82. Logarithm of conductivity vs $T^{-1/3}$. The data are for two values of V_G. After Mott *et al.* (1975).

Many of the apparent anomalies in these "ideally" localized samples, such as the Hall effect and substrate bias effects, are discussed below. It is not clear that other supposedly anomalous effects, such as the observation of magneto-oscillations or cyclotron resonance below the mobility edge, have ever been studied in "ideal" samples.

3. "Nonideal" activated conductance

As discussed in the introduction to this section, many samples are not as "ideal" as those discussed above and do not seem to conform to the Mott-Pepper model of transport in a two-dimensional system experiencing Anderson localization. Some data of this sort taken from Allen, Tsui, and DeRosa (1975) are shown in Fig. 83; they are similar to data from many sources (Fang and Fowler, 1968; Fowler, 1975; Hartstein and Fowler, 1975; Arnold, 1976; Cole, Sjöstrand, and Stiles, 1976; Tsui *et al.*, 1974). As will be discussed below, application of reverse substrate bias, resulting in a decrease in z_{av}, can sometimes change samples from nonideal to nearly ideal (Pepper, 1977a).

It can be seen in Fig. 83 that the prefactor of the exponential temperature dependence of conductivity increases with N_s. For the nonideal case it is much more difficult to define a "σ_{min}" experimentally because σ_0 varies with N_s. An approximate value is taken at the lowest nonactivated conductivity. Values below 10^{-5} S up to close to 10^{-3} S have been reported. Furthermore, there is usually strong curvature in these data, sometimes approximating the law expected for variable-range hopping at temperatures where variable-range hopping is not likely to dominate (Hartstein and Fowler, 1975a). It is in such samples that many of the apparently anomalous effects have been observed and used as evidence against an Anderson transition. Another mechanism may be at work.

Arnold (1976) has attributed such "nonideal" results to longer-range or macroscopic fluctuations in the oxide charge and the surface potential. He has attempted to explain his results in terms of a semiclassical percolation theory, necessarily with many approximations and assumptions. He assumes that near (or even below) current threshold, pools or lakes of carriers form that are at first not simply connected. They are below the percolation threshold at 0 K, and conduction can only proceed by tunneling through or by thermal excitation over the intervening barriers. [He has suggested that resonant tunneling may give rise to the structure in the field-effect mobility observed by Howard and Fang (1965), Pals and van Heck (1973), Tidey *et al.*, (1974), Voland and Pagnia (1975), and Voss (1977, 1978).] Even for higher values of the average N_s, where there are percolation paths at $T=0$, thermal excitation over the barriers could provide current paths at finite temperatures. Arnold (1974, 1976) supposes, as do Brews (1972a, 1972b, 1975a, 1975b) and Stern (1974b, 1974c) that the oxide charges have a Poisson distribution across the surface which leads to pools of the order of several hundred angstroms or more. This assumption is questionable, but calculation of the conductivity is mathematically tractable. Arnold finds that if $g_1(E_F)$ is the average conductance in the metallic regions,

$$g(E_F,V)\approx g_1(E_F)\exp([E_F-V]/k_BT), \quad V>E_F$$
$$\approx g_1(E_F), \quad V<E_F \tag{5.6}$$

where V is the energy of the local band edge. In the insulating regions he finds a conductivity

$$g_2=\left[\frac{g_1}{2\varepsilon}\right]\exp\left[\frac{\sigma^2}{2k^2T^2}+\frac{E_F}{k_BT}\right]\operatorname{erfc}\left[\frac{E_F}{\sqrt{2}\,\sigma}+\frac{\sigma}{\sqrt{2}\,kT}\right], \tag{5.7}$$

where σ is the standard deviation of the potential and ε is the fraction of space occupied by the noninsulating regions. He then uses the percolation theory of Kirkpatrick (1973) to determine the conductivity as a function of temperature. At finite temperatures he finds that

$$g=\tfrac{1}{2}(2p-1)(\sigma_1-\sigma_2)$$
$$+[\tfrac{1}{4}(2p-1)^2(g_1^2-g_2^2+g_1g_2)]^{1/2}, \tag{5.8}$$

where $p(E_F)$ is the fraction of the surface occupied by metallic regions, which reduces to a constant at $T=0$. He has fitted these expressions to experiment as shown in Fig. 84 for a sample where the oxide charge was 6×10^{11} cm^{-2}, apparently assuming a single constant mobility in the conducting regions. It should be noted that he obtained a reasonable fit and that there is a curvature in the plots over the entire range, with decreasing activation energy at lower temperatures. Sjöstrand and Stiles (1975) and Sjöstrand *et al.* (1976) had observed a saturation (below about 1 K), with the saturation conductance decreasing with N_s, of the conductance at a low temperature. This may represent the situation where conduction by thermal excitation over the barriers is no longer im-

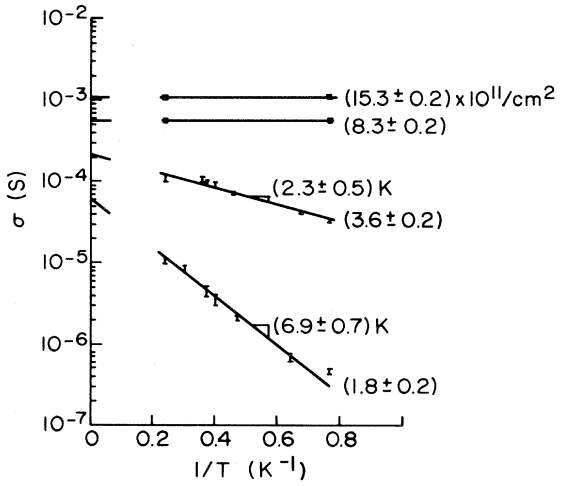

FIG. 83. Logarithm of conductivity vs T^{-1} for a nonideal sample. After Allen *et al.* (1975).

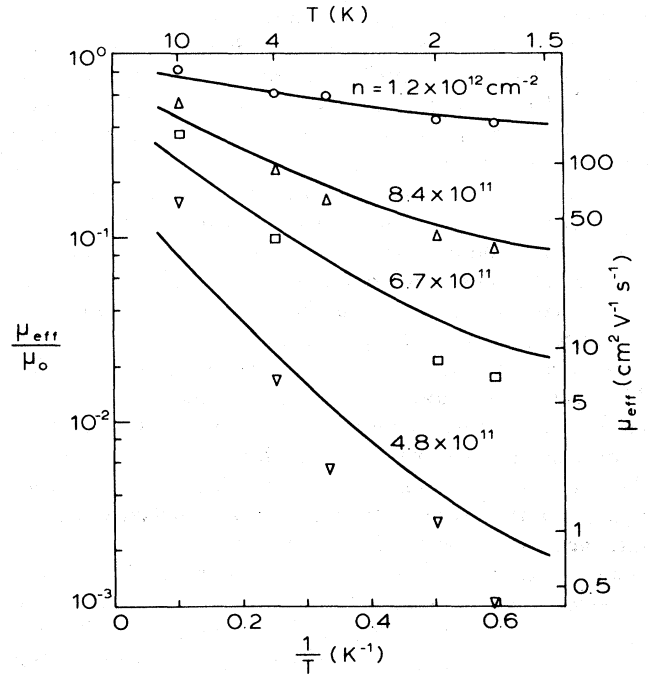

FIG. 84. Logarithm of effective mobility μ_{eff} divided by $\mu_0 = 400\ \text{cm}^2\text{V}^{-1}\text{s}^{-1}$, the value at $N_s = 1.6\times10^{12}\ \text{cm}^{-2}$. The parameter is N_s. The solid curves are a fit from Arnold's effective-medium theory. After Arnold (1976).

portant. This would imply that the percolation threshold occurs for N_s well below the value reached at the apparent minimum metallic conductivity. However, it is not yet clear that this saturation of the conductance is not an experimental artifact due to electron heating by noise. An experimentally observed variable-range hopping law is not predicted by Arnold's theory, but he remarks that the fit may be fortuitous.

Arnold's model would seem to be reasonably successful in fitting the conductance data for the nonideal samples. However, there are serious problems in fitting the model to other experiments, as discussed below. Practically, the minimum metallic conductivity, a term which is only broadly appropriate to this sort of sample, is not too well defined even experimentally because there is no common intercept for $\ln\sigma$ as a function of T^{-1} and because k_BT is much larger than the activation energy near the "mobility edge." This lack of precision in definition seems to be reflected when the reported "minimum metallic conductivities" are compared (Adkins, 1978a) for different samples from different laboratories, as shown in Fig. 85. Hartstein and Fowler (1975) had concluded from their data that $\sigma_{\min}\sim N_{\text{ox}}^{-0.5}$ but Adkins (1978a) felt that the exponent was closer to -0.85. Adkins also concluded that for many samples $\sigma_0\sim N_s^{1/2}$. Pepper (1977a) found that this result only obtained when the localized charge exceeded the oxide charge. In general, increasing the oxide charge for this type of sample decreases the dependence of the intercept, σ_0, on N_s. That is, the samples become more nearly ideal and $\sigma_{\min}$ approaches $0.1\ e^2/\hbar$. The number of states that are localized, i.e., N_s at $\sigma_{\min}$, tends to increase with N_{ox}. Hartstein and Fowler (1975a) found that it was proportional to $N_{\text{ox}}^{3/4}$.

4. Substrate bias

Substrate bias can be applied so as to change the field at the Si-SiO_2 interface, and therefore z_{av}, independently of N_s because the field is a function of both N_{depl} and N_s. Therefore, the electrons can be moved nearer or farther from the oxide charge that causes the potential fluctuations in the surface. Fowler (1975) and Lakhani and Stiles (1976a) used substrate bias to study its effects in the activated conductivity regime. Fowler found, unexpectedly, that the conductance increased rather than decreased as the electrons were forced closer to the surface. As discussed in Sec. IV, the effect of forcing the electrons closer to the surface is to increase all of the scattering mechanisms that are normally important when $E_F > E_c$. These effects have received more study by Cole, Sjöstrand, and Stiles (1976) and especially by Pepper (1977a, 1978h). In the nonideal samples, Fowler found that the conductance increased with reverse substrate bias before saturating, except at low N_s ($<10^{11}\ \text{cm}^{-2}$). Furthermore, the activation energies for constant N_s decreased with increasing reverse substrate bias. These results are shown in Fig. 86. Cole, Sjöstrand, and Stiles (1976) observed similar results for electrons, but slightly different results for holes in nonideal samples. Fowler (1975) has suggested that this effect might be due to band tails from the higher subbands that are split away by reverse substrate bias.

Pepper (1977a) found that some samples that were nonideal behaved very much like ideal samples when the carriers were forced close to the interface, or alternately ideal samples could become nonideal under the influence of forward substrate bias which pulls the carriers away from the interface, as shown for holes in Fig. 87 and for electrons in Fig. 88. In the latter case, as the electrons are pulled away from the surface, the apparent number of localized electrons seems to increase. For $N_{\text{depl}}\approx0$ the activated curves once again converge but at a value well above $0.1\ e^2/\hbar$. Pepper (1977a) has found the effect of

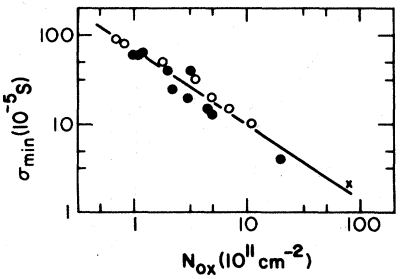

FIG. 85. Apparent minimum metallic conductivity $\sigma_{\min}$ against the net number of positive charges in the oxide N_{ox}. The gradient in the curve is -0.85. Data from Hartstein and Fowler (1975), Tsui and Allen (1975), Pepper *et al.* (1974), and Adkins (1978a). After Adkins (1978a).

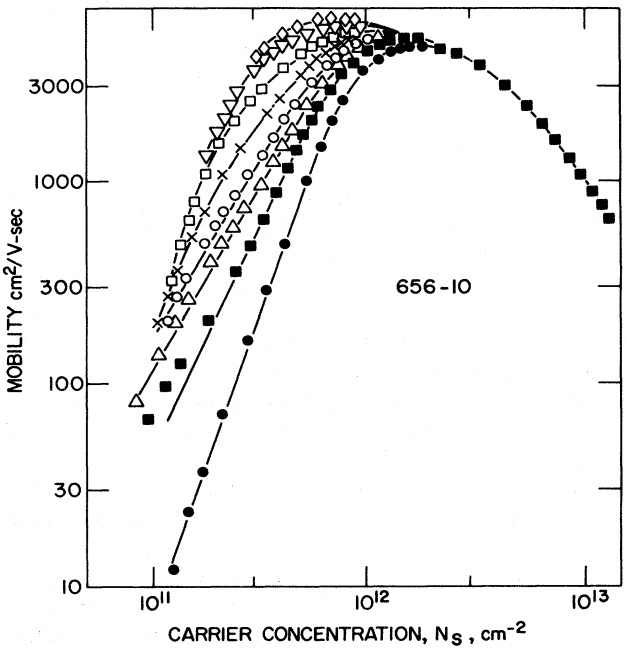

FIG. 86. Electron effective mobility as a function of inversion layer electron concentration at 4.2 K. The bulk doping level is $N_A = 1.36 \times 10^{15}$ cm^{-3} and the density of oxide charges is $N_{ox} = 9.1 \times 10^{10}$ cm^{-2}. The curves, starting with the lowest, are for substrate bias voltages $V_{sub} = 1$, 0, -1, -2, -4, -8, -16, and -32 V. At high densities the curves coincide. After Fowler (1975).

substrate bias is strongest in samples that are not radiation hard (Pepper, 1977e, 1978h). Samples that are not radiation hard have large numbers of neutral traps near the interface that trap positive charge when the samples are exposed to radiation. Similar neutral traps have been observed for electrons by Young (1980). They occur after the same annealing treatment as in samples that are not radiation hard. The electron and hole traps may be the same, although no experiments have been done to connect them. Furthermore, there is evidence of a neutral short-range scatterer in the studies of metallic conductance (Sec. IV). Pepper (1977a) supposes that these centers are dipoles, probably short-range in potential. They can easily exceed by an order of magnitude the net number of positive charges in the oxide. He suggests that when the electrons are far from the interface, the fluctuations arise primarily from the longer-range monopoles, but that when the electrons are pushed close the interface the dipoles dominate. Such an explanation would predict long-range fluctuations and nonideal behavior for moderate N_{ox}, that changes to ideal behavior either when the N_{ox} is much larger than the number of neutral centers or when N_{ox} is smaller but N_{depl} is such that the dipoles contribute most of the fluctuations. For very low doping in the substrate this transition could occur as N_s increases because N_{depl} is small. It is possible to trap either holes or electrons in these neutral centers (DiMaria, 1978), and it would be interesting to study the effect on transport in this range. One effect of hole trapping is an observed increase of the ap-

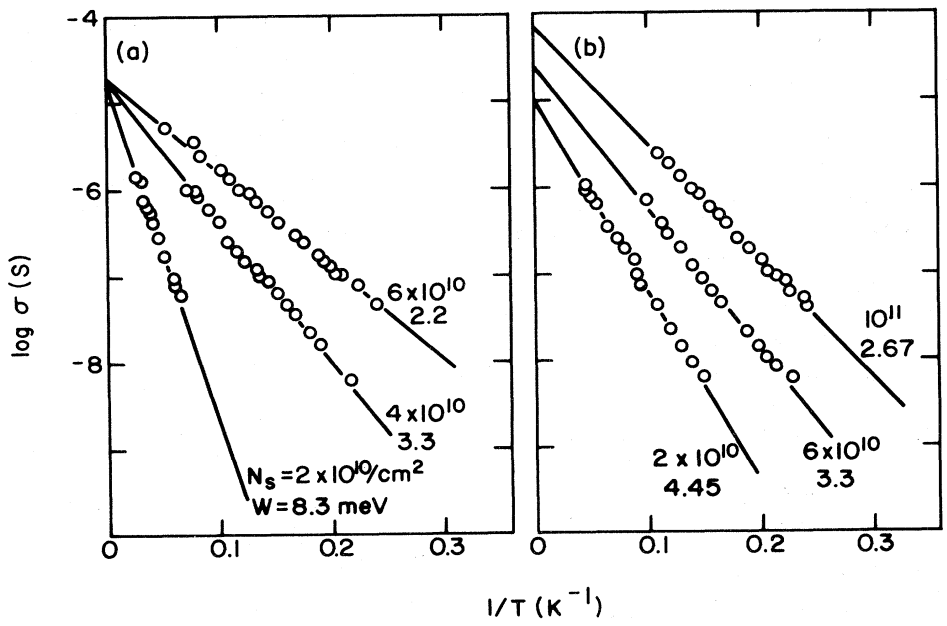

FIG. 87. The effects of substrate bias on a p-channel MOSFET. $N_{ox} = 10^{11}$ cm^{-2}. The logarithm of conductance is shown for (a) $V_{sub} = +20$ V and (b) $V_{sub} = -0.6$ V. The curves are labeled with the values of N_s[cm^{-2}] $\approx 2 \times 10^{11} V_G$[V] and the activation energy W. After Pepper (1977a).

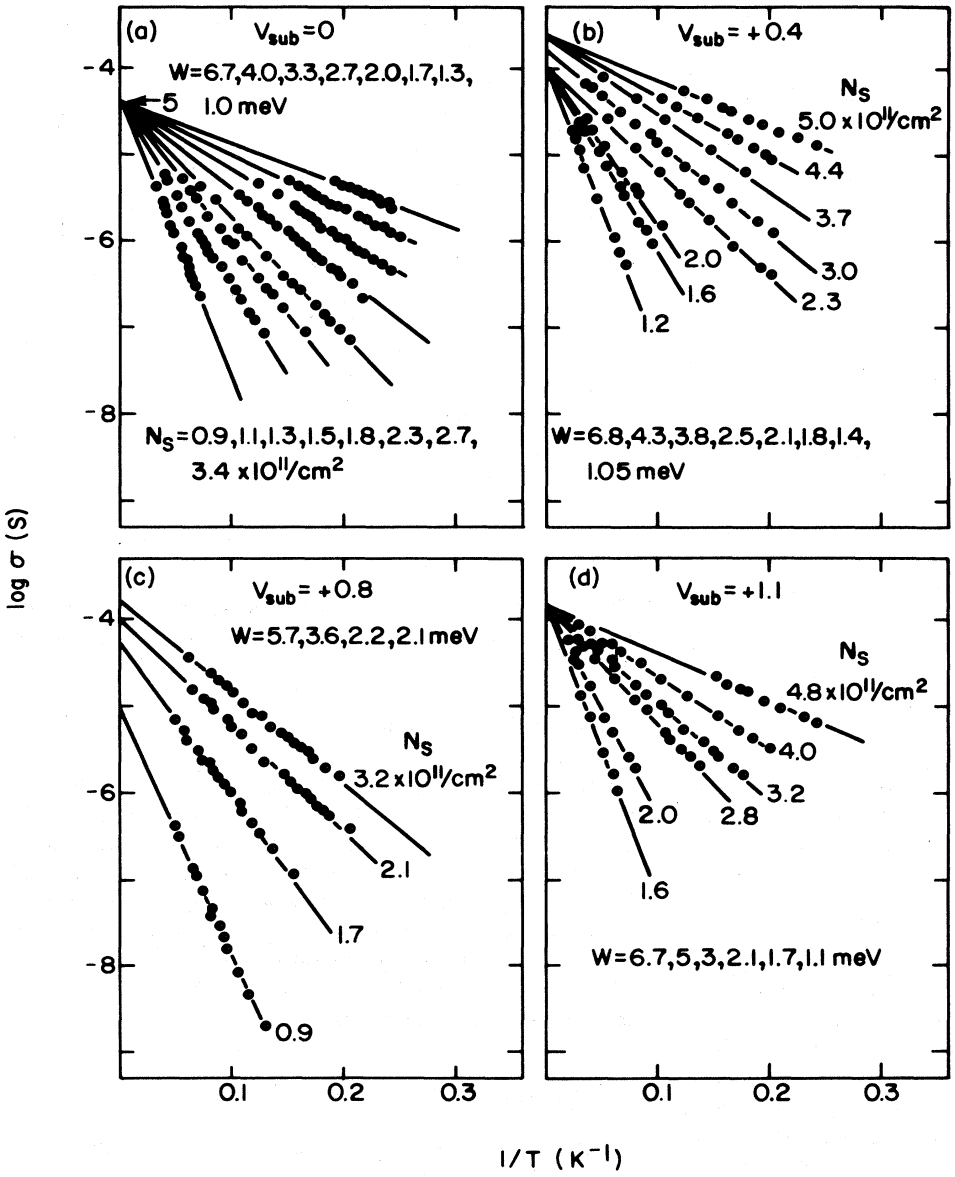

FIG. 88. Progressive effects of forward substrate bias in an n-channel MOSFET. $V_{sub}=0$, $+0.4$, $+0.8$, and $+1.1$ V. $N_{ox}=1.7\times10^{11}$ cm^{-2}. $N_A=2\times10^{15}$ cm^{-3}. $N_s[\text{cm}^{-2}]=7.5\times10^{10}V_G[\text{V}]$. Values of N_s and W are given. After Pepper (1977a).

parent density of surface states.

Pepper (1978h) has found also that if samples are prepared so as to reduce the number of neutral states or hole traps or dipoles at the interface, the usual anomalous substrate bias effects are not seen. The conductance decreases slightly as the electrons are forced closer to the interface. He has not reported on the effect on activation energies, density of states, or localization constant.

The depletion charge itself is subject to fluctuation that statistically might be expected to be fairly long range. According to Keyes (1975a, 1975b), the range might be expected to increase as N_{depl} increases, which does not seem to be consistent with Pepper's results. Keyes takes as his length scale the depletion depth. If z_{av} were more appropriate this conclusion would be different.

Thus it appears that the substrate bias experiments are not necessarily inconsistent with the discussion above of the two general types of samples with long- and short-range fluctuations. Arnold's theory (1976) has not been modified to consider the effects of substrate bias. The recent calculations of Gold and Götze (1981), in which account has been taken of the range of fluctuations to fit various "ideal" and "nonideal" data, have not yet been extended to the substrate bias data. It would be interesting to see if the fluctuation parameter does in fact decrease with negative substrate bias.

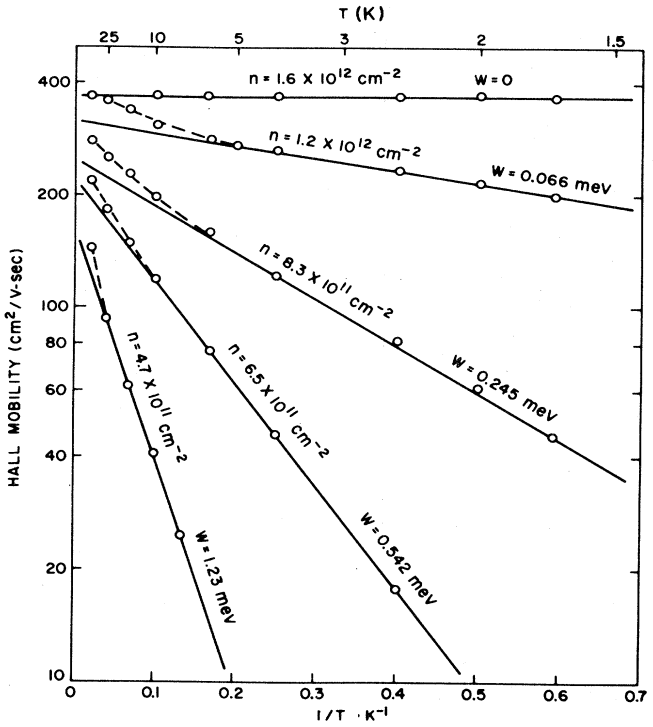

FIG. 89. Hall mobility vs T^{-1} for a p-channel sample demonstrating the activated Hall mobility in this nonideal sample. Each curve is labeled with the value of electron density N_s (here called n) and the activation energy W. After Arnold (1974).

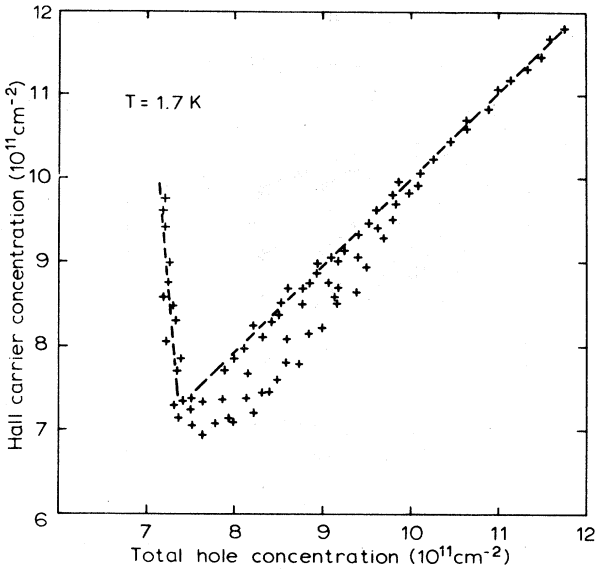

FIG. 90. $N_H=(ecR_H)^{-1}$, the value of N_s from Hall measurements, as a function of N_s from $C_{ox}(V_G-V_T)$. After Arnold and Shannon (1976).

5. Hall effect

The Hall effect in the activated regime has been regarded as anomalous since Arnold (1974) reported that the Hall mobility rather than the carrier concentration derived from the Hall effect—$(ecR_H)^{-1}$—was thermally activated as shown in Fig. 89. Arnold and Shannon (1976) further found that there was an anomalous rise in $(ecR_H)^{-1}$ with decreasing N_s somewhere close to the metallic transition in these nonideal samples, as shown in Fig. 90. In this range the Hall mobility goes to zero but the conductance remains finite. A similar but weaker structure was reported by Pollitt *et al.* (1976) for supposedly ideal samples. Similar effects have been seen by Pepper (1978f, 1978g) in samples where N_{ox}, due in this case to Na^+ ions, is relatively high (7×10^{11} cm^{-2}). He found, as may be seen in Fig. 91, that this rise disappeared as the electrons were forced by substrate bias closer to the surface and the samples became more nearly ideal. Furthermore, with reverse substrate bias the behavior that is intuitively expected for excitation to the mobility edge was found. That is, $(ecR_H)^{-1}$ was less than N_s for $\sigma<\sigma_{min}$ but equal for the metallic regime. Further, the strong temperature dependence of the mobility decreased, so that most of the temperature dependence in the activated regime was presumably in the carrier concentration. Thus these preliminary substrate bias experiments would seem to eliminate the Hall-effect anomaly in ideal samples, but more data are needed to be confident.

The case for long-range fluctuations would still seem to be anomalous. At 0 K, $(ecR_H)^{-1}$ should take on the value for the metallic regions (Juretschke *et al.*, 1956). We believe that there is no theory of the Hall effect at elevated temperatures where conductance is dominated by excitation over barriers and especially none that yields something like the experimental results.

It should be noted that Adkins (1978a, 1978b) has come to very different conclusions.

6. Other experiments

It has been observed (Tsui and Allen, 1974) that magneto-oscillations persist into the activated regime. It should be remembered that these experiments were made

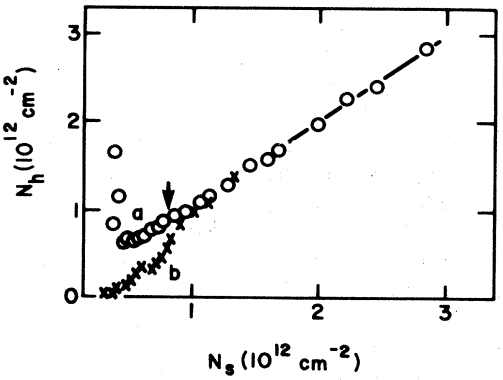

FIG. 91. $(ecR_H)^{-1}$ vs N_s for two substrate biases at 4.2 K. (a) $V_{sub}=0$. (b) $V_{sub}=-15$ V. The arrow marks a conductivity of 3×10^{-5} S ($0.12e^2/\hbar$). After Pepper (1978f).

on nonideal samples. If they correspond to Arnold's long-range fluctuation model then it would not be surprising that cyclotron orbits could exist in the pools of metallic electrons. However, it might be expected that oscillations would be considerably smeared because it would be almost unbelievable if N_s were the same in each pool. We have found no reference to measurement of magneto-oscillations below $\sigma_{\min}$ for ideal samples.

The situation is similar for cyclotron resonance experiments. It is not apparent that cyclotron resonance occurs anomalously in ideal samples. Some workers have not measured the temperature dependence of the conductance but have assumed an activated behavior. Further, there are still differences in results between different groups (Kennedy *et al.*, 1977; Kotthaus *et al.*, 1974b; Abstreiter *et al.*, 1976b; Wagner, 1976a, 1976b; Wagner and Tsui, 1979, 1980; Wagner *et al.* 1980). Both of the above experiments might be clarified with substrate bias.

Allen *et al.* (1975) carried out some very instructive and difficult experiments on 25 Ω cm samples for which the conductance data are shown in Fig. 83. The conductance was measured from 0 to about 10^{12} Hz and is shown in Fig. 92. At high N_s the data fit the Drude relationship,

$$\sigma(\omega)=\frac{N_s e^2\tau}{m(1+\omega^2\tau^2)} . \tag{5.9}$$

The scattering time τ can be determined at $\omega=0$, and the curves are fit for this value of τ. When the conductance is activated in these nonideal samples τ is determined from the intercept from Fig. 83 (for $T^{-1}=0$ and $\omega=0$). Apart from understandable scatter, the Drude curves seem to fit the data at frequencies somewhat above those corresponding to the relevant activation energies from the dc data. At lower frequencies they drop precipitously to the dc value. Allen *et al.* (1975) believe that these data cannot be explained in terms of a macroscopic fluctuation model because they believe the barriers would be shorted out at the intermediate frequencies or that the inhomogeneities would have to be unreasonably large as compared to those in other smaller samples showing similar conductance behavior. Thus this experiment may contradict all of the arguments about nonideal samples above. One possibility is that these samples are well above the percolation threshold at $T=0$, as the samples of Sjöstrand *et al.* (1974, 1976) may have been. In that case, most of the samples would be conducting, and large pools of metallic electrons might exist. This seems to be the only experiment of this sort reported, so that it is important that more be done taking advantage of newer insights gained since it was done.

Hoshino (1976) developed a theory of frequency-dependent conductance for a microscopic localization model that results in curves similar to those in to Fig. 92. One of his parameters is the power s by which the localization factor α varies [see Eq. (5.5)]. He found the best fit for $s=0.75$ in agreement with the early theory of Abram (1973) and experiments of Pepper, Pollitt, and Adkins (1974b) but not with the later data of Pollitt (1976).

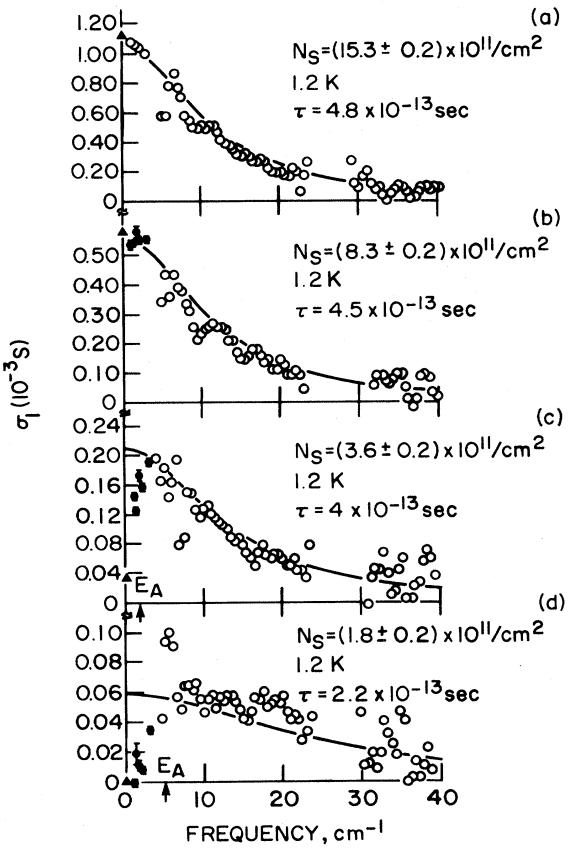

FIG. 92. Conductivity (S) at 1.2 K vs frequency in cm^{-1}. These curves correspond to the same conditions as in Fig. 83 with the dc data (Δ) taken from that figure. The open circles are data taken using an infrared spectrometer; the closed circles are from microwave measurements. The solid lines are the Drude behavior predicted from the dc conductivity, extrapolated to $T^{-1}=0$, at the indicated value of N_s. After Allen *et al.* (1975).

It should be noted that nonohmic behavior can set in at very low source-drain fields (as low as 10^{-3} V cm^{-1} in the activated regimes). Experimentally it must be avoided and/or studied. Pepper (1978g) has reviewed this subject.

7. Summary

With the exception of the frequency-dependent experiments of Allen *et al.* (1975) there seems to be some order to these disordered systems. The samples seem to fall into two classes which have been labeled ideal or nonideal, or alternatively microscopically or macroscopically disordered, or simply I or II.

I. $\sigma=\sigma_{\min}\exp[-(E_F-E_c)/k_BT]$, where $\sigma_{\min}\approx 0.1e^2/\hbar$—the ideal Anderson-localization case in two dimensions, with short-range fluctuations.

II. $\sigma=\sigma_0\exp(-W/k_BT)$, where σ_0 increases with N_s—the nonideal, macroscopic case of classical percolation, with long-range fluctuations.

However, as remarked at the beginning of this section, the existing data are not much more than a framework. Much experimental work has to be done, especially on the Hall effect and on $\sigma(\omega)$. It would be interesting if the theoretical work of Gold and Götze (1981) could be applied to Hall effect, substrate bias, and $\sigma(\omega)$.

Further, it has been long recognized (Allen and Tsui, 1974) that the correlation energies are comparable to the size of the band tails and to the binding energies of electrons to ions in the oxide, and evidence certainly exists for strongly correlated states (Adkins, 1978a, 1978b; Wilson *et al.* 1980a, 1980b). These effects are discussed below.

In all of the above discussions it has been assumed that only one set of subbands is involved for electrons on (100) surfaces. At higher temperatures (>30 K) this may not be true, and if $N_{\rm depl}$ is low or there are significant strains it may not be so at low N_s, even at 0 K. Peculiar activated and Hall-effect behavior might be expected if two sets of valleys were close together. No experiments have been reported varying the stress in the activated regime.

Note added in proof. Recently Kastalsky and Fang (1982) have reported experimental results not inconsistent with the suggestion (Fowler, 1975) that higher band tails may play a role in activated processes.

Pepper (1978c) has observed a transition from three- to two-dimensional minimum metallic conductance in an impurity band in GaAs when the thickness was reduced to several hundred angstroms. This case is more nearly similar to that studied by Knotek, Pollak, Donovan, and Kurtzman (1973) in thin amorphous Ge films than for inversion layers. The value of $\sigma_{\rm min}$ observed in the presence of a magnetic field was 2×10^{-6} S, or about $\frac{1}{10}$ of 0.1 $e^2/\hbar$, in rough agreement with the suggestion of Aoki and Kamimura (1977) that if E_c is in a Landau level $\sigma_{\rm min}$ is decreased. With no magnetic field $\sigma_{\rm min}$ was near 0.1 $e^2/\hbar$.

B. Logarithmic conductance at low temperatures

The experimental results on temperature dependence of conductance generally allow an empirical division into cases with activated conduction, as discussed in the preceding section, and cases with nonactivated conduction, as discussed in Sec. IV. Within the last few years there has been growing evidence, both experimental and theoretical, that there is an increase in resistance at very low temperatures for samples previously thought to be nonactivated or quasimetallic. Because the resistance changes are rather small—of order 10%—and because a large body of theory attributes them to two-dimensional localization in the limit of weak disorder, these effects are sometimes called weak localization effects. In this section we briefly discuss the theoretical and experimental work that has led to this new state of affairs. No attempt is made to give a definitive assessment of this rapidly developing field or to describe the theory in detail.

Localization effects are most pronounced in one-dimensional systems [see, for example, Mott and Twose (1961); Landauer (1970); Thouless and Kirkpatrick (1981)], but determination of the dimensionality of a real sample requires a careful analysis of the characteristic scale lengths, as discussed by Adkins (1977), Thouless (1977), and many later authors. A review of the status of localization in thin wires is given by Giordano (1980). Chaudhari *et al.* (1980) point out that the magnitudes of the inelastic scattering times required to account for the temperature dependence of the resistance of metallic wires at low temperatures are one or two orders of magnitude smaller than theoretically estimated. They find, however, that experiments which deduce the inelastic scattering times from an analysis of the current-voltage characteristics of superconducting wires in terms of phase-slip centers give values in approximate agreement with those deduced from the scaling theory, and therefore do not allow a definitive choice to be made between the scaling theory and the electron-electron interaction theory. Although the one-dimensional systems are of great interest, we shall not pursue them here. Most of the remaining discussion in this section will be limited to two-dimensional systems.

Work on weak localization received a major impetus from the paper of Abrahams, Anderson, Licciardello, and Ramakrishnan (1979), who gave a general discussion of localization effects for systems in one, two, and three dimensions. Their model includes the conventional strong, exponential localization, independent of dimensionality, for systems with strong disorder and proposes that two-dimensional systems will have a weak, logarithmic decrease of conductance with increasing sample length, even for weak disorder. This implies that there is no insulator-metal transition in an infinite two-dimensional sample. In contrast, three-dimensional systems exhibit a transition from activated conductivity to metallic conductivity as the degree of disorder decreases.

Indications that two-dimensional systems of noninteracting electrons have zero dc conductivity at absolute zero had also been obtained in the theoretical work by Wegner (1979) and Götze, Prelovšek, and Wölfle (1979). Vollhardt and Wölfle (1980a, 1980b) calculated the dynamical conductivity $\mathrm{Re}\sigma(\omega)\sim\omega^2$ for $\omega\to0$ using a diagrammatic self-consistent perturbation scheme for the dielectric constant. A similar self-consistent scheme has been used by Kawabata (1981a). Various numerical experiments have been performed to study the validity of the one-parameter scaling theory, but will not be discussed here.

Whether there is any connection between these results and the result, mentioned in Sec. II.E, that an arbitrarily weak attractive potential has a bound state in two dimensions, is not clear. Allen (1980) has drawn an analogy between localization and random walks for sys-

tems of one, two, and three dimensions.

The scaling theory of Abrahams *et al.* (1979) predicts a logarithmic dependence of conductance on sample length in two dimensions but does not explicitly discuss the temperature dependence of the conductance. Such discussions were given by Thouless (1977) and Anderson, Abrahams, and Ramakrishnan (1979), who related the characteristic length that appears in the scaling theory to an inelastic scattering length. Related discussions have also been given by Imry (1981). For two dimensions, the acoustic-phonon scattering rate varies as T^p, where the value of p varies between 2 and 4 depending on the dimensionality of the phonons that dominate the scattering and on the ratio of the thermal phonon wavelength to the elastic mean free path l (Thouless, 1977; Anderson *et al.*, 1979). If electron-electron scattering is the dominant inelastic process then $p=2$, but this value can be modified if effects of disorder are taken into account in the electron-electron collision process. The logarithmic dependence of conductance on sample length in the scaling theory is therefore converted to a logarithmic decrease of conductance with decreasing temperature, provided the sample length is larger than the distance a wave packet diffuses between inelastic scattering events (Thouless, 1977). This distance is of the order of the geometric mean of the elastic and inelastic mean free paths (Anderson *et al.*, 1979).

An alternative to the scaling theory which also predicts a logarithmic decrease of conductance with decreasing temperature at low temperatures was given by Altshuler, Aronov, and Lee (1980a) and by Fukuyama (1980b, 1981), who considered combined effects of electron-electron interactions and disorder. Related work has also been done by Maldague (1981). For a recent experiment on a three-dimensional system (doped bulk Si) which gives results that tend to support the prediction of the electron-electron interaction theory that there should be a conductance *increase* proportional to $T^{1/2}$ at low temperatures, see Rosenbaum, Andres, Thomas, and Lee (1981).

The predicted conductivity σ for a two-dimensional electron gas in the quasimetallic, nonactivated range has the form

$$\sigma=\sigma_0+\frac{Ce^2}{\pi^2\hbar}\ln(T/T_0)\ . \tag{5.10}$$

For the scaling theory,

$$C=g_v\alpha p/2\ , \tag{5.11}$$

with $\alpha=1$ for spin-independent scattering and $\alpha=\frac{1}{2}$ for strong spin-flip scattering (Anderson *et al.*, 1979; see also Hikami *et al.*, 1980); g_v is the valley degeneracy, which equals 2 for (100) silicon inversion layers. Fukuyama (1980d) showed that if the intervalley scattering in such a system exceeds the *inelastic* scattering rate, as is likely at low enough temperatures in a silicon inversion layer, then there is an additional factor $\frac{1}{2}$ which cancels the factor $g_v=2$ for a (100) surface. The situation for other surfaces depends on the relative magnitudes of the various intervalley scattering rates. The electron-electron interaction theory (Altshuler *et al.*, 1980a) gives

$$C=\tfrac{1}{2}(1-F)\ , \tag{5.12}$$

where F depends on the ratio of the Fermi wavelength to the screening length. F approaches 1 for strong screening and 0 for weak screening. Fukuyama (1980b, 1981) gives a slightly different coefficient because he includes additional processes which were ignored by Altshuler *et al.* In their theory, $T_0=\hbar/k_B\tau$, where τ, the electron scattering time, is generally dominated at low temperatures by elastic scattering.

Experimental evidence in support of these theories was first found for thin metal films. Dolan and Osheroff (1979) found a logarithmic resistance increase with decreasing temperature in thin films of a gold-palladium alloy. The total resistance change in the logarithmic range was $\sim 10\%$. Corresponding results for silicon inversion layers were reported by Bishop, Tsui, and Dynes (1980), as shown in Fig. 93, and by Uren, Davies, and Pepper (1980).

The experimental values of the coefficient C vary significantly. Dolan and Osheroff (1979) found values between 0.36 and 0.84 for AuPd films with thicknesses of 2—4 nm and resistances of 1—5 kΩ. Van den dries *et al.* (1981) found values of order one for clean Cu films with resistivities of 10—20 Ω, and values $\lesssim 0.5$ for films with resistivities above 100 Ω. Markiewicz and Harris (1981) measured thin, clean Pt films with thicknesses from 0.1 to 10 nm deposited on clean Si substrates. They found $C=0.75\pm0.15$, with the logarithmic temperature dependence continuing up to room temperature in the thinnest films, which were one monolayer thick. For silicon inversion layers, Bishop *et al.* (1980) reported $C=0.52\pm0.05$. Finally, for In_2O_3 films, Ovadyahu and Imry (1981) found C in the range 0.75 to 1. The clustering of these results within a factor ~ 3 for so many different systems, with electron densities and resistivities

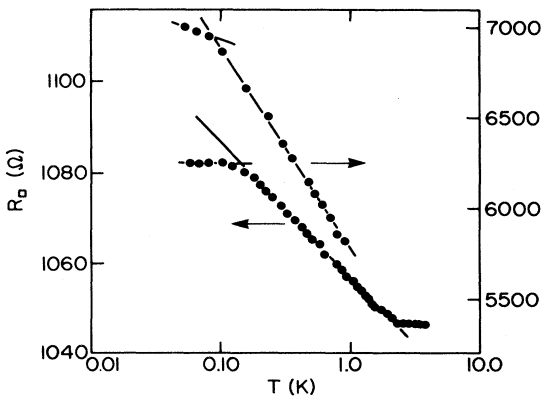

FIG. 93. Resistance of silicon inversion layers, extrapolated to zero source-drain voltage, vs absolute temperature on a logarithmic scale. The electron density is 2.03×10^{12} cm^{-2} for the upper curve and 5.64×10^{12} cm^{-2} for the lower curve. After Bishop, Tsui, and Dynes (1980).

varying over several orders of magnitude, gives support to the theories that lead to Eq. (5.10), but does not clearly distinguish between the localization theory and the electron-electron interaction theory.

The comparison of theory and experiment is somewhat ambiguous when one tries to convert from conductance to resistance if the value of T_0 is not known. Several analyses appear to include an implicit assumption that the T_0 which enters in Eq. (5.10) is close to the range of the measurements. The theories presumably contain a cutoff above which the logarithmic dependence no longer holds, but this has not been spelled out clearly in relation to experimental results.

The conductance of two-dimensional quasimetallic systems is also found to have a term logarithmic in electric field F at low fields and low temperatures. Anderson *et al.* (1979) propose that the effect is caused by simple Joule heating of the electrons. Then the analog to Eq. (5.10) in which the temperature T is replaced by the electric field F has a coefficient $C'=2C/(p'+2)$, where p' is the exponent in the temperature dependence of the rate of electron energy loss to the lattice, which is not necessarily the same as the inelastic scattering rate. Where the terms logarithmic in temperature and in electric field have both been measured, the comparison generally gives physically reasonable values of p', although there are exceptions (Uren *et al.*, 1980).

Negative magnetoresistance at low temperatures which depends only on the normal component of the magnetic field and which has an approximately logarithmic temperature dependence was observed in Si(111) inversion layers by Kawaguchi, Kitahara, and Kawaji (1978a, 1978b) before recent ideas on weak localization had developed. They attributed the effect to *s-d* scattering (Kondo effect). The first measurements showing negative magnetoresistance in inversion layers at low temperatures were those of Eisele and Dorda (1974a) and Dorda and Eisele (1974), who attributed it to interface effects (see also Sec. IV.B.3).

More recently, detailed measurements of magnetoconductance of electrons in Si inversion layers at low temperatures and low magnetic fields have been carried out by Kawaguchi and Kawaji (1980b, 1980c), as illustrated in Fig. 94, and Wheeler (1981). They compared their results with the theory of Hikami, Larkin, and Nagaoka (1980) for weak localization, which predicts under some simplifying but approximately valid conditions that

$$\sigma(H)-\sigma_0\simeq-\frac{\alpha e^2}{2\pi^2\hbar}\left[\psi\left(\frac{1}{2}+\frac{1}{\tau a}\right)-\psi\left(\frac{1}{2}+\frac{1}{\tau_{\rm in}a}\right)\right], \tag{5.13}$$

where ψ is the digamma function (Abramowitz and Stegun, 1964, p. 258), with $\psi(z)\sim\ln z-(2z)^{-1}-\cdots$ for large z, τ and $\tau_{\rm in}$ are the elastic and inelastic scattering times, respectively,

$$a=\frac{4DeH}{\hbar c}, \tag{5.14}$$

D is the diffusion constant, and $\sigma_0=e^2DD(E_F)$, where the last factor is the density of states at the Fermi energy. If the elastic scattering rate is much larger than the inelastic scattering rate, as is likely at low enough temperatures, and if $\tau a<<1$, then Eq. (5.13) leads to

$$\sigma(H)-\sigma(0)\simeq-\frac{\alpha e^2}{2\pi^2\hbar}\left[\ln\frac{1}{\tau_{\rm in}a}-\psi\left(\frac{1}{2}+\frac{1}{\tau_{\rm in}a}\right)\right] \tag{5.15}$$

at constant temperature. Hikami *et al.* (1980) also considered magnetic scattering and spin-orbit interaction, but we shall not consider those aspects of the problem here.

Kawaguchi and Kawaji (1980b) find that the coefficient α in Eq. (5.13) is between 0.5 and 0.7 and that the inelastic scattering rate is approximately given by $\tau_{\rm in}^{-1}\simeq 2\times10^{-11}$ s^{-1} $(T/4\text{ K})^{1.8}$ for a sample with $N_s=5\times10^{12}$ cm^{-2}. Their second paper (1980c) shows that the temperature dependence weakens to about the 1.3 power for $N_s=8\times10^{11}$ cm^{-2}, that the inelastic scattering time increases with increasing N_s, as shown in Fig. 95, and that the coefficient α decreases from 1 for $N_s\sim10^{12}$ cm^{-2} to about 0.6 for $N_s=6\times10^{12}$ cm^{-2}, smaller than the expected value one. The inelastic scattering rate deduced by Wheeler (1981) from his data varies approximately linearly with temperature, and decreases with increasing values of N_s, reaching a minimum near $N_s\sim6\times10^{12}$ cm^{-2}, where the next subband begins to be occupied. Wheeler finds that $\alpha=1$ in Eq. (5.13) is consistent with his measurements.

There has been no quantitative analysis yet of the mechanisms that lead to the temperature dependences and magnitudes of the inelastic scattering rates in inver-

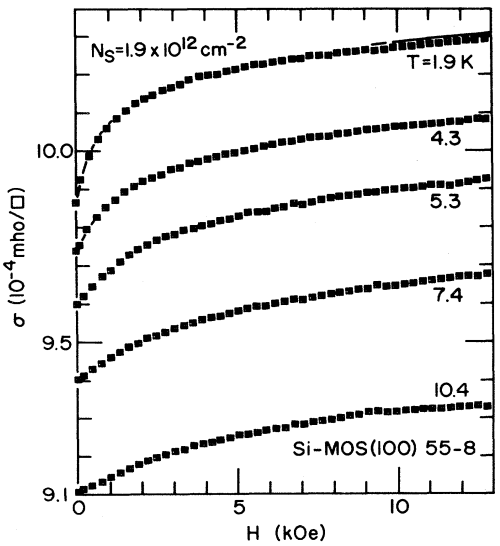

FIG. 94. Magnetic field dependence of the conductance of a Si(100) inversion layer with 1.9×10^{12} electrons per cm^2 at temperatures from 1.9 to 10.4 K. The experimental points have been fitted to the expression of Hikami *et al.* (1980) given in Eq. (5.15). After Kawaguchi and Kawaji (1980c).

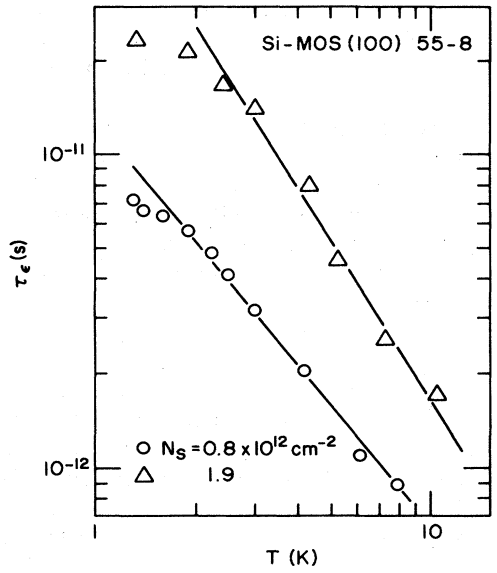

FIG. 95. Temperature dependence of the inelastic scattering time obtained from fitting experimental magnetoconductance results to the theory of Hikami *et al.* (1980). After Kawaguchi and Kawaji (1980c).

sion layers deduced from analysis of the weak localization effects. The inelastic scattering rate $1/\tau_{in}$ is expected in clean samples to vary with temperature as T^3 if bulk phonon scattering is the dominant mechanism and as T^2 if electron-electron scattering is the dominant mechanism. However, strong elastic scattering can modify these results, as shown, for example, by Schmid (1974) for bulk systems. Abrahams, Anderson, Lee, and Ramakrishnan (1981) and Uren *et al.* (1981) have shown that under these circumstances the electron-electron scattering rate at low temperatures is linear in T. If the resulting value $p=1$ is used in Eq. (5.11) with the indicated value (Fukuyama, 1980b) $g_v\alpha=1$, then $C\sim\frac{1}{2}$, which is well within the range of experimental values referred to above.

Hall-effect results have been published by Uren, Davies and Pepper (1980), as illustrated in Fig. 96, and by Bishop, Tsui, and Dynes (1981). The ratio s of the fractional change of the Hall coefficient to the fractional change of the resistivity as the temperature is changed is found to depend on the magnitude of the resistivity, varying from a value near two at resistivities of order 1 kΩ to a value approaching 0 at higher resistivities. Fukuyama (1980c, 1980e) showed that this ratio should be zero in the localization theory, for which the logarithmic corrections arise in the mobility rather than in the carrier concentration. Altshuler, Khmel'nitzkii, Larkin, and Lee (1980b) showed that the ratio is two in the electron-electron interaction model. Thus there is evidence in the Hall-effect data for the presence of both mechanisms. Kaveh and Mott (1981b) agree with the finding of Uren *et al.* (1980) that their experimental results can be understood if the localization effects are quenched at large enough magnetic fields, where the electron-electron effects then dominate. This quenching is implicit in the theory of Hikami *et al.*

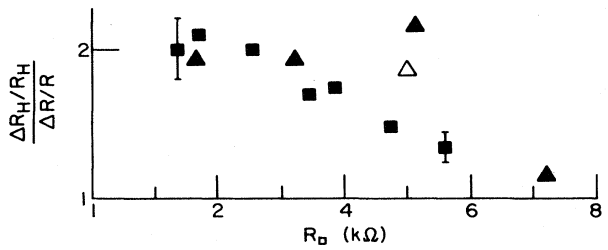

FIG. 96. Hall-coefficient change divided by conductance change vs resistance per square for silicon inversion layers. The triangles are for a magnetic field of 0.4 T and for electron concentrations of about 3×10^{11} cm^{-2} and the squares are for a magnetic field of 1.3 T and for electron concentrations from 0.8 to 2×10^{12} cm^{-2}. The solid symbols give changes with variation of source-drain field, and the open symbols give changes with variation of temperature. After Uren *et al.* (1980).

Whether a magnetic field destroys the weak localization or not is an interesting theoretical problem that has not yet been fully understood. Yoshioka, Ono, and Fukuyama (1981; see also Ono *et al.*, 1981) extended the self-consistent diagrammatic theory of Vollhardt and Wölfle (1980a, 1980b) and studied this problem. They showed that the magnetic field does not destroy the localization, although it tends to increase the spatial extent of localized wave functions. It is known that all the states cannot be localized in strong magnetic fields (see Sec. VI.D).

The experiments are quite difficult because of the small signal levels required, and consequently the experimental error bars are quite large. The best data are obtained from electron heating effects, in which the source-drain field rather than the ambient temperature is varied, because these are considerably less troublesome to carry out with precision. The determination of the detailed dependence of the Hall-effect ratio s on sample parameters and on magnetic field requires additional measurements.

The relation between localization and superconductivity is intriguing. Deutscher *et al.* (1980) found that superconductivity appears in granular aluminum films whose conductivity is in the weak localization regime, where the resistance has a logarithmic temperature dependence, but not in films whose conductivity is activated at low temperatures. [For a review of granular films, see Abeles *et al.* (1975).] Whether these results have any bearing on silicon inversion layers, for which superconductivity has been predicted (see Sec. II.D) but not yet observed, is not clear.

This sketchy account gives only a hint of the great interest in these new developments in the low-temperature conductance of quasimetallic two-dimensional systems. Apart from resolution of some of the experimental problems that have been alluded to above, the principal need is the development of a theory that includes both localization effects and electron-electron interaction. One ap-

proach, based on additivity of the two effects, has recently been described by Kaveh and Mott (1981b). The subject is likely to see considerable progress in the near future.

Note added in proof. After this manuscript was submitted, other theoretical treatments that include both localization effects and electron-electron interaction have been published. See, for example, Fukuyama (1982) for a more recent review.

C. Two-dimensional impurity bands

Silicon inversion layers afford a unique opportunity for the study of impurity levels and impurity bands because of the ease with which almost all of the relevant parameters can be varied. The theory of bound states arising from charges near the Si-SiO_2 interface was discussed in Sec. II.E. The impurity bands may be created by drifting sodium ions to the proximity of the silicon-silicon dioxide interface where they give rise to bound states in the silicon. At high enough concentrations the bound states overlap and result in impurity bands (Hartstein and Fowler, 1975b). In practice the sodium concentration that gives rise to such states may be varied between about 10^{11} and 2×10^{12} cm^{-2}. The electron concentration may be varied simply by changing the voltage on the gate electrode of a metal-oxide-silicon (MOS) device. The potential binding the electrons to the ions may be varied independently of the electron concentration by changing the potential well due to the depletion charge (Fowler, 1975) using a substrate bias between the surface contacts and the bulk of the silicon.

The existence of bound states due to ions in the SiO_2 near the Si-SiO_2 interface was suggested by Stern and Howard (1967) to explain the peaks in μ_{FE} observed by Fang and Fowler (1968) discussed in Sec. IV.B. Many of the groups who have studied these peaks since then (Kotera *et al.*, 1972b; Komatsubara *et al.*, 1974; Tidey and Stradling, 1974) have also suggested this explanation. The last cited paper suggested that the ions were "field deionized" as N_s and the binding energy increased, giving rise to the minimum in μ_{FE}. Whether these peaks are due to impurity states or to higher subbands (see Sec. IV.B) may still be an open question. Here we shall leave this question to discuss a more fully characterized and identified structure that is believed to arise from impurity bands resulting from electrons bound to sodium ions near the Si-SiO_2 interface.

Sodium ions have long been known to be mobile in the SiO_2 films on MOS structures. (See, for instance, out of a large literature, Hickmott, 1975; Boudry and Stagg, 1979; Verwey, 1979). These tend to be located near one or the other interface (DiMaria 1977, 1981; DiMaria *et al.*, 1976) and are easily drifted back and forth at or above room temperature in an electric field across the oxide, but are effectively frozen in position somewhere below 300 K. These positive sodium ions can give rise to fast states, a variety of traps in the oxide (DiMaria, 1981), macroscopic inhomogeneities giving rise to band tails (Hartstein and Fowler, 1975a), and gross inhomogeneities at least at high concentrations of about 10^{13} cm^{-2} (DiStefano, 1971; Williams and Woods, 1973; Bottoms and Guterman, 1974; DiStefano and Lewis, 1974). Evidence due to Fowler and Hartstein (1980a) implies that at least at lower densities most of the sodium at the Si-SiO_2 interface contributes fast interface donor states well below the conduction-band edge. If these states were acceptors they would dominate the scattering (Hartstein *et al.*, 1980). If they were within about 40 meV of the conduction-band edge the structure (as a function of V_G) discussed below would shift with temperature. In addition, there are bound states 15—30 meV below the conduction-band edge resulting from electrons in the silicon bound to Na^+ ions in the SiO_2 quite close to the interface. These ions cannot be neutralized by transfer of electrons from the silicon presumably because they are energetically inaccessible. In a sense, they are neutralized, or at least screened when electrons are bound to them but the SiO_2 barrier keeps most of the electronic wave function in the silicon.

If the wave functions of such states overlap, tunneling is possible between them. Thermal excitation to the mobility edge is also possible at higher temperatures. The bound states may be random in position along the surface, and because of background surface potential fluctuations or because of variation of the distance of the ions from the interface may be random in energy. The wells are shown in Fig. 97(a) with the wave functions de-

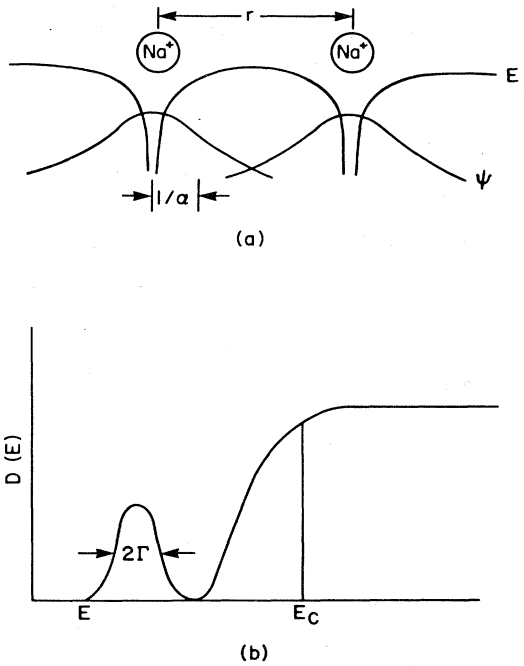

FIG. 97. (a) The potentials due to the Na^+ ions at the Si-SiO_2 interface are shown by the upper curves with wells. The overlapping wave functions which fall off as $\exp(-\alpha r)$ are also shown. (b) Density of states averaged over the surface. The impurity band is shown with a half width at half maximum of Γ. The mobility edge E_c is shown in the band tail.

caying as $\exp(-\alpha r)$. Below, in Fig. 97(b), the expected density of electron states averaged across the surface is shown with a band tail due to other fluctuations and an impurity band.

The sodium-derived impurity bands have been observed primarily by the study of conductance in the (100) surface of MOSFET devices (Hartstein and Fowler, 1975b, 1976; Hartstein *et al.*, 1978a, 1978b; Fowler and Hartstein, 1980b). Typical conductance curves as a function of gate voltage are shown in Fig. 98. The conductance peak has been reported only in the sodium-doped samples and is believed to be due to an impurity band. As may be seen, the impurity band peaks precede the onset of conduction in the first quasi-two-dimensional subband as the gate voltage is increased and negative charge is induced. At high enough Na^+ concentrations the peak is washed out. Reverse substrate bias sharpens the peak but decreases its amplitude.

The number of sodium ions has been determined in different ways which give different results. Their number and the carrier concentration remain the greatest uncertainty in these measurements. It is now believed that the best measure of their number is from the shift of threshold (onset of inversion) determined from an extrapolation of the magnetoconductance oscillations in the metallic conduction region to zero magnetic field (Fang and Fowler, 1968; Fowler and Hartstein, 1980a). This procedure results in lower values of sodium concentrations than those reported earlier for some of the same data. There could still be an error in N_{ox} of about 0.5×10^{11} cm^{-2}.

The temperature dependence of the conductance has been observed to exhibit three ranges; the two higher ranges are thermally activated and are believed to correspond to activation to the mobility edge (E_1) and nearest-neighbor hopping (E_3), and the lowest appears to be variable-range hopping (Mott, 1973). Early papers (Hartstein and Fowler, 1976, 1978) gave approximate values for E_1 and E_3. A recent paper (Fowler and Hartstein, 1980b) reports values from least-squares fits to

$$\sigma=\sigma_1\exp\left[\frac{-E_1}{k_BT}\right]+\sigma_3\exp\left[\frac{-E_3}{k_BT}\right]. \tag{5.16}$$

In Fig. 99 representative data are shown for the temperature dependence for a sample where the surface field, and therefore the binding potential, has been increased by increasing the negative substrate bias (V_{sub}). In these measurements the carrier concentrations have been fixed at the conductance maxima, which presumably correspond to the maxima of the density of states and to half-filled impurity bands. The activation energies from these curves have been widely compared (Martin and Wallis, 1976, 1978; Lipari, 1978; Vinter, 1978) with calculations of the binding energies, even though E_1 is thought to correspond to activation to the mobility edge, which does not necessarily correspond to the unperturbed conduction-band edge. These calculations are reviewed in Sec. II.E. As expected, a higher surface field forces the electrons closer to the ions in the oxide and increases both E_1 and E_3. In Fig. 100 these data are compared with the theories of Martin and Wallis and of Lipari. (Note that in both of these papers the determination of the experimental values of electric field in electrostatic units is wrong by an order of magnitude.) These theories and that of Vinter, which agrees approximately with Lipari, differ in the degree of sophistication of the trial

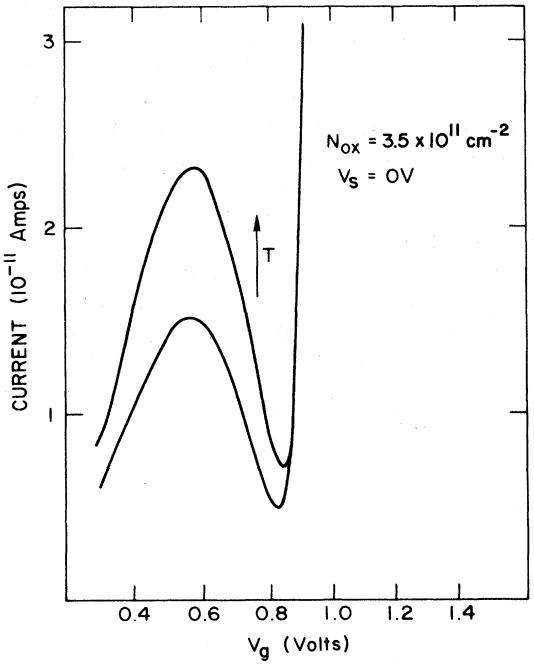

FIG. 98. Typical conductance curves near current threshold at two temperatures. The impurity-band maximum is assumed to occur at the conductance maximum. Note that the position of the maximum conductance is temperature independent. After Fowler and Hartstein (1980b).

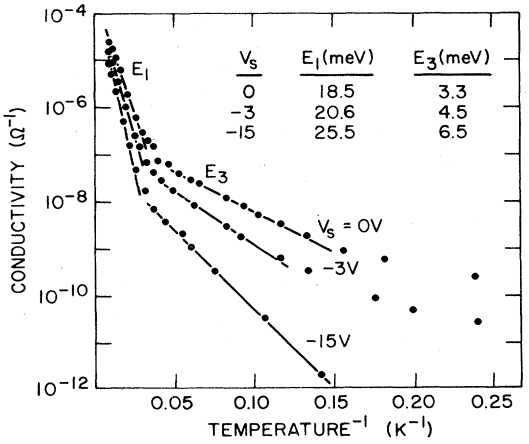

FIG. 99. Temperature dependence of the conductance at the conductance maxima for different values of substrate bias and for a substrate doping $N_A=8.9\times10^{15}$ cm^{-3}. The values of E_1 and E_3 given here are not from least-squares fits. After Fowler and Hartstein (1980b).

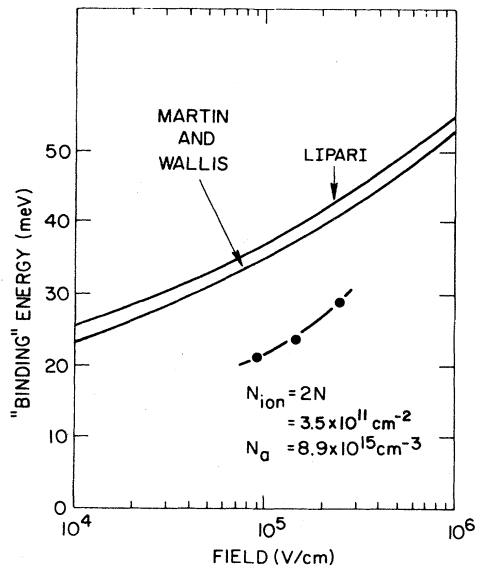

FIG. 100. Comparison of the values of E_1 from Fig. 99 with the theories of Martin and Wallis (1978) and Lipari (1978). The binding energies from theory and E_1 from experiment are compared for different values of surface field corresponding to different values of V_{sub}. After Fowler and Hartstein (1980b).

wave functions. None take screening into account. The earlier theory of Stern and Howard (1967) did, in a simple way, for strictly two-dimensional electrons. Hipólito and Campos (1979) calculated the effect of screening, but fits to the data of Fig. 100 could not distinguish between screening and displacement of the ion from the surface. All of these theories give results that are higher than the experimental results for E_1.

If screening is important, then an extrapolation of the measured values of E_1 to zero sodium concentration, and therefore $N_s=0$, should be expected to be more nearly comparable to the theory. Such data are shown in Table III and plotted in Fig. 101 for the depletion charge $N_{depl}=3.63\times10^{11}$ cm^{-2}. It may be seen that the least-squares fit to a linear curve gives a value of E_1 of 24.1 ± 0.3 meV. An error in N_{ox} probably would not affect this value by more than 1 meV. The calculated values for the binding energy for this case are 28.1 meV (Martin and Wallis, 1976, 1978), 29.3 meV (Vinter, 1978), and 29.8 meV (Lipari, 1978), where all theories assume the ion is at the interface. According to Lipari, the binding would be about 24 meV if the ions were displaced about 4 Å into the oxide (see Fig. 8). Vinter's (1978) scattering theory puts the electrons at the interface but would not be changed much by a displacement of 4 Å. A dangerous extrapolation of E_1 in Fig. 101 to high sodium concentration would result in $E_1=0$ at $N_{ox}\approx1.7\times10^{12}$ cm^{-2}. At this concentration the impurity band is observed to be merged with the band tail.

The extrapolation of the conductance in this range for activation to a mobility edge to infinite temperature should give the minimum metallic conductivity σ_{min} if the fluctuations are mostly microscopic and if the values given in Table III for the various sodium concentrations are accurate. There is no strong dependence on N_{ox}, and the average value is $(2.0\pm0.1)\times10^{-4}$ S. This is high compared to $0.12e^2/\hbar$ or 3×10^{-5} S. It is consistent with the minimum temperature-independent conductivity observed in the conduction band tail, which is not necessarily a minimum metallic conductivity (see Sec. V.A).

Table III and Fig. 101 also show E_3, which is related to the bandwidth (Miller and Abrahams, 1960), as a function of N_{ox}. The bandwidth is strongly reduced as the oxide charge is increased. It should be remembered that these data are for half-filled bands, so that both the density of states and the electron concentration increase with N_{ox}. One would expect that the effects of screening should increase with N_{ox} and that the effects of the fluctuations should be reduced by screening. The only estimates of screening effects are due to Stern (1976) and to Hipólito and Campos (1979). Stern assumed that the random potential arises from the sodium ions giving rise to the bound states and that the screening is proportional to the density of states and is equal to that of a two-dimensional electron gas $[2\pi e^2D(E)/\bar{\kappa}]$ [see Eq. (2.24)]. His iterated results do not give rise to an impurity band for the values of N_{ox} where one has been observed, so that his treatment would seem to overestimate the level broadening. The assumed screening which is possibly appropriate for free electrons is probably not right. No one has calculated the polarizability of the bound electrons for the two-dimensional case appropriate here, so that no better screening theory exists. Vinter (1978) has a more nearly appropriate theory but has applied it only to scattering in the metallic regime. The extrapolation of E_3 from Fig. 101 to zero N_{ox} gives a value of about 5 meV. This may represent the intrinsic potential fluctua-

TABLE III. Constants for activated conductivity as a function of N_{ox}. Here, N_{ox} is the oxide charge and E_1, σ_1, E_3, and σ_3 are from a least-squares fit to Eq. (5.16).

N_{ox} (10^{11} cm^{-2})	E_1 (meV)	σ_1 (10^{-4} S)	E_3 (meV)	σ_3 (S)
2.1	21.8	1.7	4.0	2.2×10^{-7}
2.9	19.9	2.4	3.5	1.6×10^{-6}
4.2	17.1	1.8	1.9	4.4×10^{-6}
4.9	16.6	1.9	1.6	4.8×10^{-6}
6.6	15.4	2.1	1.1	1.3×10^{-5}

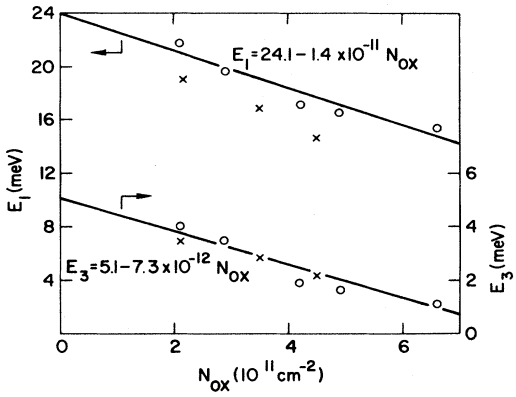

FIG. 101. The activation energies for excitation to the mobility edge, E_1, and for nearest-neighbor hopping, E_3, as functions of N_{ox}. Only the data (○) were used in the fit of the solid lines. The two sets of data are for different samples. After Fowler and Hartstein (1980b).

tions in the absence of both screening and sodium, or it may represent fluctuations in the displacement of the sodium ions from the interface.

The data for nearest-neighbor hopping can be compared to the two-dimensional hopping theory of Hayden and Butcher (1979). They predict that

$$\sigma_3=\sigma_0\exp\left[\frac{-2.39\alpha}{N_{ox}^{1/2}}\right]\exp\left[-\frac{W}{3k_BT}\right], \tag{5.17}$$

where σ_0 is proportional to $N_{ox}^{1/2}$, α appears in $\psi=\psi_0\exp(-\alpha r)$, the wave function of the bound states parallel to the surface, and W is the bandwidth for a band with a constant density of states. The extrapolation of σ_3 to $T=\infty$, σ_∞, should be proportional to $N_{ox}^{1/2}\exp(-2.39\alpha N_{ox}^{-1/2})$. Figure 102 shows these data in linearized form. A least-squares fit yields $\alpha^{-1}=69\pm2$ Å, a much larger value than previously estimated (Hartstein and Fowler, 1978). It should be remembered that this procedure assumes that α is not a function of N_{ox} even though E_1 is.

Below the temperature regime for nearest-neighbor hopping, variable-range hopping is observed. The best data for this range are shown in Fig. 103. While these data are not extensive, they reasonably fit the expected variable-range hopping law [Eq. (5.4)], where

$$T_0=27\alpha^2/\pi k_BD(E_F) \tag{5.18}$$

and where $D(E_F)$ is the density of states at the Fermi level. $D(E_F)$ was taken as N_{ox}/E_3 in the past (Hartstein and Fowler, 1978). More recently Hartstein *et al.* (1979) and Fowler and Hartstein (1980b) assumed that for a Gaussian distribution of the form $D(E)=D_{max}\times\exp(-E^2/2\Gamma^2)$ one would have $E_3=2\Gamma/3$. This was chosen in analogy with a result by Hayden and Butcher (1979) that for a constant density of states with width W, one has $E_3=W/3$. More recently Al-Sadee, Butcher, and Hayden (1981) have found that $E_3=1.2\Gamma$ for a Gaussian. The maximum density of states is related to the total number of states by $D_{max}=N_{tot}/\Gamma\sqrt{2\pi}$, and it was assumed that $N_{tot}=N_{ox}$. If $E_3=2\Gamma/3$ was substituted in Eq. (5.18), it was found for the data discussed above that $\alpha^{-1}=42$ Å. If the relation between E_3 and Γ given by Al-Sadee *et al.* was used, then $\alpha^{-1}=56$ Å. No measurements of variable-range hopping have been made as a function of substrate bias or N_{ox}, so that the effects of changing the surface field or N_{ox} are not known, unlike the situation for E_1 and E_3.

Some measurements have been made of E_1 and E_3 as functions of N_s (Hartstein *et al.*, 1979; Fowler and Hartstein, 1980b). The dependence of E_1 and E_3 on N_s is shown in Fig. 104 for different values of N_{ox}. The variation of E_1 with N_s was fitted with a Gaussian with parameters N_{tot} and Γ. The values of Γ, of the maximum density of states D_{max}, and of the integrated number of states in the Gaussian were calculated and are shown in Table IV. This procedure assumed that the bandwidth, binding energy, and mobility edge do not

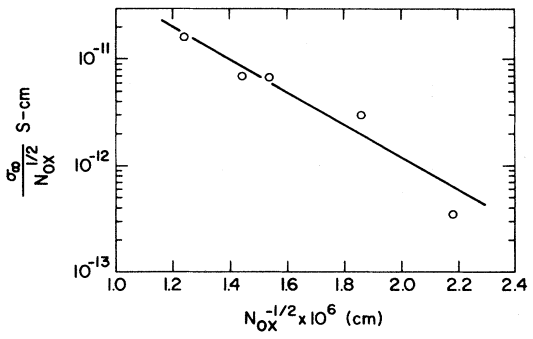

FIG. 102. Logarithm of the conductance σ_∞ from the extrapolation of the nearest-neighbor hopping as $(1/T)$ goes to 0, divided by $N_{ox}^{1/2}$, as a function of $N_{ox}^{-1/2}$. A straight line is predicted by Hayden and Butcher (1979). After Fowler and Hartstein (1980b).

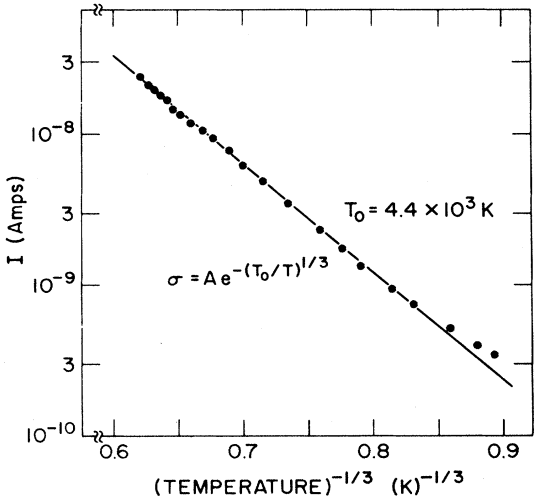

FIG. 103. Logarithm of current at the lowest temperatures vs $T^{-1/3}$. Here $N_{ox}=3.5\times10^{11}$ cm^{-2} and, at somewhat higher temperatures, $E_3=3.3$ meV. After Fowler and Hartstein (1980b).

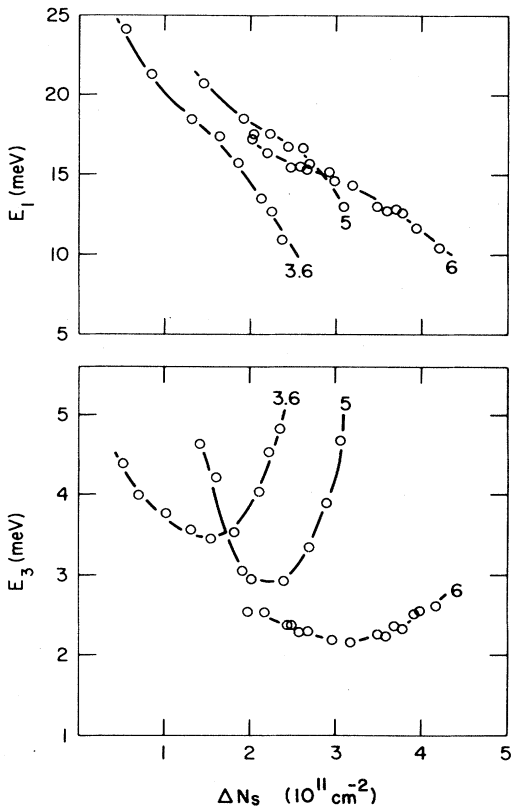

FIG. 104. E_1 and E_3 for different values of N_{ox} as functions of N_s. More accurate determination of the oxide charges gives $N_{ox}=2.1$, 3.4, and 4.5×10^{11} cm^{-2} for the three samples shown. The data for E_1 have been fitted using a Gaussian by Hartstein *et al.* (1979) and using a constant density of states by Hayden (1980). After Hartstein *et al.* (1979).

depend on the number of electrons in the band. The effects of motion of the Fermi level were not considered. The least-squares fit was relatively insensitive to the parameters. In the table, Γ is compared to $3E_3/2$ at the conductance maximum. Comparison with $E_3/1.2$ would be consistent with Al-Sadee *et al.* (1981). The data do not allow a clear choice between the two.

The dip in E_3 in the data of Fig. 104 could arise from two causes. It may arise, as has been suggested (Hartstein *et al.*, 1979), and as Hayden (1980) has confirmed for his model, from the statistics of the hopping process. In the experiments the carrier concentration rather than the Fermi level is held constant. When the Fermi level is above or below the center of the band there is a difference in the number of initial and final states, which leads to an increase in the apparent activation energy as observed. Hayden (1980) found that for a constant density of states (finite rectangular band) of width W,

$$E_3=\left[\frac{5+3[(\delta'/W')^2]}{12}\right]W,\quad \delta'<W' \tag{5.19}$$

$$E_3=\left[\frac{\delta'}{2W'}+\frac{1}{6}\right]W,\quad W'>\delta' \tag{5.20}$$

where $\delta'=\delta/k_BT$ and $W'=W/2k_BT$ and δ is the displacement of the Fermi level from the center of the band. Using these formulas and properly relating δ to N_s, he was able to get a reasonable fit to the data of Fig. 104 both for E_1 and E_3. There may in addition be a real change in the bandwidth because the screening might be expected to change as the electron density and the density of states changes. There is no explicit dependence of σ_∞, the infinite temperature extrapolation of the nearest-neighbor hopping process, on electron concentration in the theory of Hayden and Butcher (1979). This may result from the constant density of states assumed. What was observed experimentally was a monotonic increase of σ_∞ as electron density increased, as shown in Fig. 105. This is not in agreement with intuition, which would be that $\sigma_\infty\sim N_s(N_{ox}-N_s)$. A decrease of α with increasing N_s and decreasing E_1 might explain the results.

Attempts have been made to observe a second conductance peak that might correspond to a second Hubbard band, with no success. The sodium concentration has been increased to a level where one might have expected to observe metallic conduction at the maximum in the impurity band, again with negative results. An attempt to observe impurity-band conductance anisotropy in a (110) sample was inconclusive (Fowler and Hartstein, 1980b). Measurements in a magnetic field (Fowler and Hartstein, 1980b) showed the expected reduction in conductivity, but not enough measurements were made to determine the changes in the activated processes. Voss (1977, 1978) has measured the noise in these impurity bands. Good Hall-effect measurements are probably needed for really accurate determination of N_{ox} and N_s. Pepper (1978b) has made preliminary measurements, but has reported no results except when the peaks were

TABLE IV. Density of states in impurity bands. $D(E)_{max}$ is the maximum of the density of states with a distribution $\exp(-E^2/2\Gamma^2)$ and N_{tot} is the integrated value. Γ and $D(E)_{max}$ were determined by fitting to $E_1(N_s)$ in Fig. 104. The values of the activation energy E_3 used in the last column are the minimum values from Fig. 104.

N_{ox} (10^{11} cm^{-2})	$D(E)_{max}$ (10^{13} cm^{-2}eV^{-1})	N_{tot} (10^{11} cm^{-2})	Γ (meV)	$3E_3/2$ (meV)
2.1	2.1	2.6	4.8	5.2
3.5	3.4	1.5	1.8	4.3
4.5	2.1	2.3	2.1	3.3

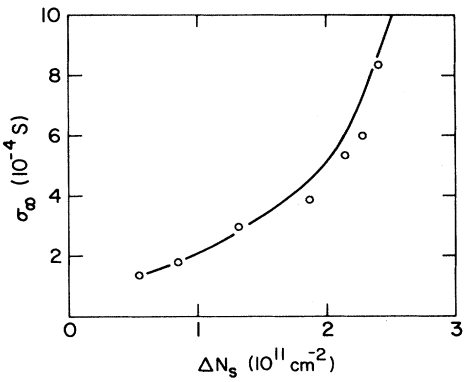

FIG. 105. σ_∞, the extrapolation of the nearest-neighbor hopping conductivity to $1/T=0$, as a function of N_s. After Fowler and Hartstein (1980b).

smeared out. No evidence of these impurity bands has been seen in the capacitance (Fowler and Hartstein, 1980a).

Even at this preliminary stage of investigation the Na^+-MOS structure has generally shown many properties expected of impurity bands. The impurity bands are somewhat different from those in compensated three-dimensional systems in that the fluctuations are not caused by the compensating ions, but rather by variation in the location of the Na^+ ions parallel and perpendicular to the surface. This system seems to offer a unique opportunity to study impurity-band phenomena. It appears that in the range of temperatures studied (>1 K) there has been no need to invoke a Coulomb gap or cooperative hopping processes (Pollak, 1980).

The ac conductivity of these samples has not been measured using the techniques of Allen *et al.* (1975). However, McCombe and Schafer (1979) and McCombe and Cole (1980) have made measurements studying the effects of sodium ions on the far-infrared absorption spectra with the field perpendicular to the surface. While their data are somewhat scanty, there is evidence of a shifted absorption peak as compared to the intersubband absorption ($E_0 \rightarrow E_1$). See Fig. 106. Because the

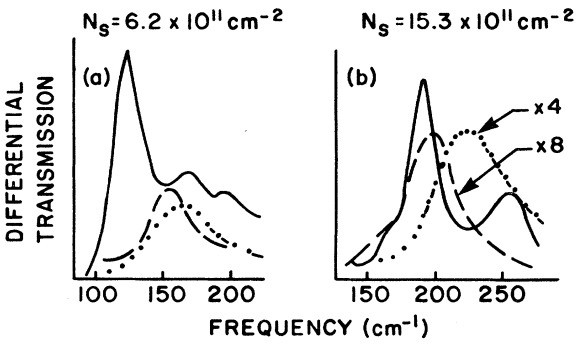

FIG. 106. Spectra for differential transmission through MOSFET samples for two values of N_s and three values of N_{ox}: —— (1.6×10^{11} cm^{-2}); ----- (7.4×10^{11} cm^{-2}); —·—·— (16.1×10^{11} cm^{-2}). After McCombe and Schafer (1979).

bound state for the higher subband is expected to be less tightly bound than the bound state for the lowest subband, the shift in transition energy is expected to be positive, and a positive shift of about 5 meV was observed. Kramer and Wallis (1979) have calculated a shift of about 10 meV. A comparison has been made in Fig. 107. This measurement does not depend on the mobility edge location as do the determinations of E_1 from conductance as a function of temperature. It may depend on the sodium and electron concentrations. One interesting result is that the impurity-band transition was observed when the Fermi level was below the conduction band, but merged with the intersubband transition when the Fermi level was in the conduction band. As can be seen in Fig. 107, the difference between the shifted and unshifted lines effectively disappears for $N_s \approx 2N_{ox}$ for $N_{ox} \approx 7.4\times10^{11}$ cm^{-2}. This may mean that the impurity bands merge with the conduction band in the presence of large numbers of free electrons.

If measurements on the band tails, discussed in Sec. V.A, are scanty, measurements on the impurity bands are more so. As should be obvious, more data are needed, especially relating to variable-range hopping as functions of N_{ox}, N_s, and V_{sub} or N_{depl}. Better data on $E_1(N_s,N_{ox},N_{depl})$ and $E_3(N_{ox},N_s,N_{depl})$ are needed. Hall-effect data are needed. Additionally, surfaces under strain where E_0 and $E_{0'}$ are interchanged have not been studied. It is clear that the opportunities afforded by an impurity-band system where so many variables may be changed relatively easily have only begun to be explored.

VI. TRANSPORT IN STRONG MAGNETIC FIELDS

When a strong magnetic field is applied normal to the inversion layer, the energy spectrum becomes discrete because the quantization of the orbital motion converts the constant density of states connected with motion parallel to the surface into a series of Landau levels. This system provides an ideal tool for the study of quantum transport phenomena, whose characteristics are not so clear in the

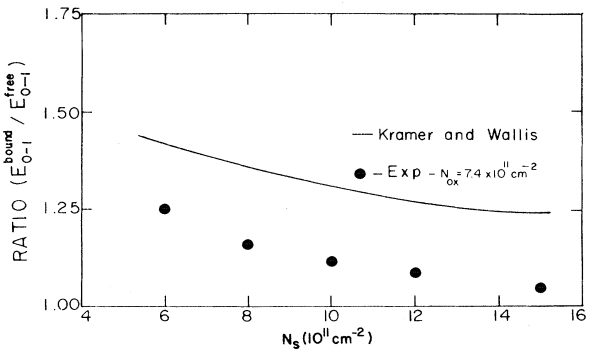

FIG. 107. Ratio of impurity-shifted transition to continuum transition as a function of N_s compared to the theoretical prediction of Kramer and Wallis (1979). The experimental results compare transition energies for samples with $N_{ox}=7\times10^{11}$ cm^{-2} and $N_{ox}\sim10^{10}$ cm^{-2}. The calculations are for isolated ions with no screening. After McCombe and Cole (1980).

usual three-dimensional systems because of the existence of the free motion in the direction parallel to magnetic fields. There have been a number of theoretical and experimental investigations on phenomena such as magnetotransport, cyclotron resonance, and magnetoplasmon effect. Effects of electron-electron interactions which play important roles in determining the subband structure and screening effects manifest themselves in various properties because of the singular nature of the density of states. The discrete density of states can also modify the localization strongly. In this section we describe various investigations related to the quantum transport phenomena mainly in the n-channel inversion layer on the silicon (100) surface.

We briefly summarize theoretical results on the broadening of Landau levels, the conductivity tensor, and dynamical properties in Sec. VI.A. Transport properties of actual inversion layers and their interpretations are given in Sec. VI.B Section VI.C is devoted to the discussion of cyclotron resonance and related dynamical properties. A rough sketch of various investigations on electron localization is given in Sec. VI.D.

A. Theory of quantum transport in a two-dimensional system

1. Static transport

Let us consider an isotropic two-dimensional system characterized by an effective mass m. In the absence of scatterers the density of states has a δ-function peak at the position of each Landau level $E=E_N$, where $E_N=(N+1/2)\hbar\omega_c$, $\omega_c=eH/mc$, and H is the strength of a magnetic field applied normal to the system. The degeneracy of each level is given by $1/2\pi l^2$ in a unit area, where l is the radius of the ground cyclotron orbit, given by $l^2=c\hbar/eH$. For $H=100$ kOe, for example, $l=81$ Å and the degeneracy is 2.5×10^{11} cm^{-2}. In the presence of scatterers each Landau level is broadened. So far many different approximations have been proposed for the calculation of such level broadening and transport properties. Among them the so-called self-consistent Born approximation is known to be most established and the simplest one free from various difficulties of divergence caused by the singular nature of the density of states. In the self-consistent Born approximation, effects of scattering from each scatterer are taken into account in the lowest Born approximation, while those of the level broadening are considered in a self-consistent way within a framework of the Green's-function formalism. This becomes equivalent to the Boltzmann transport theory in the absence of a magnetic field in the weak scattering limit, and is sufficient to demonstrate characteristics of the quantum transport in this system. In the following we briefly review the theory and summarize various characteristic results (Ando *et al.*, 1972a, 1972b; Ando and Uemura, 1974a; Ando, 1974a–1974c; Ando *et al.*, 1975).

The Hamiltonian is given by

$$\mathscr{H}=\mathscr{H}_0+\mathscr{H}_1 , \tag{6.1}$$

with

$$\mathscr{H}_0=\frac{1}{2m}\left[\mathbf{p}+\frac{e}{c}\mathbf{A}\right]^2 , \tag{6.2}$$

$$\mathscr{H}_1=\sum_i\sum_\mu v^{(\mu)}(\mathbf{r}-\mathbf{r}_i,z_i) , \tag{6.3}$$

where $v^{(\mu)}(\mathbf{r}-\mathbf{r}_i,z_i)$ is the effective two-dimensional potential of the μth kind of scatterer located at $(\mathbf{r}_i,z_i)$. We choose the symmetric gauge $\mathbf{A}=(-Hy/2,Hx/2)$. An eigenfunction of $\mathscr{H}_0$ is given by

$$\psi_{NX}(\mathbf{r})=\frac{1}{\sqrt{L}}\exp\left[i\frac{xy}{2l^2}-i\frac{Xy}{l^2}\right]\chi_N(x-X) , \tag{6.4}$$

with

$$\chi_N(x)=(2^N N!\sqrt{\pi}\,l)^{-1/2}\exp\left[-\frac{x^2}{2l^2}\right]H_N\left[\frac{x}{l}\right] , \tag{6.5}$$

where $H_N(y)$ is Hermite's polynomial and L^2 is the area of the system. The Hamiltonian is rewritten as

$$\mathscr{H}_0=\sum_{NX}E_N a_{NX}^+ a_{NX} , \tag{6.6}$$

$$\mathscr{H}_1=\sum_i\sum_\mu\sum_{NX}\sum_{N'X'}(NX\mid v^{(\mu)}(\mathbf{r}-\mathbf{r}_i,z_i)\mid N'X')a_{NX}^+ a_{N'X'} , \tag{6.7}$$

where a_{NX}^+ and a_{NX} are the creation and destruction operator, respectively. We introduce the Green's function

$$G_N(E)\delta_{NN'}\delta_{XX'}=\langle(0\mid a_{NX}(E-\mathscr{H})^{-1}a_{N'X'}^+\mid 0)\rangle \tag{6.8}$$

where $\mid 0)$ represents the vacuum state and $\langle\cdots\rangle$ means an average over all configurations of scatterers. The Green's function is diagonal with respect to Landau-level index N and center coordinate X and independent of X. The density of states $D(E)$ is given by

$$D(E)=\left[-\frac{1}{\pi}\right]\sum_{NX}\mathrm{Im}G_N(E+i0)$$

$$=\left[-\frac{1}{\pi}\right]\frac{1}{2\pi l^2}\sum_N\mathrm{Im}G_N(E+i0) . \tag{6.9}$$

The Green's function is calculated perturbationally, using iteratively

$$(E-\mathscr{H})^{-1}=(E-\mathscr{H}_0)^{-1}+(E-\mathscr{H}_0)^{-1}\mathscr{H}_1(E-\mathscr{H})^{-1} , \tag{6.10}$$

and is usually written in terms of the self-energy $\Sigma_N(E)$ as

$$G_N(E)=G_N^{(0)}(E)+G_N^{(0)}(E)\Sigma_N(E)G_N(E) , \tag{6.11}$$

with $G_N^{(0)}(E)=(E-E_N)^{-1}$.

The self-consistent Born approximation includes contributions of the diagram shown in Fig. 108 and gives

$$\Sigma_N(E)=\sum_{\mu}\sum_{i}\sum_{N'X'}\langle(NX\mid v^{(\mu)}\mid N'X')(N'X'\mid v^{(\mu)}\mid NX)\rangle G_{N'}(E)\ , \tag{6.12}$$

where

$$\sum_{i}\sum_{\mu}\sum_{X'}\langle(NX\mid v^{(\mu)}\mid N'X')(N'X'\mid v^{(\mu)}\mid NX)\rangle$$

$$=\sum_{\mu}\int dz\,N_i^{(\mu)}(z)\int d\mathbf{r}_i\int d\mathbf{r}\int d\mathbf{r}'\sum_{X'}\psi_{NX}^*(\mathbf{r})v^{(\mu)}(\mathbf{r}-\mathbf{r}_i,z_i)\psi_{N'X'}(\mathbf{r})\psi_{N'X'}^*(\mathbf{r}')v^{(\mu)}(\mathbf{r}'-\mathbf{r}_i,z_i)\psi_{NX}(r')$$

$$=2\pi l^2\sum_{\mu}\int dz\,N_i^{(\mu)}(z)\int\frac{d\mathbf{r}}{2\pi l^2}\int\frac{d\mathbf{r}'}{2\pi l^2}v^{(\mu)}(\mathbf{r},z)v^{(\mu)}(\mathbf{r}',z)J_{NN}\left[\frac{|\mathbf{r}-\mathbf{r}'|}{l}\right]J_{N'N'}\left[\frac{|\mathbf{r}-\mathbf{r}'|}{l}\right]. \tag{6.13}$$

Here we have used

$$\sum_{X}\psi_{NX}(\mathbf{r})\psi_{NX}^*(\mathbf{r}')=\frac{1}{2\pi l^2}J_{NN}\left[\frac{|\mathbf{r}-\mathbf{r}'|}{l}\right]\exp\left[i\frac{\mathbf{r}\times\mathbf{r}'}{2l^2}\right], \tag{6.14}$$

with

$$J_{NN'}(x)=(-1)^{N-N'}J_{N'N}(x)=\left[\frac{N'!}{N!}\right]^{1/2}\left[\frac{x}{\sqrt{2}}\right]^{N-N'}L_{N'}^{N-N'}\left[\frac{x^2}{2}\right]\exp\left[-\frac{x^2}{4}\right], \tag{6.15}$$

where $L_N^{\alpha}(x)$ is the associated Laguerre polynomial. In sufficiently strong magnetic fields one can neglect couplings between different Landau levels. When $E\sim E_N$, one gets

$$\Sigma_N(E)=\tfrac{1}{4}\Gamma_N^2G_N(E)\ , \tag{6.16}$$

with

$$\Gamma_N^2=4\times2\pi l^2\sum_{\mu}\int dz\,N_i^{(\mu)}(z)\int\frac{d\mathbf{r}}{2\pi l^2}\int\frac{d\mathbf{r}'}{2\pi l^2}v^{(\mu)}(\mathbf{r},z)v^{(\mu)}(\mathbf{r}',z)J_{NN}\left[\frac{|\mathbf{r}-\mathbf{r}'|}{l}\right]^2. \tag{6.17}$$

The density of states becomes

$$D(E)=\frac{1}{2\pi l^2}\sum_{N}\left[1-\left[\frac{E-E_N}{\Gamma_N}\right]^2\right]^{1/2}. \tag{6.18}$$

The density of states for each Landau level has a semielliptic form with the width Γ_N.

The nature of the level broadening Γ_N depends strongly on the range of scattering potentials. In the case of short-range scatterers ($d<l/(2N+1)^{1/2}$ where d is of the order of the range), one can replace $v^{(\mu)}(\mathbf{r},z)$ by $V^{(\mu)}(z)\delta(\mathbf{r})$ and get $\Gamma_N=\Gamma$ with

$$\Gamma^2=4\sum_{\mu}\int dz\,N_i^{(\mu)}(z)\frac{|V^{(\mu)}(z)|^2}{2\pi l^2}=\frac{2}{\pi}\hbar\omega_c\frac{\hbar}{\tau_f}\ , \tag{6.19}$$

where τ_f is the relaxation time for $H=0$ obtained by assuming the same scatterers. The level broadening is essentially the lifetime broadening and independent of the Landau level. However, it depends on the strength of the magnetic field. In the case of long-range scatterers, on the other hand, one gets

$$\Gamma_N^2\cong4\times2\pi l^2\sum_{\mu}\int dz\,N_i^{(\mu)}(z)\int\frac{d\mathbf{r}}{2\pi l^2}v^{(\mu)}(\mathbf{r},z)^2\int\frac{d\mathbf{r}'}{2\pi l^2}J_{NN}\left[\frac{|\mathbf{r}-\mathbf{r}'|}{l}\right]^2$$

$$=4\sum_{\mu}\int dz\,N_i^{(\mu)}(z)\int d\mathbf{r}\,v^{(\mu)}(\mathbf{r},z)^2=4\langle(V(\mathbf{r})-\langle V(\mathbf{r})\rangle)^2\rangle\ , \tag{6.20}$$

where $V(\mathbf{r})$ is the local potential energy. Therefore, the level broadening is of the so-called inhomogeneous type and is determined by the fluctuation of the local potential energy. If the range is comparable to the wavelength of electrons given by $l/(2N+1)^{1/2}$, the width depends on N in a complicated manner. Figure 109 gives an example of the range dependence of Γ_N for scatterers with a Gaussian potential,

$$v^{(\mu)}(\mathbf{r},z)=\frac{V^{(\mu)}(z)}{\pi d^2}\exp\left[-\frac{r^2}{d^2}\right]. \tag{6.21}$$

The width is independent of N for both short- and long-range limits and becomes smaller with increasing N for inter-

mediate ranges. The effect of the range is more important for large N because the electron wavelength becomes smaller.

The transverse conductivities σ_{xx} and σ_{yy} $(=\sigma_{xx})$ are most easily calculated with the center-migration theory (Kubo *et al.*, 1965). One has

$$\sigma_{xx}=\frac{e^2\hbar}{\pi L^2}\int dE\left[-\frac{\partial f}{\partial E}\right]\sum_{NX}\left\langle 0\left|a_{NX}X\left[\mathrm{Im}\frac{1}{E-\mathscr{H}+i0}\right]\dot{X}\left[\mathrm{Im}\frac{1}{E-\mathscr{H}+i0}\right]a_{NX}^{+}\right|0\right\rangle, \tag{6.22}$$

where $f(E)$ is the Fermi distribution function and

$$\dot{X}=\frac{1}{i\hbar}[X,\mathscr{H}]=\frac{1}{\hbar}\sum_{\mu}\sum_{i}\sum_{NX}\sum_{N'X'}\left[NX\left|l\frac{\partial v^{(\mu)}(\mathbf{r}-\mathbf{r}_i,z_i)}{\partial y}\right|N'X'\right]a_{NX}^{+}a_{N'X'}\,. \tag{6.23}$$

The conductivity can also be calculated perturbationally. One has to sum contributions of diagrams which are consistent with those taken into account in the self-energy diagram. In the self-consistent Born approximation one should include the diagram shown in Fig. 108, and one gets, in sufficiently strong magnetic fields,

$$\sigma_{xx}=\frac{e^2}{\pi^2\hbar}\int dE\left[-\frac{\partial f}{\partial E}\right]\left[\frac{\Gamma_N^{xx}}{\Gamma_N}\right]^2\left[1-\left[\frac{E-E_N}{\Gamma_N}\right]^2\right], \tag{6.24}$$

where N should be chosen in such a way that E_N is closest to E and

$$(\Gamma_N^{xx})^2=4\times 2\pi l^2\sum_{\mu}\int dz\,N_i^{(\mu)}(z)\tfrac{1}{2}\int\frac{d\mathbf{r}}{2\pi l^2}\int\frac{d\mathbf{r}'}{2\pi l^2}l\frac{\partial v^{(\mu)}(\mathbf{r},z)}{\partial y}l\frac{\partial v^{(\mu)}(\mathbf{r}',z)}{\partial y'}J_{NN}\left[\frac{|\mathbf{r}-\mathbf{r}'|}{l}\right]^2. \tag{6.25}$$

In the case of short-range scatterers one can expand $J_{NN}(x)$ with respect to x and obtain

$$(\Gamma_N^{xx})^2=(N+\tfrac{1}{2})\Gamma^2\,. \tag{6.26}$$

The peak value of σ_{xx} at zero temperature is given by

$$(\sigma_{xx})_{\mathrm{peak}}=\frac{e^2}{\pi^2\hbar}(N+\tfrac{1}{2})\,, \tag{6.27}$$

which depends only on the Landau-level index N and the natural constants and is independent of the magnetic field and the strength of scatterers. In the case of long-range scatterers one has

$$(\Gamma_N^{xx})^2=\langle(l\nabla V(\mathbf{r}))^2\rangle\,, \tag{6.28}$$

which is just the fluctuation of the gradient of the local potential energy. The transverse conductivity vanishes in the limit of long-range scatterers. Figure 110 shows peak values of σ_{xx} for scatterers with the Gaussian potential (6.21). The peak value decreases rapidly with increasing range in proportion to $(l/d)^2$.

The Hall conductivity σ_{xy} $(=-\sigma_{yx})$ can be calculated similarly (Ando *et al.*, 1975) and is given by

$$\sigma_{xy}=-\frac{N_s ec}{H}+\Delta\sigma_{xy}\,, \tag{6.29}$$

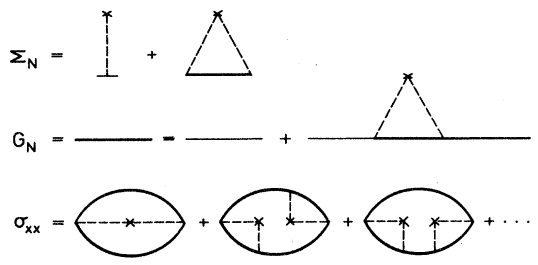

FIG. 108. A diagrammatic representation of the self-consistent Born approximation. The crosses denotes scatterers and the dotted lines represent interactions with them. The first term in the self-energy causes a trivial shift of the energy origin and can be omitted. The terms other than the first in the bottom figure do not contribute to the conductivity in strong magnetic fields.

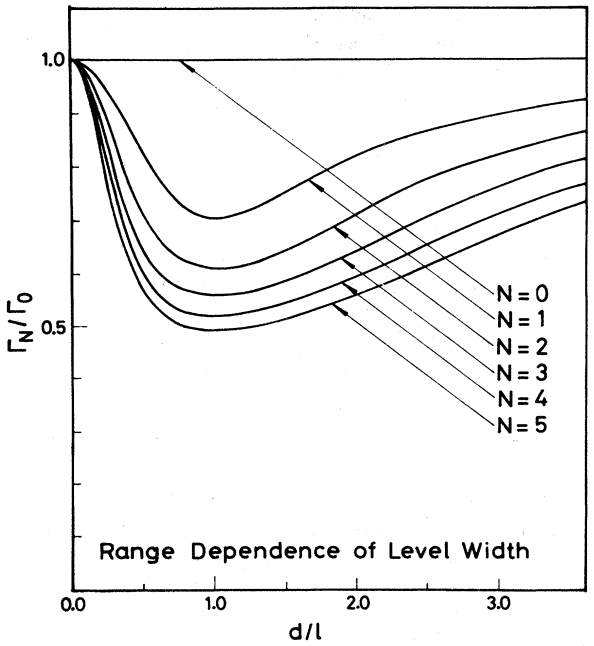

FIG. 109. The level broadening ratio Γ_N/Γ_0 as a function of the range $\alpha=d/l$ of the Gaussian potential. After Ando and Uemura (1974a).

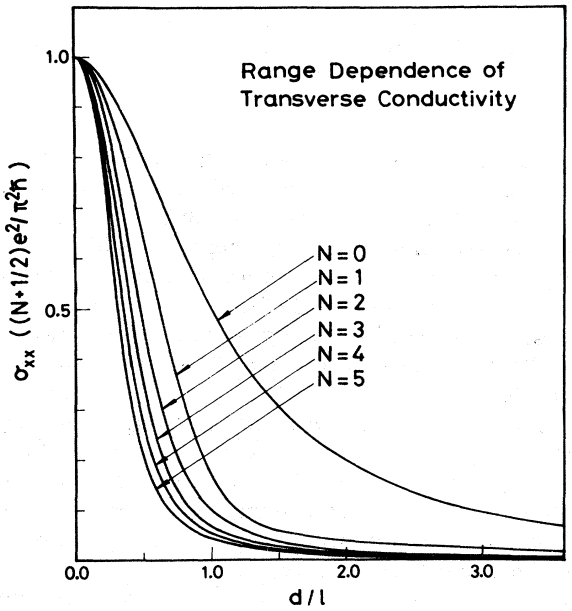

FIG. 110. The peak value of the conductivity $(\Gamma_N^{xx}/\Gamma_N)^2/(N+\frac{1}{2})$ as a function of the range $\alpha=d/l$ of the Gaussian potential. After Ando and Uemura (1974a).

with

$$\Delta\sigma_{xy}=\frac{e^2}{\pi^2\hbar}\int dE\left[-\frac{\partial f}{\partial E}\right]\frac{(\Gamma_N^{xy})^4}{\hbar\omega_c\Gamma_N^3}\left[1-\left[\frac{E-E_n}{\Gamma_N}\right]^2\right]^{3/2}. \tag{6.30}$$

In the case of short-range scatterers one gets

$$(\Gamma_N^{xy})^4=(N+\tfrac{1}{2})\Gamma^4 . \tag{6.31}$$

Thus we have a relation:

$$(\Delta\sigma_{xy})_{\text{peak}}=\frac{\Gamma}{\hbar\omega_c}(\sigma_{xx})_{\text{peak}} . \tag{6.32}$$

In the case of long-range scatterers, one has

$$(\Gamma_N^{xy})^4=4(N+\tfrac{1}{2})\langle(l\nabla V(\mathbf{r}))^2\rangle^2 , \tag{6.33}$$

which vanishes in the long-range limit.

The above results can physically be understood in terms of a simple diffusion picture, as has been shown by Uemura (1974a, 1974b). In strong magnetic fields the conduction takes place because of jumps of the center coordinates of a cyclotron orbit caused by scattering. In the case of short-range scatterers the distance of each jump is of the order of the radius of the cyclotron orbit, and the diffusion constant D^* of the center of the orbit is given by

$$D^*\sim\frac{(2N+1)l^2}{\tau} , \tag{6.34}$$

where τ is a lifetime of the orbit. Further, the uncertainty relation gives the density of states near the center of each Landau level,

$$D(E_F)\sim\frac{1}{2\pi l^2}\frac{\tau}{\hbar} . \tag{6.35}$$

Thus the Einstein relation gives

$$(\sigma_{xx})_{\text{peak}}\sim e^2D(E_F)D^*\sim\frac{e^2}{\hbar}(N+\tfrac{1}{2}) . \tag{6.36}$$

This agrees with Eq. (6.27) within a numerical factor. The above intuitive derivation of the peak value of the transverse conductivity shows that its independence of relevant quantities such as the level width and H is a consequence of a cancellation of the two effects: The probability of jumps of the center coordinate is proportional to the scattering rate. When the scattering rate is large, however, the level broadening becomes large, and consequently the jump probability decreases because of the decrease of the density of final states. A similar argument is applicable also to the case of slowly varying scatterers (Ando and Uemura, 1974a). Since the center coordinate moves according to

$$\dot{X}=\frac{l^2}{\hbar}\frac{\partial V(\mathbf{r})}{\partial y} , \tag{6.37}$$

the diffusion constant is proportional to the fluctuation of the gradient of the local potential energy. Equation (6.32) is the same as that which the classical phenomenological expressions of σ_{xx} and σ_{xy} satisfy, i.e.,

$$\begin{aligned}\sigma_{xy}&=-\frac{N_se^2\tau_f}{m}\frac{\omega_c\tau_f}{1+(\omega_c\tau_f)^2}\\&=-\frac{N_sec}{H}+\frac{1}{\omega_c\tau_f}\frac{N_se^2\tau_f}{m}\frac{1}{1+(\omega_c\tau_f)^2}\\&=-\frac{N_sec}{H}+\frac{1}{\omega_c\tau_f}\sigma_{xx} .\end{aligned} \tag{6.38}$$

This also has a simple meaning: When an electric field E_y is applied in the y direction, the center of the cyclotron motion moves in the x direction with a drift velocity $v_x=cE_y/H$, which gives rise to the Hall conductivity $-N_sec/H$. Effects of scattering can be regarded as a frictional force acting on each electron, whose strength is given by $F_x=-mv_x/\tau_f=eE_y/\omega_c\tau_f$. The current in the x direction due to this force is given by

$$\Delta j_x=\sigma_{xx}\frac{F_x}{(-e)}=\frac{1}{\omega_c\tau_f}\sigma_{xx}E_y=\Delta\sigma_{xy}E_y . \tag{6.39}$$

In magnetic fields of arbitrary strength, the problem becomes difficult because scattering processes between different Landau levels become important. Even in the simplest self-consistent Born approximation it is very difficult to get explicit expressions of the conductivity tensor, and so far only the case of short-range scatterers has been studied in detail (Ando, 1974c). It has been shown that the peak value of σ_{xx} decreases and that of $\Delta\sigma_{xy}$ increases rather slowly with decreasing magnetic field if $\omega_c\tau_f$ is sufficiently larger than unity. The conductivities and the density of states for arbitrary values of $\omega_c\tau_f$ have been calculated numerically. When $\omega_c\tau_f$ is less than unity, the oscillation becomes sinusoidal and one has

$$\sigma_{xx}=\frac{N_s e^2\tau_f}{m}\frac{1}{1+(\omega_c\tau_f)^2}\left[1-2\frac{(\omega_c\tau_f)^2}{1+(\omega_c\tau_f)^2}\frac{2\pi^2 k_B T}{\hbar\omega_c}\operatorname{csch}\frac{2\pi^2 k_B T}{\hbar\omega_c}\cos\frac{2\pi\mu}{\hbar\omega_c}\exp\left[-\frac{\pi}{\omega_c\tau_f}\right]+\cdots\right], \tag{6.40}$$

where simple parabolic bands and evenly spaced Landau levels are assumed and the chemical potential μ is assumed to be sufficiently larger than $\hbar\omega_c$. This equation enables us to extract the effective mass and the zero-field relaxation time τ_f from experimental data of the temperature dependence and magnetic field dependence of the oscillation amplitude. This will be discussed in detail in Sec. VI.B. It should be noticed that the oscillatory part of the conductivity does not contain $(\hbar\omega_c/\mu)^{1/2}$, in contrast to the result in a three-dimensional system. In a three-dimensional system the nonoscillatory part of the density of states increases as $E^{1/2}$ with increasing E because of the overlapping of the density of states of lower Landau levels corresponding to large momenta in the direction of a magnetic field, which gives rise to the factor $(\hbar\omega_c/\mu)^{1/2}$. In the two-dimensional system the nonoscillatory part of the density of states is essentially independent of E and such a factor does not exist. Nevertheless many people have used a simple formula for three dimensions containing this factor in analyzing experimental results (Niederer, 1974; Eisele *et al.*, 1976a, 1976b; Fang *et al.*, 1977). This factor does not influence the effective-mass determination, which is usually based on the temperature dependence alone.

To examine the validity of the self-consistent Born approximation, the Born series has been summed up to infinite order (the so-called single-site approximation) (Ando, 1974a). The results approach those in the self-consistent Born approximation for high concentrations of weak scatterers, i.e., when an electron feels potentials of many scatterers at the same time. In other cases we have to use the higher-order approximation. Especially when the strength of scatterers is weak enough to neglect coupling with different Landau levels and their concentration is small, the density of states associated with each Landau level has structure because of the appearance of so-called impurity bands. Such impurity bands can appear both at the low- and high-energy edges of the Landau level, depending on whether the potential is attractive or repulsive. When the potential is attractive and strong, the impurity band can appear only below the bottom of the ground Landau level. The Hall conductivity has also been calculated in higher-order approximations (Ando *et al.*, 1975). It has been noted that when each Landau level is filled at zero temperature σ_{xy} takes its classical value $-N_s ec/H$, even in the presence of localized impurity states in the strong-field limit. This problem has attracted considerable attention, as will be discussed in Sec. VI.B. An early discussion of the level broadening and transverse conductivities in a kind of single-site approximation was given by Ohta (1971a, 1971b). The important self-consistency requirement was neglected in this work, however.

The self-consistent Born approximation is not sufficient in the energy region close to the spectral edges, which is clear if we consider the unphysical sharp cutoff of the density of states. The results obtained in this approximation, especially in strong magnetic fields where the density of states vanishes between adjacent Landau levels, are therefore not suitable for a detailed analysis of the line shape of the conductivity tensor. To get reasonable results near the spectral edges, one has to take into account effects of multiple scattering. This is difficult, however, since the simple multiple-scattering correction does not give physically reasonable results because of the analyticity problem (Ando, 1974b). In the case of high concentrations of weak short-range scatterers, infinite series can be summed up to infinite order in an approximate manner. One replaces terms by a common expression for each order of the perturbation expansion and sums up the resulting asymptotic expansion. The profile of the resulting density of states is a kind of average of the elliptic form and a Gaussian form, as is shown in Fig. 111. With increasing Landau-level index N the pro-

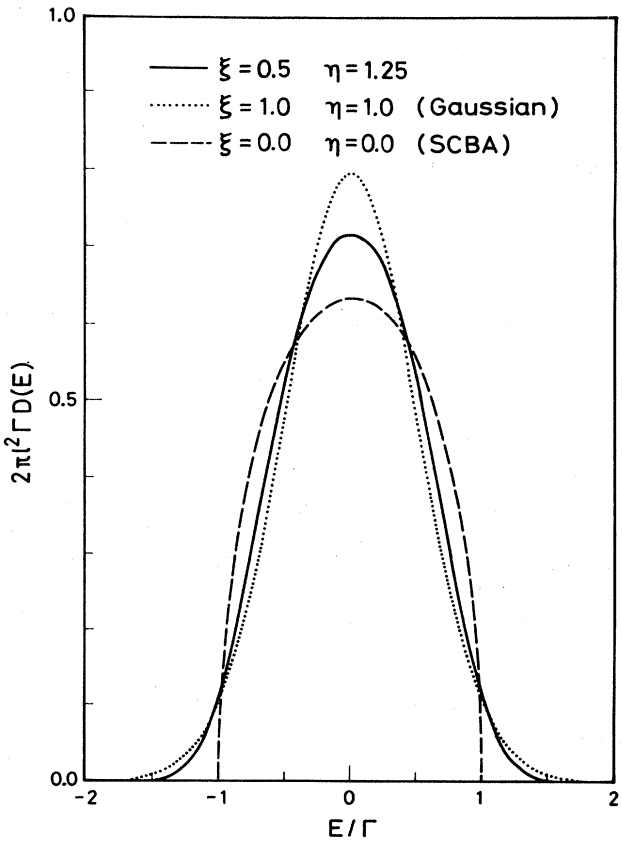

FIG. 111. The density-of-states profile of the ground Landau level calculated by approximately summing up infinite series of a perturbation expansion (the solid line). The broken line and the dotted line give the elliptic and Gaussian form, respectively. After Ando (1974b).

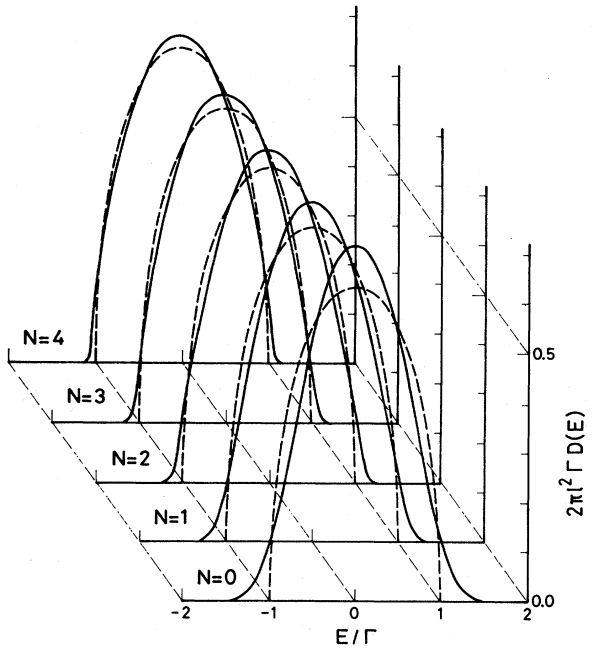

FIG. 112. The density-of-states profile of Landau levels calculated by approximately summing up infinite series of a perturbation expansion. It approaches a semielliptic form with increasing Landau-level index N. After Ando (1974b).

file approaches the result of the self-consistent Born approximation, although the density of states has low- and high-energy tails, as is shown in Fig. 112. This dependence on N is consistent with the fact that the Born approximation becomes sufficient for large kinetic energy. A similar calculation for the conductivity is difficult and has not yet been carried out.

Gerhardts (1975a, 1975b, 1976) used a method of cumulant expansion (or path-integral method) in calculating the density of states. The Green's function is written as

$$G_N(E)=\int_0^\infty dt\,\exp(-iEt)(0\,|\,a_{NX}K(t)a_{NX}^{+}\,|\,0)\,, \tag{6.41}$$

with

$$K(t)=\left\langle \exp\left[-\frac{i}{\hbar}\mathscr{H}t\right]\right\rangle . \tag{6.42}$$

In the interaction representation one gets

$$K(t)=K^0(t)\left\langle T\exp\left[-\frac{i}{\hbar}\int_0^t d\tau\,\mathscr{H}_1(\tau)\right]\right\rangle , \tag{6.43}$$

with T being a time-ordering operator,

$$\mathscr{H}_1(t)=\exp\left[\frac{i}{\hbar}\mathscr{H}_0t\right]\mathscr{H}_1\exp\left[-\frac{i}{\hbar}\mathscr{H}_0t\right], \tag{6.44}$$

and

$$K^0(t)=\exp\left[-\frac{i}{\hbar}\mathscr{H}_0t\right] . \tag{6.45}$$

A cumulant expansion of the time-ordered exponential in Eq. (6.43) gives

$$\left\langle T\exp\left[-\frac{i}{\hbar}\int_0^t d\tau\,\mathscr{H}_1(\tau)\right]\right\rangle=\exp\left[\sum_{\nu=1}^{\infty}\frac{1}{\nu!}C_\nu\right] . \tag{6.46}$$

The first-order term,

$$C_1=-\frac{i}{\hbar}t\langle\mathscr{H}_1\rangle , \tag{6.47}$$

is trivial and can be neglected. The second-order term is nontrivial and is given by

$$C_2=\left[-\frac{i}{\hbar}\right]^2 T\int_0^t d\tau\int_0^t d\tau'[\langle\mathscr{H}_1(\tau)\mathscr{H}_1(\tau')\rangle-\langle\mathscr{H}_1\rangle^2] . \tag{6.48}$$

If the lowest nontrivial term is retained one has

$$\begin{aligned}K_N(t)&=(0\,|\,a_{NX}K(t)a_{NX}^{+}\,|\,0)\\&=\exp\left[-\frac{i}{\hbar}E_Nt\right]\exp\left[-\frac{1}{\hbar^2}\sum_{\mu}\int dz\,N_i^{(\mu)}(z)2\pi l^2\sum_{N'}\int\frac{d\mathbf{r}}{2\pi l^2}\int\frac{d\mathbf{r}'}{2\pi l^2}\right.\\&\left.\times v^{(\mu)}(\mathbf{r},z)v^{(\mu)}(\mathbf{r}',z)J_{NN}\left[\frac{|\mathbf{r}-\mathbf{r}'|}{l}\right]J_{N'N'}\left[\frac{|\mathbf{r}-\mathbf{r}'|}{l}\right]\chi\left[\frac{E_{N'}-E_N}{\hbar},t\right]\right] ,\end{aligned} \tag{6.49}$$

with

$$\begin{aligned}\chi(\omega,t)&=\int_0^t d\tau\int_0^\tau d\tau'\exp[-i\omega(\tau-\tau')]\\&=\frac{t}{i\omega}+\frac{1}{\omega^2}[1-\exp(-i\omega t)] .\end{aligned} \tag{6.50}$$

In a sufficiently strong magnetic field, one gets

$$K_N(t)=\exp\left[-\frac{i}{\hbar}E_Nt\right]\exp\left[-\frac{\Gamma_N^2t^2}{8\hbar^2}\right] . \tag{6.51}$$

Thus, the density of states takes on a Gaussian form,

$$D(E)=\frac{1}{2\pi l^2}\sum_N\left[\frac{\pi}{2}\Gamma_N^2\right]^{-1/2}\exp\left[-2\frac{(E-E_N)^2}{\Gamma_N^2}\right] , \tag{6.52}$$

which is shown by the dotted line in Fig. 111. This approximation, called the lowest-order cumulant approximation, can take into account higher-order effects partially and does not cause the unphysical sharp cutoff of

the density of states. It gives, therefore, a theoretical basis, together with the calculation of Ando, for using the Gaussian form of the density of states in qualitative line-shape analysis. Figure 112 shows that the line shape calculated by Ando in higher approximation resembles the elliptic form more closely than the Gaussian for higher Landau levels. Such a result can be obtained in the present approximation only if higher-order terms in the cumulant expansion are included. It is rather difficult to calculate the transport coefficients in a consistent approximation with this method, and Gerhardts introduced a simplified approximation. The peak value obtained for the transverse conductivity is a factor $\pi/2$ as large as Eq. (6.27). The transverse conductivity remains finite in the limit of long-range scatterers. This result is unphysical, since the potentials are ineffective in this limit, and might originate from the inconsistency of the approximation for the Green's function and that for the conductivity.

The theory mentioned above can easily be extended to an anisotropic case with the electron dispersion given by two different effective masses, especially in strong magnetic fields (Ando, 1976d). The density of states and the conductivities are given by expressions similar to Eqs. (6.18), (6.24), (6.29), and (6.30), where x and y directions are chosen in the symmetry directions. The nature of the level broadening is essentially the same as in the isotropic system, as is expected. In the case of short-range scatterers the transverse conductivity is most anisotropic, and one gets

$$\sigma_{xx}=\frac{\bar{m}}{m_x}\bar{\sigma}_{xx},\quad \sigma_{yy}=\frac{\bar{m}}{m_y}\bar{\sigma}_{xx}\ , \tag{6.53}$$

where m_x and m_y are the effective masses in the x and y direction, respectively, $\bar{m}=(m_x m_y)^{1/2}$, and $\bar{\sigma}_{xx}$ is the conductivity in the isotropic system characterized by the mass $\bar{m}$ and the same scatterers. With an increase of the range the anisotropy decreases and the conductivity becomes isotropic in the case of long-range scatterers. Figure 113 shows an example of the calculated range dependence of the anisotropy for scatterers with a Gaussian potential. We can see the range dependence clearly. One can also calculate the Hall conductivity in the anisotropic system. However, the anisotropy does not affect the Hall conductivity strongly. When a magnetic field becomes weaker and mixing between different Landau levels is important, the problem becomes considerably more difficult, except in case of short-range scatterers. In the case of short-range scatterers Eq. (6.53) is valid in magnetic fields of arbitrary strength. In the case of scatterers with finite ranges, however, we cannot give any definite answers. Even the Boltzmann equation in the absence of a magnetic field can be solved only with tedious numerical calculation or only approximately.

2. Dynamical conductivity

Dynamical properties of the inversion layer are usually studied by measuring the transmission of far-infrared light incident normal to the surface. Emission can also be used (Gornik and Tsui, 1978a, 1978b; Gornik *et al.*, 1980a). Usually the wavelength of the light is much larger than the thickness of the inversion layer. The response of the system to an external electric field can be calculated by regarding the inversion layer as a conducting sheet having a two-dimensional conductivity tensor $\sigma_{\mu\nu}(\omega)$, defined by

$$J_\mu\delta(z)\exp(-i\omega t)=\sum_{\nu=x,y}\sigma_{\mu\nu}(\omega)E_\nu(z)\delta(z)\exp(-i\omega t)\ , \tag{6.54}$$

where $E_\nu(z)\exp(-i\omega t)$ is the electric field, and the sheet is assumed to be at $z=0$. Using this equation we can calculate the transmission coefficient easily (Ando, 1975a; von Ortenberg, 1975; Abstreiter *et al.*, 1976b; Chiu *et al.*, 1976; Kennedy *et al.*, 1976a). When the conductivity is not too large we can easily show that the change of the transmission of light linearly polarized in the x direction is proportional to the real part of $\sigma_{xx}(\omega)$. Thus the problem is reduced to the study of the dynamical conductivity $\sigma_{xx}(\omega)$. Note that Fabry-Perot—type multiple reflection effects due to finite layer thickness should be avoided in experiments. Otherwise various lineshape distortions can appear in the transmission (von Ortenberg; 1975; Abstreiter *et al.*, 1976b; Chiu *et al.*, 1976; Kennedy *et al.*, 1976a). Note also that the conductivity can become large and the line shape of the transmission can deviate from that of the real part of $\sigma_{xx}(\omega)$, especially at high electron concentrations. A full transmission coefficient should be used in analyzing the line shape in such cases.

The theory discussed in the previous section can be extended to the calculation of the dynamical conductivity $\sigma_{xx}(\omega)$ (Ando and Uemura, 1974d; Ando, 1975a). Here we present only some of the results obtained. In the case

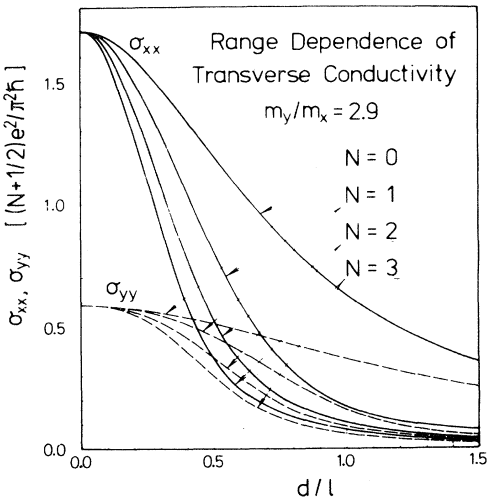

FIG. 113. An example of the range dependence of the transverse conductivity in an n-channel inversion layer on a Si(110) surface. Scatterers with a Gaussian potential are assumed. After Ando (1976d).

of short-range scatterers optical transitions between all states in adjacent Landau levels become allowed, since the level broadening is essentially the lifetime broadening. Consequently the resonance width is determined by the level width itself. In the case of long-range scatterers only the transition between states with nearly the same relative energy measured from the center of each broadened Landau level is allowed, since those states correspond to those with nearly the same position of the center of the cyclotron motion in the case of inhomogeneous broadening. The width of the resonance Γ_{CR} is determined by the fluctuation of the gradient of the local potential $V(\mathbf{r})$, i.e.,

$$\Gamma_{CR} \sim \frac{\langle (l\nabla V(\mathbf{r}))^2 \rangle}{\langle (V(\mathbf{r}) - \langle V(\mathbf{r}) \rangle)^2 \rangle^{1/2}} . \tag{6.55}$$

It is rather difficult to give an explicit expression of the width of the cyclotron resonance in general cases. Ando (1975a) has obtained the second moment of the spectrum, $\Delta(\hbar\omega)^2$, when the Fermi level lies midway between adjacent Landau levels in strong magnetic fields:

$$\begin{aligned}\Delta(\hbar\omega)^2 &= 2\pi l^2 \sum_{\mu} \int dz\, N_i(\mu)(z) \int \frac{d\mathbf{r}}{2\pi l^2} \int \frac{d\mathbf{r}'}{2\pi l^2} \left[J_{NN}\left[\frac{|\mathbf{r}-\mathbf{r}'|}{l}\right]^2 + J_{N+1N+1}\left[\frac{|\mathbf{r}-\mathbf{r}'|}{l}\right]^2 \right. \\ &\quad \left. - 2J_{NN+1}\left[\frac{|\mathbf{r}-\mathbf{r}'|}{l}\right]^2 \right] v^{(\mu)}(\mathbf{r},z) v^{(\mu)}(\mathbf{r}',z) \\ &= \sum_{\mu} \int dz\, N_i^{(\mu)}(z) \sum_{q} v_q^{(\mu)}(z)^2 [J_{NN}(lq) - J_{N+1N+1}(lq)]^2 ,\end{aligned} \tag{6.56}$$

with

$$v^{(\mu)}(\mathbf{r},z) = \sum_{q} v_q^{(\mu)}(z) \exp(i\mathbf{q}\cdot\mathbf{r}) . \tag{6.57}$$

We have $\Delta(\hbar\omega)^2 = \Gamma^2/2$ in the case of short-range scatterers. There is a possibility, however, that the actual width can be smaller than the second moment in the case of long-range scatterers. As a matter of fact Eq. (6.56) gives

$$\Delta(\hbar\omega)^2 \sim \langle (l^2\nabla^2 V(\mathbf{r}))^2 \rangle , \tag{6.58}$$

which is shown to be larger than Γ_{CR}^2 with the aid of Schwarz's inequality. Examples of $\sigma_{xx}(\omega)$ calculated in the self-consistent Born approximation for scatterers with a Gaussian potential are given in Fig. 114. With increasing range the linewidth becomes narrower than the level width. A part of this effect is the same as the difference between the usual lifetime of states and the velocity relaxation time in the absence of a magnetic field. The line shape is strongly dependent on the position of the Fermi energy, especially in the case of short-range scatterers. This is a result of the Pauli exclusion principle and the discrete nature of the density of states characteristic of the two-dimensional system. Thus it is rather difficult to define the exact width of the transition in this system at low temperatures. This strong dependence of the dynamical conductivity on the position of the Fermi level causes the appearance of quantum oscillation of the cyclotron resonance line shape at low temperatures. Usually the cyclotron resonance is observed by sweeping H at a constant $\hbar\omega$. With the change of H the Fermi level passes through many different Landau levels successively, and an oscillatory behavior appears in the cyclotron resonance line shape. The dynamical conductivity $\sigma_{xx}(\omega)$ has a dip when ω_c is smaller than ω and a peak when ω_c is larger than ω, when the Fermi level lies midway between adjacent Landau levels. The period of this quantum oscillation is determined only by the electron concentration N_s, as for the usual Shubnikov–de Haas oscillation of the static conductivity. Examples of the results of numerical calculation for an n-channel inversion layer on the Si(100) surface are shown in Fig. 115. Short-range scatterers are assumed. We can clearly see the strong quantum oscillation below 10 K. The asymmetry of the line shape is a consequence of the fact that the level width is proportional to $H^{1/2}$. The structure around $H = 30$ kOe and 20 kOe is a subharmonic structure, which is again a direct consequence of the discrete density of states of our system. Because of a coupling of different Landau levels due to scatterers, the profile of the density of states of each Landau level has a small peak at the position of other Landau levels. This structure of the density of states gives rise to the subharmonic structure at $\omega_c/\omega = \frac{1}{2}, \frac{1}{3}, \ldots$ in the two-dimensional system. In three-dimensional systems such structure might exist in the density profile, but is not strong enough to cause the subharmonic structure in the line shape since the singularity of the density of states is much weaker than in the two-dimensional system. Those are the main characteristics of the cyclotron resonance line shape in the two-dimensional system.

Prasad and Fujita (1977a–1977c, 1978; see also Fujita and Prasad, 1977; Prasad, 1978, 1980) calculated the width of the resonance using a more simplified approximation scheme. In their formalism one starts from the self-consistent Born approximation and introduces a further approximation to get an explicit expression of the dynamical conductivity. It cannot describe the detailed structure of the resonance line shape, such as the quantum oscillation and the subharmonic structure, although it is quite useful for qualitative discussion of the broadening. They obtained an expression for the width which is the same as the second moment (6.56). A different approach was used by Götze and Hajdu (1979) and

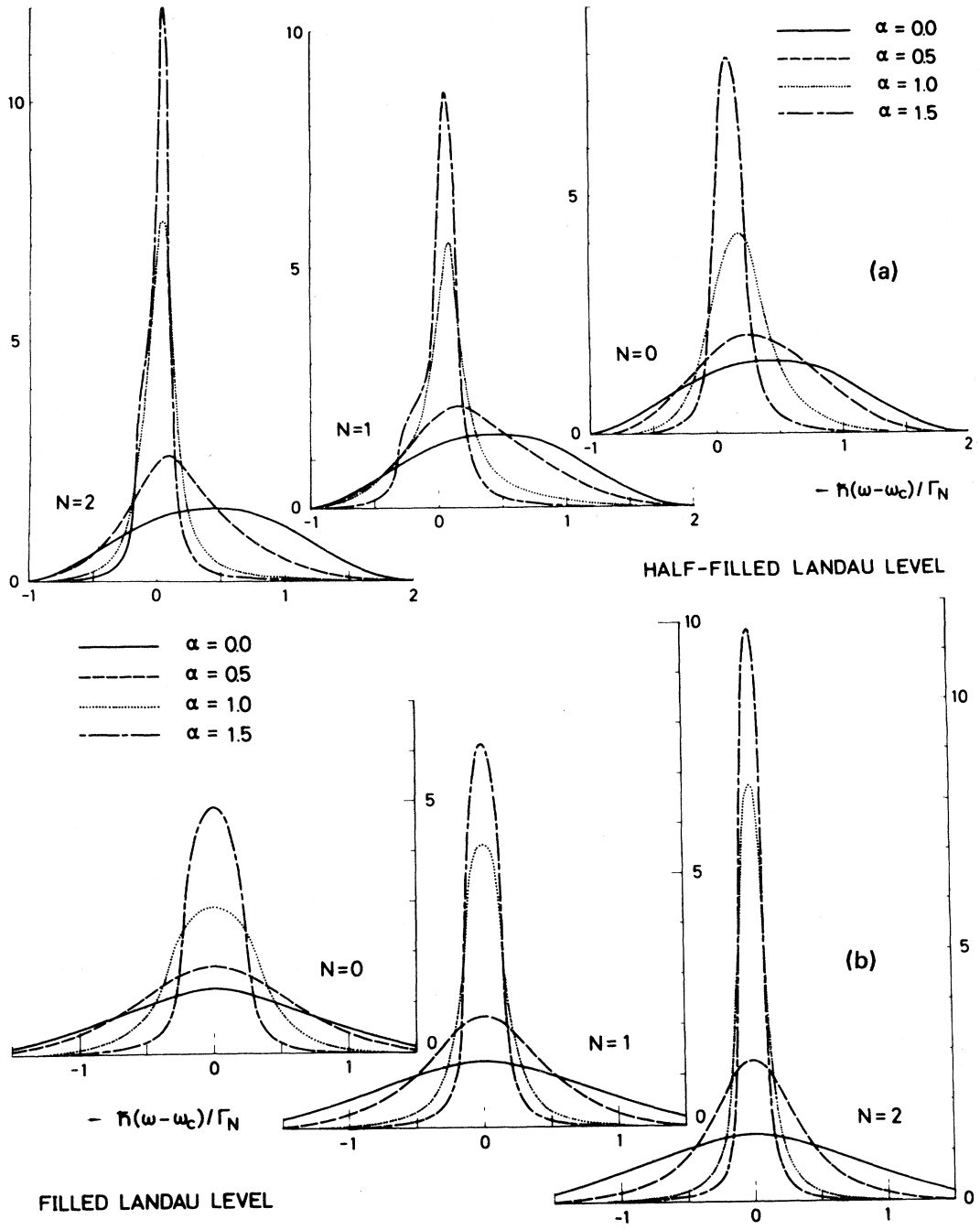

FIG. 114. Dynamical conductivity in the case of scatterers with the Gaussian potential at zero temperature. Γ_N is the level width of the Nth Landau level and $\alpha=d/l$. (a) The Fermi level lies just at the middle of the gap between the Nth and $(N+1)$th levels. (b) It lies at the center of the Nth level. Note that the peak is shifted to the higher-energy side for the half-filled case (b), especially in the case of short-range scatterers. This causes the quantum oscillation of the cyclotron resonance line shape. After Ando (1975a).

gave similar results for the broadening. Effects of phonon scattering at higher temperatures have been considered (Prasad *et al.*, 1977; Prasad, 1979). Electron-phonon interactions were also discussed by Horovitz and Madhukar (1979). Various theories have been proposed in connection with effects of electron-electron interactions. Those will be discussed in Sec. VI.C.

B. Magnetotransport in the silicon inversion layer

1. Case of strong magnetic fields

As we have seen in Sec. IV.C, the screening of scattering potentials by free carriers in the inversion layer plays an important role in determining the conductivity and

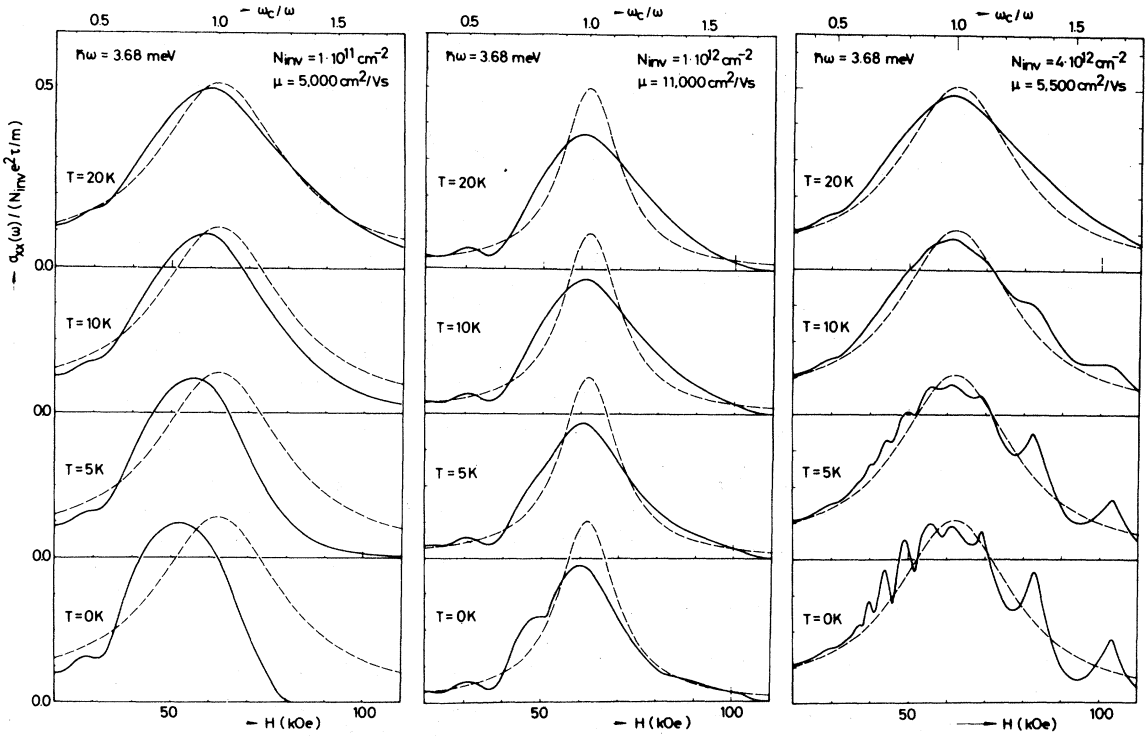

FIG. 115. Dynamical conductivity as a function of applied magnetic field in an n-channel inversion layer on a Si(100) surface. Short-range scatterers are assumed. The broken lines are obtained by the classical formula in which the Lorentzian line shape with a single relaxation time τ_f is assumed. In the calculation use has been made of $m=0.195m_0$ and $g^*=2$, and the valley splitting is ignored. $\hbar\omega=3.68$ meV. After Ando (1975a).

the mobility. Since the Thomas-Fermi screening constant is given by the density of states at the Fermi energy at zero temperature, the discrete density of states in strong magnetic fields makes the screening quite different from that in the absence of a magnetic field. Thus the application of the theory discussed in the previous section is not a simple problem in realistic inversion layers. The dielectric function in magnetic fields depends strongly on the broadening of Landau levels, which is determined by the strength of scatterers, i.e., by the screening. We have to determine the broadening and the screening in a self-consistent manner. Such a calculation has been performed only for the case in which the strong magnetic field limit is applicable, i.e., when interactions between different Landau levels can be treated perturbationally (Ando, 1977d). The assumed scatterers are charged centers, which have been assumed to be distributed almost uniformly in the oxide, and surface roughness. An example of the results for $H=100$ kOe is shown in Figs. 116 and 117. In Fig. 116 are shown the calculated mobility in the absence of a magnetic field, the width obtained from Eq. (6.19), the width Γ_N of the Landau level N where the Fermi level lies, and the second moment of cyclotron resonance. Two different moments are given, corresponding to the fact that we have two transitions, from N to $N+1$ and from $N-1$ to N. The actual width is expected to be given by an average of the two moments and might be smaller in the case of long-range scatterers. The width Γ_N depends on the position of the Fermi energy E_F and becomes very large when E_F lies at the tail region of each Landau level. The moments of the cyclotron resonance do not vary so much with N_s.

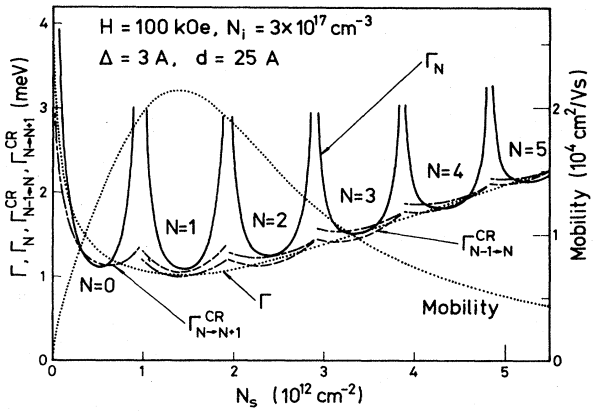

FIG. 116. Various kinds of widths calculated in the self-consistent Born approximation in an n-channel inversion layer on Si(100) for $H=100$ kOe. Charged centers in the oxide and surface roughness are assumed as dominant scatterers. The mobility at $H=0$ and the corresponding Γ are shown by the dotted lines. The level broadening Γ_N depends strongly on the position of the Fermi level, whereas the broadening of the cyclotron resonance ($\Gamma^{CR}_{N\to N+1}$, $\Gamma^{CR}_{N-1\to N}$) does not vary so much. After Ando (1977d).

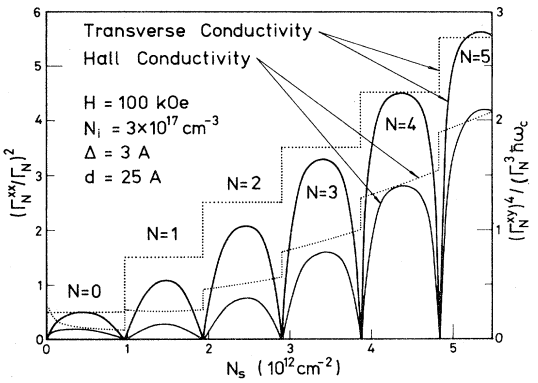

FIG. 117. Peak values of σ_{xx} and $\Delta\sigma_{xy}$ in units of $e^2/\pi^2\hbar$ in an n-channel inversion layer on a Si(100) surface at $H=100$ kOe. The corresponding results for short-range δ-potential scatterers are shown by the dotted lines. After Ando (1977d).

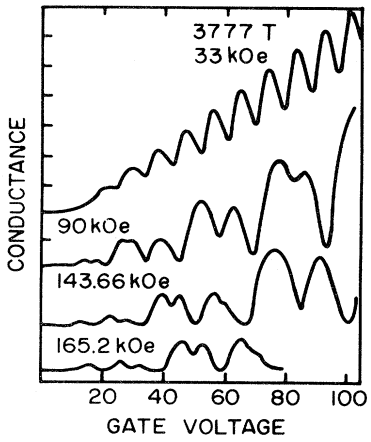

FIG. 118. The magnetoconductivity for varying magnetic fields as one crosses from the intermediate-field region to the high-field region, observed by Fowler, Fang, Howard, and Stiles (1966a, 1966b). After Stiles (1974b).

The scattering potentials become long range because of the decrease of the screening effect when E_F lies near the tails. Except for these cases, both Γ_N and the moments are given rather well by Γ. This is rather a surprising result, but is true of a relatively wide range of parameters which gives reasonable values of the mobility. In Fig. 117 the peak values of σ_{xx} and $\Delta\sigma_{xy}$ are shown together with the results for short-range scatterers, which correspond to the same value of the mobility in the absence of a magnetic field. The peak values become very small when E_F lies in the tail region, since the potentials become long range. In other cases, however, the values are again well given by the results for short-range scatterers. In weaker magnetic fields the short-range scatterer model becomes slightly worse and the finite range of scatterers becomes important, especially at low N_s. In any case, one sees that the model of short-range scatterers, which has frequently been used because of its simplicity, works rather well in discussing various qualitative features of transport in inversion layers in strong magnetic fields. However, there are some cases in which this simple model is not appropriate.

In 1966 Fowler, Fang, Howard, and Stiles (1966a, 1966b) first observed the Shubnikov–de Haas oscillation in an n-channel inversion layer on the Si(100) surface. Some of the observed results are given in Fig. 118. Although the line shape of the oscillation does not look as ideal as that subsequently observed for better samples with lower oxide charge or higher mobility, it shows all the characteristic behaviors which will be discussed later in this section. From the constant period in N_s of the oscillation and the temperature dependence of its amplitude, Fowler *et al.* confirmed that this system was a two-dimensional electron system characterized by an effective mass which is close to the conduction-band mass of Si. The spin and valley splittings were also observed in strong magnetic fields. As has been discussed in Sec. III.A, the ground electric subband in the n-channel inversion layer on the silicon (100) surface is given by the two valleys located in the [100] and [$\bar{1}$00] directions. These are degenerate within the effective-mass approximation, but the degeneracy can be lifted. This problem will be discussed in detail in Sec. VII.A.

A detailed and systematic measurement of σ_{xx} for samples having high mobility was made by Kobayashi and Komatsubara (Ando *et al.*, 1972b; Komatsubara *et al.*, 1974) after the theoretical prediction (Ando and Uemura, 1974a) of the peak value of σ_{xx}; see Eq. (6.27). An example of their results is shown in Fig. 119. The lowest four peaks correspond to the ground ($N=0$) Landau level, the next four peaks to $N=1$, and so on. The splitting of the peak into two, observed in $N=2$ and 3 Landau levels, is considered to be spin-Zeeman splitting,

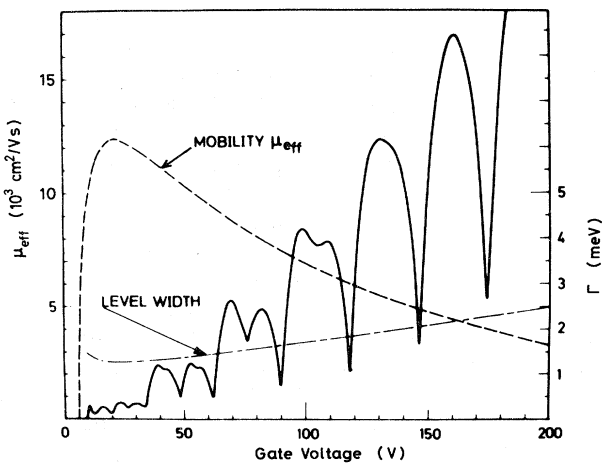

FIG. 119. An example of the oscillation of the conductivity observed by Kobayashi and Komatsubara (Ando *et al.*, 1972a; Komatsubara *et al.*, 1974) in an n-channel inversion layer on a Si(100) surface at $H=95$ kOe. The effective mobility and the corresponding level width Γ are also shown. After Ando and Uemura (1974a).

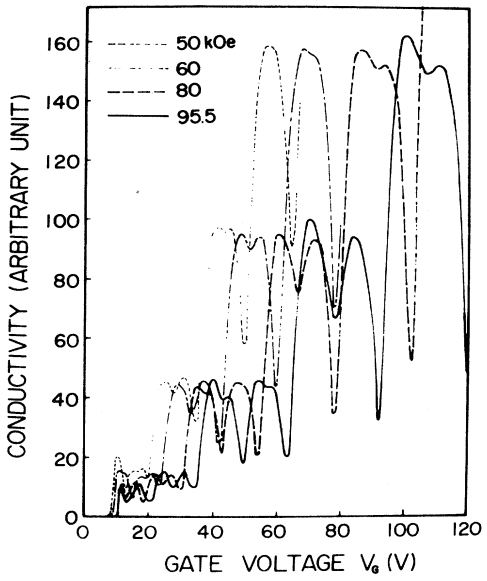

FIG. 120. Magnetoconductivity oscillations for different fields observed by Kobayashi and Komatsubara (Ando *et al.*, 1972a; Komatsubara *et al.*, 1974). After Ando *et al.* (1972a).

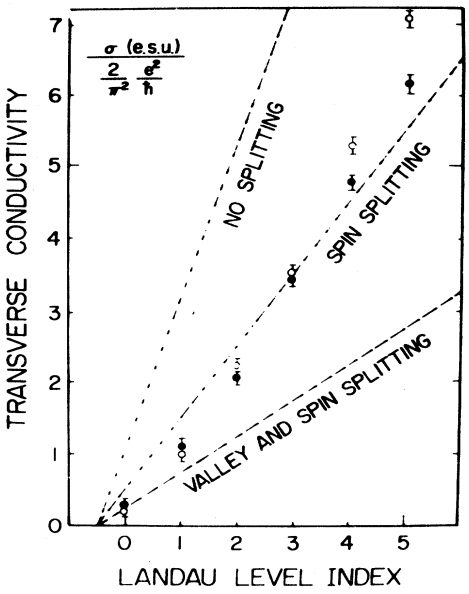

FIG. 121. The peak values of the transverse conductivity versus Landau level indices. Three broken lines represent theoretical values of the peak heights of fourfold, twofold, and no degeneracy cases, respectively. White and black circles are experimental results for two different samples at $50 < H < 95.5$ kOe and at 1.4 K. After Ando *et al.* (1972a).

and the additional splitting observed in $N=0$ and 1 is considered to be valley splitting. In Fig. 120, σ_{xx} is shown for various strengths of H. It shows clearly that the peak values are almost independent of H, which is explained by dominant short-range scatterers. The experimental peak values are plotted as a function of N in Fig. 121. If one takes into account the degree of the splittings observed experimentally, one can conclude that the theoretical peak values for short-range scatterers are in semiquantitative agreement with the experiments.

Lakhani and Stiles (1976b) also made a systematic study of the peak values of σ_{xx} for a wider range of H and for different values of substrate bias. Their peak values tend to decrease rather more rapidly with decreasing H than the theoretical prediction for very short-range scatterers. This can qualitatively be explained by the result of the calculation for realistic scatterers discussed above. Quantitatively, however, the calculated H dependence of the peak values is too large in comparison with the experiments. This suggests the existence of additional and unknown scatterers in actual inversion layers. Lakhani and Stiles suggested that intervalley scattering which couples different valleys might be important (see Sec. IV.C for more detailed discussion of scattering mechanisms). Peak values of σ_{xx} have also been studied as functions of the source-drain electric field (Kawaji and Wakabayashi, 1976; Kawaji, 1978).

As has been shown in Sec. VI.A, we can determine the broadening of levels from the Hall conductivity σ_{xy}. A measurement of the Hall conductivity σ_{xy} was first made by Igarashi, Wakabayashi, and Kawaji (1975) in strong magnetic fields. They used a wide rectangular sample (length-to-width ratio $\frac{1}{3}$) and deduced σ_{xx} and σ_{xy} from the measured source-drain current and Hall voltage. Figure 122 gives an example of their results. The experiments are qualitatively explained by the theory. For example, the theory shows that the effective width of $\Delta\sigma_{xy}$ as a function of the Fermi energy is narrower than that of σ_{xx}. This explains the experimental result that the spin splitting is resolved in $\Delta\sigma_{xy}$ but not in σ_{xx} for $N=3$. Kawaji, Igarashi, and Wakabayashi (1975) made a line-shape analysis of their results using a Gaussian form of the density of states. The spin splitting and its enhancement due to the exchange effect (see Sec. VI.B.3) was taken into account, but the valley splitting was not in the analysis. The calculated line shape is given by the

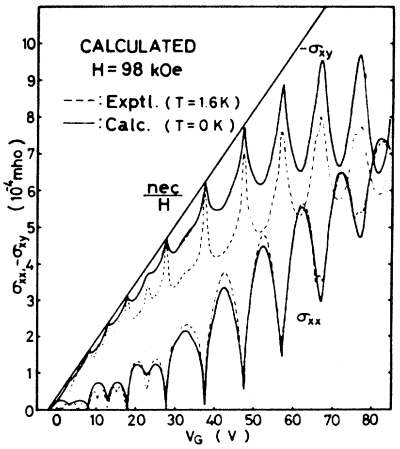

FIG. 122. The conductivities σ_{xx} and σ_{xy} measured by Igarashi, Wakabayashi, and Kawaji (1975) together with a theoretical prediction based on a line-shape analysis (Kawaji, Igarashi, and Wakabayashi, 1975). After Kawaji, Igarashi, and Wakabayashi (1975).

solid lines. The agreement is satisfactory for σ_{xx} but not so good for $\Delta\sigma_{xy}$, for which the absolute value is much larger than the theoretical one. Various possible corrections for $\Delta\sigma_{xy}$ in higher-order approximations have theoretically been considered, but are too small to explain this large disagreement (Ando *et al.*, 1975). Wakabayashi and Kawaji (1978; see also Kawaji, 1978) have shown that the observed σ_{xx} and σ_{xy} depend strongly on the sample geometry and that the simple procedure for determining σ_{xx} and σ_{xy} from measured quantities does not give correct values for the conductivity tensor. For wide samples, the value obtained for σ_{xx} is close to that observed in circular samples (the Corbino geometry) and is reasonable, but the Hall conductivity turns out to be unreasonable. For long samples, on the other hand, the transverse conductivity becomes completely different from that of circular samples. It has been suggested that a large electric field distortion near the edges of the samples is responsible. Because of these problems a direct comparison between theory and experiment was not possible for the Hall conductivity. σ_{xy} has been successfully obtained by measuring the Hall current instead of the conventional Hall voltage for wide samples (Wakabayashi and Kawaji, 1980a, 1980b). The electric field distortion is not so serious in this method. Figure 123 shows an example of the results obtained. A solid line in σ_{xy} is the result calculated from the measured σ_{xx} with $\Delta\sigma_{xy}\sim\Gamma\sigma_{xx}/\hbar\omega_c$, where Γ is obtained from the measured mobility through Eq. (6.19). One sees that the theory explains the experimental results on the absolute value of $\Delta\sigma_{xy}$ quite satisfactorily.

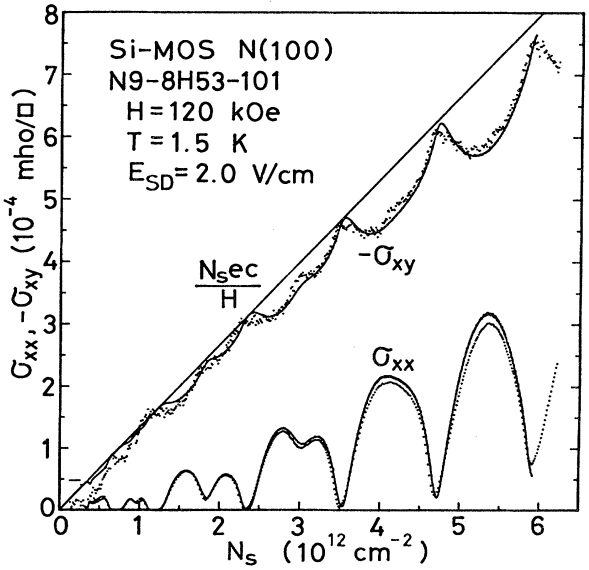

FIG. 123. The conductivities σ_{xx} and σ_{xy} (dotted curves) observed by Wakabayashi and Kawaji (1980a, 1980b) in Hall-current measurement. The solid line for the transverse conductivity represents that observed in the Corbino geometry (circular samples) giving purely σ_{xx}. The solid line for the Hall conductivity is calculated through $\Delta\sigma_{xy}=(\Gamma/\hbar\omega_c)\sigma_{xx}$ by using a measured mobility in the absence of a magnetic field. After Wakabayashi and Kawaji (1980b).

The theory discussed in Sec. VI.A predicts that $\sigma_{xy}=-N_s ec/H=Ne^2/2\pi\hbar$ when the Fermi level lies midway between adjacent Landau levels N and $N+1$ in sufficiently strong magnetic fields. In 1980 von Klitzing, Dorda, and Pepper (1980), Braun, Staben, and von Klitzing (1980), and Kawaji and Wakabayashi (1981) measured σ_{xy} on the Si(100) surface and showed that σ_{xy} is independent of N_s in the range where σ_{xx} is extremely small in comparison with its peak value. An example of the experimental results is given in Fig. 124. Von Klitzing, Dorda, and Pepper (1980) showed that the value of σ_{xy} in the flat region is given by an integer multiple of $e^2/2\pi\hbar$ to high accuracy (within a relative error of $\sim 1.5\times 10^{-5}$). They suggested further that it is possible to determine the fundamental constant $e^2/\hbar$ more accurately. This application, as well as the use of the quantum Hall effect as a possible secondary resistance standard, has attracted considerable attention and is being actively pursued in the standards laboratories of several countries (Taylor and Phillips, 1982). A review has been given by von Klitzing (1981). The quantum Hall effect has also been found in GaAs-(Al,Ga)As heterojunctions (Tsui and Gossard, 1981; Narita *et al.*, 1981a; Baraff and Tsui, 1981). These interesting developments have raised a fundamental problem on the validity of the theoretical prediction obtained in the previous section within rather simple approximations (Aoki and Ando, 1981; Prange, 1981; Laughlin, 1981).

The Hall conductivity σ_{xy} is given by Eq. (6.29). The correction $\Delta\sigma_{xy}$ arising from the presence of scatterers is

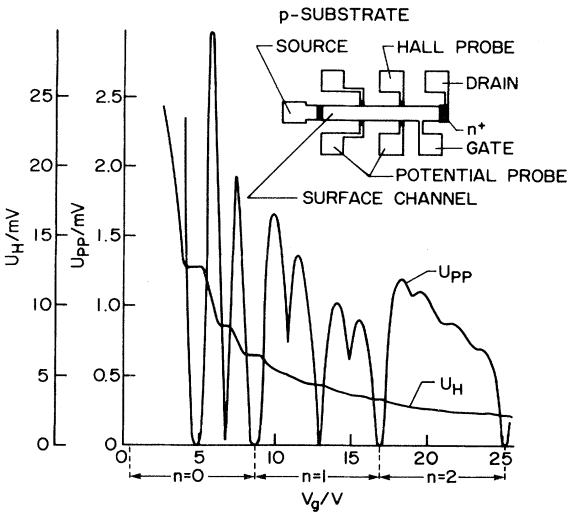

FIG. 124. Recordings of the Hall voltage, U_H, and the voltage drop between the potential probes, U_{pp}, as a function of the gate voltage at $T=1.5$ K. The magnetic field is 18 T. The oscillation up to the Landau level $n=2$ is shown. The Hall voltage and U_{pp} are proportional to ρ_{xy} and ρ_{xx}, respectively, where $\rho_{xx}=\sigma_{xx}/(\sigma_{xx}^2+\sigma_{xy}^2)$ and $\rho_{xy}=-\sigma_{xy}/(\sigma_{xx}^2+\sigma_{xy}^2)$. The inset shows a top view of the device with a length of $L=400$ μm, a width of $W=50$ μm and a distance between the potential probes of $L_{pp}=130$ μm. After von Klitzing, Dorda, and Pepper (1980).

written as (Kubo *et al.*, 1965)

$$\Delta\sigma_{xy}=\frac{e^2\hbar}{iL^2}\sum_{\alpha,\beta}\frac{f(E_\alpha)}{(E_\alpha-E_\beta+i0)^2}\times[(\alpha|\dot{X}|\beta)(\beta|\dot{Y}|\alpha)-(\alpha|\dot{Y}|\beta)(\beta|\dot{X}|\alpha)], \quad (6.59)$$

where $|\alpha)$ describes eigenstates and E_α corresponding energy. When the state $|\alpha)$ is localized, we have

$$(\alpha|\dot{X}|\beta)=\frac{1}{i\hbar}(\alpha|[X,\mathscr{H}]|\beta)=\frac{1}{i\hbar}(E_\beta-E_\alpha)(\alpha|X|\beta). \quad (6.60)$$

With the aid of $[X,Y]=il^2$, we immediately see that the contribution in $\Delta\sigma_{xy}$ of the state $|\alpha)$ is given by ec/H, which exactly cancels the corresponding term in the first term of (6.29). This means that σ_{xy} becomes flat as a function of N_s as long as the Fermi level lies in the energy region of localized states. This agrees with an intuitive picture that localized states carry no current and explains the experimental results. It can immediately be shown from Eq. (6.59) that σ_{xy} vanishes when a Landau level is completely occupied by electrons in a strong-field limit where mixing between different Landau levels is not important. Therefore, σ_{xy} is given by the same value (an integer multiple of $e^2/2\pi\hbar$) as in the absence of scatterers, even in the case when some of the states are localized. This has a simple physical meaning: The induced current in the x direction in an infinitesimal electric field E_y in the y direction is written as

$$j_x=-e\sum_{\alpha'}f(E_{\alpha'})(\alpha'|\dot{X}|\alpha')=-\frac{c}{H}\sum_{\alpha'}f(E_{\alpha'})\left[\left(\alpha'\left|\frac{\partial V}{\partial y}\right|\alpha'\right)+eE_y\right], \quad (6.61)$$

where $V(\mathbf{r})$ is the local potential energy and $|\alpha')$ is the eigenstate in the presence of E_y. In the strong-field limit we have

$$\psi_{\alpha'}(\mathbf{r})=\sum_X c_{NX}^{\alpha'}\psi_{NX}(\mathbf{r}), \quad (6.62)$$

and

$$\sum_{\alpha'}\left(\alpha'\left|\frac{\partial V}{\partial y}\right|\alpha'\right)=\frac{1}{2\pi l^2}\left\langle\frac{\partial V}{\partial y}\right\rangle=0, \quad (6.63)$$

where $\langle\cdots\rangle$ means the spatial average and use has been made of the orthogonality of $c_{NX}^{\alpha'}$ and Eq. (6.14). Therefore, we have $\Delta\sigma_{xy}=0$ when each Landau level is completely filled with electrons. In localized states wave functions deform infinitesimally in the electric field in such a way that the effective field of scatterers $(\alpha'|\partial V/\partial y|\alpha')$ exactly cancels the external field E_y. On the other hand, wave functions of some extended states deform in the opposite way because their wave functions are orthogonal to localized wave functions, and electrons move faster than $-cE_y/H$ by an amount given by the effective field due to scatterers. This extra Hall current compensates for that not carried by the localized electrons.

Under actual experimental conditions, mixing between different Landau levels cannot be neglected completely and might give rise to corrections to the value of σ_{xy}. This interesting problem has not been fully studied yet, although there is some indication that higher-order mixing effects are not important (Prange, 1981; Ando, unpublished). Laughlin (1981) has presented an argument which shows that the Hall conductivity should be exactly an integer multiple of e^2/h in arbitrary magnetic fields as long as the Fermi level lies in localized states and a gap exists in the density of extended states. The problem has also been studied by Thouless (1981).

There have been attempts to obtain the width of the Landau levels by measuring the temperature dependence of the minimum values of σ_{xx} when the Fermi level lies midway between two adjacent levels (Nicholas *et al.*, 1977, 1978; Englert and von Klitzing, 1978). If there is no overlap of the density of states of adjacent levels, σ_{xx} is determined by thermal excitation of electrons to the Landau levels and is expected to be given by

$$(\sigma_{xx})_{\min}\propto\exp\left[-\frac{\Delta E-2\Gamma}{2k_BT}\right], \quad (6.64)$$

where ΔE is the separation of the levels and Γ is their width. Nelgecting valley splitting, Nicholas *et al.* and Englert and von Klitzing determined Γ from their experimental results. The Γ's obtained in this way are considerably smaller than the width obtained from zero-field mobilities and have no simple relationship with them. This is not surprising. As has been discussed above, scattering when the Fermi level lies near the tail of Landau levels can be quite different from scattering in the absence of a magnetic field, due to the difference of the screening effect. Further, this determination of the width is closely related to the localization in strong magnetic fields (see Sec. VI.D).

Warm-electron effects in strong magnetic fields were studied theoretically by Uchimura and Uemura (1979a, 1979b). They solved an energy-balance equation for the gain from the applied electric field and the loss to the phonon system and calculated the increase of the temperature of the electron system. In spite of the discrete density of states the temperature increase does not show singular behavior as a function of the electron concentration. This is due to a cancellation of the density-of-states function appearing in the expressions for the energy loss and gain terms. The results were compared with experimental results (Kawaji and Wakabayashi, unpublished), which were estimated from comparison between the conductivities for high fields at low temperatures and for low fields at elevated temperatures. The calculated temperature rise has turned out to be slightly smaller than the experiments.

2. Shubnikov-de Haas oscillation in weak magnetic fields

When the magnetic field becomes weaker, the conductivity exhibits a sinusoidal oscillation. In general we can write it as

$$\sigma_{xx}=\int\left[-\frac{\partial f}{\partial E}\right]dE\,\sigma_{xx}(E)\ . \tag{6.65}$$

In sufficiently weak magnetic fields we have

$$\sigma_{xx}(E)=F^{(0)}(E)-\cos\frac{2\pi E}{\hbar\omega_c}F^{(1)}(E)\ , \tag{6.66}$$

where $F^{(0)}(E)$ and $F^{(1)}(E)$ are slowly varying functions of E. Thus we have at low temperatures

$$\sigma_{xx}=F^{(0)}(\mu)-\frac{2\pi^2k_BT}{\hbar\omega_c}\,\mathrm{csch}\frac{2\pi^2k_BT}{\hbar\omega_c}\cos\frac{2\pi\mu}{\hbar\omega_c}F^{(1)}(\mu)\ , \tag{6.67}$$

where μ is the chemical potential. Therefore we can determine ω_c or the effective mass m defined by $\omega_c=eH/mc$ from the temperature dependence of the oscillation amplitude of σ_{xx} if $F^{(0)}$ and $F^{(1)}$ are independent of temperature. Very early (Fowler *et al.*, 1966b) the mass was found to be $(0.21\pm0.01)m_0$ at low N_s. Smith and Stiles (1972, 1974; see also Stiles, 1974a, 1974b) made a systematic study of such temperature dependence and determined the effective mass as a function of N_s. It is about 15% enhanced from the conduction-band mass $m_t=0.191m_0$ around $N_s=1\times10^{12}$ cm^{-2} and decreases with increasing N_s. This N_s dependence is in the opposite direction to that expected from nonparabolicity and is considered to be a result of electron-electron interactions. It has provoked a lot of theoretical investigations. As has been discussed in Sec. II.F, the theoretical calculation of the mass enhancement due to electron-electron interactions explains the experimental results reasonably well. Furthermore, the enhancement has turned out to be in agreement with that estimated from the so-called subharmonic structure of the cyclotron resonance line shape (Kotthaus *et al.*, 1974a; Abstreiter *et al.*, 1976b). The position of the subharmonic structure has been shown by Ando (1976e) to be determined by the effective mass enhanced by the many-body effect. This will be discussed in more detail in Sec. VI.C.1.

Many later experiments, however, cast some doubt on the accuracy of the effective masses determined in this way. Stiles (1974b) made similar experiments in tilted magnetic fields, and obtained mass values strongly dependent on the spin splitting, although the general tendency of the mass to be enhanced, and decrease with N_s, was the same as that determined by Smith and Stiles. Lakhani, Lee, and Quinn (1976) studied effects of the substrate bias and found that the mass increased when electrons were brought close to the surface. However, the mass obtained in the absence of the substrate bias showed a completely opposite behavior to that observed by Smith and Stiles, i.e., the mass increased with N_s. Fang, Fowler, and Hartstein (1977, 1978) made a more systematic study of the temperature dependence of the Shubnikov–de Haas oscillation. They determined the mass for different values of H, substrate bias, bulk doping, and concentrations of charges in the oxide. Their conclusion is rather disappointing. According to them the masses obtained from such an analysis do not behave in a consistent way as a function of the doping and the substrate bias. If the enhancement were caused by an intrinsic effect, such as electron-electron interactions, the mass values obtained for the same N_{depl} should be the same. Their results suggest that the masses derived from an analysis of Shubnikov–de Haas oscillations depend on the detailed nature of scatterers in the system. This fact has been demonstrated by changing the concentration of charges in the oxide. For low concentrations of the oxide charges the masses obtained show behavior similar to that found by Smith and Stiles, but they show opposite N_s dependence when scattering due to the oxide charges becomes important.

There might be several possible reasons for such a strange behavior of the temperature dependence of the Shubnikov–de Haas oscillations. As has been shown in Sec. IV.C, the screening of scattering potentials by free carriers in the inversion layer plays an important role in determining the mobility. Thus the oscillatory behavior of the screening effect can cause additional temperature dependence of the term $F^{(0)}$ and $F^{(1)}$ when the oscillation amplitude is not sufficiently small. As a matter of fact, the Thomas-Fermi screening constant ($q\to0$) is given by

$$\bar{q}_s=\frac{2\pi e^2}{\bar{\kappa}}\int dE\left[-\frac{\partial f}{\partial E}\right]D(E)\ . \tag{6.68}$$

In the case of short-range scatterers we have the oscillation of $\bar{q}_s$ in weak magnetic fields, given by

$$\bar{q}_s=\frac{2\pi e^2}{\bar{\kappa}}\frac{m}{2\pi\hbar^2}\left[1-2\frac{2\pi^2k_BT}{\hbar\omega_c}\,\mathrm{csch}\frac{2\pi^2k_BT}{\hbar\omega_c}\times\cos\frac{2\pi\mu}{\hbar\omega_c}\exp\left[-\frac{\pi}{\omega_c\tau_f}\right]\right]\ , \tag{6.69}$$

where use has been made of a result (Ando, 1974c):

$$D(E)=\frac{m}{2\pi\hbar^2}\left[1-2\cos\frac{2\pi E}{\hbar\omega_c}\exp\left[-\frac{\pi}{\omega_c\tau_f}\right]\right]\ . \tag{6.70}$$

The spin and valley degeneracies have been neglected, for simplicity. There have been some theoretical investigations on the screening in magnetic fields (Lee and Quinn, 1976; Horing *et al.*, 1974; Horing and Yildiz, 1976). However, explicit expressions for the dielectric constant cannot easily be obtained for nonzero values of q, especially in the presence of level broadening due to scatterers. Further, so far there has not been any reliable theory of the Shubnikov–de Haas oscillation for realistic scatterers, and we can not rule out the possibility that such a change in the screening is responsible for the strange behavior of the effective mass. A possible tem-

perature dependence of the spin and valley splittings due to the change in the many-body effect (see Sec. VI.B.3) also affects the temperature dependence of the oscillation amplitude. Another possibility is a strong perturbation of the energy spectrum due to the existence of scatterers. In the presence of impurity-bound states, energy levels of low-lying extended states are pushed up due to quantum-mechanical interactions. Consequently the separation between adjacent Landau levels becomes smaller, causing an increase of the effective mass (Overhauser, 1978). This model predicts that the effective mass increases with impurity concentrations, which is, however, opposite to the behavior obtained by Fang, Fowler, and Hartstein (1977, 1978). An effective-mass modification caused by impurity scattering has been proposed also by Sernelius and Berggren (1980). There is no doubt that a large part of the mass enhancement and its strong dependence on the electron concentration in high-mobility samples is due to electron-electron interactions discussed in Sec. II.F. At present, however, it is hard to separate experimentally the exact contribution of the electron-electron interaction from other kinds of effects.

As is clear from Eq. (6.40), the oscillation amplitude decreases exponentially with decreasing H. This so-called Dingle factor was used to determine the relaxation time in this system. Fowler (1969, unpublished) obtained relaxation times which were in reasonable agreement with the values deduced from the mobility at high N_s but which were much larger at low N_s. Niederer (1974) made similar measurements and obtained results which were in good agreement with the mobility around the electron concentration where the mobility had a peak, but became smaller at high N_s. Lakhani, Lee, and Quinn (1976) used this method to show that the relaxation time decreased with increasing negative substrate bias. Experiments of Fang, Fowler, and Hartstein (Fang *et al.*, 1977, 1978; Hartstein and Fang, 1978) gave results in good agreement with the mobility. Although there still remain some disagreements between the experimental results, one can conclude that the relaxation time determined from the oscillation amplitude is roughly equal to the relaxation time which determines the mobility in the absence of a magnetic field. This fact is rather surprising because there is no *a priori* reason that the two kinds of relaxation times should be the same for arbitrary scatterers. It might be related to the fact that the short-range scatterer model works quite well in strong magnetic fields. Hartstein and Fang (1978) investigated the Dingle temperature ($k_B T_D = \hbar/2\pi\tau_f$) for different concentrations of charged centers in the oxide. They have found that the oxide charge dependence of the Dingle temperature agrees quite well with the theoretical prediction.

3. Spin and valley splittings

We have seen in the previous section that the observed values of σ_{xx} are explained by the theory quite well. There remains the problem of explaining the line shape of σ_{xx}, especially the observed degree of splitting for different Landau levels. The measured mobility and the level width calculated from Eq. (6.19) are shown in Fig. 119. If one assumes a g factor of two, the spin-Zeeman energy $g\mu_B H$ (typically, 1.16 meV at $H = 100$ kOe) is smaller than the level width Γ, and one cannot expect to see either the spin splitting or the valley splitting, which is even smaller than the spin splitting for low-lying Landau levels (see Sec. VII.A for a detailed discussion on the valley splitting). Further, the width is a relatively slowly varying function of N_s, and one cannot expect a large change of the degree of the splitting with increasing Landau levels observed experimentally.

In 1968 Fang and Stiles (1968) performed a celebrated experiment. In the electric quantum limit the Landau-level structure is determined by the component of a magnetic field normal to the surface, and the spin splitting is given by the total magnetic field, when the magnetic field is tilted from the normal direction (see Sec. III.D). Thus the separation of Landau levels and that of different spin states can be controlled independently. An example of observed oscillation of the transconductance $d\sigma_{xx}/dN_s$ in tilted magnetic fields is given in Fig. 125. From the characteristic change of the line shape, Fang and Stiles determined the tilt angle where the energy separations between adjacent levels $(N,\uparrow)$ and $(N,\downarrow)$, $(N,\downarrow)$ and $(N+1,\uparrow)$, are equal to each other. From such a tilt angle one gets a relation between the g factor (g_S^*) when the Fermi level lies midway between the $(N,\uparrow)$ and $(N,\downarrow)$ levels and the g factor (g_L^*) when it lies between the $(N,\downarrow)$ and $(N+1,\uparrow)$ levels,

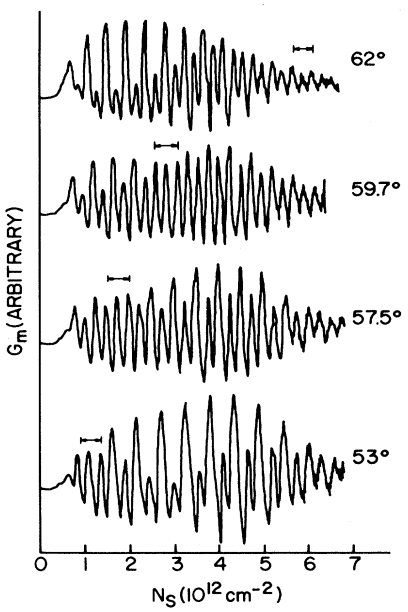

FIG. 125. Transconductance oscillations with the surface-electron concentrations at 90 kOe for different tilt angles θ. The arrows identify the surface-electron concentration at which the energy separations are equal. After Fang and Stiles (1968).

$$g_S^*\mu_B H=\frac{\hbar eH}{mc}\cos\theta-g_L^*\mu_B H\ . \tag{6.71}$$

Putting $g_L^*=g_S^*$ and using $m=m_t=0.191m_0$ they determined the g factor for various values of N_s. The g factor is strongly enhanced from the bulk value (~ 2) and increases drastically with decreasing electron concentration. Note, however, that the absolute value derived in this way can be somewhat in error if the mass is different from the bulk value.

The g-factor enhancement has been explained by the exchange effect among electrons in the Landau level. Let us assume that the number of electrons with ↑ spin is larger than that of electrons with ↓ spin because of the spin-Zeeman splitting. Electrons with ↓ spin feel more repulsive force than those with ↑ spin, since electrons with the same spin cannot be close to each other due to the Pauli exclusion principle and electrons feel stronger repulsive force from electrons with different spins. The original splitting is therefore enhanced by electron-electron interactions. Such enhancement of the g factor has been calculated by a number of authors in the weak magnetic field limit, as has been discussed in Sec. II.F. The actual experiments were performed in strong magnetic fields, where the quantization into Landau levels is appreciable. Thus the assumption that $g_L^*=g_S^*$ is actually not so good, since the difference of the numbers of electrons with ↑ and ↓ spins is different for the two cases corresponding to g_L^* and g_S^*. In strong magnetic fields the density of states becomes discrete and the difference in numbers of electrons with ↑ and ↓ spins, to which the enhancement is proportional, depends strongly on the position of the Fermi level. When the Fermi level lies at the middle of the gap between $(N,\uparrow)$ and $(N,\downarrow)$ levels, the difference becomes maximum and the g factor has a certain maximum value larger than 2. When it lies midway between the $(N,\downarrow)$ and $(N+1,\uparrow)$ levels, the difference becomes minimum and the g factor has a minimum value close to 2. Therefore the g factor oscillates with the change of N_s.

This oscillatory g factor has been calculated in the so-called screened Hartree-Fock approximation (Ando and Uemura, 1974b, 1974c; see also Uemura, 1974a, 1974b). The effective g factor is defined by

$$g^*\mu_b H=g\mu_B H+\Sigma_{N\downarrow}-\Sigma_{N\uparrow}\ . \tag{6.72}$$

Here, we have

$$\Sigma_{N\downarrow}-\Sigma_{N\uparrow}=\sum_q \frac{V(q)}{\varepsilon(q,0)}J_{NN}(lq)^2(n_{N\uparrow}-n_{N\downarrow})\ , \tag{6.73}$$

where $n_{N\sigma}$ is the filling factor of the Landau level (N,σ), which equals one when the level is filled by electrons, $V(q)$ is the Fourier transform of the effective two-dimensional electron-electron interaction given by $V(q)=(2\pi e^2/\bar{\kappa}q)F(q)$ with $F(q)$ being the form factor given by Eq. (2.51), and $\varepsilon(q,0)$ is the static dielectric function. The dielectric function is calculated within the random-phase approximation in strong magnetic fields. Since the difference of the occupations, $n_{N\uparrow}-n_{N\downarrow}$, and the dielectric function depend on the energy separation of the ↑ and ↓ spin levels, one has to determine the splitting self-consistently. An example of the results is shown in Fig. 126. The g factor oscillates with N_s, and peak values increase with increasing magnetic fields. Figure 127 shows the ratio $g^*\mu_B H/\Gamma_N$ when the Fermi level lies midway between ↑ and ↓ spin levels. The points connected by the dashed lines are the values obtained by

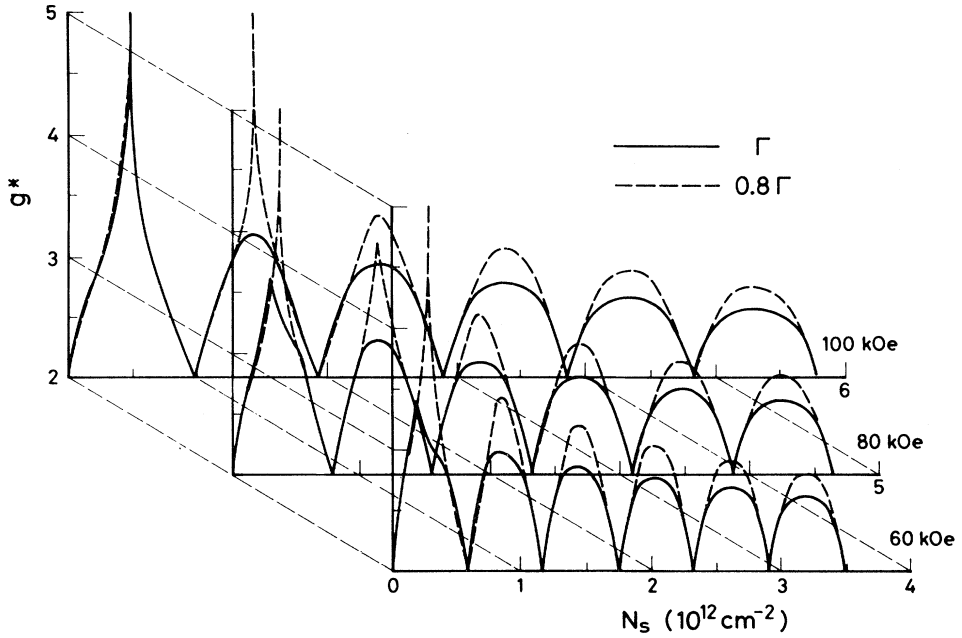

FIG. 126. Calculated oscillatory g factor as a function of the electron concentration in magnetic fields. The solid and broken lines represent the g factor for the level width $\Gamma_N=\Gamma$ and 0.8Γ, respectively. After Ando and Uemura (1974b).

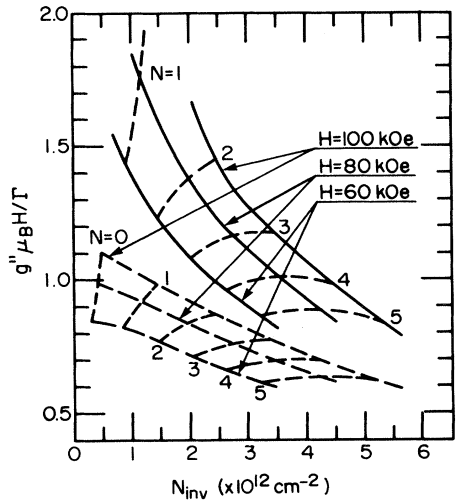

FIG. 127. The ratio of $g^*\mu_B H$, when the Fermi level lies at the middle point between ↑ and ↓ levels, to the level width Γ_N. The points connected by broken lines are the values obtained by neglecting the enhancement of the g factor ($g^*=2$). Those connected by solid lines are obtained by the values for $\Gamma_N=0.8\Gamma$ in Fig. 126. After Ando and Uemura (1974b, 1974c).

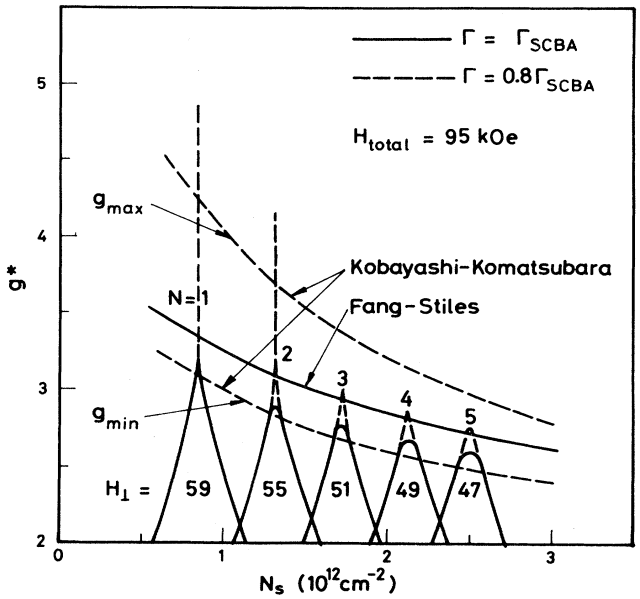

FIG. 128. Oscillatory g factor under tilted magnetic fields versus electron concentration $N_{\rm inv}$. $H_{\rm total}$ is 95 kOe. $H_\perp$ (component perpendicular to the surface) is shown in the figure. The solid and broken lines represent the g factor for $\Gamma_N=\Gamma$ and $\Gamma_N=0.8\Gamma$, respectively. The upper ($g_{\rm max}$) and lower bounds ($g_{\rm min}$) obtained by Kobayashi and Komatsubara (1974) and the value obtained by Fang and Stiles (1968) are also shown.

neglecting the enhancement of the g factor. The points connected by the solid lines are obtained by the enhanced g factor (g^*). When this ratio is larger than a certain critical value, $(g^*\mu_B H/\Gamma_N)_c$, the spin splitting can be resolved in the line shape of σ_{xx}. Although the critical value depends on the actual form of the energy dependence of σ_{xx}, it is reasonable to assume that $(g^*\mu_B H/\Gamma_N)_c \sim 1$. Therefore the theory predicts that the spin splitting should be seen in levels with $N<2$ in accordance with the experimental results.

Because of such oscillatory behavior of g^*, we cannot determine the value of g^* from Eq. (6.71) even if we know the tilt angle θ. Kobayashi and Komatsubara (1974) performed a tilted magnetic field experiment similar to that of Fang and Stiles (1968), and obtained the upper and lower bounds of the actual values of g^*. Since $g_S^* > g_L^*$ we can get $g_{\rm max}$ by putting $g_L^*=2$ and $g_{\rm min}$ by putting $g_L^*=g_S^*$. Their values are given in Fig. 128 together with the results of Fang and Stiles. Calculated values of g^* for the tilted magnetic fields experimentally found are also shown. The calculated g_S^* lies between $g_{\rm min}$ and $g_{\rm max}$ except for low Landau levels $N=0$ and 1, where the sharp cutoff of the density of states calculated in the self-consistent Born approximation causes singular results. One can conclude that the experiments are explained by the enhancement of the g factor rather well.

By further tilting magnetic fields one can bring about a situation in which the levels of $(N,\downarrow)$ and $(N+1,\uparrow)$ coincide with each other and can obtain the g factor. From the above discussion it is clear that the g factor obtained by this coincidence method can give different values of the g factor from that of Fang and Stiles (1968). Kobayashi and Komatsubara (1973; see also Komatsubara *et al.*, 1974) obtained a g factor which was very close to the bulk value of 2. There seemed to be a problem, however, concerning the determination of the tilt angle where the coincidence occurred. Landwehr, Bangert, and von Klitzing (1975) made similar experiments more carefully and showed that the g factor obtained in this coincidence method was also enhanced. The same result was obtained recently by Englert (1981). Theoretical calculation for such a large tilt angle has not yet been done, however.

Lakhani and Stiles (1973) proposed a method to measure g_S^* by considering the minimum value of σ_{xx} between adjacent levels. They assumed that all the quantities except the level separations remain unchanged with the change of H and that the minimum values of σ_{xx} depended only on the energy separation of the two adjacent levels. At a constant total magnetic field they determined the tilt angle where the average of the minimum values for the cases when the Fermi level lies at the midpoint between $(N,\downarrow)$ and $(N,\uparrow)$ levels and the midpoint between $(N,\downarrow)$ and $(N+1,\uparrow)$ levels become the same as the minimum value of σ_{xx} for the case when the Fermi level lies midway between $(N,\uparrow)$ and $(N,\downarrow)$ in the magnetic field perpendicular to the surface. They obtained experimental values of g_S^* using Eq. (6.72) assuming $g_L^*=2$. Although this seemed to be an excellent idea to determine g_S^*, the peak value of the oscillatory g factor, the basic assumption was not correct since the level broadening depends on the normal component of the applied magnetic field and changes with the tilt angle.

Englert and von Klitzing (1978) proposed an ingenious

way to determine g_L^* and g_S^* independently. They measured minimum values of σ_{xx} for different values of H at a fixed $H\cos\theta$. In such a case all the quantities like broadening and Landau-level separations are expected to remain unchanged except the spin splitting. If the densities of states of adjacent levels do not overlap, the conductivity can become nonzero due to thermal excitation of electrons into adjacent levels. Thus the magnetic field dependence of the minimum value of the σ_{xx} is given by

$$(\sigma_{xx})_{\min} \propto \exp\left[\frac{g_L^*\mu_B H}{2k_B T}\right], \tag{6.74}$$

for the case when the Fermi level lies midway between the $(N,\uparrow)$ and $(N+1,\downarrow)$ levels. They have obtained $g_L^*=2$ for $N=1$ and 2. For the case when the Fermi level lies midway between $(N,\uparrow)$ and $(N,\downarrow)$ we expect

$$(\sigma_{xx})_{\min} \propto \exp\left[-\frac{g_S^*\mu_B H}{2k_B T}\right]. \tag{6.75}$$

They obtained $g_S^* \sim 2.6$ for $N=1$. Thus they have shown that the enhancement is really caused by the exchange effect and demonstrated for the first time the oscillation of the g factor as a function of N_s. The actual values of g_S^* obtained are not accurate enough, however, because the overlapping of the densities of states of the two adjacent spin levels is still appreciable. Stronger magnetic fields will be necessary to obtain more accurate values.

At the early stages there was some controversy as to whether the observed enhancement of the spin splitting is a real one or an apparent enhancement originating from the fact that the gate voltage is proportional to the electron concentration rather than the Fermi energy (Narita *et al.*, 1973; Narita and Komatsubara, 1974; Komatsubara *et al.*, 1974; Niederer, 1974). There still seem to exist some controversies on the coincidence method for determining the spin splitting. Köhler and Roos (1979c) have raised the question whether the valley splitting seriously affects the experimental results on the spin splitting. Englert, von Klitzing, Nicholas, and Landwehr (1980; see also Englert, 1981) have argued against it.

So far we have completely disregarded the existence of the valley splitting, which plays an important role in determining the actual line shape of σ_{xx}. As will be shown in Sec. VII.A, the calculated valley splitting is roughly proportional to N_s, in contrast to the experimental results which seem to indicate that it decreases with increasing N_s. The valley splitting is enhanced in the same manner as the spin splitting by the exchange effect (Ando and Uemura 1974b), and the enhancement is much more important than for the spin splitting. Ohkawa and Uemura (1976, 1977c) took into account this enhancement in the screened Hartree-Fock approximation, using the value of the bare valley splitting calculated by them. They assumed short-range scatterers and a Gaussian form of the density of states, and calculated the line shape of σ_{xx}. An example of the results is given in Fig. 129. Characteristics of the degree of the splitting observed experimentally are qualitatively reproduced if we use widths slightly smaller than those obtained from Eq. (6.19) with the experimental mobilities. Although the assumption of short-range scatterers for the full N_s range is not realistic, one can conclude that the theory explains the experiments quite well. A complete line-

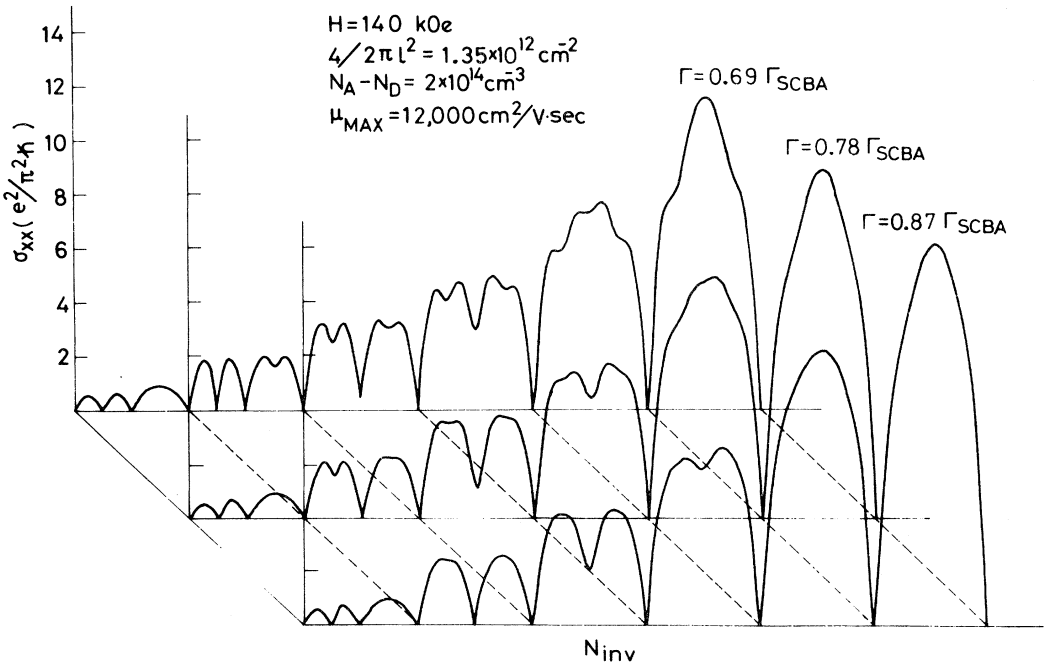

FIG. 129. Calculated transverse magnetoconductivity for several level widths as a function of electron concentration (N_{inv}). The valley and spin splittings are resolved in the lower Landau levels. "Cusps" can be seen in the Landau level $N=4$. Γ and Γ_{SCBA} in the figure correspond to Γ_N and Γ, respectively, in the text. After Ohkawa and Uemura (1976, 1977c).

shape analysis requires the self-consistent determination of the broadening and screening and proper treatment of the localization effect, in addition to the enhancement of the spin and valley splittings. Such analysis is extremely difficult, even if we know the precise nature of scatterers in this system. A more detailed discussion of the valley splitting is given in Sec. VII.A.

C. Cyclotron resonance

A brief discussion of the theory of the dynamical conductivity of a two-dimensional electron-impurity system in strong magnetic fields has been given in Sec. VI.A.2. This section deals with various problems related to cyclotron resonance in actual inversion layers.

1. Characteristics of the cyclotron resonance

Cyclotron resonance was observed for the first time in an n-channel inversion layer on the silicon (100) surface by Abstreiter, Kneschaurek, Kotthaus, and Koch (1974) and by Allen, Tsui, and Dalton (1974) independently. The quantum oscillation predicted theoretically (Ando and Uemura, 1974d; Ando, 1975a) was first observed by Abstreiter, Kotthaus, Koch, and Dorda (1976b). An example of their results is shown in Fig. 130. The magnetic fields where the Fermi level lies just at the midpoint between adjacent Landau levels are denoted by black triangles. One sees clearly that the absorption has a dip at the low magnetic field side, i.e., below $H \sim 60$ kOe, and a peak at the high magnetic field side, in agreement with the theoretical prediction. An example of corresponding theoretical line shapes is also shown. One sees the position of the quantum oscillation is in excellent agreement with the theory, although the theoretical line shape shows slightly larger amplitude. This disagreement concerning the amplitude of the quantum oscillation cannot be explained by a possible difference of the real part of $\sigma_{xx}(\omega)$ and the transmission coefficient, which was mentioned in Sec. VI.A.2. There are many possible reasons for the disagreement. The self-consistent Born approximation used in the theoretical calculation is the simplest approximation. If one considers higher-order effects, the density of states has low- and high-energy tails, where the broadening is expected to be inhomogeneous. Therefore the energy region where our simple approximation holds becomes effectively narrower, and consequently the amplitude of the quantum oscillation becomes smaller. Further, the short-range scatterer model is not strictly applicable, and the quantum oscillation decreases with increasing range of scattering potentials. Sample inhomogeneity, if present, could make the amplitude smaller. In any case one can conclude that the agreement is satisfactory.

Abstreiter, Kotthaus, Koch, and Dorda (1976b) obtained the width of the cyclotron resonance by fitting their results to a classical Lorentzian line shape and compared it with the relaxation time at $H=0$. The result is shown in Fig. 131. The width of the cyclotron

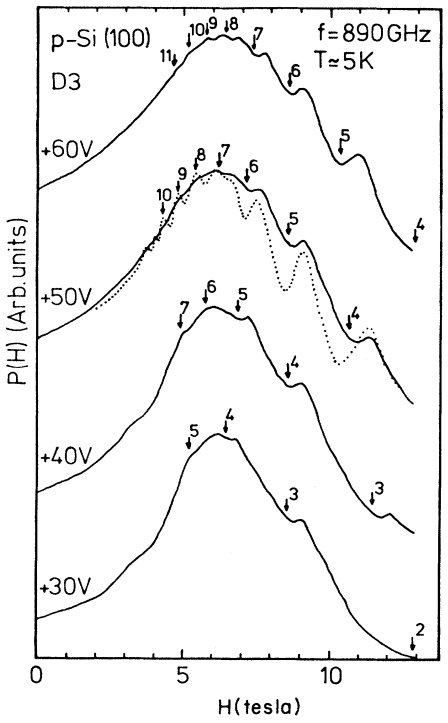

FIG. 130. Examples of cylotron resonances observed in an n-channel inversion layer on a Si(100) surface. $\hbar\omega = 3.68$ meV. $T = 5$ K. The magnetic fields where the Fermi level lies at the center of each Landau level are denoted by downward pointing arrows with corresponding Landau-level indices. The dotted line represents a theoretical prediction by Ando (1975a). The electron concentration is proportional to the gate voltage and is given approximately by 0.9×10^{12} cm^{-2} at 10 V. After Abstreiter *et al.* (1976b).

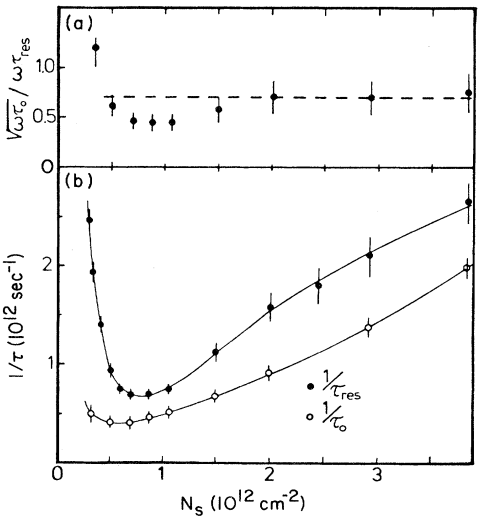

FIG. 131. Comparison of the zero-field scattering rate $1/\tau_0$ with the scattering rate at resonance $1/\tau_{res}$. The dashed line in (a) (~ 0.65) is the value predicted for short-range scatterers in the self-consistent Born approximation. Here, τ_0 corresponds to τ_f in the text. After Abstreiter *et al.* (1976b).

resonance is larger than the level broadening $\hbar/\tau_f$ at $H=0$, which is consistent with the theoretical prediction. In the upper part of the figure the ratio of the cyclotron width to the square root of $\hbar/\tau_f$ is plotted. Theoretically this ratio should be constant and is given by the broken line if scatterers are of short range and the same both at nonzero H and $H=0$. At high concentrations ($N_s > 1.5\times10^{12}$ cm^{-2}) the agreement is satisfactory. Near the electron concentration where the relaxation time has a peak, the actual width becomes smaller than the result for short-range scatterers. This suggests that actual scatterers are different from complete short-range scatterers. At very low concentrations ($N_s < 0.5\times10^{12}$ cm^{-2}) the cyclotron width becomes very large because of the inhomogeneous broadening. Abstreiter, Koch, Goy, and Couder (1976a) studied the frequency dependence of the cyclotron resonance line shape. At high N_s the experimental results were consistent with the $H^{1/2}$ dependence predicted theoretically, but they found a significant deviation from the $H^{1/2}$ dependence at low N_s, i.e., the width became almost independent of H. Wagner, Kennedy, McCombe, and Tsui (1980; see also Kennedy *et al.*, 1975a) performed a much more extensive study of the frequency dependence of the cyclotron resonance line shape for wider ranges of external frequencies. The $H^{1/2}$ dependence was found for high densities ($N_s > 1\times10^{12}$ cm^{-2}) and high fields, in agreement with the theoretical prediction. Again very little dependence on magnetic field was found at low electron concentrations. In order to explain those detailed results we need accurate knowledge of the nature of scatterers and theoretical calculation of the actual line shape for realistic scatterers. This is a very difficult task, however. Experiments with controlled concentrations of scatterers like Na^+ ions, performed quite recently (Chang and Koch, 1981), can give important information on the broadening.

Another interesting feature of the cyclotron resonance line shape in the two-dimensional system predicted theoretically (Ando, 1975a) is the appearance of the subharmonic structure. The subharmonic structure was experimentally observed by Kotthaus, Abstreiter, and Koch (1974a; see also Abstreiter *et al.*, 1976b). An example of their results is shown in Fig. 132, where the absorption derivative is plotted against H. The existence of such structure can be seen in Fig. 131, although the structure is very small. The actual position of the subharmonics is, however, shifted to the higher magnetic field side. This shift has been explained by the mass enhancement effect due to electron-electron interactions (Ando, 1976e).

Kohn (1961) has proved that the position of the cyclotron resonance is not affected by electron-electron interactions in homogeneous systems (Kohn's theorem). Although Kohn's proof is restricted only to short-range mutual interactions, the theorem is a consequence of the fact that electron-electron interactions are an internal force. In inversion layers, the presence of scatterers violates the translational invariance of the system and the theorem is actually not applicable. It suggests, however, that one should make a careful and consistent approximation in calculating dynamical conductivities which include effects of electron-electron interactions. In calculating the dynamical conductivity, one must consider an important correction called the vertex correction, which cancels the mass enhancement effect completely if applied to a homogeneous system. Landau's Fermi-liquid theory is an example of such methods, but is not adequate for the discussion of the subharmonic structure, which is a direct consequence of the complete quantization of the orbital motion.

Ando (1976e) considered a model two-dimensional system in which electrons are interacting with each other via a weak short-range potential. Within the simplest approximation (essentially Hartree-Fock) we can calculate the mass enhancement and the dynamical conductivity consistently. The resulting dynamical conductivity is given by

$$\sigma_{\pm}(\omega)=\tilde{\sigma}_{\pm}(\omega)\left[1+i\omega\left[\frac{m^*}{m}-1\right]\frac{m}{N_s e^2}\tilde{\sigma}_{\pm}(\omega)\right]^{-1}, \tag{6.76}$$

where m and m^* are the bare and dressed masses, respectively, $+$ ($-$) denotes the left (right) circularly polarized wave, and $\tilde{\sigma}_{\pm}$ is the conductivity of a noninteracting system characterized by the dressed mass m^*. If we substitute a simple classical Lorentzian line shape in the above expression we immediately see that the resonance position is determined by the bare mass m. If the line shape is quite different from the Lorentzian, however, the peak

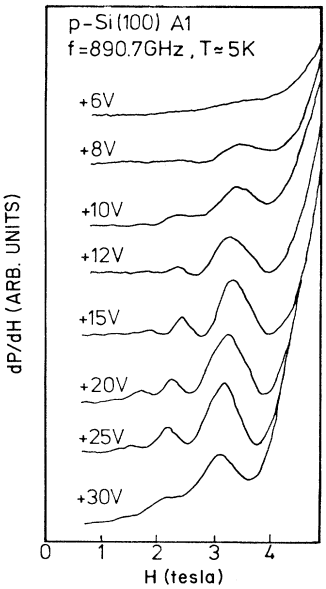

FIG. 132. Subharmonic structure in the absorption derivative for different gate voltages. $\hbar\omega=3.68$ meV. The electron concentration is roughly proportional to the gate voltage and is 1×10^{12} cm^{-2} at 10 V. The position of the subharmonic structure is shifted to the higher magnetic field side corresponding to the increase of the mass with decreasing electron concentration. After Abstreiter *et al.* (1976b).

position can be shifted. At the tails of the cyclotron resonance $\tilde{\sigma}_{\pm}(\omega)$ is small and can be neglected in the denominator of (6.76). Therefore the subharmonic structure is determined by that of $\tilde{\sigma}_{\pm}(\omega)$, i.e., by the condition that $\omega \sim n\omega_c^*$ (n is an integer larger than 2), where $\omega_c^* = eH/m^*c$. This model of electron-electron interactions is too simple and not directly applicable to actual inversion layers. However, the fact that the subharmonic structure is essentially determined by the dressed mass m^* is true of actual systems. Since the vertex correction is not important at tails, the position of the subharmonic structure is given by the difference of the quasiparticle energies of adjacent Landau levels, i.e., by m^*. Figure 133 shows an example of the line shape calculated in this model together with an experimental result of Abstreiter, Kotthaus, Koch, and Dorda (1976b). The peaks denoted by arrows correspond to the subharmonics. If we assume 8% enhancement of the mass, the position is shifted to the higher magnetic field side and agrees with the experiment. Enhancement of this order is theoretically quite reasonable. Figure 134 gives the comparison of three different experimental masses. The mass determined from the main peak is essentially independent of N_s except for the strange behavior at low N_s, while the masses determined from the temperature dependence of the amplitude of the Shubnikov-de Haas oscillation of static conductivities and from the subharmonics are enhanced and show the same N_s dependence. Thus we can say that the mass enhancement due to electron-electron interactions explains the shift of the subharmonic structure quite well.

Ting, Ying, and Quinn (1976) suggested a similar mechanism of the shift of the subharmonic structure based on a different formalism. We can generally express the dynamical conductivity as

$$\sigma_{\pm}(\omega) = \frac{iN_s e^2/m}{\omega \mp \omega_c + M(\omega)} , \tag{6.77}$$

where $M(\omega)$ is called the memory function (Götze and Wölfle, 1972). If we expand $M(\omega)$ in terms of the strength of scattering we have, to the lowest order in the strength of impurity scattering,

$$M(\omega) = \frac{1}{N_s \omega m} \sum_{\mu} \int dz\, N_i^{(\mu)}(z) \times \sum_{q} |v_q^{(\mu)}(z)|^2 q_x^2 [\varepsilon(q,\omega)^{-1} - \varepsilon(q,0)^{-1}] . \tag{6.78}$$

If such an expansion to the lowest order in the impurity concentration is meaningful, this is the exact expression to this order. In our system, however, the validity of such an expansion is highly doubtful because a self-consistent treatment is essential, as has been discussed in Sec. VI.A. One might be able to use this expression only for looking at the qualitative behavior of the conductivity. It is easy to see that the imaginary part of $M(\omega)$ has a peak near $n\omega_c^*$ due to magnetoplasmon modes (Chiu and Quinn, 1974; see also Horing and Yildiz, 1973, 1976; Horing *et al.*, 1974). Because of the dispersion of magnetoplasmon modes the actual subharmonic structure can be shifted and broadened, depending on what wave vectors q are important in scattering. In the case of short-range scatterers a wide range of q contributes to the structure, and the position of the subharmonic structure is expected to be close to $n\omega_c^*$. A later numerical calculation of the line shape based on this method, however,

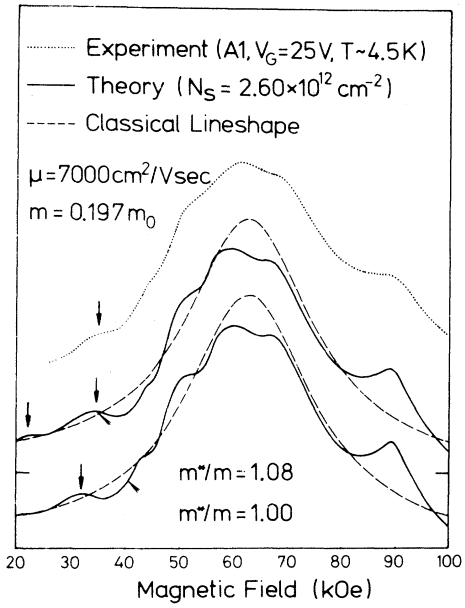

FIG. 133. An example of theoretical and experimental cyclotron resonance line shapes in an n-channel inversion layer on a Si(100) surface. The energy of the incident light is 3.68 meV. The magnetic fields given by $\omega = 2\omega_c^*$ and $\omega = 3\omega_c^*$ are shown by the arrows. After Ando (1976e).

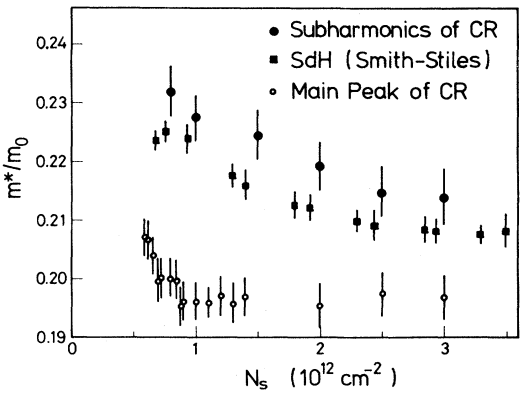

FIG. 134. A comparison of various masses in an n-channel inversion layer on a Si(100) surface. The mass obtained by putting ω equal to $2\omega_c^*$ from the position of the subharmonic structure of the cyclotron resonance (Abstreiter *et al.*, 1976b), the mass measured by Smith and Stiles (1972) under 25.9 kOe, and the mass deduced from the main peak position of the cyclotron resonance (Abstreiter *et al.*, 1976b) are shown. After Ando (1976e).

failed to give a definite subharmonic structure (Ting *et al.*, 1977).

Many-body effects on the cyclotron resonance have also been studied at high temperatures in high magnetic fields (Fukuyama, Kuramoto, and Platzman, 1978; Fukuyama, Platzman, and Anderson, 1978).

2. Cyclotron effective mass

The problem of the cyclotron mass m_c, defined by the position of the main cyclotron resonance, is in much controversy. Kotthaus, Abstreiter, Koch, and Ranvaud (1974b; see also Kotthaus, 1978, 1979, 1980; Abstreiter *et al.*, 1976b) observed an increase of m_c with decreasing N_s at low N_s ($N_s < 0.8\times10^{12}$ cm^{-2}) for the laser frequency $\hbar\omega = 3.68$ meV as is shown in Fig. 135. At still lower N_s ($N_s < 0.4\times10^{12}$ cm^{-2}) m_c decreases very rapidly, depending on the samples. At higher N_s the mass almost has a constant value close to $m_c = 0.198m_0$. This mass value is slightly larger than the bulk conduction-band mass of $m_t = 0.191m_0$, but has been shown to be consistent with the bulk mass for the same laser frequency (Abstreiter *et al.*, 1976b). Abstreiter *et al.* (1976a) studied the frequency dependence of m_c and found no systematic variation outside experimental error for N_s above 0.4×10^{12} cm^{-2}.

The reason for the increasing m_c with decreasing N_s below $N_s < 0.8\times10^{12}$ cm^{-2} is totally unknown. The decrease of m_c at even lower N_s was attributed by Kotthaus *et al.* (1974b) to perturbed cyclotron resonance due to potential fluctuations. When a slowly varying potential fluctuation $V(\mathbf{r})$ exists, the change of the frequency of the cyclotron motion is given by the curvature of the local potential, i.e., by

$$\delta(\hbar\omega_c) \cong \tfrac{1}{2}(l\nabla)^2 V(\mathbf{r}) . \tag{6.79}$$

When electrons occupy the ground Landau level completely, this shift vanishes because the curvature of the potential becomes zero on the average. At low concentrations electrons are considered to be in local potential minima where $\delta(\hbar\omega_c) > 0$, and the effective cyclotron energy becomes larger or m_c decreases. Such a shift should become appreciable roughly below the electron concentration where only the ground Landau level is occupied by electrons. This simple consideration explains the value of N_s where the rapid decrease of m_c occurs. A similar shift of the peak can appear even for short-range scatterers (Ando, 1975a). Mikeska and Schmidt (1975) examined this effect theoretically by assuming an artificial potential fluctuation and showed that the abrupt decrease of m_c observed experimentally could be explained by such a mechanism. A later temperature dependence study gave results consistent with such a model (Küblbeck and Kotthaus, 1975; Kotthaus and Küblbeck, 1976).

Similar experiments at low electron concentrations were also performed by Kennedy, Wagner, McCombe, and Tsui (1977; see also Wagner *et al.*, 1976a, 1976b, 1980; Wagner and Tsui, 1979, 1980). An example of their results is shown in Fig. 136. They found a charac-

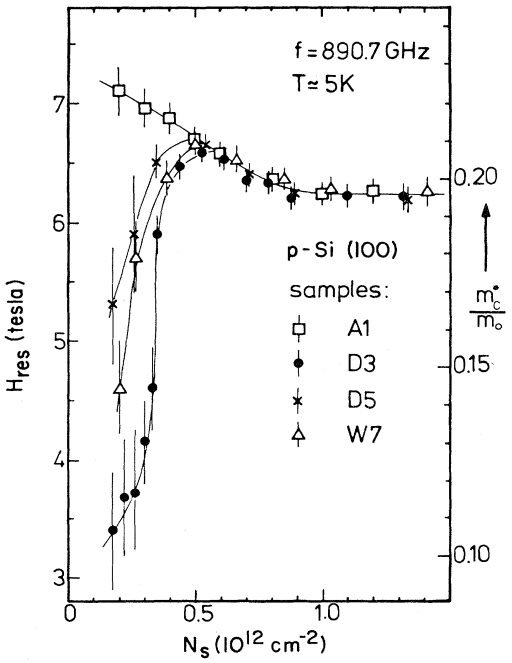

FIG. 135. Resonance magnetic field and cyclotron effective mass versus electron density (n_s) for different samples at relatively low electron concentrations. $\hbar\omega = 3.68$ meV. After Abstreiter *et al.* (1976b).

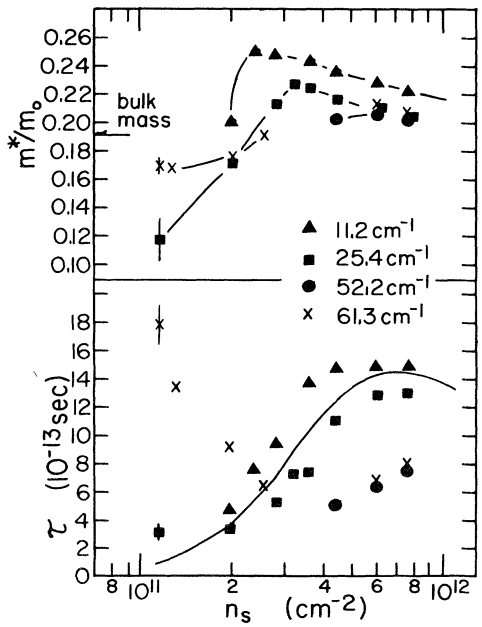

FIG. 136. The density (n_s) dependence of the cyclotron effective mass and scattering time τ at four far-infrared radiation frequencies. The lines connecting the mass data at a particular frequency are drawn as aids to the eye. A dc scattering time derived from the 4.5 K effective mobility and the band mass $m = 0.19m_0$ is shown as a solid line. After Kennedy *et al.* (1977).

teristic N_s dependence similar to that of Kotthaus *et al.* (1974b), but their m_c depended on the photon energy of the laser light, in contrast to the results of Abstreiter *et al.* (1976a). As is seen in the figure, the linewidth becomes narrower with decreasing N_s at $\hbar\omega=7.6$ meV, in contrast to the opposite behavior for lower magnetic fields. They argued that this was inconsistent with the perturbed cyclotron resonance and tried to attribute it to some phase change of the two-dimensional electron gas. Wilson, Allen, and Tsui (1980) measured the cyclotron resonance at low concentrations with the use of a far-infrared spectrometer. This technique enabled a direct observation of the frequency dependence of the conductivity at a fixed magnetic field and electron concentration, when the usual magnetic field sweep at constant frequency is not adequate for investigation of phenomena strongly dependent on the field. Figure 137 gives an example of observed resonances for $\nu=0.43$, with ν being the filling factor of the ground Landau level defined by $\nu=2\pi l^2 N_s$. The broken line shows the expected classical line shape. The peak is shifted to the higher-frequency side and the line shape is narrower than expected from the zero-field mobility. They also showed that the line shape exhibits a peculiar change as a function of the filling factor. As a possible explanation they proposed a highly correlated or crystalline ground state. As a matter of fact, a pinned charge-density-wave model (Fukuyama and Lee, 1978) gives the dotted line, which explains the observed line shape. However, it is not completely certain that the existence of a crystalline ground state is the only explanation for the behavior in the absence of any reliable theory of localization effects for realistic scatterers and that of electron solids in strong magnetic fields. The electron solid will be discussed in Sec. VII.C. A similar narrowing has also been

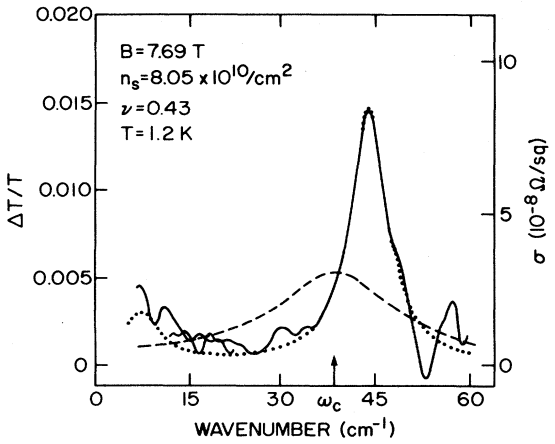

FIG. 137. Cyclotron resonance in the extreme quantum limit. The solid lines represent raw data; the structure is residual noise. The expected classical line shape is shown as a dash line. The dotted line is a theoretical calculation of the frequency response of a pinned charge-density wave with $m=0.21m_0$ and a pinning frequency $\gamma=20.2$ cm^{-1}, following Fukuyama and Lee (1978). The filling factor is 0.43. After Wilson *et al.* (1980).

observed under compressional stress (Stallhoffer *et al.*, 1976; Kotthaus, 1978, 1979).

Kennedy, Wagner, McCombe, and Tsui (1975b, 1976b; see also Wagner *et al.*, 1980) measured the frequency dependence and observed that m_c increased with decreasing frequency except at low concentrations. They showed that m_c was a function of $\omega\tau$ and proposed that this was caused by a reintroduction of electron-electron interactions caused by the presence of strong scattering. To explain this anomalous frequency dependence, Tzoar, Platzman, and Simons (1976) calculated a high-frequency conductivity neglecting the presence of magnetic fields, using the formula (6.77). They defined the mass shift by comparing a high-frequency expansion of the phenomenological expression:

$$\sigma(\omega)=\frac{iN_s e^2}{m^*(\omega+i/\tau)} \tag{6.80}$$

and that of Eq. (6.77). Naturally the calculated mass decreases with increasing frequency because such a correction should vanish in the limit of infinite ω. A similar calculation was also made by Ganguly and Ting (1977). It is not clear, however, that this enhanced mass is related to the actual resonance position. Actually what we need is the dynamical conductivity at $\omega\sim\omega_c$, which corresponds to $\omega=0$ in the absence of a magnetic field in Eq. (6.77) and has nothing to do with the calculated mass shift in the high-frequency limit. Ting, Ying, and Quinn (1977) calculated the dynamical conductivity, substituting $\varepsilon(q,\omega)$ calculated in the random-phase approximation in the presence of magnetic fields. Because the lowest-order expression has a difficulty with divergence, as has been mentioned before, they calculated $\varepsilon(q,\omega)$ in an approximation similar to the self-consistent Born approximation. Figure 138 gives an example of the comparison between observed and calculated line shapes. They obtained a slight enhancement of m_c (around 2%) which is almost independent of the frequency. So far the theories cannot give any definite conclusion on the effects of electron-electron interactions on the cyclotron resonance in this system. This is a very difficult theoretical problem, and further study is needed. More experimental work is also necessary in order to clarify important parameters which cause such differences of experimental results.

Ngai and Reinecke (1976) proposed a new model of localization effects based on localized two-electron states which have been proposed to exist in amorphous SiO_2. Using a very simplified model Hamiltonian, they claimed that the increase of m_c with decreasing N_s below 0.8×10^{12} cm^{-2} could be explained by such a model. This and related models were further investigated (Ngai and White, 1978, 1980; White and Ngai, 1978a, 1978b).

Theis (1978, unpublished) has carefully measured the cyclotron resonance at high N_s and observed an increase of m_c with increasing N_s. This behavior is consistent with the effect of the nonparabolicity of the silicon conduction band. Falicov (1976) calculated the nonparaboli-

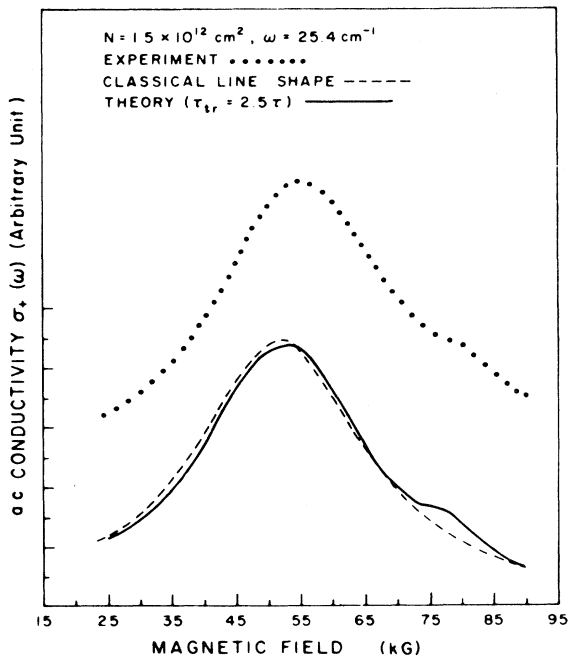

FIG. 138. Calculated and measured cyclotron resonance line shapes for electron concentration (N) of 1.5×10^{12} cm^{-2} and at $\hbar\omega=3.15$ meV. The dotted curve is from Kennedy, Wagner, McCombe, and Tsui (unpublished). After Ting *et al.* (1977).

city effect in an approximation similar to that employed by Falicov and Garcia (1975) in calculating the effective mass in p channels of silicon. He calculated the bulk Fermi surface and then cut it at k_z corresponding to the conduction-band minimum. Although the qualitative behavior of the calculated N_s dependence of m_c seems to agree with the experiments, this method is known to be inadequate in p channels (see Sec. VIII.A). More work is necessary concerning such a nonparabolicity effect.

Küblbeck and Kotthaus (1975; see also Kotthaus and Küblbeck, 1976) measured the cyclotron resonance as a function of temperature. They found a surprising result that m_c increased considerably with temperature. Kennedy, McCombe, Tsui and Wagner (1978) found no such anomalous behavior. Stallhoffer, Kotthaus, and Koch (1976) investigated the cyclotron resonance under uniaxial stress and found an increase of m_c similar to the temperature effect. These strange behaviors are related to the existence of another set of subbands associated with valleys located in differect directions in the silicon Brillouin zone and will be discussed in Sec. VII.B together with more recent experimental results.

3. Plasmon and magnetoplasmon absorption

So far we have discussed a response of the system to homogeneous external fields ($q=0$, where $\mathbf{q}$ is the two-dimensional wave vector in the direction parallel to the surface). A response to an external field with nonzero q's is also observable. Allen, Tsui, and Logan (1977; see also Tsui, Allen, Logan, Kamgar, and Coppersmith, 1978) observed the two-dimensional plasmon in the inversion layer. The two-dimensional plasmon was first observed by Grimes and Adams (1976a, 1976b; see also Grimes, 1978a) in the system of electrons trapped by the image potential on the liquid-helium surface. Allen, Tsui, and Logan made a grating structure on top of a semitransparent gate electrode, as is shown in Fig. 139. When far-infrared light is incident normal to the surface with a polarization parallel to the grating periodicity (say, x direction), the light is longitudinally modulated with the wave vectors $q_n=2\pi n/a$ ($n=1,2,\ldots$),

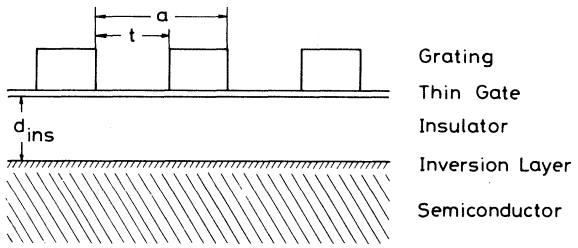

FIG. 139. A schematic illustration of the grating structure for observation of the two-dimensional plasmon in the inversion layer.

$$E_x(x,z)=\sum_{n=0} E_x(q_n,z)\exp(iq_nx-i\omega t)\,, \tag{6.81}$$

where a is the period of the grating. The strength of each component of the electric field can easily be calculated. Roughly speaking, fields with high n become relatively larger with decreasing width t of the semitransparent region of the gate, since the field is concentrated across this part while being essentially zero over the highly conductive part. Such modulation of the field is appreciable within a distance of the order of the grating period a from the gate electrode.

Usually the wavelength of such modulated far-infrared radiation is much larger than the thickness of the inversion layer, and we can still regard the layer as a conducting sheet having the two-dimensional conductivity tensor $\sigma_{\mu\nu}(\mathbf{q},\omega)$, defined by

$$J_\mu(\mathbf{q})\delta(z)\exp(i\mathbf{q}\cdot\mathbf{r}-i\omega t)=\sum_{\nu=x,y}\sigma_{\mu\nu}(\mathbf{q},\omega)\delta(z)E_\nu(\mathbf{q},z)\times\exp(i\mathbf{q}\cdot\mathbf{r}-i\omega t)\,, \tag{6.82}$$

where the sheet is assumed to be at $z=0$. Usually the capacitive reactance of the grid is small compared to the average resistive admittance of the metallization, and we can calculate the response of the inversion layer to such electric fields assuming the conductivity of the gate is infinite. Neglecting the retardation effect (infinite light velocity) and solving Poisson's equation by the image method, we can calculate the induced electric field corresponding to the induced current in the inversion layer. We have for $\mathbf{q}=(q,0)$

$$E_x^{\rm ind}(q,z) = -\frac{4\pi i}{\omega}\frac{q}{\kappa_{\rm sc}+\kappa_{\rm ins}\coth(qd_{\rm ins})} \times \exp(-q\,|\,z\,|\,)J_x(q)\,, \tag{6.83}$$

where $d_{\rm ins}$ is the thickness of the insulator (SiO_2). Therefore we have

$$J_x(q)\exp(iqx-i\omega t)\delta(z) = \tilde{\sigma}_{xx}(q,\omega)E_x(q,z)\delta(z) \times \exp(iqx-i\omega t)\,, \tag{6.84}$$

where

$$\tilde{\sigma}_{xx}(q,\omega) = \sigma_{xx}(q,\omega)\varepsilon(q,\omega)^{-1}\,, \tag{6.85}$$

with

$$\varepsilon(q,\omega) = 1+\frac{4\pi i}{\omega}\frac{q}{\kappa_{\rm sc}+\kappa_{\rm ins}\coth(qd_{\rm ins})}\sigma_{xx}(q,\omega)\,. \tag{6.86}$$

Therefore the absorption is given by

$$P = \tfrac{1}{2}\,{\rm Re}\sigma_{\rm eff}(\omega)\,|\,E_x(q=0,z=0)\,|^2\,, \tag{6.87}$$

with

$$\sigma_{\rm eff}(\omega) = \sum_{n=0}\tilde{\sigma}_{xx}(q_n,\omega)\delta_n\,, \tag{6.88}$$

where

$$|\,E_x(q_n,z=0)\,|^2 = \delta_n\,|\,E_x(q=0,z=0)\,|^2\,. \tag{6.89}$$

Under the experimental conditions the period of the grating is much larger than the length scale, and we can replace $\sigma_{xx}(q,\omega)$ by $\sigma_{xx}(\omega)$. Further, if we substitute the Drude expression $\sigma_{xx}(\omega)=iN_se^2/m\omega$ into (6.85) and (6.86) we have the resonance absorption at the position of the two-dimensional plasmon

$$\omega_p^2 = \frac{4\pi N_s e^2}{m}\frac{q}{\kappa_{\rm sc}+\kappa_{\rm ins}\coth(qd_{\rm ins})}\,, \tag{6.90}$$

with $q=q_n$. See Sec. II.D for some more discussion on the plasmon.

An example of absorption observed by Allen *et al.* (1977) is shown in Fig. 140. We can see the clear absorption due to the excitation of the plasmon ($n=1$) superposed on the Drude background, corresponding to absorption of the spatially unmodulated ($n=0$) component of the radiation field. They analyzed their data using the simple Drude formula of the conductivity (6.80) and determined the mass. They obtained a value close to $0.2m_0$ almost independent of N_s at high N_s, but found an increase of the mass with decreasing N_s at low N_s, a result similar to that observed in the cyclotron resonance (Kotthaus *et al.*, 1974b; Kennedy *et al.*, 1977). Theis, Kotthaus, and Stiles (1978a, 1978b; see also Theis, 1980; Kotthaus, 1980) observed resonances associated with higher n for various energies of far-infrared light. They analyzed their data using a mass value close to $0.2m_0$ independent of N_s and concluded that the theoretical dispersion relation (6.90) explains their results quite well. The plasmon has also been observed in emission experiments (Gornik *et al.*, 1980a).

In the presence of a magnetic field perpendicular to the surface, the plasmon resonance turns into the so-called plasma-shifted cyclotron resonance or magnetoplasmon. If we substitute $\sigma_{xx}(\omega)=iN_se^2\omega/m(\omega^2-\omega_c^2)$ into Eqs. (6.85) and (6.86) we have a resonance at $\omega^2=\omega_c^2+\omega_p^2$. Theis, Kotthaus, and Stiles (1977; see also Theis, 1980) observed such a resonance. An example of their results is given in Fig. 141. A plasma-shifted cyclotron resonance can be seen at the lower magnetic field side of the usual cyclotron resonance, and its position is shifted to lower H with increasing N_s. They found that

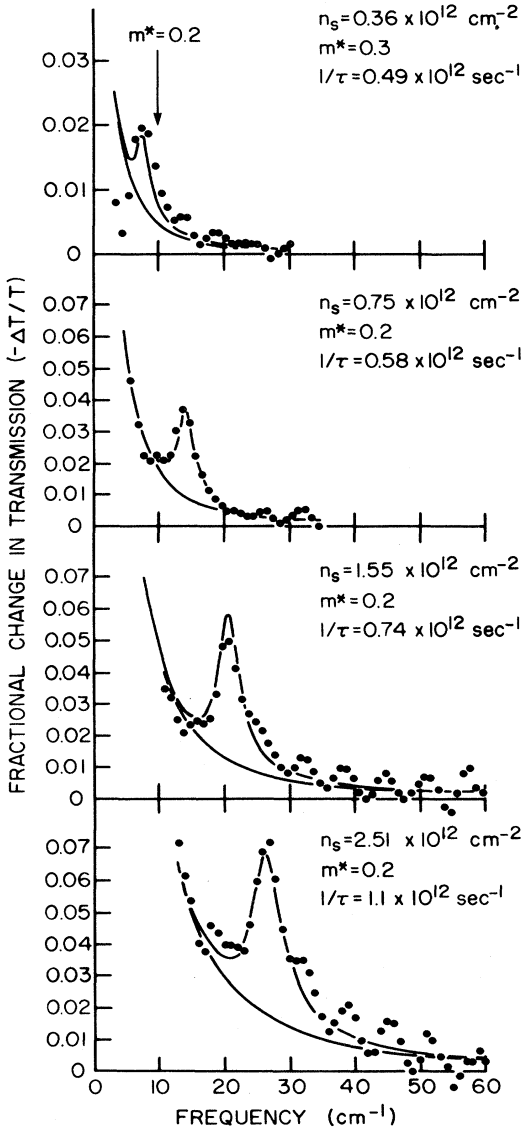

FIG. 140. Fractional change in transmission caused by inversion layer electrons at 1.2 K. Resolution is 1 cm^{-1}. Solid curves are theoretical results with indicated mass and relaxation time. The lower curve is the Drude part and the upper curve contains the plasmon absorption. After Allen *et al.* (1977).

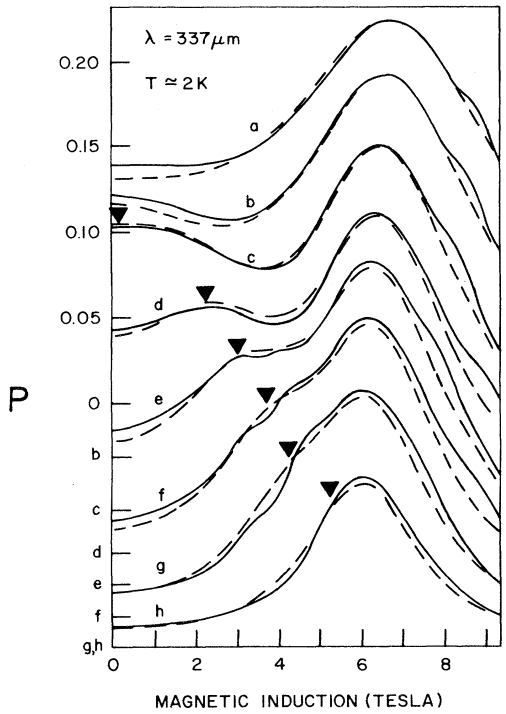

FIG. 141. Absorption as a function of magnetic field for different electron concentrations in an n-channel inversion layer on a Si(100) surface. $\hbar\omega = 3.68$ meV. The numbers in the first row at the bottom represent electron concentration N_s (called n_s in the figure) in units of 10^{12} cm^{-2}. The inverted triangles indicate the expected magnetoplasmon position. The dashed curves have been generated with the use of a classical Lorentzian line shape of the cyclotron resonance. A coupling of the magnetoplasmon with the subharmonic structure can be seen around $H \sim 35$ kOe for $N_s = 2.42 \times 10^{12}$ cm. After Theis *et al.* (1977).

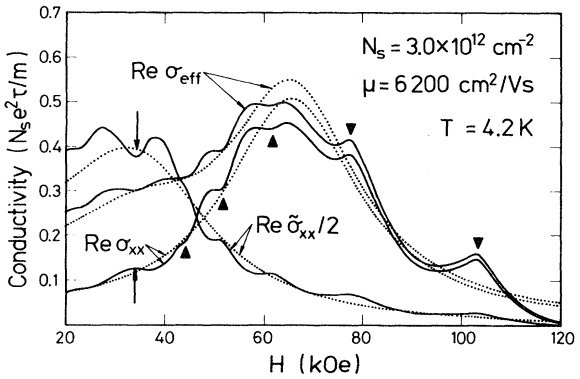

FIG. 142. Calculated dynamical conductivities for $N_s = 3 \times 10^{12}$ cm^{-2} in an n-channel inversion layer on a Si(100) surface as a function of the magnetic field normal to the surface. $\hbar\omega = 3.68$ meV. The solid lines represent the result of the self-consistent Born approximation and the dotted lines the classical. σ_{xx} gives the usual cyclotron resonance, $\tilde{\sigma}_{xx}$ the plasma-shifted cyclotron resonance, and σ_{eff} the total absorption. The positions of the plasma-shifted cyclotron resonance and the subharmonic structure are denoted by the downward and upward pointing arrows, respectively. The other structures denoted by triangles are the quantum oscillation. After Ando (1978d).

the position of the plasma-shifted cyclotron resonance agreed reasonably well with the theoretical prediction based on the simple Drude conductivity. However, they observed additional effects, i.e., a coupling of the plasma-shifted cyclotron resonance with the subharmonic structure when their positions were close to each other, i.e., for $N_s = 1.95$, 2.42, and 2.90×10^{12} cm^{-2} in Fig. 141.

A corresponding theoretical calculation of the magnetoplasmon resonance line shape was performed by Ando (1978d). An example of the results corresponding to the experimental conditions is given in Fig. 142. The position of the plasma-shifted cyclotron resonance is denoted by downward-pointing arrows and the position of the subharmonic structure by upward-pointing arrows. When the two positions are close to each other as shown in the figure, they repel each other, and the two peaks appear in the plasma-shifted cyclotron resonance $\tilde{\sigma}_{xx}(q_1,\omega)$ and also in the total absorption. If we take account of the nonzero value of q (nonlocal effect), the dynamical conductivity $\sigma_{xx}(q,\omega)$ has a resonance structure at $n\omega_c$ ($n > 1$) because of the existence of the magnetoplasmon modes (Chiu and Quinn, 1974). The coupling with such modes has been shown to be negligible under experimental conditions.

The technique of using a grating structure for the gate electrode has made it possible to observe the two-dimensional plasmon and magnetoplasmon. So far, however, we have not been able to get much new information from such observations. As is clear from the above discussion, what we need to explain the experimental observations is a precise knowledge of the local two-dimensional conductivity $\sigma_{xx}(q=0,\omega)$, which might as well be obtained from the more usual transmission-type experiments without a grating structure. Therefore a technique to get much larger wave vectors is highly desirable. At large wave vectors comparable to the Fermi wave vectors or the inverse of the thickness of the inversion layers, a variety of interesting physical effects should become accessible, such as observation of various magnetoplasmon modes (Chiu and Quinn, 1974), effects of exchange and correlation on the plasmon dispersion (Rajagopal, 1977a; Beck and Kumar, 1976), and mixing of plasmon and intersubband resonances (Dahl and Sham, 1977; Eguiluz and Maradudin, 1978a, 1978b). Attempts in this direction have been made already (Theis, 1980), and we may expect to see much more work on inversion layer plasmons in the next few years.

D. Electron localization in strong magnetic fields

It has long been known that states are localized near the edges of low-lying Landau levels in strong magnetic fields. This fact can clearly be seen even in the first experiments of Fowler, Fang, Howard, and Stiles (1966a, 1966b), where the conductance is very small for a considerable range of gate voltages between the peaks for dif-

ferent spin- and valley-split levels. This problem was left untouched for a long while and then received considerable theoretical and experimental attention. Various experimental results and corresponding theoretical models (sometimes rather speculative) have been reported.

Kawaji and Wakabayashi (1976; see also Kawaji, 1978) made a careful study of the transverse conductivity σ_{xx} in strong magnetic fields and observed the vanishing of σ_{xx} in several finite regions of N_s, indicating the existence of localized electrons at the edges of Landau levels. They have shown that the concentration of localized electrons associated with the tail of the Nth Landau levels is approximately given by $[(2N+1)2\pi l^2]^{-1}$, as is shown in Fig. 143. This roughly means that the electron wave functions become extended when the cyclotron orbit covers the whole space. They suggested as a possible explanation a two-dimensional Wigner crystal pinned by random potential fluctuations. In this model, only electrons in the Landau level where the Fermi level lies are supposed to form an electron crystal, and it becomes unstable when the condition $[(2N+1)2\pi l^2]^{-1} \sim 1$ is satisfied. This interesting experimental result has provoked various theoretical investigations.

The possibility of two-dimensional Wigner crystallization, with and without strong magnetic fields, has been studied theoretically by a number of authors. Tsukada (1976a, 1977a, 1977b) investigated the properties of the electron crystal in strong magnetic fields, extending the theory of Platzman and Fukuyama (1974) in the absence of a magnetic field. He showed that the N dependence and H dependence of the concentration of localized electrons could be similar to that obtained in the experiments of Kawaji and Wakabayashi (1976) discussed above. To explain the actual experimental values he had to assume large potential fluctuations, which he did only to stablize the Wigner crystal. In the presence of large potential fluctuations we must consider effects of the Anderson localization, however, There have been various theoretical estimates of critical concentrations in the case when electrons occupy only the ground Landau level, as will be discussed in Sec. VII.C. The results show essentially that the critical electron concentration increases with the strength of a magentic field roughly in proportion to H. However, if we consider the fact that Platzman and Fukuyama's (1974) criterion for classical electrons in the absence of a magnetic field is different by a factor of about 50 from the results of various more recent numerical experiments, those considerations can predict only qualitative behaviors. The possibility of a charge-density wave ground state originating from the mutual Coulomb interaction has been discussed also (Fukuyama, Platzman, and Anderson, 1978, 1979; Fukuyama, 1979; Kuramoto, 1978a, 1978b; Kawabata, 1978; Yoshioka and Fukuyama, 1979, 1980, 1981a, 1981b). A more detailed discussion on the electron solid in the two-dimensional system is given in Sec. VII.C.

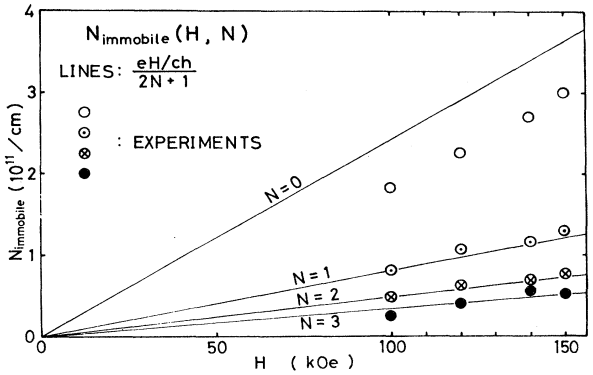

FIG. 143. Concentration of immobile electrons vs magnetic field for different Landau-level indices N observed by Kawaji and Wakabayashi (1976). The straight lines give $[2\pi l^2(2N+1)]^{-1}$.

Another possible explanation of the observed localization is the Anderson localization due to large potential fluctuations analogous to that in the absence of a magnetic field. Tsukada (1976b) assumed slowly varying potential fluctuations and calculated the density of states in the tail region of Landau levels. In the case of slowly varying potentials the center of the cyclotron motion moves according to Eq. (6.37), and the percolation of such loop orbitals around potential minima determines the delocalization of electrons. Assuming simplified circular orbits, Tsukada obtained a condition for the localization which was very close to the experimental results for the ground Landau level. For higher Landau levels such a calculation does not predict the observed N dependence, however. In actual inversion layers it is not certain whether the slowly varying limit is applicable or not, because different kinds of scatterers can contribute to scattering and because the short-range scatterer model works relatively well, as has been discussed in previous sections.

Aoki and Kamimura (1977) proposed a condition for the localization by a heuristic argument corresponding to the Ioffe–Regel condition $k_F l \sim 1$ where l is the mean free path (see, for example, Mott and Davis, 1979). Their argument is not so convincing, but leads to the existence of a minimum metallic conductivity independent of the Landau-level index. Assuming a value for the minimum metallic conductivity and using the result of σ_{xx} in the self-consistent Born approximation, they derived an expression for the concentration of localized electrons similar to the experimental results. Aoki (1977, 1978b) made a numerical study of localization in strong magnetic fields. He considered a finite system with random short-range scatterers, and calculated the density of states and electron wave functions for the ground Landau level. The results demonstrated the localization of electronic states at the tail region in agreement with a simple intuitive picture. He calculated the dynamical conductivity and showed that the conductivity became much smaller than the result of the single-site approximation when the Fermi level was in the tail region (Aoki, 1978b). The calculation was extended to the $N=1$ Landau level and showed that the region of the energy corresponding to localized states became narrower than for

$N=0$. However the calculation was not accurate enough to conclude whether this was consistent with the minimum metallic conductivity independent of N, as had been proposed by Aoki and Kamimura (1977).

Wigner crystallization and Anderson localization correspond to the two extreme limiting cases of strong electron-electron interactions and large potential fluctuations, respectively. In actual inversion layers we expect that both random potential fluctuations and electron-electron interactions are important. The interplay of the two mechanisms is one of the most difficult theoretical problems. Aoki (1978a, 1979) tried to study this problem numerically. He considered a finite system confined within a square, and calculated electronic states in the Hartree-Fock approximation in the presence of both electron-electron interactions and short-range scatterers. His calculation demonstrated the change of the electronic states from the Wigner crystal to the Anderson localization with the change of their relative strengths. In the intermediate cases the system can be regarded as a Wigner glass. Although the results look very beautiful, we could hardly say that we understand this difficult problem, since the system size is too small and we can not neglect important edge effects.

Kawaji and Wakabayashi (1977; see also Kawaji, 1978) measured the activation-type temperature dependence of the transverse conductivity when the Fermi level lies in the low-energy part of the lowest Landau level. The temperature dependence was shown to be given by a sum of two activated conductivities and to be different from the characteristic behavior of the Anderson localization:

$$\sigma_{xx}=\sigma_{\min}\exp\left[-\frac{W}{k_BT}\right], \tag{6.91}$$

where W is the energy separation between the mobility edge and the Fermi level (see, for example, Mott and Davis, 1979). They suggested that the temperature dependence might be explained by a quantum diffusion of Schottky defects in the Wigner crystal. Kawaji, Wakabayashi, Namiki, and Kusuda (1978) found that the temperature dependence was strongly sample-dependent. They showed that in samples with low mobilities, Eq. (6.91) was consistent with their results, and they obtained a minimum metallic conductivity which slightly depended on the strength of the magnetic field.

Nicholas, Stradling, and Tidey (1977) measured the temperature dependence of minimum values of σ_{xx} for different H. They showed that the existence of the mobility edge and the minimum metallic conductivity explained the behavior at sufficiently low temperatures. They obtained values of minimum metallic conductivity which are about the same as the minimum metallic conductivity in the absence of a magnetic field for the ground Landau level, but are one order of magnitude smaller for higher Landau levels. Similar experiments were extended to stronger magnetic fields and different samples, and values of minimum metallic conductivity strongly dependent on the samples were obtained (Nicholas *et al.*, 1978; see also, Nicholas, 1979). The existence of sample dependence of the minimum metallic conductivity is analogous to that in the absence of a magnetic field (see Sec. V.A), and its origin is not well understood. Nicholas *et al.* suggested that the electron concentration corresponding to the mobility edge was rather independent of the strength of the magnetic field, in contrast to the result of Kawaji and Wakabayashi (1976). This is inconsistent with the Wigner crystal and possibly favors Anderson localization. Work has been extended to lower temperatures (Nicholas *et al.*, 1979; Nicholas, Kress-Rogers, Kuchar, Pepper, Portal, and Stradling, 1980). At extremely low temperatures the dependence of σ_{xx} on the temperature is shown to deviate from Eq. (6.91) and obey

$$\sigma_{xx}\sim\sigma_0\exp\left[-\frac{B}{T^{1/3}}\right]. \tag{6.92}$$

This suggests that so-called variable-range hopping (see, for example, Mott and Davis, 1979) is a dominant conduction process.

Similar experiments were performed by Pepper (1978b) for the ground Landau level. He obtained results which were similar to those obtained by him in the absence of a magnetic field. Some samples show the beautiful characteristic behavior (6.91) for the constant minimum metallic conductivity and others do not. He could control such behavior by either applying substrate bias or changing the surface conditions. The resulting value of the minimum metallic conductivity for the ground Landau level was close to those found in other work.

Tsui (1977) extended magnetoconductivity measurements up to 220 kOe and found new fine structures resulting from localized electrons at the high-energy side of each Landau level. Those structures were very sensitive to applied source-drain electric field and disappeared for large fields.

At low concentrations, especially where only the lowest Landau level is occupied by electrons, the cyclotron resonance has been known to exhibit a peculiar behavior, as has been discussed in Sec. VI.C. The line narrowing and shifts of the peak have been linked to the existence of a highly correlated or crystalline ground state.

We have given a rough sketch of recent investigations on localization in strong magnetic fields. The present understanding of the problem is very poor, especially theoretically, and much more work is necessary in order to clarify the situation. As discussed in Sec. VI.B, the Hall conductivity has been shown experimentally to be independent of N_s in the region where σ_{xx} vanishes and given by an integer multiple of $e^2/2\pi\hbar$. This experimental result and subsequent theoretical study (Aoki and Ando, 1981) have shown that all the states in a Landau level cannot be localized in the strong-field limit. This shows that the theory of Abrahams, Anderson, Licciardello, and Ramakrishnan (1979; see V.B above) does not apply to two-dimensional systems in strong magnetic fields.

VII. OTHER ELECTRONIC STRUCTURE PROBLEMS

A. Valley splittings—beyond the effective-mass approximation

As has frequently been mentioned, the ground subband in an n-channel inversion layer on the Si(100) surface is formed from states associated with two conduction valleys located near X points in opposite $\langle 100 \rangle$ directions in the Brillouin zone. It has long been known that this valley degeneracy predicted in the effective-mass approximation is lifted in actual inversion layers, as observed in the experiments of Fowler, Fang, Howard, and Stiles (1966a, 1966b). Usually the valley splitting is observed in the Shubnikov—de Haas oscillation in strong magnetic fields and at relatively low electron concentrations, as has been discussed in Sec. VI.B. Only relatively recently have extensive investigations been performed on these interesting old phenomena. A valley splitting has been observed also on the (111) surface (Englert, Tsui, and Landwehr, 1980; see also Landwehr, 1980). The valley splitting attracted further attention in connection with observation of minigaps in the electron dispersion relation in inversion layers on Si surfaces slightly tilted from the (100). The minigaps on tilted surfaces are considered to arise from the valley splitting. However, their actual magnitudes are much larger than those predicted by straightforward extension of the mechanisms of the splitting on the exact (100) surface and remain to be understood in the future. In this section we discuss the valley splitting and related phenomena. Various mechanisms proposed theoretically and their mutual relations are briefly discussed first, and experimental attempts to determine values of the valley splitting are summarized and results are compared with theoretical predictions. Minigaps on tilted surfaces and related topics are discussed also.

1. Mechanisms of valley splittings

a. Ohkawa-Uemura theory—electric breakthrough

The problem of valley splittings in donor states of semiconductors with multivalley structure like Si and Ge was left controversial and unsolved after the formulation of the effective-mass theory (Luttinger and Kohn, 1955) and its success in explaining their excited states (Kohn and Luttinger, 1955). Many attempts have been made to explain the binding energy of the split levels originally degenerate in the effective-mass theory. However, none of them has been conclusive. Especially the so-called multivalley effective-mass theory formulated by Twose (see Appendix of Fritzsche, 1962) and its analogs have been widely used and seemed to give values of valley splittings in reasonable agreement with experiments on donors in Si and Ge. The multivalley effective-mass theory was criticized and shown to be inconsistent by a number of authors independently (see, e.g., Ohkawa, 1979a; Pantelides, 1979, and references therein). The multivalley effective-mass equation, if treated correctly, should give identical vanishing of the splitting, and various nonzero values of the valley splittings calculated based on it are incorrect. The first theoretical attempt to obtain the valley splitting in the inversion layer was made by Narita and Yamada (1974). Their method contains an inconsistency similar to that appearing in the multivalley effective-mass theory and gives an expression which depends on the choice of the energy origin. They obtained a relatively large value of the splitting which is proportional to an applied electric field. However, this result seems to originate from an artificially chosen extremely large value of the potential energy at the Si-SiO_2 interface.

Ohkawa and Uemura (1976, 1977a, 1977b) calculated the valley splitting on the Si(100) based on a naive generalization of the effective-mass formulation of Luttinger and Kohn. They constructed a $\mathbf{k}\cdot\mathbf{p}$ effective Hamiltonian which describes the lowest conduction band for $k_2=k_3=0$, where k_2 and k_3 are [010] and [001] components of the wave vector. Cardona and Pollak (1966) obtained the energy bands across the entire zone by diagonalizing a 15×15 $\mathbf{k}\cdot\mathbf{p}$ Hamiltonian. The 15 states used correspond to free-electron states having wave vectors $\langle 000 \rangle$, $\langle 111 \rangle$, and $\langle 200 \rangle$ in a unit of $2\pi/a$, with a being the lattice constant given by 5.43 Å. The calculated energy bands of silicon in the $\langle 111 \rangle$ and $\langle 100 \rangle$ directions are shown in Fig. 144. Three bands of Δ_1 symmetry, which include the lowest conduction band Δ_1^{lc}, are obtained from the 3×3 matrix,

$$\begin{bmatrix} E(\Gamma_1^u)+\frac{\hbar^2}{2m_0}k_1^2 & \frac{\hbar^2}{2m_0}Tk_1 & 0 \\ \frac{\hbar^2}{2m_0}Tk_1 & E(\Gamma_{15})+\frac{\hbar^2}{2m_0}k_1^2 & \frac{\hbar^2}{2m_0}T'k_1 \\ 0 & \frac{\hbar^2}{2m_0}T'k_1 & E(\Gamma_1^l)+\frac{\hbar^2}{2m_0}k_1^2 \end{bmatrix}, \tag{7.1}$$

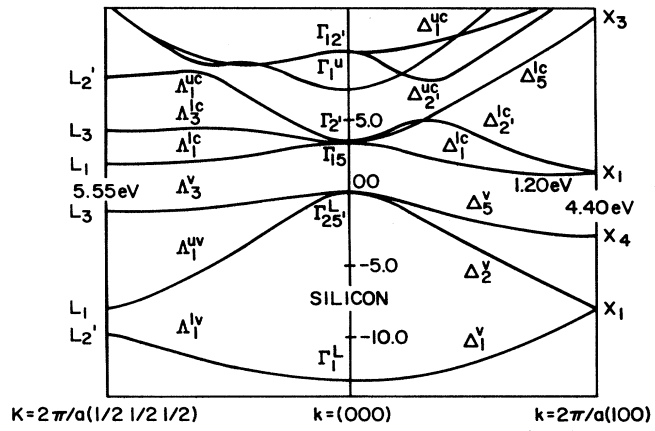

FIG. 144. Energy bands of silicon in the [111] and [100] directions of $\mathbf{k}$ space calculated in the $\mathbf{k}\cdot\mathbf{p}$ method by Cardona and Pollak (1966).

where m_0 is the free-electron mass, k_1 is the [100] component, and $E(\Gamma_{15})$, $E(\Gamma_1^u)$, and $E(\Gamma_1^l)$ are the energies of the corresponding bands at the Γ point. Ohkawa and Uemura have reduced (7.1) to the following 2×2 matrix by treating Γ_1^l perturbationally:

$$\mathscr{H}(k_1)=\begin{bmatrix} E(\Gamma_1^u)+\frac{\hbar^2}{2m_0}k_1^2 & \frac{\hbar^2}{2m_0}Tk_1 \\ \frac{\hbar^2}{2m_0}Tk_1 & E(\Gamma_{15})+\frac{\hbar^2}{2m_0}(1+S)k_1^2 \end{bmatrix}, \tag{7.2}$$

with

$$S=\frac{\hbar^2T'^2}{2m_0}\frac{1}{E(\Gamma_{15})-E(\Gamma_1^l)}. \tag{7.3}$$

If we use $E(\Gamma_1^u)-E(\Gamma_{15})=0.268$ Ry, $T=1.080$ atomic units (a.u.), and $S=0.041$, the two conduction-band minima are at $k_1=\pm k_0$ with $k_0=0.84(2\pi/a)$, which is very close to the known value of $k_0=0.85(2\pi/a)$. The effective mass at the minima is given by $m_l=1.035m_0$ in contrast to the known value of $0.916m_0$. These minor insufficiencies cause no serious errors. The bands do not have zero slope at an X point on the Brillouin-zone boundary. This degeneracy is called "sticking together" and is characteristic of the diamond structure. Because of this fact one can partly include effects of the $\Delta_{2'}$ band just above the lowest conduction band by extending (7.2) to the second Brillouin zone, i.e., one uses (7.2) also for $-4\pi/a<k_1<4\pi/a$. In the presence of an external potential the effective-mass equation is shown to be given by

$$\mathscr{H}(k_z)\mathbf{A}(k_z)+\frac{1}{2\pi}\int_{-4\pi/a}^{4\pi/a}dk_z'\,V(k_z-k_z')\mathbf{A}(k_z') =\varepsilon\mathbf{A}(k_z)\mathbf{A}(k_z), \tag{7.4}$$

where $\mathbf{A}(k_z)$ is a two-component envelope wave function and $V(k_z-k_z')$ is the Fourier transform of the external potential $V(z)$. The above is approximately transformed into a usual effective-mass equation in real space,

$$\mathscr{H}\left(\frac{1}{i}\frac{\partial}{\partial z}\right)\mathbf{F}(z)+V(z)\mathbf{F}(z)=\varepsilon\mathbf{F}(z), \tag{7.5}$$

with

$$\mathbf{F}(z)=\frac{1}{2\pi}\int_{-\infty}^{+\infty}dk_z\mathbf{A}(k_z)e^{ik_2z}. \tag{7.6}$$

Ohkawa and Uemura expanded the envelope function as

$$\mathbf{F}(z)=\sum_{n=0}\sum_{\pm}\begin{bmatrix}C_n^{(\pm)}\\ D_n^{(\pm)}\end{bmatrix}\left[\frac{b^3}{(n+1)(n+2)}\right]^{1/2} \times zL_n^2(bz)\exp(-\tfrac{1}{2}bz\pm ik_0z), \tag{7.7}$$

where

$$b^3=\frac{48\pi m_le^2}{\kappa_{sc}\hbar^2}(N_s+\tfrac{11}{32}N_{depl}), \tag{7.8}$$

and $L_n^\alpha(x)$ is the associated Laguerre polynomial. The term $n=0$ is the same as the usual variational wave function (3.25). Instead of determining $V(z)$ self-consistently they used the Hartree potential corresponding to the electron density distribution given by Eq. (3.25). The valley splitting was calculated variationally by a numerical diagonalization of a large matrix given by truncating the sum over n in Eq. (7.7) at $n=9$. The resulting valley splitting is shown in Fig. 145 and is expressed approximately by

$$\Delta E_v\sim0.15\times\frac{N_s+\frac{32}{11}N_{depl}}{10^{12}\text{ cm}^{-2}}\text{ meV}. \tag{7.9}$$

Since the above expression is essentially proportional to the effective electric field an electron feels, this mechanism has been called the electric breakthrough by Ohkawa and Uemura.

An analytic expression for the valley splitting has been obtained in a more simplified treatment of Eq. (7.5) (Ando, 1979b). Assume a trial wave function

$$\mathbf{F}^{(\pm)}=\begin{bmatrix}\sin\lambda_\pm\\ \cos\lambda_\pm\end{bmatrix}\zeta(z)\exp(\pm ik_0z). \tag{7.10}$$

The usual variational procedure in which $(\pm\,|\,\mathscr{H}+V\,|\,\pm)$ is minimized gives $\lambda_\pm$ and $\zeta(z)$. One has

$$-\frac{\hbar^2}{2m_z}\frac{d^2}{dz^2}\zeta(z)+V(z)\zeta(z)=E_0\zeta(z), \tag{7.11}$$

where $m_z\sim0.98m_0$ is slightly different from the experimental value $m_l=0.916m_0$. Since the overlap integral $(\pm\,|\,\mp)$ is extremely small, the valley splitting is obtained from the off-diagonal element $(+\,|\,\mathscr{H}+V-\varepsilon_0-E_0\,|\,-)$,

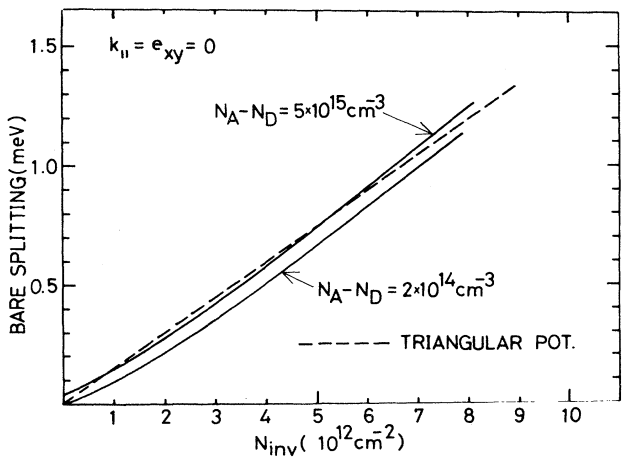

FIG. 145. The valley splitting calculated by Ohkawa and Uemura (1976, 1977b) as a function of the inversion layer electron concentration. The broken line is calculated assuming a triangular potential. The solid lines are calculated assuming nearly self-consistent potentials for two different dopings. After Ohkawa and Uemura (1977b).

where ε_0 is the energy of the bottom of the conduction band. The resulting expression, in the limit that k_0^{-1} is much smaller than the scale of the variation of $\zeta(z)$, is given by

$$\Delta E_v = \frac{\beta}{4k_0^3}\varepsilon_\Gamma |\zeta'(0)|^2 , \tag{7.12}$$

where β is a quantity close to unity, $\varepsilon_\Gamma = E(\Gamma_1^u) - E(\Gamma_{15})$, and $\zeta'(0)$ is the derivative of the wave function at $z=0$. Using an identity (3.33) it is written as

$$\Delta E_v = \alpha \left\langle \frac{\partial V(z)}{\partial z} \right\rangle , \tag{7.13}$$

with

$$\alpha = \frac{1}{4}\beta\varepsilon_\Gamma \frac{2m_z}{\hbar^2 k_0^2}\frac{1}{k_0} \sim 0.25 \text{ Å} . \tag{7.14}$$

Since the potential is determined self-consistently, we have in the electric quantum limit, where only the ground subband is occupied,

$$\left\langle \frac{\partial V(z)}{\partial z} \right\rangle = \frac{4\pi e^2}{\kappa_{sc}}\left(\tfrac{1}{2}N_s + N_{depl}\right) - \frac{(\kappa_{sc}-\kappa_{ins})e^2}{4\kappa_{sc}(\kappa_{sc}-\kappa_{ins})}\left\langle \frac{1}{z^2} \right\rangle . \tag{7.15}$$

The last term represents a contribution from a classical image force and has a relatively large contribution, as will be discussed below. The factor $\frac{1}{2}$ in the term proportional to N_s has an important meaning, as has been discussed in Sec. IV.C.2, and is a result of the exact self-consistency of $\zeta(z)$ and $V(z)$. This result (7.13) is several percent smaller than the numerical result (7.9) of Ohkawa and Uemura. This difference partly originates from the difference of $m_l = 1.035m_0$ and $m_z = 0.98m_0$ and the neglect of the self-consistency by Ohkawa and Uemura. However, such a discrepancy is certainly within the accuracy of the present approximate treatment of the conduction band.

The essential part of Eq. (7.13) is reproduced by a simpler argument. When we neglect small S in Eq. (7.2) and change the representation, we can write (7.2) to lowest order in ε_Γ as

$$\mathcal{H}(k_z) \sim \begin{bmatrix} \frac{\hbar^2}{2m_0}(k_z-k_0)^2+\varepsilon_0 & \frac{1}{2}\varepsilon_\Gamma \\ \frac{1}{2}\varepsilon_\Gamma & \frac{\hbar^2}{2m_0}(k_z+k_0)^2+\varepsilon_0 \end{bmatrix} . \tag{7.16}$$

The Hamiltonian gives two independent subbands when ε_Γ is zero. The valley splitting is given to lowest order in ε_Γ by

$$\Delta E_v \sim \varepsilon_\Gamma \left| \int_0^\infty dz\, e^{-2ik_0 z} |\zeta_0(z)|^2 \right| . \tag{7.17}$$

In the limit of large k_0, the overlapping integral is determined by a region of z where $\zeta(z)$ spatially varies most strongly, i.e., near $z=0$ where the wave function itself is continuous but its derivative changes discontinuously across $z=0$. We have

$$\int_0^\infty dz\, e^{-2ik_0 z}|\zeta(z)|^2 = \lim_{\delta\to+0}\int_0^\infty dz\, e^{-2ik_0 z-\delta z}z^2 |\zeta'(0)|^2 = \frac{2}{(2ik_0)^3}|\zeta'(0)|^2 . \tag{7.18}$$

Thus we obtain

$$\Delta E_v \sim \frac{1}{4k_0^3}\varepsilon_\Gamma |\zeta'(0)|^2 , \tag{7.19}$$

which is close to (7.12). Equation (7.19) means that the overlapping integral, and consequently the valley-valley interaction, is given by a portion of the electron density distribution within a distance from the interface of the order of the lattice constant ($\sim 2\pi/k_0$). Ohkawa and Uemura used the variational wave function (3.25) in evaluating the overlapping integral (7.18) and obtained values almost three times as large as those given by Eq. (7.9). Their elaborate numerical calculation was actually necessary only to get accurate values of the derivative of the wave function at $z=0$.

There are various insufficiencies in the Ohkawa-Uemura theory. They treated the Γ_1^l band perturbationally in Eq. (7.2). This approximation is valid near the Γ point, but might break down near the conduction-band minima. As a matter of fact, the energy separation between Δ_1^u and Δ_1^{lc} has become smaller than that between Δ_1^{uc} and Δ_1^{lc} around the X point. The analytic treatment of the 2×2 matrix Hamiltonian can easily be extended to the original 3×3 matrix Hamiltonian (7.1), which is shown to give about 20% larger splitting than Eqs. (7.13) and (7.14) (Ando, unpublished). As is clear from the above discussion, the interaction of the two Δ_1^{lc} bands at the Γ point and the resulting gap ε_Γ are the main origin of the valley splitting obtained by Ohkawa and Uemura. Figure 144 shows that $\Delta_{2'}$ bands which have been included in the extended zone scheme should have interactions at the Γ point (or at $k_1 = \pm 4\pi/a$ in the extended zone scheme). The valley-valley coupling caused by these interactions is completely neglected, but might also give a significant contribution to the splitting because the distance from the band minimum $k_1 = 0.85(2\pi/a)$ to the second edge $k_1 = 4\pi/a$ is comparable to that to the Γ point ($k_1 = 0$). There can be a problem concerning the boundary condition at the interface. The barrier height at the Si-SiO_2 interface is believed to be about 3 eV, while the gap between Δ_1^{lc} and Δ_1^{uc} at the conduction-band minima is of the order of 13 eV. Therefore, the condition that the envelope functions for both of these bands should vanish at $z=0$ may be unreasonable, and more realistic conditions should be employed. Ohkawa (1979a) later extended his theory to a

case of finite barrier heights and showed within the two-band model that the absolute value of the splitting is independent of the barrier height as long as it is much larger than the subband energy E_0. However, it is not certain that this result is applicable to many-band cases.

Effects of nonzero values of wave vectors in the direction parallel to the interface have also been studied using the $\mathbf{k}\cdot\mathbf{p}$ Hamiltonian near the X point,

$$\mathscr{H}(k_1,k_2,k_3)=\begin{bmatrix} \frac{\hbar^2}{2m_l}(k_1-k_0')^2+\frac{\hbar^2}{2m_t}(k_2^2+k_3^2) & -i\frac{\hbar^2}{2m_0}Lk_2k_3-i\Xi'_u e_{23} \\ i\frac{\hbar^2}{2m_0}Lk_2k_3+i\Xi'_\mu e_{23} & \frac{\hbar^2}{2m_l}(k_1+k_0')^2+\frac{\hbar^2}{2m_t}(k_2^2+k_3^2) \end{bmatrix}, \tag{7.20}$$

obtained by Hensel, Hasegawa, and Nakayama (1965), where k_1 is measured from the X point, $k_0'=0.15(2\pi/a)$, Ξ_u' is a deformation potential constant, and e_{23} is a shear strain. Ohkawa and Uemura (1977b) treated the off-diagonal part of Eq. (7.20) perturbationally and claimed that the valley splitting for a Landau-level N was given by

$$\Delta E_v=0.15\times\frac{N_s+\frac{32}{11}N_{\rm depl}}{10^{12}\ {\rm cm}^{-2}}\left\{1+\frac{\gamma}{8}\left[\frac{(N+\frac{1}{2})\hbar\omega_c}{10\ {\rm meV}}\right]^2+\left[\frac{\Xi_u' e_{xy}}{10\ {\rm meV}}\right]^2\right\}^{1/2} \tag{7.21}$$

(in meV in strong magnetic fields. Here γ, proportional to L^2, is a dimensionless quantity larger than unity. Ohkawa (1978b) found later that the second term in the curly bracket of (7.21) does not exist actually and that the valley splitting should be almost independent of the Landau level.

b. Sham-Nakayama theory—surface scattering

Sham and Nakayama (1978, 1979) have presented a more elegant theory of the valley splitting which includes the Ohkawa-Uemura theory as a special case. In this theory we first solve a problem of the band structure in a half-space and then construct an effective-mass equation which includes the slowly varying potential $V(z)$ but does not contain the potential of the abrupt interface. Let us consider the vicinity of the conduction-band minima $k_1=\pm k_0$. In the presence of the interface the wave function for the states with energy $\varepsilon_0+\hbar^2\kappa^2/2m_l$ is written as

$$\phi_{1\kappa}=e^{-i\kappa z}\psi_{k_0}-S_{11}e^{i\kappa z}\psi_{k_0}-S_{21}e^{i\kappa z}\psi_{-k_0}-\sum_\lambda T_{\lambda 1}\chi_\lambda\ , \tag{7.22a}$$

$$\phi_{2\kappa}=e^{-i\kappa z}\psi_{-k_0}-S_{12}e^{i\kappa z}\psi_{k_0}-S_{22}e^{i\kappa z}\psi_{-k_0}-\sum_\lambda T_{\lambda 2}\chi_\lambda\ , \tag{7.22b}$$

where $\psi_{\pm k_0}$ is the Bloch wave function at $k_1=\pm k_0$ and $k_2=k_3=0$, κ is the wave vector measured from $\pm k_0$, χ_λ is an evanescent wave corresponding to the given energy, and $m_l=0.916m_0$. The first term of the right-hand side of Eq. (7.22a) represents an incoming wave with wave vector $k_0-\kappa$ propagating toward the interface, and the second and third terms are scattered waves with $k_0+\kappa$ and $-k_0+\kappa$, respectively. The quantity S_{ij} is called the S matrix. If there is no intrinsic interface state around the conduction-band edge, the S matrix for sufficiently small κ is given by

$$S=\begin{bmatrix} 1-2ia_s\kappa & -\alpha^*\kappa \\ \alpha\kappa & 1-2ia_s\kappa \end{bmatrix}, \tag{7.23}$$

where a_s is called the scattering length. In the interior of the semiconductor where the evanescent waves have died down, the asymptotic wave functions become

$$\Psi_{1\kappa}=\phi_{1\kappa}-\tfrac{1}{2}\alpha\kappa\phi_{2\kappa} \sim 2\sin\kappa(z-a_s)\psi_{k_0}-i\alpha\kappa\cos\kappa(z-a_s)\psi_{-k_0}\ , \tag{7.24a}$$

$$\Psi_{2\kappa}=\phi_{2\kappa}+\tfrac{1}{2}\alpha^*\kappa\phi_{1\kappa} \sim 2\sin\kappa(z-a_s)\psi_{-k_0}+i\alpha^*\kappa\cos\kappa(z-a_s)\psi_{k_0}\ . \tag{7.24b}$$

The effective position of the boundary for the asymptotic wave functions is given by the scattering length a_s. These $\Psi_{1\kappa}$ and $\Psi_{2\kappa}$ for positive values of κ form the basis set in treating bound states due to an external potential.

Since electrons in the inversion layer exist in the interior, and the external potential $V(z)$ is sufficiently slowly varying, the wave function can be expanded as

$$\Psi=\sum_{v=1,2}\int_0^\infty\frac{d\kappa}{2\pi}A_v(z)\Psi_{v\kappa}\ . \tag{7.25}$$

We choose the origin of z at $z=a_s$, for simplicity. The matrix elements of $V(z)$ are evaluated in the approximation of the slowly varying potential and by neglecting intervalley terms such as $(\psi_{k_0}\,|\,V\,|\,\psi_{-k_0})$. The diagonal element becomes

$$(\Psi_{v\kappa}\,|\,V\,|\,\Psi_{v\kappa'})=V(\kappa-\kappa')-V(\kappa+\kappa')\ , \tag{7.26}$$

$$V(\kappa)=\int_{-\infty}^{+\infty}dz\,V(\,|\,z\,|\,)e^{-i\kappa z}\ . \tag{7.27}$$

The off-diagonal element becomes

$$(\Psi_{1\kappa}\,|\,V\,|\,\Psi_{2\kappa'})=W(\kappa-\kappa')-W(\kappa+\kappa')\ , \tag{7.28}$$

where $W(\kappa)$ is the Fourier transform of $W(z)$, defined by

$$W(z)=\frac{\alpha^*}{2i}\frac{\partial V(z)}{\partial z}\ ,\quad z>0 \tag{7.29}$$

and $W(-z)=W(z)$. If we define

$$A_v(z)=\int_0^\infty \frac{d\kappa}{\pi}\sin\kappa z A_v(\kappa)\ , \tag{7.30}$$

we have the coupled equations

$$\begin{bmatrix} \frac{\hbar^2}{2m_1}\frac{d^2}{dz^2}+V(z)\partial z & -\frac{i}{2}\alpha^*\frac{\partial V(z)}{\partial z} \\ \frac{i}{2}\alpha\frac{\partial V(z)}{\partial z} & -\frac{\hbar^2}{2m_l}\frac{d^2}{dz^2}+V(z) \end{bmatrix}\begin{bmatrix} A_1(z) \\ A_2(z) \end{bmatrix}$$
$$=\varepsilon\begin{bmatrix} A_1(z) \\ A_2(z) \end{bmatrix}\ . \tag{7.31}$$

with the boundary condition that $A_1(0)=A_2(0)=0$. When only the diagonal part is retained, the usual single-valley effective-mass equation is recovered,

$$-\frac{\hbar^2}{2m_l}\frac{d^2}{dz^2}\zeta(z)+V(z)\zeta(z)=E_0\zeta(z)\ , \tag{7.32}$$

with $A_1(z)=A_2(z)=\zeta(z)$. The lowest-order perturbation gives the valley splitting,

$$\Delta E_v=|\alpha|\left\langle\frac{\partial V(z)}{\partial z}\right\rangle . \tag{7.33}$$

Therefore, the problem has been reduced to that of obtaining the quantity α, i.e., the off-diagonal element of the S matrix. This has been called the surface scattering mechanism.

There have been controversies as to whether the electric breakthrough mechanism of Ohkawa and Uemura and the surface scattering of Sham and Nakayama are essentially equivalent or completely independent (Ohkawa, 1978a, 1979a; Nakayama and Sham, 1978). As can easily be understood from the derivation of (7.19), the presence of the abrupt interface plays an important role even in the electric breakthrough formalism. Further, Eq. (7.33) is quite similar to (7.13). The similarity of the expressions obtained in both theories suggests that they are not independent of each other. Nakayama and Sham (1978) have calculated α in the two-band model ($S=0$) considered by Ohkawa and Uemura as

$$\alpha=\frac{2m_0\varepsilon_\Gamma}{k_0\hbar^2T^2}=0.23\ \text{Å}\ , \tag{7.34}$$

which agrees with Eq. (7.14) except for some minor differences arising from terms with higher order in $2m_0\varepsilon_\Gamma/\hbar^2T^2$. Thus one can conclude that the Sham-Nakayama theory contains the Ohkawa-Uemura theory as a special case and that the electric breakthrough mechanism is essentially equivalent to the surface scattering mechanism.

Sham and Nakayama evaluated α for $k_x=k_y=0$ employing the $\mathbf{k}\cdot\mathbf{p}$ band structure model of Cardona and Pollack (1966). They used a model for the interface of an infinite barrier in a plane at a distance z_0 from a (100) atomic plane and calculated α as a function of z_0. For a given energy just above the conduction-band edge, the 3×3 matrix associated with the Δ_1 symmetry (7.1) yields four Bloch states $\pm k_0\pm\kappa$ close to the minima. The 5×5 $\Delta_{2'}$ matrix yields four evanescent waves with wave vectors $\pm0.095i$ a.u. and $\pm0.835i$ a.u., neglecting terms of $O(\kappa^2)$. Evanescent waves of symmetry other than Δ_1 and $\Delta_{2'}$ are ignored since they are incompatible with the $\bar{\Gamma}_1$ symmetry in the plane parallel to the interface (Jones, 1966). We expand these Bloch and evanescent waves in terms of the plane waves of symmetry $\bar{\Gamma}_1$ at $z=z_0$:

$$\begin{aligned}
\xi_1(\mathbf{r})&=1\ ,\\
\xi_2(\mathbf{r})&=2\left[\cos\frac{2\pi}{a}x\cos\frac{2\pi}{a}y\cos\frac{2\pi}{a}z_0\right.\\
&\qquad\left.+\sin\frac{2\pi}{a}x\sin\frac{2\pi}{a}y\sin\frac{2\pi}{a}z_0\right]\ ,\\
\xi_3(\mathbf{r})&=2\left[\cos\frac{2\pi}{a}x\cos\frac{2\pi}{a}y\sin\frac{2\pi}{a}z_0\right.\\
&\qquad\left.-\sin\frac{2\pi}{a}x\sin\frac{2\pi}{a}y\cos\frac{2\pi}{a}z_0\right]\ ,\\
\xi_4(\mathbf{r})&=\cos\frac{4\pi}{a}x+\cos\frac{4\pi}{a}y\ .
\end{aligned} \tag{7.35}$$

The Bloch waves ψ_k of Δ_1 symmetry are expanded at $z=z_0$ as

$$\psi_k(\mathbf{r},z=z_0)=\sum_{i=1}^{4}c_i(k)\xi_i(\mathbf{r})\ , \tag{7.36}$$

and the evanescent waves χ_λ of $\Delta_{2'}$ symmetry are given by

$$\chi_\lambda(\mathbf{r},z=z_0)=\sum_{i=1}^{4}b_{i\lambda}\xi_i(\mathbf{r})\ , \tag{7.37}$$

where the coefficients $c_i(k)$ and $b_{i\lambda}$ can be determined by the original $\mathbf{k}\cdot\mathbf{p}$ Hamiltonian and its basis plane waves. In particular, one has $c_4(k)=0$. The S matrix can be obtained by substituting Eqs. (7.36) and (7.37) into the right-hand side of (7.22) and imposing the condition that the left-hand side should vanish. One gets

$$\begin{aligned}
&c_i(k_0-\kappa)-S_{11}c_i(k_0+\kappa)-S_{21}c_i(-k_0+\kappa)\\
&\quad-\sum_{\lambda=1}^{2}T_{\lambda1}b_{i\lambda}=0\ ,
\end{aligned} \tag{7.38a}$$

$$\begin{aligned}
&c_i(-k_0-\kappa)-S_{12}c_i(k_0+\kappa)-S_{22}c_i(-k_0+\kappa)\\
&\quad-\sum_{\lambda=1}^{2}T_2b_{i\lambda}=0\ ,
\end{aligned} \tag{7.38b}$$

for $i=1\sim4$. These constitute a set of eight equations

which determine eight unknown S_{ij} and $T_{\lambda j}$. In Fig. 146, the resulting $|\alpha|$ is plotted as a function of z_0. We have $|\alpha|=0.43$ Å except in the extreme neighborhood of $z_0=0.047a$, where the energy of an interface state present in the model crosses the conduction-band minima and α diverges due to a resonance scattering. We can discard the possibility of such resonances in Si-SiO_2 systems, since it would be impossible to form an inversion layer if there were intrinsic interface states near the conduction-band edge. Sham and Nakayama have chosen $|\alpha|=0.43$ Å. This value of α is almost twice as large as that calculated in the two-band model of Ohkawa and Uemura. This large enhancement is partly due to the inclusion of additional couplings of the two valleys neglected in the two-band model, as has been discussed previously, and due to intervalley interactions through intrinsic interface states.

Schulte (1979, 1980a) calculated directly the energy levels of the system described by the $\mathbf{k}\cdot\mathbf{p}$ Hamiltonian of Cardona and Pollak within the model of a constant external electric field (the triangular potential approximation) and the abrupt interface, which is the same as used by Sham and Nakayama. He replaced the constant field by a staircase potential and expanded the wave function for each small interval of z in terms of four Bloch waves and four evanescent waves obtained by Sham and Nakayama. Those functions are joined smoothly at each step edge. The resulting valley splitting or the value of $|\alpha|$ is almost the same as that of Sham and Nakayama, which confirms the validity of the effective-mass approximation for the external potential $V(z)$. The k_x and k_y dependence of α was studied within the same model and shown to give very small distortion of the Fermi line (Schulte, 1980b).

Within the model of the infinite potential at the interface, the Sham-Nakayama theory is certainly more complete and gives a more accurate value of the valley splitting. However, the validity of the model is highly doubtful in actual inversion layers, especially if it is literally

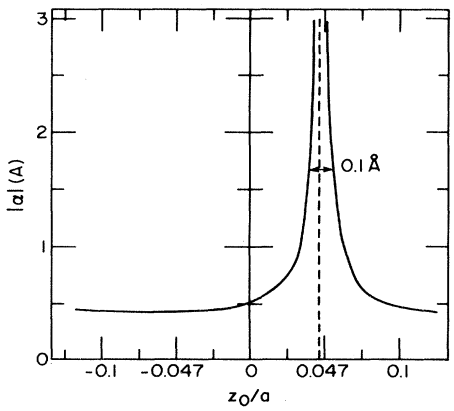

FIG. 146. The coefficient $|\alpha|$ of the intervalley scattering matrix for the conduction-band edge on a Si(100) surface as a function of the interface position, from a crystal plane at $z_0=0$ to midway between two crystal planes, at $z_0=\pm a/8$. After Sham and Nakayama (1979).

extended to many-band Hamiltonians. The Si-SiO_2 interface is not yet understood in detail, although various experiments have already been started to investigate its microscopic structure (see, for example, Pantelides, 1978b, and Sec. III.E). The interface is expected to be sharp, but SiO_2 is known to be amorphous, and a thin transition layer of several angstroms of SiO_x, where x is between 0 and 2, is thought to exist at the interface. This has been discussed in Sec. III.E. The wave function in the vicinity of the interface, which determines the intervalley couplings, is actually very sensitive to such microscopic structures. It is hardly possible to conclude, therefore, that the value of α obtained by Sham and Nakayama is more appropriate in actual inversion layers than that of Ohkawa and Uemura. At present one can discuss only the order of magnitude of the valley splitting. Further, there may well be a problem of misorientation effects in actual systems, as will be discussed below.

Nakayama (1980) has presented a calculation of α based on an LCAO (linear combination of atomic orbitals) version of the Sham-Nakayama theory. For bulk silicon he has used a semiempirical LCAO model of Pandey and Phillips (1976), which consists of $3s$ and $3p$ atomic orbitals whose interaction parameters are determined so as to fit to known band energies. A very simple model is taken for the oxide and interface region: An infinitely large diagonal atomic energy is assumed in the oxide and a diagonal shift Δ is assumed for all atomic orbitals for Si atoms in the interface layer. The values of $|\alpha|$ and a_s are calculated as functions of Δ. Both $|\alpha|$ and a_s are shown to vary strongly and exhibit resonance behavior as Δ varies. Furthermore, the absolute values of $|\alpha|$ and a_s are quite sensitive to the choice of the LCAO parameters. Although this model is much too simplified, and its relation to the actual Si-SiO_2 system is not clear, the results suggest that the valley splitting is extremely sensitive to models of the interface, and its accurate value could be obtained theoretically only if the detailed structure of the interface were well understood.

There are some problems in estimation of $F_{\rm eff}=\langle \partial V(z)/\partial z\rangle$ in addition to that of $|\alpha|$. As a matter of fact, $F_{\rm eff}$ is quite sensitive to treatment of the image potential. Sham and Nakayama (1979) evaluated $F_{\rm eff}$ assuming the image potential,

$$V_I(z)=\frac{e^2(\kappa_{\rm sc}-\kappa_{\rm ins})}{4\kappa_{\rm sc}(\kappa_{\rm sc}+\kappa_{\rm ins})(z+\delta)}\ , \tag{7.39}$$

where δ is a cutoff distance of the order of the lattice constant. They used the more accurate variational wave function (3.34). Figure 147 shows the resulting $N_{\rm eff}$, which is defined by $F_{\rm eff}=2\pi e^2 N_{\rm eff}/\kappa_{\rm sc}$, as a function of N_s for $N_{\rm depl}=0$. The modification of the image potential by a finite δ of the order of the lattice constant a affects the energy levels rather weakly but changes $F_{\rm eff}$ drastically. This fact can be another source of uncertainty in the exact theoretical estimation of the valley splitting.

As has been shown in Eq. (7.24), the effective interface

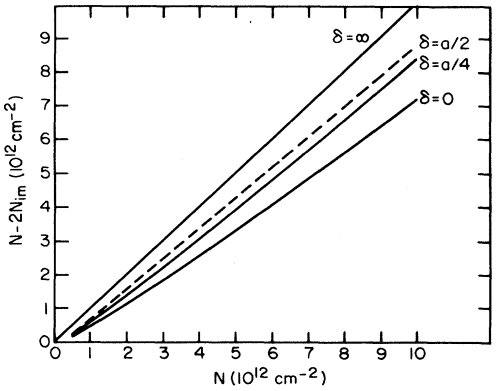

FIG. 147. The effective electron concentration $N_s-2N_{\rm im}$, defined by $F_{\rm eff}=2\pi e^2(N_s-2N_{\rm im})/\kappa_{\rm sc}$, as a function of the electron concentration N_s (called N in the figure) when $N_{\rm depl}=0$ for various values of the distance parameter δ which modifies the denominator of the image potential. In the case of infinite δ (no image force), one gets $N_{\rm im}=0$. After Sham and Nakayama (1979).

for the envelope function should be placed at the scattering length $z=a_s$, which can depend on the interface boundary conditions. In the presence of a perturbing potential $V(z)$ the effective-mass approximation gives an energy shift of the subband by an amount

$$\Delta E=a_s\left.\frac{\partial V(z)}{\partial z}\right|_{z=0} \tag{7.40}$$

with respect to that obtained under the condition that the envelope function vanishes at $z=0$. This does not affect the energy separations of the subbands associated with the two valleys which we have considered and which are assumed to be occupied by electrons. However, this effect can shift the relative energies of the subbands for different sets of valleys. We have

$$\Delta E_{0'0}=(a_s'-a_s)\left\langle\frac{\partial V(z)}{\partial z}\right\rangle_{0'}, \tag{7.41}$$

where a_s' is the scattering length for the four valleys which present a lighter normal effective mass and $\langle\partial V(z)/\partial z\rangle_{0'}$ is the average of the field for the 0′ subband. Sham and Nakayama (1979) have shown that a_s' is rather sensitive to the position of the interface z_0 in their $\mathbf{k}\cdot\mathbf{p}$ infinite-barrier model. Nakayama (1980) obtained an interface-induced increase of $E_{0'0}$ of the order of meV in his LCAO model. This behavior is opposite to the result of Stern (1977), who found that effects of interface grading make $E_{0'0}$ smaller than in the case of an abrupt interface, as has been discussed in Sec. III.E. The possible existence of internal strains in the vicinity of the interface affects the relative positions of E_0 and $E_{0'}$ subbands. In any case, the energy difference $E_{0'0}$ is quite sensitive to the actual interface condition. Since SiO_2 is amorphous, the scattering length a_s can vary spatially. This fluctuating a_s can be another source of electron scattering. The effect is similar to that of the interface roughness considered in Sec. IV.C.

c. Kümmel's theory—spin-orbit interaction

Kümmel (1975) proposed a mechanism for the valley splitting which is completely different from the two mentioned above, namely spin-orbit coupling. One may write the wave function in the presence of an external potential as

$$\Psi(\mathbf{r},z)=\int\frac{dk_z}{2\pi}F(k_z)\psi_{k_z}(\mathbf{r},z), \tag{7.42}$$

where $F(k_z)$ is the envelope function and $\psi_{k_z}(\mathbf{r},z)$ is the Bloch function of the conduction band for $k_x=k_y=0$. In the presence of the potential $V(z)=eFz$, the envelope function satisfies

$$\varepsilon(k_z)F(k_z)+eF\left[\frac{1}{i}\frac{\partial}{\partial k_z}+X(k_z)\right]F(k_z)=\varepsilon F(k_z), \tag{7.43}$$

where the F before the bracket is the electric field, $\varepsilon(k)$ is the dispersion of the conduction band, and

$$X(k_z)=\frac{1}{\Omega}\int_\Omega d\mathbf{R}\,u_{k_z}^*(\mathbf{R})\frac{\partial}{\partial k_z}u_{k_z}(\mathbf{R}), \tag{7.44}$$

where Ω is the volume of a unit cell and $u_{k_z}(\mathbf{R})$ is the periodic part of the Bloch function. Assuming that $F(k_z)$ has nonzero values only around the minima $\pm k_0$, Kümmel has obtained two series of subbands whose energies are shifted by $eFX(\pm k_0)$ from the energy levels calculated in the usual effective-mass equation. In the absence of a spin-orbit interaction u_{k_z} can be chosen as real and $X(\pm k_0)$ can be set zero. In its presence, however, $X(\pm k_0)$ can be nonzero and $X(+k_0)=-X(-k_0)$. Thus the spin-orbit coupling may give rise to a valley splitting

$$\begin{aligned}\Delta E_v&=2\,|X(\pm k_0)|\,eF\\&=2\,|X(\pm k_0)|\left\langle\frac{\partial V(z)}{\partial z}\right\rangle.\end{aligned} \tag{7.45}$$

This is the spin-orbit mechanism proposed by Kümmel. Since the spin-orbit interaction is not important in the conduction-band edge of silicon, it is not certain whether such a mechanism really contributes a sizable amount to the valley splitting in actual inversion layers. Estimation of $X(\pm k_0)$ requires understanding of the detailed band structure and has not been done yet. Kümmel claims that $|X(\pm k_0)|$ takes a nonzero value which is one order of magnitude smaller than the lattice constant. There have been arguments as to whether a nonzero value of $|X(\pm k_0)|$ can give the splitting given by (7.45) to lowest order (Campo *et al.*, 1978; Ando, unpublished).

2. Valley splittings on Si(100)

a. Many-body effects

A typical example of the Shubnikov—de Haas oscillation of the transverse conductivity in strong magnetic

fields (Kawaji, Wakabayashi, and Kusuda, unpublished) is given in Fig. 148. A similar figure has also been given in Sec. VI.B. The lowest two Landau levels ($N=0$ and 1) show splitting of the peak into four. The larger splitting is the spin-Zeeman splitting and the additional one is considered to be the valley splitting. The Landau level $N=2$ exhibits a small valley splitting. For $N=3$, only the spin splitting is resolved in magnetic fields below 150 kOe, and a characteristic structure called a cusp by Ohkawa and Uemura (1976, 1977c) appears above $H\sim 150$ kOe, as is denoted by an arrow. For higher Landau levels no splittings are resolved. Therefore, the valley splittings disappear at high concentrations. On the other hand, calculated valley splittings, as discussed in Sec. VII.A.1, are extremely small at low N_s and increase roughly in proportion to N_s. Such characteristic behavior of the line shape is closely related to the problem of the level broadening effect. As has been discussed in Sec. VI.B estimated level widths of Landau levels are typically $1.5\sim 2$ meV in $H\sim 100$ kOe and much larger than the valley splitting predicted theoretically. Further, the width does not increase so rapidly with N_s as to explain the rapid change of the line shape of the Shubnikov–de Haas oscillation. It is clear, therefore, that simple inclusion of the bare valley splitting cannot account for the experimental results and that the additional enhancement of the splitting, which is the same as that of the spin splitting as discussed in detail in Sec. VI.B, is crucial.

A schematic illustration of the relative motions of Landau levels with different spins and valleys is given in Fig. 149, where the spin orientations are denoted by ↑ and ↓ and the valleys by + and −. The occupied levels suffer a self-energy shift roughly proportional to their occupation and inversely proportional to the screening of the system. Therefore, the enhancement oscillates as a function of the electron occupation of the levels. Ohkawa and Uemura (1976, 1977c) calculated the self-energy shift in the screened Hartree-Fock approximation used by Ando and Uemura (1974b, 1974c) for the explanation of the spin splitting, using their value of the bare valley splitting and taking a Gaussian form as the density of states of each level. An example of calculated line shapes of the Shubnikov–de Haas oscillation has been given in Fig. 129, which explains the characteristic feature of the experimental results. Although there remain various problems in such a line-shape analysis such as electron localization effects discussed in Sec. VI.D, they clearly demonstrated the importance of the exchange enhancement effect in explaining the experimental results.

Rauh and Kümmel (1980a–1980c) extended the calculation of Ohkawa and Uemura to nonzero temperatures and calculated the maximum enhanced valley splitting when the position of the chemical potential is midway between the valley energy levels (the cases A and F in Fig. 149). They have demonstrated that with the increase of temperature and enhanced splitting stays approximately constant at its zero temperature value and then drastically drops down around a certain temperature of the order of the bare valley splitting. At higher temperatures the valley splitting is not resolved. This rapid decrease occurs due to a twofold positive feedback mechanism: With increasing temperature the difference in occupation numbers of the two valleys decreases and the screening increases simultaneously.

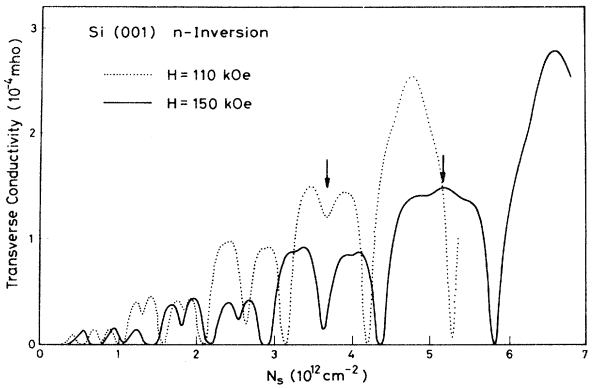

FIG. 148. Examples of transverse conductivity observed by Kawaji, Wakabayashi, and Kusuda (unpublished) in an n-channel inversion layer on a Si(100) surface. The arrows indicate positions of $N=3$ Landau levels. After Ando (1980a).

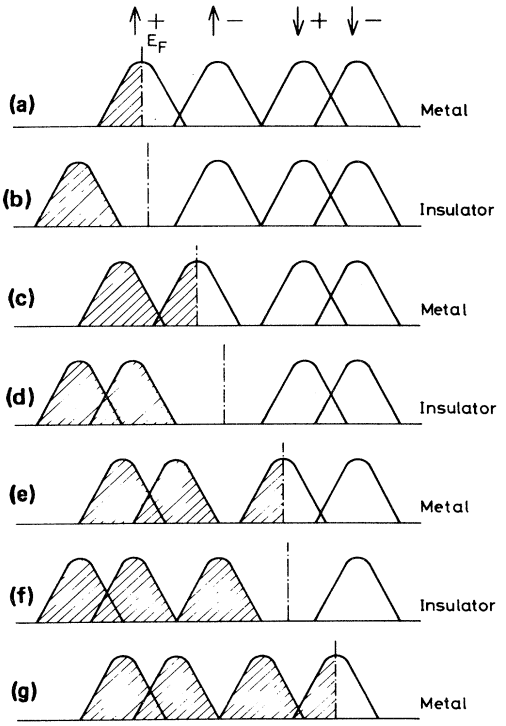

FIG. 149. A schematic sketch of the enhancement of the spin and valley splittings. The occupied level suffers a self-energy shift proportional to its occupation and inversely proportional to the screening of the system. The enhancement is large in an insulating situation, and small in a metallic situation. After Ohkawa and Uemura (1977c).

b. Experimental determination of the valley splitting

The line shape of the Shubnikov–de Haas oscillation calculated by Ohkawa and Uemura does not necessarily mean that their value of the bare valley splitting agrees with experiments. This is because the actual splitting, according to their calculation, is dominated by many-body enhancement, especially at low electron concentrations. It should be noticed that the enhancement due to the exchange effect is still appreciable and cannot be neglected even at higher electron concentrations where the valley splitting is not resolved in the Shubnikov–de Haas oscillations. This makes experimental determination of the valley splitting quite difficult and ambiguous, although one can get some information on the splitting from the experimental results.

Let us first focus our attention on the characteristic difference of the line shape of the peak for $N=3$ (denoted by arrows) in Fig. 148. At $H=110$ kOe the peak shows only the spin splitting, which means that the energy separation of the levels $N=(3,\downarrow,+)$ and $(3,\uparrow,-)$ when the Fermi level lies midway between them is larger than that of the levels $(3,\uparrow,-)$ and $(3,\uparrow,+)$ when the Fermi level lies at the corresponding middle point. Although this relation holds for the level separations modified by the strong many-body enhancement, one can safely assume that the same is applicable to the energy levels in the absence of the enhancement effect. Therefore, one can conclude that the valley splitting is smaller than half of the spin splitting around the peak electron concentration, i.e., $\Delta E_v < \mu_B H$, with μ_B being the Bohr magneton. The line shape at $H=150$ kOe, on the other hand, shows that the valley splitting is slightly larger than half of the spin splitting. In this way one can obtain such upper and lower bounds (sometimes the exact values) of the bare valley splitting from line-shape analysis in different magnetic fields. One can be more precise in the case of tilted magnetic fields because the spin splitting is determined by the total magnetic field. Figure 150 gives an example of results of the line-shape analysis done by Kawaji, Wakabayashi, and Kusuda (unpublished), together with the theoretical results of Ohkawa and Uemura (1976, 1977b) and of Sham and Nakayama (1978, 1979), in the case of no cutoff of the image potential. Both theoretical results become about 10% larger than those shown in the figure if one chooses $\delta \sim a/4$ in Eq. (7.39). The bare valley splitting for $N=3$ seems to lie between the two theoretical curves. Note, however, that the theoretical results are shown in the figure only for visual aid and are not meant to be compared with the experimental results because of various uncertainties originating from the model of the interface.

The most naive determination of the valley splitting should be possible in lower magnetic fields where the Landau-level separation $\hbar\omega_c$ is comparable to the valley splitting (Stiles, 1979; see also Ando, 1979b). An example of the Landau-level structure for $H=25$ kOe is shown in Fig. 151 together with a schematic illustration of the Shubnikov–de Haas oscillation of the conductivity. The result of Sham and Nakayama (1979) for $\delta=0$ is assumed, and the many-body enhancement is completely neglected for simplicity. Although the valley splitting is small and not resolved, the Shubnikov–de Haas oscillation should show a characteristic phase change of π at the electron concentration where the valley splitting is half of the Landau-level separation (around $N_s=3.8\times 10^{12}$ cm^{-2} in Fig. 151). Such a phase change did not attract much attention until quite recently, and the experimental situation is still unclear. This is mainly because of its strong sample dependence. Some samples seem to exhibit such a phase change at high electron concentrations but others do not. Stiles (1979) reexamined earlier experimental results of weak-field Shubnikov–de Haas oscillations of various samples systematically. The phase change does not happen in all samples, but the behavior is nearly the same for all samples from a given wafer. He has found also that such a phase change even occurs twice or more in some samples for a certain range of applied magnetic fields, suggesting an oscillatory behavior of the valley splitting as a function of N_s. Figure 150 contains a single experimental result obtained by Kawaji, Wakabayashi and Kusuda (unpublished). The valley splitting is much smaller than those in strong magnetic fields. Note that the splitting determined in this way contains the exchange enhancement, which cannot be neglected even at small magnetic fields, and that the bare

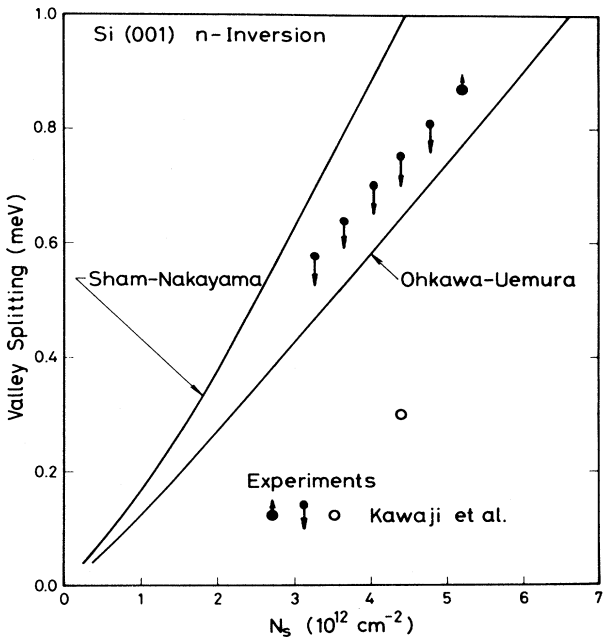

FIG. 150. Upper and lower bounds (black dots with a downward and upward pointing arrow, respectively) obtained from a line-shape analysis of magnetoconductance oscillations in strong magnetic fields by Kawaji, Wakabayashi, and Kusuda (unpublished). Theoretical predictions by Ohkawa and Uemura (1977b) and by Sham and Nakayama (1979) for $\delta=0$ are also shown. A phase change of the Shubnikov–de Haas oscillation in weak magnetic fields gives the data point shown by a small circle. After Ando (1980).

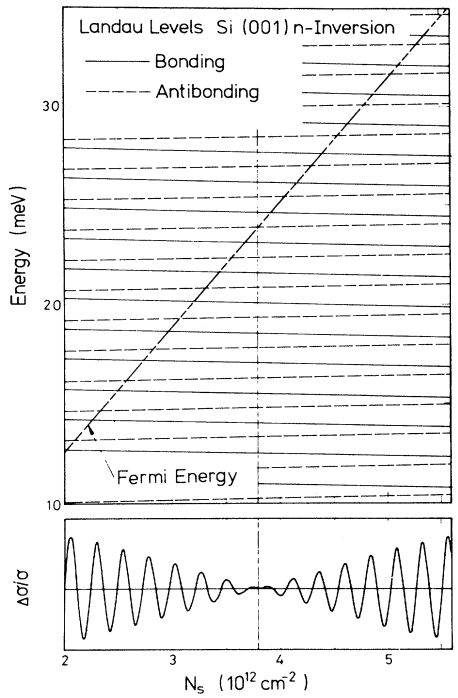

FIG. 151. Schematic illustration of the Landau-level energy and the Shubnikov–de Haas oscillation of the conductivity as a function of electron concentration N_s in $H=25$ kOe. The thin solid lines and broken lines represent the bonding and antibonding levels, respectively, and the dot-dot-dashed line the position of the Fermi energy in the absence of magnetic field. The vertical dot-dashed line at 3.8×10^{12} cm^{-2} shows the electron concentration where the valley splitting is one-half of the Landau-level separation. The oscillation changes its phase at this electron concentration. After Ando (1979b).

splitting is even smaller. One sees, therefore, that the valley splitting depends on magnetic field rather strongly.

Actually there have been many other attempts to determine the value of the valley splitting. Köhler and co-workers (Köhler *et al.*, 1978; Köhler and Roos, 1979a, 1979b; Köhler, 1980) tried to determine the valley splitting using a slightly different argument of the phase change of the Shubnikov–de Haas oscillation in tilted magnetic fields. Von Klitzing (1980) analyzed the Fermi-energy dependence of the transverse conductivity by tilting a magnetic field and keeping its normal component fixed. He has obtained maximum allowed values (upper bounds) of the valley splitting from such an analysis. Oscillations in strong magnetic fields as a function of the substrate bias were studied by Nicholas *et al.* (1980a), who demonstrated a strong sample dependence of the absolute value of the splitting and an increase of the splitting with increasing $N_{\rm depl}$. More recently Nicholas, von Klitzing, and Englert (1980) performed a line-shape analysis of the conductivity in strong magnetic fields in a way similar to that discussed above by varying $N_{\rm depl}$ and the tilt angle of the magnetic field. They showed, for the first time, that the valley splitting increases linearly as a function of $N_{\rm depl}$, in agreement with a theoretical prediction. In all these works, however, the important many-body effect has not been considered explicitly. Therefore, the values of the valley splitting cannot be compared directly with the theoretical values, although their qualitative behavior is expected to be correct. We do not give a detailed account of these experiments here, since they require quite complicated arguments on the level structure and the line shape of the conductivity.

c. Misorientation effects

Ando (1979a) has suggested that crystallographic misorientations of the surface can affect the valley splitting. Since the valley splitting is a result of coupling of the two valleys located near the opposite ends of the Brillouin zone, a slight tilt of the interface from the (100) direction can give rise to a large change in the splitting. Suppose that the interface is tilted by θ. The Fermi lines associated with the two valleys projected to the interface plane ($k_z=0$) are separated by an amount of $2k_0\sin\theta$ in the k_x-k_y plane. Therefore, if we neglect coupling of different Landau levels of the two valleys, we get

$$\Delta E_v' \sim \Delta E_v \, | J_{NN}(2k_0 l \sin\theta) | \ , \tag{7.46}$$

where ΔE_v is the valley splitting for $\theta=0$, $J_{NN}(x)$ is the overlapping integral of the Landau levels, and $l^2=c\hbar/eH$ is the radius of the ground cyclotron orbit. For sufficiently large N,

$$J_{NN}(2k_0 l \sin\theta) \sim J_0[(2N+1)^{1/2} 2k_0 l \sin\theta] \sim J_0[2k_0 R_c \sin\theta] \ , \tag{7.47}$$

where $J_0(x)$ is the Bessel function of the zeroth order and R_c is the classical cyclotron radius. Since $k_0^{-1}\sim1$ Å and $l\sim100$ Å typically, very small values of θ (of the order of 0.5°) are sufficient to modify the splitting drastically. Further, the effect is larger for high Landau levels and weak magnetic fields. Examples of results of numerical calculations in which couplings between different Landau levels are also included are given in Fig. 152, where the valley splitting of the Landau level where the Fermi level lies is plotted against N_s for $H=25$ and 150 kOe. Effects are enormous, especially in weak magnetic fields, and even give rise to an oscillatory behavior which can be understood from Eq. (7.47). This can be a candidate to explain the experimental results of Stiles (1979) mentioned above. Additional valley-valley interactions through an X point are present for nonzero values of k_x and k_y and can become important in the case of large misorientations.

There can be various sources of nonzero values of θ in actual inversion layers. Since experimental accuracy of the determination of the crystallographic orientation is usually limited to $\sim0.5°$, usual MOSFETs are believed to have misorientations of the same order. Actual samples have the so-called interface roughness, whose exact nature is not well known (see Secs. IV.B and IV.C) and which can give rise to a large-scale (slowly varying) de-

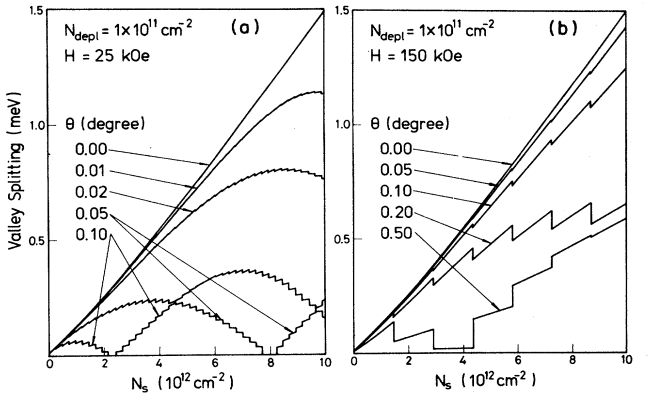

FIG. 152. Calculated valley splittings of the Landau level where the Fermi level lies at zero temperature as a function of the electron concentration N_s for different values of the tilt angle θ in (a) $H=25$ kOe and (b) 150 kOe. $N_{\rm depl}=0.1\times10^{12}$ cm^{-2}. After Ando (1979b).

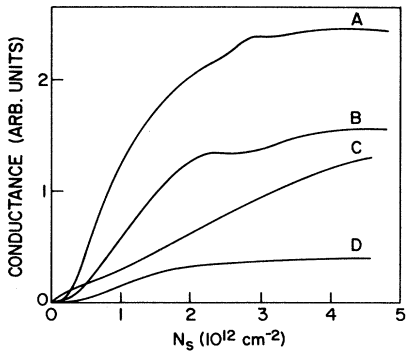

FIG. 153. Observed conductivity on various tilted surfaces as a function of the electron concentration n_s. Curve A, σ_{yy}; curve B, σ_{xx} in n channel on a Si(811) surface at low temperature; curve C, σ_{yy} on a Si(811) surface at high temperature (77 K); curve D, p channel on a Si(811) surface. After Cole *et al.* (1977).

formation of the interface similar to misorientations. These are almost uncontrollable experimentally and can cause valley splittings which are strongly sample dependent, especially in lower magnetic fields. Therefore, the misorientation effect can explain various strange behaviors of the splitting which are observed experimentally. There are some problems, however, in applying the above simple-minded theory to actual systems. The tilt angle of 0.5° corresponds to a distance of several hundred angstroms along the surface for each lattice constant step, which might cast some doubt on the meaning of such a small tilt angle. The interface might locally be flatter than expected and directed in the exact (100) direction, which weakens the misorientation effect, especially in strong magnetic fields where the cyclotron radius is sufficiently small. Thus the effective tilt angle can depend on the strength of the field through the radius of the cyclotron orbit.

3. Minigaps on vicinal planes of Si(100)

Cole, Lakhani, and Stiles (1977; see also Stiles *et al.*, 1977) have observed an anomalous structure in the electron concentration dependence of the conductivity in an n-channel inversion layer on the Si(811) surface. The (811) surface was tilted only 10° from the exact (100) surface and both the subband structure and transport properties were expected to be almost the same as those on (100). Examples of observed conductivities are given in Fig. 153. Let us choose in the following the x and y directions in $[\bar{2}88]$ and $[0\bar{1}1]$, respectively, and the z direction in [811]. The conductivities in the principal directions, σ_{xx} and σ_{yy}, exhibit a double-dip (or W-shape) and single-peak structure, respectively. Such structures disappear at high temperatures and do not seem to exist in p-channel layers. Figure 154 shows observed Shubnikov–de Haas oscillations of the y component conductivity ($\partial\sigma_{yy}/\partial N_s$) as a function of the electron concentration N_s. An oscillation with large amplitude appears above $N_s\sim3.2\times10^{12}$ cm^{-2} in weak magnetic fields. This oscillation has longer period in N_s than the usual one which can be seen at smaller concentrations ($N_s<2.5\times10^{12}$ cm^{-2}). From the period and the temperature dependence of the oscillation amplitude Cole *et al.* have obtained the concentration of electrons participating in the oscillation and their effective mass. The results are given in Fig. 155. One sees that the electron dispersion relation for high concentrations is highly nonparabolic. Such anomalous behavior was explained by assuming a minigap in the two-dimensional dispersion relation caused by the existence of a one-dimensional superlattice potential. A minigap which is about 4 meV at $N_s=3\times10^{12}$ cm^{-2} and increases linearly with N_s seems to explain all the characteristics of the observed results.

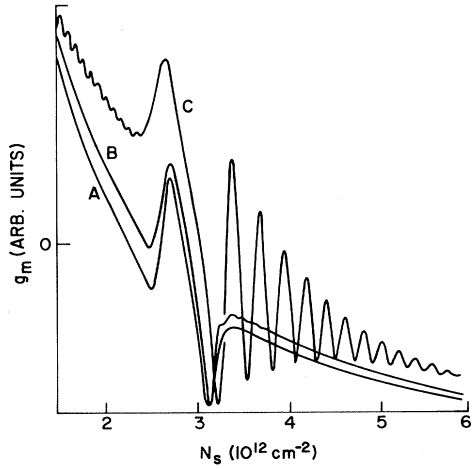

FIG. 154. Transconductance $d\sigma_{yy}/dn_s$ on Si(811) at 1.5 K for different magnetic fields. Curve A, $H=0$; curve B, $H=3$ kOe; curve C, $H=8$ kOe. After Cole *et al.* (1977).

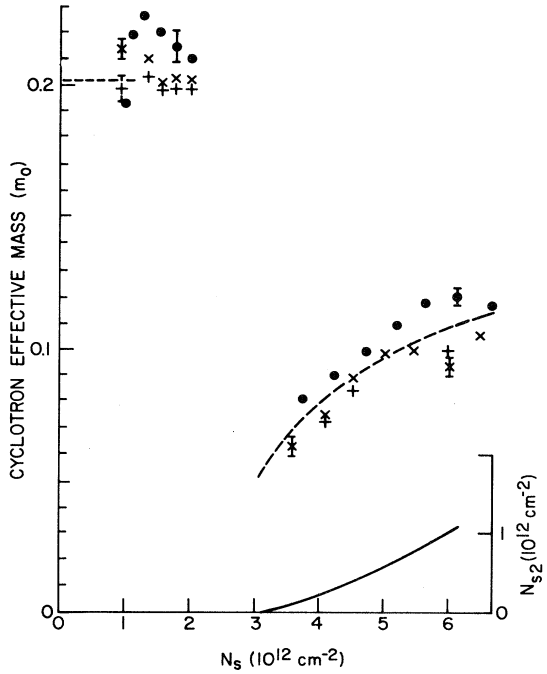

FIG. 155. Measured effective masses as a function of the electron concentration on a Si(811) surface. The solid curve is the measured number of carrier in the lens orbit. The dashed curves are the expected values for the one-dimensional superlattice model. After Cole *et al.* (1977).

The structures of the conductivities are caused by the change in the density of states and electron velocities near the minigap. Electrons in the upper lens orbit cause the Shubnikov–de Haas oscillation with a longer period and a larger amplitude. From the electron concentration corresponding to the anomalous peak of σ_{yy}, one can determine the period of the superlattice potential to be 104 Å. This is different from the expected step period 31.4 Å at the Si-SiO_2 interface. The origin of the assumed superlattice potential has remained unknown. Other surfaces have also been studied (Lakhani *et al.*, 1978). The (511) surface (tilted 16°) has been shown to exhibit a similar expected behavior, whereas a striking difference occurs on the (23 2 2) surface (tilted $\sim 7°$).

Sham, Allen, Kamgar, and Tsui (1978) have proposed an alternative model in which minigaps result from the removal, by valley-valley interactions, of the valley degeneracies at crossings of the surface subbands obtained by projecting the bulk dispersion to the plane parallel to the interface ($k_z=0$). This so-called valley projection model predicts that the minigap occurs at the electron concentration where the Fermi wave number measured from the bottom reaches $0.15(2\pi/a)\sin\theta$, where θ is the surface tilt angle. This electron concentration explains the position of the gap observed on the (811) and (911) surfaces. Tsui, Sturge, Kamgar, and Allen (1978) later made a systematic study of the tilt-angle dependence and confirmed the valley projection model.

Although the position of the minigap can be explained, the size of the observed minigaps is much larger than the valley splitting on the exact (100) surface and is not understood yet. For tilt angles like $\theta\sim 10°$ valley-valley interactions through the X point are expected to be important. One can estimate the value of the minigap from Eq. (7.20) in a manner similar to that discussed previously (Sham, 1979a; Ohkawa, 1978b, 1979b, 1980). One obtains

$$\begin{bmatrix} k_1 \\ k_2 \\ k_3 \end{bmatrix} = \begin{bmatrix} -\sin\theta & 0 & \cos\theta \\ \cos\theta\cos\phi & -\sin\phi & \sin\theta\cos\phi \\ \cos\theta\sin\phi & \cos\phi & \sin\theta\cos\phi \end{bmatrix} \begin{bmatrix} k_x \\ k_y \\ k_z \end{bmatrix}, \tag{7.48}$$

where ϕ is the azimuthal angle of the surface direction with respect to the [010] direction and the x direction has been chosen in the direction of the tilt. In the absence of shear strains e_{23} the minigap at $k_x=k_y=0$ is given to the lowest order in L and θ as

$$\Delta E_v \sim \left| i\frac{\hbar^2}{2m_0} L \int_0^\infty dz\, \zeta_0^*(z) e^{-ik'_0 z \frac{1}{2}} k_z^2 \sin\theta \sin(2\phi) \zeta_0(z) e^{-ik'_0 z} \right| \sim \frac{L}{4k'_0}\frac{m_l}{m_0}\sin^2\theta\,|\sin 2\phi|\left\langle \frac{\partial V(z)}{\partial z}\right\rangle, \tag{7.49}$$

where $\langle \partial V(z)/\partial z\rangle$ is given by Eq. (7.15). This value depends strongly on θ and ϕ. For the (911) surface, for example, it gives 0.6 meV at $N_s\sim 3\times 10^{12}$ cm^{-2} by putting $\theta\sim 10°$ and $\phi=\pi/4$. This number is much smaller than that observed by Cole *et al.* (1977). One can calculate the gap for nonvanishing k_x and k_y, which shows that the gap depends rather strongly on k_x and k_y.

Various experiments have been performed to obtain the value of the minigap. Sham, Allen, Kamgar, and Tsui (1978) observed far-infrared optical absorption across the minigap on the (811) surface. Figure 156 shows an example of observed dynamical conductivities, $\sigma_{xx}(\omega)$ and $\sigma_{yy}(\omega)$, when the Fermi level lies at the center of the minigap. The y component of conductivity is close to the Drude conductivity given by the observed mobility, while the x component exhibits a clear interband transition. Since the largest valley-valley coupling occurs at $k_x=0$ where the two valleys are degenerate, the predominant contribution to the optical transition comes from regions of k_x-k_y space close to the points where the two Fermi circles in the absence of a minigap cross each other. One can expect, therefore, that such optical mea-

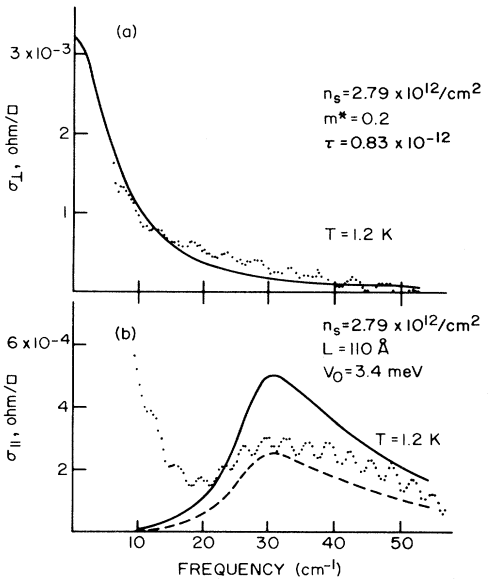

FIG. 156. Optical conductivity vs frequency on a Si(911) surface observed by Sham, Allen, Kamgar, and Tsui (1978). (a) σ_{yy}; (b) σ_{xx}. The solid and dashed curves in (b) represent theoretical predictions based on the superlattice model and the valley projection model, respectively.

surements give the minigap at these points, while the structure of the static conductivities gives the minigap at $k_x=k_y=0$. Far-infrared absorption has also been observed by other workers (Tsui, Allen, Logan, Kamgar, and Coppersmith, 1978; Cole *et al.*, 1978; Sesselmann *et al.*, 1979; see also Kotthaus, 1980) and has been investigated extensively on various surfaces with different tilt angles by Sesselmann and Kotthaus (1979) and by Kamgar, Sturge, and Tsui (1980). The results show that the minigap increases with the tilt angle and N_s, in qualitative agreement with the theoretical prediction based on Eq. (7.20). However, the absolute value is much larger than the theoretical one. Far-infrared emission resulting from radiative decay of electronic excitations across the minigap has also been observed (Tsui and Gornik, 1978; Tsui, Gornik, and Müller, 1979; Gornik and Tsui, 1978a, 1978b; Gornik *et al.*, 1980a) and used for the investigation of the N_s and θ dependence of the gap. The condition of the onset of the magnetic breakthrough in the Shubnikov–de Haas oscillation (see, for example, Pippard, 1962), $\Delta E_v \sim (\hbar\omega_c E_F)^{1/2}$, has explicitly been employed by Kusuda and Kawajii (unpublished) and by Okamoto, Muro, Narita, and Kawaji (1980). Roughly speaking, the minigap obtained in this way is expected to be the same as the optical minigap. Although this method cannot determine the absolute value, it can describe the qualitative behavior such as the N_s and θ dependence. Effects of substrate bias have not been fully studied yet. Cole, Lakhani, and Stiles (1977) have shown that the minigap increases with increasing depletion field proportional to N_{depl}, consistent with the theoretical prediction given in Eq. (7.49). Gornik, Schawarz, Lindemann, and Tsui (1980a) have suggested from experiments on far-infrared emission that the minigap is a function of (N_s+N_{depl}), in disagreement with Eq. (7.49).

All the experiments mentioned above indicate existence of a large θ-independent term in the expression of the minigap. One possible candidate for this large term is existence of large strains which might originate from the tilting of the interface. In the presence of a strain the off-diagonal term $i\Xi_u' e_{23}$ of Eq. (7.20) gives rise to a θ-independent valley splitting. Since the overlapping integral of the wave functions of the two valleys is dominated by the region of z close to the interface, strains extremely localized in the vicinity of the interface are sufficient. In this case, however, such localized strains cannot be described by Eq. (7.20). The amount of strain can depend on the tilt angle, which might cause additional θ dependence of the minigap. A possible appearance of interface states near the conduction-band edge on tilted surfaces and resulting resonance interactions of the two valleys, as demonstrated by Sham and Nakayama on the exact (100) surface within a $\mathbf{k}\cdot\mathbf{p}$ infinite barrier model, is another candidate. One needs experimental study of the minigap on samples made by different preparation techniques to give an answer.

Equation (7.49) suggests that the valley splitting can strongly depend on the azimuthal angle ϕ. Such a dependence has been studied by several groups, but is still in controversy. Sesselmann and co-workers (Sesselmann *et al.*, 1979; Sesselmann and Kotthaus, 1979) have suggested from measurements of optical absorptions and static conductivities that the minigap on (n 10) surfaces ($\phi=0$) is much smaller than on the (n 11), consistent with the $\sin 2\phi$ dependence of Eq. (7.49). Stiles (1979) obtained a minigap on (n 10) surfaces similar to those on the (n 11) although the structure of the conductivity is much weaker. Kusuda and Kawaji (unpublished) obtained, from the condition for magnetic breakthrough, minigaps on (n 10) which are about half of the corresponding gaps on (n 11) with the same tilt angle. It is not certain at present whether such contradictory results originate from a large k_x and k_y dependence of the minigap or are inherent in its strong dependence on interface conditions.

The valley projection model predicts a possibility of appearance of many other higher minigaps (Tsui, Sturge, Kamgar, and Allen, 1978; Tsui, Kamgar, and Sturge, 1979). Figure 157 shows the E vs k_x relation of inversion layer electrons on surfaces tilted by θ from (100). In the extended zone scheme and if minigaps are neglected, it consists of two parabolas centered at $k_x=\pm k_0$, with $k_0=0.85(2\pi/a)$, one from each of the two $\langle 100\rangle$ valleys. The model assumes that projection of the reciprocal lattice vector, $(4\pi/a,0,0)$, onto the surface gives a surface reciprocal lattice vector $\mathbf{Q}=(Q,0)$ with $Q=(4\pi/a)\sin\theta$ in the tilting direction. Consequently minigaps in the surface bands can appear whenever these bands cross each other in the periodic zone scheme, as is illustrated in Fig. 157. The minigaps occurring at $k_x=0$, $\pm Q/2$, $\pm 2Q/2$, ... arise from valley-valley interactions, while the interaction of degenerate states from the same valley

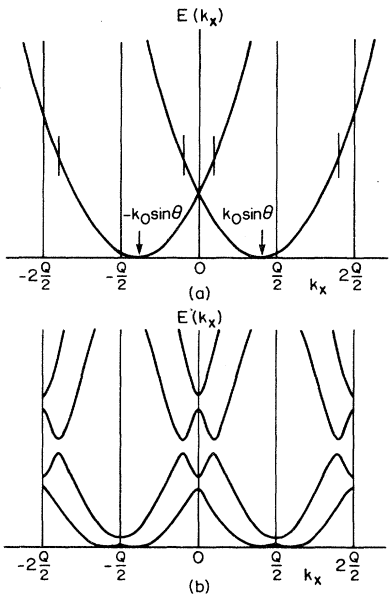

FIG. 157. E vs k_x relation of inversion layer electrons on surfaces tilted by an angle θ from (100): (a) in the extended-zone scheme in the absence of valley-valley interactions and (b) in the periodic-zone scheme with degeneracies at band crossings removed. $Q=(4\pi/a)\sin\theta$. After Tsui, Sturge, Kamgar, and Allen (1978).

will result in the minigaps at $k_x=\pm(2\pi/a-k_0)\sin\theta$. Therefore one can expect minigaps to appear with increasing electron concentration N_s at $k_F=(2\pi/a-k_0)\sin\theta$, $k_0\sin\theta$, $(2\pi/a)\sin\theta$, $(4\pi/a-k_0)\sin\theta$, ..., where $k_F=(\pi N_s)^{1/2}$. Tsui, Sturge, Kamgar, and Allen (1978) observed at expected positions anomalies in the second derivatives of conductivities with respect to N_s associated with those additional higher minigaps [$k_F=0.85(2\pi/a)\sin\theta$, $(2\pi/a)\sin\theta$, and $1.15(2\pi/a)\sin\theta$] on (n 11) surfaces with large n. Optical absorption was observed across the second minigap $0.85(2\pi/a)\sin\theta$ and gave a gap which is similar in magnitude to the first minigap corresponding to the same N_s and tilt angle (Tsui, Sturge, Kamgar, and Allen, 1978; Kamgar *et al.*, 1980). Far-infrared emission also gives some of these higher minigaps (Gornik *et al.*, 1980a).

When electrons are confined within an extremely narrow region close to the interface plane, and the momentum $\hbar k_z$ in the direction perpendicular to the interface spreads out in the whole momentum space, the two-dimensional reciprocal lattice vectors **G** can be obtained by projecting the corresponding reciprocal lattice vectors in three dimension onto the interface plane (Volkov and Sandomirskii, 1978, 1979; Sham, 1979a). This projection can give reciprocal lattice points in two dimensions which are different from those obtained in the simple valley projection model discussed above. One can show that on the (n 11) surface $G_x=m(2\pi/a)\sin\theta$ for even n and $G_x=m(4\pi/a)\sin\theta$ for odd n, where m is an integer. The two-dimensional Brillouin zone becomes a half of that obtained previously in the k_x direction for even n. Although this does not affect the electron concentration corresponding to the lowest minigap, it can give rise to additional higher gaps on (n 11) surfaces with even n. Those new minigaps have not yet been observed, however. In the case of the (23 2 2) surface, the same argument gives $G_x=m(\pi/a)\sin\theta$, and even k_F or the electron concentration corresponding to the lowest minigap can be different from that predicted in the simple valley projection model (Volkov and Sandomirskii, 1978). It is not certain whether this new gap explains the observed anomalous behavior on the (23 2 2) surface (Lakhani *et al.*, 1978). Such new minigaps can certainly exist in principle. However, if we consider that couplings between bands which are quite far apart in momentum space are needed, there might be some doubt as to whether they have values big enough to be observable experimentally.

Although there is no doubt about the existence of a minigap on tilted surfaces, there remains a problem as to whether the minigap due to the valley splitting explains details of the anomalous behavior of the transport observed experimentally. Actually the inversion layer on the tilted surfaces provides an ideal system where one can study effects of nonparabolicity and band gaps in the dispersion relation on transport phenomena. Transport properties of such a system have been investigated theoretically (Ando, 1979d; see also Ando, 1980a). The model assumes a gap independent of k_x and k_y to describe the dispersion around the lowest minigap on tilted surfaces and short-range scatterers as a main mechanism which limits the electron mobility. The model of short-range scatterers has been shown to explain various characteristics of the quantum transport in the inversion layer, as has been discussed in Sec. VI. The transport coefficients $\sigma_{xx}(\omega)$ and $\sigma_{yy}(\omega)$ have been calculated within the model both in the presence and in the absence of a magnetic field and both for $\omega=0$ and for $\omega\neq0$. Figure 158 shows an example of calculated density of states and static conductivities as a function of the Fermi energy. The energy is measured from the bottom of the subbands in the absence of their coupling and is normalized by the Fermi energy corresponding to the crossing of the two subbands. The scattering strength is parametrized by the level broadening in the absence of a minigap Γ_0, which is given for the present example by 0.15. The minigap lies between 0.7 and 1.3. The density of states shows structure near the bottom and the top of the gap, reflecting a logarithmic divergence and a step-function—like increase, respectively. This sharp structure has been smoothed by the level broadening effect. Both σ_{xx} and σ_{yy} exhibit a small peak when the Fermi level crosses the minigap, and σ_{xx} has a larger peak. This is quite different from the characteristic feature of the experiments shown in Fig. 153. Experimentally σ_{yy} has a peak, while σ_{xx} has a W-shaped structure. Similar disagreements have been shown to exist also in the Shubnikov—de Haas oscillation and the dynamical conductivities describing the minigap absorption. The various anomalies in the transport coefficients associated

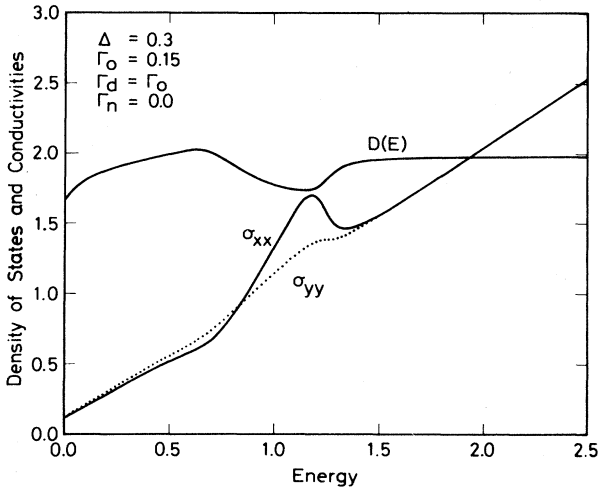

FIG. 158. An example of the density of states $D(E)$ and conductivities σ_{xx} and σ_{yy} calculated in a model system. The minigap lies between 0.7 and 1.3. After Ando (1979d).

with the existence of the minigap are very sensitive to the presence of intervalley scattering, which has been completely ignored. Figure 159 gives an example in the presence of intervalley scattering, i.e., in the case when 25% of the mobility is determined by intervalley scattering. The y component is not affected, but σ_{xx} now exhibits a W-shaped structure in agreement with experiments. Both the Shubnikov–de Haas oscillations and the dynamical conductivities are strongly modified by such intervalley scattering and now explain the experimental features. We see, therefore, that the existence of minigaps explains various characteristics of transport only if we assume the presence of a sizable amount of intervalley scattering at low temperatures. This suggests the existence of scatterers with short ranges of atomic scales in the inversion layer. It is not certain whether

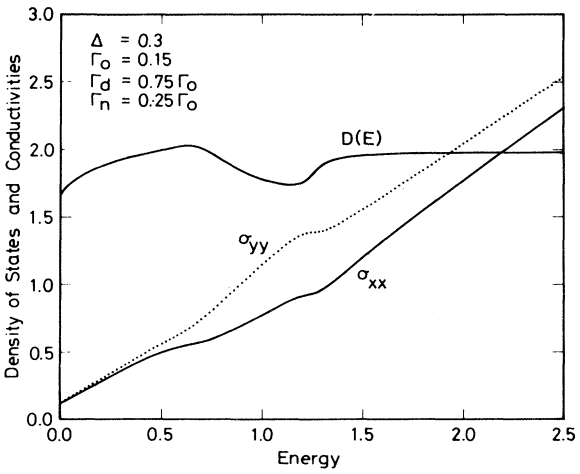

FIG. 159. An example of the density of states and conductivities calculated in a model system. A weak intervalley scattering has been included. After Ando (1979d).

such scatterers are inherent in interface conditions on tilted surfaces or common to all the different surfaces. Detailed experimental investigations of Shubnikov–de Haas oscillations in this system have been carried out by Matheson and Higgins (1982).

B. Valley degeneracy and stress effects

1. Valley degeneracy on Si(111) and (110)

As has been discussed in Sec. III, the multivalley structure of the conduction band of Si can give various valley degeneracy factors g_v on different surfaces. Constant-energy ellipsoids of the conduction band of Si are schematically illustrated in Fig. 5. The six valleys will be denoted by a, b, c, d, e, and f, following the notation of Kelly and Falicov (1977a). Sometimes we will call the valleys a and d 1 valleys and the valleys b and f 2 valleys. For the Si(100) geometry, valleys a and d (the 1 valleys) present their major axes and a high effective mass normal to the surface, while the other four have their major axes in the plane of the surface and present a lower normal effective mass. Consequently the ground subband consists of the 1 valleys on the (100) surface, giving $g_v=2$. All the experimental results have confirmed this expectation except for the existence of a small valley splitting arising from the deviation from the simple effective-mass approximation. A similar consideration gives $g_v=4$ and $g_v=6$ for the ground subband on the (110) and (111) surface, respectively. Until quite recently, however, all the experiments failed to observe any valley degeneracy factor other than $g_v=2$ on these surfaces. The puzzling problem of the valley degeneracy has excited much controversy.

Although experimental study on the Si (110) and (111) surfaces began simultaneously with that on the (100) surface, the low electron mobility has long prevented detailed investigation on those surfaces. The Shubnikov–de Haas effect was first reported by Lakhani and Stiles (1975a) and Neugebauer, von Klitzing, Landwehr, and Dorda (1975, 1976). These two groups found that $g_v=2$ on both surfaces. The degeneracy factor g_v was determined unambiguously from the Shubnikov–de Haas period by using the electron concentration which is proportional to an applied gate voltage and by the orbital degeneracy of the Landau level, $1/2\pi l^2$ with $l^2=c\hbar/eH$. Occupation of higher subbands was not observed for a wide range of electron concentration. The latter authors obtained the effective mass and the effective g factor by extending the usual method employed on the (100) surface. These quantities were shown to be enhanced and to decrease with increasing electron concentration. This behavior is essentially the same as on the (100) surface.

The relative energies of the valleys can be shifted in the presence of stresses, as is well known in the case of bulk samples. There can be built-in stress fields in an MOS structure. As a result of thermally grown SiO_2 on

Si, for example, stresses develop on cooling to room or lower temperature because of the different thermal expansion coefficients of Si and SiO_2 (and also of metallic gate electrode). However, such stresses caused by the thermal mismatch are known to be less than 10^8 dyn cm^{-2} (Jaccodine and Schlegel, 1966; Whelam *et al.*, 1967; Conru, 1976; Jacobs and Dorda, 1978) and are too small to account for the observed lifting of the valley degeneracy. Further, any stress fields along the plane of the interface cannot remove the degeneracy $g_v=4$ on the (110) surface. Therefore, such a macroscopic uniform stress mechanism can be ruled out for removal of the valley degeneracy.

Effects of uniaxial stresses applied externally were later studied on the (111) surface (Tsui and Kaminsky, 1976b; Dorda *et al.*, 1976). Occupation of other subbands was not observed even for stresses up to 2×10^9 dyn cm^{-2}. The mobility, which was isotropic in spite of $g_v=2$, became anisotropic in the presence of a stress. This anisotropy roughly corresponds to that estimated from the effective-mass anisotropy for the occupation of a single set of valleys.

Tsui and Kaminsky (1976b) proposed the existence of inhomogeneous stresses at the interface arising from mismatch between the Si—Si bonds in Si and Si—O—Si bonds in SiO_2. The interface is assumed to be divided into small domains of uniaxial stresses, and within each domain the uniaxial stress lowers two of the sixfold-degenerate subbands in energy. In this model the domains are supposed to be randomly oriented, and the mobility is isotropic in the absence of external stresses. When a uniaxial stress is applied to the sample, the domains with favorable stress directions grow, which causes mobility anisotropy.

Kelly and Falicov (1976, 1977a; see also Falicov, 1979) proposed that a large intervalley electron-electron interaction mediated by phonons could give rise to a broken-symmetry ground state with a valley degeneracy lower than the usual paramagnetic occupation of the sixfold and fourfold valley degeneracy on the (111) and (110) surface, respectively. This theory will be discussed in detail in a subsequent section. It was claimed that the so-called charge-density wave (CDW_β) state, in which the two "right-angle" valleys are coupled, giving two degenerate subbands ($g_v=2$), is realized on the (111) surface. Since there are three possible ways of coupling, this CDW_β state would lead to domain structure.

Extensive investigations were made on the problem of valley degeneracy by Dorda and co-workers (Dorda *et al.*, 1976, 1978, 1980; Eisele, 1978). They measured the mobility anisotropy and Shubnikov—de Haas oscillations carefully in the presence of various different uniaxial stresses. The valley degeneracy was always 2 throughout their investigations. However, the anisotropic mobility behaved just as expected from the usual electron transfer from the six valleys to an appropriate set of valleys with the increase of stress. It was concluded that the stress mechanism was unlikely because the valley degeneracy of 2 required local stresses much larger than the applied stress, whereas the behavior of the mobility suggested that local inhomogeneous stresses were of the same order as the applied stress. They also measured the temperature dependence of the anisotropic mobility and found a kinklike structure around $T\sim272$ K for $N_s=5.4\times10^{12}$ cm^{-2} on the (111) surface. They argued that this temperature corresponded to a critical temperature at which the first-order phase transition occured from the charge-density wave state to the usual paramagnetic state. This temperature was, however, almost independent of the strength of applied stresses, and much larger than a predicted critical temperature which is of the order of the Fermi energy.

Some information on the nature of the ground state can be obtained from intersubband optical absorptions. On the (111) and (110) surfaces the electron motions parallel and perpendicular to the surface are coupled with each other because of the anisotropic and tilted configuration of the valleys. Consequently intersubband transitions can be induced by an electric field parallel to the surface. In such a simple transmission geometry, the depolarization effect and exciton effect can be different from those in the usual transmission line geometry. Ando, Eda, and Nakayama (1977) have shown that the depolarization effect and a part of the exciton effect disappear when the state has a full symmetry, i.e., $g_v=6$ on the (111) surface and $g_v=4$ on the (110) surface. When electrons occupy only two opposite valleys under sufficiently strong stresses, on the other hand, the spectrum has been shown to be the same as that for the transmission line geometry. Nakayama (1978) examined resonance spectra of both geometries for possible models of the ground state on the (111) surface, i.e., the normal state ($g_v=6$), stress-induced states ($g_v=2$), and charge-density wave state with and without domain structure. A characteristic feature of the spectra was shown to depend on the symmetry of the ground state and the size of the domain in a complicated way. A comparison of the resonance line shapes in the different geometries can be used for distinguishing a possible ground state among those so far proposed. There has been some progress on this direction experimentally (Kamgar, unpublished; McCombe and Cole, 1980; Cole and McCombe, 1980). However, the results are still preliminary and no definite conclusion has been deduced so far.

2. Stress effects on Si(100)

When a compressional stress is applied, for example, along the [010] direction, the 2 valleys located in the same direction are lowered in energy with respect to the 1 valleys. Consequently the separation between E_0 and $E_{0'}$ becomes smaller. Tsui and Kaminsky (1975b, 1976a) found a change in the oscillation period at high electron concentrations in an unstressed sample and suggested occupation of higher subbands. In the presence of uniaxial compressional stresses such a period change was shown to occur at lower electron concentrations, which suggest-

ed the simultaneous occupation of E_0 and $E_{0'}$ subbands because of the decrease of their energy separation caused by stresses.

The electron transfer under stress provides an interesting theoretical problem, since electron-electron interactions are known to be important in our system. Takada and Ando (1978) studied this problem in the case when a compressional stress was applied in the [010] direction. They assumed variational wave functions of the type given by Eq. (3.34), with parameters b_1 for the 1 valleys and b_2 for the 2 valleys. The total energy E at a concentration N_s and under a given stress characterized by the energy splitting of the 1 and 2 valleys in the bulk was calculated as a function of b_1, b_2, N_1, and N_2, where N_1 and N_2 are concentrations for the corresponding valleys ($N_1+N_2=N_2$). The parameters b_1 and b_2 were determined so as to minimize $E(b_1,b_2,N_1,N_2)$ at a given N_1, and the resulting energy was then minimized with respect to N_1. This procedure is a natural extension of the method described in Sec. III.A, where only a single subband is considered. Kawaji, Hatanaka, Nakamura, and Onga (1976) discussed the subband structure of silicon on sapphire in the Hartree approximation using this method and assuming the wave functions of the type given by Eq. (3.25). Takada and Ando extended this method to higher approximations such as the Hartree-Fock and random-phase approximation. This approach has the merit of being able to describe the change in the electron density distribution caused by exchange and correlation effects, which could be included in the perturbation method considered by Vinter (1975a, 1976) and by Ohkawa (1976a, 1976b) only if intersubband mixings are taken into account. As a matter of fact, it gives a density distribution of electrons in good agreement with the results of the density-functional calculation (Ando, 1976a, 1976b) in the single-subband case.

An example of the calculated "phase diagram" is shown in Fig. 160, where the stresses at which the electron transfer begins or ends are plotted against the electron concentration. The Hartree approximation (the dotted lines) always predicts a continuous electron transfer and also a large range of the stress where electrons occupy both the 1 and 2 valleys. This is related to the Fermi-level "pinning" which occurs when a higher subband having a large spatial extent begins to be occupied, as has been discussed in Sec. III.A. The Hartree-Fock approximation gives an abrupt first-order transfer between the two sets of valleys up to $N_s \sim 1\times10^{12}$ cm^{-2}. Even above $N_s \sim 10^{12}$ cm^{-2} there are jumps in N_1 and N_2 at the beginning and the end of the transfer. When the correlation is included in the random-phase approximation, the region of the abrupt transfer is reduced to below $N_s \sim 2\times10^{11}$ cm^{-2} since the correlation greatly reduces the exchange effect.

Vinter (1979b) studied the same problem in the density-functional formulation. He extended the approximation scheme used by Ando (1976a, 1976b) to the case when electrons occupy both the 1 and 2 valleys. The exchange-correlation potentials for the 1 and 2 valleys

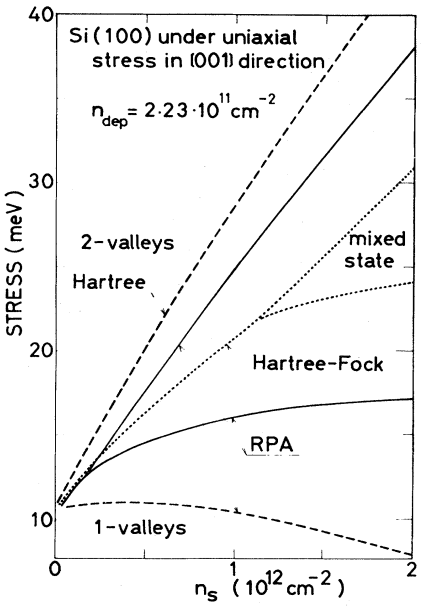

FIG. 160. A phase diagram in an n-channel inversion layer on a Si(100) surface under uniaxial compressional stresses in the Hartree, Hartree-Fock, and random-phase approximations. The mixed state shows the coexistent region of the two kinds of valleys. After Takada and Ando (1978).

can differ from each other and were chosen to be the exchange-correlation part of the chemical potential of those electrons in a uniform electron gas with the local electron densities $n_1(z)$ and $n_2(z)$. This procedure is similar to the spin-density-functional formalism for a spin-polarized system (von Barth and Hedin, 1972; Gunnarson and Lundqvist, 1976). The results were shown to be in reasonable agreement with those calculated by Takada and Ando with a different method. Tews (1978) has presented a calculation of the subband structure within a quite simplified approximation.

Experimental piezoresistance study started quite early (Dorda, 1970, 1971a, 1971b; Dorda *et al.*, 1972a, 1972b; Dorda, Friedrich, and Preuss, 1972; Dorda and Eisele, 1973; see also Dorda, 1973). Following this pioneering work, the study of stress effects was continued by Dorda and co-workers. They employed two methods in applying stresses to MOS transistors: Narrow slabs containing one row of devices were mounted on one side, whereas the other free end was bent upwards or downwards, giving rise to uniaxial compression or tension at the surface. This method could produce stresses up to $|P| \sim 3.2\times10^9$ dyn cm^{-2} in the [010] direction. Larger mechanical pressure was achieved by direct compression ($|P| \sim 5\times10^9$ dyn cm^{-2}). Using bulk deformation constants, values of $\Delta/P \sim 8.4\times10^{-9}$ meV dyn cm^{-2} were obtained where Δ is the difference of the bottoms of the 1 and 2 valleys.

The effective mass was determined from the usual temperature dependence of the amplitude of the Shubnikov–de Haas oscillation and found to increase

considerably with applied compressional stresses in the [010] direction (Eisele *et al.*, 1976a, 1976b). A later more systematic investigation revealed that it varied from $0.2m_0$ to $0.45m_0$ sharply with stress at sufficiently low electron concentrations like $N_s < 10^{12}$ cm^{-2} (Eisele *et al.*, 1977). The latter $0.45m_0$ is close to theoretically predicted $0.42m_0$ of the 2 valleys. This seemed to suggest that the complete electron transfer really takes place under stresses. No clear indication of simultaneous occupation of the four valleys was observed, although the oscillation amplitude became extremely small around the crossover stresses.

The Shubnikov–de Haas effect was also studied by Englert *et al.* (1978). The valley degeneracy was again found to remain 2 for stresses up to $P \sim 3.3 \times 10^9$ dyn cm^{-2}, although some disturbance of the phase was observed for moderate stresses and electron concentrations. They could not observe change in the period even at high concentrations similar to that found by Tsui and Kaminsky (1975b). Instead, the conductivity exhibited a phase shift of the oscillation by an amount of π in comparison with the phase in the absence of stress. This was attributed to a result of the mass increase from $0.2m_0$ to $0.45m_0$ mentioned above, which makes the spin splitting larger than half of the Landau-level separation and can cause the phase change, as has been discussed in Sec. VI.B in connection with effects of tilted magnetic fields.

Relaxation times and mobilities in the presence of stresses have also been studied (Eisele *et al.*, 1976c; Dorda *et al.*, 1978; Gesch *et al.*, 1978). Details will not be discussed, as they are contained in the review by Eisele (1978). Here, we note the result of Gesch, Eisele, and Dorda (1978), who measured the field-effect mobility defined by $\mu_{FE} = \partial\sigma / e\partial N_s$ as a function of uniaxial compressional stress in the [010] direction. Usually μ_{FE} increases rapidly and then decreases slowly with N_s in the absence of stresses. With increasing stresses the peak N_s was found to be shifted to higher electron concentrations and then μ_{FE} had a double-peak structure as a function of the electron concentration. This behavior was related to the electron transfer effect. Assuming that $E_0 \sim E_{0'}$ around the dip position Gesch *et al.* estimated $E_{0'0}$ in the absence of a stress. They showed that the estimated values coincided with the corresponding theoretical result of Ando (1976b).

Takada (1979) studied the mobility under stress theoretically, assuming simultaneous occupation of the E_0 and $E_{0'}$ subbands. It was shown that the mobility of electrons in the $E_{0'}$ subbands limited by surface roughness and charged centers in the oxide increased considerably (more than a factor 10) when electrons occupied both the subbands. He suggested the importance of other kinds of scatterers, and especially neutral impurities, as a candidate. The results qualitatively explain the observed behavior. See also Sec. IV.C.3 for more discussion on related problems.

The calculations by Takada and Ando (1978) and by Vinter (1979b) show that as soon as both subbands contain electrons, the Fermi energy is almost pinned to the $E_{0'}$ subband, and for all practical purposes the number of electrons in the $E_{0'}$ stays constant, especially at relatively low concentrations. Thus only the electrons that go into the E_0 subband show up in the Shubnikov–de Haas oscillations in a "gate voltage sweep." This could explain why only a single period is seen in the N_s sweep, why a change of phase upon increasing the electron concentration at higher stresses was observed by Englert *et al.* (1978), and why only the mass corresponding to the $E_{0'}$ subband or the one corresponding to the E_0 can be determined from the temperature dependence of the oscillation amplitude. In a magnetic sweep at a constant N_s, however, one usually expects that two periods in $1/H$ should show up, or at least the period observed corresponding to one of the systems should change with pressure because of the change in the population of that subband system. No evidence of this was seen experimentally (Eisele *et al.*, 1976b; Eisele, 1978).

Large compressional stresses can also be produced on MOSFETs made by silicon grown on sapphire films. A large difference in thermal expansion coefficients causes a large lateral (anisotropic) stress in the Si films on cooling from the deposition temperature. Various properties, such as anisotropies in the electron mobility, elastoresistance, and magnetoresistance, were studied and explained by the anisotropic two-dimensional dispersion relation corresponding to the two valleys with the density-of-states effective mass $m_d \sim 0.42m_0$ which were lowered in energy due to the stress.

Kawaji, Hatanaka, Nakamura, and Onga (1976) observed a hump in the electron mobility versus gate voltage curves in n-channel layers on silicon on $(\bar{1}012)$ Al_2O_3. The hump was attributed to electron population of the usual E_0 subband with increasing N_s. The Shubnikov–de Haas effect was also studied (Hatanaka *et al.*, 1978; see also Kawaji, 1978). Considering that $\hbar\omega_c \sim 2\mu_B H$, they assumed that each peak did not have a spin degeneracy and concluded that the ground subband consisted of the fourfold-degenerate 2 and 3 valleys. Later experiments in tilted magnetic fields (von Klitzing *et al*, 1977; Hatanaka *et al.*, 1978; Englert, Landwehr, Pontcharra, and Dorda, 1980) revealed, however, that each peak consisted of two Landau levels of electrons with different spins (i.e., $g_v = 2$). This was considered to be due to the enhancement of the g factor caused by the exchange effect. An enhancement of the g factor similar to that in the absence of a stress gives $g^*\mu_B H \sim \hbar\omega_c$, which predicts that each peak consists of the $(N, \downarrow)$ and $(N+1, \uparrow)$ levels, and that the total degeneracy of the ground Landau level should be a half of that of higher Landau levels. A careful examination of the oscillation period by Wakabayashi, Hatanaka, and Kawaji (1979) showed, however, that the ground Landau level had the same degeneracy as others, which let them choose a different model in which $g^*\mu_B H \sim 2\hbar\omega_c$. This model gave an extremely large value of the g factor. The oscillation amplitude became extremely small near the electron concentration corresponding to the mobility hump. Again,

no clear change in the oscillation period was observed.

More information can be obtained from cyclotron resonance experiments. Before going into a discussion of stress effects, let us consider the cyclotron resonance at high temperatures in the absence of a stress, since the increase of the temperature causes electron occupation of the $E_{0'}$ subband and is expected to give rise to effects similar to those of compressional stresses. Küblbeck and Kotthaus (1975; see also Kotthaus and Küblbeck, 1976) obtained a surprising result on the temperature dependence of the cyclotron resonance in the absence of external stresses. An example of their results is shown in Fig. 161. The cyclotron mass deduced from the peak position and the broadening increased drastically with increasing temperature. The temperature effect was shown to be enormous at low electron concentrations and to become smaller with increasing concentration. Around $N_s \sim 10^{12}$ cm^{-2}, for example, the effective mass increased by as much as 30% between 4.2 and 65 K. In intersubband optical transitions under similar conditions, Kneschaurek and Koch (1977) found a new transition, suggesting the population of the $E_{0'}$ subband. Naively this would lead to two cyclotron resonances corresponding to $m_c \sim 0.2m_0$ and $0.42m_0$. However, the cyclotron resonance experiment showed only a single peak which shifted to the high magnetic field side with increasing temperature.

Cyclotron resonance under stress was investigated by Stallhofer, Kotthaus, and Koch (1976). They failed to see two peaks, even under their largest compressional stresses, but observed only a single peak which exhibited an increase of the cyclotron mass with decreasing electron concentration, as at high temperatures. The mass became as large as $0.42m_0$, the effective mass of the $E_{0'}$ subband, at sufficiently low concentrations. They also found a peculiar behavior of the line narrowing at low concentrations under the influence of stresses.

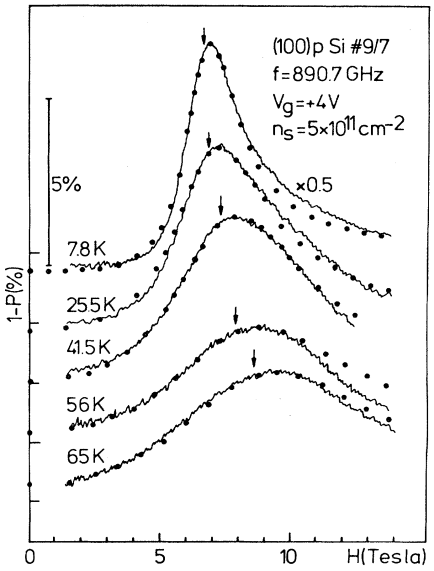

FIG. 161. Cyclotron resonance in an n-channel inversion layer on a Si(100) surface at different temperatures for $N_s \sim 5\times 10^{11}$ cm^{-2}. The dots are fits of the classical expression to the line shape. Values for m_c/m_0 of 0.210, 0.217, 0.232, 0.252, and 0.272, and for $\omega\tau_{\rm res}$ of 6, 3.2, 2.5, 2, and 1.8 were obtained for temperatures of 7.8, 25.5, 41.5, 56, and 65 K, respectively. The corresponding values of the resonance magnetic field are marked by arrows. After Küblbeck and Kotthaus (1975).

In systems consisting of two kinds of electrons with different masses, Kohn's theorem is no longer valid and electron-electron interactions can directly modify the cyclotron resonance positions. Takada and Ando (1978) calculated the dynamical conductivity $\sigma_{xx}(\omega)$ in Landau's Fermi-liquid theory and studied such effects. Effects of electron-electron scatterings on relaxation times were neglected. They found that the resonance peaks for corresponding electrons were both shifted to the higher magnetic field side (mass enhancement). Further, the peak shift for electrons with a lower mass was shown to be much larger than that for electrons with a higher mass, and the resonance intensity was found to be modified by interactions in such a way that the intensity for electrons with a small mass was enhanced considerably. In the limit of strong interactions, there remains essentially a single peak which lies around a certain average of the positions of the original two peaks. This is a result of the fact that both kinds of electrons move in a correlated way when interactions are strong enough. With the use of the Fermi-liquid parameters calculated by the use of the subband structure discussed previously, they calculated the resonance line shape under stress. They demonstrated that the line shape could behave as if it had a single peak which shifted from the positoin corresponding to the 2 valleys to that corresponding to the 1 valleys with increasing N_s at a fixed stress when the line broadening was large enough ($\omega\tau \sim 2$). This qualitatively explains the observed behavior of the cyclotron resonance under stress, but quantitatively stronger electron-electron interactions were shown to be needed to fully account for the experiments.

Appel and Overhauser (1978) proposed an alternative effect of electron-electron scattering on the cyclotron resonance. They calculated the dynamical conductivity using kinetic equations for the total currents J_1 and J_2 of electrons of the 1 and 2 valleys, respectively. In addition to the ordinary scattering term $-J_i/\tau$ ($i=1,2$) describing effects of impurity scattering, they added a term characterized by an electron-electron collision time τ_e. This new scattering term, which makes each carrier relax to a common velocity, was first proposed by Kukkonen and Maldague (1976) and arises because scattering among electrons with different masses does not preserve the total velocity. This τ_e was shown to make the resonance peaks for the two kinds of electrons come closer together, and to merge into a single peak in the limit of short τ_e, because the scattering reduces the relative velocities of their cyclotron motions. The collision rate $1/\tau_e$ is proportional to $(k_BT)^2+(\hbar\omega/2\pi)^2$ at low temperatures and for a small frequency, ω, of an external field because of the presence of the sharp Fermi surfaces. This effect

is, therfore, independent of that studied by Takada and Ando (1978), which does not vanish in the limit of small T and ω. Appel and Overhauser made a rough estimate of τ_e using an expression for a three-dimensional system and claimed that both the temperature effect of Kùblbeck and Kotthaus (1975) and the stress effect at low temperatures could be explained by the similar electron occupation of the 1 and 2 valleys.

Takada (1980a) incorporated the two effects within a framework of the Fermi-liquid theory and investigated the relative importance of the above-mentioned two effects. He showed that $1/\tau_e$, if calculated more accurately, is one order of magnitude smaller than that estimated by Appel and Overhauser and is not important at low temperatures like $T<10$ K. It could become important at high temperatures like $T\sim 77$ K. As is well known, the Fermi-liquid theory is valid only when $\hbar\omega << E_F$ and $k_B T << E_F$, where E_F is a typical Fermi energy. However, these conditions were often not satisfied experimentally. Ting (1980) extended a memory-functional method used by Ganguly and Ting (1977) to the two-carrier system and calculated the dynamical conductivity to the lowest order in the Coulomb interaction between electrons of different valleys. Although the validity of such an approximation is not clear, he obtained essentially the same conclusion as that of Takada. Tzoar and Platzman (1979) calculated the high-frequency limit of the conductivity in the absence of a magnetic field and showed that effects of electron collisions could be represented by a frequency-dependent relaxation time. Then, they extended the results to a lower-frequency side by a phenomenological argument. The resulting expression was similar to that of Ting (1980), in which a magnetic field was set equal to zero. All the above-mentioned investigations treat a magnetic field semiclassically or neglect it completely, and the quantization of the orbital motion is completely neglected. Perhaps strong magnetic field effects might be most crucial under actual experimental conditions, since the cyclotron energy is comparable to the typical Fermi energy.

3. Kelly-Falicov theory

To explain the observed reduction of the valley degeneracy factor g_v on the Si(111) and (110) surfaces discussed previously, Kelly and Falicov (1976, 1977a) proposed a charge-density wave (CDW) ground state resulting from a large phonon-mediated intervalley electron exchange interaction. As an illustrated example let us consider a model Hamiltonian for a two-valley system (Paulus, 1978):

$$\begin{aligned}\mathscr{H}=&\sum_{k\sigma}[\varepsilon_a(\mathbf{k})a^+_{\mathbf{k}\sigma}a_{\mathbf{k}\sigma}+\varepsilon_b(\mathbf{k})b^+_{\mathbf{k}\sigma}b_{\mathbf{k}\sigma}]\\&+\tfrac{1}{2}V\sum_{kk'q\sigma\sigma'}(a^+_{\mathbf{k}\sigma}a_{\mathbf{k}-\mathbf{q}\sigma}+b^+_{\mathbf{k}\sigma}b_{\mathbf{k}-\mathbf{q}\sigma})\\&\times(a^+_{\mathbf{k}'\sigma'}a_{\mathbf{k}'+\mathbf{q}\sigma'}+b^+_{\mathbf{k}'\sigma'}b_{\mathbf{k}'+\mathbf{q}\sigma'})\\&+U\sum_{kk'q\sigma\sigma'}a^+_{\mathbf{k}\sigma}b_{\mathbf{k}'+\mathbf{q}\sigma}b^+_{\mathbf{k}'\sigma'}a_{\mathbf{k}-\mathbf{q}\sigma'}\ .\end{aligned}\tag{7.50}$$

Here, $a^+_{\mathbf{k}\sigma}$ and $b^+_{\mathbf{k}\sigma}$ are the creation operators for electrons in valleys a and b, respectively, and the wave vector $\mathbf{k}$ is measured from each valley minimum. The second term proportional to V represents the usual Coulomb repulsion, and the last term describes an intervalley interaction introduced by Kelly and Falicov. Usually this term is extremely small for the Coulomb interaction, since it includes a large momentum transfer. Kelly and Falicov assumed that U arose from a phonon-mediated interaction, as discussed by Cohen (1964), and took a large negative value.

Let us consider the stability of a charge-density wave state in the unrestricted Hartree Fock approximation. The charge-density wave state is characterized by the nonvanishing expectation value of the product $a^+_{\mathbf{k}\sigma}b_{\mathbf{k}\sigma}$ and $b^+_{\mathbf{k}\sigma}a_{\mathbf{k}\sigma}$. In the Hartree Fock approximation

$$\begin{aligned}\mathscr{H}=&\sum_{k\sigma}[\varepsilon_a(\mathbf{k})a^+_{\mathbf{k}\sigma}a_{\mathbf{k}\sigma}+\varepsilon_b(\mathbf{k})b^+_{\mathbf{k}\sigma}b_{\mathbf{k}\sigma}\\&-V^*\sum_{k\sigma}(a^+_{\mathbf{k}\sigma}b_{\mathbf{k}\sigma}+b^+_{\mathbf{k}\sigma}a_{\mathbf{k}\sigma})+2\Delta^2V^*\ ,\end{aligned}\tag{7.51}$$

with

$$\Delta=\sum_k\langle b^+_{\mathbf{k}\sigma}a_{\mathbf{k}\sigma}\rangle\ ,\tag{7.52}$$

where $V^*=V-2U$, and we have neglected unimportant terms which contain the usual $\langle a^+_{\mathbf{k}\sigma}a_{\mathbf{k}\sigma}\rangle$ or $\langle b^+_{\mathbf{k}\sigma}b_{\mathbf{k}\sigma}\rangle$ and assumed that Δ is real. Further, we assume that

$$\varepsilon_a(\mathbf{k})=\varepsilon_b(\mathbf{k})=\frac{\hbar^2}{2m}k^2=\varepsilon(k)\ ,\tag{7.53}$$

for simplicity. The term "charge-density wave" stems from the fact that the state with a nonvanishing Δ gives rise to an electron density which varies spatially with a wave vector given by the difference of the positions of the two valleys in the two-dimensional $\mathbf{k}$ space. In terms of the bonding and antibonding combinations,

$$\alpha_{\mathbf{k}\sigma}=\frac{(a_{\mathbf{k}\sigma}+b_{\mathbf{k}\sigma})}{\sqrt{2}};\quad \beta_{\mathbf{k}\sigma}=\frac{(a_{\mathbf{k}\sigma}-b_{\mathbf{k}\sigma})}{\sqrt{2}}\ ,\tag{7.54}$$

we have

$$\begin{aligned}\mathscr{H}=&\sum_{k\sigma}[\varepsilon(k)-\Delta V^*]\alpha^+_{\mathbf{k}\sigma}\alpha_{\mathbf{k}\sigma}\\&+\sum_{k\sigma}[\varepsilon(k)+\Delta V^*]\beta^+_{\mathbf{k}\sigma}\beta_{\mathbf{k}\sigma}+2\Delta^2V^*\ ,\end{aligned}\tag{7.55}$$

with

$$\Delta=\tfrac{1}{2}\sum_k[\langle\alpha^+_{\mathbf{k}\sigma}\alpha_{\mathbf{k}\sigma}\rangle-\langle\beta^+_{\mathbf{k}\sigma}\beta_{\mathbf{k}\sigma}\rangle]\ .\tag{7.56}$$

Introduce the Fermi energy E_F in the case of vanishing Δ, i.e., $N_s=2(2m/2\pi\hbar^2)E_F$. Then the total energy becomes

$$\begin{aligned}E=&\frac{2m}{2\pi\hbar^2}\left[E_F^2-\left[1-\frac{2\pi\hbar^2}{mV^*}\right]\Delta^2V^{*2}\right]\quad(\Delta V^*<E_F)\ ,\\=&\frac{2m}{2\pi\hbar^2}\left[\left[2-\frac{mV^*}{2\pi\hbar^2}\right]E_F^2\right.\\&\left.+\frac{2\pi\hbar^2}{mV^*}\left[\Delta V^*\frac{mV^*}{2\pi\hbar^2}E_F\right]^2\right]\quad(\Delta V^*>E_F)\ .\end{aligned}\tag{7.57}$$

This gives $\Delta=0$ for $\delta<1$ and $\Delta=(m/2\pi\hbar^2)E_F$ for $\delta>1$, where $\delta=mV^*/2\pi\hbar^2$ is a dimensionless coupling constant. One sees, therefore, that the first-order transition from the usual paramagnetic ground state to the charge-density wave state occurs at $\delta=(m/2\pi\hbar^2)(V-2U)=1$. In the charge-density wave state only the bonding state (α) is occupied by electrons, since the $2\Delta V^*$ is larger than $2E_F$, which means the reduction of the valley degeneracy. At finite temperatures, on the other hand, the transition is of the second order. The gap equation (7.56) becomes

$$\Delta=\frac{\delta}{2}k_BT\ln\frac{1+\exp[(\Delta V^*+\mu)/k_BT]}{1+\exp[(-\Delta V^*+\mu)/k_BT]}\ , \tag{7.58}$$

where μ is the chemical potential. This critical temperature T_c is given by the condition that (7.58) does not have a solution except $\Delta=0$, and becomes

$$k_BT_c=-E_F/\ln\left[1-\frac{1}{\delta}\right]\ . \tag{7.59}$$

This shows that the critical temperature is always of the order of the Fermi energy except in the vicinity of $\delta=1$.

In actual inversion layers on the (111) surface the problem is slightly more complicated. The model Hamiltonian is given by

$$\begin{aligned}\mathcal{H}=&\sum_{k\sigma}[\varepsilon_a(\mathbf{k})a^+_{\mathbf{k}\sigma}a_{\mathbf{k}\sigma}+\cdots]\\&+\sum_{qkk'\sigma\sigma'}\tfrac{1}{2}V[a^+_{\mathbf{k}\sigma}a_{\mathbf{k}-q\sigma}+\cdots][a^+_{\mathbf{k}'\sigma'}a_{\mathbf{k}'+\mathbf{q}\sigma'}+\cdots]\\&+\sum_{qkk'\sigma\sigma'}U_\alpha[a^+_{\mathbf{k}\sigma}d_{\mathbf{k}'+\mathbf{q}\sigma}d^+_{\mathbf{k}'\sigma'}a_{\mathbf{k}-\mathbf{q}\sigma'}+\cdots]\\&+\sum_{qkk'\sigma\sigma'}U_\beta[a^*_{\mathbf{k}\sigma}b_{\mathbf{k}'+\mathbf{q}\sigma}b^+_{\mathbf{k}'\sigma}a_{\mathbf{k}-\mathbf{q}\sigma'}+\cdots]\ ,\end{aligned} \tag{7.60}$$

where the first term is the kinetic energy of electrons of the 6 valleys (*a*, *b*, *c*, *d*, *e*, and *f*), the second term represents the usual intravalley term dominated by the Coulomb repulsion, the third the intervalley exchange between the valleys along the same axis, and the last between the valleys at right angles to each other. The last two terms are assumed to be attractive phonon-mediated interactions (U_α, $U_\beta<0$). In the above Hamiltonian four-valley terms such as a^+bd^+e, etc., which are considered to have the same order of magnitude as a^+bb^+a, are neglected.

Kelly and Falicov examined the total energy of various less exotic states of the above Hamiltonian in the unrestricted Hartree-Fock approximation (both for positive and negative U's for completeness). It was shown that there were two types of charge-density wave states, driven by U_α and U_β. The CDW$_\alpha$ solution couples two opposite valleys, pushing one below the Fermi level, while the other four valleys remain uncoupled and unoccupied. It is characterized by a nonvanishing correlation $\Delta_{ad\uparrow}=\pm\Delta_{ad\downarrow}=N_s/4$ and the occupation number $A_\sigma=D_\sigma=N_s/4$, where

$$\Delta_{ad\sigma}=\sum_k\langle a^+_{\mathbf{k}\sigma}d_{\mathbf{k}\sigma}\rangle,\quad A_\sigma=\sum_k\langle a^+_{\mathbf{k}\sigma}a_{\mathbf{k}\sigma}\rangle,\ \text{etc.} \tag{7.61}$$

The valley degeneracy factor becomes unity. The CDW$_\beta$ state couples four valleys into two pairs, pushing two below the Fermi level while the remaining two valleys are uncoupled and unoccupied. It has the occupation multiplicity of 2 and is characterized by

$$\begin{aligned}&\Delta_{bf\uparrow}=\pm\Delta_{bf\downarrow}=\Delta_{ce\uparrow}=\pm\Delta_{ce\downarrow}\ ,\\&B_\sigma=C_\sigma=E_\sigma=F_\sigma=N_s/8\ .\end{aligned} \tag{7.62}$$

Examples of the phase diagrams as a function of U_β and V are shown in Fig. 162 for several different values of U_α/U_β. The phase diagrams depend strongly on the ratio U_α/U_β. According to Cohen (1964), the phonon-mediated electron-electron interaction U varies as $(\omega_{\Delta\mathbf{k}})^{-2}$, where $\omega_{\Delta\mathbf{k}}$ is the appropriate phonon frequency of the wave vector equal to the intervalley $\mathbf{k}$ vector. By using both the selection rules of Lax and Hopfield (1961) and the phonon spectrum of Martin (1969), Kelly and

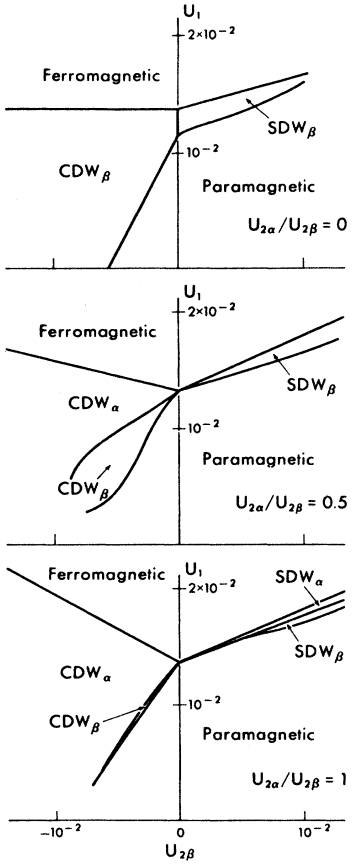

FIG. 162. Phase diagram for Si(100) inversion layer ground state. U_1, $U_{2\alpha}$, and $U_{2\beta}$ correspond to V, U_α, and U_β, respectively, in the text. U_1, $U_{2\alpha}$, and $U_{2\beta}$ are given in a unit of 10^{-12} eV cm^{-2}. SDW means spin-density wave states. After Kelly and Falicov (1977a).

Falicov estimated U_α/U_β to be somewhat less than unity. Keeping the observed $g_v=2$ in mind, they suggested that the sample was in the CDW_β regime for the actual experimentally accessible range of N_s.

In the CDW_β phase, the C_{3v} symmetry of the (111) surface is reduced to mirror symmetry, and domains of different CDW_β solutions, each with just one of the three possible $\mathbf{q}$ vectors, should appear. Consequently the transport properties will be isotropic for random distribution of such domains, and the anisotropy will appear under uniaxial stress as just one density-wave domain is preferentially driven. Therefore the existence of the CDW_β state can explain the main features of the experimental findings on the (111) surface.

The CDW_β causes various other effects. Since the two valleys with different effective masses are coupled, the Fermi line is distorted and the density-of-states effective mass at the Fermi level is enhanced. Further, this distortion allows optical transitions from the bonding to antibonding states in an electric field parallel to the surface (Kelly and Falicov, 1977b). Drew (1978) suggested the appearance of harmonics in the cyclotron resonance at $\omega=(2n+1)\omega_c$, with n being an integer.

On the Si(110) surface the two-dimensional effective-mass tensors for the four heavy-normal-mass valleys are identical, and the possible density-wave solutions, while they alter the occupied valley degeneracy, do not affect the effective masses. The nonvanishing intervalley correlations, Δ_{ab} for example, merely split the bands rigidly apart. The simple model considered above is applicable to this surface. The phase of the paramagnetic occupation of two valleys ($g_v=2$) becomes stable for values of U_α and U_β corresponding to the CDW_β phase on the (111) surface, thus explaining the observed $g_v=2$ on the (110) surface. A similar model was also applied to various surfaces of Ge and GaP where the conduction-band minima possess different symmetries (Kelly and Falicov, 1977c).

On the Si(100) surface a similar consideration predicts the usual ground state with $g_v=2$ (Kelly and Falicov, 1976, 1977a). When the energies of the 1 and 2 valleys are close to each other under a uniaxial compressional stress in the [010] direction, two valleys, a and b for example, can be coupled into bonding and antibonding combinations, and it becomes favorable to establish a charge-density wave ground state if the intervalley interaction U_β is sufficiently strong. This stress-induced CDW was proposed by Kelly and Falicov (1977d, 1977e, 1978) to account for various anomalous behaviors of the experiments mentioned earlier. The application of the previous theory is straightforward. The only difference is that one is now dealing with the coupling of two valleys having different normal effective masses and has to consider the change in the wave functions for electron motion in the z direction normal to the surface. Kelly and Falicov assumed the same envelope function of the form given by Eq. (3.25) for both kinds of valleys and minimized the total energy calculated in the unrestricted Hartree-Fock approximation with respect to the variational parameter.

Kelly and Falicov assumed extremely large values of V ($V\sim 54\times 10^{12}\ \mathrm{cm}^{-2}\,\mathrm{meV}$), for which a discontinuous first-order transition always takes place between the 1 valleys and 2 valleys, even for vanishing U's. Their results show as a function of the stress a first-order transition from paramagnetic occupation of the 1 valleys to a charge-density wave state and a second-order transition from the charge-density wave state to paramagnetic occupation of the 2 valleys for sufficiently large values of U_α and U_β (comparable to V). Correspondingly the effective mass changed discontinously from $\sim 0.2m_0$ to intermediate values and then continuously to the high effective mass $\sim 0.42m_0$. If we look at the effective mass as a function of the electron concentration under stress, the effective mass remains $\sim 0.42m_0$ till some electron concentration which depends on stress, decreases continuously, and then drops discontinuously to $\sim 0.2m_0$. Throughout these transitions the occupied valley degeneracy remains 2. Similar phase changes were shown to occur as a function of temperature (Kelly and Falicov, 1977e, 1978). With increasing temperature at a constant stress and electron concentration, electrons occupied the 2 valleys as well, even if they were only in the 1 valleys at zero temperature. At sufficiently high temperatures the number of electrons in the 2 valleys could become much larger than that of electrons in the 1 valleys because of the difference in their effective masses. It was demonstrated that for certain values of stress and the electron concentration successive transitions similar to those which occur as a function of stress could take place as a function of temperature. These results seem to explain at least qualitatively the experimental results of the temperature and stress dependence of the cyclotron resonance (Küblbeck and Kotthaus, 1975; Stallhofer *et al.*, 1976). Effects of strong magnetic fields were studied and shown to modify the phase boundary slightly (Kelly and Falicov, 1977f).

Some additional work was subsequently done on the properties of charge-density wave states. Nakayama (1978) suggested the so-called triple charge-density wave as a possible ground state on the Si(111) surface. This state is characterized by nonvanishing correlations, $\Delta_{ac\sigma}=\Delta_{ce\sigma}=\Delta_{ea\sigma}$ and $\Delta_{bd\sigma}=\Delta_{df\sigma}=\Delta_{fb\sigma}$. This was briefly treated by Kelly and Falicov (1977a) and claimed to be unstable with respect to the CDW_α and/or CDW_β states. Actually, however, the state can be lower in energy than the other states. It also has $g_v=2$. Since the trigonal symmetry of the surface is retained, one need not assume the existence of a domain structure to explain the observed isotropic conductivities. On the other hand, Kelly (1978a) argued that the triple CDW state could easily be taken over by the CDW_β state in the presence of a small built-in stress. Effects of four-valley terms neglected in the Hamiltonian (7.60) were studied by Quinn and Kawamoto (1978) and by Kelly (1978a). Especially the former paper showed that the CDW_β and/or triple CDW states were more stabilized against the CDW_α state by their inclusion. Ono and Paulus

(1979) calculated low-lying collective excitations in the charge-density wave state within the simple two-valley model and found acoustic-phonon—like modes related to the phase oscillation of the charge-density wave and fluctuation of the population difference between the two valleys.

As we have seen, the Kelly-Falicov theory seems to explain qualitatively various anomalous and unexplained features of experimental results on the (111) and (110) surfaces and on the (100) surface under stresses. In spite of such a success the magnitude of the assumed parameters of the model Hamiltonian poses a serious problem. Kelly and Falicov (1976, 1977a) tried to estimate V assuming a three-dimensional screened Coulomb potential and leaving the screening constant as an adjustable parameter. This procedure is certainly not appropriate. There might be several different ways to estimate V from more elaborate treatment of the electron-electron Coulomb interaction discussed in Sec. II.F. One way is to note that the effective g factor calculated in the Hartree-Fock approximation from the Hamiltonian (7.50) for $U=0$ is given by

$$g^*=2\left[1-\frac{m}{2\pi\hbar^2}V\right]^{-1}. \tag{7.63}$$

A comparison of the above with the result of Sec. II.F. leads to the conclusion that $mV/2\pi\hbar^2$ lies between 0.3 and 0.4 for the electron concentration $1\times10^{12}\ \mathrm{cm}^{-2}<N_s<5\times10^{12}\ \mathrm{cm}^{-2}$ on the Si(100) surface. This gives $5<V<8\times10^{12}\ \mathrm{cm}^2\,\mathrm{meV}$, which is one order of magnitude smaller than that assumed by Kelly and Falicov (1977d, 1977e) to explain the stress effect on the (100) surface. For nonvanishing U_α the g factor is given by

$$g^*=2\left[1-\frac{m}{2\pi\hbar^2}(V+U_\alpha)\right]^{-1}, \tag{7.64}$$

on the (100) surface in the absence of stress. Therefore, the enhancement of the g factor is reduced if U_α is negative. If we consider the fact that the observed g factor is actually enhanced and is well explained by the conventional theory, we must place $|U_\alpha|$ as being much less than $5\times10^{12}\ \mathrm{cm}^2\,\mathrm{meV}$. Kelly (1978b) estimated the phonon-mediated intervalley interactions U_α and U_β in the bulk within a tight-binding formulation. The results are given by $U_\alpha\sim-0.11\times10^{12}\ \mathrm{cm}^2\,\mathrm{meV}$ and $U_\beta\sim-0.25\times10^{12}\ \mathrm{cm}^2\,\mathrm{meV}$, which are nearly two orders of magnitude smaller than the values necessary for the charge-density wave ground state. He suggested, however, that near the Si-SiO_2 interface phonon selection rules might be relaxed and the phonon-mediated interactions could be enhanced from the bulk values. Recently Kelly and Hanke (1981b) carried out a detailed calculation of the phonon-mediated electron-electron interaction and its enhancement near the Si-SiO_2 interface. They found the effect to be too weak to lead by itself to the density-wave effects predicted by Kelly and Falicov.

Beni and Rice (1979) argued that in Si all intervalley exchange interactions are negligible in comparison with the direct Coulomb interactions, on the ground that calculations of the electron-hole-liquid binding energy in bulk Si can be fully explained by neglecting intervalley exchange interactions. They compared the energy of the states with $g_v=6$ and 2 on the Si(111) surface and showed that the state with $g_v=6$ is lower in energy for usually accessible electron concentrations.

Although the smallness of the parameters makes the proposed charge-density wave ground state highly unlikely, a definite conclusion can be obtained only experimentally. The best way to check the existence of such a broken-symmetry ground state is to observe characteristic phenomena which appear only in the charge-density wave phase and not in the usual phase. The optical transitions between the bonding and antibonding states and the harmonics of the cyclotron resonances might be a good candidate.

4. Additional developments

In the last few years various experimental results have appeared which apparently contradict previous ones and are unfavorable to the Kelly-Falicov theory. Tsui and Kaminsky (1979, 1980) studied the Shubnikov—de Haas oscillations in a large number of MOSFETs on the Si(111) surface prepared under various experimental conditions. They observed the expected sixfold valley degeneracy in some devices fabricated in a way different from that for samples which showed $g_v=2$. The influence of uniaxial stress was also studied and the expected change in the valley degeneracy was observed. It was suggested that the previously observed $g_v=2$ was not an intrinsic effect caused by electron-electron interactions but more likely was related to the condition of the interface of the device. However, it is still unclear what the changes are at the Si-SiO_2 interface for different oxidation procedures and how such changes are related to the valley degeneracy of the electronic state of the inversion layer. The expected fourfold degeneracy has also been observed on the (110) surface (Stiles, 1980). Roos and Köhler (1980) argued that $g_v=2$ could not explain Shubnikov—de Haas oscillations observed on the (110) and (111) surfaces in tilted magnetic fields.

An attempt has been made to apply external biaxial stress on the (100) surface so that the four valleys of the heavy-mass band should be equally lowered and the expected fourfold degeneracy and mixed sixfold bands may be observed under favorable conditions (Fang, 1980). The desired isotropic biaxial stress was created by the differential expansion coefficient of the Si and a suitable epoxy. The situation is quite similar to that of silicon on sapphire except that the lateral stress on sapphire is anisotropic. Unfortunately, Fang failed to observe the fourfold degeneracy, possibly because of slight anisotropy of stress. However, he could study the heavy-mass band in detail in the highly compressed sample. A phase reversal of the Shubnikov—de Haas oscillation was observed at an electron concentration depending on temperature.

This was attributed to the N_s and temperature dependence of the exchange-enhanced g factor. As has already been discussed above in connection with the experimental results of Englert, Landwehr, von Klitzing, Dorda, and Gesch (1978), the spin splitting is larger than half of the Landau-level separation at low concentrations. At high electron concentrations the situation becomes just the opposite because of the decrease of the effective g factor. In a sample under moderate stress the Shubnikov–de Haas oscillation suggests occurrence of transitions at two different electron concentrations. The transition at lower concentration ($N_s \sim 1.9\times 10^{12}$ cm^{-2}) is accompanied by a small phase shift. The period remains unchanged by the transitions. The transition at higher concentration ($N_s \sim 4\times 10^{12}$ cm^{-2}) is accompanied by a small phase shift and the period is increased by about 15% after the transition. The latter transition is similar to the one previously observed by Tsui and Kaminsky (1975) and the former resembles that reported by Eisele *et al.* (1977). Both the phase and period change do not support the charge-density wave ground state.

Cyclotron resonance at elevated temperatures was also studied by Kennedy, Wagner, McCombe, and Tsui (1977). No appreciable temperature dependence of the cyclotron effective mass was observed, in contrast to the experiments of Küblbeck and Kotthaus (1975). The dependence of the cyclotron mass at high temperatures on the depletion charge was studied by Stallhofer, Miosga, and Kotthaus (1978). In the original experiments on the temperature dependence by Küblbeck and Kotthaus and on the stress dependence by Stallhofer, Kotthaus, and Koch (1976), the samples were continuously illuminated with band-gap radiation, and the local Fermi level at the interface was much higher than that in the bulk (the quasiaccumulation layer). It was demonstrated that the temperature dependence of the resonance position became smaller with increasing $N_{\rm depl}$ and disappeared in the large $N_{\rm depl}$ limit. These experiments strongly suggest that the change in the cyclotron effective mass with temperature is related to the occupation of the heavy-mass subband $E_{0'}$. Although the above mentioned experiments are not inconsistent with the charge-density wave ground state, the experimentally observed temperature dependence of the intersubband optical absorption spectrum cannot readily be interpreted within the framework of the Kelly-Falicov theory. Kneschaurek and Koch (1977) observed that with rising temperature a new peak grows and the resonance lines originating from the E_0 subband shift and diminish in amplitude. This behavior was attributed to the electron occupation of the $E_{0'}$ subband. The existence of two distinct resonance lines indicated at least the presence of two distinct types of electrons at high temperatures, contrary to the prediction of Kelly and Falicov.

The stress effect on the cyclotron resonance on Si(100) has been reexamined. Stallhofer, Kotthaus, and Abstreiter (1979) and Abstreiter, Stallhofer, and Kotthaus (1980) observed for the first time two distinct cyclotron resonance peaks under stress except at low carrier concentrations and high temperatures. The compression quoted by the earlier work (Stallhofer *et al.*, 1976) was found to be overestimated by a factor of 3. The cyclotron effective masses deduced from the resonance peaks agree well with the expected value for the E_0 subband but are more than 10% higher than predicted for the $E_{0'}$ subband. The dependence on the depletion charge was also studied and shown to be consistent with the expectation that $E_{0'0}$ increased with $N_{\rm depl}$. From the stress dependence of the relative population they extracted $E_{0'}-E_F$ in the absence of a stress as ~ 6 meV roughly independent of N_s. This number is smaller than theoretically predicted for an accumulation layer (Ando, 1976b), which is, however, consistent with the intersubband optical absorption spectrum at high temperatures (Kneschaurek and Koch, 1977). The electron concentration in a given subband can also be extracted from the period of the quantum oscillation of the cyclotron resonance, as has been discussed in Sec. VI.A. With increasing stress the quantum oscillation of the cyclotron resonance for the E_0 subband was found to increase in period (decrease in electron concentration). This change in the population of the E_0 subband agreed with the one obtained from the relative strength of the two peaks. The quantum oscillation was, however, observed to disappear under high stresses, possibly due to the existence of some inhomogeneities in the stress, and such comparison was not possible for a wide range of the stress.

These new observations can be well understood within the conventional theory, and completely contradict the Kelly-Falicov theory. The relative occupation of the 1 and 2 valleys extracted from the experiments is explained by the theoretical results of Takada and Ando (1978) and of Vinter (1979b), although one has to assume smaller $E_{0'0}$ for a given strength of stress. The shifts of the peaks when both kinds of valleys are occupied can be explained by the usual electron-electron interaction (Takada and Ando, 1978; Takada, 1980), and the behavior at high temperatures is consistent with the prediction of Appel and Overhauser (1978). Therefore, the cyclotron resonance under stress seems to be perfectly explainable without introducing the charge-density wave ground state. However, the problem of the valley degeneracy still remains unexplained. Gesch, Dorda, Stallhoffer, and Kotthaus (1979) measured the Shubnikov–de Haas oscillation on the same sample used for the cyclotron resonance under identical conditions and found that the oscillation period always gave a valley degeneracy of two. In order to reconcile the two contradicting experimental results, they suggested a domain model where the domain sizes were large enough for cyclotron orbits to exist, and in each domain only one of the subbands was occupied. Such a model is, however, highly doubtful if we consider the fact that the various characteristics of the cyclotron resonance are explained as has been mentioned above. Vinter and Overhauser (1980) suggested the possibility of explaining this valley degeneracy paradox in terms of the discreteness of the density of states in two dimensions. When the energy level is completely

discrete, the Fermi level is always pinned to some Landau levels, and the oscillation of the density of states is determined only by the degeneracy of Landau levels with the same energy. Therefore, slight lifting of the degeneracy of Landau levels associated with different sets of valleys can give rise to the valley degeneracy of 2 instead of 6 on Si(111). The argument is not convincing, however, since they must assume extremely narrow Landau-level width to explain the experimental results. The problem of the stress effect and the valley degeneracy remains open at present.

C. Electron lattice

1. Introduction

As first pointed out by Wigner (1934, 1938), the electron system will adopt a configuration of the lowest potential energy and crystallize into a lattice when the potential energy dominates the kinetic energy. In the Wigner lattice (or crystal, solid, etc.) each electron becomes localized about a lattice site. For a two-dimensional electron gas with a density per unit area $N_s=(\pi r_0^2)^{-1}$, the mean potential energy per electron becomes

$$\langle V\rangle=\frac{e^2}{r_0}=e^2\pi^{1/2}N_s^{1/2}\ . \tag{7.65}$$

At zero temperature (called the quantum regime) the kinetic energy becomes $\langle K\rangle=\pi N_s\hbar^2/2m$. Therefore crystallization will occur at sufficiently low concentrations. At sufficiently high temperatures (called the classical regime) the kinetic energy is given by k_BT and crystallization will occur at high concentrations. Usually the inversion layer at sufficiently low electron concentrations corresponds to the quantum regime, and the classical regime is hardly realizable. On the other hand, the electron system on liquid helium is in the classical regime.

We can get a qualitative picture of the shape and nature of the phase diagram by setting

$$\Gamma\equiv\frac{\langle V\rangle}{\langle K\rangle}\ , \tag{7.66}$$

the ratio of the average potential energy to the average kinetic energy, equal to a constant Γ_m along the melting curve. Figure 163 shows a phase diagram obtained by Platzman and Fukuyama (1974) in this way. At high temperatures, where $\langle K\rangle=k_BT$, the melting curve becomes

$$N_s=(\Gamma_m k_BT/\pi^{1/2}e^2)^2\ , \tag{7.67}$$

and at zero temperature the melting occurs at $N_s=N_c$ with

$$N_c=\frac{4m^2e^4}{\pi\hbar^4\Gamma_m^2}=\frac{4}{\pi a_B^2}\frac{1}{\Gamma_m^2}\ , \tag{7.68}$$

where $a_B=\hbar^2/me^2$. If we introduce $r_s=r_0/a_B$ as usual, we have $r_s=(\pi/4)^{1/2}\Gamma_m$ at the melting point.

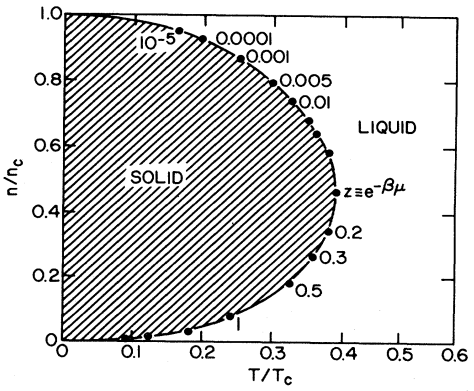

FIG. 163. Parametrized phase diagram of the two-dimensional system. The shaded region corresponds to the crystal phase. $n_c=4/\pi a_B^2\Gamma^2$. $k_BT_c=2e^4m/\hbar^2\Gamma^2$. After Platzman and Fukuyama (1974).

In the three-dimensional system the Wigner crystal is believed to have a body-centered cubic lattice (Fuchs, 1935), since it has the lowest static lattice energy among several possible lattice structures. There have been a number of different estimates of the critical r_s denoted by r_{sc} at which the "Wigner transition" is expected to occur at zero temperature. These estimates have varied over a wide range, say from 5 to 700. [See also a review paper by Care and March (1975) for more detailed discussion in three dimensions.] Wigner ascribed to each electron a fixed potential energy $-e^2/r_0$ and a zero-point energy $3\hbar\omega/2$, with $\omega^2=e^2/mr_0$ and compared their sum with the energy of the liquid phase calculated in the lowest order. He obtained $6\le r_{sc}\le 10$. Carr (1961) calculated the energy of the lattice state and obtained $r_{sc}\sim 5$ from the behavior of the lowest-order anharmonic contribution. Mott (1961), on the other hand, used as the zero-point energy that of a particle in a spherical cavity of radius r_0 and obtained $r_{sc}\sim 20$. The most common method of estimating r_{sc} is by using the Lindemann melting criterion, which states that melting will occur when the root-mean-square electron displacement $\langle u^2\rangle_{\rm av}$ is some fraction δ of the square of the intersite separation r_0. Nozières and Pines (1958) calculated $\langle u^2\rangle_{\rm av}$ on the assumption that only longitudinal vibrations at frequency ω_p with $\omega_p^2=4\pi ne^2/m$ contributed, and obtained $r_{sc}\sim 20$ for the known empirical value $\delta=\frac{1}{4}$. However, this method is very dependent on the choice of δ, as was pointed out by Coldwell-Horsfall and Maradudin (1960). As a matter of fact, we have $r_{sc}=\delta^{-4}/12$ in the Nozières-Pines theory, which gives $r_{sc}\sim 20$ for $\delta\sim\frac{1}{4}$ and $r_{sc}\sim 1$ for $\delta\sim\frac{1}{2}$. Further, the result also depends strongly on the way in which $\langle u^2\rangle_{\rm av}$ is determined. If we use the harmonic frequencies of Carr (1961), one has $r_{sc}\cong 6\delta^{-4}$, which gives $r_{sc}\sim 1536$ for $\delta\sim\frac{1}{4}$ and $r_{sc}\sim 96$ for $\delta\sim\frac{1}{2}$. Kugler (1969) obtained $r_{sc}\sim 21.9$, calculating the frequency of transverse phonons in the renormalized harmonic approximation (or self-consistent harmonic approximation). This approximation has been widely used in the calculation of the phonon spectra of rare gas solids

(see, for example, Koehler, 1966, 1968; Werthamer, 1969). Kugler then attempted to estimate the effects of anharmonicity not contained in the self-consistent harmonic approximation and found that deviations from the harmonic result could become important at much higher values of r_s, i.e., around $r_s \sim 700$. De Wette (1964) estimated that r_{sc} lay between 47 and 100 by a criterion for the appearance of bound states for an electron in a single-particle potential well. This criterion was later reexamined by Van Horn (1967) to give $r_{sc} \sim 27$. Isihara (1972) obtained $r_{sc} = 14.4$ by the Padé approximant interpolation of the ground-state energy. More recently Shore, Zaremba, Rose, and Sander (1979) used a density-functional theory and obtained $r_{sc} \sim 26$ from the condition that a nonuniform electron distribution in a Wigner-Seitz sphere becomes stable. Such a wide variation of predicted critical r_s reflects the difficulty of the problem, and the whole subject of the transition density remains rather open.

In the two-dimensional system the problem becomes more difficult since the meaning of the two-dimensional crystal is not well understood yet. Peierls (1935) has shown that thermal motion of long-wavelength phonons will destroy the long-range crystalline order of a two-dimensional solid in the sense that the mean-square deviation of an atom from its equilibrium position increases logarithmically with the size of the system, and Bragg peaks of the diffraction pattern are broad instead of sharp. The absence of long-range order of the conventional form has been proved by Mermin (1968) with the use of rigorous Bogoliubov's inequalities. He has suggested, however, that the thermal motion does not necessarily destroy the correlation in orientation of crystal axes at large distances.

Kosterlitz and Thouless (1973) proposed that the melting is associated with a transition from an elastic to a fluid response to small external shear strains, i.e., the solid phase supports a long-wavelength transverse phonon, but the fluid phase does not. As a criterion for such a solid-liquid phase transition, they proposed a change in the sign of the free energy of a dislocation. In the solid state there are no free dislocations in equilibrium, and above the melting temperature there is some concentration of dislocations which can move freely under the influence of an arbitrarily small shear stress.

Nelson and Halperin (Halperin and Nelson, 1978; Nelson and Halperin, 1979; Nelson, 1978; Halperin, 1979, 1980) extended the theory of dislocation-mediated melting and found that melting should occur in two stages with increasing temperature. The state just above the melting temperature does not have the properties of an isotropic liquid, but is a new type of liquid-crystal phase termed the hexatic phase, in which there is quasi-long-range order of the orientation of nearest-neighbor bonds. With increasing temperature the hexatic phase becomes unstable to the formation of free disclinations and a transition occurs to an isotropic phase.

It is not obvious that the above-mentioned general theory of the two-dimensional solid-liquid transition is directly applicable to the electron solid which is determined by the long-range Coulomb force. As a matter of fact, the Coulomb potential does not satisfy a condition assumed by Mermin (1968).

A review of various aspects of the electron crystal in two dimensions has been given by Fukuyama (1979).

2. The two-dimensional electron crystal

Crandall and Williams (1971) first suggested that an ordered state might minimize the potential energy of electrons on the liquid helium surface by forming a two-dimensional electron crystal. Independently Chaplik (1972a) discussed the possibility of crystallization of charge carriers in low-density inversion layers. Several people investigated properties of the two-dimensional Wigner crystal assuming its presence.

There seems to be little doubt about the fact that the two-dimensional Wigner solid forms a hexagonal lattice. Meissner, Namaizawa, and Voss (1976) calculated the ground-state static potential energy E_0, defined by

$$E_0 = \frac{1}{N} \sum_{i<j} \frac{e^2}{|\mathbf{r}_i^0 - \mathbf{r}_j^0|} , \tag{7.69}$$

where N is the number of electrons and $\mathbf{r}_i^0$ is the equilibrium position of the ith electron. They obtained $E_0 = -2.21/r_s$ Ry for the hexagonal lattice. Bonsall and Maradudin (1976, 1977) performed calculation of E_0 for the five two-dimensional Bravais lattices and showed that the hexagonal lattice has the lowest energy. Strictly speaking, one has to add the zero-point energy of the lattice vibration and compare the total energy. This can be especially important for the comparison of the hexagonal and square lattices, which have static energies very close to each other. As will be discussed below, however, the square lattice is unstable for long-wavelength shear waves.

In a harmonic approximation the spectrum of lattice vibrations is determined by the Hamiltonian

$$\mathscr{H} = \frac{1}{2m} \sum_i \mathbf{p}_i^2 + \tfrac{1}{2} \sum_{ij} \sum_{\alpha,\beta=x,y} \Phi_{\alpha\beta}(ij) u_{i\alpha} u_{j\beta} , \tag{7.70}$$

where $\mathbf{u}_i = \mathbf{r} - \mathbf{r}_i^0$ is the displacement vector relative to the lattice site $\mathbf{r}_i^0$, and $\Phi_{\alpha\beta}(ij)$ is the force-constant tensor, defined by

$$\begin{aligned} \Phi_{\alpha\beta}(ij) &= -\frac{1}{m} \frac{\partial}{\partial r_\alpha} \frac{\partial}{\partial r_\beta} v(r) \Big|_{\mathbf{r}=\mathbf{r}_{ij}^0}, \quad i \neq j \\ &= \frac{1}{m} \sum_{k \neq i} \frac{\partial}{\partial r_\alpha} \frac{\partial}{\partial r_\beta} v(r) \Big|_{\mathbf{r}=\mathbf{r}_{ik}^0}, \quad i = j \end{aligned} \tag{7.71}$$

with $v(r) = e^2/r$, and $\mathbf{r}_{ij}^0 = \mathbf{r}_i^0 - \mathbf{r}_j^0$. The two eigenvalues of the Fourier transform

$$\Phi_{\alpha\beta}(\mathbf{k}) = \sum_j \Phi_{\alpha\beta}(ij) \exp(-i\mathbf{k}\cdot\mathbf{r}_{ij}^0) \tag{7.72}$$

give the squared vibrational frequencies

$$\omega_{\mathbf{k}\pm}^2=\tfrac{1}{2}\{\Phi_{xx}(\mathbf{k})+\Phi_{yy}(\mathbf{k}) \pm[[\Phi_{xx}(\mathbf{k})-\Phi_{yy}(\mathbf{k})]^2+4\Phi_{xy}(\mathbf{k})^2]^{1/2}\}\ , \tag{7.73}$$

where the upper and lower branches become the longitudinal and transverse phonon frequencies, respectively, in the long-wavelength limit. In terms of the polarization vector $\mathbf{e}(\mathbf{k}\lambda)$, which satisfies

$$\sum_{\beta=x,y}\Phi_{\alpha\beta}(\mathbf{k})e_\beta(\mathbf{k}\lambda)=\omega_\lambda^2(\mathbf{k})e_\alpha(\mathbf{k}\lambda)\ , \tag{7.74}$$

the above can be written as

$$\omega_\lambda^2(\mathbf{k})=-\frac{1}{m}\sum_{i<j}\sum_{\alpha,\beta}e_\alpha(\mathbf{k}\lambda)e_\beta(\mathbf{k}\lambda)[1-\exp(i\mathbf{k}\cdot\mathbf{r}_{ij}^0)] \times\frac{\partial}{\partial r_\alpha}\frac{\partial}{\partial r_\beta}v(r)\bigg|_{\mathbf{r}=\mathbf{r}_{ij}^0}\ . \tag{7.75}$$

To see the long-wavelength limit we can use an expansion in reciprocal lattice space,

$$\Phi_{\alpha\beta}(\mathbf{k})=\frac{2\pi N_s e^2}{m}\left[\frac{k_\alpha k_\beta}{k}+\sum_{G\neq 0}\left[\frac{(k+G)_\alpha(k+G)_\beta}{|\mathbf{k}+\mathbf{G}|}-\frac{G_\alpha G_\beta}{|\mathbf{G}|}\right]\right]\ . \tag{7.76}$$

For long wavelengths the frequency of the longitudinal phonon is determined by the first term of Eq. (7.76) and

$$\omega_l^2(k)=\frac{2\pi N_s e^2}{m}k\ . \tag{7.77}$$

This is independent of the lattice structure and is the same as the plasma frequency of the two-dimensional electron gas (or liquid). For the transverse phonon, on the other hand, the term including summations over nonzero reciprocal lattice vectors becomes important and the dispersion becomes linear, i.e., $\omega_\lambda(k)=c_{\rm ph}k$.

Crandall (1973) calculated the phonon spectrum of the square lattice, but his calculation seems to contain errors. Platzman and Fukuyama (1974) made a crude estimate for the hexagonal lattice. More accurate calculations were later performed by Meissner *et al.* (1976) and by Bonsall and Maradudin (1976, 1977). It was found that the transverse branch in the $\langle 10\rangle$ direction is imaginary in the square lattice, which implies that the square lattice is unstable against shear forces in this direction. A similar instability has also been found for the honeycomb lattice (Meissner and Flammang, 1976). In the hexagonal lattice, on the other hand, the frequency is positive everywhere in the Brillouin zone and the transverse mode becomes isotropic in the long-wavelength limit, as is expected. Meissner *et al.* (1976) and Bonsall and Maradudin (1976, 1977) also calculated the zero-point vibrational energy in the hexagonal lattice.

There have been several attempts to determine the critical temperature or electron concentration at which the two-dimensional Wigner solid melts. Platzman and Fukuyama (1974) applied the self-consistent harmonic approximation proposed by Kugler (1969) in a three-dimensional system. In this approximation the normal mode frequencies are given by

$$\omega_\lambda(\mathbf{k})^2=\frac{1}{m}\sum_{i<j}\sum_{\alpha,\beta}[1-\exp(i\mathbf{k}\cdot\mathbf{r}_{ij}^0)] \times e_\alpha(\mathbf{k}\lambda)e_\beta(\mathbf{k}\lambda)\left\langle\frac{\partial}{\partial r_{i\alpha}}\frac{\partial}{\partial r_{i\beta}}v(r_{ij})\right\rangle\ , \tag{7.78}$$

where $\langle\cdots\rangle$ means the average over the phonon distribution at temperature T and $\mathbf{r}_{ij}=\mathbf{r}_i-\mathbf{r}_j$. This constitutes an equation which self-consistently determines $\omega_\lambda(\mathbf{k})$. It was solved by assuming a longitudinal plasmon mode given by Eq. (7.77) and an isotropic transverse mode having a velocity $c_{\rm ph}$, i.e., $\omega_t(k)=c_{\rm ph}k$, and by determining $c_{\rm ph}$ in a self-consistent manner. The melting of the crystal is related to the vanishing of a self-consistent solution. One of the remarkable features of their results is that the phonon frequency increases with the fluctuation, suggesting that the solid becomes harder in the presence of fluctuations. The transverse phonon velocity in the vicinity of the melting temperature is even higher than that at zero temperature (the value calculated in the harmonic approximation). This is because in two dimensions interaction between broadened charge distributions is larger than between point charges if the broadening is small enough. Platzman and Fukuyama found $\Gamma_m=2.8$ at high temperatures (the classical regime) and $r_s=4.5$ ($\Gamma_m\sim 3$) at zero temperature. These values are extremely small, and it is hard to believe that the system really crystallizes under these conditions.

Thouless (1978) used the Kosterlitz-Thouless (1973) theory of dislocation-mediated melting to discuss melting of the two-dimensional electron crystal. In this theory, there are supposed to be no isolated dislocations at low temperatures, and melting takes place when the free energy of a dislocation changes sign. The energy of an isolated dislocation with Burgers vector of magnitude b (the lattice constant) is given by

$$E=\frac{c_{\rm ph}\rho^2 b^2}{4\pi}\ln\frac{L^2}{b^2}\ , \tag{7.79}$$

where $c_{\rm ph}$ is the velocity of the transverse phonon, ρ is the mass per unit area, and L^2 is the area of the system. Since there are approximately L^2/b^2 possible positions for the dislocation, the entropy is given by

$$S=k_B\ln\frac{L^2}{b^2}\ . \tag{7.80}$$

Therefore, the melting temperature T_m is

$$k_B T_m=\frac{c_{\rm ph}\rho^2 b^2}{4\pi}\ . \tag{7.81}$$

Using the value of $c_{\rm ph}$ calculated by Bonsall and Maradudin (1977) at zero temperature, Thouless obtained $\Gamma_m\cong 79$ in the classical regime. This number is much

larger than that of Platzman and Fukuyama. The actual value of Γ_m has been expected to be larger than the above, since as the melting temperature is approached from below, bound dislocation pairs appear, and these reduce the rigidity modulus below its zero-temperature value [opposite to the behavior found by Platzman and Fukuyama (1974) in the self-consistent harmonic approximation].

Morf (1979) employed a molecular dynamic simulation to calculate the temperature dependence of the rigidity modulus and found that the low-frequency shear modulus decreases slowly with increasing T until $T\sim 0.9T_m$, and drops rapidly as T approaches T_m due to nonlinear phonon interactions. A melting temperature was calculated by solving the renormalization group equations of Halperin and Nelson with the use of this rigidity modulus and the dislocation core energy (Fisher *et al.*, 1979a) and gave $\Gamma_m=128$.

Hockney and Brown (1975) carried out a computer experiment using a molecular-dynamic method for a system of 10^4 classical point charges confined to move in a plane. They discussed a lambdalike anomaly in the electronic specific heat at $\Gamma=95$, which they took to be a transition between a fluid and a polycrystalline phase. All other calculated properties (internal energy, pair correlation function, and structure factor) varied smoothly through the phase transition. More recent numerical experiments have failed to confirm the anomaly in the specific heat and have found the phase transition at larger values of Γ. It has been suggested that the system was not allowed sufficient time to reach thermal equilibrium in the Hockney-Brown simulation (Gann *et al.*, 1979; Morf, 1979). A Monte Carlo calculation by Gann, Chakravarty, and Chester (1979) places the melting transition in the range $110\leq\Gamma_m\leq 140$. The experimental observation of coupled plasmon-ripplon resonances on the liquid helium surface by Grimes and Adams (1979, 1980) gives $\Gamma_m\sim 135$.

The dislocation theory of the melting of the two-dimensional electron solid seems to work quite well in the classical regime. The value of Γ_m estimated in the self-consistent harmonic approximation (Platzman and Fukuyama, 1974) is, on the other hand, almost two orders of magnitude smaller than the actual value. Since the self-consistent harmonic approximation for phonons assumes that the lattice vibrations are nearly harmonic, it cannot take proper account of effects of local disorders like dislocations which play important roles in the melting of the lattice. The dislocation theory is not applicable to the quantum regime, since it is essentially classical. There have been some attempts to include quantum-mechanical effects (Fukuyama, 1980a; Fukuyama and Yoshioka, 1980a). So far there is no reliable theory in the quantum regime.

3. Electron crystals in magnetic fields

There have been various investigations on magnetic field effects on the two-dimensional electron crystal. Let us first consider the vibrational spectrum in the harmonic approximation. Effects of a magnetic field applied perpendicular to the plane can be taken into account quasiclassically by replacing $\mathbf{p}_i$ in Eq. (7.70) by $\mathbf{p}_i+e\mathbf{A}(\mathbf{r}_i)/c$, where $\mathbf{A}(\mathbf{r})$ is the vector potential. Then

$$H=\frac{1}{2m}\sum_i[\mathbf{p}_i+\frac{e}{c}\mathbf{A}(\mathbf{r}_i)]^2+\frac{m}{2}\sum_{\mu,\nu}\Phi_{\mu\nu}(ij)u_{i\mu}u_{j\nu}\,. \tag{7.82}$$

When we introduce the phonon Green's function defined by

$$D_{\mu\nu}(ij;i\omega_n)=\tfrac{1}{2}\int_{-\beta}^{\beta}d\tau e^{i\omega_n\tau}\langle T_\tau u_{i\mu}(\tau)u_{j\nu}\rangle\,, \tag{7.83}$$

where $\beta=1/k_BT$, $\omega_n=2\pi nk_BT$, T_τ is a time-ordering operator, and n is an integer, we have

$$\omega_n^2D_{\mu\nu}(ij)+\omega_n\omega_c\varepsilon_{\mu\nu}D_{\mu\nu}(ij)+\sum_l\sum_{\alpha=x,y}\Phi_{\mu\alpha}(il)D_{\alpha\nu}(lj)=\frac{1}{m}\delta_{ij}\delta_{\mu\nu}\,, \tag{7.84}$$

with $\varepsilon_{xy}=1$, $\varepsilon_{yx}=-1$, and $\varepsilon_{\mu\nu}=0$, otherwise. In terms of the Fourier transform, one has

$$D(\mathbf{k})^{-1}=m\begin{bmatrix}\omega_n^2+\Phi_{xx}(\mathbf{k}) & \omega_n\omega_c+\Phi_{xy}(\mathbf{k})\\ -\omega_n\omega_c+\Phi_{yx}(\mathbf{k}) & \omega_n^2+\Phi_{yy}(\mathbf{k})\end{bmatrix}. \tag{7.85}$$

The eigenfrequencies of phonons, $\omega_\pm^2(\mathbf{k})$, are determined by $\det D(\mathbf{k})^{-1}=0$ as

$$\omega_\pm^2=\tfrac{1}{2}\{\omega_l^2+\omega_t^2+\omega_c^2\pm[(\omega_l^2+\omega_t^2+\omega_c^2)^2-4\omega_l^2\omega_t^2]^{1/2}\}\,, \tag{7.86}$$

where ω_l and ω_t are frequencies of longitudinal and transverse phonons in the absence of a magnetic field and $\omega_c=eH/mc$. The above expression was first derived by Chaplik (1972a).

In the long-wavelength limit we have

$$\omega_+\to\omega_c\,, \tag{7.87}$$

$$\omega_-\to\frac{1}{\omega_c}\left[\frac{2\pi N_se^2}{m}\right]^{1/2}c_{\rm ph}k^{3/2}\,. \tag{7.88}$$

We see that the cyclotron frequency, which is $\omega_+(k=0)$, is unchanged even in the crystalline state, in agreement with Kohn's (1961) theorem. Because of interactions with the cyclotron motion the transverse phonon becomes softened and is proportional to $k^{3/2}$.

With the use of the above spectrum the orbital magnetization was calculated by Chaplik (1972a) and later also be Fukuyama and McClure (1975). Fukuyama (1976a) studied the qualitative behavior of dynamical conductivities and effects of impurity pinning. The phonon spectrum in a magnetic field has also been discussed by Meissner (1976, 1978).

There have been various discussions as to whether a magnetic field tends to stabilize the electron crystal. Lozovik and Yudson (1975a) suggested that the solid phase became more stable in the presence of a magnetic field.

They used a simple Einstein model of phonons with a frequency $\omega_0 \sim \omega_p (k \sim \pi/b)$ in the absence of a field and argued that the amplitude $\langle u^2 \rangle_{\rm av} = \hbar/m\omega$ of the zero-point oscillations decreased and consequently the crystal was more favored, since ω is given by $(\omega_0^2+\omega_c^2)^{1/2}$ in a magnetic field. This discussion, however, does not take into account the ω_- mode, which is proportional to $k^{3/2}$ in the long-wavelength limit. If one uses the usual expression of the mean displacement in the absence of a magnetic field,

$$\langle u^2 \rangle_{\rm av} = \frac{1}{mN} \sum_{\mathbf{k}} \sum_{\lambda} \frac{1}{\omega_\lambda(\mathbf{k})} (n_{\lambda\mathbf{k}} + \tfrac{1}{2}) , \tag{7.89}$$

one might expect the melting temperature to become smaller in a magnetic field because of the softening of the ω_- mode. In Eq. (7.89) N is the total number of electrons and $n_{\lambda\mathbf{k}}$ is the Bose occupation number of phonons with a frequency $\omega_\lambda(\mathbf{k})$. As a matter of fact, there have been several arguments based on the above that the electron crystal would melt in a strong magnetic field (Fukuyama, 1975; Chaplik, 1977a, 1977b).

In a magnetic field, however, Eq. (7.89) is not valid. A correct expression is

$$\begin{aligned} \langle u^2 \rangle_{\rm av} &= k_B T \sum_n \frac{1}{N} \sum_{\mathbf{k}} [D_{xx}(\mathbf{k}) + D_{yy}(\mathbf{k})] \\ &= \frac{1}{mN} \sum_k \left[\frac{2\omega_+^2 - \omega_l^2 - \omega_t^2}{\omega_+(\omega_+^2 - \omega_-^2)} (n_{\mathbf{k}+} + \tfrac{1}{2}) \right. \\ &\quad \left. + \frac{2\omega_-^2 - \omega_l^2 - \omega_t^2}{\omega_-(\omega_-^2 - \omega_+^2)} (n_{\mathbf{k}-} + \tfrac{1}{2}) \right] . \end{aligned} \tag{7.90}$$

In the long-wavelength limit ($k \to 0$) the second term in the large parentheses becomes

$$\frac{\omega_l}{\omega_t \omega_c} (n_{\mathbf{k}-} + \tfrac{1}{2}) , \tag{7.91}$$

which means that the magnetic field works rather to stabilize the solid phase. Fukuyama (1976b) calculated $\langle u^2 \rangle_{\rm av}$ at zero temperature, where it does not diverge, and showed that application of magnetic fields enhanced the localization of electrons in spite of the fact that the phonon was softened by the field. A similar conclusion was reached by Lozovik, Musin, and Yudson (1979).

Jonson and Srinivasan (1977) extended the Platzman-Fukuyama calculation in the self-consistent harmonic approximation to the case in a magnetic field. They showed that the magnetic field tends to crystallize electrons and increases the melting temperature monotonically. This was also suggested from comparison of the free energy of the liquid and solid phases. Lerner and Lozovik (1978c) also discussed magnetic field effects.

So far, the magnetic field has been treated quasiclassically, and the quantization of the orbital motion and the discrete energy spectrum in the two-dimensional system have not been considered explicitly. Actually, it is possible that electrons belonging to each Landau level form a kind of crystal when their concentrations are sufficiently small, although all the electrons can not form a Wigner solid. Such a possibility was studied theoretically by Tsukada (1976a, 1977a, 1977b). When one neglects interactions between different Landau levels, the Hamiltonian is expressed in terms of center coordinates of the cyclotron orbit. Assuming that the center coordinates form a hexagonal lattice, Tsukada determined vibrational frequencies in the self-consistent harmonic approximation and showed that the electrons could form a lattice when the occupation ratio of each Landau level, $\nu = 2\pi l^2 N_s$ with $l^2 = c\hbar/eH$, was sufficiently small ($\nu \sim 0.3$ and 0.17 for the ground and first excited Landau level, respectively) for the n-channel inversion layer on Si(100). These numbers are too small to explain experimental results observed in the Si inversion layer by Kawaji and Wakabayashi (1976). Tsukada also considered effects of impurities, assuming that they would tend to stabilize the crystal.

In magnetic fields the x and y components of the center coordinates of a cyclotron orbit, X and Y, do not commute with each other, i.e., $[X, Y] = XY - YX = il^2$, which makes the system different from a simple classical system. In the strong-field limit where $\nu << 1$ is satisfied, this incommutability is unimportant and the system becomes classical. The melting temperature of the electron lattice is, therefore, given by Eq. (7.81) in the Kosterlitz-Thouless theory. Fukuyama and Yoshioka (1980b) estimated quantum effects, i.e., effects of noncommuting X and Y, on the shear modulus within a harmonic approximation. It has been shown that the quantum effects cannot be neglected and reduce the melting temperature already around $\nu \sim 0.1$. Electron crystals in strong fields have been discussed also by Canel (1978) and by Doman (1979).

Fukuyama, Platzman, and Anderson (1978, 1979) calculated the free energy within the Hartree-Fock approximation and suggested that the usual phase with a uniform electron density distribution becomes unstable against the formation of charge-density waves at temperatures well above the melting temperature of the electron lattice. This instability may be obtained as follows. The dielectric function describing response of the system is written as

$$\varepsilon(q) = 1 + \frac{2\pi e^2}{q} \Pi(q) . \tag{7.92}$$

If we consider only the lowest ($N = 0$) Landau level, we have

$$\Pi(q) \cong \exp\left[\frac{-q^2 l^2}{2} \right] \frac{1}{2\pi l^2} \int dE \left[-\frac{\partial f}{\partial E} \right] \delta \left[\frac{E - \hbar\omega_c}{2} \right] , \tag{7.93}$$

in the Hartree (random-phase) approximation, where $f(E)$ is the Fermi distribution function. At sufficiently high temperatures the above is reduced to

$$\Pi(q) \cong \exp\left[\frac{-q^2 l^2}{2} \right] \frac{1}{2\pi l^2} \frac{\nu(1-\nu)}{k_B T} . \tag{7.94}$$

In the Hartree-Fock approximation exchange can be taken into account by replacing $\Pi(q)$ by $\Pi(q)/$

$[1-2\pi l^2(e^2/l)I(q)\Pi(q)]$, where

$$I(q)=\left[\frac{\pi}{2}\right]^{1/2}\exp\left[\frac{-q^2l^2}{4}\right]I_0\left[\frac{q^2l^2}{4}\right], \tag{7.95}$$

with $I_0(x)$ being the modified Bessel function. The dielectric function vanishes at $T=T_c$ $[\cong 0.557\nu(1-\nu)e^2/l]$ around $q=q_0$ $(\cong 1.568/l)$, corresponding to the instability toward charge-density wave formation. The wavelength of the charge-density wave is independent of the electron concentration and determined by the exchange matrix element $I(q)$. It has been expected that as the temperature is lowered, the period and harmonic content of the charge-density wave change, evolving towards an anharmonic electron solid.

Electronic properties of the charge-density wave ground state have been investigated within the Hartree-Fock approximation (Kuramoto, 1978a, 1978b; Kawabata, 1978; Yoshioka and Fukuyama, 1979, 1980, 1981b). Kuramoto and Kawabata concluded that the charge-density wave state was a kind of zero-gap semiconductor, i.e., there was not an energy gap at the Fermi level, for $\nu=\frac{1}{2}$ (half-filled Landau level). However, a later calculation (Yoshioka and Fukuyama, 1979, 1980, 1981a) has shown that the charge-density wave state is essentially an electron lattice and has a large gap at the Fermi level. Dynamical properties of the impurity pinning of phasons of the charge-density wave have been studied (Fukuyama and Lee, 1978). Kawabata (1980) discussed effects of charge-density wave fluctuations on the conductivity.

All discussion of the charge-density wave instability has been made within the mean-field-type Hartree-Fock approximation. It is not so certain, therefore, that the results can describe real features of actual two-dimensional systems. Especially the instability at high temperatures as $T_c\sim 0.557\nu(1-\nu)e^2/l$ may critically depend on the nature of the approximation. As can easily be seen, the charge-density wave formation with $q\sim q_0$ at T_c originates purely from the exchange interaction, which is known to be overestimated in the Hartree-Fock approximation. Fukuyama, Platzman, and Anderson (1979) suggested that T_c does not represent the actual melting temperature of the charge-density wave, but rather a kind of transition temperature between an essentially gaslike phase and a phase with charge-density waves but no long-range order. Wilson, Allen, and Tsui (1980) have tried to explain recent experiments on cyclotron resonance at low electron concentrations in a Si inversion layer by the existence of such short-range order of charge-density waves. See Sec. VI.C for more details on the cyclotron resonance.

VIII. SYSTEMS OTHER THAN *n*-CHANNEL Si

A. Si *p*-channel layers

The investigation of *p*-channel silicon inversion layers began in earnest even before that of *n* channels. Especially in the mid-1960's the literature on *p*-channel devices exceeded that on *n* channels because many semiconductor companies concentrated their efforts on them. Some information may be found in the papers by Murphy (1964), Leistiko, Grove, and Sah (1965), Colman, Bate, and Mize (1968), Sato, Takeishi, and Hara (1969), Murphy, Berz, and Flinn (1969), Cheng (1974), Hess, Englert, Neugebauer, Landwehr, and Dorda (1977), and Guzev, Gurtov, Rzhanov, and Frantsuzov (1979), among others. The two-dimensional properties of *p*-channel devices are more difficult to observe than those of *n*-channel devices primarily because the effective masses are higher and the mobilities are lower. Furthermore, the theory is more difficult because of the complex nature of the warped valence bands.

The powerful experimental methods like the Shubnikov–de Haas effect or infrared spectroscopy, which can give direct information about electric subbands, were applied more recently. Surface quantum oscillations in *p*-channel inversion layers have been studied on the (110), (111), and (100) surfaces by von Klitzing, Landwehr, and Dorda (1974a–1974c) and on the (111) and (100) surfaces by Lakhani, Stiles, and Cheng (1974). From the temperature dependence of the amplitude of the Shubnikov–de Haas oscillations both groups determined the effective mass as a function of the hole concentration. They showed that the effective mass increased considerably with N_s. There is a large discrepancy between these two experimental results. Mass values obtained by Lakhani *et al.* (1974) are about twice as large as those of von Klitzing *et al.* As will be discussed below, different theories appeared which agreed with either set of experimental results. This caused quite a controversy. On the (110) surface von Klitzing *et al.* (1974a) observed a second set of oscillations associated with the occupation of the first excited subband above $N_s=3.2\times 10^{12}$ cm^{-2}.

Hole cyclotron resonance was observed by Kotthaus and Ranvaud (1977) on the (100), (110), and (111) surfaces. By fitting a classical line shape to experimental data they determined the effective mass. The masses obtained from the cyclotron resonance turned out to agree with those determined from Shubnikov–de Haas oscillations by von Klitzing *et al.* The reasons why Lakhani *et al.* obtained mass values about a factor of two larger than the actual ones are not understood yet and might originate from bad quality of their samples.

Intersubband optical transitions were studied in inversion and accumulation layers on the (100) surface by Kneschaurek, Kamgar, and Koch (1976) and on the (110) and (111) surfaces by Kamgar (1977). Resonance line shapes were broader than corresponding ones in *n*-channel layers. The line shape turned out to be extremely broad in accumulation layers. The temperature dependence was also studied briefly (Kamgar, 1977).

The band structure of the valence band in the vicinity of the Γ point is known to be described by the 6×6 matrix Hamiltonian (Luttinger and Kohn, 1955),

$$\mathcal{H}_0=\begin{bmatrix}\mathcal{H}_{\mathbf{k}\cdot\mathbf{p}} & 0\\ 0 & \mathcal{H}_{\mathbf{k}\cdot\mathbf{p}}\end{bmatrix}+\mathcal{H}_{so}, \tag{8.1}$$

where $\mathscr{H}_{\mathbf{k}\cdot\mathbf{p}}$ given by

$$\begin{bmatrix} \frac{\hbar^2}{2m_0}K^2+Lk_1^2+M(k_2^2+k_3^2) & Nk_1k_2 & Nk_1k_3 \\ Nk_1k_2 & \frac{\hbar^2}{2m_0}K^2+Lk_2^2+M(k_3^2+k_1^2) & Nk_2k_3 \\ Nk_1k_3 & Nk_2k_3 & \frac{\hbar^2}{2m_0}K^2+Lk_3^2+M(k_1^2+k_2^2) \end{bmatrix} . \tag{8.2}$$

and

$$H_{\mathrm{so}}=-\frac{\Delta}{3}\begin{bmatrix} 1 & i & 0 & 0 & 0 & -1 \\ -i & 1 & 0 & 0 & 0 & i \\ 0 & 0 & 1 & 1 & -i & 0 \\ 0 & 0 & 1 & 1 & -i & 0 \\ 0 & 0 & i & i & 1 & 0 \\ -1 & -i & 0 & 0 & 0 & 1 \end{bmatrix} , \tag{8.3}$$

where $\mathbf{K}=(k_1,k_2,k_3)$ and $K=|\mathbf{K}|$. This Hamiltonian has been obtained by the $\mathbf{k}\cdot\mathbf{p}$ perturbation for p-like wave functions at the Γ point. In the approximation that the spin-orbit splitting of the $p_{3/2},p_{1/2}$ levels is sufficiently large, one has approximate expressions of the dispersion relation for the heavy and light holes:

$$E(\mathbf{K})=AK^2\pm[B^2K^2+C^2(k_1^2k_2^2+k_2^2k_3^2+k_3^2k_1^2)]^{1/2} , \tag{8.4}$$

and for the spin-splitoff level:

$$E(K)=-\Delta+AK^2 , \tag{8.5}$$

where

$$\begin{aligned} A&=\tfrac{1}{3}(L+2M)+\frac{\hbar^2}{2m_0} , \\ B&=\tfrac{1}{3}(L-M) , \\ C^2&=\tfrac{1}{3}[N^2-(L-M)^2] . \end{aligned} \tag{8.6}$$

The band parameters L, M, N, and Δ have been determined by microwave cyclotron resonances and effects of uniaxial stresses (Dresselhaus, Kip, and Kittel, 1955; Dexter, Zeiger, and Lax, 1956; Hensel and Feher, 1963). Because of the degeneracy at $k_1=k_2=k_3=0$, the dispersion cannot be expressed in terms of the usual effective-mass tensor for the heavy and light holes. One sees that the band is highly nonparabolic and anisotropic. Because of the existence of inversion symmetry each band has Kramers degeneracy.

In principle the extension of the subband structure calculation in n channels to that in p channels is straightforward. As usual we choose the z direction normal to the surface. The subband structure can be obtained by solving the coupled effective-mass equation

$$\left[\mathscr{H}_0\left[k_x,k_y,\frac{1}{i}\frac{\partial}{\partial z}\right]+V(z)\right]\frac{1}{L}e^{ik_xx+ik_yy}\zeta_{ik_xk_y}(z)$$
$$=E_i(k_x,k_y)\frac{1}{L}e^{ik_xx+ik_yy}\zeta_{ik_xk_y}(z) , \tag{8.7}$$

with the boundary condition that $\zeta_{ik_xk_y}(z=0)=\zeta_{ik_xk_y}(z=\infty)=0$. The potential $V(z)$ should be determined self-consistently in the Hartree approximation. The actual numerical procedure is, however, very tedious, and several simplifications have been tried.

The simplest procedure proposed by several authors (Colman *et al.*, 1968; Sato *et al.*, 1969) is to cut the three-dimensional energy contour $E(k_x,k_y,k_z)$ of the heavy hole in the bulk at $k_z=\pm k_0$ with $k_0=(2m|E_0|/\hbar^2)^{1/2}$, where m is an appropriate effective mass and E_0 is the energy of the bottom of the ground subband calculated in a triangular potential approximation. This gives a two-dimensional E vs $\mathbf{k}$ relation. Such a simple estimation has been used for a rough explanation of the anisotropy of mobility at room temperature.

Falicov and Garcia (1975) slightly improved the above approximation. Instead of putting $k_z=\pm k_0$ in the bulk dispersion of the heavy hole, they determined the $E(\mathbf{k})$ relation by minimizing the expression

$$E_0(k_x,k_y)=\int_{-\infty}^{\infty}\frac{dk_z}{2\pi}E(k_x,k_y,k_z)\int_0^{\infty}dz\,e^{-ik_zz}|\zeta(z)|^2$$
$$+\int_0^{\infty}dz\,V(z)|\zeta(z)|^2 , \tag{8.8}$$

where $\zeta(z)$ is a variational wave function of the usual form (3.25). From the area $A(E)$ in the k_x-k_y space given by $E=E(\mathbf{k})$, they calculated a classical cyclotron mass

$$m_c=\frac{\hbar^2}{2\pi}\frac{\partial A(E)}{\partial E}\bigg|_{E=E_F} . \tag{8.9}$$

The calculated effective mass was coincident with experimental results of Lakhani *et al.* (1974) on the (111) and (100) surfaces, but turned out to be about twice as large as more exact experimental results of von Klitzing *et al.* (1974a–1974c) and of Kotthaus and Ranvaud (1977).

One sees that such simplified treatment is not appropriate in p channels. This originates from the degeneracy at the Γ point and large off-diagonal elements of the matrix Hamiltonian (8.1). In the theories mentioned above, k_z appearing in the off-diagonal elements has been replaced by some effective k_0 and the matrix has then been diagonalized. When an inversion layer is formed, however, terms linear in k_z become much smaller, as has been suggested by Landwehr, Bangert, von Klitzing, Englert, and Dorda (1976). This can easily be seen if one

considers the fact that $\langle k_z \rangle = 0$ for a bound state. Consequently, such theories overestimate effects of the off-diagonal elements and give too large an effective mass.

Garcia and Falicov (1975a, 1975b) and Garcia (1976) made attempts to calculate the subband structure using a single-band effective-mass equation by assuming an appropriate isotropic effective mass determined in the simplified theory. The accuracy of their calculated results is highly doubtful, however, for the reasons mentioned above.

More rigorous calculations of the subband structure were performed independently by Bangert and coworkers (Bangert *et al.*, 1974; Bangert and Landwehr, 1976; see also Landwehr, 1975) and by Ohkawa and Uemura (1975; see also Uemura, 1976). Both groups solved the 6×6 matrix effective-mass equation (8.7) at zero temperature in the absence of a magnetic field. The former authors expanded $\zeta_{ik_xk_y}$ into a linear combination of six Airy functions and diagonalized a matrix Hamiltonian for different sets of points in the k_x-k_y plane. Self-consistency was established iteratively using the calculated electron density as the initial distribution for the next step. The effective mass was calculated by (8.9) semiclassically. Ohkawa and Uemura used a similar method except that they used a more complicated set of trial functions.

The calculations revealed that the ground subband could be approximately regarded as the heavy hole, the first excited subband as the light hole, and the second excited subband as the excited state of the heavy hole. Figure 164 shows an example of Fermi lines of the ground subband for the three major surfaces calculated by Ohkawa and Uemura (1975). The dispersion is highly nonparabolic. Further, the spin degeneracy is lifted except at $k_x = k_y = 0$, even in the absence of a magnetic field. This lifting is considered to arise from the spin-orbit interaction and breaking of the inversion symmetry, and is larger for excited subbands. Such splittings have never been observed experimentally, however.

For the (110) surface, the calculation of Bangert *et al.* (1974) predicts that the first excited subband becomes populated at $N_s \sim 4\times10^{12}$ cm^{-2} for $N_{\text{depl}} = 1.3\times10^{11}$ cm^{-2}, while that of Ohkawa and Uemura (1975) predicts $N_s \simeq 2.8\times10^{12}$ cm^{-2}. Both calculations neglect the image potential. This difference arises partly because of slight differences of values of band parameters used in the two calculations. Insufficiencies of the number of basis wave functions might be another possible reason. The experimental value found by von Klitzing *et al.* (1974a) is $N_s \simeq 3.2\times10^{12}$ cm^{-2}.

Calculated effective masses on the three major surfaces, i.e., (100), (110), and (111), are compared with experimental results determined by Shubnikov–de Haas oscillations (von Klitzing *et al.*, 1974a–1974c) and cyclotron resonances (Kotthaus and Ranvaud, 1977) in Fig. 165. Experimental results of Lakhani, Stiles, and Cheng (1974) and theoretical results of Falicov and Garcia (1975) are also shown. Although there exist slight differences between the results of Bangert *et al.* and of

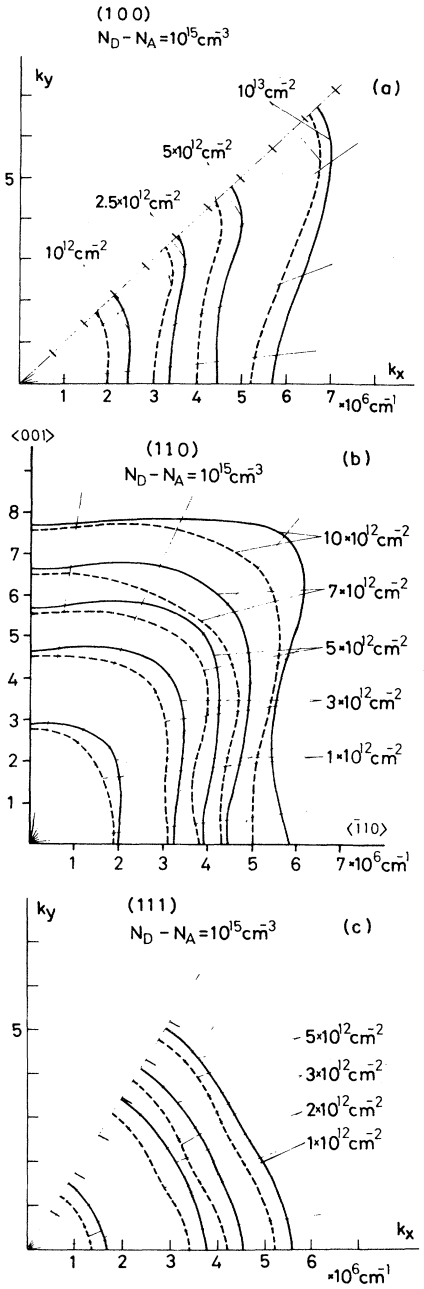

FIG. 164. The Fermi line of the ground subband in *p*-channel inversion layers on Si: (a) (100); (b) (110); (c) (111). The solid and dashed curves are for two spin-split levels. The electron concentration for each curve is given in the figure. After Ohkawa and Uemura (1975).

Ohkawa and Uemura and between the experimental results of von Klitzing *et al.* and of Kotthaus and Ranvaud, they are in reasonable agreement.

The effect of exchange and correlation on the subband structure was studied by Ohkawa (1976b) in a crude approximation. He neglected the nonparabolicity and calculated the self-energy shift of the subbands associated with the heavy hole using a parabolic dispersion on the

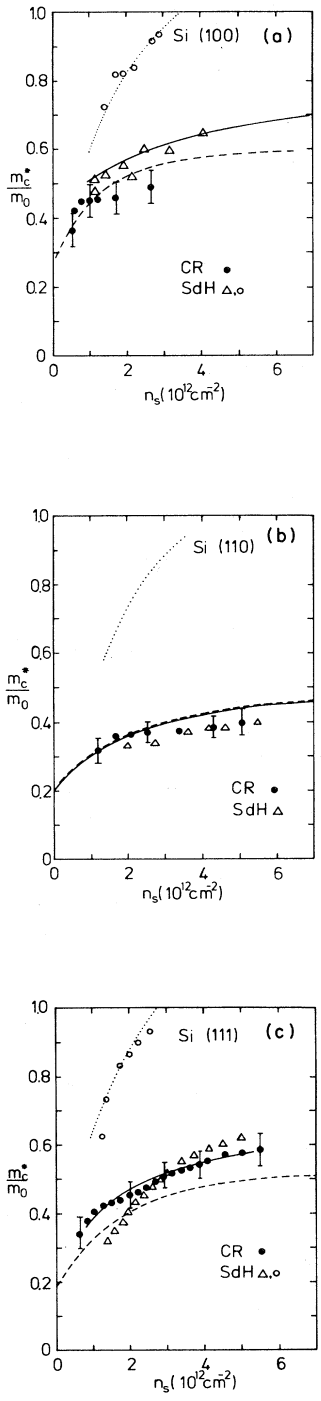

FIG. 165. Cyclotron effective mass m_c^* vs electron concentration n_s for p-channel inversion layers on (a) (100), (b) (110), and (c) (111) surfaces of Si. $\hbar\omega = 3.68$ meV. $T \sim 10$ K. Typical absolute errors are indicated by the error bars for m_c^* (black dots) determined by the cyclotron resonance (Kotthaus and Ranvaud, 1977). Shubnikov–de Haas experiments give the open circles (Lakhani *et al.*, 1974) and the triangles (von Klitzing *et al.*, 1974a–1974c). Theoretical results are represented by solid lines (Ohkawa and Uemura, 1975), dashed lines (Bangert *et al.*, 1974), and dotted lines (Falicov and Garcia, 1975). After Kotthaus and Ranvaud (1977).

(100) surface. As had been expected, the many-body correction to the subband energy level was shown to be as important as in n-channel layers, while the correction to the effective mass was small. Although calculations have never been made for the light-hole subband, the shift of that subband is also expected to be appreciable. Thus the coincidence between theory and experiment concerning the concentration at which the first excited subband becomes occupied by holes on the (110) surface must be accidental.

Intersubband optical transitions from the ground to the second excited subband (heavy-hole subbands) have the largest oscillator strength. Transitions to the first excited subband are not strictly forbidden but have been shown to be small (Ohkawa, 1976b). The energy difference between the ground and the second excited subband calculated by Ohkawa, crudely including the many-body shift, seems to coincide with the resonance energy measured by Kneschaurek *et al.* (1976) on the (100) surface. However, additional corrections like the depolarization effect and its local field effect, which appear in the optical absorption, are expected to be as important as in n-channel layers. Reliable theoretical estimation of these corrections seems very difficult, and we do not know whether the coincidence is accidental or not.

B. The III-V and related compounds

Investigations of space-charge layers on narrow-gap III-V semiconductors also started in the mid-1960s (Kawaji *et al.*, 1965; Chang and Howard, 1965; Kawaji and Kawaguchi, 1966; Kawaji and Gatos, 1967a, 1967b). However, the difficulty of obtaining samples with good quality has long prevented progress in this system. We first summarize results of theoretical investigations of the energy-level structure and then discuss experimental results for the more widely studied materials.

1. Energy-level structure

In narrow-gap III-V semiconductors with the zinc-blende structure, the bottom of the conduction band and the top of the valence band are located at the Γ point in the Brillouin zone. A schematic illustration of the band structure is shown in Fig. 166. The band structure near the Γ point is well described by a simplified version (Bowers and Yafet, 1959) of a $\mathbf{k}\cdot\mathbf{p}$ Hamiltonian obtained by Kane (1957) from one s-like and three p-like basis wave functions:

$$\mathscr{H} = \begin{bmatrix} \mathscr{H}_{++} & \mathscr{H}_{+-} \\ \mathscr{H}_{-+} & \mathscr{H}_{--} \end{bmatrix}, \tag{8.10}$$

with

$$\mathscr{H}_{\pm\pm}=\begin{bmatrix} \hbar^2K^2/2m_0 & Pk_{\pm}/\sqrt{2} & \pm Pk_{\mp}/\sqrt{6} & \pm Pk_{\mp}/\sqrt{3} \\ Pk_{\pm}/\sqrt{2} & -\varepsilon_G+\hbar^2K^2/2m_0 & 0 & 0 \\ \pm Pk_{\pm}/\sqrt{6} & 0 & -\varepsilon_G+\hbar^2K^2/2m_0 & 0 \\ \pm Pk_{\pm}/\sqrt{3} & 0 & 0 & -\Delta-\varepsilon_G+\hbar^2K^2/2m_0 \end{bmatrix}, \tag{8.11}$$

$$\mathscr{H}_{+-}=\mathscr{H}_{-+}=\begin{bmatrix} 0 & 0 & \sqrt{2/3}\,Pk_3 & -Pk_3/\sqrt{3} \\ 0 & 0 & 0 & 0 \\ \sqrt{2/3}\,Pk_3 & 0 & 0 & 0 \\ -Pk_3/\sqrt{3} & 0 & 0 & 0 \end{bmatrix}, \tag{8.12}$$

where $k_{\pm}=k_1\pm ik_2$ and $K^2=k_1^2+k_2^2+k_3^2$. The band parameters are

$$P=\frac{\hbar}{m_0}\langle iS\,|\,p_z\,|\,Z\rangle\ , \tag{8.13}$$

and

$$\Delta=i\frac{3\hbar}{4m_0^2c^2}\left\langle X\left|\frac{\partial V}{\partial x}p_y-\frac{\partial V}{\partial y}p_x\right|Y\right\rangle, \tag{8.14}$$

where V is the periodic crystal potential. In the above expression, the bases are

$$|iS\uparrow\rangle\ ,$$
$$2^{-1/2}\,|(X+iY)\uparrow\rangle\ ,$$
$$6^{-1/2}\,|(X-iY)\uparrow\rangle+(\tfrac{2}{3})^{1/2}\,|Z\downarrow\rangle\ ,$$
$$3^{-1/2}\,|(X-iY)\uparrow\rangle-3^{-1/2}\,|Z\downarrow\rangle\ ,$$
$$|iS\downarrow\rangle\ ,$$

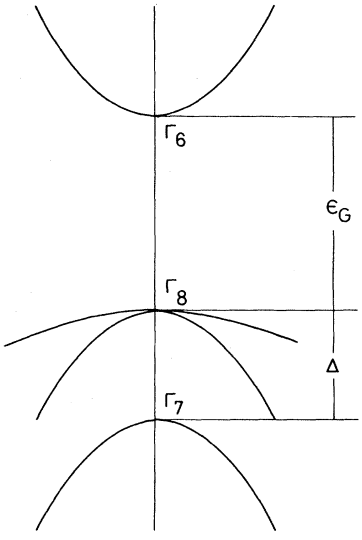

FIG. 166. A schematic illustration of the band structure in III-V semiconductors near the Γ point. Γ_6 is the conduction band, Γ_8 gives the heavy and light holes, and Γ_7 is called the spin-splitoff band.

$$2^{-1/2}\,|(X-iY)\downarrow\rangle\ ,$$
$$-6^{-1/2}\,|(X+iY)\downarrow\rangle+(\tfrac{2}{3})^{-1/2}\,|Z\uparrow\rangle\ ,$$

and

$$-3^{-1/2}\,|(X+iY)\downarrow\rangle-3^{-1/2}\,|Z\uparrow\rangle$$

in that order. Actually, the expression shown above is the Hamiltonian for the diamond structure, and the lack of inversion symmetry in the zinc-blende structure gives rise to additional terms. However, such corrections are usually small and are neglected. For discussion of the valence-band structure additional terms, second-order in $\mathbf{k}\cdot\mathbf{p}$, should be included as in the case of p channels of silicon. The above Hamiltonian is considered to be sufficient for the conduction band. In the presence of a magnetic field we add the spin-Zeeman energy and replace $k_i\rightarrow k_i+eA_i/c$ with $\mathbf{H}=\nabla\times\mathbf{A}$. The usual elimination of off-diagonal elements leads to the effective-mass expression

$$\varepsilon(K)=\frac{\hbar^2K^2}{2m}-\tfrac{1}{2}g\mu_BH\sigma\ , \tag{8.15}$$

with

$$\frac{1}{m}=\frac{1}{m_0}+\frac{2}{3}\frac{P^2(3\varepsilon_G+2\Delta)}{\hbar^2\varepsilon_G(\varepsilon_G+\Delta)}\ , \tag{8.16}$$

$$g=2-\frac{4}{3}\frac{m_0\Delta P^2}{\hbar^2\varepsilon_G(\varepsilon_G+\Delta)}\ . \tag{8.17}$$

For InSb, for example, we have $\varepsilon_G=238$ meV, $\Delta=900$ meV, $m=0.013m_0$, and $g=-51$.

In contrast to p channels of Si where the band structure is also described by a complicated matrix Hamiltonian, there is no well-established method of calculating the subband structure for semiconductors with a narrow gap. Effects of the interface or the surface on the band structure are not understood, and it is not yet clear what kinds of boundary conditions should be used for envelope wave functions at the interface. The change in the charge-density distribution when the inversion layer is formed is not necessarily determined by excess electrons in the inversion layer alone. Deformed wave functions of valence bands, whose effects are usually included in terms of the dielectric constant κ_{sc} in case of wide-gap materials, might play an important role. In addition to

such fundamental problems there is also a practical difficulty in actual calculations. The usual variational principle, which works in the case of p channels of Si, is not applicable in this system because the energy spectrum extends from minus infinity to plus infinity. In spite of these difficulties there have been various attempts to calculate the subband structure.

Ohkawa and Uemura (1974a, 1974b) tried to solve the effective-mass equation

$$\sum_j [\mathscr{H}_{ij}+V(z)\delta_{ij}]\zeta_j(k,z)\exp(i\mathbf{k}\cdot\mathbf{r}) = \varepsilon\zeta_i(k,z)\exp(i\mathbf{k}\cdot\mathbf{r}) , \quad (8.18)$$

for a given surface potential $V(z)$. They neglected the kinetic energy corresponding to the free electron and eliminated the components of the wave function except those associated with the Γ_6 conduction band, i.e., ζ_1 and ζ_5. The resulting equation for ζ_1 and ζ_5 is given by

$$\left[\frac{\hbar^2 k_z^2}{2m}-\lambda_\pm(k,z)\right]\phi_\pm(z)=0 , \quad (8.19)$$

with

$$\phi_\pm(k,z)=\frac{1}{\sqrt{2}}(-\varepsilon_G+V-\varepsilon)^{1/2}\left[\zeta_1\mp\frac{k_+}{k}\zeta_5\right] . \quad (8.20)$$

For simplicity they treated the case of $\Delta\to\infty$ and obtained

$$\lambda_\pm(k,z)=\varepsilon-\frac{\hbar^2k^2}{2m}-V(z)-\frac{(V(z)-\varepsilon)^2}{\varepsilon_G} - \frac{3\hbar^2(\partial V/\partial z)}{8m(-\varepsilon_G+V-\varepsilon)^2} + \frac{\hbar^2(\partial^2V/\partial z^2)}{4m(-\varepsilon_G+V-\varepsilon)} \pm \frac{\hbar^2(\partial V/\partial z)}{4m(-\varepsilon_G+V-\varepsilon)}k . \quad (8.21)$$

They solved the above equation using the WKB method:

$$\int_0^{z_0} dz\left[\frac{2m}{\hbar^2}\lambda_\pm(k,z)\right]^{1/2}=(n+\tfrac{3}{4})\pi , \quad n=0,1,\ldots \quad (8.22)$$

where z_0 is a turning point of $\lambda_\pm(k,z)$. The results were used to analyze experimental results of $Hg_{0.79}Cd_{0.21}Te$ by Antcliffe, Bate, and Reynolds (1971).

An important conclusion deduced from (8.21) by Ohkawa and Uemura was that the spin splitting arising from the lack of inversion symmetry of the applied electric field was given by $kP^2\langle\partial V/\partial z\rangle/\varepsilon_G$ (Ohkawa and Uemura, 1974a, 1974b; Uemura, 1974a). When one uses $\langle\partial V/\partial z\rangle\sim F_{\text{eff}}$, where F_{eff} is an appropriate average of the effective electric field acting on electrons, the splitting is large and could cause a reversal of ordering of Landau levels in $Hg_{1-x}Cd_xTe$. However, this result was later criticized by Ando (Därr *et al.*, 1976). The simplest argument is as follows: The potential $V(z)$ appearing in Eq. (8.21) contains also the potential of the interface barrier. Although the amplitude of wave functions near the interface is very small, the expectation value of the derivative of the potential remains nonzero and cancels the term associated with the electric field for $z>0$. Thus one must put $\langle\partial V/\partial z\rangle=0$ in the above expression. Otherwise electrons are accelerated in the negative z direction and can not stay in the inversion layer. One sees, therefore, that the spin splitting does not appear in the lowest order but in the third order with respect to the last term of (8.21). This argument does not seem to be valid if the barrier height is larger than the band gap. However, one can easily show that the requirement of the boundary condition, $\zeta_1(0)=\zeta_5(0)=0$, leads to the same conclusion. In deriving Eq. (8.19) one must take a derivative of the potential to eliminate other components of the wave function. One should be very careful in estimating such derivatives since the singular interface barrier potential can be crucial.

Arai (unpublished) expanded $\zeta_i(k,z)$ as

$$\zeta_i(k,z)=\sum_{l=0} a_l^{(i)}(k)\zeta_l^{(0)}(z) , \quad (8.23)$$

where $\zeta_l^{(0)}(z)$ satisfies

$$\left[-\frac{\hbar^2}{2m'}\frac{d^2}{dz^2}+V(z)\right]\zeta_l^{(0)}(z)=E_l^{(0)}\zeta_l^{(0)}(z) , \quad (8.24)$$

with the boundary condition $\zeta_l^{(0)}(0)=\zeta_l^{(0)}(\infty)=0$. Here, m' is an appropriately estimated effective mass at a given electron concentration. He used $l=0,\ldots,6$ as the basis. Therefore one has to diagonalize a 56×56 matrix for different values of k. Arai assumed that 14 levels with the "highest" energies corresponded to the conduction band and calculated the electron density and the potential $V(z)$ self-consistently. The subband structure in an n-channel inversion layer on InSb determined in this way turned out to be in excellent agreement with experiments on the subband structure, such as subband energy separations and the effective mass. Arai also estimated tunneling from an inversion layer state to the bulk valence-band state and showed that it was negligible for InSb. The spin splitting turned out to be extremely small in comparison with the prediction of Ohkawa and Uemura, as had been expected. There remain several problems even in such an elaborate calculation. There is no *a priori* reason to choose the 14 highest levels out of 56 resulting levels because the usual variational principle does not exist. The assumed basis wave functions are considered to be reasonable for the conduction band but cannot describe state corresponding to the valence band. Therefore it is highly doubtful that the calculation contains effects of the change in interband interactions caused by the surface potential, which was crucial in p channels of Si.

Takada and Uemura (1977) used a simplified approximation similar to that employed by Falicov and Garcia (1975) in p channels of Si. The bulk dispersion relation was approximated by

$$\varepsilon(K)=\varepsilon_G\left[\left[1+\frac{2\hbar^2K^2}{m\varepsilon_G}\right]^{1/2}-1\right] , \quad (8.25)$$

and the subband structure was determined variationally with the use of Eq. (3.34) for the ground subband and an orthogonal trial function for the first excited subband. Effects of higher subbands were included in a very crude way. In spite of the crudeness of the approximation the results turned out to be in reasonable agreement with those of Arai in InSb, especially for low electron concentrations where occupation of higher excited subbands was not appreciable. It is not yet clear why the simplification works well for the conduction band in narrow-gap semiconductors but does not for the valence band of Si. One possible reason is that, in p channels of Si, wave functions of heavy and light holes overlap each other and mixing between them caused by the surface potential is very important, while in n-channel layers of narrow-gap semiconductors the states associated with the conduction band and the valence band are spatially separated and mutual mixing is not important as long as tunneling effects are negligible. Takada and Uemura also investigated the possibility of occupation of subbands associated with conduction-band valleys having a heavy effective mass. The lowest such valleys are believed to exist at the L point in InAs, InSb, and GaAs (see, for example, Phillips, 1973; Aspnes, 1976). They showed that a subband associated with heavy-mass valleys could be populated at sufficiently high concentrations because its kinetic energy corresponding to the motion in the z direction does not increase so much due to the large effective mass. This is similar to the situation in an n-channel layer on Si(100) under high uniaxial stresses. This approximation scheme has been refined significantly by Takada, Arai, Uchimura, and Uemura (1980a, 1980b), who obtained a subband structure in good agreement with experiments and calculated also optical spectra for both parallel and perpendicular polarization of the electric field.

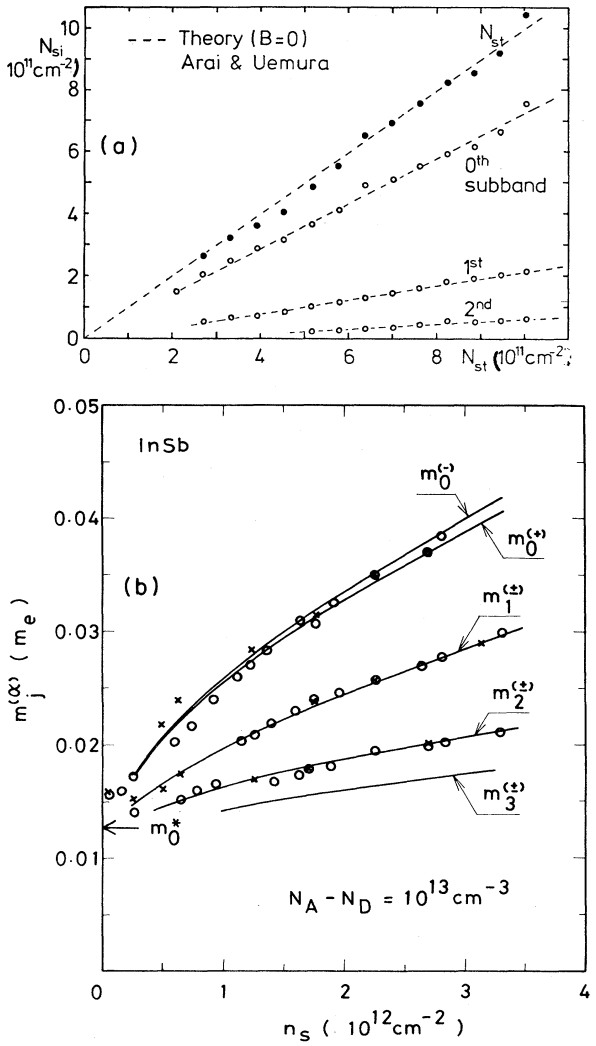

FIG. 167. Subband occupation N_{si} (a) and cyclotron effective mass m_{ci}^* (b) of the ith subband in an n-channel inversion layer on InSb vs electron density. The theoretical values (dashed lines) are taken from Arai (unpublished) for the subband occupation and from Takada *et al.* (1980b) for the effective mass. After Därr and Kotthaus (1978) and Takada *et al.* (1980b).

2. InSb

Extensive investigations of n-channel space-charge layers on InSb have been performed. The conduction band of InSb is characterized by a small effective mass and is highly nonparabolic, as has been discussed in a previous section. Preliminary work on the low-temperature conduction was started in the 1960s (Kawaji *et al.*, 1965; Chang and Howard, 1965; Kawaji and Gatos, 1967a; Komatsubara *et al.*, 1969). Kotera, Katayama, and Komatsubara (1972a) succeeded in observing Shubnikov–de Haas oscillations in elaborately prepared MOSFET samples with SiO_2-insulated gates. The complicated oscillations showed occupation of more than two subbands and were analyzed in terms of two subband levels in a triangular potential well. The intricacies of the subband structure in narrow-gap materials were not appreciated at that stage, however.

A thorough investigation of the quantum oscillations was later made by Därr and co-workers (Därr and Kotthaus, 1978; Därr *et al.*, 1978). They observed beautiful Shubnikov–de Haas oscillations and determined subband occupations which are shown in Fig. 167 together with the theoretical prediction of Arai. For densities up to $N_s \sim 10^{12}$ cm^{-2} three subbands are partially filled. The good agreeement between the theory and the experiments seems to suggest that interband effects are still unimportant up to this electron concentration.

The cyclotron resonance has also been observed (Därr *et al.*, 1975, 1978), although not yet fully published. The resonance contains separate lines from each subband because the strong nonparabolicity makes the effective mass subband dependent. The cyclotron masses deduced from the resonance fields seem to be in reasonable agreement with the theoretical result, especially in low magnetic fields. Further, the resonance amplitudes have been shown to be related reasonably well to the occupancy determined from the Shubnikov–de Haas oscillations.

A weak but distinct peak was observed on the high-

field tail of the cyclotron resonance when the magnetic field was tilted from the normal to the surface (Därr *et al.*, 1976). This resonance was attributed to a spin resonance since its position was essentially determined by the total magnetic field when the field was tilted and was close to that expected from the bulk g value. The intensity seemed to depend strongly on the tilt angle and disappeared when the magnetic field was exactly perpendicular to the surface. However, its mechanism and the tilt angle dependence have not been fully understood yet. In a narrow-gap semiconductor with strong spin-orbit interaction and nonparabolicity, spin resonances can be induced by usual electric-dipole transitions. This so-called electric-dipole-induced electron spin resonance was first observed in bulk $Hg_{1-x}Cd_xTe$ by Bell (1962) and in bulk InSb by McCombe and Wagner (1971). Its matrix element was calculated for the bulk by Sheka (1964) and is given by

$$v_- = v_x - iv_y \cong -\frac{\hbar}{m_s} k_z \frac{2\varepsilon_G + \Delta}{\varepsilon_G(\varepsilon_G + \Delta)} \frac{\hbar eH}{m_s c} , \qquad (8.26)$$

where $m_s = 2m/|g^*|$ and the magnetic field H is in the z direction. It is clear that the matrix element given by (8.26) vanishes in the inversion layer because $\langle k_z \rangle = 0$. The k-linear term discussed in the previous section could give rise to a large spin resonance matrix element, even for the magnetic field normal to the surface, if $\langle \partial V/\partial z \rangle$ were set equal to F_{eff}. The experimental results also show that one must put $\langle \partial V/\partial z \rangle \cong 0$ and that such a large k-linear splitting of the spin degeneracy does not exist. In tilted magnetic fields where mixing between different subbands and Landau levels is appreciable, the spin resonance seems to become strong, but the mechanism is not yet established because of the difficulty of the problem.

Direct intersubband optical absorptions were observed by Beinvogl and Koch (1977) in the configuration where incident infrared light was chosen to be normal to the surface. Because of the nonparabolicity, the electron motion parallel to the surface couples with the perpendicular motion, which can give rise to intersubband transitions even in this configuration (Beinvogl *et al.*, 1978). There is no net polarization of electrons in the direction normal to the surface, and the resonance is not affected by the depolarization effect which is important in Si inversion layers, as has been discussed in Sec. III.C. The observed resonance energies, E_{10}, E_{20}, and E_{21}, seemed at first to agree well with the theoretical result. Experiments by Wiesinger, Beinvogl, and Koch (1979) have revealed, however, that the resonance lines are actually observed as doublets. The temperature dependence of the resonance has also been investigated. The resonance positions have been shown to shift to the lower-energy side in contrast to the prediction in the simple Hartree approximation for Si inversion layers, as discussed in Sec. III.A. Induced free electrons and holes might be responsible for such anomalous temperature dependence. These problems remain to be explained in the future.

3. InAs

It has been known from anomalous behavior of the Hall coefficient that surfaces of p-type InAs crystals can be inverted and natural n-channel inversion layers can be formed. The study of inversion layers on InAs began quite early. Kawaji and co-workers (Kawaji and Kawaguchi, 1966; Kawaji and Gatos, 1967b) studied the conductivity of an inversion layer on etched surfaces both in the presence and in the absence of a magnetic field. The electron concentration was controlled by a mylar-foil-insulated gate. The mobility was found to increase with carrier density, consistent with ionized impurity scattering in the quantized surface channel. The surface magnetoresistance exhibited oscillatory variations which were most likely quantum oscillations.

Work was later extended to surfaces cleaved in air, where charges at the surface cause a strong band bending and an inversion layer with an extremely high electron concentration $N_s \sim 10^{13}$ cm^{-2} (Kawaji, 1968; Kawaji and Kawaguchi, 1968). Anomalous changes of the resistivity and magnetoresistance were observed below 4 K. The resistivity was found to drop rapidly around 3 K and to become extremely small below 2 K. This resistivity change disappeared in the presence of a magnetic field. This anomaly was primarily analyzed in terms of scattering by localized spins, but was considered to be caused by fluctuation effects in two-dimensional superconductors (Kawaji, Miki, and Kinoshita, 1975). The transition temperature was estimated as 2.7 K. The superconductivity has not been observed by other groups, however.

Takada and Uemura (1976) investigated various possible mechanisms which could give rise to superconductivity in the inversion layer. Because of the small density of states near the Fermi energy, phonons alone are not sufficient to support superconductivity. Takada and Uemura suggested as the most probable mechanism acoustic plasmons existing in multicarrier systems like space-charge layers on III-V compound semiconductors. It was suggested that acoustic plasmons play a similar role for the superconductivity of carriers in the subband with high electron concentrations to that played by the acoustic phonons in metals. Takada and Uemura estimated the coupling constant from an integral kernel of a gap equation and showed that superconductivity was possible at high electron concentrations if the acoustic-plasmon mechanism was combined with phonon mechanisms. Properties of acoustic plasmons were later studied by Takada in various cases (Takada, 1977). More recently Takada (1978, 1980b) numerically solved the gap equation including electron-electron interactions in the random-phase approximation and found that the plasmon itself could cause the superconductivity when the electron concentration was not too high and not too low. He suggested that the experimentally observed high T_c could be explained if a heavy effective mass and a small dielectric constant were assumed. The problem is still open because the calculation includes various approximations and unknown parameters concerning the

subband structure at high concentrations like 10^{13} cm^{-2}. It is not certain whether the plasmon alone can give rise to the superconductivity in principle. (See Sec. II.F.1 for references to related theoretical work by Hanke and Kelly on superconductivity in silicon).

Tsui (1970a—1970c, 1971b, 1972, 1973, 1975a, 1975b) extensively studied n-channel accumulation layers on degenerate InAs (2.2×10^{16} cm$^{-3} < N_D - N_A < 1.6\times10^{18}$ cm^{-3}), where bound charge states coexist with free charge in the surface region. He employed tunneling of electrons through an interface barrier to determine the bound-state energies. The derivative of the tunneling conductance with respect to the applied bias voltage showed a dip when the bottom of a subband coincided with the Fermi energy of the metal gate. Energies of two bound states were determined at low bulk carrier densities, while only a single level was found at high densities. An example of observed conductance is given in Fig. 168. For magnetic fields perpendicular to the interface the conductance showed quantum oscillations associated with Landau levels of the bound state, which could directly determine the cyclotron mass of subband carriers. The cyclotron masses were found to increase with the applied magnetic field, reflecting the nonparabolicity of the conduction band. The diamagnetic energy shift caused by a magnetic field parallel to the surface discussed in Sec. III.D was observed first in these tunneling experiments (Tsui, 1971a).

The screening of an external electric field by free bulk carriers in the vicinity of the surface of degenerate semiconductors was theoretically investigated in different approximations by Appelbaum and Baraff (1971a—1971c; see also Baraff and Appelbaum, 1972) in considerable detail. By a self-consistent Hartree-type calculation they showed that bound surface states could exist even in the absence of external electric field when the electron concentration was sufficiently large. This bound state is a result of a deficiency of negative charges arising from the existence of the large barrier potential at the surface. Their self-consistent calculation gave results at least in qualitative agreement with the experiments of Tsui. A quantitative comparison is not possible because of the importance of the nonparabolicity on actual InAs accumulation layers. Effects of a magnetic field perpendicular to the surface on the bound-state energy were also studied. Landau quantization of surface carriers, rather than quantization of bulk carriers, was shown to be a main cause of the quantum oscillation of the bound-state energy. This was confirmed by the experiments of Tsui (1972).

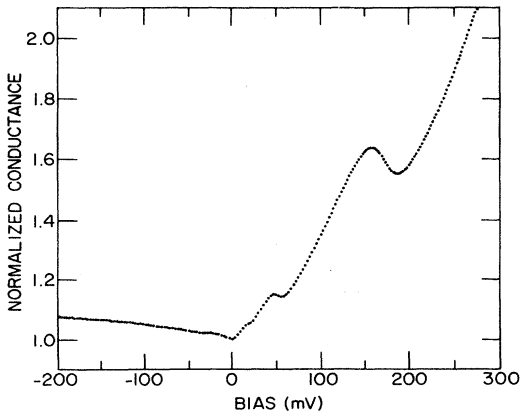

FIG. 168. Normalized conductance vs bias on an n-type InAs-oxide-Pb tunnel junction observed by Tsui (1971b). The bulk carrier concentration is 2.2×10^{16} cm^{-3}. The conductance shows structures when the Fermi level of Pb crosses the bottoms of the subbands (E_0 at $\sim$180 meV and E_1 at $\sim$50 MeV). The structure around 20 meV corresponds to crossing the conduction-band edge of the bulk InAs.

InAs has again become a subject of active experimental investigations. A space-charge layer with tunable N_s has been created on n-type epitaxial layers grown on GaAs substrate material (Wagner *et al.*, 1978; Washburn and Sites, 1978; Washburn *et al.*, 1979). In these experiments the bulk doping is much smaller ($N_D - N_A \sim 2\times10^{15}$ cm^{-3}) than in the samples used by Tsui, and the existence of free carriers is not so important. Subband occupations have been determined from quantum oscillations of surface conductivity, and three subbands have been shown to be occupied by electrons up to $N_s \sim 2.5\times10^{12}$ cm^{-2}. Resonant Raman scattering has been reported, and LO phonons coupled to intersubband excitations have been observed (Ching *et al.*, 1980). Intersubband transitions have also been observed by absorption and reflection experiments (Reisinger and Koch, 1981). Clear evidence of the presence of mixed electric and magnetic subbands (see also Sec. III.D) has been observed in a magnetic field parallel to the surface (Doezema *et al.*, 1980). Comparison of experimental mobility results (Kawaji and Kawaguchi, 1966; Baglee *et al.*, 1980) for electrons in InAs inversion layers with theoretical estimates by Moore and Ferry (1980c) shows surface roughness scattering to be important over the entire range of N_s values covered, from $\sim10^{11}$ to 2×10^{12} cm^{-2} (Baglee *et al.*, 1981).

4. InP

There have been attempts to make high-quality MIS structures on GaAs, which have been motivated by the hope of applying such devices to the fabrication of large-scale integrated circuits operating at multigigabit data rates. They have been unsuccessful, however, because of large surface-state densities which are observed on this semiconductor. In contrast with GaAs, the III-V compound InP has turned out to have lower surface-state densities, and an inversion layer has been produced on p-type materials. Its transport properties have been studied at room temperature, generally in the context of metal-insulator-semiconductor device characterization (see, for example, Roberts *et al.*, 1977, 1978; Lile *et al.*, 1978, Kawakami and Okamura, 1979; Meiners *et al.*, 1979; and Baglee *et al.*, 1980). For a review of materials aspects of work on field-effect transistors using com-

pound semiconductors, see Wieder (1980, 1981).

Low-temperature experiments are beginning to be carried out. Several preliminary results have been reported, such as Shubnikov–de Haas oscillations (von Klitzing *et al.*, 1980a, 1980b) and cyclotron resonance (Cheng and Koch, 1981).

5. $Hg_{1-x}Cd_xTe$

Both HgTe and CdTe have the zinc-blende structure, and the edges of both the conduction and valence bands are located at the Γ point. In HgTe the deep potential well of the heavy Hg ion pulls down the energy of the s-like state, which has a large electron density distribution around the ion core. Consequently HgTe has the so-called inverted ordering of the bands, i.e., the s-like Γ_6 band lies below the p-like Γ_8 band. The band gap is about 0.28 eV at low temperatures. On the other hand, CdTe has a structure similar to that of InSb and InAs. The band gap is about 1.6 eV. Therefore band crossing occurs in the $Hg_{1-x}Cd_xTe$ alloys, near $x=0.146$ at low temperatures. For $x>0.146$ the alloys can be regarded as narrow-gap semiconductors, while for $x<0.146$ they are semimetals. These materials are ideal for studying band mixing effects.

Antcliffe, Bate, and Reynolds (1971) observed oscillatory magnetoresistance in naturally inverted surfaces of p-type $Hg_{1-x}Cd_xTe$ ($x=0.21$) with the band gap $\varepsilon_G=68$ meV and the band-edge mass $m=0.06m_0$ at 4.2 K. Several sets of oscillations were recorded, and the electron concentrations were determined from the oscillation periods. Various samples were found to have different surface electron densities between 1 and 7×10^{11} cm^{-2}. The effective mass was obtained from the temperature dependence of the oscillation amplitudes and was found to vary from sample to sample according to the electron concentration. The results were analyzed with the use of the subband structure calculated in the WKB approximation for a triangular potential and the simplified bulk dispersion relation $\hbar^2K^2/2m=\varepsilon(1+\varepsilon/\varepsilon_G)$. The analysis showed that only the ground subband was occupied, which led Antcliffe *et al.* to conclude that different sets of quantum oscillations observed in a single sample were associated with different regions of the surface having different electron concentrations. A later more elaborate analysis of Ohkawa and Uemura (1974a, 1974b) suggested that at least two subbands could be occupied by electrons. Ohkawa and Uemura calculated the effective mass with the use of an appropriately parametrized potential and obtained reasonable agreement with the experiments.

Narita, Kuroda, and co-workers (Kuroda and Narita, 1976; Narita and Kuroda, 1977; Narita *et al.*, 1979) constructed an MIS structure of $Hg_{1-x}Cd_xTe$ ($x=0.165$, 0.180, and 0.185) using a thin mylar foil as an insulator. They could vary the surface charge concentration between 0 and 8×10^{11} cm^{-2}. Surface cyclotron resonance was observed from electrons in various subbands. Shubnikov–de Haas oscillations of the surface conductivity were also obtained, using nonresonant microwave absorptions. They could determine the cyclotron masses and the electron occupation ratios of various subbands. The results were compared with a calculation of Takada and Uemura (unpublished), who extended their method (Takada and Uemura, 1977) for III-V semiconductors to $Hg_{1-x}Cd_xTe$. The experimental results were in disagreement with the calculation and seemed to be explained if one assumed that the actual surface charge density for a given gate voltage was about half of that determined experimentally.

Thuillier and Bazenet (1979) made capacitance measurements in a magnetic field and obtained electron concentrations of various subbands. The results turned out to be explained by the calculation of Takada and Uemura. The origin of such disagreement between different experiments is not known.

C. Space-charge layers on other materials

1. Ge

A superb natural insulating oxide and a good-quality interface have made Si the obvious choice for MOSFETs, and a great deal of physical research has been done on the quantized electronic states on Si surfaces. Surface and interface transport properties of germanium have also been the concern of physical research. However, the natural oxide of Ge is unstable, and Ge has been known to have high density of interface states, which has made sophisticated research like that on Si surfaces very difficult. In spite of the difficulties, various experiments have been carried out on Ge surfaces.

Germanium has four very anisotropic conduction-band minima at the Brillouin-zone edge in the $\langle 111\rangle$ directions, which are characterized by longitudinal and transverse effective masses $m_l=1.6m_0$ and $m_t=0.08m_0$, respectively. The valley which has its longitudinal mass perpendicular to the surface gives rise to one ladder of subbands denoted by 0,1,2, . . . , whereas the other three valleys give rise to another, higher-lying ladder of subbands, 0′,1′,2′, ... Although the situation is quite similar to that on Si(100), there are two features significantly different from Si(100). First, the effective mass normal to the surface of the unprimed subbands is larger than that in Si, while the density of states is much smaller because of the small transverse mass and the lack of valley degeneracy. This means that the Fermi energy increases much faster with the electron concentration, so that several excited subbands are readily filled by electrons. Second, the large-mass anisotropy and thereby a small normal effective mass for the 0′ subband push it up in energy drastically. As a matter of fact, a density-functional calculation of Vinter (1979a) predicts that E_1 starts to be occupied below $N_s=3\times10^{11}$ cm^{-2} and E_2 below 1×10^{12} cm^{-2} and that $E_{0'}$ is very close to E_3. In contrast, $E_{0'}$ is close to E_1 on the Si(100) surface.

Weber, Abstreiter, and Koch (1976) prepared a metal-

insulator-semiconductor (MIS) structure on the (111) surface of p-type Ge using mylar foil as an insulator. Because the samples lack source-drain contacts, microwave absorption was used to measure the surface conductivity. They observed distinct Shubnikov–de Haas oscillations and cyclotron resonances originating from electrons in the surface subbands. A single period of quantum oscillation observed up to $N_s \sim 6.2 \times 10^{12}$ cm^{-2} indicated a single occupied subband and gave the subband occupancy of only $\sim 20\%$ of the charge N_s. They proposed that about 80% of the induced charge occupied bound surface states.

Binder, Germanova, Huber, and Koch (Binder *et al.*, 1979a, 1979b) prepared better samples by coating Ge surfaces with a dielectric lacquer layer. They observed additional Shubnikov–de Haas oscillations, supposed to arise from electrons in the ground subband. Figure 169 gives some examples of the magneto-oscillation spectrum of (111) Ge, where S_0 and S_1 are series of peaks associated with the ground and the first excited subbands, respectively. Only S_1 was observed, and S_0 was not observed in the previous experiments (Weber *et al.*, 1976). This is probably because the smaller binding length of the ground subband results in stronger scattering from surface charges and imperfections and a poor mobility. Figure 170 shows the subband occupation numbers of electrons determined from the oscillation periods, together with those calculated by Vinter (1979a). The observation of S_0 certainly explains the main part of the electrons "missing" in the earlier experiment. However, there still remain some electrons which do not show up in the Shubnikov–de Haas oscillations. Further, the agreement between the theoretical and experimental results is not perfect. It has been suggested that the 0′ subband is for some reason possibly much lower in energy than predicted and the Fermi level is strongly pinned at $E_{0'}$ because of its large density of states. Intersubband optical absorptions have also been observed in Ge, and the resulting resonance energies for the 0→1 and 0→2 transitions are in reasonable agreement with theoretical estimations (Scholz and Koch, 1980).

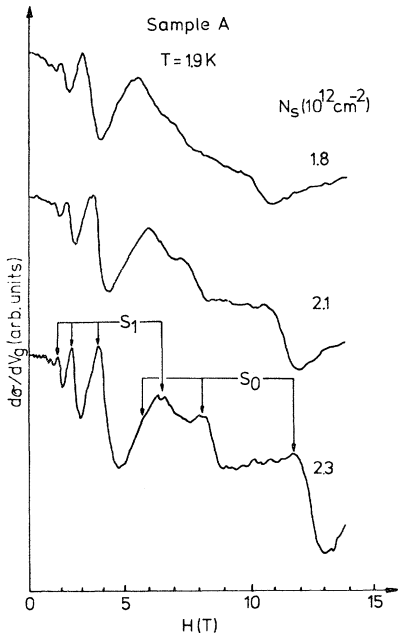

FIG. 169. Magnetoconductivity of an n-channel inversion layer on a Ge(111) surface. S_0 and S_1 are series of peaks associated with the ground and the next-higher-lying subband. After Binder *et al.* (1979a).

2. Te

Tellurium is another elemental semiconductor on which surface subbands have been examined extensively. The Te crystal is characterized by its distinctive chain structure with large anisotropy and no center of inversion. Both the valence-band maxima and the conduction-band minima are known to be in the vicinity of a corner (called the H point) of the hexagonal Brillouin zone. Pure crystals of this material are p-type degenerate, with hole concentrations rarely less than 10^{14} cm^{-3}, and it has been impossible to synthesize n-type samples. Consequently the valence-band structure has been the object of interest and has been studied extensively. It has been found that the valence band takes the so-called camel-back shape and the Fermi surface has a dumbell-like form owing to a large k-linear term originating from the lack of inversion symmetry. There has not been so much work on the conduction band because of the lack of n-type bulk samples. Therefore the inversion layer is especially important, since it provides an excellent tool for the study of electrons in the conduction band.

Investigations of surface properties began rather early. From field-effect experiments (Silbermann *et al.*, 1971) it was deduced that usually an accumulation layer is

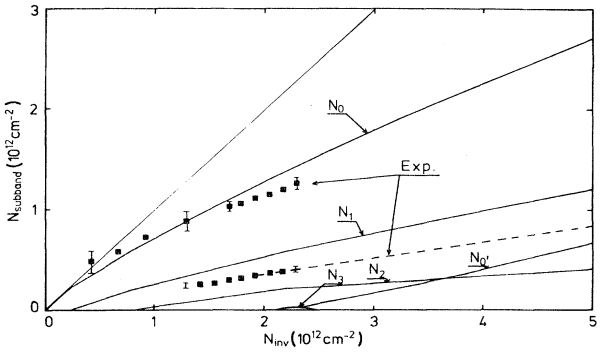

FIG. 170. Comparison between calculated (Vinter, 1979a) and observed (Binder *et al.*, 1979a) population of subbands as a function of total energy density in an n-channel inversion layer on a Ge(111) surface. N_{inv} corresponds to N_s in the text and N_i represents the population of the ith subband. The broken line represents earlier experimental results (Weber *et al.*, 1976). After Vinter (1979a).

present at the surface of pure Te single crystals. This accumulation could be so much enhanced by chemical treatment that surface carriers confined in surface subbands could show up in quantum oscillations of bulk sample resistance in magnetic fields (von Klitzing and Landwehr, 1971). Extensive investigations were later performed in both accumulation and inversion layers on the (0001) and (1$\bar{1}$00) surfaces (Silbermann *et al.*, 1974; Silbermann and Landwehr, 1975, 1976). The work employed a metal-insulator-semiconductor (MIS) structure in which insulating mylar foils were loosely mounted on chemically polished surfaces. This technique made it possible to vary surface hole concentration over a wide range and also generate electron inversion layers. On the (0001) surface up to four periods for holes were identified in surface quantum oscillations. The distribution of holes in each subband was determined from the period. The effective masses were also obtained from the temperature dependence of the oscillation amplitude. However, electron signals were observed only with difficulty. On the (1$\bar{1}$00) surface many periods were observed for both electrons and holes. They gave $g_v g_s = 2$ for both cases, where g_v and g_s are the spin and the valley degeneracy factor, respectively. However, the total charge density deduced from the assignments revealed that about 10% of the total charge calculated from the applied voltage was missing. Additional work has been performed for inversion layers on both surfaces (Bouat and Thuillier, 1974, 1977, 1978a, 1978b), and two periods have been identified in the quantum oscillations.

A self-consistent calculation of surface subbands has been done within a simplified treatment for the accumulation layer on the (0001) surface (Kaczmarek and Bangert, 1977). The calculation predicts that six electric subbands are occupied for experimentally available hole concentrations. It has been suggested that two subbands are very close to the Fermi energy and do not contribute to Shubnikov–de Haas oscillations. Calculated charge distributions among the remaining four subbands are in excellent agreement with experimental results. However, the enhancement of the effective masses from the bulk value cannot be fully accounted for by the calculation. Kaczmarek and Bangert (1980) also performed calculations for inversion layers on the (0001) and (1$\bar{1}$00) surfaces in magnetic fields normal to the surface. A large k-linear term has been shown to remove the spin degeneracy. Calculated subband occupations and effective masses roughly explain the experimental results of Shubnikov–de Haas oscillations and cyclotron resonances.

Cyclotron resonance has been observed in both accumulation and inversion layers (von Ortenberg and Silbermann, 1975, 1976). Figure 171 shows an example of the cyclotron resonance spectra of electrons and holes on the (0001) surface for two different wavelengths. The resonance line shape has a common pseudosplitting due to bulk hole absorptions, which makes the line-shape analysis rather complicated. The cyclotron mass increases considerably with the hole concentration in the

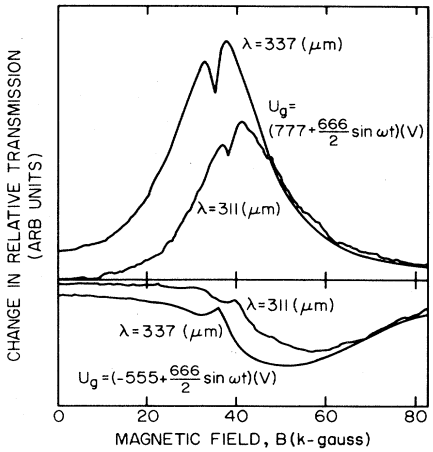

FIG. 171. Cyclotron resonance spectra of electrons (upper panel) and holes (lower panel) on a Te(0001) surface for radiation of two different wavelenghts ($\lambda = 311$ and 337 μm). Sharp dips, which cause the common pseudosplitting of the line shape, are due to bulk hole cyclotron resonances. After von Ortenberg and Silbermann (1976).

accumulation case, while it is almost independent of the electron concentration in the inversion case. Investigation of the frequency dependence of the cyclotron resonance has revealed an anomalous increase of the effective mass at low frequencies in both accumulation and inversion layers on the (0001) and (1$\bar{1}$00) surface (von Ortenberg *et al.*, 1979; von Ortenberg, 1980). The reason for this anomalous behavior cannot be explained by nonparabolicity and remains unresolved.

3. PbTe

The IV-VI compound PbTe has the NaCl crystal structure, and its conduction band has multiple minima at the L points of the Brillouin zone of the fcc lattice. Because of the small direct energy gap at L ($\varepsilon_G = 0.19$ eV at 4.2 K), the conduction band is highly nonparabolic. Extrinsic carriers are generated by deviations of stoichiometry, and no freeze-out of these carriers has been detected at any temperature. The electron Fermi surface consists of four elongated ellipsoids with their major axes oriented along the ⟨111⟩ directions. The transverse mass m_t and the longitudinal mass m_l at the band minima are $m_t \sim 0.02 m_0$ and $m_l \sim 0.2 m_0$. The static dielectric constant is extremely large, $\kappa_{sc} \sim 1000$, reflecting the unusual lattice properties of the lead salts, which makes the system quite different from other narrow-gap semiconductors like InSb and HgCdTe.

The accumulation layer on the (100) surface of n-type PbTe has been studied in electron tunneling through PbTe-oxide-Pb junctions (Tsui *et al.*, 1974; Tsui, 1975b). A natural accumulation layer with a fixed electron concentration of about 2×10^{13} cm^{-2} is observed on PbTe with bulk electron concentration of 1.2×10^{18} cm^{-3}. Existence of three quantized levels is suggested from dips in the tunneling currents. The depth of the surface poten-

tial well is also obtained. A perpendicular magnetic field gives rise to oscillations in the tunneling current, which give the Landau-level structure in the accumulation layer. It has been demonstrated that Landau levels of different subbands interact strongly with each other, possibly because of strong nonparabolicity. Ion-bombarded surfaces have been studied (Tsui, Kaminsky, and Schmidt, 1978), and four occupied electron subbands were observed for both PbTe-oxide-Pb and PbTe-oxide-Sn junctions. Tunneling through PbTe-Au Schottky barriers was also observed.

The nonparabolicity effect was considered in a two-band $\mathbf{k}\cdot\mathbf{p}$ model by Lin-Chung (1979), who assumed a parametrized surface potential and calculated the subband energies in the WKB approximation. The scheme was essentially the same as that for III-V compounds proposed earlier by Ohkawa and Uemura (1974a, 1974b). Comparison with experiments requires a full self-consistent calculation, however.

An inversion layer has been created on (111) surfaces of epitaxially grown p-type materials with bulk hole concentration 7×10^{16} cm^{-3} (Schaber *et al.*, 1977). The surface electron density is tuned using a mylar-foil-insulated gate electrode. Distinct Shubnikov–de Haas oscillations have been observed. However, the number of carriers at a given gate voltage which contribute to the oscillations has been found to be only about 5% of the total number expected. Cyclotron resonance was later observed in this system (Schaber *et al.*, 1978; Schaber and Doezema, 1979). The reflectivity was measured, since the frequency of the radiation used was within the restrahlen band of PbTe. Further, circularly polarized radiation was used to distinguish the surface electron contribution from bulk hole resonances. Figure 172 shows an example of observed spectra for the electron active mode. The difference of the reflectivities for $V_G=V_T$ and $V_G=V_G(N_s)$ is plotted against applied magnetic field. The large dip around $H\sim23$ kOe corresponds to cyclotron resonances of electrons in the a valley which presents the major axis in the direction normal to the surface, and a weak structure around 50 kOe corresponds to those of electrons in three b valleys whose major axes form an angle of 70.53° with the surface normal. A line-shape analysis suggests electron occupation of several subbands associated with the a valley and a few associated with the b valleys. This fact has been shown to be consistent with a calculation in a triangular potential approximation. The effective masses deduced from the resonance positions are close to the bulk cyclotron mass rather than the predicted two-dimensional one. Further, the b-valley resonances split with tilting of the magnetic field, as shown in the figure. This suggests that the surface field is so weak—because of the large static dielectric constant—that the binding length is larger than the cyclotron radius and the electron motion is three-dimensional. The occupation of the b valleys explains the absence of electrons mentioned previously.

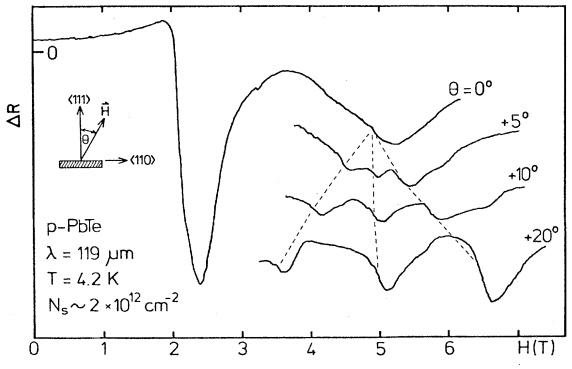

FIG. 172. Differential magnetoreflectivity of an n-channel inversion layer on a PbTe(111) surface. A large dip around 2.3 T is due to cyclotron resonance of electrons in the a valley. A weak b-valley cyclotron resonance around $H=5$ T splits into three dips with tilting magnetic field. This suggests the three-dimensional nature of the system.

4. ZnO

ZnO is the only example of the class II-VI materials for which surface transport has been seriously examined. Various methods have been proposed to create n-channel accumulation layers on ZnO crystals (for reviews see, for example, Many, 1974; Göpel and Lampe, 1980). The conductivities and Hall conductivities of the polar Zn and O surfaces and the prism surface have been measured for vacuum-cleaved surfaces with annealing treatments in atomic hydrogen and oxygen atmospheres (Heiland and Kunstmann, 1969; Kohl and Heiland, 1977; Kohl *et al.*, 1978). Very strong accumulation layers ($N_s\sim10^{14}$ cm^{-2}) have been obtained with voltage pulses applied in an electrolyte, and the density of induced charge has been measured as a function of the surface barrier height (Eger *et al.*, 1975, 1976; Eger and Goldstein, 1979). Corresponding theoretical calculation of the subband structure gives results in reasonable agreement with the experiments. Extremely strong accumulation layers were produced also by illuminating ZnO crystals in vacuum with band-gap light and by exposure to thermalized He^+ ions. The Hall and field-effect mobilities have been measured as a function of the electron concentration. Papers by the Aachen group (Kohl and Heiland, 1977; Kohl *et al.*, 1978; Moormann *et al.*, 1980; Veuhoff and Kohl, 1981) have reported that at low carrier concentrations the mobility oscillates as N_s varies, for reasons which are not well understood. At higher electron concentrations they and the group at Jerusalem (Goldstein *et al.*, 1977; Grinshpan *et al.*, 1979; Nitzan *et al.*, 1979) find smoother variations. Mobilities are of order 100 cm^{2}V^{-1}s^{-1} at room temperature, less than half of a calculated value based on polar phonon scattering (Roy *et al.*, 1980). At temperatures below 100 K the mobilities exceed 1000 cm^{2}V^{-1}s^{-1}. At the highest values of N_s, of order 10^{14} cm^{-2} and above, interface roughness is thought to dominate and the mobilities fall below 100 cm^{2}V^{-1}s^{-1}.

A large negative magnetoresistance has been observed (Goldstein and Grinshpan, 1977; Goldstein *et al.*, 1979) which varies as $(B/T)^2$ over a considerable range of magnetic fields and temperatures and reaches values over 2% for $B/T \sim 0.1$ T K^{-1}. It has been suggested that positive surface charges which conglomerate into large clusters with large magnetic moments may be the main scatterers in such systems. The energy-loss spectrum of low-energy electrons has been observed and analyzed in terms of two-dimensional plasmons (Goldstein *et al.*, 1980; Many *et al.*, 1981).

D. Heterojunctions, quantum wells, and superlattices

1. Structures

A superlattice arises when a periodic spatial modulation is imposed and lowers the effective dimensionality of a system. The simplest example relevant to the present discussion is the superposition of a periodic potential, as produced by a sound wave (Keldysh, 1962), a composition variation (Esaki and Tsu, 1970), or an impurity concentration modulation (Döhler, 1972a, 1972b) on an otherwise homogeneous three-dimensional system. Superlattices have also been proposed in two-dimensional systems (Bate, 1977; Ginzburg and Monarkha, 1978; Petrov, 1978; Stiles, 1978; Ferry, 1981).

The development of crystal growth techniques such as molecular-beam epitaxy (Cho and Arthur, 1976; Esaki and Chang, 1976) and metalorganic chemical vapor deposition (Dupuis and Dapkus, 1979) has made possible the growth of semiconductors with controlled changes of composition and doping on a very fine scale. The first man-made semiconductor superlattice was reported by Blakeslee and Aliotta (1970), who used chemical vapor deposition to make $GaAs_{1-x}P_x$ structures. Heterostructures which exhibit two-dimensional electron effects have also been made using liquid-phase epitaxy (Tsui and Logan, 1979). In this section we shall briefly discuss some of the structures that have been made in the past ten or so years and shall consider some of their properties, with particular reference to two-dimensional behavior and quantum effects. The role of the many people involved in the preparation of improved materials and structures, cited only peripherally in this article, has been a key factor in the advances that have been made in the electronic properties and the device applications of these systems.

Figure 173 shows the energy-band diagram of a GaAs-$Ga_{1-x}Al_xAs$ heterojunction, with the band-gap discontinuity that arises in the presence of an abrupt composition change. The quasitriangular potential well can confine electrons (see, for example, van Ruyven, Bluyssen, and Williams, 1979) and can lead to quantum effects similar to those seen in inversion layers. Two heterojunctions can be combined to give a quantum well, for example a thin layer of GaAs surrounded by layers of $Ga_{1-x}Al_xAs$. Such structures, with central layers too thick to show quantum effects, have been used for many years in double-heterostructure lasers (Kressel and Butler, 1977; Casey and Panish, 1978) to confine both carriers and light. As the thickness of the central layer becomes comparable to the Fermi wavelength $2\pi/k_F$, quantum effects become important and modify the energy-level structure of the system. If many such wells with adjoining barriers are combined in a regular array, a superlattice is formed.

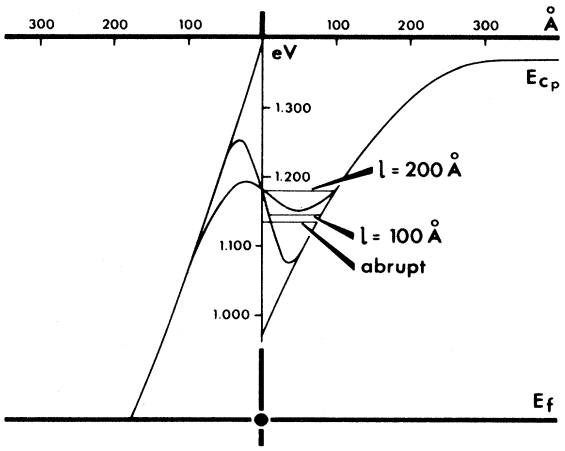

FIG. 173. Schematic drawing of the conduction-band edge at a GaAs-$Al_{0.4}Ga_{0.6}As$ heterojunction with an abrupt composition change or a transition layer graded over 10 or 20 nm. The position of the lowest quantum level is indicated by the horizontal line for each of the three cases. After van Ruyven *et al.* (1979).

The combinations of materials from which heterojunctions—and therefore quantum wells and superlattices—can be made is limited by material constraints such as reasonable matching of lattice parameters and absence of large densities of interface states. The possibility of using more than two materials has been considered by Esaki, Chang, and Mendez (1981). Reviews of superlattices have been given by Shik (1974), Dingle (1975a, 1975b), Sai-Halasz (1979, 1980), Chang and Esaki (1980), and Döhler (1981).

A superlattice that does not involve heterojunctions was considered by Döhler (1972a, 1972b, 1979, 1981). It is called a "nipi" structure and is made by alternating donor and acceptor doping. Because the band bending arises from space-charge effects, the spatial period of such structures is generally larger than for heterojunction superlattices and the barriers are generally less sharp. These structures are now beginning to be realized and their possibilities are being explored (Ploog *et al.*, 1981a, 1981b; Künzel *et al.*, 1981; Döhler *et al.*, 1981). One interesting feature is that one can contact the *n*-type layers and the *p*-type layers separately and apply a voltage difference to modulate the potential variations and the effective energy gap for optical transitions.

2. Energy levels

Energy levels can be calculated most easily for a quantum well—or for a thin film— if one assumes an abrupt

interface and an inifinite barrier height. Then in effective-mass approximation the energy levels are given by

$$E=\frac{\hbar^2}{2m_z}\frac{\pi^2}{d^2}n^2+\frac{\hbar^2k^2}{2m}, \tag{8.27}$$

where d is the well width, m_z is the effective mass for motion perpendicular to the walls, and k and m are the wave vector and effective mass for motion parallel to the walls. This spectrum shows increasing level spacing with increasing quantum number n, which is opposite to the behavior in a triangular well. See Eq. (3.24).

If the barrier height is finite and if the carriers inside the barrier have properties not too different from those in the well, e.g., they arise from the same band extremum, then the simple effective-mass approximation can still be used to calculate an envelope wave function provided the proper boundary conditions (Harrison, 1961; see also Price, 1962) are used to match the envelope functions at the barrier plane. More complex cases are mentioned briefly in Sec. III.E.

The energy-level structure of a quantum well has been confirmed in a number of experiments, including optical experiments mentioned below and tunneling measurements, for example those of Chang, Esaki, and Tsu (1974b) shown in Fig. 174.

If many quantum wells are arranged periodically the energy levels for motion in the z direction will interact as the wave functions of adjacent wells begin to overlap inside the barrier. The superlattice periodicity creates a new, smaller Brillouin zone in the k_z direction. The discrete quantum levels of widely spaced wells are replaced by a series of energy bands called minibands. Their energy bandwidth increases as the barrier height and width decrease. An example of the dependence of superlattice energy-band structure on layer width is shown in Fig. 175, where the motion parallel to the layers has not been included.

If the materials from which a quantum well or a superlattice is formed have such different properties that carriers at a given energy have wave functions attached to different band extrema, then the simple envelope-function approach considered above no longer applies. The wave functions must include contributions from more than one Bloch function, and the matching of wave functions at the heterojunction must be done microscopically. This situation applies for example, to the InAs-GaSb system, first discussed by Sai-Halasz, Tsu, and Esaki (1977), for which the energy gaps of the two constituents are so poorly aligned that valence-band levels in one constituent can be at a higher energy than conduction-band levels in the other constituent (see Fig. 176). This system is expected to be semimetallic when the superlattice layers are thick, and to be semiconducting for thin layers, in which quantum effects move the levels apart. This expectation has been confirmed by Chang *et al.* (1979). Properties of the InAs-GaSb system have been reviewed by Chang and Esaki (1980) and Döhler (1980).

Bastard (1981b) and White and Sham (1981) have shown how the effective-mass approximation can be generalized to treat band overlap problems like those of the

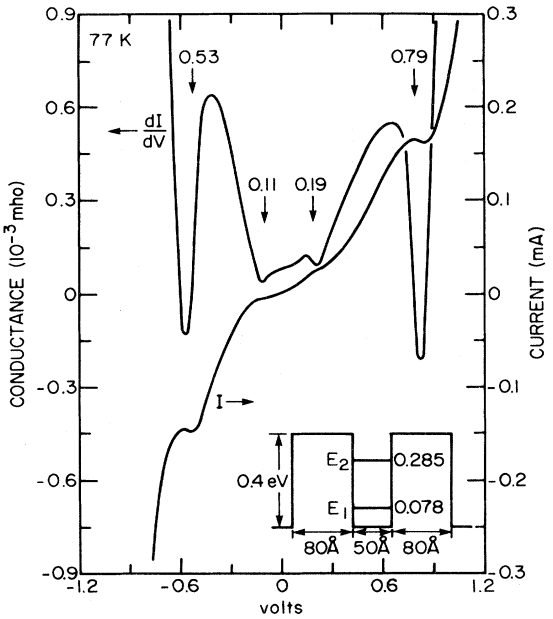

FIG. 174. Conductance versus voltage perpendicular to the layers for the GaAs-$Ga_{0.3}Al_{0.7}As$ double-barrier structure shown in the inset. The structures at -0.11 and 0.19 V are attributed to a drop of about 0.08 V across each $Ga_{0.3}Al_{0.7}As$ barrier, making the band edge in the adjoining bulk n-GaAs resonant with the first quantum level in the central GaAs well. The structures at -0.53 and 0.79 V are similarly attributed to resonance with the second quantum level. After Chang *et al.* (1974b).

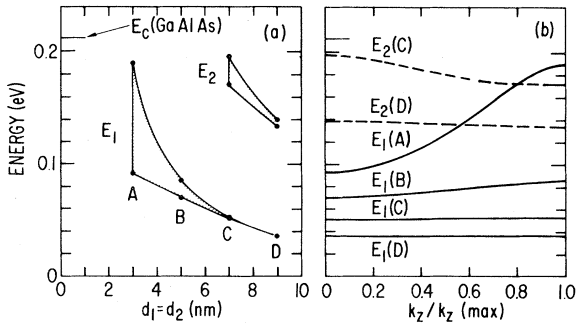

FIG. 175. (a) Calculated band edges of the lowest and first excited minibands in a superlattice with GaAs and $Ga_{0.8}Al_{0.2}As$ layers each having the indicated thickness. The barrier height is taken to be 0.21 eV, and the electron effective mass in both layers is taken to be $0.07m_0$. (b) Dispersion of the energy of the bottom of the lowest miniband versus normalized wave vector in the direction of the superlattice axis. Cases A, B, C, and D correspond to $d_1=d_2=3$, 5, 7, and 9 nm, respectively. The dashed curves give the dispersion of the bottom of the first excited miniband for cases C and D. Unpublished results courtesy of L. L. Chang.

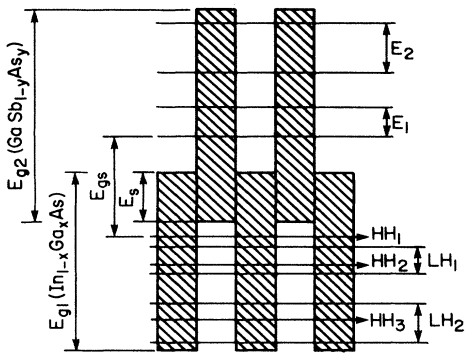

FIG. 176. Schematic energy diagram of an $In_{1-x}Ga_xAs$-$GaSb_{1-y}As_y$ superlattice. The shaded regions are the energy gaps of the respective layers. The calculated energies of electron and hole minibands are indicated on the right for parameters corresponding to a semiconducting state. After Sai-Halasz *et al.* (1978a).

InAs-GaSb system. Calculations of energy levels that go beyond the effective-mass approximation have been carried out by a number of authors, including Mukherji and Nag (1975), Caruthers and Lin-Chung (1978), Sai-Halasz, Esaki, and Harrison (1978b), Ihm, Lam, and Cohen (1979), Madhukar and Nucho (1979), Schulman and McGill (1977, 1979a, 1979b), Schulte (1979, 1980a), and Ivanov and Pollman (1980). When charged impurities, and therefore band curvature, are present the energy levels must be calculated self-consistently, as has been done, for example, by Ando and Mori (1979; see also Mori and Ando, 1980a).

3. Optical properties

The energy levels expected in heterojunctions, quantum wells, and superlattices are most directly verified by optical measurements. The transmission measurements of Dingle, Wiegmann, and Henry (1974) for a GaAs-$Ga_{1-x}Al_xAs$ system, shown in Fig. 177, displayed major structure identified with electron quantum levels, with some additional splitting attributed to hole quantum levels. Peaks out to electron quantum number 7 have been fitted to a model (Dingle, 1975b), although the analysis of hole levels, which has not been published in detail, may require additional work in view of complex valence-band structure.

Because GaAs-(Al,Ga)As quantum wells and superlattices confine both electrons and holes in the same layer, exciton effects are expected to be significant—probably even more significant than in a three-dimensional system because the hydrogenic levels in two dimensions are deeper than those in three dimensions (see Sec. II. E). The excitonic effects were recognized in the paper of Dingle *et al.* (1974), and have been more quantitatively considered by Keldysh (1979b). Weaker excitonic effects are expected in superlattices of the InAs-GaSb type that confine electrons and holes in adjoining layers. Optical

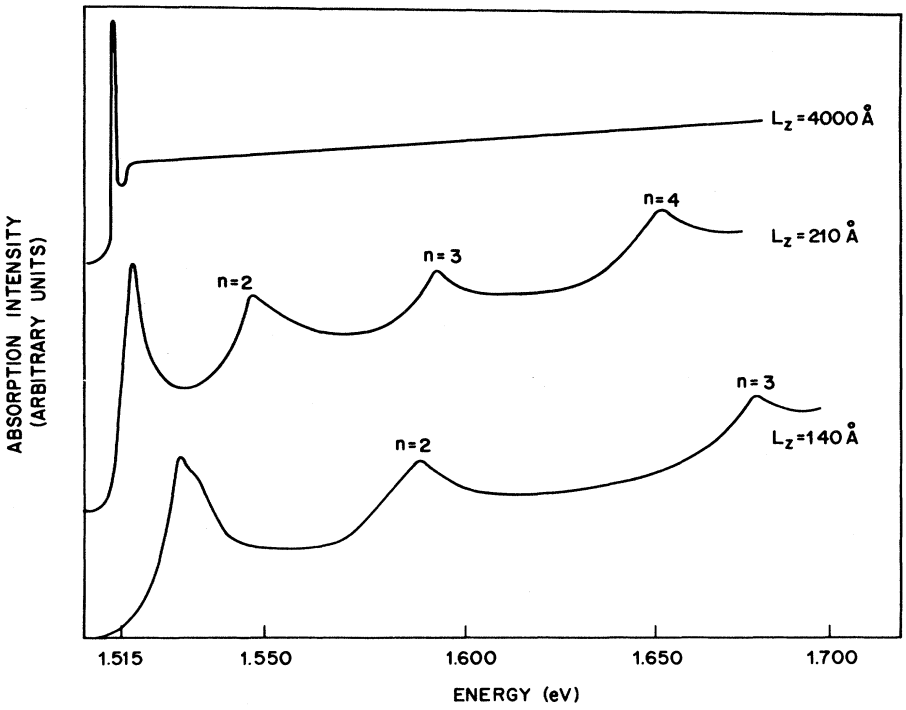

FIG. 177. Optical absorption of GaAs layers 14, 21, and 400 nm thick between $Al_{0.2}Ga_{0.8}As$ confining layers, showing peaks associated with electron quantum levels. The splitting of the lowest peak for the thinnest layer is attributed to light- and heavy-hole quantum levels in the valence band. After Dingle *et al.* (1974).

absorption in such structures has been reported by Chang, Sai-Halasz, Esaki, and Aggarwal (1981). Effects of confinement in quantum wells or superlattices on bound states associated with charged impurities have been considered by a number of authors, including Keldysh (1979a), Arutyunyan and Nerkararyan (1981), and Bastard (1981a).

Quantization effects in narrow potential wells can significantly affect lasing properties (see, for example, van der Ziel *et al.*, 1975; Holonyak *et al.*, 1980a). It has been suggested that the two-dimensionality of the energy spectrum in a quantum well leads to a slower increase of threshold current density with temperature than in lasers with thicker active layers (Chin *et al.*, 1980; Hess *et al.*, 1980). Lasing at a phonon sideband of the electronic transition in a GaAs-based quantum well heterostructure has been reported by Holonyak *et al.* (1980b), but contrary evidence has been reported by Weisbuch *et al.* (1981b). The possible role of clustering in ternary alloys, its effect on energy levels and optical transitions in quantum wells and heterostructures, and its dependence on growth conditions are also under active discussion (Holonyak *et al.*, 1980c, 1981a, 1981b; Miller and Tsang, 1981; Miller, Weisbuch, and Gossard, 1981). Luminescence and lasing are being actively explored to characterize the electronic states of quantum wells (see, for example, Holonyak *et al.*, 1980a; Miller *et al.*, 1981a–1981c; Vojak *et al.*, 1980; Weisbuch *et al.*, 1980, 1981a; Voisin *et al.*, 1981) but will not be discussed further here. Some of the underlying theoretical questions have been examined by Satpathy and Altarelli (1981).

The first measurements of Raman scattering by a superlattice were made by Manuel *et al.* (1976). They related the energy dependence of the resonant Raman cross section for longitudinal-optical (LO) phonon scattering to the electronic energy-level structure of the superlattice. Sai-Halasz, Pinczuk, Yu, and Esaki (1978c, 1978d) attributed a Raman scattering peak near the GaAs LO phonon energy in a GaAs-$Ga_{0.75}Al_{0.25}As$ superlattice to umklapp processes associated with the smaller Brillouin zone of the superlattice. The effect of zone folding on the phonons is not thought to play a role in their samples, which had periods of 12 and 20 nm. Merlin *et al.* (1980a, 1980b) attribute the extra peak seen by Sai-Halasz *et al.* to phonon anisotropy that gives different energies for longitudinal phonons moving parallel and perpendicular to the layers. Breaking of selection rules by defects is required if this explanation is to account for the observed results. Additional work is required to test the two alternative explanations. The fine structure that Merz, Barker, and Gossard (Merz *et al.*, 1977; Barker *et al.*, 1978) had seen is attributed by Merlin *et al.* to effects of Raman scattering in air near the surface of the sample and is absent when the measurements are made in vacuum.

The most pronounced effects in the previous experiments occur for Raman scattering near the LO phonon energies of the constituent materials of the superlattice, i.e., between 280 and 400 cm^{-1} for systems based on GaAs and AlAs. In addition, Colvard, Merlin, Klein, and Gossard (1980) find two sharp peaks at 63 and 67 cm^{-1} in a superlattice whose unit cell has 1.36 nm of GaAs and 1.14 nm of AlAs. These peaks are attributed to effects of Brillouin-zone folding. Superlattices have been found to give selective absorption for phonons whose wavelength is twice the superlattice period (Narayanamurti *et al.*, 1979).

Resonant electronic Raman scattering is a powerful technique that has been used to study quantum levels in heterojunctions, shown in Fig. 178 (Abstreiter and Ploog, 1979), in quantum wells, shown in Fig. 179 (Pinczuk *et al.*, 1980b), and in doping superlattices (Döhler *et al.*, 1981). The configuration with parallel polarization of the incident and backscattered beams is sensitive to collective excitation modes, while the perpendicular polarization configuration is sensitive to single-particle spin-flip excitations. Theoretical considerations regarding resonance enhancements and spin-flip versus non-spin-flip transitions were discussed by Burstein, Pinczuk, and Buchner (1979) and Burstein, Pinczuk, and Mills (1980). One interesting aspect of the Raman scattering measure-

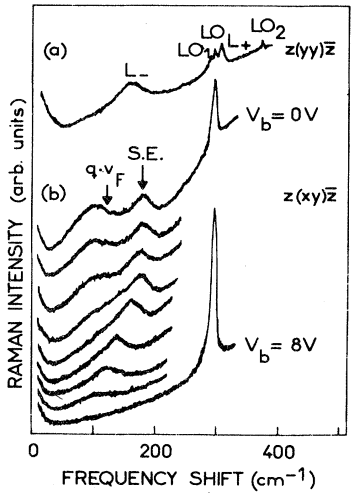

FIG. 178. Resonant Raman scattering from a GaAs-$Al_{0.2}Ga_{0.8}As$ heterostructure at 2 K excited by 1.92 eV photons. The upper curve shows backscattered light in the parallel polarization configuration. The peaks correspond to phonons in the doped GaAs adjoining the heterojunction (L_+ and L_-), in the GaAs Schottky barrier at the surface (LO), and in the undoped AlGaAs substrate (LO_1 and LO_2). The lower series of curves, for the perpendicular polarization configuration, shows a free-electron Raman peak with an upper cutoff at a value of qv_F given by the product of the backscattering wave vector times the indicated Fermi velocity of the GaAs layer, a sharp GaAs LO phonon peak associated with the Schottky barrier, and a peak attributed to subband excitation of the electrons at the heterojunction. The curves are for a series of increasing reverse voltages applied across the Schottky barrier. Increasing values of V increase the barrier thickness and decrease the carrier concentrations, first in the GaAs layer and then in the interfacial accumulation layer. After Abstreiter and Ploog (1979).

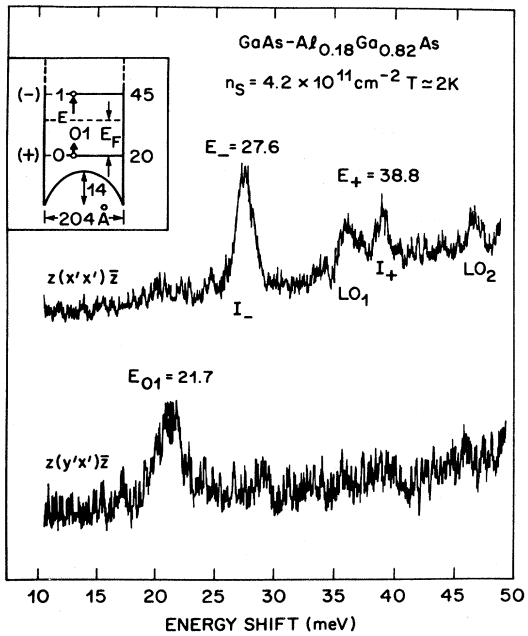

FIG. 179. Resonant Raman scattering for a modulation-doped superlattice with GaAs and $Al_{0.18}Ga_{0.82}As$ layers, each 20 nm thick. The upper curve, for parallel polarization of the incident and backscattered light (incident photon energy = 1.935 eV) shows two peaks, with subscripts + and −, attributed to coupled collective modes of the charge-density intersubband transition 0→1 and a GaAs LO phonon, as well as the LO phonon peaks of the GaAs and (Al,Ga)As layers. The lower peak, for perpendicular polarization, is attributed to a spin-flip 0→1 single-particle transition. The inset shows the calculated energies of the lowest subbands and the band bending. All the energies are in meV. After Pinczuk *et al.* (1980b).

ments is that the depolarizing fields which enter into optical absorption, as discussed in Sec. III.C, are present for the parallel polarization configuration but are absent for the perpendicular polarization configuration, which allows their effects to be experimentally determined. For additional details on these points and on the coupling of plasmon modes and intersubband excitations, see Pinczuk *et al.* (1980b, 1980c, 1981a) and Abstreiter *et al.* (1981).

Miller, Tsang, and Nordland (1980) showed that electrons in GaAs-(Al,Ga)As quantum wells excited by circularly polarized light achieve greater values of spin polarization than in bulk GaAs. The increase arises from the splitting of the degeneracy at the top of the valence band by the quantum well potential. These authors studied spin-dependent recombination as well as spin polarization, but were unable to explain all of the observed results quantitatively. Alvarado, Cicacci, and Campagna (1981) recently showed that spin-polarized electrons can be obtained by combining a superlattice with a surface having negative electron affinity.

4. Transport properties

The first paper on superlattices (Esaki and Tsu, 1970) proposed that carriers moving across the layers of a superlattice would constitute a realization of a Bloch oscillator, a system in which a carrier moving in a periodic potential with spatial period d under the influence of an electric field F traverses the Brillouin zone (or, in the present case, minizone) periodically with frequency $\nu_B = edF/h$ (see, for example, Wannier, 1959; the Bloch frequency appears to have been first written down explicitly by Zener, 1934). The realization of such periodic motion requires that $\nu_B\tau > 1$, where τ is the scattering time. Esaki and Tsu (1970) and Lebwohl and Tsu (1970) showed that such a system exhibits negative differential conductivity (see also Tsu and Döhler, 1975). Price (1973) found that this effect is obliterated (i.e., the differential mobility is positive, and in fact approaches a positive peak) near the Bloch frequency. Esaki, Chang, Howard, Rideout, Ludeke, and Schul (Esaki *et al.*, 1972; Chang *et al.*, 1973) reported a weak negative differential conductance in a GaAs-(Al,Ga)As superlattice, but this is not evidence for the Bloch oscillator, which remains a tantalizing concept. Some related theoretical concepts are cited by Churchill and Holmstrom (1981).

Transport properties of carriers in superlattices are controlled in part by the same mechanisms that limit the mobility of electrons in silicon inversion layers. One important difference arises from the polar nature of most superlattice materials, which enhances phonon scattering. Calculations of scattering mechanisms in superlattices and related two-dimensional electronic systems have been carried out by Ferry (1978c, 1979), Hess (1979), Mori and Ando (1980a, 1980b), Price (1981a, 1981c), and Basu and Nag (1980, 1981). Although the formal expressions for the lattice scattering mobility are different from those for three-dimensionless systems, the numerical values of the mobility and of its temperature dependence for a GaAs-based superlattice or heterojunction near 100 K are comparable to those in bulk GaAs for typical layer parameters if the carrier concentration is low enough that screening effects can be neglected (Price, unpublished).

Coulomb scattering by impurities can be reduced in superlattices if the impurities are placed in the layers with the higher energy gap and the carriers are confined in the layers with the lower energy gap. This technique, called modulation doping, allows the carriers and the impurities to be spatially separated and results in higher mobilities than would obtain for uniform doping. It was suggested in an unpublished 1969 report by Esaki and Tsu and was first published and applied to GaAs-based superlattices by Dingle, Störmer, Gossard and Wiegmann (1978). Still higher mobilities can be obtained by separating the carriers from the ions by an undoped spacer layer. Low-temperature mobilities considerably higher than those obtained for Si inversion layers have been obtained in this way, as illustrated in Fig. 180. Part of the increase can be attributed to the smaller mass of electrons in GaAs ($0.07m_0$) than in (001) Si inversion layers ($0.19m_0$).

The prospects of improved device performance (see, for example, Mimura *et al.*, 1980, 1981; Mimura and Fuku-

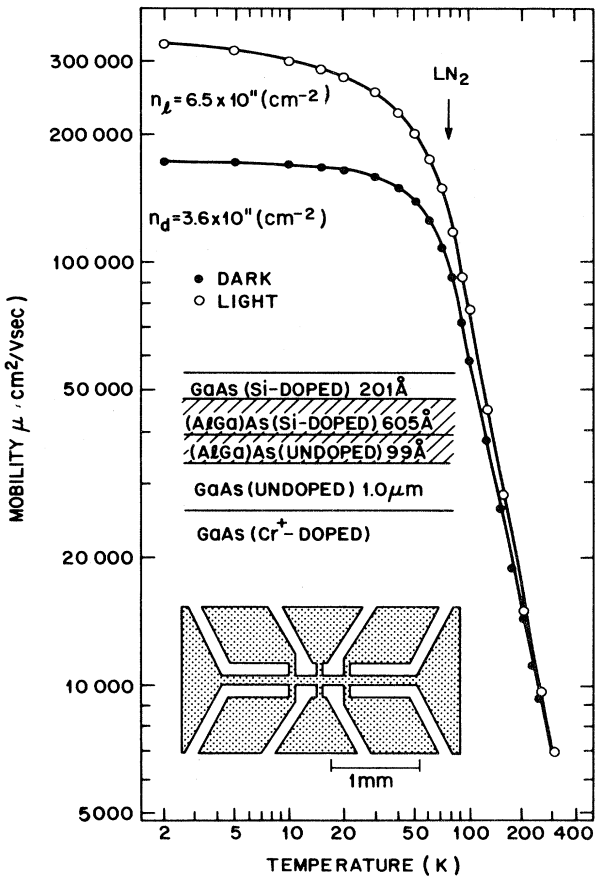

FIG. 180. Electron mobility in a modulation-doped GaAs-$Al_{0.31}Ga_{0.69}As$ heterostructure. A 10 nm undoped layer separates the doped (Al,Ga)As from the electrons in the undoped GaAs. The lower curve is for the sample in the dark, with 3.6×10^{11} electrons per cm^2 in the channel. The increased electron concentration in the upper curve is a result of long-lived carriers induced by light. After Störmer *et al.* (1981b).

ta, 1980) have stimulated active programs to grow GaAs heterostructures and measure their transport properties. Among the groups that have reported transport measurements are those at Bell Laboratories (Dingle *et al.*, 1978; Störmer *et al.*, 1979a—1979c, 1981a—1981c; Störmer, 1980; Tsui *et al.*, 1981), Cornell University (Wang *et al.*, 1981; Judaprawira *et al.*, 1981), the University of Illinois (Drummond *et al.*, 1981a—1981e; Witkowski *et al.*, 1981a, 1981b), and Rockwell (Coleman *et al.*, 1981b) in the United States, as well as groups in France (Delagebeaudeuf *et al.*, 1980; Delescluse *et al.*, 1981), and Japan (Hiyamizu *et al.*, 1980, 1981a, 1981b; Narita *et al.*, 1981a, 1981b). This long list, by no means complete, shows the intense interest—and competition—in this field. As data accumulate, comparisons of the experiments with theories for the scattering in these systems can become more detailed and systematic. Some comparisons, especially on the role of modulation doping and the use of undoped spacer layers, have already been made (see, for example, Drummond *et al.*, 1981e) and show that phonon scattering is the limiting mechanism in the highest-mobility structures down to below 77 K, with Coulomb scattering dominant near liquid helium temperatures. The advantages of very high mobilities at low temperatures are reduced in device applications by the strong decrease of mobility in modest source-drain fields at these temperatures (see, for example, Drummond *et al.*, 1981a; Morkoç, 1981).

Most transport measurements in superlattices, heterojunctions, and quantum wells have been for electrons, but Störmer and Tsang (1980) have reported measurements on holes at a GaAs-(Al,Ga)As heterojunction interface.

5. Magnetotransport

A magnetic field perpendicular to a layer of a two-dimensional system quantizes the motion along the layer and leads to the characteristic Shubnikov—de Haas oscillations in magnetoconductance. Such experiments have been widely used to probe the two-dimensionality of carriers in superlattices. Note, however, that a gate voltage cannot be used to control carrier concentration as easily in a superlattice as in an inversion or accumulation layer. Thus oscillatory magnetotransport measurements have been made by varying the magnetic field rather than the carrier concentration. One of the key tests of two-dimensional character is the behavior of the oscillations as the field is tilted from the normal to the layers. A strictly two-dimensional system will have oscillations that follow the normal component of the field. Magnetoconductance experiments along these lines have been carried out (Chang *et al.*, 1977; Dingle, 1978; Sakaki *et al.*, 1978). An example is shown in Fig. 181. There is evidence that magnetic breakdown can cause transitions between different subbands under appropriate conditions (Chang *et al.*, 1977).

The magnetophonon effect, which arises when the LO phonon energy is a multiple or a submultiple of the Landau energy $\hbar\omega_c$, has been observed in the second derivative of resistance with respect to magnetic field (with B in the range 5 to 18 T) in GaAs-(Al,Ga)As interfaces and superlattices by Tsui, Englert, Cho, and Gossard (1980). Two-dimensional magnetophonon effects have been considered theoretically by Korovin, Pavlov, and Éshpulatov (1980) and by Das Sarma and Madhukar (1980b).

A striking effect induced by magnetic fields is the transition of the InAs-GaSb superlattice from a semimetallic state to a semiconducting state as Landau levels cross the Fermi level (Kawai *et al.*, 1980).

Cyclotron resonance of electrons has been observed in GaAs-(Al,Ga)As heterojunction by Störmer *et al.* (1979b) and in an InAs-GaSb superlattice by Bluyssen *et al.* (1979). The mass values in both cases are within 10% of the values expected from a simple model. Magnetoabsorption measurements on InAs-GaSb superlattices (Guldner *et al.*, 1980; Maan *et al.*, 1981) show both cyclotron resonance and oscillatory interband magnetoabsorption, and allow experimental determination of parameters of the electronic band structure which are in

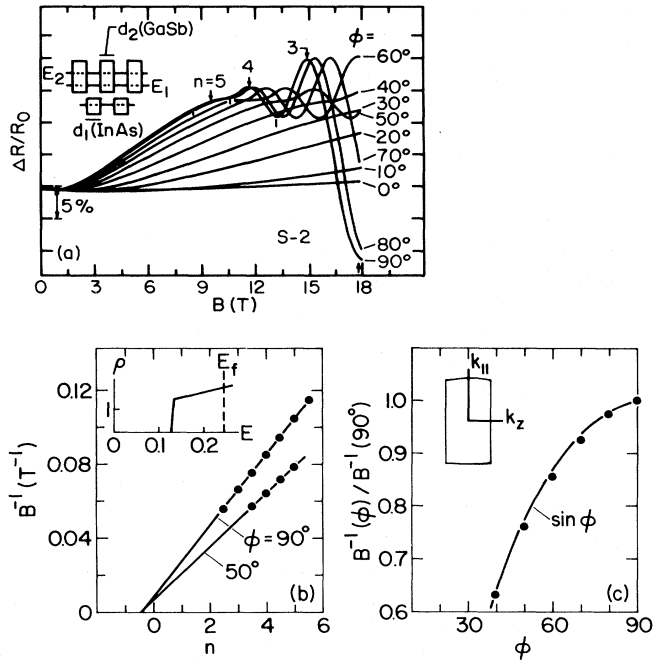

FIG. 181. Magnetoresistance oscillations at 4.2 K for electrons in a superlattice with InAs and GaSb layers each 9 nm thick. The upper figure shows the relative resistance change vs magnetic field B for fields inclined at various angles ϕ to the layers. The lower left figure shows the fan diagram for the oscillation extrema, and its inset shows the approximate density of states, in units of 10^{10} cm^{-2}meV^{-1} vs energy in eV. The lower right figure shows the angular dependence of the increment of $1/B$, confirming the sinϕ behavior expected for a two-dimensional electron gas. Its inset shows the approximate Fermi surface in the $k_{||}-k_z$ plane. After Sakaki *et al.* (1978).

good agreement with those expected theoretically.

Speculations about electron crystallization and charge-density waves in two-dimensional systems have influenced work on superlattices. Tsui, Störmer, Gossard, and Wiegmann (1980) observed conductance behavior at high fields and low temperatures which could not be explained by one-electron models, and which they attributed to a correlated state. The evidence, as in the case of inversion layers, is still inconclusive.

Work on heterojunctions, quantum wells, and superlattices is developing rapidly, and much of the work reported here may be superseded soon. Part of the interest stems from the possibility of device applications and part from the rapid development of molecular-beam epitaxy and other methods of device fabrication.

E. Thin films

Quantum effects in thin films have been known for a long time, both in connection with magnetic quantization (see, for example, Erukhimov and Tavger, 1967) which arises when the sample thickness is comparable to the diameter of a Landau orbit, and in connection with "electrical" quantization, which arises when the sample thickness is comparable to a typical electron wavelength. The energy-level structure in the latter case is given in lowest approximation by Eq. (8.27). It will be modified by interface effects and by the detailed energy-band structure of the material. The theory of size quantization in thin films has been studied extensively by Bezák (1966a, 1966b), Cottey (1970, 1972, 1973, 1975, 1976, 1978, 1980), Volkov and Pinsker (1976, 1977, 1979), Zaĭužny (1978, 1979a, 1979b, 1981a–1981c; Zaĭužny and Pilat, 1979), and by many other authors. For a review of early experimental work, see, for example, Lutskii (1970).

Quantum size effects have been observed in the optical properties of a number of materials, including InSb (Filatov and Karpovich, 1969a, 1969b) and PbTe (Salashchenko *et al.*, 1975). Quantum size effects are also seen in tunneling spectra, for example in Bi thin films (Korneev *et al.*, 1970).

Transport properties of films are also sensitive to quantum size effects. In thick films, surface scattering perturbs the electron motion, as has been well reviewed by Greene (1969a, 1969b). In thin films, where the motion perpendicular to the film is quantized, the formal treatment is rather different, and is closer to the treatment required for inversion layers. Work on thin-film transport properties, which in part predates the corresponding results for inversion layers, has been discussed by Demikhovskii and Tavger (1964), Chaplik and Éntin (1968), and Baskin and Éntin (1969), among others, and has been reviewed by Tavger and Demikhovskii (1968).

$Bi_8Te_7S_5$ is a striking thin-film material which cleaves in units of five atomic layers. Its electrical and optical properties have been extensively studied by Soonpaa and co-workers. See Soonpaa (1976a, 1976b, 1978a) for an account of this work and for references to earlier papers. The system shows indications of minimum metallic conductivity (Soonpaa, 1978b), discussed for inversion layers in Sec. V. Magnetotransport properties (Undem *et al.*, 1977; Soonpaa, 1979) and localization effects (Soonpaa, 1980) have also been investigated.

F. Layer compounds and intercalated graphite

In this section we allude briefly to two important classes of materials that also show aspects of two-dimensional electronic structure. The first class consists of the layer compounds, of which there are many examples, including GaSe and related materials and $TaSe_2$ and related materials. Many properties of the layer compounds have been reviewed in the series of books edited by Mooser (1976), including the volumes edited by Lévy (1976) and by Lee (1976); see also the conference proceedings edited by van Bruggen, Haas, and Myron (1980, part A) and by Nishina, Tanuma, and Myron (1981). Charge-density waves in layer compounds (DiSalvo, 1976; Williams, 1976) are easier to verify than in inversion layers or superlattices because they produce measurable lattice displacement.

Graphite and intercalated graphite constitute another

large family of materials with quasi-two-dimensional electronic properties. Intercalation effects are also widely studied in the layer compounds. For collections of papers dealing with these subjects, see, for example, Vogel and Hérold (1977), van Bruggen *et al.* (1980, part B), and Nishina *et al.* (1981). The subject has been reviewed by Dresselhaus and Dresselhaus (1981).

The two kinds of materials briefly noted in this section both have large bodies of literature, and have developed largely independently of the two-dimensional systems described in this review. One major difference is that the layer compounds and intercalated graphite both have electron densities of order 10^{15} cm^{-2} per layer, much larger than the densities in inversion layers, superlattices, or on liquid helium. Thus the energy scales, and the approximations that are useful, are considerably different for the two classes of systems.

Plasma oscillations in superlattices and in layer compounds and intercalated graphite can be strongly affected by coupling of the electromagnetic field from layer to layer. Theoretical treatments of this problem were briefly mentioned in Sec. II. D. An experiment on plasmon dispersion in a layered system was carried out by Mele and Ritsko (1980) on intercalated graphite.

G. Electron-hole system

For some time, a system consisting of spatially separated two-dimensional electrons and holes has been a subject of theoretical study. Such a structure can, for example, be realized in a sandwich structure of a *p*-type semiconductor, a thin insulator, and an *n*-type semiconductor. Semiconductor heterostructures grown by the molecular-beam epitaxy technique may be another candidate (see Sec. VIII. D). Although experimental observation has not been reported, the theoretical investigation has been motivated by a new mechanism of superconductivity. In this section a brief description of various investigations related to such two-dimensional electron-hole systems is given.

As has been well known, a pairing interaction between electrons and holes in an electron-hole system can give rise to a transition to the so-called "excitonic phase" (see, e.g., Halperin and Rice, 1968). In the case of a usual semimetal or a semiconductor with a narrow gap, the pairing leads only to a rearrangement of the band scheme, i.e., to a transition to an excitonic insulator. In fact, superconductivity is impossible in an excitonic insulator by virtue of the local electrical neutrality. Moreover, the presence of interband transitions of the pairing quasiparticles lifts the degeneracy of the system with respect to the phase of the order parameter, which makes superfluidity impossible. If the pairing is produced between spatially separated electrons and holes, however, tunneling processes between the paired quasiparticles can be negligibly weak and the system can go over the excitonic superfluid state. The superfluid motion of pairs of spatially separated electrons and holes corresponds to undamped currents flowing through different regions of the system in opposite directions. This is the new mechanism of superconductivity proposed first by Lozovik and Yudson (1975b, 1976a, 1976b) and later independently by Shevchenko (1976).

Electronic properties of the excitonic phase have been investigated in the Hartree-Fock approximation for spatially separated electron-hole systems with circular Fermi lines (Lozovik and Yudson, 1975b, 1976a–1976c, 1977a, Shevchenko, 1976, 1977). It has been shown that the system possesses a majority of the properties of a superconductor, but not the Meissner effect. The transition temperature, which is of the order of the gap Δ at the Fermi level, has been shown to be as large as ~ 100 K for an optimum choice of the values of the parameters such as the insulator thickness, the dielectric constants, and the effective masses. Lozovik and Yudson suggested that possible consequences of electron-hole superconductivity that could be observed experimentally are the existence of an an energy gap 2Δ in the two-dimensional dynamical conductivity and antiparallel superconducting currents in noncontacting coaxial cylindrical films.

There have been many other investigations on this and related systems. They include, for example, effects of weak electron-hole tunneling processes (Lozovik and Yudson, 1977b; Klyuchnik and Lozovik, 1978b, 1979; Lozovik and Klyuchnik, 1980), extension to periodic layered structures with spatially separated electrons and holes (Shevchenko and Kulik, 1976; Shevchenko, 1977; Kulik and Shevchenko, 1977), and effects of high magnetic fields perpendicular to the layer (Kuramoto and Horie, 1978). The possibility of a dipole-solid phase in which dipoles consisting of paired electrons and holes form a hexagonal lattice has also been suggested in both the presence and the absence of magnetic fields (Yoshioka and Fukuyama, 1978).

Two-dimensional electron-hole systems can also be produced, for example, in size-quantized semimetal films and quantized semiconductor films or layered semiconductors with nonequilibrium electrons and holes. Although superfluidity is impossible in these systems, various kinds of phase transitions can occur as in three-dimensional electron-hole systems. Investigations have been directed to, for example, the ground-state energy of an electron-hole liquid (Kuramoto and Kamimura, 1974; Andryushin and Silin, 1976b; Andryushin, 1976), an excitonic transition (Lozovik and Yudson, 1976b; Klyuchnik and Lozovik, 1978a; Andryushin and Silin, 1979), and effects of strong magnetic fields (Lerner and Lozovik, 1977, 1978a, 1978d, 1979a, 1979b, 1980a, 1980b).

H. Electrons on liquid helium

Electrons on liquid helium constitute a special kind of quasi-two-dimensional space-charge layer that shares some general features with the other electronic systems we have discussed, but differs from them in other ways. As we shall see, this system is scaled down in many respects—most notably the energy separations and the attainable electron densities. But small is beautiful, be-

cause mobilities are very high, allowing spectroscopy to be carried out with greater precision than for space-charge layers in semiconductors.

We shall give only a brief discussion of the properties of electrons on liquid helium to emphasize the relationship of this system to the semiconductor space-charge layers that are our principal concern. Fortunately the interested reader can consult several good reviews, including those of Cole (1974), Shikin and Monarkha (1975), Crandall (1976), Grimes (1978a), Shikin (1978a), Williams (1980), and Édel'man (1980).

The most notable development in this field has been the observation of crystallization of electrons on the surface of liquid helium at low temperatures by Grimes and Adams (1979). This result is discussed in the more general context of electron crystals in Sec. VII. C, and some details are also given below. In this section we give a brief description of some of the basic properties of the electrons on liquid helium and related substrates and of some of the experimental and theoretical approaches that have been used to study them.

An electron outside a dielectric medium with dielectric constant κ feels an attractive image potential energy

$$V(z)=-\frac{\kappa-1}{\kappa+1}\frac{e^2}{4z} \tag{8.28}$$

when the dielectric occupies the half-space $z<0$. In the particular case of liquid helium, whose dielectric constant is 1.0572 at 1 K (Chan *et al.*, 1977), this gives a very weak force. There is also a potential step of order 1 eV (Schoepe and Rayfield, 1973; Broomall and Onn, 1975) which keeps electrons out of the liquid helium. In many experiments the image potential is supplemented by applying an electric field F, sometimes called the pressing field or holding field, across two planar electrodes located above and below the surface. If we assume, as in the usual approximation for inversion layers, that the barrier can be taken to be inifinite and that the interface is abrupt, then the Schrödinger equation

$$-\frac{\hbar^2}{2m}\frac{d^2\psi_n}{dz^2}+[V(z)+eFz]\psi_n(z)=E_n\psi_n \tag{8.29}$$

can be solved with the boundary conditions $\psi(0)=\psi(\infty)=0$ to find the bound states. The subbands are given by adding the free-electron kinetic energy $\hbar^2k^2/2m$ to the eigenvalues E_n.

With the image potential of Eq. (8.28), the Schrödinger equation (8.29) when $F=0$ is the same as for the hydrogen atom, and the bound states are given by

$$E_n=-\left[\frac{\kappa-1}{\kappa+1}\right]^2\frac{me^4}{32\hbar^2}\frac{1}{n^2},\quad n=1,2,3,\ldots. \tag{8.30}$$

Solutions of the Schrödinger equation including the electric field term have been obtained variationally (Grimes *et al.*, 1976) and analytically (Hipólito *et al.*, 1978). Some mathematical aspects of the solutions have been considered by Rau (1977) and O'Connell (1978). Transitions between these energy levels lie at microwave frequencies for electrons on helium. They were first seen by Grimes and Brown (1974), and are illustrated in Fig. 182, taken from Zipfel, Brown, and Grimes (1976a). The energy-level differences for zero electric field are about 5% larger than those predicted by Eq. (8.30). The discrepancy is attributed to interface effects, which have been discussed in Sec. III. E. Several model calculations that give a good fit to the results of Grimes *et al.* are briefly discussed in that section.

Lambert and Richards (1981) recently reported results of microwave measurements extending to higher pressing fields. They compared their measured splittings, extrapolated to zero surface charge, with Stern's (1978b and unpublished) calculations and found agreement within 1 GHz. These results are illustrated in Figs. 183 and 184. Lambert and Richards (1980, 1981) also pointed out that correlations between the electrons in the layer influence the measured splittings, and determined one moment

$$K=0.70656N_s^{-3/2}\int_0^\infty g(r)r^{-2}dr \tag{8.31}$$

of the radial distribution function $g(r)$ to be approximately 10% bigger than the value for a hexagonal lattice. This result is consistent with theoretical estimates for the electron density range covered by their measurements. Correlations also affect the rate of electron escape from the surface, as discussed by Iye, Kōno, Kajita, and Sasaki (1980).

Plasmons in a two-dimensional system were first observed for electrons on liquid helium (Grimes and Adams, 1976a, 1976b). The dependence of the plasma frequency on the wave vector follows the expected dispersion, including the boundary effects from the cavity walls. Plasmon dispersion is discussed more generally in Secs. II.D and VI.C.3.

Cyclotron resonance of electrons on liquid helium is a rich subject that has been actively studied both experimentally and theoretically. Both the cyclotron linewidth and its position are influenced by the interaction of the

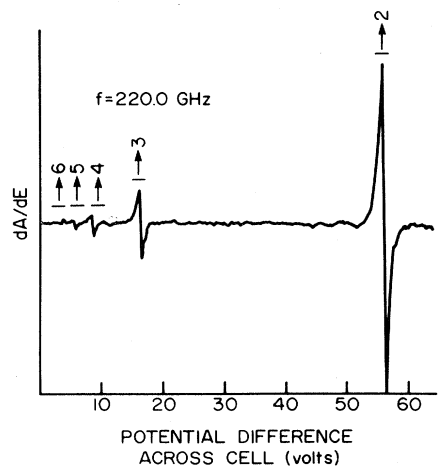

FIG. 182. Derivative of the microwave power vs the potential difference across a cell with a layer of electrons on the surface of liquid helium. The cell height is 0.32 cm and the bath temperature is 1.2 K. After Zipfel *et al.* (1976a).

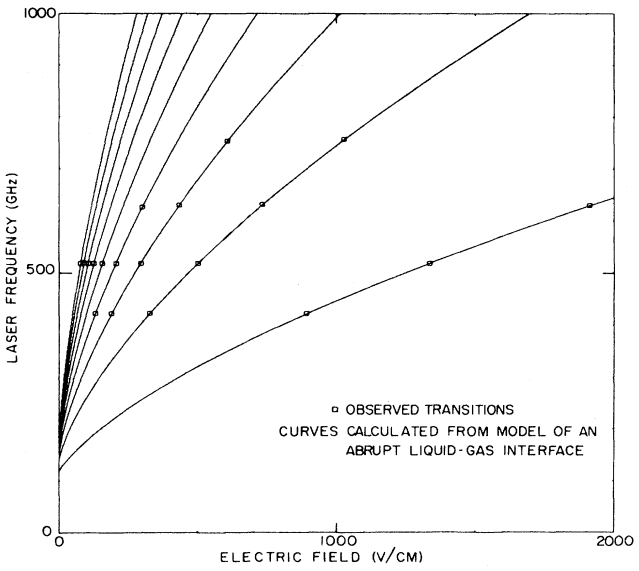

FIG. 183. Measured energy-level splittings of electrons on liquid helium vs the pressing electric field (squares) and splittings calculated assuming an abrupt helium surface with an infinite barrier height (lines). After Lambert and Richards (1981).

electrons with each other and with the helium surface. Comprehensive experimental results have been published by Édel'man (1979). The work is well reviewed by Monarkha and Shikin (1980) and is not covered here. Dykman (1980) has discussed the effect of electron ordering on cyclotron resonance.

The mobility of electrons on liquid helium has been measured directly (see, for example, Bridges and McGill, 1977) and has been deduced from the linewidth of cyclotron resonance (Brown and Grimes, 1972) and of the plasmon modes (Grimes and Adams, 1976a, 1976b). At high vapor density the mobility is limited by scattering from helium atoms in the vapor, and at lower densities it is limited by scattering from ripplons, which are hydrodynamic modes of the helium surface. At temperatures below about 0.7 K the latter mechanism dominates. Mobilities up to 10^7 cm^2 V^{-1} s^{-1} have been observed, as shown in Fig. 185.

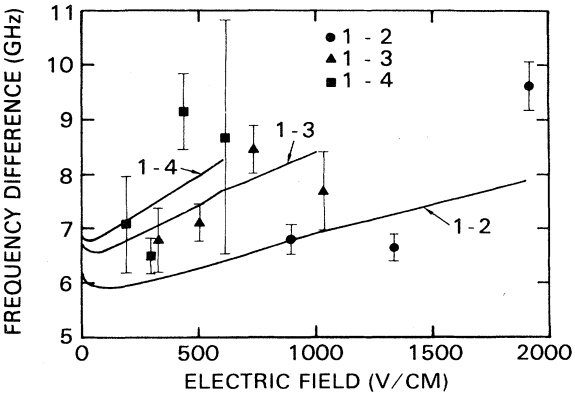

FIG. 184. Difference between the measured and calculated splittings of Fig. 183 (points) and differences calculated by Stern (1978b and unpublished) using a graded interface model (lines). After Lambert and Richards (1981).

The density of electrons on liquid helium is limited to values below $\sim 2\times 10^9$ cm^{-2} by an instability (Gor'kov and Chernikova, 1973; see also Williams and Crandall, 1971) which leads to discharge of the electrons to the bottom electrode or out the sides of the film (see, for example, Volodin *et al.*, 1977; Khaikin, 1978b) at higher densities. The available density range includes the range in which electron crystallization can be expected on the basis of the theoretical considerations described in Sec. VII. C.

Electrons on a thin film of liquid helium are attracted not only by the image potential of the helium but also by the stronger image potential of the substrate. The resulting binding energies can be much larger than for bulk liquid helium, but the electrons can tunnel to the substrate if the film is thin enough. This system has been discussed theoretically by Cole (1971), Sander (1975), Shikin and Monarkha (1975), and Jackson and Platzman (1981). Volodin, Khaikin, and Édel'man (1976) found that the maximum attainable electron density is higher in such a system than for electrons on bulk liquid helium.

Experimental evidence for an electron crystal was found by Grimes and Adams (1979), who observed resonant frequencies predicted by Fisher, Halperin, and Platzman (1979b) for a hexagonal lattice (sometimes loosely called a triangular lattice) of electrons coupled to the surface modes of the liquid helium. These oscillations disappear above a transition temperature which depends on density and corresponds to $\Gamma_m = 137 \pm 15$, where Γ is the ratio of potential energy to kinetic energy given in Eq. (7.66). Fisher (1980b) quotes a value

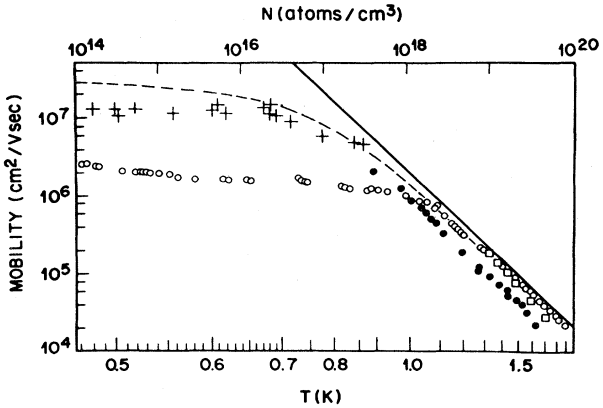

FIG. 185. Electron mobility parallel to the He surface versus temperature and He vapor density. The solid line is calculated for vapor-atom scattering only (Brown and Grimes, 1972). The dashed line is calculated for both ripplon and vapor-atom scattering (Saitoh, 1977). The experimental data points are from: full circles, Sommer and Tanner (1971); open squares, Brown and Grimes (1972); plus signs, Grimes and Adams (1976b); open circles, Rybalko *et al.* (1975). After Grimes (1978a).

$\Gamma_m = 131 \pm 7$ from more recent work of Grimes and Adams. He has also briefly discussed the order of the transition. Kalia, Vashishta, and de Leeuw (1981) find a first-order transition from a molecular dynamics calculation. A large first-order transition appears to be ruled out experimentally. The experimental results of Grimes and Adams are illustrated in Fig. 186. Mehrotra and Dahm (1979) have predicted that the linewidth of phonon resonances in this system drops upon crystallization and then increases again to a peak as the temperature is lowered below the crystallization temperature.

Confirming evidence of crystallization has been obtained by Deville *et al.* (1980; see also Marty *et al.*, 1980) from observation of optical modes of electrons coupled to surface deformations of the liquid helium. They find a transition for $N_s \sim T^{1.8\pm0.2}$, as opposed to the T^2 dependence of Eq. (7.67) which is confirmed by Grimes and Adams. If the results of Deville *et al.* are fitted to a T^2 dependence, they give $\Gamma_m = 118 \pm 10$.

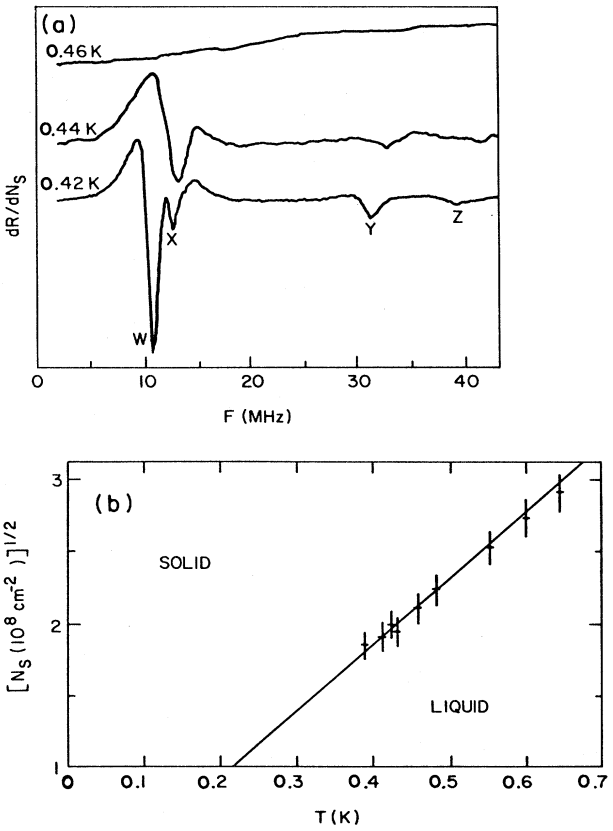

FIG. 186. (a) Experimental traces displaying the sudden appearance with decreasing temperature of coupled plasmon-ripplon resonances associated with a hexagonal electron lattice on the surface of liquid helium. The letters identify modes of the system as described by Fisher *et al.* (1979b). (b) Portion of the solid-liquid phase boundary for a classical, two-dimensional sheet of electrons. The data points denote the melting temperatures measured at various values of the electron density N_s. The line is for $\Gamma_m = 137$, where Γ is the ratio of potential energy to kinetic energy. After Grimes and Adams (1979).

Hot-electron effects have been widely discussed for electrons on liquid helium. Good introductions to the experimental and theoretical work are the theoretical papers of Monarkha and Sokolov (1979) and of Saitoh and Aoki (1978b). One consequence of electron heating is the appearance of abrupt changes for small increases in applied power, as seen, for example, in cyclotron resonance (Édel'man, 1977a) and in plasmon standing-wave resonance (Grimes, 1978a). These effects are attributed to excitation of electrons to higher subbands, where they have different spatial distributions and scattering rates than in the lowest subband. Another prediction of hot-electron calculations (Monarkha, 1979b) is a different dependence of mobility on the pressing field when the electrons are in the fluid phase and when they are in the ordered phase. Such a change has been observed by Rybalko, Esel'son, and Kovdrya (1979) and is in fair agreement with the crystallization parameters found by Grimes and Adams.

Most of the work on liquid helium has been on ^{4}He. There has been some work on electrons bound to the surface of liquid ^{3}He (Édel'man, 1977b, 1979), whose dielectric constant is only 1.0425 at 1 K (Kierstead, 1976), leading to a weaker image potential and shallower, more extended energy levels which are more easily deformed by an external field. Volodin and Édel'man (1979) have measured the energy-level splittings between the lowest subband and the first two excited subbands. They find deviations of order 3—4% from the hydrogenic spectrum [Eq. (8.30)] and conclude that the deviations can be accounted for by a liquid-vapor interface similar to or slightly wider than that of ^{4}He. Iye (1980) has measured the temperature dependence of mobility for electrons on ^{3}He, and finds the mobility to be limited by gas atom scattering down to 0.5 K. Electron binding has also been reported on the surface of liquid hydrogen and crystalline neon and hydrogen by Troyanovskii, Volodin, and Khaikin (1979a, 1979b).

The interaction between electrons and the surface of liquid helium admits of a state in which electrons cluster together and form a dimple on the helium surface (Williams and Crandall, 1971). Application of a pressing field can lead to softening of coupled electron-ripplon modes and to an instability which causes the electrons to form a hexagonal dimple lattice, in which each dimple holds about 10^7 electrons (Leiderer and Wanner, 1979; Ikezi, 1979; Shikin and Leiderer, 1980; Mel'nikov and Meshkov, 1981). Ebner and Leiderer (1980) have studied the development of the dimple instability on a time scale of seconds for a range of electron densities. Other types of nonlinear deformations of the surface have recently been described by Giannetta and Ikezi (1981). Mode softening and dimple crystals also occur for ions trapped at the boundary between liquid ^{3}He and ^{4}He (Leiderer *et al.*, 1978; Wanner and Leiderer, 1979; Leiderer, 1979). Another system of massive particles is formed by electrons and their surrounding bubbles inside the liquid helium, which must be held to the surface by a pressing field (see, for example, Cole, 1974; Williams and

Theobald, 1980). Electrons can also line the surface of a bubble in liquid helium (Shikin, 1978b).

I. Magnetic-field-induced surface states in metals

Surface Landau levels can be induced in metals in the presence of a magnetic field parallel to the surface, and manifest themselves as oscillations in the microwave impedance of the sample versus magnetic field. The surface component of the Fermi velocity of electrons within the skin depth induces an effective force perpendicular to the surface, which in turn induces quantum levels much like those in inversion layers. Because of the small value of the equivalent electric field, the level spacings correspond to frequencies of order 10^{11} Hz for magnetic fields of order 100 G, and vary as $H^{2/3}$. This subject was pursued in the late 1960s and early 1970s (Khaikin, 1968; Nee *et al.*, 1968; Azbel, 1969, Sec. 13; Doezema and Koch, 1972), and there has been some more recent work (see, for example, Silin and Tolkachev, 1979). The scattering of electrons in magnetic surface states in metals (Prange and Nee, 1968; Prange, 1969; Koch and Murray, 1969; Mertsching and Fischbeck, 1970) is controlled by mechanisms which in part are similar to those that operate in inversion and accumulation layers in semiconductors.

Levels similar to those described here for normal metals are also found at the surface of type-I superconductors (see, for example, Koch and Pincus, 1967; Maldonado and Koch, 1970).

IX. OUTLOOK

The scope of this review and of the bibliography shows that the study of electronic properties of two-dimensional systems has flourished in the past ten years. The versatility that follows from easily varied carrier concentrations and other system parameters has been widely exploited, and the importance of many-body effects has been clearly established. Electrons near the $Si\text{-}SiO_2$ interface, on the surface of liquid helium, and in the more recently explored heterojunction systems provide nearly ideal physical realizations of a two-dimensional electron gas. However, except for electrons on helium, factors like impurites, strains, interface roughness, and other sources of inhomogeneities complicate the understanding—and in some cases the reproducibility—of some observed phenomena. Many of the subjects covered in our review cannot be considered to be fully understood and await new approaches or more comprehensive study.

Many new propects are opening. The advent of heterostructures with electrons of very high mobility and therefore very long mean free paths, as well as the increased ability to make very small structures, allows the reduction of dimensionality in some physical sense from two to one. Increased sophistication and increasing entry of new workers into the field has led to continuing innovation both experimentally and theoretically. There is still opportunity for discovering new phenomena, new techniques, new structures, and new applications. We expect that this field will continue to be fruitful for some years.

ACKNOWLEDGMENTS

We are grateful to the many colleagues who have assisted us during the preparation of this review through discussions and correspondence and by providing preprints and figures. To those who may have deferred plans to write review articles of their own we apologize for the long time it has taken to complete this manuscript. We thank L. L. Chang, M. Inoue, S. Lai, B. D. McCombe, M. Pepper, P. J. Price, and P. J. Stiles for helpful contributions to this article, and Maryann Pulice for typing parts of Secs. I, IV, and V.

APPENDIX: CHARACTERISTIC SCALE VALUES

In this section we give numerical values for some of the characteristic lengths, energies, and other quantities that arise in discussing the electronic properties of semiconductor space-charge layers. Although equations in the remainder of the text are in cgs units, we shall give them here both in cgs and in *Système International* (SI) units. To convert from SI units to cgs units, replace ε_0 by $1/4\pi$. See the list of symbols at the beginning of this article for definitions of symbols not defined below.

The expressions given here are often valid only under certain conditions. Refer to the relevant places in the text for a more complete discussion.

Most numerical values in this section are normalized to the values for electrons in silicon (100) inversion layers at low temperatures with only the lowest subband occupied. The material parameters used are:

κ_{sc} = static dielectric constant of silicon = 11.5,
κ_{ins} = static dielectric constant of oxide = 3.9,
m = effective mass for motion parallel to the interface = $0.19m_0$,
m_z = effective mass for motion perpendicular to the interface = $0.916m_0$.

The mass values are from Hensel, Hasegawa, and Nakayama (1965), the silicon dielectric constant is from Bethin, Castner, and Lee (1974), and the oxide dielectric constant is from Grove (1967; p. 103). Slightly different values may have been used elsewhere in the text and in the papers cited.

1. Quantities related to charge

C_{ins}, *insulator capacitance.*

$$C_{ins} = \frac{\kappa_{ins}}{4\pi d_{ins}} \quad \text{(cgs)} ,$$

$$C_{\rm ins}=\frac{\varepsilon_0\kappa_{\rm ins}}{d_{\rm ins}}\ \ ({\rm SI})\ ,$$

$$C_{\rm ins}[{\rm pF/cm^2}]=34.53\left[\frac{100\ {\rm nm}}{d_{\rm ins}}\right]\left[\frac{\kappa_{\rm ins}}{3.9}\right]\ .$$

N_s, space-charge layer carrier density, $\sim C_{\rm ins}(V_G-V_T)/e$.

$$N_s[{\rm cm^{-2}}]=2.155\times10^{11}\,|\,V_G-V_T\,|\,[{\rm V}]\times\left[\frac{100\ {\rm nm}}{d_{\rm ins}}\right]\left[\frac{\kappa_{\rm ins}}{3.9}\right]\ ,$$

where V_G and V_T are the gate voltage and the threshold voltage, respectively. This relation is an approximate one, and applies to strongly inverted or accumulated space-charge layers.

$N_{\rm depl}$, depletion layer charges per unit area.

$$N_{\rm depl}=\left[\frac{\kappa_{\rm sc}\phi_d(N_A-N_D)}{2\pi e}\right]^{1/2}\ \ ({\rm cgs})\ ,$$

$$N_{\rm depl}=\left[\frac{2\varepsilon_0\kappa_{\rm sc}\phi_d(N_A-N_D)}{e}\right]^{1/2}\ \ ({\rm SI})\ ,$$

$$N_{\rm depl}[{\rm cm^{-2}}]=1.127\times10^{11}(\phi_d[{\rm V}])^{1/2}\times\left[\frac{N_A-N_D}{10^{15}\ {\rm cm^{-3}}}\right]^{1/2}\left[\frac{\kappa_{\rm sc}}{11.5}\right]^{1/2}\ ,$$

where ϕ_d is the band bending in the depletion layer, including the substrate voltage $\phi_{\rm sub}$, if any. See Eqs. (3.9)—(3.13).

$F_{\rm ins}$, electric field in insulator.

$$|F_{\rm ins}|=\frac{4\pi e(N_s+N_{\rm depl})}{\kappa_{\rm ins}}\ \ ({\rm cgs})\ ,$$

$$|F_{\rm ins}|=\frac{e(N_s+N_{\rm depl})}{\varepsilon_0\kappa_{\rm ins}}\ \ ({\rm SI})\ ,$$

$$|F_{\rm ins}|[{\rm V/cm}]=4.640\times10^5\left[\frac{N_s+N_{\rm depl}}{10^{12}\ {\rm cm^{-2}}}\right]\left[\frac{3.9}{\kappa_{\rm ins}}\right]\ ,$$

if there is no charge in the insulator or at the semiconductor-insulator interface. Because SiO_2 has a maximum dielectric breakdown field of about 10^7 V/cm, the value of $N_s+N_{\rm depl}$ in Si cannot exceed about 2×10^{13} cm^{-2}.

F_s, electric field just inside the semiconductor.

$$|F_s|=\frac{4\pi e(N_s+N_{\rm depl})}{\kappa_{\rm sc}}\ \ ({\rm cgs})\ ,$$

$$|F_s|=\frac{e(N_s+N_{\rm depl})}{\varepsilon_0\kappa_{\rm sc}}\ \ ({\rm SI})\ ,$$

$$|F_s|[{\rm V/cm}]=1.574\times10^5\left[\frac{N_s+N_{\rm depl}}{10^{12}\ {\rm cm^{-2}}}\right]\left[\frac{11.5}{\kappa_{\rm sc}}\right]\ .$$

2. Quantities related to distance

z_d, depletion layer thickness.

$$z_d=\left[\frac{\kappa_{\rm sc}\phi_d}{2\pi e(N_A-N_D)}\right]^{1/2}\ \ ({\rm cgs})\ ,$$

$$z_d=\left[\frac{2\kappa_{\rm sc}\varepsilon_0\phi_d}{e(N_A-N_D)}\right]^{1/2}\ \ ({\rm SI})\ ,$$

$$z_d[\mu{\rm m}]=1.127(\phi_d[{\rm V}])^{1/2}\left[\frac{10^{15}\ {\rm cm^{-3}}}{N_A-N_D}\right]^{1/2}\left[\frac{\kappa_{\rm sc}}{11.5}\right]^{1/2}\ ,$$

where ϕ_d is the band bending in the depletion layer, including the substrate voltage $\phi_{\rm sub}$, if any. See Eqs. (3.9)—(3.13). Typical values of z_d range from 0.1 to 10 μm.

$z_0\equiv z_{00}$, average distance of electrons from the interface with only the lowest subband occupied.

$$z_0=\left[\frac{9\kappa_{\rm sc}\hbar^2}{16\pi m_z e^2 N^*}\right]^{1/3}\ \ ({\rm cgs})\ ,$$

$$z_0=\left[\frac{9\kappa_{\rm sc}\varepsilon_0\hbar^2}{4m_z e^2 N^*}\right]^{1/3}\ \ ({\rm SI})\ ,$$

$$z_0[{\rm nm}]=2.283\left[\frac{10^{12}\ {\rm cm^{-2}}}{N^*}\right]^{1/3}\times\left[\frac{\kappa_{\rm sc}}{11.5}\right]^{1/3}\left[\frac{0.916m_0}{m_z}\right]^{1/3}\ ,$$

where $N^*=N_{\rm depl}+\frac{11}{32}N_s$. Typical values of z_0 range from 1 to 10 nm or more. See also Fig. 12.

$k_F=(2\pi N_s/g_v)^{1/2}$, Fermi wave vector.

$$k_F[{\rm cm^{-1}}]=1.772\times10^6\left[\frac{N_s}{10^{12}\ {\rm cm^{-2}}}\right]^{1/2}\left[\frac{2}{g_v}\right]^{1/2}\ .$$

$\lambda_F=2\pi/k_F$, Fermi wavelength.

$$\lambda_F[{\rm nm}]=35.45\left[\frac{10^{12}\ {\rm cm^{-2}}}{N_s}\right]^{1/2}\left[\frac{g_v}{2}\right]^{1/2}\ .$$

$v_F=\hbar k_F/m$, Fermi velocity.

$$v_F[{\rm cm/s}]=1.080\times10^7\left[\frac{N_s}{10^{12}\ {\rm cm^2}}\right]^{1/2}\times\left[\frac{2}{g_v}\right]^{1/2}\left[\frac{0.19m_0}{m}\right]\ .$$

a^*, effective Bohr radius using semiconductor dielectric constant.

$$a^*=\frac{\kappa_{\rm sc}\hbar^2}{me^2}\ \ ({\rm cgs})\ ,$$

$$a^*=\frac{4\pi\varepsilon_0\kappa_{\rm sc}\hbar^2}{me^2}\ \ ({\rm SI})\ ,$$

$$a^*[\text{nm}]=3.203\left[\frac{\kappa_{sc}}{11.5}\right]\left[\frac{0.19m_0}{m}\right].$$

$\bar{a}^*$, effective Bohr radius using average dielectric constant of semiconductor and insulator.

$$\bar{a}^*=\frac{\bar{\kappa}\hbar^2}{me^2}\ \text{(cgs)},$$

$$\bar{a}^*=\frac{4\pi\varepsilon_0\bar{\kappa}\hbar^2}{me^2}\ \text{(SI)},$$

$$\bar{a}^*[\text{nm}]=2.145\left[\frac{\bar{\kappa}}{7.7}\right]\left[\frac{0.19m_0}{m}\right].$$

$q_s=2g_v/a^*$, screening wave vector (long-wavelength, low-temperature limit; one subband occupied) using semiconductor dielectric constant [see Eqs. (2.24) and (2.28)].

$$q_s[\text{cm}^{-1}]=1.249\times10^7\left[\frac{11.5}{\kappa_{sc}}\right]\left[\frac{g_v}{2}\right]\left[\frac{m}{0.19m_0}\right].$$

$\bar{q}_s=2g_v/\bar{a}^*$, screening wave vector (long-wavelength, low-temperature limit; one subband occupied) using average dielectric constant of semiconductor and insulator [see Eqs. (2.24) and (2.28)]:

$$\bar{q}_s[\text{cm}^{-1}]=1.865\times10^7\left[\frac{7.7}{\bar{\kappa}}\right]\left[\frac{g_v}{2}\right]\left[\frac{m}{0.19m_0}\right].$$

$r_s=(\pi N_s)^{-1/2}$, Wigner-Seitz radius.

$$r_s[\text{nm}]=5.642\left[\frac{10^{12}\ \text{cm}^{-2}}{N_s}\right]^{1/2},$$

$$\frac{r_s}{a^*}=1.761\left[\frac{10^{12}\ \text{cm}^{-2}}{N_s}\right]^{1/2}\left[\frac{11.5}{\kappa_{sc}}\right]\left[\frac{m}{0.19m_0}\right],$$

$$\frac{r_s}{\bar{a}^*}=2.631\left[\frac{10^{12}\ \text{cm}^{-2}}{N_s}\right]^{1/2}\left[\frac{7.7}{\bar{\kappa}}\right]\left[\frac{m}{0.19m_0}\right].$$

The dimensionless ratio r_s/a^* or $r_s/\bar{a}^*$ is often called simply r_s. It varies from about 1 to 10 or more for the usual range of carrier concentrations in silicon inversion layers.

3. Quantities related to energy

$D(E)=g_v m/\pi\hbar^2$, density of states in the lowest subband.

$$D(E)[\text{cm}^{-2}\text{eV}^{-1}]=1.587\times10^{14}\left[\frac{g_v}{2}\right]\left[\frac{m}{0.19m_0}\right],$$

where a spin degeneracy $g_s=2$ has been assumed.

$E_F=N_s/D(E)$, Fermi energy at absolute zero, one subband occupied.

$$E_F[\text{meV}]=6.300\left[\frac{N_s}{10^{12}\ \text{cm}^{-2}}\right]\left[\frac{2}{g_v}\right]\left[\frac{0.19m_0}{m}\right].$$

E_i, quantum levels in a constant electric field F_s [see Eq. (3.24)].

$$E_i\sim\left[\frac{\hbar^2}{2m_z}\right]^{1/3}\left[\frac{3\pi}{2}eF_s(i+\tfrac{3}{4})\right]^{2/3},$$

$$E_i[\text{meV}]\sim61.15(i+\tfrac{3}{4})^{2/3}\left[\frac{N_{\text{depl}}}{10^{12}\ \text{cm}^{-2}}\right]^{2/3}\times\left[\frac{11.5}{\kappa_{sc}}\right]^{2/3}\left[\frac{0.916m_0}{m_z}\right]^{1/3},$$

where we used $F_s=eN_{\text{depl}}/\kappa_{sc}\varepsilon_0$. The three lowest levels are $E_0=50.9$ meV, $E_1=88.9$ meV, and $E_2=120.1$ meV, all multiplied by the last three factors above.

Ry*, *effective rydberg using semiconductor dielectric constant.*

$$\text{Ry}^*=\frac{me^4}{2\kappa_{sc}^2\hbar^2}\ \text{(cgs)},$$

$$\text{Ry}^*=\frac{me^4}{32\pi^2\varepsilon_0^2\kappa_{sc}^2\hbar^2}\ \text{(SI)},$$

$$\text{Ry}^*[\text{meV}]=19.55\left[\frac{m}{0.19m_0}\right]\left[\frac{11.5}{\kappa_{sc}}\right]^2.$$

$\overline{\text{Ry}}^*$, *effective rydberg using average dielectric constant of semiconductor and insulator.*

$$\overline{\text{Ry}}^*=\frac{me^4}{2\bar{\kappa}^2\hbar^2}\ \text{(cgs)},$$

$$\overline{\text{Ry}}^*=\frac{me^4}{32\pi^2\varepsilon_0^2\bar{\kappa}^2\hbar^2}\ \text{(SI)},$$

$$\overline{\text{Ry}}^*[\text{meV}]=43.60\left[\frac{m}{0.19m_0}\right]\left[\frac{7.7}{\bar{\kappa}}\right]^2.$$

$\hbar\omega_p$, two-dimensional plasmon energy for wave vector q in thick-insulator limit [see Eq. (2.42)].

$$\omega_p=\left[\frac{2\pi N_s e^2 q}{\bar{\kappa}m}\right]^{1/2}\ \text{(cgs)},$$

$$\omega_p=\left[\frac{N_s e^2 q}{2\bar{\kappa}\varepsilon_0 m}\right]^{1/2}\ \text{(SI)},$$

$$\hbar\omega_p[\text{meV}]=6.865\left[\frac{q}{10^5\ \text{cm}^{-1}}\right]^{1/2}\left[\frac{N_s}{10^{12}\ \text{cm}^{-2}}\right]^{1/2}\times\left[\frac{0.19m_0}{m}\right]^{1/2}\left[\frac{7.7}{\bar{\kappa}}\right]^{1/2},$$

$$\left[\frac{\omega_p}{2\pi c}\right][\text{cm}^{-1}]=55.37\left[\frac{q}{10^5\ \text{cm}^{-1}}\right]^{1/2}\left[\frac{N_s}{10^{12}\ \text{cm}^{-2}}\right]^{1/2}\times\left[\frac{0.19m_0}{m}\right]^{1/2}\left[\frac{7.7}{\bar{\kappa}}\right]^{1/2}.$$

$\hbar\omega_p$, two-dimensional plasmon energy for wave vector q in

thin-insulator limit [see Eq. (2.43)].

$$\omega_p = q\left[\frac{4\pi N_s e^2 d_{\rm ins}}{\kappa_{\rm ins} m}\right]^{1/2} \quad \text{(cgs)},$$

$$\omega_p = q\left[\frac{N_s e^2 d_{\rm ins}}{\kappa_{\rm ins}\varepsilon_0 m}\right]^{1/2} \quad \text{(SI)},$$

$$\hbar\omega_p[\text{meV}] = 4.314\left[\frac{q}{10^5\ \text{cm}^{-1}}\right]\left[\frac{d_{\rm ins}}{10\ \text{nm}}\right]^{1/2} \times\left[\frac{N_s}{10^{12}\ \text{cm}^{-2}}\right]^{1/2}\left[\frac{0.19m_0}{m}\right]^{1/2}\left[\frac{3.9}{\kappa_{\rm ins}}\right]^{1/2},$$

$$\left[\frac{\omega_p}{2\pi c}\right][\text{cm}^{-1}] = 34.79\left[\frac{q}{10^5\ \text{cm}^{-1}}\right]\left[\frac{d_{\rm ins}}{10\ \text{nm}}\right]^{1/2} \times\left[\frac{N_s}{10^{12}\ \text{cm}^{-2}}\right]^{1/2}\left[\frac{0.19m_0}{m}\right]^{1/2}\left[\frac{3.9}{\kappa_{\rm ins}}\right]^{1/2}.$$

The depletion layer is assumed to be much thicker than the oxide.

4. Quantities related to magnetic field

$\hbar\omega_c$, Landau-level separation.

$$\hbar\omega_c = \frac{eH\hbar}{mc} \quad \text{(cgs)},$$

$$\hbar\omega_c = \frac{eB\hbar}{m} \quad \text{(SI)},$$

$$\hbar\omega_c[\text{meV}] = 0.6093B[\text{T}]\left[\frac{0.19m_0}{m}\right].$$

$1\ \text{T} = 10^4$ G.

$g\mu_B B$, spin splitting.

$$g\mu_B B[\text{meV}] = 0.1158B[\text{T}]\frac{g}{2},$$

where μ_B (cgs) $= e\hbar/2m_0c$, μ_B (SI) $= e\hbar/2m_0$.

eB/h, carriers per magnetic quantum level, spin and valley splittings resolved.

$$\frac{eB}{h}[\text{cm}^{-2}] = 2.418\times10^{10}B[\text{T}].$$

l, size of lowest cyclotron orbit.

$$l = \left[\frac{\hbar c}{eH}\right]^{1/2} \quad \text{(cgs)},$$

$$l = \left[\frac{\hbar}{eB}\right]^{1/2} \quad \text{(SI)},$$

$$l[\text{nm}] = 25.66(B[\text{T}])^{-1/2}.$$

5. Quantities related to mobility

$\tau = m\mu/e$, scattering time.

$$\tau[\text{ps}] = 1.080\left[\frac{m}{0.19m_0}\right]\left[\frac{\mu}{10^4\ \text{cm}^2\,\text{V}^{-1}\,\text{s}^{-1}}\right].$$

$l = v_F\tau = \hbar k_F\mu/e$, low-temperature mean free path.

$$l[\text{nm}] = 65.82\left[\frac{\mu}{10^4\ \text{cm}^2\,\text{V}^{-1}\,\text{s}^{-1}}\right]\left[\frac{k_F}{10^6\ \text{cm}^{-1}}\right],$$

$$l[\text{nm}] = 116.7\left[\frac{\mu}{10^4\ \text{cm}^2\,\text{V}^{-1}\,\text{s}^{-1}}\right]\left[\frac{N_s}{10^{12}\ \text{cm}^{-2}}\right]^{1/2}.$$

$\Gamma_\tau = \hbar/2\tau$, level broadening.

$$\Gamma_\tau[\text{meV}] = 0.3047\left[\frac{0.19m_0}{m}\right]\left[\frac{10^4\ \text{cm}^2\,\text{V}^{-1}\,\text{s}^{-1}}{\mu}\right].$$

$k_F l$, Fermi wave vector times mean free path $= E_F/\Gamma_\tau$.

$$\omega_c\tau = \mu[m^2\,\text{V}^{-1}\,\text{s}^{-1}]B[\text{T}] = 10^{-8}\mu[\text{cm}^2\,\text{V}^{-1}\,\text{s}^{-1}]H[\text{Oe}].$$

N_A, bulk acceptor concentration, versus room-temperature bulk resistivity ρ, for nominally uncompensated p-type silicon (after Sze, 1969).

ρ [Ω cm]	N_A [cm^{-3}]
0.1	5×10^{17}
1	1.5×10^{16}
10	1.4×10^{15}
100	1.4×10^{14}

BIBLIOGRAPHY

This bibliography attempts to give fairly complete coverage of the electronic properties of inversion and accumulation layers at semiconductor-insulator interfaces and of recent work on the properties of electrons on the surface of liquid helium. Some papers dealing with related fields, such as thin films, heterojunctions, quantum well structures, and superlattices, and with some general aspects of two-dimensional systems have also been included. We have excluded most papers dealing with devices, radiation effects, and interface states. Not all papers in the bibliography are referred to in the text.

Abeles, B., P. Sheng, M. D. Coutts, and Y. Arie, 1975, "Structure and electrical properties of granular metal films," Adv. Phys. **24**, 407–461.

Abessonova, L. N., V. N. Dobrovol'skii, and Yu. S. Zharkikh, 1975, "Scattering of holes appearing near cleaved germanium surfaces under energy quantizing conditions," Fiz. Tekh. Poluprovodn. **9**, 957-960 [Sov. Phys.—Semicond. **9**, 626–627 (1975)].

Abessonova, L. N., V. N. Dobrovol'skii, Yu. S. Zharkikh, G.

K. Ninidze, and O. S. Frolov, 1976, "Anomalous behavior of the carrier mobility in inversion channels on the surface of oxidized silicon," Fiz. Tekh. Poluprovodn. **10**, 665–668 [Sov. Phys.—Semicond. **10**, 397–399 (1976)].

Abowitz, G., E. Arnold, and E. A. Leventhal, 1967, "Surface states and $1/f$ noise in MOS transistors," IEEE Trans. Electron Devices **ED-14**, 775–777.

Abrahams, E., P. W. Anderson, P. A. Lee, and T. V. Ramakrishnan, 1981, "Quasiparticle lifetime in disordered two-dimensional metals," Phys. Rev. B **24**, 6783–6789.

Abrahams, E., P. W. Anderson, D. C. Licciardello, and T. V. Ramakrishnan, 1979, "Scaling theory of localizations: Absence of quantum diffusion in two dimensions," Phys. Rev. Lett. **42**, 673–676.

Abrahams, E., P. W. Anderson, and T. V. Ramakrishnan, 1980, "Non-Ohmic effects of Anderson localization," Philos. Mag. B **42**, 827–833.

Abram, R. A., 1973, "Localized states in inverted silicon-silicon dioxide interfaces," J. Phys. C **6**, L379–L381.

Abramowitz, M., and I. A. Stegun, eds., 1964, *Handbook of Mathematical Functions* (National Bureau of Standards Applied Mathematics Series, No. 55) (U.S. Government Printing Office, Washington)

Abstreiter, G., 1980, "Electronic properties of the two-dimensional system at $GaAs/Al_xGa_{1-x}As$ interfaces," Surf. Sci. **98**, 117–125.

Abstreiter, G., P. Kneschaurek, J. P. Kotthaus, and J. F. Koch, 1974, "Cyclotron resonance of electrons in an inversion layer on Si," Phys. Rev. Lett. **32**, 104–107.

Abstreiter, G., J. F. Koch, P. Goy, and Y. Couder, 1976a, "Frequency dependence of surface cyclotron resonance in Si," Phys. Rev. B **14**, 2494–2497.

Abstreiter, G., J. P. Kotthaus, J. F. Koch, and G. Dorda, 1976b, "Cyclotron resonance of electrons in surface space-charge layers on silicon," Phys. Rev. B **14**, 2480–2493.

Abstreiter, G., and K. Ploog, 1979, "Inelastic light scattering from a quasi-two-dimensional electron system in $GaAs-Al_xGa_{1-x}As$ heterojunctions," Phys. Rev. Lett. **42**, 1308–1311.

Abstreiter, G., P. Stallhofer, and J. P. Kotthaus, 1980, "Effects of uniaxial stress on the cyclotron resonance in inversion layers on Si(100)," Surf. Sci. **98**, 413–415.

Abstreiter, G., Ch. Zeller, and K. Ploog, 1981, "Study of $GaAs-Al_xGa_{1-x}As$ multilayer systems by resonant inelastic light scattering techniques," in *Gallium Arsenide and Related Compounds, 1980,* edited by H. W. Thim (Institute of Physics, Bristol), pp. 741–749.

Adachi, T., and C. R. Helms, 1979, "Electron energy loss spectroscopy studies of the $Si-SiO_2$ interface," Appl. Phys. Lett. **35**, 199–201.

Adkins, C. J., 1977, "Maximum metallic resistance," Philos. Mag. **36**, 1285–1289.

Adkins, C. J., 1978a, "Threshold conduction in inversion layers," J. Phys. C **11**, 851–883.

Adkins, C. J. 1978b, "The Hall effect in inversion layers," Philos. Mag. B **38**, 535–548.

Adkins, C. J., 1979a, "Effective medium theory of conductivity and Hall effect in two dimensions," J. Phys. C **12**, 3389–3393.

Adkins, C. J., 1979b, "Application of effective medium theory to inversion layers," J. Phys. C **12**, 3395–3400.

Adkins, C. J., S. Pollitt, and M. Pepper, 1976, " The Anderson transition in silicon inversion layers," J. Phys. (Paris) **37**, Colloques, C4-343–C4-347.

Agarwal, G. K., J. S. Thakur, and K. N. Pathak, 1981, "Sum rules for the current correlation functions of a two-dimensional classical electron liquid," Phys. Lett. A **84**, 213–215.

Agranovich, [V.] M., and B. P. Antonyuk, 1974, "Excitons and instability of the dielectric state in quasi-one-dimensional and quasi-two-dimensional structures," Zh. Eksp. Teor. Fiz. **67**, 2352–2356 [Sov. Phys.—JETP **40**, 1167–1169 (1975)].

Agranovich, V. M., B. P. Antonyuk, and A. G. Mal'shukov, 1976, "New mechanism of exciton self-localization in quasi-one-dimensional and quasi-two-dimensional semiconductors," Zh. Eksp. Teor. Fiz. Pis'ma Red. **23**, 492–495 [JETP Lett. **23**, 448–450 (1976)].

Agranovich, V. M., B. P. Antonyuk, E. P. Ivanova, and A. G. Mal'shukov, 1977, "Self-localization of excitons in quasi-one-dimensional and quasi-two-dimensional semiconductors," Zh. Eksp. Teor. Fiz. **72**, 614–624 [Sov. Phys.—JETP **45**, 322–327 (1977)].

Alferieff, M. E. and C. B. Duke, 1968, "Energy and lifetime of space-charge-induced localized states," Phys. Rev. **168**, 832–842.

Alig, R. C., 1976, "Optical properties of a dense two-dimensional electron gas," RCA Rev. **37**, 206–219.

Allen, P. B., 1980, "Electron localisation in a random potential: A random walk analogue," J. Phys. C **13**, L667–L669.

Allen, S. J., Jr., D. C. Tsui, and J. V. Dalton, 1974, "Far infrared cyclotron resonance in the inversion layer of Si," Phys. Rev. Lett. **32**, 107–110.

Allen, S. J., Jr., D. C. Tsui, and F. DeRosa, 1975, "Frequency dependence of the electron conductivity in the silicon inversion layer in the metallic and localized regimes," Phys. Rev. Lett. **35**, 1359–1362.

Allen, S. J., Jr., D. C. Tsui, and B. Vinter, 1976, "On the absorption of infrared radiation by electrons in semiconductor inversion layers," Solid State Commun. **20**, 425–428.

Allen, S. J., Jr., D. C. Tsui, and R. A. Logan, 1977, "Observation of the two-dimensional plasmon in silicon inversion layers," Phys. Rev. Lett. **38**, 980–983.

Allgaier, R. S., and J. B. Restorff, 1979, "Improved weak-field magnetoresistance analysis for (001)-oriented thin films and surface layers with cubic or tetragonal symmetry," J. Appl Phys. **50**, 402–405.

Allgaier, R. S., J. B. Restorff, and B. Houston, 1979a, "Unified weak-field magnetoresistance phenomenology for cubic and noncubic {001}-and {111}-oriented epitaxial films and surface layers," Appl. Phys. Lett. **34**, 158–159.

Allgaier, R. S., J. B. Restorff, and B. Houston, 1979b, "Unified weak-field magnetoresistance phenomenology for (111)-oriented thin films and surface layers with cubic, trigonal, and hexagonal symmetries," Phys. Rev. B **19**, 6155–6163.

Al-Sadee, S. R., P. N. Butcher, and K. J. Hayden, 1981, "Dependence of the hopping conductivity exponent on band shape for two-dimensional impurity bands," Philos. Mag. B **43**, 173–175.

Altshuler, B. L., and A. G. Aronov, 1978, "Influence of electron-electron correlation on the resistivity of dirty metals," Zh. Eksp. Teor. Fiz. Pis'ma Red. **27**, 700–702 [JETP Lett. **27**, 662–664 (1978)].

Altshuler, B. L., and A. G. Aronov, 1981, "Electron density of states and energy relaxation time in magnetic field," Solid State Commun. **38**, 11–15.

Altshuler, B. L., A. G. Aronov, and P. A. Lee, 1980a, "Interaction effects in disordered Fermi systems in two dimensions," Phys. Rev. Lett. **44**, 1288–1291.

Altshuler, B. L., D. Khmel'nitzkii, A. I. Larkin, and P. A. Lee, 1980b, "Magnetoresistance and Hall effect in a disordered two-dimensional electron gas," Phys. Rev. B **22**, 5142–5153.

Altwein, M., and H. Finkenrath, 1975, "Quantum size effect in SnTe observed by tunnel experiments," Phys. Status Solidi B **72**, 413–419.

Alvarado, S. F., F. Ciccacci, and M. Campagna, 1981, "GaAs–$Al_xGa_{1-x}As$ superlattices as sources of polarized photoelectrons," Appl. Phys. Lett. **39**, 615–617.

Ambegaokar, V., B. I. Halperin, and J. S. Langer, 1971, "Hopping conductivity in disordered systems," Phys. Rev. B **4**, 2612–2620.

Anderson, P. W., 1958, "Absence of diffusion in certain random lattices," Phys. Rev. **109**, 1492–1505.

Anderson, P. W., 1981, "New method for scaling theory of localization. II. Multichannel theory of a 'wire' and possible extension to higher dimensionality," Phys. Rev. B **23**, 4828–4836.

Anderson, P. W., E. Abrahams, and T. V. Ramakrishnan, 1979, "Possible explanation of nonlinear conductivity in thin-film metal wires," Phys. Rev. Lett. **43**, 718–720.

Ando, T., 1974a, "Theory of quantum transport in a two-dimensional electron system under magnetic fields. II. Single-site approximation under strong fields," J. Phys. Soc. Japan **36**, 1521–1529.

Ando, T., 1974b, "Theory of quantum transport in a two-dimensional electron system under magnetic fields. III. Many-site approximation," J. Phys. Soc. Japan **37**, 622–630.

Ando, T., 1974c, "Theory of quantum transport in a two-dimensional electron system under magnetic fields. IV. Oscillatory conductivity," J. Phys. Soc. Japan **37**, 1233–1237.

Ando, T., 1975a, "Theory of cyclotron resonance lineshape in a two-dimensional electron system," J. Phys. Soc. Japan **38** 989–997.

Ando, T., 1975b, "Subband structure of an accumulation layer under strong magnetic fields," J. Phys. Soc. Japan **39**, 411–417.

Ando, T., 1976a, "Density-functional calculation of subband structure on semiconductor surfaces," Surf. Sci. **58**, 128–134.

Ando, T., 1976b, "Density-functional calculation of sub-band structure in accumulation and inversion layers," Phys. Rev. B **13**, 3468–3477.

Ando, T., 1976c, "Lineshape of inter-subband optical transitions in space charge layers," Z. Phys. B **24**, 33–39.

Ando, T., 1976d, "Quantum transport in an anisotropic two-dimensional system under strong magnetic fields," Z. Phys. B **24**, 219–226.

Ando, T., 1976e, "Mass enhancement and subharmonic structure of cyclotron resonance in an interacting two-dimensional electron gas," Phys. Rev. Lett. **36**, 1383–1385.

Ando, T., 1977a, "Inter-subband optical transitions in a surface space-charge layer," Solid State Commun. **21**, 133–136.

Ando, T., 1977b, "Inter-subband optical absorption in an inversion layer on a semiconductor surface in magnetic fields," Solid State Commun. **21**, 801–804.

Ando, T., 1977c, "Inter-subband optical absorption in space-charge layers on semiconductor surfaces," Z. Phys. B **26**, 263–272.

Ando, T., 1977d, "Screening effect and quantum transport in a silicon inversion layer in strong magnetic fields," J. Phys. Soc. Japan **43**, 1616–1626.

Ando, T., 1978a, "Electron-electron interaction and electronic properties of space charge layers on semiconductor surfaces," Surf. Sci. **73**, 1–18.

Ando, T., 1978b, "Subband structure and inter-subband absorption in an accumulation layer in strong magnetic fields," J. Phys. Soc. Japan **44**, 475–481.

Ando, T., 1978c, "Broadening of inter-subband transitions in image-potential-induced surface states outside liquid helium," J. Phys. Soc. Japan **44**, 765–773.

Ando, T., 1978d, "Theory of magnetoplasmon resonance lineshape in the silicon inversion layer," Solid State Commun. **27**, 895–899.

Ando, T., 1979a, "Theory of intersubband-cyclotron combined resonance in the silicon accumulation layer," in *Physics of Semiconductors, 1978,* edited by B. L. H. Wilson (Institute of Physics, Bristol), pp. 1219–1222.

Ando, T., 1979b, "Valley splitting in the silicon inversion layer: Misorientation effect," Phys. Rev. B **19**, 3089–3095.

Ando, T., 1979c, "Theory of intersubband cyclotron combined resonances in the silicon space-charge layer," Phys. Rev. B **19**, 2106–2116.

Ando, T., 1979d, "Minigap and transport in a two-dimensional electron system," J. Phys. Soc. Japan **47**, 1595–1605.

Ando, T., 1980a, "Valley splitting and related phenomena in Si inversion layers," Surf. Sci. **98**, 327–349.

Ando, T., 1980b, "Many-body effects in the space charge layers," in *Proceedings of the 15th International Conference on the Physics of Semiconductors, Kyoto* [J. Phys. Soc. Japan **49**, Suppl. A, 929–936 (1980)].

Ando, T., 1981a, "Magnetic quantization and transport in a semiconductor superlattice," in *Physics in High Magnetic Fields,* edited by S. Chikazumi and M. Miura (Springer, Berlin), pp. 301–304.

Ando, T., 1981b, "Electronic properties of a semiconductor superlattice, III. Energy levels and transport in magnetic fields," J. Phys. Soc. Japan **50**, 2978–2984.

Ando, T., T. Eda, and M. Nakayama, 1977, "Optical absorption in surface space-charge layers of anisotropic and tilted valley systems," Solid State Commun. **23**, 751–754.

Ando, T., Y. Matsumoto, and Y. Uemura, 1972a, "Theory of quantum galvanomagnetic effects in the inversion layer of semiconductors," in *Proceedings of the 11th International Conference on the Physics of Semiconductors, Warsaw* (PWN–Polish Scientific, Warsaw), Vol. 1, pp. 294–305.

Ando, T., Y. Matsumoto, Y. Uemura, Mineo Kobayashi, and K. F. Komatsubara, 1972b, "Transverse magnetoconductivity of a two-dimensional electron gas," J. Phys. Soc. Japan **32**, 859.

Ando, T., Y. Matsumoto, and Y. Uemura, 1975, "Theory of Hall effect in a two-dimensional electron system," J. Phys. Soc. Japan **39**, 279–288.

Ando, T., and S. Mori, 1979 "Electronic properties of a semiconductor superlattice. I. Self-consistent calculation of subband structure and optical spectra," J. Phys. Soc. Japan **47**, 1518–1527.

Ando, T., and Y. Uemura, 1974a, "Theory of quantum transport in a two-dimensional electron system under magnetic fields. I. Characteristics of level broadening and transport under strong fields," J. Phys. Soc. Japan **36**, 959–967.

Ando, T., and Y. Uemura, 1974b, "Theory of oscillatory g factor in an MOS inversion layer under strong magnetic fields," J. Phys. Soc. Japan **37**, 1044–1052.

Ando, T., and Y. Uemura, 1974c, "Oscillation of effective g factor in MOS inversion layers under strong magnetic fields," in *Proceedings of the Second International Conference on Solid Surfaces, Kyoto* [Jpn. J. Appl. Phys., Suppl. 2, Pt. 2,

329—332 (1974)].
Ando, T., and Y. Uemura, 1974d, "Theory of cyclotron resonance line shape in MOS inversion layers," in *Proceedings of the 12th International Conference on the Physics of Semiconductors, Stuttgart,* edited by M. H. Pilkuhn (Teubner, Stuttgart), pp. 724—728.
Andreev, A. F., 1971, "Interaction of conduction electrons with a metal surface," Usp. Fiz. Nauk **105**, 113—124 [Sov. Phys.—Usp. **14**, 609—615 (1972)].
Andryushin, E. A., 1976, "Ground-state energy of a layered electron-hole liquid," Fiz. Tverd. Tela (Leningrad) **18**, 2493—2498 [Sov. Phys.—Solid State **18**, 1457—1460 (1976)].
Andryushin, E. A., L. V. Keldysh, A. A. Sanina, and A. P. Silin, 1980, "Electron-hole liquid in thin semiconductor films," Zh. Eksp. Teor. Fiz. **79**, 1509—1517 [Sov. Phys.—JETP **52**, 761—765 (1980)].
Andryushin, E. A., and A. P. Silin, 1976a, "On the theory of the collective phenomena in quasi-two-dimensional semiconductors," Solid State Commun. **20**, 453—456.
Andryushin, E. A., and A. P. Silin, 1976b, "Two-dimensional electron-hole liquid," Fiz. Tverd. Tela (Leningrad) **18**, 2130—2132 [Sov. Phys.—Solid State **18**, 1243—1244 (1976)].
Andryushin, E. A., and A. P. Silin, 1979, "Phase diagram of a two-dimensional electron-hole system," Fiz. Tverd. Tela (Leningrad) **21**, 219—222 [Sov. Phys.—Solid State **21**, 129—130 (1979)].
Andryushin, E. A., and A. P. Silin, 1980, "Excitons in thin semiconductor films," Fiz. Tverd. Tela (Leningrad) **22**, 2676—2680 [Sov. Phys.—Solid State **22**, 1562—1564 (1980)].
Antcliffe, G. A., R. T. Bate, and R. A. Reynolds, 1971, "Oscillatory magnetoresistance from an *n*-type inversion layer with nonparabolic bands," in *The Physics of Semimetals and Narrow Gap Semiconductors,* edited by D. L. Carter and R. T. Bate (Pergamon, Oxford); J. Phys. Chem. Solids **32**, Suppl. 1, 499—510.
Aoki, H., 1977 "Computer simulation of two-dimensional disordered electron systems in strong magnetic fields," J. Phys. C **10**, 2583—2593.
Aoki, H., 1978a, "Numerical study of two-dimensional Wigner glass in strong magnetic fields," Surf. Sci. **73**, 281—290.
Aoki, H., 1978b, "Transport properties of two-dimensional disordered electron systems in strong magnetic fields," J. Phys. C **11**, 3823—3834.
Aoki, H., 1979, "Effect of coexistence of random potential and electron-electron interaction in two-dimensional systems: Wigner glass," J. Phys. C **12**, 633—645.
Aoki, H., and T. Ando, 1981, "Effect of localization on the Hall conductivity in the two-dimensional system in strong magnetic fields," Solid State Commun. **38**, 1079—1082.
Aoki, H., and H. Kamimura, 1977, "Anderson localization in a two-dimensional electron system under strong magnetic fields," Solid State Commun. **21**, 45—47.
Aoki, M., H. Katto, and E. Yamada, 1977, "Low-frequency $1/f$ noise in MOSFET's at low current levels," J. Appl. Phys. **48**, 5135—5140.
Aoki, T., and M. Saitoh, 1979, "Theory of hot electrons on the liquid ^{4}He surface II," J. Phys. Soc. Japan **46**, 423—431.
Aoki, T., and M. Saitoh, 1980, "Theory of cyclotron resonance of hot electrons on the liquid ^{4}He," J. Phys. Soc. Japan **48**, 1929—1936.
Apostol, M., 1975, "Plasma frequency of the electron gas in layered structures," Z. Phys. B **22**, 13—19.
Appel, J., and A. W. Overhauser 1978, "Cyclotron resonance in two interacting electron systems with application to Si inversion layers," Phys. Rev. B **18**, 758—767.
Appelbaum, J. A., and G. A. Baraff, 1971a, "Effect of magnetic field on the energy of surface bound states," Phys. Rev. B **4**, 1235—1245.
Appelbaum, J. A., and G. A. Baraff, 1971b, "Parametric approach to surface screening of a weak external electric field," Phys. Rev. B **4**, 1246—1250.
Appelbaum, J. A., and G. A. Baraff, 1971c, "Self-induced deficiency state in degenerate semiconductors," Phys. Rev. Lett. **26**, 1432—1435.
Arnold, E., 1974, "Disorder-induced carrier localization in silicon surface inversion layers," Appl. Phys. Lett. **25**, 705—707.
Arnold, E., 1976, "Conduction mechanism in bandtails at the Si-SiO_2 interface," Surf. Sci. **58**, 60—70.
Arnold, E., 1978, "Comment on the frequency dependence of electron conductivity in the silicon inversion layer in the metallic and localized regimes," Phys. Rev. B **17**, 4111—4113.
Arnold, E., and G. A. Abowitz, 1966, "Effect of surface states on electron mobility in Si surface inversion layers," Appl. Phys. Lett. **9**, 344—346.
Arnold, E., and H. Schauer, 1978, "Measurement of interface state density in MNOS structures," Appl. Phys. Lett. **32**, 333—335.
Arnold, E., and J. M. Shannon, 1976, "Anomalous Hall effect and carrier transport in bandtails at the Si-SiO_2 interface," Solid State Commun. **18**, 1153—1156.
Arora, V. K., and F. G. Awad, 1981, "Quantum size effect in semiconductor transport," Phys. Rev. B **23**, 5570—5575.
Arutyunyan, G. M., and Kh. V. Nerkararyan, 1981, "Special features of the Coulomb interaction in periodic semiconductor structures," Fiz. Tverd. Tela (Leningrad) **23**, 225—228 [Sov. Phys.—Solid State **23**, 127—129 (1981)].
Asche, M., and O. G. Sarbei, 1981, "Electron-phonon interaction in *n*-Si," Phys. Status Solidi B **103**, 11—50.
Aspnes, D. E., 1976, "GaAs lower conduction-band minima: Ordering and properties," Phys. Rev. B **14**, 5331—5343.
Aspnes, D. E., and J. B. Theeten, 1979, "Optical properties of the interface between Si and its thermally grown oxide," Phys. Rev. Lett. **43**, 1046—1050.
Aymeloglu, S., and J. N. Zemel, 1976a, "Field effect studies on *n*-channel (100) MOSFET's at 4.2 to 77 K," Surf. Sci. **58**, 98—103.
Aymeloglu, S., and J. N. Zemel, 1976b, "Freeze-out effects on *n*-channel MOSFET's," IEEE Trans. Electron Devices **ED-23**, 466—470.
Azbel, M. Ya., 1969, "Problems of the electron theory of metals. IV. Thermodynamic and kinetic properties of metals in a magnetic field," Usp. Fiz. Nauk **98**, 601—651 [Sov. Phys.—Usp. **12**, 507—533 (1970)].
Azbel, M. Ya., 1981, "Localization in thin wires," Phys. Rev. Lett. **46**, 675—678.
Babichenko, V. S., L. V. Keldysh, and A. P. Silin, 1980, "Coulomb interaction in thin semiconductor and semimetal filaments," Fiz. Tverd. Tela (Leningrad) **22**, 1238—1240 [Sov. Phys.—Solid State **22**, 723—724 (1980)].
Baccarani, G., A. M. Mazzone, and C. Morandi, 1974, "The diffuse scattering model of effective mobility in the strongly inverted layer of MOS transistors," Solid-State Electron. **17**, 785—789.
Baccarani, G., and A. M. Mazzone, 1975, "The influence of an energy-dependent relaxation time on the specular and diffuse scattering models of surface conduction in MOS structures," Solid-State Electron. **18**, 718—720.

Baglee, D. A., D. K. Ferry, C. W. Wilmsen, and H. H. Wieder, 1980, "Inversion layer transport and properties of oxides on InAs," J. Vac. Sci. Technol. **17**, 1032–1036.

Baglee, D. A., D. H. Laughlin, B T. Moore, B. L. Eastep, D. K. Ferry, and C. W. Wilmsen, 1981, "Inversion layer transport and insulator properties of the indium-based III-V's," in *Gallium Arsenide and Related Compounds, 1980,* edited by H. W. Thim (Institute of Physics, Bristol), pp. 259–265.

Bangert, E., K. von Klitzing, and G. Landwehr, 1974, "Self consistent calculations of electric subbands in *p*-type silicon inversion layers," in *Proceedings of the 12th International Conference on the Physics of Semiconductors, Stuttgart,* edited by M. H. Pilkuhn (Teubner, Stuttgart), pp. 714–718.

Bangert, E., and G. Landwehr, 1976, "Self-consistent calculations of electric subbands in *p*-type silicon inversion layers," Surf. Sci. **58**, 138–140.

Banville, M., A. Caillé, and M. J. Zuckerman, 1980, "Interaction of interface plasmons and longitudinal optical phonons in multilayer structures in the presence of transverse conductivity," Phys. Rev. B **21**, 355–363.

Baraff, G. A., and J. A. Appelbaum, 1972, "Effect of electric and magnetic fields on the self-consistent potential at the surface of a degenerate semiconductor," Phys. Rev. B **5**, 475–497.

Baraff, G. A., and D. C. Tsui, 1981, "Explanation of quantized-Hall-resistance plateaus in heterojunction inversion layers," Phys. Rev. B **24**, 2274–2277.

Barber, M. N., 1980, "Phase transitions in two dimensions," Phys. Rep. **59**, 375–409.

Bardeen, J., and W. Shockley, 1950, "Deformation potentials and mobilities in non-polar crystals," Phys. Rev. **80**, 72–80.

Bargmann, V., 1952, "On the number of bound states in a central field of force," Proc. Natl. Acad. Sci. (U.S.) **38**, 961–966.

Barker, A. S., J. L. Merz, and A. C. Gossard, 1978, "Study of zone-folding effects on phonons in alternating monolayers of GaAs-AlAs," Phys. Rev. B **17**, 3181–3196.

Bartelink, D. J., 1980, "Surface depletion and inversion in semiconductors with arbitrary dopant profiles," Appl. Phys. Lett. **37**, 220–223.

Bartkowski, M., M. Jałochowski, Z. Korczak, M. Subotowicz, and M. Załużny, 1979, "Quantum size effect in PbTe," in *Physics of Semiconductors, 1978,* edited by B. L. H. Wilson (Institute of Physics, Bristol), pp. 745–748.

Baru, V. G., and E. V. Grekov, 1980, "Gas-liquid phase transition in quasi-two-dimensional electron gas in magnetic semiconductors," Fiz. Tverd. Tela (Leningrad) **22**, 802–806 [Sov. Phys.—Solid State **22**, 467–470 (1980)].

Baru, V. G., and E. V. Grekov, 1981, "Van der Waals theory of the phase transition of quasi-two-dimensional electron gas in magnetic semiconductors," Phys. Status Solidi B **105**, 369–376.

Baskin, É. M., A. V. Chaplik, and M. V. Éntin, 1972, "Localized electron states in thin layers due to geometric defects of the surface," Zh. Eksp. Teor. Fiz. **63**, 1077–1082 [Sov. Phys.—JETP **36**, 566–569 (1973)].

Baskin, É. M., and M. V. Éntin, 1969, "Electron scattering and the conductivity of a film with surface defects," Zh. Eksp. Teor. Fiz. **57**, 460–468 [Sov. Phys.–JETP **30**, 252–256 (1970)].

Baskin, É. M., and M. V. Éntin, 1974, "Transport effects in the vicinity of a semiconductor surface under strong band-bending conditions," Fiz. Tekh. Poluprovodn. **8**, 64–73 [Sov. Phys.—Semicond. **8**, 37–42 (1974)].

Baskin, É. M., L. N. Magarill, and M. V. Éntin, 1978, "Two-dimensional electron-impurity system in a strong magnetic field," Zh. Eksp. Teor. Fiz. **75**, 723–734 [Sov. Phys.—JETP **48**, 365–370].

Bass, F. G., V. V. Zorchenko, and V. I. Shashora, 1980, "Stark-cyclotron resonance in semiconductors with a superlattice," Zh. Eksp. Teor. Fiz. Pis'ma Red. **31**, 345–347 [JETP Lett. **31**, 314–317 (1980)].

Bastard, G., 1981a, "Hydrogenic impurity states in a quantum well: A simple model." Phys. Rev. B **24**, 4714–4722.

Bastard, G., 1981b, "Superlattice band structure in the envelope-function approximation," Phys. Rev. B **24**, 5693–5697.

Basu, P. K., 1976, "On the validity of Matthiessen's Rule in the calculation of surface carrier mobility," Indian J. Pure Appl. Phys. **14**, 767–768.

Basu, P. K., 1977, "High-field drift velocity of silicon inversion layers—A Monte Carlo calculation," J. Appl. Phys. **48**, 350–353.

Basu, P. K. 1978a, "Monte Carlo calculation of the drift velocity of electrons and holes in high electric fields in silicon MOSFETs," Surf. Sci. **73**, 156–159.

Basu, P. K., 1978b, "Monte Carlo calculation of hot electron drift velocity in silicon (100)-inversion layer by including three subbands," Solid State Commun. **27**, 657–660.

Basu, P. K., 1979, "Correct form of energy-balance equation for intervalley and intersubband scattering in semiconductors," Phys. Rev. B **19**, 4100–4106.

Basu, P. K., and B. R. Nag, 1980, "Lattice scattering mobility of a two-dimensional electron gas in GaAs," Phys. Rev. B **22**, 4849–4852.

Basu, P. K., and B. R. Nag, 1981, "Piezoelectric scattering in quantized surface layers in semiconductors," J. Phys. C **14**, 1519–1522.

Bate, R. T., 1977, "Electrically controllable superlattice," Bull. Am. Phys. Soc. **22**, 407.

Batra, I. P., 1978, "Electronic structure investigations of two allotropic forms of SiO_2: α-quartz and β-cristobalite," in *The Physics of SiO_2 and its Interfaces,* edited by S. T. Pantelides (Pergamon, New York), pp. 65–69.

Bauer, R. S., J. C. McMenamin, R. Z. Bachrach, A. Bianconi, L. Johansson, and H. Petersen, 1979, "Bonding at the Si(111)-SiO_2 interface: Stoichiometry and kinetics probed with synchrotron radiation photoemission spectroscopies," in *Physics of Semiconductors, 1978,* edited by B. L. H. Wilson (Institute of Physics, Bristol), pp. 797–800.

Bauer, R. S., J. C. McMenamin, H. Petersen, and A. Bianconi, 1978, "Initial stages of SiO_2 formation on Si(111)," in *The Physics of SiO_2 and its Interfaces,* edited by S. T. Pantelides (Pergamon, New York), pp. 401–406.

Baus, M., 1978, "Collective modes and dynamic structure factor of a two-dimensional electron solid," J. Stat. Phys. **19**, 163–176.

Baus, M., 1980a, "Absence of long-range order with long-range potentials," J. Stat. Phys. **22**, 111–119.

Baus, M., 1980b, "Theoretical evidence for the existence of the self-diffusion constant of two-dimensional electron liquids," J. Phys. C **13**, L41–L43.

Baus, M., and J. Bosse, 1980, "Comments on self-diffusion in two-dimensional electron liquids," Phys. Rev. A **22**, 2284–2285.

Baus, M., and J.-P. Hansen, 1980, "Statistical mechanics of simple Coulomb systems," Phys. Rep. **59**, 1–94.

Beck, D. E., and P. Kumar, 1976, "Plasma oscillation of a charge layer at an insulator surface," Phys. Rev. B **13**,

2859—2864; **14**, 5127(E).

Beinvogl, W., H. D. Drew, and F. Koch, 1978, "On the resonant excitation of electron subbands on the surface of InSb," in *Physics of Narrow Gap Semiconductors,* edited by J. Rauluszkiewicz, M. Górska, and E. Kaczmarek (PWN—Polish Scientific, Warsaw), pp. 411—416.

Beinvogl, W., A. Kamgar, and J. F. Koch, 1976, "Influence of a magnetic field on electron subbands in a surface space-charge layer," Phys. Rev. B **14**, 4274—4280.

Beinvogl, W., and J. F. Koch, 1977, "Spectroscopy of electron subband levels in an inversion layer on InSb," Solid State Commun. **24**, 687—690; Surf. Sci. **73**, 547—548 (extended abstract) (1978).

Beinvogl, W., and J. F. Koch, 1978, "Intersubband-cyclotron combined resonance in a surface space charge layer," Phys. Rev. Lett. **40**, 1736—1739.

Bell, R. J., W. T. Bousman, Jr., G. M. Goldman, and D. G. Rathbun, 1967, "Surface and bulk impurity eigenvalues in the shallow donor impurity theory," Surf. Sci. **7**, 293—301.

Bell, R. L., 1962, "Electric dipole spin transition in InSb," Phys. Rev. Lett. **9**, 52—54.

Belyavskii, V. I., 1978, "Optical absorption by impurities in a semiconductor with a superlattice," Fiz. Tverd. Tela (Leningrad) **20**, 2821—2822 [Sov. Phys.—Solid State **20**, 1630—1631 (1978)].

BenDaniel, D. J., and C. B. Duke, 1966, "Space-charge effects on electron tunneling," Phys. Rev. **152**, 683—692.

Bendow, B., 1971, "Theory of the effect of finite crystal size on the frequencies and intensities of impurity absorption lines in semiconductors," Phys. Rev. B **3**, 1999—2003.

Beni, G., and T. M. Rice, 1979, "Stability of the six-valley state of the Si(111) *n*-type inversion layer," Phys. Rev. B **20**, 5390—5393.

Berezinskii, V. L., 1970, "Destruction of long-range order in one-dimensional and two-dimensional systems having a continuous symmetry group. I. Classical systems," Zh. Eksp. Teor. Fiz. **59**, 907—920 [Sov. Phys.—JETP **32**, 493—500 (1971)].

Berezinskii, V. L., 1971, "Destruction of long-range order in one-dimensional and two-dimensional systems possessing a continuous symmetry group. II. Quantum systems," Zh. Eksp. Teor. Fiz. **61**, 1144—1156 [Sov. Phys.—JETP **34**, 610—616 (1972)].

Bergman, D. J., and T. M. Rice, 1977, "Possibility of a spin-density-wave or a valley-density-wave in the ground state of a two-dimensional electron fluid," Solid State Commun. **23**, 59—62.

Bergman, D. J., T. M. Rice, and P. A. Lee, 1977, "Fluctuations, Coulomb effects, and long-range order in incommensurate charge-density-wave structures," Phys. Rev. B **15**, 1706—1718.

Bers, A., J. H. Cafarella, and B. E. Burke, 1973, "Surface mobility measurement using acoustic surface waves," Appl. Phys. Lett. **22**, 399—401.

Berz, F., 1970a, "Theory of low frequency noise in Si MOST's," Solid-State Electron, **13**, 631—647.

Berz, F., 1970b, "Ionized impurity scattering in silicon surface channels," Solid-State Electron, **13**, 903—906.

Berz, F., 1975a, Comment on "Measurements and interpretation of low frequency noise in FET's," IEEE Trans. Electron Devices **ED-22**, 293—294.

Berz, F., 1975b, "The surface space charge layer," in *Surface Physics of Phosphors and Semiconductors,* edited by C. G. Scott and C. E. Reed (Academic, New York), pp. 143—220.

Berz, F., and C. G. Prior, 1970, "Test of McWhorter's model of low-frequency noise in Si M.O.S.T.s," Electron. Lett. **6**, 595—597.

Bethin, J., T. G. Castner, and N. K. Lee, 1974, "Polarizabilities of shallow donors in silicon," Solid State Commun. **14**, 1321—1324.

Bezák, V., 1966a, "The degenerate semiconductor thin films. I—The Fermi energy," J. Phys. Chem. Solids **27**, 815—820.

Bezák, V., 1966b, "The degenerate semiconductor thin films. II—The longitudinal electric conductivity," J. Phys. Chem. Solids **27**, 821—834.

Binder, J., K. Germanova, A. Huber, and F. Koch, 1979a, "Space-charge layers on Ge surfaces. I. dc Conductivity and Shubnikov—de Haas effect," Phys. Rev. B **20**, 2382—2390.

Binder, J., A. Huber, K. Germanova, and F. Koch, 1979b, "Space-charge layers on Ge surfaces. II. High-frequency conductivity and cyclotron resonance," Phys. Rev. B **20**, 2391—2394.

Bishop, D. J., D. C. Tsui, and R. C. Dynes, 1980, "Nonmetallic conduction in electron inversion layers at low temperatures," Phys. Rev. Lett. **44**, 1153—1156.

Bishop, D. J., D. C. Tsui, and R. C. Dynes, 1981, "Observation of a non-Ohmic Hall resistivity at low temperatures in a two-dimensional electron gas," Phys. Rev. Lett. **46**, 360—363.

Blakeslee, A. E. and C. F. Aliotta, 1970, "Man-made superlattice crystals," IBM J. Res. Dev. **14**, 686—688.

Blanc, J., C. J. Buiocchi, M. S. Abrahams, and W. E. Ham, 1977, "The Si/SiO_2 interface examined by cross-sectional transmission electron microscopy," Appl. Phys. Lett. **30**, 120—122.

Blanc, J., 1978, "A revised model for the oxidation of Si by oxygen," Appl. Phys. Lett. **33**, 424—426.

Bliek, L. M., 1974, "The influence of Landau level broadening on the Shubnikov—de Haas effect in two-dimensional conductors," in *Proceedings of the 12th International Conference on the Physics of Semiconductors, Stuttgart,* edited by M. H. Pilkuhn (Teubner, Stuttgart), pp. 729—733.

Bloss, W. L., and L. J. Sham, 1979, "Exciton effect in silicon inversion layer," Bull. Am. Phys. Soc. **24**, 437.

Bloss, W. L., L. J. Sham, and B. Vinter, 1979, "Interaction-induced transition at low densities in silicon inversion layer," Phys. Rev. Lett. **43**, 1529—1532; Surf. Sci. **98**, 250—255 (1980).

Bloss, W. L., S. C. Ying, and J. J. Quinn, 1981, "Exchange-correlation effects in silicon (111) inversion layers: Strain-enhanced valley-occupancy phase transitions," Phys. Rev. B **23**, 1839—1842.

Bloss, W. L., S. C. Ying, J. J. Quinn, T. Cole, and B. D. McCombe, 1980, "Exchange-correlation effects in silicon inversion layers: Valley occupancy phase transitions," in *Proceedings of the 15th International Conference on the Physics of Semiconductors, Kyoto* [J. Phys. Soc. Japan **49**, Suppl. A, 963—966 (1980)].

Bluyssen, H., J. C. Maan, P. Wyder, L. L. Chang, and L. Esaki, 1979, "Cyclotron resonance in an InAs-GaSb superlattice," Solid State Commun. **31**, 35—38.

Bonsall, L., and A. A. Maradudin, 1976, "Some dynamical properties of a two-dimensional Wigner crystal," Surf. Sci. **58**, 312—319.

Bonsall, L., and A. A. Maradudin, 1977, "Some static and dynamical properties of a two-dimensional Wigner crystal," Phys. Rev. B **15**, 1959—1973.

Bose, S. M., 1976, "Electron correlations in a two-dimensional electron gas," Phys. Rev. B **13**, 4192—4195.

Bottka, N., and M. E. Hills, 1978, "Internal electroabsorption in inverted heterostructures: An optical method for probing epitaxial layers," Appl. Phys. Lett. **33**, 765–767.

Bottoms, W. R., and D. Guterman, 1974, "Electron beam probe studies of semiconductor-insulator interfaces," J. Vac. Sci. Technol. **11**, 965–971.

Bouat, J., and J. C. Thuillier, 1974, "Surface quantum transport in MOS structure on tellurium," in *Proceedings of the 5th Conference on Solid State Devices, Tokyo, 1973* [J. Japan Soc. Appl. Phys. **43**, Suppl., 327–331].

Bouat, J., and J. C. Thuillier, 1977, "Surface quantum oscillations in tellurium inversion layers," Phys. Lett. A **62**, 523–525.

Bouat, J., and J. C. Thuillier, 1978a, "Surface quantum transport in tellurium inversion layers," Surf. Sci. **73**, 528–536.

Bouat, J., and J. C. Thuillier, 1978b, "Calculation of surface quantum levels in tellurium inversion layers," J. Phys. (Paris) **39**, 1193–1197.

Boudry, M. R., and J. P. Stagg, 1979, "The kinetic behavior of mobile ions in the Al-SiO_2-Si system," J. Appl. Phys. **50**, 942–950.

Bowers, R., and Y. Yafet, 1959, "Magnetic susceptibility of InSb," Phys Rev. **115**, 1165–1172.

Brattain, W. H., and J. Bardeen, 1953, "Surface properties of germanium," Bell Syst. Tech. J. **32**, 1–41.

Braun, E., E. Staben, and K. von Klitzing, 1980, "Experimental determination of h/e^2 by the quantized Hall resistance in MOSFETs," PTB-Mitteilungen **90**, 350–351.

Brews, J. R., 1972a, "Surface potential fluctuations generated by interface charge inhomogeneities in MOS devices," J. Appl. Phys. **43**, 2306–2313.

Brews, J. R., 1972b, "Admittance of an MOS device with interface charge inhomogeneities," J. Appl. Phys. **43**, 3451–3455.

Brews, J. R., 1973a, "Limitations on photoinjection studies of charge distributions close to interfaces in MOS capacitors," J. Appl. Phys. **44**, 379–384.

Brews, J. R., 1973b, "Correcting interface-state errors in MOS doping profile determinations," J. Appl. Phys. **44**, 3228–3231.

Brews, J. R., 1975a, "Theory of the carrier-density fluctuations in an IGFET near threshold," J. Appl. Phys. **46**, 2181–2192.

Brews, J. R., 1975b, "Carrier density fluctuations and the IGFET mobility near threshold," J. Appl. Phys. **46**, 2193–2203.

Brews, J. R., 1977, Comments on "A new approach to the theory and modeling of IGFET's" IEEE Trans. Electron Devices **ED-24**, 1369–1370.

Brews, J. R., 1978, "A charge-sheet model of the MOSFET," Solid-State Electron. **21**, 345–355.

Brews, J. R., 1981, "Physics of the MOS transistor," in *Silicon Integrated Circuits,* edited by D. Kahng (Suppl. 2 of *Applied Solid State Science,* edited by R. Wolfe) (Academic, New York), Part A, pp. 1–120.

Brews, J. R., and A. D. Lopez, 1973, "A test for lateral nonuniformities in MOS devices using only capacitance curves," Solid-State Electron. **16**, 1267–1277.

Bridges, F., and J. F. McGill, 1977, "Mobility of electrons on the surface of liquid helium," Phys. Rev. B **15**, 1324–1339.

Brinkman, W. F., and T. M. Rice, 1973, "Electron-hole liquids in semiconductors," Phys. Rev. B **7**, 1508–1523.

Broomall, J. R., and D. G. Onn, 1975, "Surface electron barriers for helium-3 and helium-4: Experimental study of density dependence," in *Proceedings of the 14th International Conference on Low Temperature Physics,* edited by M. Krusius and M. Vuorio (North-Holland, Amsterdam), Vol. 1, pp. 439–442.

Broux, G., R. Van Overstraeten, and G. Declerck, 1975, "Experimental results on fast surface states and $1/f$ noise in M.O.S. transistors," Electron. Lett. **11**, 97–98.

Brown, E., 1969, "Effect of a tangential magnetic field on surface inversion layer states," IBM Research Report RC 2629 (unpublished).

Brown, T. R., and C. C. Grimes, 1972, "Observation of cyclotron resonance in surface-bound electrons on liquid helium," Phys. Rev. Lett. **29**, 1233–1236.

Brown, T. R., and R. W. Hockney, 1976, "A phase transition in a classical electron film," Surf. Sci. **58**, 295–296.

Burstein, E., A. Pinczuk, and S. Buchner, 1979, "Resonance inelastic light scattering by charge carriers at semiconductor surfaces," in *Physics of Semiconductors, 1978,* edited by B. L. H. Wilson (Institute of Physics, Bristol), pp. 1231–1234.

Burstein, E., A. Pinczuk, and D. L. Mills, 1980, "Inelastic light scattering by charge carrier excitations in two-dimensional plasmas: Theoretical considerations," Surf. Sci. **98**, 451–468.

Butcher, P. N., 1980, "Calculation of hopping transport coefficients," Philos. Mag. B **42**, 799–824.

Butcher, P. N., and K. J. Hayden, 1977, "Analytical formulae for d.c. hopping conductivity. Degenerate hopping in wide bands," Philos. Mag. **36**, 657–676.

Butcher, P. N., K. J. Hayden, and J. A. McInnes, 1977, "Analytical formulae for d.c. hopping conductivity," Philos. Mag. **36**, 19–32.

Caillé, A., and M. Banville, 1976, "The interaction of the two-dimensional plasmon with the surface plasmons in an MOS structure," Solid State Commun. **19**, 951–954.

Caillé, A., M. Banville, and M. J. Zuckermann, 1977, "Interaction of interface plasmons and longitudinal optical phonons in a multilayer structure," Solid State Commun. **24**, 805–808.

Calabrese, E., and W. B. Fowler, 1978, "Electronic energy-band structure of α quartz," Phys. Rev. B **18**, 2888–2896.

Calinon, R., Ph. Choquard, E. Jamin, and M. Navet, 1980, "On the equation of state of the 2-D Wigner model," in *Ordering in Two Dimensions,* edited by S. K. Sinha (Elsevier–North-Holland, New York), pp. 317–320.

Campo, A., and R. Kümmel, 1981, "Valley splitting in (001), (011) and (111) Si MOSFETs," Solid State Commun. **37**, 433–435.

Campo, A., R. Kümmel, and H. Rauh, 1978, "Spin-orbit interaction and many-body effects in surface states of silicon MOSFETs," Surf. Sci. **73**, 342–349.

Canali, C., G. Manni, R. Minder, and G. Ottaviani, 1975, "Electron and hole drift velocity measurements in silicon and their empirical relation to electric field and temperature," IEEE Trans. Electron Devices **ED-22**, 1045–1047.

Canel, E., 1978, "On the two-dimensional Wigner lattice in a magnetic field," Surf. Sci. **73**, 350–356.

Canel, E., M. P. Matthews, and R. K. P. Zia, 1972, "Screening in very thin films," Phys. Kondens. Materie **15**, 191–200.

Caplan, P. J., E. H. Poindexter, B. E. Deal, and R. R. Razouk, 1980, "EPR defects and interface states on oxidized (111) and (100) silicon," in *The Physics of MOS Insulators,* edited by G. Lucovsky, S. T. Pantelides, and F. L. Galeener (Pergamon, New York), pp. 306–310.

Cardona, M., and F. H. Pollak, 1966, "Energy-band structure of germanium and silicon: The $\mathbf{k}\cdot\mathbf{p}$ method," Phys. Rev. **142**, 530–543.

Care, C. M., and N. H. March, 1975, "Electron crystalliza-

tion," Adv. Phys. **24**, 101–116.
Carr, W. J., Jr., 1961, "Energy, specific heat, and magnetic properties of the low-density electron gas," Phys. Rev. **122**, 1437–1446.
Caruthers, E., and P. J. Lin-Chung, 1978, "Pseudopotential calculations for ultrathin layer heterostructures," J. Vac. Sci. Technol. **15**, 1459–1464.
Casey, H. C., Jr., and M. B. Panish, 1978, *Heterostructure Lasers* (Academic, New York).
Castner, T. G., N. K. Lee, G. S. Cieloszyk, and G. L. Salinger, 1975, "Dielectric anomaly and the metal-insulator transition in *n*-type Si," Phys. Rev. Lett. **34**, 1627–1630.
Ceperley, D., 1978, "Ground state of the fermion one-component plasma: A Monte Carlo study in two and three dimensions," Phys. Rev. B **18**, 3126–3138.
Chakravarti, A. N., A. K. Chowdhury, K. P. Ghatak, and D. R. Choudhury, 1980, "On the modification of the Einstein relation for inversion layers on narrow gap semiconductors in a strong electric field," Phys. Status Solidi A **59**, K211–K215.
Chakravarty, S., and C. Dasgupta, 1980, "Absence of crystalline order in two dimensions," Phys. Rev. B **22**, 369–372.
Chalupa, J., 1975, "Equation of state of a classical electron layer," Phys. Rev. B **12**, 4–9.
Cham, K. M., and R. G. Wheeler, 1980a, "Electron-phonon interactions in *n*-type silicon inversion layers at low temperatures," Surf. Sci. **98**, 210 (abstract).
Cham, K. M., and R. G. Wheeler, 1980b, "Temperature-dependent resistivities in silicon inversion layers at low temperatures," Phys. Rev. Lett. **44**, 1472–1475.
Chan, M., M. Ryschkewitsch, and H. Meyer, 1977, "The dielectric constant in liquid and solid ^{4}He," J. Low Temp. Phys. **26**, 211–228.
Chang, C.-A., A. Segmüller, L. L. Chang, and L. Esaki, 1981, "Ge-GaAs superlattices by molecular beam epitaxy," Appl. Phys. Lett. **38**, 912–914.
Chang, H. R., and F. Koch, 1981, "Cyclotron resonance at Na^+-doped Si-SiO_2 interfaces," Solid State Commun. **38**, 1189–1192.
Chang, H. R., H. Reisinger, F. Schäffler, J. Scholz, K. Wiesinger, and F. Koch, 1980, "Developments in subband spectroscopy," in *Proceedings of the 15th International Conference on the Physics of Semiconductors, Kyoto* [J. Phys. Soc. Japan **49**, Suppl. A, 955–958].
Chang, L. L., 1978, "Sub-band dimensionality in semiconductor superlattices," Surf. Sci. **73**, 226–228.
Chang, L. L., 1980, "Semiconductor-semimetal transitions in InAs-GaSb superlattices," in *Proceedings of the 15th International Conference on the Physics of Semiconductors, Kyoto,"* [J. Phys. Soc. Japan **49**, Suppl. A, 997–1004].
Chang, L. L., and L. Esaki, 1980, "Electronic properties of InAs-GaSb superlattices," Surf. Sci. **98**, 70–89.
Chang, L. L., L. Esaki, W. E. Howard, R. Ludeke, and G. Schul, 1973, "Structures grown by molecular beam epitaxy," J. Vac. Sci. Technol. **10**, 655–662.
Chang, L. L., L. Esaki, A. Segmüller, and R. Tsu, 1974a, "Resonant electron tunneling in semiconductor barrier structures," in *Proceedings of the 12th International Conference on the Physics of Semiconductors, Stuttgart,* edited by M. H. Pilkuhn (Teubner, Stuttgart), pp. 688–692.
Chang, L. L., L. Esaki, and R. Tsu, 1974b, "Resonant tunneling in semiconductor double barriers," Appl. Phys. Lett. **24**, 593–595.
Chang, L. L., and W. E. Howard, 1965, "Surface inversion and accumulation of anodized InSb," Appl. Phys. Lett. **7**, 210–212.
Chang, L. L., N. Kawai, G. A. Sai-Halasz, R. Ludeke, and L. Esaki, 1979, "Observation of semiconductor-semimetal transitions in InAs-GaSb superlattices," Appl. Phys. Lett. **35**, 939–942.
Chang, L. L., N. J. Kawai, E. E. Mendez, C.-A. Chang, and L. Esaki, 1981, "Semimetallic InAs-GaSb superlattices to the heterojunction limit," Appl. Phys. Lett. **38**, 30–32.
Chang, L. L., and R. Ludeke, 1975, "Molecular-beam epitaxy," in *Epitaxial Growth, Part A,* edited by J. W. Matthews (Academic, New York), pp. 37–72.
Chang, L. L., G. A. Sai-Halasz, L. Esaki, and R. L. Aggarwal, 1981, "Spatial separation of carriers in InAs-GaSb superlattices," J. Vac. Sci. Technol. **19**, 589–591.
Chang, L. L., H. Sakaki, C. A. Chang, and L. Esaki, 1977, "Shubnikov–de Haas oscillations in a semiconductor superlattice," Phys. Rev. Lett. **38**, 1489–1493.
Chaplik, A. V., 1970, "Impurity scattering of electrons in thin films," Zh. Eksp. Teor. Fiz. **59**, 2110–2115 [Sov. Phys.—JETP **32**, 1143–1145 (1971)].
Chaplik, A. V., 1971a, "Energy spectrum and electron scattering processes in inversion layers," Zh. Eksp. Teor. Fiz. **60**, 1845–1852 [Sov. Phys.—JETP **33**, 997–1000 (1971)].
Chaplik, A. V., 1971b, "Some features of the temperature dependence of the conductivity of thin films," Fiz. Tekh. Poluprovodn. **5**, 1900–1903 [Sov. Phys.—Semicond. **5**, 1651–1653 (1972)].
Chaplik, A. V., 1972a, "Possible crystallization of charge carriers in low-density inversion layers," Zh. Eksp. Teor. Fiz. **62**, 746–753 [Sov. Phys.—JETP **35**, 395–398 (1972)].
Chaplik, A. V., 1972b, "Magnetic surface levels in semiconductors," Fiz. Tekh. Poluprovodn. **6**, 1760–1764 [Sov. Phys.—Semicond. **6**, 1516–1519 (1973)].
Chaplik, A. V., 1977a, "Phase diagram of a two-dimensional Wigner crystal in a magnetic field," Zh. Eksp. Teor. Fiz. **72**, 1946–1952 [Sov. Phys.—JETP **45**, 1023–1026 (1977)].
Chaplik, A. V., 1977b, "Phase diagram of the two-dimensional (TD) electron crystal in a magnetic field," in *Proceedings of the Seventh International Vacuum Congress and the Third International Conference on Solid Surfaces, Vienna,* edited by R. Dobrozemsky, F. Rüdenauer, F. P. Viehböck, and A. Breth (Berger, Horn, Austria), Vol. I, pp. 399–401.
Chaplik, A. V., 1978, "Two-dimensional plasmons on the surface of piezocrystal," Solid State Commun. **27**, 1297–1300.
Chaplik, A. V., 1980, "Amplification of two-dimensional plasma waves in superlattices," Zh. Eksp. Teor. Fiz. Pis'ma Red. **32**, 529–532 [JETP Lett. **32**, 509–512].
Chaplik, A. V., and M. V. Éntin, 1968, "Energy spectrum and electron mobility in a thin film with non-ideal boundary," Zh. Eksp. Teor. Fiz. **55**, 990–998 [Sov. Phys.—JETP **28**, 514–517 (1969)].
Chaplik, A. V., and M. V. Éntin, 1970, "Absorption of light by free carriers in a thin film with non-ideal surface," Zh. Eksp. Teor. Fiz. **59**, 857–864 [Sov. Phys.—JETP **32**, 468–471 (1971)].
Chaplik, A. V., and M. V. Éntin, 1971, "Charged impurities in very thin layers," Zh. Eksp. Teor. Fiz. **61**, 2496–2503 [Sov. Phys.—JETP **34**, 1335–1339 (1972)].
Chaplik, A. V., and M. V. Krasheninnikov, 1980, "Two-dimensional plasmons (2DP) and acoustic waves in crystals," Surf. Sci. **98**, 533–552.
Chaplik, A. V., and L. D. Shvartsman, 1979, "Magnetic surface levels in Schottky barriers," Fiz. Tekh. Poluprovodn. **13**, 169–170 [Sov. Phys.—Semicond. **13**, 96–97 (1979)].

Chaudhari, P., A. N. Broers, C. C. Chi, R. Laibowitz, E. Spiller, and J. Viggiano, 1980, "Phase-slip and localization diffusion lengths in amorphous W-Re alloys," Phys. Rev. Lett. **45**, 930–932.

Chaudhari, P., and H.-U. Habermeier, 1980a, "Quantum localization in amorphous W-Re alloys," Phys. Rev. Lett. **44**, 40–43.

Chaudhari, P., and H.-U. Habermeier, 1980b, "One-dimensional quantum localization in amorphous W-Re films," Solid State Commun. **34**, 687–689.

Chen, J. T. C., and R. S. Muller, 1974, "Carrier mobilities at weakly inverted Si surfaces," J. Appl. Phys. **45**, 828–834.

Chen, W. P., Y. J. Chen, and E. Burstein, 1976, "The interface EM modes of a 'surface quantized' plasma layer on a semiconductor surface," Surf. Sci. **58**, 263–265.

Cheng, A., and P. M. Platzman, 1978, "Shift in cyclotron resonance of electrons on liquid helium surfaces," Solid State Commun. **25**, 813–815.

Cheng, H. C., and F. Koch, 1981, "Magnetoconductance studies on InP surfaces," Solid State Commun. **37**, 911–913.

Cheng, Y. C., 1969, "On the temperature dependence of MOS threshold," Phys. Lett. A **29**, 444–445.

Cheng, Y. C., 1971, "On the scattering of electrons in magnetic and electric surface states by surface roughness," Surf. Sci. **27**, 663–666.

Cheng, Y. C., 1972, "Electron mobility in an MOS inversion layer," in *Proceedings of the 3rd Conference on Solid State Devices, Tokyo, 1971* [J. Japan Soc. Appl. Phys. **41**, Suppl., 173–180].

Cheng, Y. C., 1973a, "Effect of charge inhomogeneities on silicon surface mobility," J. Appl. Phys. **44**, 2425–2427.

Cheng, Y. C., 1973b, "A proposed experiment to measure surface roughness in Si/SiO_2 system," Surf. Sci. **40**, 433–438.

Cheng, Y. C., 1974, "The influence of surface on hole mobility in metal-oxide-silicon structure," in *Proceedings of the Second International Conference on Solid Surfaces, Kyoto* [Jpn. J. Appl. Phys. Suppl. 2, Pt. 2, 363–366].

Cheng, Y. C., 1977, "Electronic states at the silicon-silicon dioxide interface," Prog. Surf. Sci. **8**, 181–218.

Cheng, Y. C., and E. A. Sullivan, 1973a, "Scattering of charge carriers in Si surface layers," J. Appl. Phys. **44**, 923–925.

Cheng, Y. C., and E. A. Sullivan, 1973b, "Relative importance of phonon scattering to carrier mobility in Si surface layer at room temperature," J. Appl. Phys. **44**, 3619–3625.

Cheng, Y. C., and E. A. Sullivan, 1973c, "On the role of scattering by surface roughness in silicon inversion layers," Surf. Sci. **34**, 717–731.

Cheng, Y. C., and E. A. Sullivan, 1974, "Effect of Coulomb scattering on silicon surface mobility," J. Appl. Phys. **45**, 187–192.

Chernikova, D. M., 1976, "Charged helium surface in a capacitor," Fiz. Nizk. Temp. **2**, 1374–1378 [Sov. J. Low Temp. Phys. **2**, 669–671 (1976)].

Cheung, N. W., L. C. Feldman, P. J. Silverman, and I. Stensgaard, 1979, "Studies of the $Si-SiO_2$ interface by MeV ion channeling," Appl. Phys. Lett. **35**, 859–861.

Chin, R., N. Holonyak, Jr., B. A. Vojak, K. Hess, R. D. Dupuis, and P. D. Dapkus, 1980, "Temperature dependence of threshold current for quantum-well $Al_xGa_{1-x}As$-GaAs heterostructure laser diodes," Appl. Phys. Lett. **36**, 19–21.

Ching, L. Y., E. Burstein, S. Buchner, and H. H. Wieder, 1980, "Resonant Raman scattering at InAs surfaces in MOS junctions," in *Proceedings of the 15th International Conference on the Physics of Semiconductors, Kyoto* [J. Phys. Soc. Japan **49**, Suppl. A, 951–954].

Chiu, K. W., T. K. Lee, and J. J. Quinn, 1976, "Infrared magneto-transmittance of a two-dimensional electron gas," Surf. Sci. **58**, 182–184.

Chiu, K. W., and J. J. Quinn, 1974, "Plasma oscillations of a two-dimensional electron gas in a strong magnetic field," Phys. Rev. B **9**, 4724–4732.

Cho, A. Y., and J. R. Arthur, 1976, "Molecular beam epitaxy," in *Progress in Solid State Chemistry,* edited by J. O. McCaldin and G. Somorjai (Pergamon, Oxford), Vol. 10, pp. 157–191.

Choudhuri, D. Ray, and D. Chattopadhyay, 1979, "First order intervalley scattering in silicon inversion layers," Solid State Commun. **32**, 1053–1054.

Choudhury, D. R., P. K. Basu, and A. N. Chakravarti, 1976a, "Effect of the surface electric field on the specific heat of semiconductor inversion layers," Phys. Status Solidi A **36**, K65–K69.

Choudhury, D. R., P. K. Basu, and A. N. Chakravarti, 1976b, "On the modification of the Einstein relation for semiconductor inversion layers," Phys. Status Solidi A **38**, K85–K88.

Choudhury, D. R., A. K. Choudhury, and A. N. Chakravarti, 1980, "Effect of a quantizing magnetic field on the capacitance of MOS structures of small-gap semiconductors," Appl. Phys. **22**, 145–148.

Chroboczek, J., D. I. Aladashvili, and L. Sosnowski, 1974, "Magnetically controlled surface conduction in *p*-type InSb at liquid helium temperatures," in *Proceedings of the 12th International Conference on the Physics of Semiconductors, Stuttgart,* edited by M. H. Pilkuhn (Teubner, Stuttgart), pp. 698–702.

Churchill, J. N., and F. E. Holmstrom, 1981, "Comments on the existence of Bloch oscillations," Phys. Lett. A **85**, 453–456.

Clark, T. D., 1974, "Quantum size effect in the electrical conductivity of $Bi_8Te_7S_5$," J. Phys. Chem. Solids **35**, 9–13.

Coen, R. W., and R. S. Muller, 1980, "Velocity of surface carriers in inversion layers on silicon," Solid-State Electron. **23**, 35–40.

Cohen, M. L., 1964, "Superconductivity in many-valley semiconductors and in semimetals," Phys. Rev. **134**, A511–A521.

Coldwell-Horsfall, R. A., and A. A. Maradudin, 1960, "Zero-point energy of an electron lattice," J. Math. Phys. **1**, 395–404.

Cole, M. W., 1971, "Electronic surface states of a dielectric film on a metal substrate," Phys. Rev. B **3**, 4418–4422.

Cole, M. W., 1974, "Electronic surface states of liquid helium," Rev. Mod. Phys. **46**, 451–464.

Cole, T., J. P. Kotthaus, T. N. Theis, and P. J. Stiles, 1978, "High frequency conductivity of two-dimensional electrons in a superlattice," Surf. Sci. **73**, 238–239.

Cole, T., A. A. Lakhani, and P. J. Stiles, 1976, "Fine structure in the field effect mobility of MOS transistors," Surf. Sci. **58**, 56–59.

Cole, T., A. A. Lakhani, and P. J. Stiles, 1977, "Influence of a one-dimensional superlattice on a two-dimensional electron gas," Phys. Rev. Lett. **38**, 722–725.

Cole, T., A. A. Lakhani, and P. J. Stiles, 1981, "Effect of reverse substrate bias on the minigap in Si inversion layers," Solid State Commun. **39**, 127–132.

Cole, T., and B. D. McCombe, 1980, "Valley degeneracy and intersubband spectroscopy in (111) and (110) Si inversion layers," in *Proceedings of the 15th International Conference*

on the Physics of Semiconductors, Kyoto [J. Phys. Soc. Japan **49**, Suppl. A, 959–962].

Cole, T., B. D. McCombe, J. J. Quinn, and R. K. Kalia, 1981, "Evidence for a valley-occupancy transition in Si inversion layers at low electron densities," Phys. Rev. Lett. **46**, 1096–1099.

Cole, T., M. E. Sjöstrand, and P. J. Stiles, 1976, "Activated channel conductivity in silicon inversion layers at high temperatures," Surf. Sci. **58**, 91–97.

Coleman, J. J., P. D. Dapkus, W. D. Laidig, B. A. Vojak, and N. Holonyak, Jr., 1981a, "High-barrier cluster-free $Al_xGa_{1-x}As$-AlAs-GaAs quantum-well heterostructure laser," Appl. Phys. Lett. **38**, 63–65.

Coleman, J. J., P. D. Dapkus, and J. J. J. Yang, 1981b, "Single-interface enhanced mobility structures by metalorganic chemical vapour deposition," Electron. Lett. **17**, 606–608.

Colman, D., R. T. Bate, and J. P. Mize, 1968, "Mobility anisotropy and piezoresistance in silicon *p*-type inversion layers," J. Appl. Phys. **39**, 1923–1931.

Colvard, C., R. Merlin, M. V. Klein, and A. C. Gossard, 1980, "Observation of folded acoustic phonons in a semiconductor superlattice," Phys. Rev. Lett. **45**, 298–301.

Combescot, M., and C. Benoit à la Guillaume, 1981, "Two-dimensional electrons-holes droplets in superlattices," Solid State Commun. **39**, 651–654.

Combescot, M., and P. Nozières, 1972, "Condensation of excitons in germanium and silicon," J. Phys. C **5**, 2369–2392.

Conru, H. W., 1976, "Measuring small-area Si/SiO_2 interface stress with SEM," J. Appl. Phys. **47**, 2079–2081.

Conwell, E. M., 1967, *High Field Transport in Semiconductors* (Academic, New York).

Cooper, J. A., Jr., and D. F. Nelson, 1981, "Measurement of the high-field drift velocity of electrons in inversion layers on silicon," IEEE Electron Device Lett. **EDL-2**, 171–173.

Cottey, A. A. 1970, "Intraband transitions in the quantum size effect," J. Phys. C **3**, L167–L169.

Cottey, A. A., 1972, "Band theory of quantum size effect," J. Phys. C **5**, 2591–2598.

Cottey, A. A., 1973, "Quantum size effect with arbitrary surface potential," J. Phys. C **6**, 2446–2458.

Cottey, A. A., 1975, "Theory of infrared spectrum of size-quantized films," J. Phys. C **8**, 4135–4146.

Cottey, A. A., 1976, "Intraband dipole matrix elements of a sized-quantized film," J. Phys. C **9**, 2365–2373.

Cottey, A. A., 1978, "Band theory of size-quantized electron states in thin crystalline films," Phys. Status Solidi B **88**, 207–219.

Cottey, A. A., 1980, "Theory of tunneling into size-quantized films with application to lead," Phys. Status Solidi B **102**, 577–583.

Crandall, R. S., 1973, "Collective modes of a two-dimensional Wigner crystal," Phys. Rev. A **8**, 2136–2142.

Crandall, R. S., 1974a, "Lifetime of surface state electrons on liquid ^{4}He. I. Free electron," Phys. Rev. A **9**, 1297–1304.

Crandall, R. S., 1974b, "Lifetime of surface state electrons on liquid ^{4}He. II. Electron lattice," Phys. Rev. A **10**, 1370–1379.

Crandall, R. S., 1975, "Hot electrons on liquid helium," Phys. Rev. B **12**, 119–124.

Crandall, R. S., 1976, "Properties of surface state electrons on liquid helium," Surf. Sci. **58**, 266–282.

Crandall, R. S., and R. Williams, 1971, "Crystallization of electrons on the surface of liquid helium," Phys. Lett. A **34**, 404–405.

Dahl, D. A., and L. J. Sham, 1977, "Electrodynamics of quasi-two-dimensional electrons," Phys. Rev. B **16**, 651–661.

Dandekar, N. V., A. Madhukar, and D. N. Lowy, 1980, "Study of the electronic structure of model (110) surfaces and interfaces of semi-infinite III-V compound semiconductors: The GaSb-InAs system," Phys. Rev. B **21**, 5687–5705.

Därr, A., A. Huber, and J. P. Kotthaus, 1978, "Magnetoconductivity and cyclotron resonance in inversion layers on *p*-InSb," in *Physics of Narrow Gap Semiconductors,* edited by J. Rauluszkiewicz, M. Górska, and E. Kaczmarek (PWN–Polish Scientific, Warsaw), pp. 417–422.

Därr, A., and J. P. Kotthaus, 1978, "Magnetotransport in an inversion layer on *p*-InSb," Surf. Sci. **73**, 549–552.

Därr, A., J. P. Kotthaus, and T. Ando, 1976, "Electron spin resonance in an inversion layer on InSb," in *Proceedings of the 13th International Conference on the Physics of Semiconductors, Rome,* edited by F. G. Fumi (North-Holland, Amsterdam), pp. 774–777.

Därr, A., J. P. Kotthaus, and J. F. Koch, 1975, "Surface cyclotron resonance in InSb," Solid State Commun. **17**, 455–458.

Das, M. B., 1969, "Physical limitations of MOS structures," Solid-State Electron. **12**, 305–336.

Das, M. B., and J. M. Moore, 1974, "Measurements and interpretation of low-frequency noise in FET's," IEEE Trans. Electron Devices **ED-21**, 247–257.

Das, P., D. K. Ferry, and A. H. Barr, 1978, "The transient response of quasi-two-dimensional semiconductors under hot electron conditions," Surf. Sci. **73**, 147–155.

Dasgupta, B. B., 1980, "Effects of a perpendicular electric field on a quasi-two-dimensional system: Hydrogenic model," J. Phys. Chem. Solids **41**, 89–93.

Dasgupta, B. B., and R. S. Sorbello, 1980, "Electromigration in a quasi-two-dimensional electron gas: Theory of driving force," Phys. Rev. B **21**, 4196–4201.

Dash, J. G., 1975, *Films on Solid Surfaces* (Academic, New York).

Das Sarma, S., 1980, "Self-consistent theory of screening in a two-dimensional electron gas under strong magnetic field," Solid State Commun. **36**, 357–360.

Das Sarma, S., 1981, "Two-dimensional level broadening in the extreme quantum limit," Phys. Rev. B **23**, 4592–4596.

Das Sarma, S., R. K. Kalia, M. Nakayama, and J. J. Quinn, 1979, "Stress and temperature dependence of subband structure in silicon inversion layers," Phys. Rev. B **19**, 6397–6406.

Das Sarma, S., and A. Madhukar, 1980a, "Formation of an anomalous acoustic plasmon in spatially separated plasmas," Surf. Sci. **98**, 563–570.

Das Sarma, S., and A. Madhukar, 1980b, "Study of electron-phonon interaction and magneto-optical anomalies in two-dimensionally confined systems," Phys. Rev. B **22**, 2823–2836.

Das Sarma, S., and A. Madhukar, 1981a, "Collective modes of spatially separated, two-component, two-dimensional plasma in solids," Phys. Rev. B **23**, 805–815.

Das Sarma, S., and A. Madhukar, 1981b, "Ideal vacancy induced band gap levels in lattice matched thin superlattices: The GaAs-AlAs(100) and GaSb-InAs(100) systems," J. Vac. Sci. Technol. **19**, 447–452.

Das Sarma, S., and B. Vinter, 1981a, "Temperature-dependent many-body effects on the electronic properties of space-charge layers," Phys. Rev. B **23**, 6832–6835.

Das Sarma, S., and B. Vinter, 1981b, "Effect of impurity

scattering on the distribution function in two-dimensional Fermi systems," Phys. Rev. B **24**, 549–553.

Davies, R. A., M. J. Uren, and M. Pepper, 1981, "Magnetic separation of localisation and interaction effects in a two-dimensional electron gas at low temperatures," J. Phys. C **14**, L531–L537.

Declerck, G., R. Van Overstraeten, and G. Broux, 1974, "Discussion of the surface-potential fluctuations caused by oxide charge fluctuations," J. Appl. Phys. **45**, 2593–2595.

de Jongh, L. J., and A. R. Miedema, 1974, "Experiments on simple magnetic model systems," Adv. Phys. **23**, 1–260.

Delagebeaudeuf, D., P. Delescluse, P. Etienne, M. Laviron, J. Chaplart, and N. T. Linh, 1980, "Two-dimensional electron gas M.E.S.F.E.T. structure," Electron. Lett. **16**, 667–668.

Delescluse, P., M. Laviron, J. Chaplart, D. Delagebeaudeuf, and N. T. Linh, 1981, "Transport properties in GaAs-$Al_xGa_{1-x}As$ heterostructures and MESFET application," Electron. Lett. **17**, 342–344.

Demikhovskii, V. Ya., and B. A. Tavger, 1964, "Electron scattering by acoustic vibrations in thin semiconductor films," Fiz. Tverd. Tela (Leningrad) **6**, 960–962 [Sov. Phys.—Solid State **6**, 743–744 (1964)].

Deutscher, G., B. Bandyopadhyay, T. Chui, P. Lindenfeld, W. L. McLean, and T. Worthington, 1980, "Transition to localization in granular aluminum films," Phys. Rev. Lett. **44**, 1150–1153.

Deville, G., F. Gallet, D. Marty. J. Poitrenaud, A. Valdes, and F. I. B. Williams, 1980, "Detection of ordering of electrons on liquid helium," in *Ordering in Two Dimensions,* edited by S. K. Sinha (Elsevier–North-Holland, New York), pp. 309–312.

de Wette, F. W., 1964, "Note on the electron lattice," Phys. Rev. **135**, A287–A294.

Dexter, R. N., H. J. Zeiger, and B. Lax, 1956, "Cyclotron resonance experiments in silicon and germanium," Phys. Rev. **104**, 637–644.

DiMaria, D. J., 1977, "Room-temperature conductivity and location of mobile sodium ions in the thermal silicon dioxide layer of a metal-silicon dioxide-silicon structure," J. Appl. Phys. **48**, 5149–5151.

DiMaria, D. J., 1978, "The properties of electron and hole traps in thermal silicon dioxide layers grown on silicon," in *The Physics of SiO_2 and its Interfaces,* edited by S. T. Pantelides (Pergamon, New York), pp. 160–178.

DiMaria, D. J., 1981, "Capture and release of electrons on Na^+-related trapping sites in the SiO_2 layer of metal-oxide-semiconductor structures at temperature between 77°K and 296°K," J. Appl. Phys. **52**, 7251–7260.

DiMaria, D. J., J. M. Aitken, and D. R. Young, 1976, "Capture of electrons into Na^+-related trapping sites in the SiO_2 layer of MOS structures at 77°K," J. Appl. Phys. **47**, 2740–2743.

Dingle, R., 1975a, "Optical and electronic properties of thin $Al_xGa_{1-x}As$/GaAs heterostructures," Crit. Rev. Solid State Sci. **5**, 585–590.

Dingle, R., 1975b, "Confined carrier quantum states in ultrathin semiconductor heterostructures," in *Festkörperprobleme (Advances in Solid State Physics),* edited by H. J. Queisser (Pergamon-Vieweg, Braunschweig), Vol. XV, pp. 21–48.

Dingle, R., 1978, "Magnetic field induced carrier dimensionality change in a semiconductor superlattice," Surf. Sci. **73**, 229–231.

Dingle, R., A. C. Gossard, and W. Wiegmann, 1975, "Direct observation of superlattice formation in a semiconductor heterostructure," Phys. Rev. Lett. **34**, 1327–1330.

Dingle, R., H. L. Störmer, A. C. Gossard, and W. Wiegmann, 1978, "Electron mobilities in modulation-doped semiconductor heterojunction superlattices," Appl. Phys. Lett. **33**, 665–667.

Dingle, R., H. L. Störmer, A. C. Gossard, and W. Wiegmann, 1980, "Electronic properties of the GaAs-AlGaAs interface with applications to multi-interface heterojunction superlattices," Surf. Sci. **98**, 90–100.

Dingle, R., W. Wiegmann, and C. H. Henry, 1974, "Quantum states of confined carriers in very thin $Al_xGa_{1-x}As$-GaAs-$Al_xGa_{1-x}As$ heterostructures," Phys. Rev. Lett. **33**, 827–830.

DiSalvo, F. J., 1976, "Charge density waves in layered compounds," Surf. Sci. **58**, 297–311.

DiStefano, T. H., 1971, "Barrier inhomogeneities on a Si-SiO_2 interface by scanning internal photoemission," Appl. Phys. Lett. **19**, 280–282.

DiStefano, T. H., 1976, "Field dependent internal photoemission probe of the electronic structure of the Si-SiO_2 interface," J. Vac. Sci. Technol. **13**, 856–859.

DeStefano, T. H., and J. E. Lewis, 1974, "The influence of sodium on the Si-SiO_2 interface," J. Vac. Sci. Technol. **11**, 1020–1027.

Djurik, Z., Ž. Spasojević, and D. Tjapkin, 1976, "Electron ground state in the semiconductor inversion layer and low frequency MIS capacitance," Solid-State Electron. **19**, 931–934.

Dobrovol'skii, V. N., and Yu. S. Zharkikh, 1970, "Scattering of holes of a two-dimensional gas near cleaved germanium surface," Phys. Status Solidi **42**, K33–K35.

Dobrovol'skii, V. N., and Yu. S. Zharkikh, 1971, "Scattering of holes of a two-dimensional gas near germanium surfaces cleaved in liquid nitrogen," Phys. Status Solidi A **6**, 655–663.

Dobrovol'skii, V. N., Yu. S. Zharkikh, and L. N. Abessonova, 1971, "Scattering of carriers in inversion channels in metal-oxide-silicon structures," Fiz. Tekh. Poluprovodn. **5**, 723–729 [Sov. Phys.—Semicond. **5**, 633–638 (1971)].

Doezema, R. E., and J. F. Koch, 1972, "Magnetic surface levels in Cu—Observation and analysis of microwave resonances and determination of Fermi velocities," Phys. Rev. B **5**, 3866–3882.

Doezema, R. E., M. Nealon, and S. Whitmore, 1980, "Hybrid quantum oscillations in a surface space-charge layer," Phys. Rev. Lett. **45**, 1593–1596.

Döhler, G. H., 1972a, "Electron states in crystals with '*nipi*-superstructure'," Phys. Status Solidi B **52**, 79–92.

Döhler, G. H., 1972b, "Electrical and optical properties of crystals with '*nipi*-superstructure'," Phys. Status Solidi B **52**, 533–545.

Döhler, G. H., 1976a, "Influence of intervalley transitions on the photoconductivity in *n*-type Si ⟨100⟩ inversion layers," Solid State Commun. **18**, 633–636.

Döhler, G. H., 1976b, "Intervalley transitions in inversion layers," J. Vac. Sci. Technol. **13**, 903–907.

Döhler, G. H., 1978, "Ultrathin doping layers as a model for 2D systems," Surf. Sci. **73**, 97–105.

Döhler, G. H., 1979, "Doping superlattices," J. Vac. Sci. Technol. **16**, 851–856.

Döhler, G. H., 1980, "Electron-hole subbands at the GaSb-InAs interface," Surf. Sci. **98**, 108–116.

Döhler, G. H., 1981, "Semiconductor superlattices—A new material for research and applications," Physica Scripta **24**,

430—439.
Döhler, G. H., H. Künzel, D. Olego, K. Ploog, P. Ruden, H. J. Stolz, and G. Abstreiter, 1981, "Observation of tunable band gap and two-dimensional subbands in a novel GaAs superlattice," Phys. Rev. Lett. **47**, 864—867.
Döhler, G. H., R. Tsu, and L. Esaki, 1975, "A new mechanism for negative differential conductivity in superlattices," Solid State Commun. **17**, 317—320.
Dolan, G. J., and D. D. Osheroff, 1979, "Nonmetallic conduction in thin metal films at low temperatures," Phys. Rev. Lett. **43**, 721—724; **43**, 1690(E).
Doman, B. G. S., 1979, "The two-dimensional Wigner crystal in a magnetic field," J. Phys. C **12**, 3757—3760.
Domany, E., and S. Sarker, 1979, "Renormalization-group study of Anderson localization," Phys. Rev. B **20**, 4726—4729.
Don, K. Z., I. G. Neizvestnyi, V. N. Ovsyuk, and Yu. A. Rzhanov, 1979, "The anomalous Hall factor in electron inversion channels in germanium," Zh. Eksp. Teor. Fiz. Pis'ma Red. **30**, 189—192 [JETP Lett. **30**, 174—176 (1979)].
Doniach, S., and B. A. Huberman, 1979, "Topological excitations in two-dimensional superconductors," Phys. Rev. Lett. **42**, 1169—1172.
Dorda, G., 1970, "Effective mass change of electrons in silicon inversion layers observed by piezoresistance," Appl. Phys. Lett. **17**, 406—408.
Dorda, G., 1971a, "Piezoresistance in quantized conduction bands in silicon inversion layers," J. Appl. Phys. **42**, 2053—2060.
Dorda, G., 1971b, "The band splitting in silicon inversion layers," in *Proceedings of the International Conference on the Physics and Chemistry of Semiconductor Heterojunctions and Layer Structures,* edited by G. Szigeti, Z. Bodó, G. Gergely, G. Pataki, J. Pócza, J. Schanda, I. Szép, and Mrs. A. Valkó (Akadémiai Kiadó, Budapest), Vol. V, pp. 83—90.
Dorda, G., 1973, "Surface quantization in semiconductors," in *Festkörperprobleme (Advances in Solid State Physics),* edited by H. J. Queisser (Pergamon-Vieweg, Braunschweig), Vol. XIII, pp. 215—239.
Dorda, G., 1974, "Transport properties of semiconductor surface layers," Electrón. Fisc. Apli. **17**, 203—208.
Dorda, G., and I. Eisele, 1973, "Piezoresistance in *n*-type silicon inversion layers at low temperatures," Phys. Status Solidi A **20**, 263—273.
Dorda, G., and I. Eisele, 1974, "Negative and positive magnetoresistance related to surface states in silicon inversion layers," in *Proceedings of the 12th International Conference on the Physics of Semiconductors, Stuttgart,* edited by M. H. Pilkuhn (Teubner, Stuttgart), pp. 704—708.
Dorda, G., I. Eisele, and H. Gesch, 1978, "Many-valley interactions in silicon inversion layers," Phys. Rev. B **17**, 1785—1798.
Dorda, G., I. Eisele, and E. Preuss, 1972a, "Energy level differences in surface quantization measured by piezoresistance effect," Solid State Commun. **11**, 1625—1628.
Dorda, G., I. Eisele, and E. Preuss, 1972b, "Surface quantization observed by piezoresistance and Hall effect measurements in *p*-type silicon inversion layers," in *Proceedings of the 11th International Conference on the Physics of Semiconductors, Warsaw* (PWN—Polish Scientific, Warsaw), Vol. 2, pp. 1468—1473.
Dorda, G., I. Eisele, E. Soutschek, E. Vass, and K. Hess, 1977, "Electron transport at the Si-SiO_2 interface," in *Proceedings of the Seventh International Vacuum Congress and the Third International Conference on Solid Surfaces, Vienna,* edited by R. Dobrozemsky, F. Rüdenauer, F. P. Viehböck, and A. Breth (Berger, Horn, Austria), Vol. I, pp. 563—565.
Dorda, G., H. Friedrich, and E. Preuss, 1972, "Band structure investigation on *p*-type silicon inversion layers by piezoresistance and mobility measurements," J. Vac. Sci. Technol. **9**, 759—761.
Dorda, G., H. Gesch, and I. Eisele, 1976, "Valley degeneracy and mobility anisotropy under mechanical stress on (111) silicon inversion layers," Solid State Commun. **20**, 429—432.
Dorda, G., H. Gesch, and I. Eisele, 1980, "Anomalous behaviour of the electron transport on (110) and (111) silicon surfaces," Surf. Sci. **98**, 407—412.
Dresselhaus, G., A. F. Kip, and C. Kittel, 1955, "Cyclotron resonance of electrons and holes in silicon and germanium crystals," Phys. Rev. **98**, 368—384.
Dresselhaus, M. S., and G. Dresselhaus, 1981, "Intercalation compounds of graphite," Adv. Phys. **30**, 139—326.
Drew, H. D., 1978, "Charge-density wave induced cyclotron resonance harmonics on Si(111) inversion layers," Surf. Sci. **73**, 498—499.
Drummond, T. J., M. Keever, W. Kopp, H. Morkoç, K. Hess, B. G. Streetman, and A. Y. Cho, 1981a, "Field dependence of mobility in $Al_{0.2}Ga_{0.8}As$/GaAs heterojunctions at very low fields," Electron. Lett. **17**, 545—547.
Drummond, T. J., W. Kopp, and H. Morkoc, 1981b, "Three period (Al,Ga)As/GaAs heterostructures with extremely high mobilities," Electron. Lett. **17**, 442—444.
Drummond, T. J., W. Kopp, H. Morkoç, K. Hess, A. Y. Cho, and B. G. Streetman, 1981c, "Effect of background doping on the electron mobility of (Al,Ga)As/GaAs heterostructures," J. Appl. Phys. **52**, 5689—5690.
Drummond, T. J., H. Morkoç, and A. Y. Cho, 1981d, "Dependence of electron mobility on spatial separation of electrons and donors in $Al_xGa_{1-x}As$/GaAs heterostructures," J. Appl. Phys. **52**, 1380—1386.
Drummond, T. J., H. Morkoç, K. Hess, and A. Y. Cho, 1981e, "Experimental and theoretical electron mobility of modulation doped $Al_xGa_{1-x}As$/GaAs heterostructures grown by molecular beam epitaxy," J. Appl. Phys. **52**, 5231—5234.
Duke, C. B., 1967a, "Optical absorption due to space-charge-induced localized states," Phys. Rev. **159**, 632—644; **164**, 1214(E) (1967); **177**, 1394(E) (1969).
Duke, C. B., 1967b, "Continuously-variable infrared line absorption due to narrow space-charge channels," Phys. Lett. A **24**, 461—463.
Duke, C. B., 1968, "Quantum theory of transport in narrow channels," Phys. Rev. **168**, 816—831.
Duke, C. B., and C. E. Swenberg, 1968, "Quantum effects in narrow channels at semiconductor surfaces," in *Proceedings of the Ninth International Conference on the Physics of Semiconductors, Moscow* (Nauka, Leningrad), Vol. 2, pp. 745—749.
Dupuis, R. D., and P. D. Dapkus, 1979, "Preparation and properties of $Ga_{1-x}Al_xAs$-GaAs heterostructure lasers grown by metalorganic chemical vapor deposition," IEEE J. Quant. Electron. **QE-15**, 128—135.
D'yakonova, M. I., and A. V. Khaetskii, 1981, "Surface states in a gapless semiconductor," Zh. Eksp. Teor. Fiz. Pis'ma Red. **33**, 115—118 [JETP Lett. **33**, 110—113 (1981)].
Dykman, M. I., 1976, "Theory of nondegenerate two-dimensional electrons interacting with phonons in quantizing magnetic fields," Phys. Status Solidi B **74**, 547—559.
Dykman, M. I., 1978, "Theory of cyclotron resonance of two-dimensional electrons interacting with surface and volume

phonons," Phys. Status Solidi B **88**, 463–475.
Dykman, M. I., 1980a, "Toward the theory of cyclotron resonance of two-dimensional electrons on a liquid helium surface," Fiz. Nizk. Temp. **6**, 560–566 [Sov. J. Low Temp. Phys. **6**, 268–271 (1980)].
Dykman, M. I., 1980b, "Cyclotron resonance of two-dimensional electrons forming Wigner crystal," Solid State Commun. **35**, 753–757.
Dynes, R. C., J. P. Garno, and J. M. Rowell, 1978, "Two-dimensional electrical conductivity in quench-condensed metal films," Phys. Rev. Lett. **40**, 479–482.
Eagles, D. M., 1967, "Predicted transition temperature of very thin films and whiskers of superconducting semiconductors—Application to $SrTiO_3$," Phys. Rev. **164**, 489–497.
Eagles, D. M., 1969, "Possible pairing without superconductivity at low carrier concentrations in bulk and thin-film superconducting semiconductors," Phys. Rev. **186**, 456–463.
Eagles, D. M., 1971, "Tunneling results on In-$SrTiO_3$ barriers interpreted as confirmation of the theory of transitions from large to nearly small polarons," Phys. Status Solidi B **48**, 407–417.
Eaves, L., R. A. Hoult, R. A. Stradling, R. J. Tidey, J. C. Portal, and S. Askenazy, 1975, "Fourier analysis of magnetophonon and two-dimensional Shubnikov–de Haas magnetoresistance structure," J. Phys. C **8**, 1034–1053.
Ebner, W., and P. Leiderer, 1980, "Development of the dimple instability on liquid ^{4}He," Phys. Lett. A **80**, 277–280.
Echenique, P. M., and J. B. Pendry, 1976a, "Scattering of ^{4}He atoms from the surface of liquid ^{4}He at 30 mK," J. Phys. C **9**, 3183–3191.
Echenique, P. M., and J. B. Pendry, 1976b, "Reflectivity of liquid ^{4}He surfaces to ^{4}He atoms," Phys. Rev. Lett. **37**, 561–563.
Édel'man, V. S., 1976, "Effective mass of electrons localized over the surface of liquid helium," Zh. Eksp. Teor. Fiz. Pis'ma Red. **24**, 510–513 [JETP Lett. **24**, 468–471 (1976)].
Édel'man, V. S., 1977a, "Nonlinear cyclotron resonance of electrons localized over the surface of liquid helium," Zh. Eksp. Teor. Fiz. Pis'ma Red. **25**, 422–425 [JETP Lett. **25**, 394–397 (1977)].
Édel'man, V. S., 1977b, "Observation of electrons localized over the surface of liquid ^{3}He," Zh. Eksp. Teor. Fiz. Pis'ma Red. **26**, 647–650 [JETP Lett. **26**, 493–495 (1977)].
Édel'man, V. S., 1979, "Investigation of the resonance properties of electrons localized above liquid ^{3}He and ^{4}He," Zh. Eksp. Teor. Fiz. **77**, 673–691 [Sov. Phys.—JETP **50**, 338–348 (1979)].
Édel'man, V. S., 1980, "Levitated electrons," Usp. Fiz. Nauk. **130**, 675–706 [Sov. Phys.—Usp. **23**, 227–244 (1980)].
Edel'shtein, V. M., 1980, "Conductivity of a two-dimensional electron gas," Zh. Eksp. Teor. Fiz. Pis'ma Red. **31**, 60–62 [JETP Lett. **31**, 55–58 (1980)].
Edwards, D. O., and P. P. Fatouros, 1978, "Theory of atomic scattering at the free surface of liquid ^{4}He," Phys. Rev. B **17**, 2147–2159.
Edwards, D. O., and W. F. Saam, 1978, "The free surface of liquid helium," in *Progress in Low Temperature Physics,* edited by D. F. Brewer (North-Holland, Amsterdam), Vol. VIIA, pp. 283–369.
Edwards, J. T., and D. J. Thouless, 1972, "Numerical studies of localization in disordered systems," J. Phys. C **5**, 807–820.
Edwards, S. F., M. B. Green, and G. Srinivasan, 1977, "The density [of] states of electrons in a disordered material," Philos. Mag. **35**, 1421–1424.
Eger, D., and Y. Goldstein, 1979, "Quantization effects in ZnO accumulation layers in contact with an electrolyte," Phys. Rev. B **19**, 1089–1097.
Eger, D., A. Many, and Y. Goldstein, 1975, "Very strong accumulation layers on ZnO surfaces," Phys. Lett. A **55**, 197–198.
Eger, D., A. Many, and Y. Goldstein, 1976, "Quantum properties of strong accumulation layers on ZnO surfaces," Surf. Sci. **58** 18–24.
Eguiluz, A., T. K. Lee, J. J. Quinn, and K. W. Chiu, 1975, "Interface excitations in metal-insulator-semiconductor structures," Phys. Rev. B **11**, 4989–4993.
Eguiluz, A., and A. A. Maradudin, 1978a, "Electromagnetic modes of an inversion layer," Surf. Sci. **73**, 437–445.
Eguiluz, A., and A. A. Maradudin, 1978b, "Electromagnetic modes of an inversion layer on a semiconductor surface," Ann. Phys. (N.Y.) **113**, 29–78.
Eguiluz, A. G., A. A. Maradudin, and R. J. Elliott, 1981, "Vibration modes of a two-dimensional Wigner lattice coupled to ripplons on a liquid-helium surface," Phys. Rev. B **24**, 197–217.
Ehrenreich, H., and M. H. Cohen, 1959, "Self-consistent field approach to the many-electron problem," Phys. Rev. **115**, 786–790.
Eisele, I., 1978, "Stress and intersubband correlation in the silicon inversion layer," Surf. Sci. **73**, 315–337.
Eisele, I., and G. Dorda, 1974a, "Negative magnetoresistance in *n*-channel (100) silicon inversion layers," Phys. Rev. Lett. **32**, 1360–1363.
Eisele, I., and G. Dorda, 1974b, "Surface states in the conduction band region of Si," Solid State Commun. **15**, 1391–1394.
Eisele, I., H. Gesch, and G. Dorda, 1976a, "Mechanical stress influence on effective masses in Si inversion layers," Surf. Sci. **58**, 169–177.
Eisele, I., H. Gesch, and G. Dorda, 1976b, "Surface quantum oscillations in (100) inversion layers under uniaxial stress," Solid State Commun. **18**, 743–746.
Eisele, I., H. Gesch, and G. Dorda, 1976c, "Evidence for mobility domains in (100) silicon inversion layers," Solid State Commun. **20**, 677–680.
Eisele, I., H. Gesch, and G. Dorda, 1977, "Effective masses in (100) silicon inversion layers," Solid State Commun. **22**, 185–188.
Englert, Th., 1981, "Electron transport in silicon inversion layers at high magnetic fields," in *Physics in High Magnetic Fields,* edited by S. Chikazumi and M. Miura (Springer, Berlin), pp. 274–283.
Englert, Th., G. Abstreiter, and J. Pontcharra, 1980, "Determination of existing stress in silicon films on sapphire substrate using Raman spectroscopy," Solid-State Electron. **23**, 31–33.
Englert, Th., and G. Landwehr, 1976, "Magneto-transport properties of silicon inversion layers at low carrier densities," Surf. Sci. **58**, 217–226.
Englert, Th., G. Landwehr, J. Pontcharra, and G. Dorda, 1980, "Inversion layers in silicon on insulating substrates," Surf. Sci. **98**, 427–436.
Englert, Th., G. Landwehr, K. von Klitzing, G. Dorda, and H. Gesch, 1978, "Surface quantum oscillations in silicon (100) inversion layers under uniaxial pressure," Phys. Rev. B **18**, 794–802; Surf. Sci. **73**, 338–339.
Englert, Th., D. C. Tsui, and G. Landwehr, 1980, "Observa-

tion of valley splitting in (111) n-type silicon inversion layers," Solid State Commun. **33**, 1167—1169.

Englert, Th., D. C. Tsui, and R. A. Logan, 1981, "A plasma resonance study of valley transfer in (001) Si inversion layers," Solid State Commun. **39**, 483—486.

Englert, Th., and K. von Klitzing, 1978, "Analysis of ρ_{xx} minima in surface quantum oscillations on (100) n-type silicon inversion layers," Surf. Sci. **73**, 70—80.

Englert, Th., K. von Klitzing, R. J. Nicholas, G. Landwehr, G. Dorda, and M. Pepper, 1980, "On the electronic g-factor in n-type silicon inversion layers," Phys. Status Solidi B **99**, 237—242.

Engström, L., and K.-F. Berggren, 1980, "Quantisation of electron states in a two-dimensional GaAs impurity band at low carrier concentrations," J. Phys. C **13**, 6477—6481.

Éntin, M. V., 1969, "Surface mobility of electrons with quantizing band bending," Fiz. Tverd. Tela (Leningrad) **11**, 958—961 [Sov. Phys.—Solid State **11**, 781—783 (1969)].

Épshtein, É. M., 1979, "Plasma oscillations in a superlattice subjected to a strong electric field," Fiz. Tverd. Tela (Leningrad) **21**, 1719—1722 [Sov. Phys.—Solid State **21**, 986—987 (1979)].

Erukhimov, M. Sh., and B. A. Tavger, 1967, "Quantum longitudinal galvanomagnetic phenomena in thin semiconductor and semimetal films," Zh. Eksp. Teor. Fiz. **53**, 926—935 [Sov. Phys.—JETP **26**, 560—565 (1968)].

Esaki, L. and L. L. Chang, 1974, "New transport phenomenon in a semiconductor 'superlattice'," Phys. Rev. Lett. **33**, 495—498.

Esaki, L., and L. L. Chang, 1976, "Semiconductor superfine structures by computer-controlled molecular beam epitaxy," Thin Solid Films **36**, 285—298.

Esaki, L. and L. L. Chang, 1979, "Semiconductor superlattices in high magnetic fields," J. Magn. Magn. Mater. **11**, 208—215.

Esaki, L., L. L. Chang, W. E. Howard, and V. L. Rideout, 1972, "Transport properties of GaAs-GaAlAs superlattice," in *Proceedings of the 11th International Conference on the Physics of Semiconductors, Warsaw* (PWN—Polish Scientific, Warsaw), Vol. 1, pp. 431—437.

Esaki, L., L. L. Chang, and E. E. Mendez, 1981, "Polytype superlattices and multi-heterojunctions," Jpn. J. Appl. Phys. **20**, L529—L532.

Esaki, L., and R. Tsu, 1970, "Superlattice and negative differential conductivity in semiconductors," IBM J. Res. Dev. **14**, 61—65.

Esel'son, B. N., A. S. Rybalko, and Yu. Z. Kovdrya, 1979, "Investigation of the mobility and current-voltage characteristics of surface electrons in helium," Fiz. Nizk. Temp. **5**, 1354—1358 [Sov. J. Low Temp. Phys. **5**, 641—643 (1980)].

Esel'son, B. N., A. S. Rybalko, and S. S. Sokolov, 1980a, "Investigation of the surface electron mobility in liquid He^4 and weak solutions of He^3 in He^4," Fiz. Nizk. Temp. **6**, 1120—1129 [Sov. J. Low Temp. Phys. **6**, 544—548 (1980)].

Esel'son, B. N., A. S. Rybalko, and S. S. Sokolov, 1980b, "Investigation of the liquid crystal phase transition in a system of electrons localized on the surface of liquid helium," Fiz. Nizk. Temp. **6**, 1130—1136 [Sov. J. Low Temp. Phys. **6**, 549—551 (1980)].

Essam, J. W., 1980, "Percolation theory," Rep. Prog. Phys. **43**, 833—912.

Evans, E., and D. L. Mills, 1973, "Interaction of slow electrons with the surface of a model dielectric: Theory of surface polarons," Phys. Rev. B **8**, 4004—4018.

Ezawa, H., 1971, "Phonons in a half space," Ann. Phys. (N.Y.) **67**, 438—460.

Ezawa, H., 1976, "Inversion layer mobility with intersubband scattering," Surf. Sci. **58**, 25—32.

Ezawa, H., S. Kawaji, T. Kuroda, and K. Nakamura, 1971a, "Electron mobility in a semiconductor inversion layer: Possible contribution from bulk phonons," Surf. Sci. **24**, 659—662.

Ezawa, H., S. Kawaji, and K. Nakamura, 1971b, "Surfons and the electron mobility in a semiconductor inversion layer," Surf. Sci. **27**, 218—220.

Ezawa, H., S. Kawaji, and K. Nakamura, 1974, "Surfons and the electron mobility in silicon inversion layers," Jpn. J. Appl. Phys. **13**, 126—155; **14**, 921—922(E) (1975).

Ezawa, H., T. Kuroda, and K. Nakamura, 1971, "Electrons and 'surfons' in a semiconductor inversion layer," Surf. Sci. **24**, 654—658.

Falicov, L. M., and N. Garcia, 1975, "Hole cyclotron masses in silicon MOS devices," Solid State Commun. **17**, 473—476.

Falicov, L. M., 1976, "Non-parabolicity and transverse mass of electron carriers in silicon," Solid State Commun. **18**, 669—671.

Falicov, L. M., 1979, "Density waves in one, two and three dimensions," in *Physics of Semiconductors, 1978*, edited by B. L. H. Wilson (Institute of Physics, Bristol), pp. 53—62.

Fang, F. F., 1980, "Effect of biaxial stress on Si(100) inversion layers," Surf. Sci. **98**, 416—426.

Fang, F. F., and A. B. Fowler, 1968, "Transport properties of electrons in inverted silicon surface," Phys. Rev. **169**, 619—631.

Fang, F. F., and A. B. Fowler, 1970, "Hot electron effects and saturation velocities in silicon inversion layers," J. Appl. Phys. **41**, 1825—1831.

Fang, F. F., A. B. Fowler, and A. Hartstein, 1977, "Effective mass and collision time of (100) Si surface electrons," Phys. Rev. B **16**, 4446—4454.

Fang, F. F., A. B. Fowler, and A. Hartstein, 1978, "On the effective mass and collision time of (100) Si surface electrons," Surf. Sci. **73**, 269—271.

Fang, F. F., and W. E. Howard, 1966, "Negative field-effect mobility on (100) Si surfaces," Phys. Rev. Lett. **16**, 797—799.

Fang, F. F., and P. J. Stiles, 1968, "Effects of a tilted magnetic field on a two-dimensional electron gas," Phys. Rev. **174**, 823—828.

Fang, F. F., and S. Triebwasser, 1964a, "Carrier surface scattering in silicon inversion layers," Appl. Phys. Lett. **4**, 145—147.

Fang, F. F., and S. Triebwasser, 1964b, "Carrier surface scattering in silicon inversion layers," IBM J. Res. Dev. **8**, 410—415.

Feldman, L. C., P. J. Silverman, J. S. Williams, T. E. Jackman, and I. Stensgaard, 1978a, "Use of thin Si crystals in backscattering—Channeling studies of the Si-SiO_2 interface," Phys. Rev. Lett. **41**, 1396—1399.

Feldman, L. C., I. Stensgaard, P. J. Silverman, and T. E. Jackman, 1978b, "Studies of the Si-SiO_2 interface by MeV ion scattering," in *The Physics of SiO_2 and its Interfaces*, edited by S. T. Pantelides (Pergamon, New York), pp. 344—350.

Fell, B., J. T. Chen, J. Hardy, M. Prasad, and S. Fujita, 1978, "Theory of the mobility of electrons limited by charged impurities in two dimensions," J. Phys. Chem. Solids **39**, 221—224.

Ferrell, R. A., 1958, "Predicted radiation of plasma oscillations in metal films," Phys. Rev. **111**, 1214—1222.

Ferry, D. K., 1976a, "Optical and intervalley scattering in

quantized inversion layers in semiconductors," Surf. Sci. **57**, 218–228.
Ferry, D. K., 1976b, "First-order optical and intervalley scattering in semiconductors," Phys. Rev. B **14**, 1605–1609.
Ferry, D. K., 1976c, "Hot-electron effects in silicon quantized inversion layers," Phys. Rev. B **14**, 5364–5371.
Ferry, D. K., 1976d, "Electron transport in silicon inversion layers," in *Proceedings of the 13th International Conference on the Physics of Semiconductors, Rome,* edited by F. G. Fumi (North-Holland, Amsterdam), pp. 758–761.
Ferry, D. K., 1977a, "Energy relaxation to acoustic phonons in quasi-two-dimensional semiconductors," Solid State Commun. **22**, 127–128.
Ferry, D. K., 1977b, "Critical concentration of hot carriers in a quasi-two-dimensional semiconductor," Phys. Lett. A **60**, 243–244.
Ferry, D. K., 1978a, "Transport of hot carriers in semiconductor quantized inversion layers," Solid-State Electron. **21**, 115–121.
Ferry, D. K., 1978b, "Warm electrons in degenerate quasi-two-dimensional semiconductors," Surf. Sci. **73**, 136–146.
Ferry, D. K., 1978c, "Scattering by polar-optical phonons in a quasi-two-dimensional semiconductor," Surf. Sci. **75**, 86–91.
Ferry, D. K. 1979, "The transport of electrons in quantized inversion and accumulation layers in III-V compounds," Thin Solid Films **56**, 243–252.
Ferry, D. K., 1981, "Charge instabilities in lateral superlattices under conditions of population inversion," Phys. Status Solidi B **106**, 63–71.
Ferry, D. K., and P. Das, 1977, "Microwave hot electron effects in semiconductor quantized inversion layers," Solid-State Electron. **20**, 355–359.
Fetter, A. L., 1973, "Electrodynamics of a layered electron gas. I. Single layer," Ann. Phys. (N.Y.) **81**, 367–393.
Fetter, A. L., 1974a, "Electrodynamics of a layered electron gas. II. Periodic array," Ann. Phys. (N.Y.) **88**, 1–25.
Fetter, A. L., 1974b, "Electrodynamics and thermodynamics of a classical electron surface layer," Phys. Rev. B **10**, 3739–3745.
Fetter, A. L., and J. D. Walecka, 1971, *Quantum Theory of Many-Particle Systems* (McGraw-Hill, New York).
Filatov, O. N., and I. A. Karpovich, 1969a, "Dependence of the width of the forbidden band of indium antimonide films on the thickness," Fiz. Tverd. Tela (Leningrad) **11**, 805–806 [Sov. Phys.—Solid State **11**, 655–656 (1969)].
Filatov, O. N., and I. A. Karpovich, 1969b, "Structure of the absorption band edge of thin indium antimonide films," Fiz. Tverd. Tela (Leningrad) **11**, 1637–1640 [Sov. Phys.—Solid State **11**, 1328–1330 (1969)].
Fischer, B., and M. W. Klein, 1975, "Magnetic and nonmagnetic impurities in two-dimensional metals," Phys. Rev. B **11**, 2025–2029.
Fischer, G., and H. Hoffmann, 1980, "Oscillations of the electrical conductivity with film thickness in very thin platinum films," Solid State Commun. **35**, 793–796.
Fischer, W., E. P. Jacobs, I. Eisele, and G. Dorda, 1978, "Electron mobility in Si-MOSFETs with an additional implanted channel," Chem. Eng. Science **33**, 689–692; Solid-State Electron. **22**, 225–228 (1979).
Fisher, D. S., 1980a, "Flux-lattice melting in thin-film superconductors," Phys. Rev. B **22**, 1190–1199.
Fisher, D. S., 1980b, "Two dimensional Wigner crystallization and electrons on helium," in *Ordering in Two Dimensions,* edited by S. K. Sinha (North-Holland, New York), pp. 189–192.
Fisher, D. S., B. I. Halperin, and R. Morf, 1979a, "Defects in the two-dimensional electron solid and implications for melting," Phys. Rev. B **20**, 4692–4712.
Fisher, D. S., B. I. Halperin, and P. M. Platzman, 1979b, "Phonon-ripplon coupling and the two-dimensional electron solid on a liquid-helium surface," Phys. Rev. Lett. **42**, 798–801.
Fisher, D. S., and V. B. Shikin, 1980, "Spectrum of electron-ripplon system on the surface of liquid helium in the presence of a magnetic field normal to this surface," Zh. Eksp. Teor. Fiz. Pis'ma Red. **31**, 228–230 [JETP Lett. **31**, 208–210 (1980)].
Fleishman, L., and P. W. Anderson, 1980, "Interactions and the Anderson transition," Phys. Rev. B **21**, 2366–2377.
Fleishman, L., D. C. Licciardello, and P. W. Anderson, 1978, "Elementary excitations in the Fermi glass," Phys. Rev. Lett. **40**, 1340–1343.
Flinn, I., G. Bew, and F. Berz, 1967, "Low frequency noise in MOS field effect transistors," Solid-State Electron. **10**, 833–845.
Flügge, S., and H. Marschall, 1952, *Rechenmethoden der Quantentheorie,* 2nd ed. (Springer, Berlin), Problem 24.
Fomin, N. V., 1967, "Quantum theory of space charge capacitance," Fiz. Tverd. Tela (Leningrad) **9**, 616–623 [Sov. Phys.—Solid State **9**, 474–479 (1967)].
Fonash, S. J., 1973, "Effects of stress on metal-oxide-semiconductor structures," J. Appl. Phys. **44**, 4607–4615.
Fowler, A. B., 1975, "Substrate bias effects on electron mobility in silicon inversion layers at low temperatures," Phys. Rev. Lett. **34**, 15–17.
Fowler, A. B., 1982, "Transport in inversion layers," in *Band Theory and Transport Properties,* edited by William Paul (Vol. 1 of *Handbook on Semiconductors,* edited by T. S. Moss) (North-Holland, Amsterdam), pp. 599–616.
Fowler, A. B., F. F. Fang, and F. Hochberg, 1964, "Hall measurements on silicon field effect transistor structures," IBM J. Res. Dev. **8**, 427–429.
Fowler, A. B., F. F. Fang, W. E. Howard, and P. J. Stiles, 1966a, "Magneto-oscillatory conductance in silicon surfaces," Phys. Rev. Lett. **16**, 901–903.
Fowler, A. B., F. F. Fang, W. E. Howard, and P. J. Stiles, 1966b, "Oscillatory magneto-conductance in Si surfaces," in *Proceedings of the International Conference on the Physics of Semiconductors, Kyoto* [J. Phys. Soc. Japan **21**, Suppl., 331–335].
Fowler, A. B., and A. Hartstein, 1980a, "Techniques for determining threshold," Surf. Sci. **98**, 169–172.
Fowler, A. B., and A. Hartstein, 1980b, "Impurity bands in inversion layers," Philos. Mag. B **42**, 949–959.
Fowler, W. B., P. M. Schneider, and E. Calabrese, 1978, "Band structures and electronic properties of SiO_2," in *The Physics of SiO_2 and its Interfaces,* edited by S. T. Pantelides (Pergamon, New York), pp. 70–74.
Frankl, D. R., 1967, *Electrical Properties of Semiconductor Surfaces* (Pergamon, New York).
Frankl, D. R., 1974, "Surface states," Crit. Rev. Solid State Sci. **4**, 455–475.
Freedman, R., 1978, "Some properties of a charged two-dimensional Fermi liquid," Phys. Rev. B **18**, 2482–2483.
Frenzel, H., and P. Balk, 1980, "Interface width and structure of the Si-SiO_2 layer on oxidized Si," in *The Physics of MOS Insulators,* edited by G. Lucovsky, S. T. Pantelides, and F. L. Galeener (Pergamon, New York), pp. 246–249.

Fried, B. D., and S. D. Conte, 1961, *The Plasma Dispersion Function* (Academic, New York).
Friedman, L., 1978, "The Hall effect in ordered and disordered systems," Philos. Mag. B **38**, 467–476.
Friedman, L., and M. Pollak, 1978, "Hall mobility due to hopping-type conduction in disordered systems," Philos. Mag. B **38**, 173–189.
Friedrich, H., and J. Stillger, 1970, "Die Beweglichkeit von Ladungsträgern in Stromkanal von MOS-Transistoren," Solid-State Electron, **13**, 1049–1053.
Friend, R. H., and D. Jérome, 1979, "Periodic lattice distortions and charge density waves in one- and two-dimensional metals," J. Phys. C **12**, 1441–1477.
Fritzsche, D., 1980, "Interface studies on InP MIS inversion FET's with SiO_2 gate insulation," in *Insulating Films on Semiconductors, 1979,* edited by G. G. Roberts and M. J. Morant (Institute of Physics, Bristol), pp. 258–265.
Fritzsche, H., 1962, "Effect of stress on the donor wave functions in germanium," Phys. Rev. **125**, 1560–1567.
Fu, H.-S., and C. T. Sah, 1972, "Theory and experiments on surface $1/f$ noise," IEEE Trans. Electron Devices **ED-19**, 273–285.
Fuchs, K., 1935, "A quantum mechanical investigation of the cohesive forces of metallic copper," Proc. R. Soc. London **151**, 585–602.
Fuchs, K., 1938, "The conductivity of thin metallic films according to the electron theory of metals," Proc. Cambridge Phil. Soc. **34**, 100–108.
Fujita, S., and M. Prasad, 1977, "Theory of cyclotron resonance lineshape for an electron-impurity system in two dimensions," J. Phys. Chem. Solids **38**, 1351–1353.
Fukuyama, H., 1975, "Two-dimensional Wigner crystal under magnetic field," Solid State Commun. **17**, 1323–1326.
Fukuyama, H., 1976a, "Two-dimensional Wigner crystal in magnetic fields," Surf. Sci. **58**, 320–324.
Fukuyama, H., 1976b, "Two-dimensional Wigner crystallization caused by magnetic field," Solid State Commun. **19**, 551–554.
Fukuyama, H., 1979, "Wigner solid in two-dimension," in *Physics of Low-Dimensional Systems (Proceedings of Kyoto Summer Institute, 1979),* edited by Y. Nagaoka and S. Hikami (Publication Office, Progress of Theoretical Physics, Kyoto), pp. 145–175.
Fukuyama, H., 1980a, "Quantum effects on melting temperature of two-dimensional Wigner solid," J. Phys. Soc. Japan **48**, 1841–1852.
Fukuyama, H., 1980b, "Effects of interactions on non-metallic behaviors in two-dimensional disordered systems," J. Phys. Soc. Japan **48**, 2169–2170.
Fukuyama, H., 1980c, "Hall effect in two-dimensional disordered systems," J. Phys. Soc. Japan **49**, 644–648.
Fukuyama, H., 1980d, "Effects of intervalley impurity scattering on the non-metallic behavior in two-dimensional systems," J. Phys. Soc. Japan **49**, 649–651.
Fukuyama, H., 1980e, "Conductivity and Hall effect in two-dimensional disordered systems," in *Proceedings of the 15th International Conference on the Physics of Semiconductors, Kyoto* [J. Phys. Soc. Japan **49**, Suppl. A, 987–990].
Fukuyama, H., 1980f, "Non-metallic behaviors of two-dimensional metals and effect of intervalley impurity scattering," Prog. Theor. Phys. Suppl. **69**, 220–231.
Fukuyama, H., 1981, "Effects of mutual interactions in weakly localized regime of disordered two-dimensional systems. I. Magnetoresistance and spin-susceptibility," J. Phys. Soc. Japan **50**, 3407–3414.
Fukuyama, H., 1982, "Theory of weakly localized regime of the Anderson localization in two dimensions," Surf. Sci. **113**, 489–504.
Fukuyama, H., Y. Kuramoto, and P. M. Platzman, 1978, "Coulomb interaction effects on cyclotron resonance in 2D systems," Surf. Sci. **73**, 491–493.
Fukuyama, H., Y. Kuramoto, and P. M. Platzman, 1979, "Many-body effect on level broadening and cyclotron resonance in two-dimensional systems under strong magnetic field," Phys. Rev. B **19**, 4980–4985.
Fukuyama, H., and P. A. Lee, 1978, "Pinning and conductivity of two-dimensional charge-density waves in magnetic fields," Phys. Rev. B **18**, 6245–6252.
Fukuyama, H., and J. W. McClure, 1975, "Orbital magnetic moment of two-dimensional Wigner crystal," Solid State Commun. **17**, 1327–1330.
Fukuyama, H., P. M. Platzman, and P. W. Anderson, 1978, "The two-dimensional electron gas in a strong magnetic field," Surf. Sci. **73**, 374–378.
Fukuyama, H., P. M. Platzman, and P. W. Anderson, 1979, "Two-dimensional electron gas in a strong magnetic field," Phys. Rev. B. **19**, 5211–5217.
Fukuyama, H., and D. Yoshioka, 1980a, "Quantum effects on melting temperature of two-dimensional Wigner solid," Surf. Sci. **98**, 11–16.
Fukuyama, H., and D. Yoshioka, 1980b, "Quantum effects on melting temperature of two-dimensional Wigner solid in strong magnetic fields," J. Phys. Soc. Japan **48**, 1853–1860.
Gabovich, A. M., L. G. Il'chenko, E. A. Pashitskii, and Yu. A. Romanov, 1978, "Screening of charges and Friedel oscillations of the electron density in metals having differently shaped Fermi surfaces," Zh. Eksp. Teor. Fiz. **75**, 249–264 [Sov. Phys.—JETP **48**, 124–131 (1978)].
Ganguly, A. K., and C. S. Ting, 1977, "Temperature dependence of dynamic conductivity of electrons in the surface inversion layer of semiconducting silicon," Phys. Rev. B **16**, 3541–3545.
Gann, R. C., S. Chakravarty, and G. V. Chester, 1979, "Monte Carlo simulation of the classical two-dimensional one-component plasma," Phys. Rev. B **20**, 326–344.
Garcia, N., 1976, "Self-consistent numerical solution of p-type inversion layers in silicon MOS devices," Solid State Commun. **18**, 1021–1024.
Garcia, N., and L. M. Falicov, 1975a, "Localized states of p-type inversion layers in semiconductor field-effect transistors," Phys. Rev. B **11**, 728–731.
Garcia, N., and L. M. Falicov, 1975b, "Variation with Fermi level of the hole cyclotron masses in silicon and germanium," Solid State Commun. **16**, 891–894.
Garner, C. M., I. Lindau, C. Y. Su, P. Pianetta, and W. E. Spicer, 1979, "Electron-spectroscopic studies of the early stages of the oxidation of Si," Phys. Rev. B **19**, 3944–3956.
Gaydon, B. G., 1973, "The low temperature strain sensitivity of MOS transistors," Solid-State Electron. **16**, 147–154.
Gergel', V. A., and R. A. Suris, 1978, "Fluctuation of the surface potential in metal-insulator-conductor structures," Zh. Eksp. Teor. Fiz. **75**, 191–203 [Sov. Phys.—JETP **48**, 95–101 (1978)].
Gerhardts, R. R., 1975a, "Path-integral approach to the two-dimensional magneto-conductivity problem. I. General formulation of the approach," Z. Phys. B **21**, 275–283.
Gerhardts, R. R., 1975b, "Path-integral approach to the two-dimensional magneto-conductivity problem. II. Application

to n-type (100)-surface inversion layers of p-silicon," Z. Phys. B **21**, 285–294.

Gerhardts, R. R., 1976, "Cumulant approach to the two-dimensional magneto-conductivity problem," Surf. Sci. **58**, 227–234.

Gerhardts, R. R., 1981a, "Transition to an anharmonic charge-density wave of a two-dimensional electron gas in a strong magnetic field," Phys. Rev. B **24**, 1339–1349.

Gerhardts, R. R., 1981b, "Wigner transition temperature of a two-dimensional electron gas in a strong magnetic field," Phys. Rev. B **24**, 4068–4071.

Gersten, J. I., 1980a, "Theory of surface plasmarons," Surf. Sci. **92**, 579–592.

Gersten, J. I., 1980b, "Theory of surface plasmarons. II. The effect of a finite thickness of the accumulation layer," Surf. Sci. **97**, 206–218.

Gesch, H., G. Dorda, P. Stallhofer, and J. P. Kotthaus, 1979, "Comparison of Shubnikov–de Haas effect and cyclotron resonance on Si(100) MOS transistors under uniaxial stress," Solid State Commun. **32**, 543–546.

Gesch, H., I. Eisele, and G. Dorda, 1977, "p-Type inversion layers under mechanical stress," in *Proceedings of the Seventh International Vacuum Congress and the Third International Conference on Solid Surfaces, Vienna,* edited by R. Dobrozemsky, F. Rüdenauer, F. P. Viehböck, and A. Breth (Berger, Horn, Austria), Vol. I, pp. 559–562.

Gesch, H., I. Eisele, and G. Dorda, 1978, "Pressure dependence of structure in the mobility of (100) silicon inversion layers," Surf. Sci. **73**, 81–89.

Giannetta, R. W., and H. Ikezi, 1981, "Nonlinear deformation of the electron-charged surface of liquid ^{4}He," Phys. Rev. Lett. **47**, 849–852.

Ginzburg, Vl. L., and Yu. P. Monarkha, 1978, "Surface electrons in helium over macroscopic periodic structures," Fiz. Nizk. Temp. **4**, 1236–1239 [Sov. J. Low Temp. Phys. **4**, 580–582 (1978)].

Giordano, N., 1980, "Experimental study of localization in thin wires," Phys. Rev. B **22**, 5635–5654.

Giordano, N., W. Gilson, and D. E. Prober, 1979, "Experimental study of Anderson localization in thin wires," Phys. Rev. Lett. **43**, 725–728.

Glasser, M. L., 1977, "Pair correlation function for a two-dimensional electron gas," J. Phys. C **10**, L121–L123.

Glasser, M. L., 1980, "Two-dimensional electron gas in a magnetic field: Polarizability," Phys. Rev. B **22**, 472–473.

Glasser, M. L., 1981, "Specific heat of electron gas of arbitrary dimensionality," Phys. Lett. A **81**, 295–296.

Glew, R. W., and M. Halberstadt, 1981, "Modulation doped GaAs-GaAlAs multilayer structures," in *Gallium Arsenide and Related Compounds, 1980,* edited by H. W. Thim (Institute of Physics, Bristol), pp. 731–740.

Gnädinger, A. P., and H. E. Talley, 1970, "Quantum mechanical calculation of the carrier distribution and the thickness of the inversion layer of a MOS field-effect transistor," Solid-State Electron. **13**, 1301–1309.

Goetzberger, A., 1967, "Behavior of MOS inversion layers at low temperature," IEEE Trans. Electron Devices **ED-14**, 787–789.

Goetzberger, A., V. Heine, and E. H. Nicollian, 1968, "Surface states in silicon from charges in the oxide coating," Appl. Phys. Lett. **12**, 95–97.

Goetzberger, A., E. Klausmann, and M. J. Schulz, 1976, "Interface states on semiconductor/insulator surfaces," Crit. Rev. Solid State Sci. **6**, 1–43.

Goetzberger, A., and M. Schulz, 1973, "Fundamentals of MOS technology," in *Festkörperprobleme (Advances in Solid State Physics),* edited by H. J. Queisser (Pergamon-Vieweg, Braunschweig), Vol. XIII, pp. 309–336.

Goetzberger, A., and S. M. Sze, 1969, "Metal-insulator-semiconductor (MIS) physics," in *Applied Solid State Science,* edited by R. Wolfe and L. J. Kriessman (Academic, New York), Vol. 1, pp. 153–238.

Gold, A., and W. Götze, 1981, "The conductivity of strongly disordered two-dimensional systems," J. Phys. C **14**, 4049–4066.

Goldstein, Y., and Y. Grinshpan, 1977, "Negative magnetoresistance in very strong accumulation layers on ZnO surfaces," Phys. Rev. Lett. **39**, 953–956.

Goldstein, Y., Y. Grinshpan, and A. Many, 1979, "Negative magnetoresistance in quantized accumulation layers on ZnO surfaces," Phys. Rev. B **19**, 2256–2265.

Goldstein, Y., A. Many, D. Eger, Y. Grinshpan, G. Yaron, and M. Nitzan, 1977, "Extreme accumulation layers on ZnO surfaces due to He^+ ions," Phys. Lett. A **62**, 57–58.

Goldstein, Y., A. Many, I. Wagner, and J. Gersten, 1980, "ELS studies of quantized accumulation layers on ZnO surfaces," Surf. Sci. **98**, 599–612.

Goodman, A. M., and J. J. O'Neill, Jr., 1966, "Photoemission of electrons from metals into silicon dioxide," J. Appl. Phys. **37**, 3580–3583.

Goodman, B., and W. M. Polansky, 1976, "Local mass of (110) Ge surface inversion layer electrons," Bull. Am. Phys. Soc. **21**, 342.

Göpel, W., and U. Lampe, 1980, "Influence of defects on the electronic structure of zinc oxide surfaces," Phys. Rev. B **22**, 6447–6462.

Gor'kov, L. P., and D. M. Chernikova, 1973, "Concerning the structure of a charged surface of liquid helium," Zh. Eksp. Teor. Fiz. Pis'ma Red. **18**, 119–122 [JETP Lett. **18**, 68–70 (1973)].

Gor'kov, L. P., and D. M. Chernikova, 1976, "Mode of stability loss of charged helium surface," Dokl. Akad. Nauk SSSR **228**, 829–832 [Sov. Phys.—Dokl. **21**, 328–330 (1976)].

Gor'kov, L. P., A. I. Larkin, and D. E. Khmel'nitskii, 1979, "Particle conductivity in a two-dimensional random potential," Zh. Eksp. Teor. Fiz. Pis'ma Red. **30**, 248–252 [JETP Lett. **30**, 228–232 (1979)].

Gornik, E., R. Schawarz, G. Lindemann, and D. C. Tsui, 1980a, "Emission spectroscopy on two-dimensional systems," Surf. Sci. **98**, 493–504.

Gornik, E., R. Schawarz, D. C. Tsui, A. C. Gossard, and W. Wiegmann, 1980b, "Far infrared emission from 2D electrons at the GaAs-$Al_xGa_{1-x}As$ interface," Solid State Commun. **38**, 541–545; in *Proceedings of the 15th International Conference on the Physics of Semiconductors, Kyoto* [J. Phys. Soc. Japan **49**, Suppl. A, 1029–1032].

Gornik, E., and D. C. Tsui, 1976, "Voltage-tunable far-infrared emission from Si inversion layers," Phys. Rev. Lett. **37**, 1425–1428.

Gornik, E., and D. C. Tsui, 1978a, "Far infrared emission from hot electrons in Si-inversion layers," Solid-State Electron. **21**, 139–142.

Gornik, E., and D. C. Tsui, 1978b, "Cyclotron and subband emission from Si inversion layers," Surf. Sci. **73**, 217–221.

Götze, W., and J. Hajdu, 1979, "On the theory of the transverse dynamic magneto-conductivity in two-dimensional electron-impurity systems," Solid State Commun. **29**, 89–92.

Götze, W., P. Prelovšek, and P. Wölfle, 1979, "Localization of

particles in a two-dimensional random potential," Solid State Commun. **30**, 369–373.
Götze, W., and P. Wölfle, 1972, "Homogeneous dynamical conductivity of simple metals," Phys. Rev. B **6**, 1226–1238.
Grebenshchikov, Yu. B., and V. V. Korneev, 1977, "Mott Exciton spectrum in a thin semiconductor in a magnetic field," Fiz. Tverd. Tela (Leningrad) **19**, 2143–2149 [Sov. Phys.—Solid State **19**, 1255–1258 (1977)].
Grecu, D., 1973, "Plasma frequency of the electron gas in layered structures," Phys. Rev. B **8**, 1958–1961.
Greene, R. F., 1964, "Surface transport," Surf. Sci. **2**, 101–113.
Greene, R. F., 1969a, "Electron transport and scattering near crystal surfaces," in *Molecular Processes on Solid Surfaces,* edited by E. Drauglis, R. D. Gretz and R. J. Jaffee (McGraw-Hill, New York), pp. 239–263.
Greene, R. F., 1969b, "Transport and scattering near crystal surfaces," in *Solid State Surface Science,* edited by M. Green (M. Dekker, New York), Vol. I, pp. 87–132.
Greene, R. F., 1972, "The connection between the thermodynamics of chemisorption on semiconductor surfaces and surface scattering of carriers," Thin Solid Films **13**, 179–183.
Greene, R. F., 1974, "Surface electron transport," Crit. Rev. Solid State Sci. **4**, 477–497.
Greene, R. F., 1975, "Carrier scattering at elemental and compound semiconductor interfaces," Crit. Rev. Solid State Sci. **5**, 345–351.
Greene, R. F., D. Bixler, and R. N. Lee, 1971, "Semiconductor surface electrostatics," J. Vac. Sci. Technol. **8**, 75–79.
Greene, R. F., and J. Malamas, 1973, "Scattering of carriers in semiconductors by screened surface charges," Phys. Rev. B **7**, 1384–1392.
Greene, R. F., and R. W. O'Donnell, 1966, "Scattering of conduction electrons by localized surface charges," Phys. Rev. **147**, 599–602.
Grimes, C. C., 1978a, "Electrons in surface states on liquid helium," Surf. Sci. **73**, 379–395.
Grimes, C. C., 1978b, "Structure of the electron gas at the surface of liquid helium," J. Phys. (Paris) **39**, Colloques, C6-1352–C6-1357.
Grimes, C. C., 1979, "Cyclotron resonance in a two-dimensional electron gas on helium surfaces," J. Magn. Magn. Mater. **11**, 32–38.
Grimes, C. C., and G. Adams, 1976a, "Plasmons in a sheet of electrons on liquid helium," Surf. Sci. **58**, 292–294.
Grimes, C. C., and G. Adams, 1976b, "Observation of two-dimensional plasmons and electron-ripplon scattering in a sheet of electrons on liquid helium," Phys. Rev. Lett. **36**, 145–148.
Grimes, C. C., and G. Adams, 1979, "Evidence for a liquid-to-crystal phase transition in a classical, two-dimensional sheet of electrons," Phys. Rev. Lett. **42**, 795–798.
Grimes, C. C., and G. Adams, 1980, "Crystallization of electrons on the surface of liquid helium," Surf. Sci. **98**, 1–7.
Grimes, C. C., and T. R. Brown, 1974, "Direct spectroscopic observation of electrons in image-potential states outside liquid helium," Phys. Rev. Lett. **32**, 280–283.
Grimes, C. C., T. R. Brown, M. L. Burns, and C. L. Zipfel, 1976, "Spectroscopy of electrons in image-potential-induced surface states outside liquid helium," Phys. Rev. B **13**, 140–147.
Grinshpan, Y., M. Nitzan, and Y. Goldstein, 1979, "Hall mobility of electrons in quantized accumulation layers on ZnO surfaces," Phys. Rev. B **19**, 1098–1107.
Grosvalet, J., 1968, "Phénomènes de transport en surface dans les semi-conducteurs," J. Phys. (Paris) **29**, Colloques, C2-59–C2-64.
Grosvalet, J., C. Jund, C. Motsch, and R. Poirier, 1966, "Experimental study of semiconductor surface conductivity," Surf. Sci. **5**, 49–80.
Grove, A. S., 1967, *Physics and Technology of Semiconductor Devices* (Wiley, New York).
Grunthaner, F. J., P. J. Grunthaner, R. P. Vasquez, B. F. Lewis, J. Maserjian, and A. Madhukar, 1979, "High-resolution x-ray photoelectron spectroscopy as a probe of local atomic structure: Application to amorphous SiO_2 and the Si-SiO_2 interface," Phys. Rev. Lett. **43**, 1683–1686.
Grunthaner, F. J., and J. Maserjian, 1978, "Chemical structure of the transitional region of the SiO_2/Si interface," in *The Physics of SiO_2 and its Interfaces,* edited by S. T. Pantelides (Pergamon, New York), pp. 389–395.
Gryukanov, M. F., and V. V. Korneev, 1978, "Plasma surface states of electrons in a semiconductor subjected to a quantizing magnetic field," Fiz. Tekh. Poluprovodn. **12**, 861–865 [Sov. Phys.—Semicond. **12**, 508–510 (1978)].
Guldner, Y., J. P. Vieren, P. Voisin, M. Voos, L. L. Chang, and L. Esaki, 1980, "Cyclotron resonance and far-infrared magneto-absorption experiments in semimetallic InAs-GaSb superlattices," Phys. Rev. Lett. **45**, 1719–1722.
Gulyaev, Yu. V., and R. A. Gusparian, 1980, "Acoustoelectronic phenomena in the systems with quantum size effects," Surf. Sci. **98**, 553–562.
Gunnarson, O., and B. I. Lundqvist, 1976, "Exchange and correlation in atoms, molecules, and solids by the spin-density functional formalism," Phys. Rev. B **13**, 4274–4298.
Guzev, A. A., V. A. Gurtov, A. V. Rzhanov, and A. A. Frantsuzov, 1979, "Hole mobility in inversion layers of MOS structures with superthin gate dielectric," Phys. Status Solidi A **56**, 61–73.
Guzev, A. A., G. L. Kuryshev, and S. P. Sinitsa, 1970a, "Mobility of holes in silicon inversion layers in metal-dielectric-semiconductor structures," Fiz. Tverd. Tela (Leningrad) **4**, 2043–2047 [Sov. Phys.—Semicond. **4**, 1755–1759 (1971)].
Guzev, A. A., G. L. Kuryshev, and S. P. Sinitsa, 1970b, "Scattering mechanisms in inversion channels of MIS structures on silicon," Phys. Status Solidi A **14**, 41–50.
Hahn, P. O., and M. Henzler, 1981, "Influence of oxidation parameters on atomic roughness at the Si-SiO_2 interface," J. Appl. Phys. **52**, 4122–4127.
Halperin, B. I., 1979, "Superfluidity, melting, and liquid-crystal phases in two dimensions," in *Physics of Low-Dimensional Systems (Proceedings of Kyoto Summer Institute, 1979),* edited by Y. Nagaoka and S. Hikami (Publication Office, Progress of Theoretical Physics, Kyoto), pp. 53–124.
Halperin, B. I., 1980, "Theory of melting in two dimensions," Surf. Sci. **98**, 8–10.
Halperin, B. I., and T. M. Rice, 1968, "The excitonic state at the semiconductor-semimetal transition," Solid State Phys. **21**, 115–192.
Halperin, B. I., and D. R. Nelson, 1978, "Theory of two-dimensional melting," Phys. Rev. Lett. **41**, 121–124; 519(E).
Hamilton, E. M., 1972, "Variable range hopping in a non-uniform density of states," Philos. Mag. **26**, 1043–1045.
Handler, P., and S. Eisenhour, 1964, "Transport properties of light and heavy holes in the space charge region of a clean and water covered (111) germanium surface," Surf. Sci. **2**, 64–74.
Hanke, W., and M. J. Kelly, 1980a, "Surface superconductivity

and the metal-oxide-semiconductor system," Phys. Rev. Lett. **45**, 1203–1206.

Hanke, W., and M. J. Kelly, 1980b, "Mechanisms of superconductivity at semiconductor interfaces," in *Proceedings of the 15th International Conference on the Physics of Semiconductors, Kyoto* [J. Phys. Soc. Japan **49**, Suppl. A, 991–994].

Hanni, R. S., and J. M. J. Madey, 1978, "Shielding by an electron surface layer," Phys. Rev. B **17**, 1976–1983.

Hansen, J. P., D. Levesque, and J. J. Weis, 1979, "Self-diffusion in the two-dimensional classical electron gas," Phys. Rev. Lett. **43**, 979–982.

Harrison, W. A., 1961, "Tunneling from an independent-particle point of view," Phys. Rev. **123**, 85–89.

Hartstein, A., and F. F. Fang, 1978, "Variation of the Shubnikov–de Haas amplitudes with ionic scattering in silicon inversion layers," Phys. Rev. B **18**, 5502–5505.

Hartstein, A., and A. B. Fowler, 1975a, "High temperature 'variable range hopping' conductivity in silicon inversion layers," J. Phys. C **8**, L249–L253.

Hartstein, A., and A. B. Fowler, 1975b, "Oxide-charge-induced impurity level in silicon inversion layers," Phys. Rev. Lett. **34**, 1435–1437.

Hartstein, A., and A. B. Fowler, 1976, "Conductivity in a two-dimensional impurity band," in *Proceedings of the 13th International Conference on the Physics of Semiconductors, Rome,* edited by F. G. Fumi (North-Holland, Amsterdam), pp. 741–745.

Hartstein, A., and A. B. Fowler, 1978, "Impurity bands in inversion layers," Surf. Sci. **73**, 19–30.

Hartstein, A., A. B. Fowler, and M. Albert, 1979, "Variation of the conductivity in a 2-D impurity band with Fermi level position," in *Physics of Semiconductors, 1978,* edited by B. L. H. Wilson (Institute of Physics, Bristol), pp. 1001–1004.

Hartstein, A., A. B. Fowler, and M. Albert, 1980, "Temperature dependence of scattering in the inversion layer," Surf. Sci. **98**, 181–190.

Hartstein, A., T. H. Ning, and A. B. Fowler, 1976, "Electron scattering in silicon inversion layers by oxide [charge] and surface roughness," Surf. Sci. **58**, 178–181.

Hasegawa, H., and T. Sawada, 1980, "On the distribution and properties of interface states at compound semiconductor–insulator interfaces," Surf. Sci. **98**, 597–598.

Hatanaka, K., S. Onga, Y. Yasuda, and S. Kawaji, 1978, "Magnetoconductivity oscillations and inversion layer subbands in silicon on sapphire," Surf. Sci. **73**, 170–178.

Hattori, T., and T. Nishina, 1978, "Studies of Si/SiO_2 interfaces and SiO_2 by XPS," in *The Physics of SiO_2 and its Interfaces,* edited by S. T. Pantelides (Pergamon, New York), pp. 379–383.

Hayden, K. J., 1980, "Carrier-density dependence of the activation energies associated with hopping in two-dimensional impurity bands," Philos. Mag. B **41**, 619–624.

Hayden, K. J., and P. N. Butcher, 1979, "Analysis of hopping conduction in impurity bands in inversion layers," Philos. Mag. B **38**, 603–617.

Haydock, R., 1981, "The electronic structure of weak, random, two- and three-dimensional potentials," Philos. Mag. B **43** 203–218.

Hebard, A. F., and A. T. Fiory, 1980, "Recent experimental results on vortex processes in thin-film superconductors," in *Ordering in Two Dimensions,* edited by S. K. Sinha (Elsevier–North-Holland, New York), pp. 181–187.

Hedin, L., 1965, "New method for calculating the one-particle Green's function with application to the electron-gas problem," Phys. Rev. **139**, A796–A823.

Heiland, G., E. Mollwo, and F. Stöckmann, 1959, "Electronic processes in zinc oxide," Solid State Phys. **8**, 191–323.

Heiland, G., and P. Kunstmann, 1969, "Polar surfaces of zinc oxide crystals," Surf. Sci. **13**, 72–84.

Heinrichs, J., 1978, "Density-of-states tails, fluctuation states, and mobility edges in systems with randomly distributed impurities," Phys. Rev. B **17**, 3051–3062.

Helms, C. R., 1979, "Morphology and electronic structure of $Si-SiO_2$ interfaces and Si surfaces," J. Vac. Sci. Technol. **16**, 608–614.

Helms, C. R., N. M. Johnson, S. A. Schwarz, and W. E. Spicer, 1978a, "Auger sputter profiling studies of the $Si-SiO_2$ interface," in *The Physics of SiO_2 and its Interfaces,* edited by S. T. Pantelides (Pergamon, New York), pp. 366–372.

Helms, C. R., Y. E. Strausser, and W. E. Spicer, 1978b, "Observation of an intermediate chemical state of silicon in the Si/SiO_2 interface by Auger sputter profiling," Appl. Phys. Lett. **33**, 767–769.

Hensel, J. C., and G. Feher, 1963, "Cyclotron resonance experiments in uniaxially stressed silicon: Valence band inverse mass parameters and deformation potentials," Phys. Rev. **129**, 1041–1062.

Hensel, J. C., H. Hasegawa, and M. Nakayama, 1965, "Cyclotron resonance in uniaxially stressed silicon. II. Nature of the covalent bond," Phys. Rev. **138**, A225–A238.

Henzler, M., 1975, "Electronic transport at surfaces," in *Surface Physics of Materials,* edited by J. M. Blakely (Academic, New York), Vol. I, pp. 241–278.

Henzler, M., 1978, "Quantitative evaluation of random distributed steps at interfaces and surfaces," Surf. Sci. **73**, 240–251.

Henzler, M., and F. W. Wulfert, 1976, "Determination of atomic steps at the interface $Si-SiO_2$," in *Proceedings of the 13th International Conference on the Physics of Semiconductors, Rome,* edited by F. G. Fumi (North-Holland, Amsterdam), pp. 669–672.

Herman, F., I. P. Batra, and R. V. Kasowski, 1978, "Electronic structure of a model $Si-SiO_2$ interface," in *The Physics of SiO_2 and its Interfaces,* edited by S. T. Pantelides (Pergamon, New York), pp. 333–338.

Herman, F., D. J. Henderson, and R. V. Kasowski, 1980, "Electronic structure of vacancies and interstitials in SiO_2," in *The Physics of MOS Insulators,* edited by G. Lucovsky, S. T. Pantelides, and F. L. Galeener (Pergamon, New York), pp. 107–110.

Herring, C., and E. Vogt, 1956, "Transport and deformation-potential theory for many-valley semiconductors with anisotropic scattering," Phys. Rev. **101**, 944–961.

Hess, K., 1975, "Anisotropic impurity scattering in electrically quantized inversion layers," Solid State Commun. **17**, 157–159.

Hess, K., 1976, "Magnetoresistance of *n*-silicon inversion layers in the Ohmic and in the hot-electron range," Surf. Sci. **58**, 235–237.

Hess, K., 1978a, "Review of experimental aspects of hot electron transport in MOS structures," Solid-State Electron. **21**, 123–132.

Hess, K., 1978b, "Energy relaxation to acoustic phonons in surface inversion layers," Solid State Commun. **25**, 191–192.

Hess, K., 1979, "Impurity and phonon scattering in layered structures," Appl. Phys. Lett. **35**, 484–486.

Hess, K., G. Dorda, and C. T. Sah, 1976a, "The current-voltage characteristics of field-effect transistors with short

channels," Solid State Commun. **19**, 471—473.
Hess, K., Th. Englert, T. Neugebauer, G. Landwehr, and G. Dorda, 1976b, "Non-Ohmic effects in *p*-type silicon inversion layers," in *Proceedings of the 13th International Conference on the Physics of Semiconductors, Rome,* edited by F. G. Fumi (North-Holland, Amsterdam), pp. 746—749.
Hess, K., T. Englert, T. Neugebauer, G. Landwehr, and G. Dorda, 1977, "Hot-carrier effects in high magnetic fields in silicon inversion layers at low temperatures: *p*-channel," Phys. Rev. B **16**, 3652—3659.
Hess, K., A. Neugroschel, C. C. Shiue, and C. T. Sah, 1975, "Non-Ohmic electron conduction in silicon surface inversion layers at low temperatures," J. Appl. Phys. **46**, 1721—1727.
Hess, K., and C. T. Sah, 1974a, "Warm and hot carriers in silicon surface-inversion layers," Phys. Rev. B **10**, 3375—3386.
Hess, K., and C. T. Sah, 1974b, "Hot carriers in silicon surface inversion layers," J. Appl. Phys. **45**, 1254—1257.
Hess, K., and C. T. Sah, 1975, "Dipole scattering at the Si-SiO_2 interface," Surf. Sci. **47**, 650—654.
Hess, K., and P. Vogl, 1979, "Remote polar phonon scattering in silicon inversion layers," Solid State Commun. **30**, 807—809.
Hess, K., B. A. Vojak, N. Holonyak, Jr., R. Chin, and P. D. Dapkus, 1980, "Temperature dependence of threshold current for a quantum-well heterostructure laser," Solid-State Electron. **23**, 585—589.
Hickmott, T. W., 1975, "Thermally stimulated ionic conductivity of sodium in thermal SiO_2," J. Appl. Phys. **46**, 2583—2598.
Hickmott, T. W., 1980, "Dipole layers at the metal-SiO_2 interface," J. Appl. Phys. **51**, 4269—4281.
Hikami, S., A. I. Larkin, and Y. Nagaoka, 1980, "Spin-orbit interaction and magnetoresistance in the two dimensional random system," Prog. Theor. Phys. **63**, 707—710.
Hines, D. F., and N. E. Frankel, 1979, "Charged Bose gas in two dimensions. Zero magnetic field," Phys. Rev. B **20**, 972—983.
Hipólito, O., 1979, "Ground-state energy of strongly bound charged particles on surfaces," J. Phys. C **12**, 4667—4672.
Hipólito, O., and V. B. Campos, 1979, "Screening effects in *n*-type Si inversion layers," Phys. Rev. B **19**, 3083—3088.
Hipólito, O., J. R. D. de Felício, and G. A. Farias, 1978, "Electron bound states on liquid helium," Solid State Commun. **28**, 365—368.
Hiyamizu, S., T. Mimura, T. Fujii, and K. Nanbu, 1980, "High mobility of two-dimensional electrons at the GaAs/*n*-AlGaAs heterojunction interface," Appl. Phys. Lett. **37**, 805—807.
Hiyamizu, S., T. Mimura, T. Fujii, K. Nanbu, and H. Hashimoto, 1981a, "Extremely high mobilities of two-dimensional electron gas in selectively doped GaAs/*N*-AlGaAs heterojunction structures grown by MBE," Jpn. J. Appl. Phys. **20**, L245—L248.
Hiyamizu, S., K. Nanbu, T. Mimura, T. Fujii, and H. Hashimoto, 1981b, "Room-temperature mobility of two-dimensional electron gas in selectively doped GaAs/*N*-AlGaAs heterojunction structures," Jpn. J. Appl. Phys. **20**, L378—L380.
Hockney, R. W., and T. R. Brown, 1975, "A lambda transition in a classical electron film," J. Phys. C **8**, 1813—1822.
Hohenberg, P., and W. Kohn, 1964, "Inhomogeneous electron gas," Phys. Rev. **136**, B864—B871.
Holm-Kennedy, J. W., 1974, "New effect in insulated-gate field-effect transistors: Transverse voltage anisotropy at the inverted silicon surface," Phys. Rev. Lett. **32**, 111—114.
Holonyak, N., Jr., R. M. Kolbas, W. D. Laidig, M. Altarelli, R. D. Dupuis, and P. D. Dapkus, 1979, "Phonon-sideband MO-CVD quantum-well $Al_xGa_{1-x}As$-GaAs heterostructure laser," Appl. Phys. Lett. **34**, 502—505.
Holonyak, N., Jr., R. M. Kolbas, R. D. Dupuis, and P. D. Dapkus, 1980a, "Quantum-well heterostructure lasers," IEEE J. Quant. Electron. **QE-16**, 170—185.
Holonyak, N., Jr., R. M. Kolbas, W. D. Laidig, B. A. Vojak, K. Hess, R. D. Dupuis, and P. D. Dapkus, 1980b, "Phonon-assisted recombination and stimulated emission in quantum-well $Al_xGa_{1-x}As$-GaAs heterostructures," J. Appl. Phys. **51**, 1328—1337.
Holonyak, N., Jr., W. D. Laidig, B. A. Vojak, K. Hess, J. J. Coleman, P. D. Dapkus, and J. Bardeen, 1980c, "Alloy clustering in $Al_xGa_{1-x}As$-GaAs quantum-well heterostructures," Phys. Rev. Lett. **45**, 1703—1706.
Holonyak, N., Jr., W. D. Laidig, M. D. Camras, H. Morkoç, T. J. Drummond, and K. Hess, 1981a, "Clustering and phonon effects in $Al_xGa_{1-x}As$-GaAs quantum-well heterostructure lasers grown by molecular beam epitaxy," Solid State Commun. **40**, 71—74.
Holonyak, N., Jr., W. D. Laidig, K. Hess, J. J. Coleman, and P. D. Dapkus, 1981b, "Alloy clustering in $Al_xGa_{1-x}As$," Phys. Rev. Lett. **46**, 1043.
Holyavko, V. N., V. P. Dragunov, B. V. Morozov, E. M. Skok, and N. B. Velchev, 1976, "Study of the size quantization in *p*-type silicon inversion layers by means of magnetoresistance," Phys. Status Solidi B **75**, 423—432.
Holz, A., 1980a, "Dislocation formalism in crystals with long-range interactions," Phys. Rev. B **22**, 3678—3691.
Holz, A., 1980b, "Defect states and phase transition in the two-dimensional Wigner crystal," Phys. Rev. B **22**, 3692—3705; and in *Ordering in Two Dimensions,* edited by S. K. Sinha (Elsevier—North-Holland, New York), pp. 313—316.
Holz, A., and J. T. N. Medeiros, 1978, "Melting transition of two-dimensional crystals," Phys. Rev. B **17**, 1161—1174.
Hönlein, W., K. von Klitzing, and G. Landwehr, 1980, "Influence of the MOS surface channel on a channel-to-source contact diode characteristic," Surf. Sci. **98**, 167—168; and in *Insulating Films on Semiconductors, 1979,* edited by G. G. Roberts and M. J. Morant (Institute of Physics, Bristol), pp. 133—139.
Hooge, F. N., T. G. M. Kleinpenning, and L. K. J. Vandamme, 1981, "Experimental studies on $1/f$ noise," Rep. Prog. Phys. **44**, 479—532.
Horing, N. J. M., E. Kamen, and M. Orman, 1981, "2D plasma layer conductivity tensor in high magnetic field," Physica **105B**, 115—119.
Horing, N. J. M., and J. J. LaBonney, 1979, "DHVA oscillations in the correlation energy of a two-dimensional quantum plasma," J. Magn. Magn. Mater. **11**, 73—75.
Horing, N. J. M., M. Orman, E. Kamen, and M. L. Glasser, 1981, "Analysis of the two-dimensional quantum plasma conductivity tensor," Phys. Lett. A **85**, 378—382.
Horing, N. J. M., M. Orman, and M. Yildiz, 1974, "Magnetoconductivity tensor of a two-dimensional plasma in a quantizing magnetic field," Phys. Lett. A **48**, 7—8.
Horing, N. J. M., and M. Yildiz, 1973, "Magnetic field effects on slab surface plasmons in the local limit," Phys. Lett. A **44**, 386—388.
Horing, N. J. M., and M. Yildiz, 1976, "Quantum theory of longitudinal dielectric response properties of a two dimensional plasma in a magnetic field," Ann. Phys. (N.Y.) **97**,

216—241.
Horovitz, B., and A. Madhukar, 1979, "Electron-phonon interaction and cyclotron resonance in two-dimensional electron gas," Solid State Commun. **32**, 695—698.
Hoshino, K., 1976, "Optical conductivity of two-dimensional disordered system," J. Phys. Soc. Japan **41**, 1453—1458.
Hoshino, K., and M. Watabe, 1976, "Density of states and conductivity for two-dimensional Anderson model," Solid State Commun. **18**, 1111—1113.
Houghton, A., A. Jevicki, R. D. Kenway, and A. M. M. Pruisken, 1980, "Noncompact σ models and the existence of a mobility edge in disordered electronic systems near two dimensions," Phys. Rev. Lett. **45**, 394—397.
Howard, W. E., and F. F. Fang, 1965, "Low temperature effects in Si FETs," Solid-State Electron. **8**, 82—83.
Howard, W. E., and F. F. Fang, 1976, "The effects of higher sub-band occupation in (100) Si inversion layers," Phys. Rev. B **13**, 2519—2523.
Hsing, C. J., D. P. Kennedy, A. D. Sutherland, and K. M. van Vliet, 1979, "Quantum mechanical determination of the potential and carrier distributions in the inversion layer of metal-oxide-semiconductor devices," Phys. Status Solidi A **56**, 129—141.
Hsing, C. J., D. P. Kennedy, K. M. van Vliet, and A. D. Sutherland, 1980, "Inversion layer carrier mobility in metal-oxide-semiconductor devices," Phys. Status Solidi A **57**, 683—690.
Hu, C. C., J. Pearse, K. M. Cham, and R. G. Wheeler, 1978, "Photoconductivity measurements related to intersubband transitions in silicon MOSFET structures," Surf. Sci. **73**, 207—216.
Hu, G., and W. C. Johnson, 1980, "Relationship between trapped holes and interface states in MOS capacitors," Appl. Phys. Lett. **36**, 590—592.
Huang, H.-M., Y. M. Shih, and C.-W. Woo, 1974, "Electronic surface states on liquid helium," J. Low Temp. Phys. **14**, 413—418.
Huang, W., J. Rudnick and A. J. Dahm, 1977, "Sound modes of a two-dimensional electron gas bound to a helium film," J. Low Temp. Phys. **28**, 21—27.
Hubbard, J., 1957, "The description of collective motions in terms of many-body perturbation theory," Proc. R. Soc. London Ser. A **240**, 539—560.
Hubbard, J., 1958, "The description of collective motions in terms of many-body perturbation theory II. The correlation energy of a free-electron gas," Proc. R. Soc. London Ser. A **243**, 336—352.
Huybrechts, W. J., 1978, "Ground-state energy and effective mass of a polaron in a two-dimensional surface layer," Solid State Commun. **28**, 95—97.
Igarashi, T., J. Wakabayashi, and S. Kawaji, 1975, "Hall effect in silicon inversion layers under strong magnetic fields," J. Phys. Soc. Japan **38**, 1549.
Ignatov, A. A., 1980, "Dielectric nature of high-frequency properties of thin semiconductor films," Fiz. Tekh. Poluprovodn. **14**, 1582—1586 [Sov. Phys.—Semicond. **14**, 937—939 (1980)].
Ihm, J., P. K. Lam, and M. L. Cohen, 1979, "Electronic structure of the [001] InAs-GaSb superlattice," Phys. Rev. B **20**, 4120—4125.
Ikezi, H., 1979, "Macroscopic electron lattice on the surface of liquid helium," Phys. Rev. Lett. **42**, 1688—1690; **43**, 238(E).
Ikezi, H., and P. M. Platzman, 1981, "Stability of helium films charged with electrons," Phys. Rev. B **23**, 1145—1148.
Imry, Y., 1979, "Long range order in two dimensions," Crit. Rev. Solid State Mater. Sci. **8**, 157—174.
Imry, Y., 1981, "Comments on the scaling theory of localization and conduction in disordered systems," Phys. Rev. B **24**, 1107—1110.
Imry, Y., and L. Gunther, 1971, "Fluctuations and physical properties of the two-dimensional crystal lattice," Phys. Rev. B **3**, 3939—3945.
Inkson, J. C., and K. B. Ma, 1979, "Effect of electron-electron scattering on electrical conduction in inversion layers," J. Phys. C **12**, 3941—3949.
Ioriatti, L., and A. Isihara, 1980, "A logarithmic singularity in the specific heat of a two-dimensional electron gas," Phys. Status Solidi B **97**, K65—K69.
Ipri, A. C., 1973, "Accumulation- and inversion-layer Hall mobilities in silicon films on sapphire," Appl. Phys. Lett. **22**, 16—18.
Ishibashi, T., Y. Suzuki, and H. Okamoto, 1981, "Photoluminescence of an AlAs/GaAs superlattice grown by MBE in the 0.7—0.8 μm wavelength region," Jpn. J. Appl. Phys. **20**, L623—L626.
Ishizaka, A., S. Iwata, and Y. Kamigaki, 1979, "Si-SiO_2 interface characterization by ESCA," Surf. Sci. **84**, 355—374.
Ishizaka, A., and S. Iwata, 1980, "Si-SiO_2 interface characterization from angular dependence of x-ray photoelectron spectra," Appl. Phys. Lett. **36**, 71—73.
Isihara, A., 1972, "Crystallization of an electron gas," Phys. Kondens. Mater. **15**, 225—229.
Isihara, A., 1980, "Thermal and magnetic properties of two-dimensional electrons," Surf. Sci. **98**, 31—40.
Isihara, A., and L. Ioriatti, 1980a, "Exact evaluation of the second-order exchange energy of two-dimensional electron fluid," Phys. Rev. B **22**, 214—219.
Isihara, A., and L. C. Ioriatti, Jr., 1980b, "Application of a dielectric function to the exchange energy and specifc heat of a two-dimensional electron gas," Physica **103A**, 621—629.
Isihara, A., and D. Y. Kojima, 1979, "Study of two-dimensional electrons in a magnetic field. II. Intermediate field," Phys. Rev. B **19**, 846—855.
Isihara, A., and M. Mukai, 1981, "Cyclotron resonance of Si (001) inversion layers," Phys. Rev. B **24**, 7408—7411.
Isihara, A., and T. Toyoda, 1976, "Spatial correlations of a two-dimensional electron gas," Z. Phys. B **23**, 389—394.
Isihara, A., and T. Toyoda, 1977a, "Correlation energy of 2-D electrons," Ann. Phys. (N.Y.) **106**, 394—406; **114**, 497(E) (1978).
Isihara, A., and T. Toyoda, 1977b, "The ground state energy of a 2-D electron gas (Addendum)," Z. Phys. B **26**, 216; **29**, 70(E) (1978).
Isihara, A., and T. Toyoda, 1979, "Study of a two-dimensional electron gas in a magnetic field. I. Weak field," Phys. Rev. B **19**, 831—845.
Isihara, A., and T. Toyoda, 1980, "Two-dimensional electron gas at finite temperature," Phys. Rev. B **21**, 3358—3365.
Ito, R., 1972, "Quantum-limit piezoresistance of n-type inversion layers of silicon and germanium," J. Appl. Phys. **43**, 735—737.
Itoh, N., and S. Ichimaru, 1980, "Harmonic lattice model for the internal energy of the classical two-dimensional, one-component plasma fluid," Phys. Rev. B **22**, 1459—1460.
Itoh, N., S. Ichimaru, and S. Nagano, 1978, "Lattice model for the two-dimensional electron liquid," Phys. Rev. B **17**, 2862—2865.
Ivanov, I., and J. Pollmann, 1980, "Microscopic approach to

the quantum size effect in superlattices," Solid State Commun. **32**, 869–872.

Iye, Y., 1980, "Mobility of electrons in the surface state of liquid helium," J. Low Temp. Phys. **40**, 441–451.

Iye, Y., K. Kōno, K. Kajita, and W. Sasaki, 1979, "Escape rate of two-dimensional electrons on a liquid helium surface around 1 K," J. Low Temp. Phys. **34**, 539–550.

Iye, Y., K. Kōno, K. Kajita, and W. Sasaki, 1980, "Electron escape from the image-potential-induced surface states on liquid helium," J. Low Temp. Phys. **38**, 293–310.

Jaccodine, R. J., and W. A. Schlegel, 1966, "Measurement of strains at Si-SiO_2 interface," J. Appl. Phys. **37**, 2429–2434.

Jackman, T. E., J. R. MacDonald, L. C. Feldman, P. J. Silverman, and I. Stensgaard, 1980, "(100) and (110) Si-SiO_2 interface studies by MeV ion backscattering," Surf. Sci. **100**, 35–42.

Jackson, S. A., and P. M. Platzman, 1981, "Polaronic aspects of two-dimensional electrons on films of liquid He," Phys. Rev. B **24**, 499–502.

Jacoboni, C., C. Canali, G. Ottaviani, and A. Alberigi Quaranta, 1977, "A review of some charge transport properties of silicon," Solid-State Electron. **20**, 77–89.

Jacobs, E. P., and G. Dorda, 1978, "Mechanical stress at the (111)Si surface covered by SiO_2 and Al-SiO_2 layers," Surf. Sci. **73**, 357–364.

Jaklevic, R. C., and J. Lambe, 1975, "Experimental study of quantum size effects in thin metal films by electron tunneling," Phys. Rev. B **12**, 4146–4160.

Janak, J. F., 1969, "g Factor of the two-dimensional interacting electron gas," Phys. Rev. **178**, 1416–1418.

Jindal, R. P., and A. van der Ziel, 1978, "Carrier fluctuation noise in a MOSFET channel due to traps in the oxide," Solid-State Electron. **21**, 901–903.

Joannopoulos, J. D., and R. B. Laughlin, 1977, "Interface phonon states in amorphous Si-SiO_2," in *Amorphous and Liquid Semiconductors,* edited by W. E. Spear (Centre for Industrial Consultancy and Liaison, University of Edinburgh), pp. 487–489.

Johannessen, J. S., and T. A. Fjeldly, 1977, "The effect of as-grown oxide thickness and oxidation temperature on the electronic properties of Si-SiO_2 structures," in *Proceedings of the Seventh International Vaccum Congress and the Third International Conference on Solid Surfaces, Vienna,* edited by R. Dobrozemsky, F. Rüdenauer, F. P. Viehböck, and A. Breth (Berger, Horn, Austria), Vol. I, pp. 579–582.

Johannessen, J. S., W. E. Spicer, and Y. E. Strausser, 1976, "An Auger analysis of the Si-SiO_2 interface," J. Appl. Phys. **47**, 3028–3037.

Johnson, N. M., D. J. Bartelink, and J. P. McVittie, 1979, "Measurement of interface defect states at oxidized silicon surfaces by constant capacitance DLTS," J. Vac. Sci. Technol. **16**, 1407–1411.

Johnson, N. M., D. K. Biegelsen, and M. D. Moyer, 1980, "Characteristic defects at the Si-SiO_2 interface," in *The Physics of MOS Insulators,* edited by G. Lucovsky, S. T. Pantelides, and F. L. Galeener (Pergamon, New York), pp. 311–315.

Johnson, P. N., and H. H. Soonpaa, 1971, "Contact potential change accompanying size effect semimetal to semiconductor transition," in *The Physics of Semimetals and Narrow Gap Semiconductors,* edited by D. L. Carter and R. T. Bate (Pergamon, Oxford); J. Phys. Chem. Solids **32**, Suppl. 1, 121–123.

Jones, R. O., 1966, "Surface representations and complex band structure of a diamond-type semiconductor," Proc. Phys. Soc. London **89**, 443–451.

Jonson, M., 1976, "Electron correlations in inversion layers," J. Phys. C **9**, 3055–3071.

Jonson, M., and G. Srinivasan, 1977, "Magnetic field induced Wigner transition in inversion layers," Solid State Commun. **24**, 61–64.

Jonson, M., and G. Srinivasan, 1978, "The MOSFET inversion layer: The conductivity of a localized highly correlated phase," Phys. Scr. **18**, 476–480.

Judaprawira, S., W. I. Wang, P. C. Chao, C. E. C. Wood, D. W. Woodard, and L. F. Eastman, 1981, "Modulation-doped MBE GaAs/n-$Al_xGa_{1-x}As$ MESFETs," IEEE Electron Device Lett. **EDL-2**, 14–15.

Juretschke, H. S., R. Landauer, and J. A. Swanson, 1956, "Hall effect and conductivity in porous media," J. Appl. Phys. **27**, 838–839.

Kaczmarek, E., and E. Bangert, 1977, "Calculation of surface states in accumulation layer of tellurium," Solid State Commun. **22**, 165–168.

Kaczmarek, E., and E. Bangert, 1980, "Inversion layers of tellurium in magnetic fields," J. Phys. C **13**, 695–704.

Kajita, K., Y. Iye, K. Kōno, and W. Sasaki, 1978, "Escape rate of two-dimensional electrons on liquid helium surface," Solid State Commun. **27**, 1379–1383.

Kalia, R. K., S. Das Sarma, M. Nakayama, and J. J. Quinn, 1978, "Temperature dependence of many-body effects in inversion layers," Phys. Rev. B **18**, 5564–5566.

Kalia, R. K., S. Das Sarma, M. Nakayama, and J. J. Quinn, 1978, "Temperature dependence of the subband energies in semiconducting surface inversion layers: Exchange and correlation effects," in *Physics of Semiconductors, 1978,* edited by B. L. H. Wilson (Institute of Physics, Bristol), pp. 1247–1250.

Kalia, R. K., G. Kawamoto, J. J. Quinn, and S. C. Ying, 1980, "A simplified treatment of exchange and correlation in semiconducting surface inversion layers," Solid State Commun. **34**, 423–426.

Kalia, R. K., and J. J. Quinn, 1978, "Exchange instabilities in an n-type silicon inversion layer," Phys. Rev. B **17**, 1383–1387.

Kalia, R. K., P. Vashishta, and S. W. de Leeuw, 1981, "Melting of a two-dimensional electron lattice," Phys. Rev. B **23**, 4794–4797.

Kamgar, A., 1977, "Inter-subband spectroscopy in hole space charge layers on (110) and (111) Si surfaces," Solid State Commun. **21**, 823–826.

Kamgar, A., 1979, "Temperature dependence of many-body effects in Si accumulation layers: An experimental observation," Solid State Commun. **29**, 719–722.

Kamgar, A., and P. Kneschaurek, 1976, "Spectroscopy of surface charge layers on p-type Si," Surf. Sci. **58**, 135–137.

Kamgar, A., P. Kneschaurek, W. Beinvogl, and J. F. Koch, 1974a, "Spectroscopy of space charge layers on n-type Si," in *Proceedings of the 12th International Conference on the Physics of Semiconductors, Stuttgart,* edited by M. H. Pilkuhn (Teubner, Stuttgart), pp. 709–713.

Kamgar, A., P. Kneschaurek, G. Dorda, and J. F. Koch, 1974b, "Resonance spectroscopy of electron levels in a surface accumulation layer," Phys. Rev. Lett. **32**, 1251–1254.

Kamgar, A., M. D. Sturge, and D. C. Tsui, 1978, "Photoconductivity and absorption measurements on (100) and (911) Si MOSFETs," Surf. Sci. **73**, 166–169.

Kamgar, A., M. D. Sturge, and D. C. Tsui, 1980, "Optical

measurements of the minigaps in electron inversion layers on vicinal planes of Si(001)," Phys. Rev. B **22**, 841—847.

Kamgar, A., D. C. Tsui, and M. D. Sturge, 1977, "On the discrepancies between absorption and photoconductivity measurements in silicon inversion layers," Solid State Commun. **24**, 47—50.

Kamieniecki, E., 1979, "Ion-electron (configurational) interface states in MOS structures," Appl. Phys. Lett. **35**, 807—809.

Kamins, T. I., and N. C. MacDonald, 1968, "Measurements of the scattering of conduction electrons by surface charges," Phys. Rev. **167**, 754—758.

Kane, E. O., 1957, "Band structure of indium antimonide," J. Phys. Chem. Solids **1**, 249—261.

Kane, E. O., 1978, "Pollmann-Büttner variational method for excitonic polarons," Phys. Rev. B **18**, 6849—6855.

Kaplan, J. I., and M. L. Glasser, 1969, "g Factors for an interacting electron gas," Phys. Rev. **186**, 958.

Kaplan, R., 1979, "Periodic stepped structure on vicinal planes of (100) silicon," in *Physics of Semiconductors, 1978,* edited by B. L. H. Wilson (Institute of Physics, Bristol), pp. 1351—1354.

Kaplan, R., 1980, "LEED study of the stepped surface of vicinal Si(100)," Surf. Sci. **93**, 145—158.

Kaplit, M., and J. N. Zemel, 1968, "Capacitance observations of Landau levels in surface quantization," Phys. Rev. Lett. **21**, 212—215.

Karpushin, A. A., 1968, "Theory of shallow surface states," Fiz. Tverd. Tela (Leningrad) **10**, 3515—3518 [Sov. Phys.—Solid State **10**, 2793—2795 (1969)].

Karpushin, A. A., 1969, "Theory of surface donor states in silicon and germanium," Fiz. Tverd. Tela (Leningrad) **11**, 2163—2166 [Sov. Phys.—Solid State **11**, 1748—1750 (1970)].

Karpushin, A. A., and A. V. Chaplik, 1967, "Interaction of carriers with surface defects having a dipole moment," Fiz. Tekh. Poluprovodn. **1**, 1043—1046 [Sov. Phys.—Semicond. **1**, 870—872 (1968)].

Kassabov, J., N. Velchev, and V. Gancheva, 1974, "On the effect of gate oxide thickness upon the Hall mobility and other magneto-electrical characteristics in MOST structures," Solid-State Electron. **17**, 41—45.

Kastalsky, A., and F. F. Fang, 1982, "Effect of subband splitting on Si inversion layers," Surf. Sci. **113**, 153—160.

Katayama, Y., N. Kotera, and K. F. Komatsubara, 1970, "Oscillatory magnetoconductance and negative photoconductivity of quantized electrons in surface inversion layer of InSb," in *Proceedings of the Tenth International Conference on the Physics of Semiconductors, Cambridge, Massachusetts,* edited by S. P. Keller, J. C. Hensel, and F. Stern (U. S. Atomic Energy Commission, Oak Ridge, Tennessee), pp. 464—468.

Katayama, Y., N. Kotera, and K. F. Komatsubara, 1971, "Tunable infrared detector using photoconductivity of the quantized surface inversion layer of MOS transistor," in *Proceedings of the 2nd Conference on Solid State Devices, Tokyo, 1970* [J. Japan Soc. Appl. Phys. **40**, Suppl., 214—218].

Katayama, Y., K. Narita, Y. Shiraki, M. Aoki, and K. F. Komatsubara, 1977, "Conductance anomalies and electronic states in silicon inversion layers near threshold at low temperatures," J. Phys. Soc. Japan **42**, 1632—1639.

Katayama, Y., K. Narita, Y. Shiraki, T. Shimada, and K. F. Komatsubara, 1976, "Conductance enhancement of inversion layer electrons near threshold at low temperatures," in *Proceedings of the 13th International Conference on the Physics of Semiconductors, Rome,* edited by F. G. Fumi (North-Holland, Amsterdam), pp. 750—753.

Katayama, Y., I. Yoshida, N. Kotera, and K. F. Komatsubara, 1972, "Differential negative resistance of n-type inversion layer in silicon MOS field-effect transistor," Appl. Phys. Lett. **20**, 31—33.

Katto, H., M. Aoki, and E. Yamada, 1977, "Low-frequency noise in MOSFET's at low current levels," in *Proceedings of the Symposium on 1/f Fluctuations, Tokyo* (Institute of Electrical Engineers of Japan, Tokyo), pp. 148—155.

Kaveh, M., and N. F. Mott, 1981a, "Diffusion and logarithmic corrections to the conductivity of a disordered non-interacting 2D electron gas: Power law localisation," J. Phys. C **14**, L177—L182.

Kaveh, M., and N. F. Mott, 1981b, "Electron correlations and logarithmic singularities in density of states and conductivity of disordered two-dimensional systems," J. Phys. C **14**, L183—L190.

Kaveh, M., M. J. Uren, R. A. Davies, and M. Pepper, 1981, "Localization in disordered two dimensional systems and the universal dependence on diffusion length," J. Phys. C **14**, 413—419.

Kawabata, A., 1978, "Hartree-Fock solution of CDW of two-dimensional electron gas in magnetic field," Solid State Commun. **28**, 547—550.

Kawabata, A., 1980, "Many-body effects on the transverse conductivity of two-dimensional electron systems in strong magnetic fields," Surf. Sci. **98**, 276—282.

Kawabata, A., 1981a, "A self-consistent treatment of Anderson localization," Solid State Commun. **38**, 823—825.

Kawabata, A., 1981b, "Positive magnetoresistance induced by Zeeman splitting in two-dimensional systems," J. Phys. Soc. Japan **50**, 2461—2462.

Kawaguchi, Y., H. Kato, and S. Kawaji, 1974, "Electrical properties of Cs covered real Si surfaces," in *Proceedings of the Second International Conference on Solid Surfaces, Kyoto,"* [Jpn. J. Appl. Phys., Suppl. 2, Pt. 2, 429—432].

Kawaguchi, Y., and S. Kawaji, 1976, "Impurity band conduction in cesium adsorbed n-channel Si inversion layers," Surf. Sci. **58**, 33—41.

Kawaguchi, Y., and S. Kawaji, 1980a, "Lattice scattering mobility of n-inversion layers in Si(100) at low temperatures," Surf. Sci. **98**, 211—217.

Kawaguchi, Y., and S. Kawaji, 1980b, "Negative magnetoresistance in silicon (100) MOS inversion layers," J. Phys. Soc. Japan **48**, 699—700.

Kawaguchi, Y., and S. Kawaji, 1980c, "Negative magnetoresistance in a two-dimensional random system of Si-MOS inversion layers," in *Proceedings of the 15th International Conference on the Physics of Semiconductors, Kyoto* [J. Phys. Soc. Japan **49**, Suppl. A, 983—986].

Kawaguchi, Y., H. Kitahara, and S. Kawaji, 1978a, "Negative magnetoresistance in a two-dimensional impurity band in cesiated p-Si(111) surface inversion layers," Surf. Sci. **73**, 520—527.

Kawaguchi, Y., H. Kitahara, and S. Kawaji, 1978b, "Angular dependent negative magnetoresistance in Si-MOS (111) inversion layers," Solid State Commun. **26**, 701—703.

Kawaguchi, Y., T. Suzuki, and S. Kawaji, 1980, "Carrier concentration dependence and temperature dependence of mobility in silicon (100) n-channel inversion layers at low temperatures," Solid State Commun. **36**, 257—259.

Kawai, N. J., L. L. Chang, G. A. Sai-Halasz, C.-A. Chang, and L. Esaki, 1980, "Magnetic field-induced semimetal-to-semiconductor transition in InAs-GaSb superlattice," Appl. Phys. Lett. **36**, 369—371.

Kawaji, S., 1968, "Anomalous resistance and magnetoresistance in two dimensional transport in InAs," in *Proceedings of the Ninth International Conference on the Physics of Semiconductors, Moscow* (Nauka, Leningrad), Vol. 2, pp. 730–734.

Kawaji, S., 1969, "The two-dimensional lattice scattering mobility in a semiconductor inversion layer," J. Phys. Soc. Japan **27**, 906–908.

Kawaji, S., 1978, "Quantum galvanomagnetic experiments in silicon inversion layers under strong magnetic fields," Surf. Sci. **73**, 46–69.

Kawaji, S., H. Ezawa, and K. Nakamura, 1972, "Semiconductor inversion layers and phonons in half-space," J. Vac. Sci. Technol. **9**, 762–768.

Kawaji, S., and H. C. Gatos, 1967a, "The role of surface treatment in the field effect anomaly of *n*-type InSb at high magnetic fields," Surf. Sci. **6**, 362–368.

Kawaji, S., and H. C. Gatos, 1967b, "Electric field effect on the magnetoresistance of indium arsenide surfaces in high magnetic fields," Surf. Sci. **7**, 215–228.

Kawaji, S., K. Hatanaka, K. Nakamura, and S. Onga, 1976, "Mobility hump and inversion layer subbands in Si on sapphire," J. Phys. Soc. Japan **41**, 1073–1074.

Kawaji, S., H. Huff, and H. C. Gatos, 1965, "Field effect on magnetoresistance in *n*-type indium antimonide," Surf. Sci. **3**, 234–242.

Kawaji, S., T. Igarashi, and J. Wakabayashi, 1975, "Quantum galvanomagnetic effect in *n*-channel silicon inversion layers under strong magnetic fields," Prog. Theor. Phys. Suppl. **57**, 176–186.

Kawaji, S., and Y. Kawaguchi, 1966, "Galvanomagnetic properties of surface layers in indium arsenide," in *Proceedings of the International Conference on the Physics of Semiconductors, Kyoto* [J. Phys. Soc. Japan **21**, Suppl., 336–340].

Kawaji, S., and Y. Kawaguchi, 1968, "A new type of anomalous magnetoresistance in two dimensional transport in InAs," J. Phys. Soc. Japan **24**, 963.

Kawaji, S., S. Miki, and T. Kinoshita, 1975, "Superconductivity in InAs surfaces," J. Phys. Soc. Japan **39**, 1631–1632.

Kawaji, S., M. Namiki, and N. Hoshi, 1980, "Anderson localization in silicon MOS inversion layers at low densities," J. Phys. Soc. Japan **49**, 1637–1638.

Kawaji, S., and J. Wakabayashi, 1976, "Quantum galvanomagnetic properties of *n*-type inversion layers on Si (100) MOSFET," Surf. Sci. **58**, 238–245.

Kawaji, S., and J. Wakabayashi, 1977, "Temperature dependence of the magnetoconductivity in the ground Landau level in silicon inversion layers," Solid State Commun. **22**, 87–91.

Kawaji, S., and J. Wakabayashi, 1981, "Temperature dependence of transverse and Hall conductivities of silicon MOS inversion layers under strong magnetic fields," in *Physics in High Magnetic Fields*, edited by S. Chikazumi and M. Miura (Springer, Berlin), pp. 284–287.

Kawaji, S., J. Wakabayashi, M. Namiki, and K. Kusuda, 1978, "Electron localization in silicon inversion layers under strong magnetic fields," Surf. Sci. **73**, 121–128.

Kawakami, T., and M. Okamura, 1979, "InP/Al_2O_3 *n*-channel inversion-mode M.I.S.F.E.T.s using sulphur-diffused source and drain," Electron. Lett. **15**, 502–504.

Kawamoto, G., R. Kalia, and J. J. Quinn, 1980, "Effect of the electron-phonon interaction on the subband structure of inversion layers in compound semiconductors," Surf. Sci. **98**, 589–596.

Kawamoto, G. H., J. J. Quinn, and W. L. Bloss, 1981, "Subband structure of *n*-channel inversion layers on polar semiconductors," Phys. Rev. B **23**, 1875–1886.

Kazarinov, R. F., and Yu. V. Shmartsev, 1971, "Optical phenomena due to the carriers in a semiconductor with a superlattice," Fiz. Tekh. Poluprovodn. **5**, 800–802 [Sov. Phys.—Semicond. **5**, 710–711 (1971)].

Kazarinov, R. F., and R. A. Suris, 1971, "Possibility of the amplification of electromagnetic waves in a semiconductor with a superlattice," Fiz. Tekh. Poluprovodn. **5**, 797–800 [Sov. Phys.—Semicond. **5**, 707–709 (1971)].

Kazarinov, R. F., and R. A. Suris, 1972, "Electric and electromagnetic properties of semiconductors with a superlattice," Fiz. Tekh. Poluprovodn. **6**, 148–162 [Sov. Phys.—Semicond. **6**, 120–131 (1972)].

Keldysh, L. V., 1962, "Effect of ultrasonics on the electron spectrum of crystals," Fiz. Tverd. Tela (Leningrad) **4**, 2265–2267 [Sov. Phys.—Solid State **4**, 1658–1659 (1962)].

Keldysh, L. V., 1979a, "Coulomb interaction in thin semiconductor and semimetal films," Zh. Eksp. Teor. Fiz. Pis'ma Red. **29**, 716–719 [JETP Lett. **29**, 658–661 (1979)].

Keldysh, L. V., 1979b, "Polaritons in thin semiconducting films," Zh. Eksp. Teor. Fiz. Pis'ma Red. **30**, 244–249 [JETP Lett. **30**, 224–227 (1979)].

Kelly, M. J., 1978a, "Broken symmetry states in *n*-type silicon inversion layers," J. Phys. C **11**, 4239–4250.

Kelly, M. J., 1978b, "The phonon-mediated intervalley electron-electron interaction in silicon," Solid State Commun. **27**, 717–719.

Kelly, M. J., and L. M. Falicov, 1976, "Electronic structure of inversion layers in many-valley semiconductors," Phys. Rev. Lett. **37**, 1021–1024.

Kelly, M. J., and L. M. Falicov, 1977a, "Electronic ground state of inversion layers in many-valley semiconductors," Phys. Rev. B **15**, 1974–1982.

Kelly, M. J., and L. M. Falicov, 1977b, "Optical properties of charge-density-wave ground states for inversion layers in many-valley semiconductors," Phys. Rev. B **15**, 1983–1987.

Kelly, M. J., and L. M. Falicov, 1977c, "Broken-symmetry ground states in *n*-type inversion layers of Ge and GaP," J. Phys. C **10**, 1203–1209.

Kelly, M. J., and L. M. Falicov, 1977d, "Applied stresses, cyclotron masses and charge-density waves in silicon inversion layers," Solid State Commun. **22**, 447–450.

Kelly, M. J., and L. M. Falicov, 1977e, "Stress and temperature dependence of the electronic properties of *n*-type silicon inversion layers," J. Phys. C **10**, 4735–4752.

Kelly, M. J., and L. M. Falicov, 1977f, "Magnetic fields and the stability of charge-density-wave ground-states in silicon inversion layers," Solid State Commun. **24**, 535–537.

Kelly, M. J., and L. M. Falicov, 1978, "The dependence of the electronic ground state of *n*-type silicon inversion layers on stress, temperature, magnetic field and gate voltage," Surf. Sci. **73**, 303–314.

Kelly, M. J., and W. Hanke, 1981a, "Surface superconductivity and the MOS system," Phys. Rev. B **23**, 112–123.

Kelly, M. J., and W. Hanke, 1981b, "Electron-phonon interaction at a silicon surface," Phys. Rev. B **23**, 924–927.

Kennedy, T. A., B. D. McCombe, D. C. Tsui, and R. J. Wagner, 1978, "Temperature and band-gap-light dependence of far IR resonant magnetotransmission in Si inversion layers," Surf. Sci. **73**, 500–502.

Kennedy, T. A., R. J. Wagner, B. D. McCombe, and D. C. Tsui, 1975a, "Frequency dependence of cyclotron resonance in Si inversion layers," Crit. Rev. Solid State Sci. **5**, 391–395.

Kennedy, T. A., R. J. Wagner, B. D. McCombe, and D. C. Tsui, 1975b, "Frequency-dependent cyclotron effective masses in Si inversion layers," Phys. Rev. Lett. **35**, 1031–1034.

Kennedy, T. A., R. J. Wagner, B. D. McCombe, and J. J. Quinn, 1976a, "Lineshape distortions in FIR cyclotron resonance of MOS structures," Solid State Commun. **18**, 275–278.

Kennedy, T. A., R. J. Wagner, B. D. McCombe, and D. C. Tsui, 1976b, "Frequency dependent effective masses in Si inversion layers at metallic densities," Surf. Sci. **58**, 185–186.

Kennedy, T. A., R. J. Wagner, B. D. McCombe, and D. C. Tsui, 1977, "Far infrared resonant magnetoabsorption in low density Si inversion layers," Solid State Commun. **22**, 459–462.

Keyes, R. W., 1975a, "Effect of randomness in the distribution of impurity ions on FET thresholds in integrated electronics," IEEE J. Solid-State Circuits **SC-10**, 245–257.

Keyes, R. W., 1975b, "The effect of randomness in the distribution of impurity ions on FET thresholds," Appl. Phys. **8**, 251–259.

Keyes, R. W., 1976, "Accumulation and inversion layers on semiconductor surfaces," Comments Solid State Phys. **7**, 53–58.

Khaikin, M. S., 1968, "Magnetic surface levels," Usp. Fiz. Nauk. **96**, 409–440 [Sov. Phys.—Usp. **11**, 785–801 (1968)]; Adv. Phys. **18**, 1–40 (1969).

Khaikin, M. S., 1978a, "Stationary levels of the electron in the field of a polarized neutral particle," Zh. Eksp. Teor. Fiz. Pis'ma Red. **27**, 706–709 [JETP Lett. **27**, 668–670 (1978)].

Khaikin, M. S., 1978b, "Cinematographic investigation of bubblons in superfluid helium," J. Phys. (Paris) **39**, Colloques, C6-1295–C6-1297.

Khaikin, M. S., A. M. Trojanovsky, and A. P. Volodin, 1980, "Levels of charges at surface of dielectrics," Surf. Sci. **98**, 66–67.

Khor, K. E., and P. V. Smith, 1971, "Localization of electron states in two-dimensional disordered potential arrays," J. Phys. C **4**, 2029–2040.

Kierstead, H. A., 1976, "Dielectric constant and molar volume of saturated liquid ^{3}He and ^{4}He," J. Low Temp. Phys. **23**, 791–805.

Kingston, R. H., and S. F. Neustadter, 1955, "Calculation of the space charge, electric field, and free carrier concentration at the surface of a semiconductor," J. Appl. Phys. **26**, 718–720.

Kirkpatrick, S., 1973, "Percolation and conduction," Rev. Mod. Phys. **45**, 574–588.

Kirkpatrick, S., 1979, "Models of disordered materials," in *Ill Condensed Matter,* edited by R. Balian, R. Maynard, and G. Toulouse (North-Holland, Amsterdam), pp. 323–403.

Klaassen, F. M., 1971, "Characterization of low $1/f$ noise in MOS transistors," IEEE Trans. Electron Devices **ED-18**, 887–891.

Kleppmann, W. G., 1976, "Influence of electron-electron interactions on the localization of surface states," J. Phys. C **9**, L207–L210.

Kleppmann, W. G., and R. J. Elliott, 1975, "The Wigner transition in a magnetic field," J. Phys. C **8**, 2729–2736.

Klyuchnik, A. V., and Yu. E. Lozovik, 1978a, "Two-dimensional dielectric electron-hole liquid," Fiz. Tverd. Tela (Leningrad) **20**, 625–627 [Sov. Phys.—Solid State **20**, 364 (1978)].

Klyuchnik, A. V., and Yu. E. Lozovik, 1978b, "Interband transitions and currents in systems with e-h pairing," J. Phys. C **11**, L483–L487.

Klyuchnik, A. V., and Yu. E. Lozovik, 1979, "Effect of interband transitions on the current states in systems with electron-hole pairing," Zh. Eksp. Teor. Fiz. **76**, 670–686 [Sov. Phys.—JETP **49**, 335–343 (1979)].

Kneschaurek, P., A. Kamgar, and J. F. Koch, 1976, "Electronic levels in surface space charge layers on Si(100)," Phys. Rev. B **14**, 1610–1622.

Kneschaurek, P., and J. F. Koch, 1977, "Temperature dependence of the electron intersubband resonance on (100) Si surfaces," Phys. Rev. B **16**, 1590–1596.

Knotek, M. L., 1975, "Temperature and thickness dependence of low temperature transport in amorphous silicon films: A comparison to amorphous germanium," Solid State Commun. **17**, 1431–1433.

Kobayashi, Michisuke, J. Mizuno, and I. Yokota, 1975, "Magnetoplasma oscillation of a layered electron gas," J. Phys. Soc. Japan **39**, 18–21.

Kobayashi, Mineo, and K. F. Komatsubara, 1973, "Determination of g-factor of electrons in n-type Si surface inversion layers," Solid State Commun. **13**, 293–296.

Kobayashi, Mineo, and K. F. Komatsubara, 1974, "On the experimental g factor of conduction electrons in n-type inversion layer on silicon (100) surface," in *Proceedings of the Second International Conference on Solid Surfaces, Kyoto* [Jpn. J. Appl. Phys. Suppl. 2, Pt. 2, 343–346].

Kobayashi, S., F. Komori, Y. Ootuka, and W. Sasaki, 1980, "ln$T$ dependence of resistivity in two-dimensionally coupled fine particles of Cu," J. Phys. Soc. Japan **49**, 1635–1636.

Koch, J. F., 1975, "The dynamics of conduction electrons in surface space charge layers," in *Festkörperprobleme (Advances in Solid State Physics),* edited by H. J. Queisser (Pergamon-Vieweg, Braunschweig), Vol. XV, pp. 79–112.

Koch, J. F., 1976a, "Spectroscopy of surface space charge layers," Surf. Sci. **58**, 104–127.

Koch, J. F., 1976b, "Spectroscopy of surface space charge layers," J. Vac. Sci. Technol. **13**, 897–898.

Koch, F., 1979, "Electronic properties of insulator-semiconductor interfaces," Surf. Sci. **80**, 110–124.

Koch, F., 1980, "Those other space-charge layers," Surf. Sci. **98**, 571–588.

Koch, F., 1981, "Electric subbands in a magnetic field," in *Physics in High Magnetic Fields,* edited by S. Chikazumi and M. Miura (Springer, Berlin), pp. 262–273.

Koch, J. F., and T. E. Murray, 1969, "Electron scattering at a rough surface," Phys. Rev. **186**, 722–727.

Koch, J. F., and P. A. Pincus, 1967, "Microwave absorption by magnetic-field-induced surface states in superconductors," Phys. Rev. Lett. **19**, 1044–1046.

Koehler, T. R., 1966, "Exact matrix elements of a crystal Hamiltonian between harmonic-oscillator wave functions," Phys. Rev. **144**, 789–798.

Koehler, T. R., 1968, "New theory of lattice dynamics at 0°K," Phys. Rev. **165**, 942–950.

Kogan, V. G., and V. Z. Kresin, 1969, "Light absorption in a thin film in the presence of a quantum size effect," Fiz. Tverd. Tela (Leningrad) **11**, 3230–3235 [Sov. Phys.—Solid State **11**, 2618–2622 (1969)].

Kohl, D., C. Becker, G. Heiland, U. Niggebrügge, and P. Balk, 1981, "Hall measurements on MOSFET devices prepared by TCE oxidation," J. Phys. C **14**, 553–558.

Kohl, D., and G. Heiland, 1977, "Anomalous behaviour of electron mobility in space charge layers," Surf. Sci. **63**, 96–103.

Kohl, D., H. Moorman, and G. Heiland, 1978, "Correlated behavior of Hall mobility and work function in the case of accumulation layers on ZnO crystals," Surf. Sci. **73**, 160–162.

Köhler, H., 1980, "Valley splitting in *n*-type inverted silicon MOSFET surfaces," Surf. Sci. **98**, 378–389.

Köhler, H., and M. Roos, 1979a, "Quantitative determination of the valley splitting in *n*-type inverted silicon (100) MOSFET surfaces," Phys. Status Solidi B **91** 233–241.

Köhler, H., and M. Roos, 1979b, "The influence of the valley splitting and lineshape in the density of states on the quantum oscillations of *n*-type (100) inverted silicon MOSFET surfaces," Phys. Status Solidi B **92**, 489–494.

Köhler, H., and M. Roos, 1979c, "Evidence for a Landé-factor $g=2$ in *n*-type inverted silicon MOSFET surfaces," Phys. Status Solidi B **95**, 107–115.

Köhler, H., M. Roos, and G. Landwehr, 1978, "Magnetic field dependence of the valley splitting in *n*-type inverted silicon MOSFET surfaces," Solid State Commun. **27**, 955–959.

Kohn, W., 1961, "Cyclotron resonance and de Haas–van Alphen oscillations of an interacting electron gas," Phys. Rev. **123**, 1242–1244.

Kohn, W., and J. M. Luttinger, 1955, "Theory of donor states in silicon," Phys. Rev. **98**, 915–922.

Kohn, W., and L. J. Sham, 1965, "Self-consistent equations including exchange and correlation effects," Phys. Rev. **140**, A1133–A1138.

Komatsubara, K. F., H. Kamioka, and Y. Katayama, 1969, "Electrical conductivity in an *n*-type surface inversion layer of InSb at low temperature," J. Appl. Phys. **40**, 2940–2944.

Komatsubara, K. F., K. Narita, Y. Katayama, N. Kotera, and Mineo Kobayashi, 1974, "Transport properties of conduction electrons in *n*-type inversion layers in (100) surfaces of silicon," J. Phys. Chem. Solids **35**, 723–740.

Komiyama, S., H. Eyferth, and J. P. Kotthaus, 1980, "Phonon-induced intersubband resonance in an inversion layer," in *Proceedings of the 15th International Conference on the Physics of Semiconductors, Kyoto* [J. Phys. Soc. Japan **49**, Suppl. A, 687–690].

Komori, F., S. Kobayashi, Y. Ootuka, and W. Sasaki, 1981, "Experimental study of electron localization in a two-dimensional metal," J. Phys. Soc. Japan **50**, 1051–1052.

Kōno, K., Y. Iye, K. Kajita, S. Kobayashi, and W. Sasaki, 1980, "Electron escape from the image-potential-induced surface states on liquid helium," Surf. Sci. **98**, 17–21.

Konstantinov, O. V., and A. Ya. Shik, 1970, "Plasma surface states in semiconductors," Zh. Eksp. Teor. Fiz. **58**, 1662–1674 [Sov. Phys.—JETP **31**, 891–897 (1970)].

Korneev, O. N., V. N. Lutskii, and M. I. Elinson, 1970, "Investigation of the electron energy spectrum in bismuth films using the tunnel effect," Fiz. Tverd. Tela (Leningrad) **12**, 1333–1335 [Sov. Phys.—Solid State **12**, 1049–1050 (1970)].

Korneev, V. V., 1977, "Transverse conductivity of thin semiconductor films due to the scattering by acoustic phonons in quantizing magnetic fields," Fiz. Tverd. Tela (Leningrad) **19**, 357–363 [Sov. Phys.—Solid State **19**, 205–209 (1977)].

Korneev, V. V., 1978, "Thermomagnetic coefficients in a size-quantized semiconducting film," Zh. Eksp. Teor. Fiz. **74**, 1477–1482 [Sov. Phys.—JETP **47**, 773–776 (1978)].

Korneev, V. V., F. R. Ulinich, and N. A. Usov, 1978, "Screening of an electric field and of the Coulomb interaction in quantized films located in strong magnetic fields," Fiz. Tverd. Tela (Leningrad) **20**, 2448–2452 [Sov. Phys.—Solid State **20**, 1413–1415 (1978)].

Korotkikh, V. L., A. L. Musatov, and V. D. Shadrin, 1978, "Influence of size-effect quantization of energy levels in semiconductors on the photoelectric emission," Zh. Eksp. Teor. Fiz. Pis'ma Red. **27**, 652–655 [JETP Lett. **27**, 616–619 (1978)].

Korovin, L. I., S. T. Pavlov, and B. É. Éshpulatov, 1980, "Effect of optical phonons on magnetooptic absorption by a two-dimensional electron gas," Fiz. Tverd. Tela (Leningrad) **22**, 130–134 [Sov. Phys.—Solid State **22**, 74–77 (1980)].

Koshkin, V. M., and K. A. Katrunov, 1979, "Superlattice and quantum-size effect (QSE) in the intercalated crystals," Zh. Eksp. Teor. Fiz. Pis'ma Red. **29**, 205–209 [JETP Lett. **29**, 183–186 (1979)].

Kosterlitz, J. M., and D. J. Thouless, 1973, "Ordering, metastability and phase transitions in two-dimensional systems," J. Phys. C **6**, 1181–1203.

Kosterlitz, J. M., and D. J. Thouless, 1978, "Two-dimensional physics," in *Progress in Low Temperature Physics* (North-Holland, Amsterdam), Vol. VIIB, pp. 371–433.

Kotera, N., Y. Katayama, and K. F. Komatsubara, 1972a, "Magnetoconductance oscillations of *n*-type inversion layers in InSb surfaces," Phys. Rev. B **5**, 3065–3078.

Kotera, N., Y. Katayama, I. Yoshida, and K. F. Komatsubara, 1972b, "Two-dimensional impurity states in an *n*-type inversion layer of silicon," J. Vac. Sci. Technol. **9**, 754–757.

Kotthaus, J. P., 1978, "High frequency magnetoconductivity in space charge layers on semiconductors," Surf. Sci. **73**, 472–490.

Kotthaus, J. P., 1979, "Spectroscopy of semiconductor inversion layers in high magnetic fields," J. Magn. Magn. Mater. **11**, 20–25.

Kotthaus, J. P., 1980, "Spectroscopy of quasi-two-dimensional space charge layers," in *Proceedings of the 15th International Conference on the Physics of Semiconductors, Kyoto* [J. Phys. Soc. Japan **49**, Suppl. A, 937–945].

Kotthaus, J. P., G. Abstreiter, and J. F. Koch, 1974a, "Subharmonic structure of cyclotron resonance in an inversion layer on Si," Solid State Commun. **15**, 517–519.

Kotthaus, J. P., G. Abstreiter, J. F. Koch, and R. Ranvaud, 1974b, "Cyclotron resonance of localized electrons on a Si surface," Phys. Rev. Lett. **34**, 151–154.

Kotthaus, J. P., and H. Küblbeck, 1976, "Temperature dependence of the cyclotron resonance in electron inversion layers on Si," Surf. Sci. **58**, 199–201.

Kotthaus, J. P., and R. Ranvaud, 1977, "Cyclotron resonance of holes in surface space charge layers on Si," Phys. Rev. B **15**, 5758–5762.

Kovchavtsev, A. P., 1979, "Tunnel currents in the Au-SiO_2-Si system with the oxide film 16–36 Å thick," Fiz. Tverd. Tela (Leningrad) **21**, 3055–3060 [Sov. Phys.—Solid State **21**, 1758–1762 (1979)].

Krafcsik, I., and D. Marton, 1979, "Experimental study of the charge model of interface states," Phys. Lett. A **71**, 245–248.

Kramer, B., A. MacKinnon, and D. Weaire, 1981, "Numerical study of conductivity for the Anderson model in two and three dimensions," Phys. Rev. B **23**, 6357–6370.

Kramer, G. M., and R. F. Wallis, 1979, "Theory of impurity-shifted intersubband transitions in *n*-type inversion layers on (100) silicon," in *Physics of Semiconductors, 1978,* edited by B. L. H. Wilson (Institute of Physics, Bristol), pp. 1243–1246.

Krasheninnikov, M. V., and A. V. Chaplik, 1978, "Plasma-acoustic waves on the surface of a piezoelectric crystal," Zh. Eksp. Teor. Fiz. **75**, 1907–1918 [Sov. Phys.—JETP **48**, 960–966 (1978)].

Krasheninnikov, M. V., and A. V. Chaplik, 1979, "Resonance excitation of hypersound by two-dimensional plasmons," Zh. Eksp. Teor. Fiz. **76**, 1812–1815 [Sov. Phys.—JETP **49**, 921–923 (1979)].

Krasheninnikov, M. V., and A. V. Chaplik, 1980, "Instabilities of two-dimensional plasma waves," Zh. Eksp. Teor. Fiz. **79**, 555–560 [Sov. Phys.—JETP **52**, 279–282 (1980)].

Krasheninnikov, M. V., and A. V. Chaplik, 1981, "Two-dimensional plasma waves in superlattices," Fiz. Tekh. Poluprovodn. **15**, 32–39 [Sov. Phys.—Semicond. **15**, 19–23 (1981)].

Krasheninnikov, M. V., M. B. Sultanov, and A. V. Chaplik, 1979, "Interaction between two-dimensional plasmons and acoustic waves caused by the deformation potential," Zh. Eksp. Teor. Fiz. **77**, 1636–1642 [Sov. Phys.—JETP **50**, 821–824 (1979)].

Kressel, H., and J. K. Butler, 1977, *Semiconductor Lasers and Heterojunction LEDs* (Academic, New York).

Kress-Rogers, E., R. J. Nicholas, Th. Englert, and M. Pepper, 1981, "Two-dimensional conductivity in the contact regions of silicon MOSFETs," J. Phys. C **13**, L619–L622.

Krivanek, O. L. and J. H. Mazur, 1980, "The structure of ultrathin oxide on silicon," Appl. Phys. Lett. **37**, 392–394.

Krivanek, O. L., T. T. Sheng, and D. C. Tsui, 1978a, "A high-resolution electron microscopy study of the Si-SiO_2 interface," Appl. Phys. Lett. **32**, 437–439.

Krivanek, O. L., D. C. Tsui, T. T. Sheng, and A. Kamgar, 1978b, "A high-resolution electron microscopy study of the Si-SiO_2 interface," in *The Physics of SiO_2 and its Interfaces*, edited by S. T. Pantelides (Pergamon, New York), pp. 356–361.

Krowne, C. M., and J. W. Holm-Kennedy, 1974a, "Energy relaxation of electrons in the (100) *n*-channel of a Si-MOSFET. I. Bulk phonon treatment," Surf. Sci. **46**, 197–231.

Krowne, C. M., and J. W. Holm-Kennedy, 1974b, "Energy relaxation of electrons in the (100) *n*-channel of a Si-MOSFET. II. Surface phonon treatment," Surf. Sci. **46**, 232–250.

Küblbeck, H., and J. P. Kotthaus, 1975, "Temperature-dependent cyclotron mass of inversion-layer electrons in Si," Phys. Rev. Lett. **35**, 1019–1022.

Kubo, R., S. J. Miyake, and N. Hashitsume, 1965, "Quantum theory of galvanomagnetic effect at extremely strong magnetic fields," Solid State Phys. **17**, 269–364.

Kugler, A. A., 1969, "Anharmonic contributions to vibrational properties of the Wigner electron lattice," Ann. Phys. (N.Y.) **53**, 133–173.

Kukkonnen, C. A., and P. M. Maldague, 1976, "Electron-hole scattering and the electrical resistivity of the semimetal TiS_2," Phys. Rev. Lett. **37**, 782–785.

Kukushkin, L. S., 1980, "Optical analogy in the problem of galvanomagnetic properties of a quasi-two-dimensional conductor," Zh. Eksp. Teor. Fiz. **78**, 1020–1029 [Sov. Phys.—JETP **51**, 515–519 (1980)].

Kulik, I. O., and S. I. Shevchenko, 1977, "Excitonic 'superfluidity' in low-dimensional crystals," Solid State Commun. **21**, 409–411.

Kümmel, R., 1975, "Theory of valley-splitting in surface quantum states of silicon MOSFETs," Z. Phys. B **22**, 223–230.

Künzel, H., G. H. Döhler, A. Fischer, and K. Ploog, 1981, "Modulation of two-dimensional conductivity in a molecular beam epitaxially grown GaAs bulk space-charge system," Appl. Phys. Lett. **38**, 171–174.

Kuramoto, Y., 1978a, "Charge density waves of two-dimensional electrons in strong magnetic fields," J. Phys. Soc. Japan **44**, 1035–1036.

Kuramoto, Y., 1978b, "Classical and quantum two-dimensional Wigner crystal in strong magnetic fields," J. Phys. Soc. Japan **45**, 390–396.

Kuramoto, Y., and C. Horie, 1978, "Two-dimensional excitonic phase in strong magnetic fields," Solid State Commun. **25**, 713–716.

Kuramoto, Y., and H. Kamimura, 1974, "Theory of two-dimensional electron-hole liquids—Application to layer-type semiconductors," J. Phys. Soc. Japan **37**, 716–723.

Kuroda, T., and S. Narita, 1976, "Cyclotron resonance in an *n*-type inversion layer on $Hg_{1-x}Cd_xTe$ alloy," J. Phys. Soc. Japan **41**, 709–710.

Kurosawa, T., and S. Nagahashi, 1978, "On Gunn instability in two-dimensional semiconductors," J. Phys. Soc. Japan **45**, 707–708.

Kvon, Z. D., I. G. Neizvestnyi, V. N. Ovsyuk, and G. A. Yagunova, 1980, "Charge-carrier transport anisotropy in the inversion channels on high-index silicon surfaces," Zh. Eksp. Teor. Fiz. Pis'ma Red. **32**, 370–373 [JETP Lett. **32**, 346–348 (1980)].

LaBonney, J. J., Jr., and N. J. M. Horing, 1977, "Exchange energy of a two dimensional quantum plasma in a magnetic field," Surf. Sci. **64**, 437–456.

Lado, F., 1978, "Hypernetted-chain solutions for the two-dimensional classical electron gas," Phys. Rev. B **17**, 2827–2832.

Lai, W. Y., L. Y. Liou, and C. S. Ting, 1981, "Effect of intervalley electron-electron interaction on the resistivity of electrons in Si surface inversion layers," Phys. Rev. B **24**, 935–942.

Laidig, W. D., N. Holonyak, Jr., M. D. Camras, B. A. Vojak, K. Hess, J. J. Coleman, and P. D. Dapkus, 1981, "Quenching of stimulated phonon emission in $Al_xGa_{1-x}As$-GaAs quantum-well heterostructures," Solid State Commun. **38**, 301–304.

Lakhani, A. A., T. Cole, and P. J. Stiles, 1978, "Superlattice and a two-dimensional electron gas," Surf. Sci. **73**, 223–225.

Lakhani, A. A., T. Cole, and P. J. Stiles, 1981, "Substrate bias effects on subband separation and interband scattering in Si (110) *p*-channel MOSFETs," Solid State Commun. **39**, 569–572.

Lakhani, A. A., T. K. Lee, and J. J. Quinn, 1976, "Dependence on substrate bias of the effective mass and Dingle temperature of electrons in the surface inversion layer of silicon," Surf. Sci. **58**, 213–216.

Lakhani, A. A., and P. J. Stiles, 1973, "Experimental study of oscillatory values of g^* of a two-dimensional electron gas," Phys. Rev. Lett. **31**, 25–28.

Lakhani, A. A., and P. J. Stiles, 1975a, "Shubnikov–de Haas oscillations in *n*-type inversion layers on (110) and (111) surfaces of Si," Phys. Lett. A **51**, 117–118.

Lakhani, A. A., and P. J. Stiles, 1975b, "Modification of the magnetoconductance of a two-dimensional electron gas by altering the boundary conditions in the third dimension," Solid State Commun. **16**, 993–996.

Lakhani, A. A., and P. J. Stiles, 1976a, "Effect of substrate bias on the mobility and scattering time of electrons in Si inversion layers," Surf. Sci. **58**, 193–198.

Lakhani, A. A., and P. J. Stiles, 1976b, "Critical tests of the theory of magnetoconductance in two dimensions," Phys. Rev. B **13**, 5386–5391.

Lakhani, A. A., P. J. Stiles, and Y. C. Cheng, 1974, "Oscillatory magnetoconductance of *p*-type inversion layers in Si sur-

faces," Phys. Rev. Lett. **32**, 1003—1006.
Lambert, D. K., and P. L. Richards, 1980, "Measurement of local disorder in a two-dimensional electron fluid," Phys. Rev. Lett. **44**, 1427—1429.
Lambert, D. K., and P. L. Richards, 1981, "Far-infrared and capacitance measurements of electrons on liquid helium," Phys. Rev. B **23**, 3282—3290.
Landau, L. D., 1956, "The theory of a Fermi liquid," Zh. Eksp. Teor. Fiz. **30**, 1058—1064 [Sov. Phys.—JETP **3**, 920—925 (1957)].
Landau, L. D., and E. M. Lifshitz, 1977, *Quantum Mechanics* 3rd ed. (Pergamon, Oxford).
Landauer, R., 1970, "Electrical resistance of disordered one-dimensional lattices," Philos. Mag. **21**, 863—867.
Landwehr, G., 1975, "Quantum transport in silicon inversion layers," in *Festkörperprobleme (Advances in Solid State Physics)*, edited by H. J. Queisser (Pergamon-Vieweg, Braunschweig), Vol. XV, pp. 49—77.
Landwehr, G., 1977, "Semiconductor cyclotron resonance: Transport and surface phenomena," J. Opt. Soc. Am. **67**, 922—928.
Landwehr, G., 1980, "Recent results of high magnetic field experiments on MOSFETs in Grenoble," Surf. Sci. **98**, 321—326.
Landwehr, G., E. Bangert, and K. von Klitzing, 1975, "Surface quantum oscillations in silicon," in *Physique sous Champs Magnétiques Intenses, Grenoble, 1974* (Colloques Internationaux No. 242, Éditions du Centre National de la Recherche Scientifique, Paris), pp. 177—185.
Landwehr, G., E. Bangert, K. von Klitzing, Th. Englert, and G. Dorda, 1976, "Comments on the hole mass in silicon inversion layers," Solid State Commun. **19**, 1031—1035.
Lang, N. D., and W. Kohn, 1970, "Theory of metal surfaces: Charge density and surface energy," Phys. Rev. B **1**, 4555—4568.
Larkin, A. I., 1980, "Reluctance of two-dimensional systems," Zh. Eksp. Teor. Fiz. Pis'ma Red. **31**, 239—243 [JETP Lett. **31**, 219—223 (1980)].
Last, B. J., and D. J. Thouless, 1971, "Percolation theory and electrical conductivity," Phys. Rev. Lett. **27**, 1719—1721.
Lau, K. H., and W. Kohn, 1978, "Indirect long-range oscillatory interaction between adsorbed atoms," Surf. Sci. **75**, 69—85.
Laughlin, R. B., 1981, "Quantized Hall conductivity in two dimensions," Phys. Rev. B **23**, 5632—5633.
Laughlin, R. B., J. D. Joannopoulos, and D. J. Chadi, 1978, "Electronic states of Si-SiO_2 interfaces," in *The Physics of SiO_2 and its Interfaces*, edited by S. T. Pantelides, (Pergamon, New York), pp. 321—327.
Laughlin, R. B., J. D. Joannopoulos, and D. J. Chadi, 1980, "Theory of the electronic structure of the Si-SiO_2 interface," Phys. Rev. B **21**, 5733—5744.
Laur, J., and T. S. Jayadevaiah, 1973, "Carrier concentration in the inversion layer of an MOS field effect transistor," Solid-State Electron. **16**, 644—646.
Lax, M., and J. J. Hopfield, 1961, "Selection rules connecting different points in the Brillouin zone," Phys. Rev. **124**, 115—123.
Lebwohl, P. A., and R. Tsu, 1970, "Electrical transport properties in a superlattice," J. Appl. Phys. **41**, 2664—2667.
Lee, P. A. (editor), 1976, *Optical and Electrical Properties* (Vol. 4 of *Physics and Chemistry of Materials with Layered Structures*, edited by E. Mooser) (Reidel, Dordrecht).
Lee, P. A., 1979, "Real-space scaling studies of localization," Phys. Rev. Lett. **42**, 1492—1494.
Lee, P. A., 1980, "Scaling studies of localization," J. Noncryst. Solids **35—36**, 21—28.
Lee, P. A., and D. S. Fisher, 1981, "Anderson localization in two dimensions," Phys. Rev. Lett. **47**, 882—885.
Lee, P. A., and T. M. Rice, 1979, "Electric field depinning of charge density waves," Phys. Rev. B **19**, 3970—3980.
Lee, T. K., and J. J. Quinn, 1975, "Fermi liquid theory of two dimensional electron liquid: Magnetoplasma waves," Phys. Rev. B **11**, 2144—2147.
Lee, T. K., and J. J. Quinn, 1976, "Quantum oscillations in screening in a two-dimensional electron gas," Surf. Sci. **58**, 148—152.
Lee, T. K., C. S. Ting, and J. J. Quinn, 1975a, "Electron-electron interactions in the surface inversion layer of a semiconductor," Solid State Commun. **16**, 1309—1312.
Lee, T. K., C. S. Ting, and J. J. Quinn, 1975b, "Landau interaction function for electrons in the surface inversion layer of a semiconductor: A test of many-body theory," Phys. Rev. Lett. **35**, 1048—1050.
Lee, T. K., C. S. Ting, and J. J. Quinn, 1976, "Microscopic calculation of the Fermi liquid interaction constants for electrons in the surface inversion layer of a semiconductor," Surf. Sci. **58**, 246—251.
Leiderer, P., 1979, "Charged interface of ^{3}He-^{4}He mixtures. Softening of interfacial waves," Phys. Rev. B **20**, 4511—4517.
Leiderer, P., and M. Wanner, 1979, "Structure of the dimple lattice on liquid ^{4}He," Phys. Lett. A **73**, 189—192.
Leiderer, P., M. Wanner, and W. Schoepe, 1978, "Ions at the critical interface of ^{3}He-^{4}He mixtures," J. Phys. (Paris) **39**, C6-1328—C6-1333.
Leistiko, O., Jr., A. S. Grove, and C. T. Sah, 1965, "Electron and hole mobilities in inversion layers on thermally oxidized silicon surfaces," IEEE Trans. Electron Devices **ED-12**, 248—254.
Lekner, J., and J. R. Henderson, 1978, "The surface of liquid ^{4}He, based on the idea that $\Pi_{i<j} f(r_{ij})$ describes a droplet," J. Low Temp. Phys. **31**, 763—784.
Lenzlinger, M. and E. H. Snow, 1969, "Fowler-Nordheim tunneling into thermally grown SiO_2," J. Appl. Phys. **40**, 278—283.
Lerner, I. V., and Yu. E. Lozovik, 1977, "Two-dimensional electron-hole liquid in the strong magnetic field," Solid State Commun. **23**, 453—458.
Lerner, I. V., and Yu. E. Lozovik, 1978a, "Quasi two-dimensional electron-hole liquid in strong magnetic fields," Zh. Eksp. Teor. Fiz. **74**, 274—287 [Sov. Phys.—JETP **47**, 140—147 (1978)].
Lerner, I. V., and Yu. E. Lozovik, 1978b, "Interaction of quasiparticles near the interface of two media," Fiz. Tverd. Tela (Leningrad) **20**, 2241—2245 [Sov. Phys.—Solid State **20**, 1293—1295 (1978)].
Lerner, I. V., and Yu. E. Lozovik, 1978c, "On the crystallization of two-dimensional electron system in strong magnetic field," Solid State Commun. **25**, 205—208.
Lerner, I. V., and Yu. E. Lozovik, 1978d, "Phase diagram of quasi-zero-dimensional electron-hole system," Zh. Eksp. Teor. Fiz. Pis'ma Red. **27**, 497—499 [JETP Lett. **27**, 467—470 (1978)].
Lerner, I. V., and Yu. E. Lozovik, 1979a, "Thermodynamics of electrons in a quantized semimetal film in high magnetic field," Zh. Eksp. Teor. Fiz. **76**, 1136—1150 [Sov. Phys.—JETP **49**, 576—583 (1979)].
Lerner, I. V., and Yu. E. Lozovik, 1979b, "Electron-hole rear-

rangements in two-dimensional semimetals in high magnetic fields," J. Phys. C **12**, L501–L505.
Lerner, I. V., and Yu. E. Lozovik, 1980a, "Phase transitions in two-dimensional electron-hole systems in high magnetic fields," J. Low Temp. Phys. **38**, 333–352.
Lerner, I. V., and Yu. E. Lozovik, 1980b, "Mott exciton in a quasi-two-dimensional semiconductor in a strong magnetic field," Zh. Eksp. Teor. Fiz. **78**, 1167–1175 [Sov. Phys.—JETP **51**, 588–592 (1980)].
Lerner, I. V., and Yu. E. Lozovik, 1980c, "Correlation energy and excitation spectra of two-dimensional electron-hole systems in high magnetic fields," Solid State Commun. **36**, 7–13.
Lerner, I. V., Yu. E. Lozovik, and D. R. Musin, 1981, "Spatially separated electron-hole system in high magnetic fields," J. Phys. C **14**, L311–L315.
Levine, J. D., 1965, "Nodal hydrogenic wave functions of donors on semiconductor surfaces," Phys. Rev. **140**, A586–A589.
Lévy, F. (editor), 1976, *Crystallography and Crystal Chemistry of Materials with Layered Structures* (Vol. 2 of *Physics and Chemistry of Materials with Layered Structures,* edited by E. Mooser) (Reidel, Dordrecht).
Lewicki, G., and J. Maserjian, 1975, "Oscillations in MOS tunneling," J. Appl. Phys. **46**, 3032–3039.
Licari, J. J., 1979, "Polaron self-energy in a dielectric slab," Solid State Commun. **29**, 625–628.
Licciardello, D. C., 1977, "Is 30,000 ohms the maximum two-dimensional resistance?" Comments Solid State Phys. **8**, 61–66.
Licciardello, D. C., and H. H. Soonpaa, 1980, "Variable range hopping in a thin crystal," Surf. Sci. **98**, 225–226.
Licciardello, D. C., and D. J. Thouless, 1975a, "Constancy of minimum metallic conductivity in two dimensions," Phys. Rev. Lett. **35**, 1475–1478.
Licciardello, D. C., and D. J. Thouless, 1975b, "Conductivity and mobility edges for two-dimensional disordered systems," J. Phys. C **8**, 4157–4170.
Licciardello, D. C., and D. J. Thouless, 1976a, "Universality and transport in two-dimensional disordered systems," Surf. Sci. **58**, 89–90.
Licciardello, D. C., and D. J. Thouless, 1976b, "On the extent of the localized wavefunction," J. Phys. C **9**, L417–L419.
Licciardello, D. C., and D. J. Thouless, 1977, "Fluctuations of the localized wave function," Commun. Phys. **2**, 7–8.
Licciardello, D. C. and D. J. Thouless, 1978, "Conductivity and mobility edges in disordered systems II. Further calculations for the square and diamond lattices," J. Phys. C **11**, 925–936.
Lieneweg, U., 1980, "Frequency response of charge transfer in MOS inversion layers," Solid-State Electron. **23**, 577–583.
Lile, D. L., D. A. Collins, L. G. Meiners, and L. Messik, 1978, "*n*-channel inversion-mode InP M.I.S.F.E.T.," Electron. Lett. **14**, 657–659.
Lin-Chung, P. J., 1979, "Quantized surface states in an accumulation layer of *n*-PbTe," in *Physics of Semiconductors, 1978,* edited by B. L. H. Wilson (Institute of Physics, Bristol), pp. 1223–1226.
Lindemann, G., E. Gornik, R. Schawarz, and D. C. Tsui, 1981, "Cyclotron emission from GaAs and InP," in *Gallium Arsenide and Related Compounds, 1980,* edited by H. W. Thim (Institute of Physics, Bristol), pp. 631–638.
Lindhard, J., 1954, "On the properties of a gas of charge particles," K. Dan. Vidensk. Selsk. Mat.-Fys. Medd. **28** (8), 1–57.
Lipari, N. O., 1978, "Electronic states of impurities localized at or near semiconductor-insulator interfaces," J. Vac. Sci. Technol. **15**, 1412–1416.
Litovchenko, V. G., 1978, "Characteristics of quasi-two-dimensional excitons and plasmons at various concentrations," Surf. Sci. **73**, 446–471.
Long, D., 1960, "Scattering of conduction electrons by lattice vibrations in silicon," Phys. Rev. **120**, 2024–2032.
Lozovik, Yu. E., S. M. Apenko, and A. V. Klyuchnik, 1980, "Two-dimensional electron crystal in magnetic field. Topological phase transitions and stability region," Solid State Commun. **36**, 485–492.
Lozovik, Yu. E., and A. V. Klyuchnik, 1980, "Current states and domains in systems with electron-hole pairing," J. Low Temp. Phys. **38**, 761–775.
Lozovik, Yu. E., D. R. Musin, and V. I. Yudson, 1979, "Range of existence of a two-dimensional electron crystal in a strong magnetic field," Fiz. Tverd. Tela (Leningrad) **21**, 1974–1977 [Sov. Phys.—Solid State **21**, 1132–1134 (1979)].
Lozovik, Yu. E., and V. N. Nishanov, 1976, "Wannier-Mott excitons in layer structures and near an interface of two media," Fiz. Tverd. Tela (Leningrad) **18**, 3267–3272 [Sov. Phys.—Solid State **18**, 1905–1908 (1976)].
Lozovik, Yu. E., and V. I. Yudson, 1975a, "Crystallization of two-dimensional electron gas in a magnetic field," Zh. Eksp. Teor. Fiz. Pis'ma Red. **22**, 26–28 [JETP Lett. **22**, 11–12 (1975)].
Lozovik, Yu. E., and V. I. Yudson, 1975b, "Feasibility of superfluidity of paired spatially separated electrons and holes; a new superconductivity mechanism," Zh. Eksp. Teor. Fiz. Pis'ma Red. **22**, 556–559 [JETP Lett. **22**, 274–276 (1975)].
Lozovik, Yu. E., and V. I. Yudson, 1976a, "Superconductivity at dielectric pairing of spatially separated quasiparticles," Solid State Commun. **19**, 391–393.
Lozovik, Yu. E., and V. I. Yudson, 1976b, "A new mechanism for superconductivity: Pairing between spatially separated electrons and holes," Zh. Eksp. Teor. Fiz. **71**, 738–753 [Sov. Phys.—JETP **44**, 389–397 (1976)].
Lozovik, Yu. E., and V. I. Yudson, 1976c, "Electron-hole superconductor in electromagnetic fields," Fiz. Tverd. Tela (Leningrad) **18**, 1962–1966 [Sov. Phys.—Solid State **18**, 1142–1144 (1976)].
Lozovik, Yu. E., and V. I. Yudson, 1976d, "Excitonic insulator transition in thin films," Phys. Lett. A **56**, 393–394.
Lozovik, Yu. E., and V. I. Yudson, 1977a, "Electron-hole superconductivity. Influence of structure defects," Solid State Commun. **21**, 211–215.
Lozovik, Yu. E., and V. I. Yudson, 1977b, "The phase fixation in the systems with *e-h* pairing; Collective modes and current states," Solid State Commun. **22**, 117–122.
Lucovsky, G., and D. J. Chadi, 1980, "A microscopic model for the Q_{ss} defect at the Si/SiO_2 interface," in *The Physics of MOS Insulators,* edited by G. Lucovsky, S. T. Pantelides, and F. L. Galeener (Pergamon, New York), pp. 301–305.
Lucovsky, G., S. T. Pantelides, and F. L. Galeener, eds., 1980, *The Physics of MOS Insulators* (Pergamon, New York).
Lundqvist, B. I., 1967a, "Single-particle spectrum of the degenerate electron gas I. The structure of the spectral weight function," Phys. Kondens. Mater. **6**, 193–205.
Lundqvist, B. I., 1967b, "Single-particle spectrum of the degenerate electron gas II. Numerical results for electrons coupled to plasmons," Phys. Kondens. Mater. **6**, 206–217.
Lutskii, V. N., 1970, "Quantum size effect—Present state and perspectives of experimental investigations," Phys. Status

Solidi A **1**, 199–220.
Lutskii, V. N., and E. P. Fesenko, 1968, "Some possibilities for investigating the structure of electronic spectra using the quantum-size effect," Fiz. Tverd. Tela (Leningrad) **10**, 3661–3663 [Sov. Phys.—Solid State **10**, 2902–2904 (1968)].
Lutskii, V. N., and T. N. Pinsker, 1980, "Quantum size effect in films and new method for investigating the band structure of solids," Thin Solid Films **66**, 55–69.
Luttinger, J. M., and W. Kohn, 1955, "Motion of electrons and holes in perturbed periodic fields," Phys. Rev. **97**, 869–883.
Ma, K. B., and J. C. Inkson, 1978, "Possible-re-evaporation of two-dimensional Wigner crystals at extremely low densities," J. Phys. C **11**, L411–L415.
Ma, T. P., and R. C. Barker, 1974, "Surface-state spectra from thick-oxide MOS tunnel junctions," Solid-State Electron. **17**, 913–929.
Maan, J. C., Y. Guldner, J. P. Vieren, P. Voisin, M. Voos, L. L. Chang, and L. Esaki, 1981, "Three dimensional character of semimetallic InAs-GaSb superlattices," Solid State Commun. **39**, 683–686.
Mackie, F. D., and C.-W. Woo, 1978, "Surface structure of liquid ^{4}He," Phys. Rev. B **18**, 529–535.
Madhukar, A., 1977, "Coupled electron-phonon system in two dimensions and its implications for inversion layers," Solid State Commun. **24**, 11–14.
Madhukar, A., N. V. Dandekar, and R. N. Nucho, 1979, "Two-dimensional effects and effective masses in InAs/GaSb (100) superlattices," J. Vac. Sci. Technol. **16**, 1507–1511.
Madhukar, A., and S. Das Sarma, 1980, "Electron-phonon coupling and resonant magneto-phonon effect in optical behavior of two-dimensionally confined charge carriers," Surf. Sci. **98**, 135–142.
Madhukar, A., and R. N. Nucho, 1979, "The electronic structure of InAs/GaSb (001) superlattices — two dimensional effects," Solid State Commun. **32**, 331–336.
Maeda, H., 1970, "Negative mass effect and the energy dispersion of carriers in MOS inversion layers: Possibility of a novel solid state oscillator," in *Proceedings of the 1st Conference on Solid State Devices, Tokyo, 1969* [J. Japan Soc. Appl. Phys. **39** Suppl., 185–191].
Maeda, H., 1972, "Electron conductivity-mass anisotropy in silicon MOS inversion layers," J. Phys. Soc. Japan **32**, 575.
Maekawa, S., and H. Fukuyama, 1981, "Magnetoresistance in two-dimensional disordered systems: Effects of Zeeman splitting and spin-orbit scattering," J. Phys. Soc. Japan **50**, 2516–2524.
Mahan, G. D., 1974, "Electron interaction with surface modes," in *Elementary Excitations in Solids, Molecules, and Atoms,* edited by J. T. Devreese, A. B. Kunz, and T. C. Collins (Plenum, London), Part B, pp. 93–130.
Maldague, P. F., 1978a, "Many-body corrections to the polarizability of the two-dimensional electron gas," Surf. Sci. **73**, 296–302.
Maldague, P. F., 1978b, "Effect of exchange on charge density waves in layered compounds," Solid State Commun. **26**, 133–135.
Maldague, P. F., and D. M. Nicholson, 1980, "A variational approach to the ground state of the two-dimensional electron gas," Physica **99B**, 250–254.
Maldague, P. F., 1981, "Quantum diffusion and divergent fluctuations in disordered metals," Phys. Rev. B **23**, 1719–1728.
Maldonado, J. R., and J. F. Koch, 1970, "Surface states in superconducting indium," Phys. Rev. B **1**, 1031–1039.
Manuel, P., G. A. Sai-Halasz, L. L. Chang, C.-A. Chang, and L. Esaki, 1976, "Resonant Raman scattering in a semiconductor superlattice," Phys. Rev. Lett. **37**, 1701–1704.
Many, A., 1974, "Relation between physical and chemical processes on semiconductor surfaces," Crit. Rev. Solid State Sci. **4**, 515–539.
Many, A., Y. Goldstein, and N. B. Grover, 1965, *Semiconductor Surfaces* (North-Holland, Amsterdam).
Many, A., I. Wagner, A. Rosenthal, J. I. Gersten, and Y. Goldstein, 1981, "Plasmas on quantized accumulation layers on ZnO surfaces," Phys. Rev. Lett. **46**, 1648–1651.
Marchand, A., and N. Lumbroso, 1960, "Magnetic susceptibility of a two-dimensional electron gas with an energy proportional to k^n," in *Proceedings of the Fourth Conference on Carbon,* (Pergamon, Oxford), pp. 189–195.
Margalit, S., A. Neugroschel, and A. Bar-Lev, 1972, "Redistribution of boron and phosphorous in silicon after two oxidation steps used in MOST fabrication," IEEE Trans. Electron Devices ED-**19**, 861–868.
Margoninsky, Y., and D. Eger, 1979, "The influence of ion bombardment and annealing on the conductivity of the polar ZnO (000$\bar{1}$) surface," Surf. Sci. **80**, 579–585.
Markiewicz, R. S., and L. A. Harris, 1981, "Two-dimensional resistivity of ultrathin metal films," Phys. Rev. Lett. **46**, 1149–1153.
Martin, B. G., and R. F. Wallis, 1976, "Theory of bound states associated with *n*-type inversion layers on silicon (001) surfaces," in *Proceedings of the 13th International Conference on the Physics of Semiconductors, Rome,* edited by F. G. Fumi (North-Holland, Amsterdam), pp. 792–795.
Martin, B. G., and R. F. Wallis, 1978, "Theory of bound states associated with *n*-type inversion layers on silicon," Phys. Rev. B **18**, 5644–5648.
Martin, R. M., 1969, "Dielectric screening model for lattice vibrations of diamond-structure crystals," Phys. Rev. **186**, 871–884.
Marty, D., J. Poitrenaud, and F. I. B. Williams, 1980, "Observation of liquid-to-crystal transition in a two-dimensional electronic system," J. Phys. (Paris) Lett. **41**, L311–L314.
Maschke, K., H. Overhof, and P. Thomas, 1974, "On variable range hopping near the Fermi energy. Two-dimensional systems," Phys. Status Solidi B **62**, 113–122.
Maserjian, J., 1974, "Tunneling in thin MOS structures," J. Vac. Sci. Technol. **11**, 996–1003.
Matheson, T. G., and R. J. Higgins, 1980, "Magnetic breakdown in the tipped Si 'superlattice'," in *Proceedings of the 15th International Conference on the Physics of Semiconductors Kyoto* [J. Phys. Soc. Japan **49**, Suppl. A, 967–970].
Matheson, T. G., and R. J. Higgins, 1982, "Tunneling in tilted Si inversion layers," Phys. Rev. B **25**, 2633–2644.
Matsumoto, Y., and Y. Uemura, 1974, "Scattering mechanism and low temperature mobility of MOS inversion layers," in *Proceedings of the Second International Conference on Solid Surfaces, Kyoto* [Jpn. J. Appl. Phys. Suppl. **2**, Pt. 2, 367–370].
McCombe, B. D., and T. Cole, 1980, "Intersubband spectroscopy of inversion layers in the principal surfaces of silicon: Many-body and 'impurity' effects," Surf. Sci. **98**, 469–480.
McCombe, B. D., R. T. Holm, and D. E. Schafer, 1979, "Frequency domain studies of intersubband optical transitions in Si inversion layers," Solid State Commun. **32**, 603–608.
McCombe, B. D., and D. E. Schafer, 1979, "Effects of Na^+ ions on far IR optical spectroscopy of Si inversion layers," in *Physics of Semiconductors, 1978,* edited by B. L. H. Wilson (Institute of Physics, Bristol), pp. 1227–1230.

McCombe, B. D., and R. J. Wagner, 1971, "Electric-dipole excited electron spin resonance in InSb," Phys. Rev. B **4**, 1285–1288.

McNutt, M. J., and C. T. Sah, 1974a, "High frequency space charge layer capacitance of strongly inverted semiconductor surfaces," Solid-State Electron. **17**, 377–385.

McNutt, M. J., and C. T. Sah, 1974b, "Effects of spatially inhomogeneous oxide charge distribution on the MOS capacitance-voltage characteristics," J. Appl. Phys. **45**, 3916–3921.

McNutt, M. J., and C. T. Sah, 1975, "Experimental observations of the effects of oxide charge inhomogeneity on fast surface state density from high-frequency MOS capacitance-voltage characteristics," Appl. Phys. Lett. **26**, 378–380.

McNutt, M. J., and C. T. Sah, 1976, "Exact capacitance of a lossless MOS capacitor," Solid-State Electron. **19**, 255–257.

McNutt, M. J., and C. T. Sah, 1978, "Experimental MOS *C-V* data in strong inversion," IEEE Trans. Electron Devices ED-**25**, 847–848.

McSkimin, H. J., 1953, "Measurement of elastic constants at low temperatures by means of ultrasonic waves — Data for silicon and germanium single crystals, and for fused silica," J. Appl. Phys. **24**, 988–997.

McTague, J. P., M. Nielsen, and L. Passell, 1980, "Structure and phase transitions in physisorbed monolayers," in *Ordering in Strongly Fluctuating Condensed Matter Systems,* edited by T. Riste (Plenum, New York), pp. 195–220.

Mehrotra, R., and A. J. Dahm, 1979, "Linewidths of resonances in a two-dimensional Wigner lattice on a liquid-helium surface," Phys. Rev. Lett. **43**, 467–470.

Meiners, L. G., D. L. Lile, and D. A. Collins, 1979, "Inversion layers on InP," J. Vac. Sci. Technol. **16**, 1458–1461.

Meissner, G., 1970, "Crystallization instabilities in highly anharmonic crystals," Phys. Rev. B **1**, 1822–1830.

Meissner, G., 1976, "Magnetic field dependence of vibrational excitations in a two-dimensional triangular Wigner crystal," Z. Phys. B **23**, 173–176.

Meissner, G., 1978, "Collective excitations and electrodynamic behavior of electrons in a three-layer structure," Surf. Sci. **73**, 411–418.

Meissner, G., and A. Flammang, 1976, "Dynamical instability of two-dimensional honeycomb Wigner crystal," Phys. Lett. A **57**, 277–278.

Meissner, G., H. Namaizawa, and M. Voss, 1976, "Stability and image-potential-induced screening of electron vibrational excitations in a three-layer structure," Phys. Rev. B **13**, 1370–1376.

Mele, E. J., and J. J. Ritsko, 1980, "Dielectric response and intraband plasmon dispersion in stage-1 $FeCl_3$ intercalated graphite," Solid State Commun. **33**, 937–940.

Mel'nikov, V. I., and S. V. Meshkov, 1981, "Instability of a charged surface of liquid helium," Zh. Eksp. Teor. Fiz. Pis'ma Red. **33**, 222–226 [JETP Lett. **33**, 211–214 (1981)].

Mendez, E. E., C.-A. Chang, L. L. Chang, L. Esaki, and F. H. Pollak, 1980, "Electroreflectance study of semiconductor superlattices," in *Proceedings of the 15th International Conference on the Physics of Semiconductors, Kyoto* [J. Phys. Soc. Japan **49**, Suppl. A, 1009–1012].

Mendez, E. E., L. L. Chang, G. Landgren, R. Ludeke, L. Esaki, and F. H. Pollak, 1981, "Observation of superlattice effects on the electronic bands of multilayer heterostructures," Phys. Rev. Lett. **46**, 1230–1234.

Merlin, R., C. Colvard, M. V. Klein, H. Morkoç, A. Y. Cho, and A. C. Gossard, 1980a, "Raman scattering in superlattices: Anisotropy of polar phonons," Appl. Phys. Lett. **36**, 43–45.

Merlin, R., C. Colvard, M. V. Klein, H. Morkoç, A. C. Gossard, and A. Y. Cho, 1980b, "Phonon folding and anisotropy in GaAs-AlAs superlattices," in *Proceedings of the 15th International Conference on the Physics of Semiconductors, Kyoto* [J. Phys. Soc. Japan **49**, Suppl. A, 1021–1023].

Mermin, N. D., 1968, "Crystalline order in two dimensions," Phys. Rev. **176**, 250–254; Phys. Rev. B **20**, 4762(E) (1979).

Mertsching, J., and H. J. Fischbeck, 1970, "Surface scattering of electrons in magnetic surface states," Phys. Status Solidi **41**, 45–56.

Merz, J. L., A. S. Barker, Jr., and A. C. Gossard, 1977, "Raman scattering and zone-folding effects for alternating monolayers of GaAs-AlAs," Appl. Phys. Lett. **31**, 117–119.

Mikeska, H. J., and H. Schmidt, 1975, "Cyclotron resonance of electrons in localized surface states," Z. Phys. B **20**, 43–48.

Millea, M. F., and A. H. Silver, 1978, "Influence of the free surface on the electrical behavior of metal contacts to *p*-InAs," J. Vac. Sci. Technol. **15**, 1362–1369.

Miller, A., and E. Abrahams, 1960, "Impurity conduction at low concentrations," Phys. Rev. **120**, 745–755.

Miller, R. C., R. Dingle, A. C. Gossard, R. A. Logan, W. A. Nordland, Jr., and W. Wiegmann, 1976, "Laser oscillation with optically pumped very thin GaAs-$Al_xGa_{1-x}As$ multilayer structures and conventional double heterostructures," J. Appl. Phys. **47**, 4509–4517.

Miller, R. C., D. A. Kleinman, and A. C. Gossard, 1979, "Electron spin orientation in optically pumped GaAs-$Al_xGa_{1-x}As$ multilayer structures," in *Physics of Semiconductors, 1978,* edited by B. L. H. Wilson (Institute of Physics, Bristol), pp. 1043–1046.

Miller, R. C., D. A. Kleinman, O. Munteanu, and W. T. Tsang, 1981a, "New transitions in the photoluminescence of GaAs quantum wells," Appl. Phys. Lett. **39**, 1–3.

Miller, R. C., D. A. Kleinman, W. A. Nordland, Jr., and A. C. Gossard, 1981b, "Luminescence studies of optically pumped quantum wells in GaAs-$Al_xGa_{1-x}As$ multilayer structures," Phys. Rev. B **22**, 863–871.

Miller, R. C., D. A. Kleinman, W. T. Tsang, and A. C. Gossard, 1981c, "Observation of the excited level of excitons in GaAs quantum wells," Phys. Rev. B **24**, 1134–1136.

Miller, R. C., and W. T. Tsang, 1981, "Al-Ga disorder in $Al_xGa_{1-x}As$ alloys grown by molecular beam epitaxy," Appl. Phys. Lett. **39**, 334–335.

Miller, R. C., W. T. Tsang, and W. A. Nordland, Jr., 1980, "Spin-dependent recombination in GaAs," Phys. Rev. B **21**, 1569–1575.

Miller, R. C., C. Weisbuch, and A. C. Gossard, 1981, "Alloy clustering in $Al_xGa_{1-x}As$," Phys. Rev. Lett. **46**, 1042 (Comment).

Mima, K., and H. Ikezi, 1978, "Propagation of nonlinear waves on an electron-charged surface of liquid helium," Phys. Rev. B **17**, 3567–3575.

Mimura, T., and M. Fukuta, 1980, "Status of the GaAs metal-oxide-semiconductor technology," IEEE Trans. Electron Devices ED-**27**, 1147–1155.

Mimura, T., S. Hiyamizu, T. Fujii, and K. Nanbu, 1980, "A new field-effect transistor with selectively doped GaAs/*n*-$Al_xGa_{1-x}As$ heterojunctions," Jpn. J. Appl. Phys. **19**, L225–L227.

Mimura, T., K. Joshin, S. Hiyamizu, K. Hikosaka, and M. Abe, 1981, "High electron mobility transistor logic," Jpn. J. Appl. Phys. **20**, L598–L600.

Missman, R., and P. Handler, 1959, "Hall mobility of a cleaned germanium surface," J. Phys. Chem. Solids **8**, 109–111.

Miyazaki, T., I. Yoshida, Y. Katayama, and N. Kotera, 1971, "Surface electron mobility of silicon with various gate insulator structures," in *Proceedings of the 2nd Conference on Solid State Devices, Tokyo, 1970* [J. Japan Soc. Appl. Phys. **40** Suppl., 199–204].

Mochán, L., and R. G. Barrera, 1981, "Optical properties of quasi-two-dimensional systems: Nonlocal effects," Phys. Rev. B **23**, 5707–5718.

Mon, K. K., K. Hess, and J. D. Dow, 1981, "Deformation potentials of superlattices and interfaces," J. Vac. Sci. Technol. **19**, 564–566.

Monarkha, Yu. P., 1978, "Influence of shortwave surface excitations of liquid helium on damping effects in a two-dimensional electron gas," Fiz. Nizk. Temp. **4**, 1093–1104 [Sov. J. Low Temp. Phys. **4**, 515–520 (1978)].

Monarkha, Yu. P., 1979a, "Conductivity of a two-dimensional Wigner crystal of surface electrons in helium in a rapidly alternating electrical field," Fiz. Nizk. Temp. **5**, 950–952 [Sov. J. Low Temp. Phys. **5**, 451–452 (1979)].

Monarkha, Yu. P., 1979b, "The possibility of studying the spectrum of short-wave surface excitations of liquid helium using nonlinear current-voltage characteristics of the two-dimensional electron gas," Fiz. Nizk. Temp. **5**, 994–1004 [Sov. J. Low Temp. Phys. **5**, 470–474 (1979)].

Monarkha, Yu. P., 1980a, "On the theory of electron-ripplon resonances in a two-dimensional Wigner crystal on a liquid-helium surface," Fiz. Nizk. Temp. **6**, 685–697 [Sov. J. Low Temp. Phys. **6**, 331–337 (1980)].

Monarkha, Yu. P., 1980b, "Dynamic properties of a two-dimensional electronic crystal on a helium surface in a strong magnetic field," Fiz. Nizk. Temp. **6**, 852–857 [Sov. J. Low Temp. Phys. **6**, 413–415 (1980)].

Monarkha, Yu. P., 1980c, "Coupling of the phonons of a two-dimensional Wigner crystal with the second surface sound in helium and surface waves of a solid substrate," Fiz. Nizk. Temp. **6**, 949–952 [Sov. J. Low Temp. Phys. **6**, 462–463 (1980)].

Monarkha, Yu. P., 1980d, "Influence of a magnetic field on the stability of the charged surface of a liquid dielectric," Fiz. Nizk. Temp. **6**, 1352–1355 [Sov. J. Low Temp. Phys. **6**, 660–661 (1980)].

Monarkha, Yu. P., and V. B. Shikin, 1975, "Theory of a two-dimensional Wigner crystal of surface electrons in helium," Zh. Eksp. Teor. Fiz. **68**, 1423–1433 [Sov. Phys. — JETP **41**, 710–714 (1975)].

Monarkha, Yu. P., and V. B. Shikin, 1980, "Cyclotron resonance for electrons in surface states on liquid helium," Surf. Sci. **98**, 41–60.

Monarkha, Yu. P., and S. S. Sokolov, 1979, "A theory of current instabilities of a charged liquid helium surface," Fiz. Nizk. Temp. **5**, 1283–1291 [Sov. J. Low Temp. Phys. **5**, 605–609 (1979)].

Monarkha, Yu. P., S. S. Sokolov, and V. B. Shikin, 1981, "Effective mass of surface electrons in helium under non-equilibrium conditions," Solid State Commun. **38**, 611–614.

Moore, B. T., and D. K. Ferry, 1980a, "Hall measurements on trap states in *n*-channel Si MOSFETs at 77 K," Solid State Commun. **33**, 509–511.

Moore, B. T., and D. K. Ferry, 1980b, "Remote polar phonon scattering in Si inversion layers," J. Appl. Phys. **51**, 2603–2605.

Moore, B. T., and D. K. Ferry, 1980c, "Scattering of inversion layer electrons by oxide polar mode generated interface phonons," J. Vac. Sci. Technol. **17**, 1037–1040.

Moore, J. S., and P. Das, 1979, "The transient response of hot electrons in quasi-two-dimensional semiconductors," J. Appl. Phys. **50**, 8082–8086.

Moormann, H., D. Kohl, and G. Heiland, 1980, "Variations of work functions and surface conductivity on clean cleaved zinc oxide surfaces by annealing and by hydrogen adsorption," Surf. Sci. **100**, 302–314.

Mooser, E. (managing editor), 1976-, *Physics and Chemistry of Materials with Layered Structures* (Reidel, Dordrecht) (see also Lee, 1976; Lévy, 1976).

More, R. M., 1975, "Surface roughness scattering of electrons in semiconductors and semimetals," J. Phys. C **8**, 3810–3816.

Morf, R. H., 1979, "Temperature dependence of the shear modulus and melting of the two-dimensional electron solid," Phys. Rev. Lett. **43**, 931–935.

Mori, S., and T. Ando, 1979, "Intersubband scattering effect on the mobility of a Si (100) inversion layer at low temperatures," Phys. Rev. B **19**, 6433–6441.

Mori, S., and T. Ando, 1980a, "Electronic properties of a heavily-doped *n*-type GaAs-$Ga_{1-x}Al_xAs$ superlattice," Surf. Sci. **98**, 101–107.

Mori, S., and T. Ando, 1980b, "Electronic properties of a semiconductor superlattice II. Low temperature mobility perpendicular to the superlattice," J. Phys. Soc. Japan **48**, 865–873.

Morkoç, H., 1981, "Current transport in modulation doped (Al,Ga)As/GaAs heterostructures. Applications to high speed FETs," IEEE Electron Device Lett. **EDL–2**, 260–262.

Mott, N. F., 1961, "The transition to the metallic state," Philos. Mag. **6**, 287–309.

Mott, N. F., 1966, "The electrical properties of liquid mercury," Philos. Mag. **13**, 989–1014.

Mott, N. F., 1967, "Electrons in disordered structures," Adv. Phys. **16**, 49–144.

Mott, N. F., 1968, "Conduction in glasses containing transition metal ions," J. Non-cryst. Solids **1**, 1–17.

Mott, N. F., 1973, "Conduction in amorphous materials," Electronics & Power **19**, 321–324.

Mott, N. F., 1974a, *Metal-Insulator Transitions* (Taylor and Francis, London).

Mott, N. F., 1974b, "Conduction in non-crystalline systems X. Mobility and percolation edges," Philos. Mag. **29**, 613–639.

Mott, N. F., 1975, "Coulomb gap and low-temperature conductivity of disordered systems," J. Phys. C **8**, L239–L240.

Mott, N. F., 1976a, "The metal-insulator transition in an impurity band," J. Phys. (Paris) **37**, Colloques, C4-301–C4-306.

Mott, N. F., 1976b, "Some properties of the mobility edge in disordered systems," Commun. Phys. **1**, 203–206.

Mott, N. F., 1978, "Some comments and suggestions on the Hall effect in non-crystalline systems," Philos. Mag. B **38**, 549–553.

Mott, N. F., and E. A. Davis, 1979, *Electronic Processes in Non-Crystalline Materials*, 2nd ed. (Clarendon, Oxford).

Mott, N. F., and M. Kaveh, 1981, "The conductivity of disordered systems and the scaling theory," J. Phys. C **14**, L659–L664.

Mott, N. F., M. Pepper, S. Pollitt, R. H. Wallis, and C. J. Adkins, 1975, "The Anderson transition," Proc. R. Soc. London Ser. A **345**, 169–205.

Mott, N. F., and W. D. Twose, 1961, "The theory of impurity conduction," Adv. Phys. **10**, 107–163.

Mukherji, D., and B. R. Nag, 1975, "Miniband parameters of semiconductor superlattices," Solid-State Electron. **18** 1107–1109.

Mukherji, D., and B. R. Nag, 1980, "Transverse electron effective mass in a semiconductor superlattice," Phys. Rev. B **21**, 5857–5859.

Müller, W., and I. Eisele, 1980, "Velocity saturation in short channel field effect transistors," Solid State Commun. **34**, 447–449.

Muls, P. A., G. J. Declerck, and R. J. Van Overstraeten, 1978, "Characteristics of the MOSFET operating in weak inversion," in *Advances in Electronics and Electron Physics,* edited by L. Marton (Academic, New York), Vol. 47, pp. 197–266.

Murayama, Y., Y. Kamigaki, and E. Yamada, 1972, "Differential negative resistance (DNR) in *n*-channel MOSFETs of silicon," in *Proceedings of the 3rd Conference on Solid State Devices, Tokyo, 1971* [J. Japan Soc. Appl. Phys. **41** Suppl., 133–140].

Murphy, N. St. J., 1964, "Surface mobility of holes in thermally oxidized silicon measured by the field effect and the Hall effect," Surf. Sci. **2**, 86–92.

Murphy, N. St. J., F. Berz, and I. Flinn, 1969, "Carrier mobility in silicon MOST's," Solid-State Electron. **12**, 775–786.

Nagai, T., and A. Onuki, 1978, "Melting of the two-dimensional electron solid," J. Phys. C **11**, L681–L684.

Nagano, S., S. Ichimaru, and N. Itoh, 1980, "Correlational properties of two-dimensional electron systems in the surface states on liquid helium," Surf. Sci. **98**, 22–29.

Nagano, S., S. Ichimaru, H. Totsuji, and N. Itoh, 1979, "Lifetime of surface-state electrons on liquid helium: Relation with the chemical potential of the electron liquid," Phys. Rev. B **19**, 2449–2456.

Nakamura, K., 1976, "Hot electrons in Si inversion layer," Surf. Sci. **58**, 48–55.

Nakamura, K., H. Ezawa, and K. Watanabe, 1980a, "Many-body effects in the Si metal-oxide-semiconductor inversion layer: Subband structure," Phys. Rev. B **22** 1892–1904.

Nakamura, K., K. Watanabe, and H. Ezawa, 1978, "Many-body effects in the subband structure of Si-MOS inversion layer," Surf Sci. **73**, 258–265.

Nakamura, K., K. Watanabe, and H. Ezawa, 1980b, "Many-body effects and the electron mobility in Si inversion layers at room temperature," Surf. Sci. **98**, 202–209.

Nakao, K., 1979, "Electronic band structure of superlattices in magnetic fields," J. Phys. Soc. Japan **46**, 1669–1670.

Nakayama, M., 1974a, "Theory of surface waves coupled to surface carriers," J. Phys. Soc. Japan **36**, 393–398.

Nakayama, M., 1974b, "Theory of magnetoplasma surface waves coupled to surface carriers," in *Proceedings of the Second International Conference on Solid Surfaces, Kyoto* [Jpn. J. Appl. Phys., Suppl. 2, Pt. 2, 901–904].

Nakayama, M., 1975, "Theory of electromagnetic response of solid surfaces," J. Phys. Soc. Japan **39**, 265–274.

Nakayama, M., 1977a, "On the strip transmission line spectroscopy of the inter-subband transition of MOS charge layer," Solid State Commun. **21**, 587–589.

Nakayama, M., 1977b, "Electromagnetic response of surface states," in *Proceedings of the Seventh International Vacuum Congress and the Third International Conference on Solid Surfaces, Vienna,* edited by R. Dobrozemsky, F. Rüdenauer, F. P. Viehböck, and A. Breth (Berger, Horn, Austria), Vol. I, pp. 395–398.

Nakayama, M., 1978, "Optical spectrum of inter-subband transition in *n*-Si (111) MOS charge layer," Surf. Sci. **73**, 510–517.

Nakayama, M., 1980, "Effect of the interface on electronic structure of *n*-Si MOS charge layer," Surf. Sci. **98**, 358–365.

Nakayama, M., and L. J. Sham, 1978, "Surface-induced valley splitting in *n*-channel (001) silicon-MOS charge layer," Solid State Commun. **28**, 393–396.

Namaizawa, H., 1980, "Self-consistent Debye-Waller factors of the electron solid on liquid helium," Solid State Commun. **34**, 607–610.

Narayanamurti, V., H. L. Störmer, M. A. Chin, A. C. Gossard, and W. Wiegmann, 1979, "Selective transmission of high-frequency phonons by a superlattice: The 'dielectric' phonon filter," Phys. Rev. Lett. **43**, 2012–2016.

Narita, K., and K. F. Komatsubara, 1974, "On the *g* factor for electrons in *n*-type silicon surface inversion layers," in *Proceedings of the Second International Conference on Solid Surfaces, Kyoto* [Jpn. J. Appl. Phys. Suppl. 2, Pt. 2, 347–350].

Narita, K., S. Takaoka, and K. F. Komatsubara, 1973, "On the *g*-factor for electrons in *n*-type Si surface inversion layers," Solid State Commun. **12**, 1221–1224.

Narita, K., and E. Yamada, 1974, "Valley-orbit splitting of the states in surface inversion layers," in *Proceedings of the 12th International Conference on the Physics of Semiconductors, Stuttgart,* edited by M. H. Pilkuhn (Teubner, Stuttgart), pp. 719–723.

Narita, S., and T. Kuroda, 1977, "Far-infra-red cyclotron resonance in the inversion layer on *p*-$Hg_{1-x}Cd_xTe$," Nuovo Cimento B **39**, 834–839.

Narita, S., T. Kuroda, and Y. Nisida, 1979, "Study of *n*-surface inversion layers of $Hg_{1-x}Cd_xTe$ alloys," in *Physics of Semiconductors, 1978,* edited by B. L. H. Wilson (Institute of Physics, Bristol), pp. 1235–1238.

Narita, S., S. Takeyama, W. B. Luo, S. Hiyamizu, K. Nanbu, and H. Hashimoto, 1981a, "Galvanomagnetic study of 2-dimensional electron gas in $Al_xGa_{1-x}As$/GaAs heterojunction FET," Jpn. J. Appl. Phys. **20**, L443-L446.

Narita, S., S. Takeyama, W. B. Luo, S. Hiyamizu, K. Nanbu, and H. Hashimoto, 1981b, "Magnetoconductance investigations of $Al_xGa_{1-x}As$/GaAs heterojunction FET in strong magnetic fields," Jpn. J. Appl. Phys. **20**, L447–L450.

Nash, J. G., and J. W. Holm-Kennedy, 1974, "Determination of intervalley electron-phonon deformation potential constants in *n*-silicon by analysis of high electric field transport properties," Appl. Phys. Lett. **25**, 507–509.

Nedorezov, S. S., 1966, "Oscillations of the electronic thermodynamic characteristics of a metal film at high pressures," Zh. Eksp. Teor. Fiz. **51**, 1575–1586 [Sov. Phys. — JETP **24**, 1061–1067 (1967)].

Nedorezov, S. S., 1970, "Space quantization in semiconductor films," Fiz. Tverd. Tela (Leningrad) **12**, 2269–2276 [Sov. Phys. — Solid State **12**, 1814–1819 (1970)].

Nee, T. W., J. F. Koch, and R. E. Prange, 1968, "Surface quantum states and impedance oscillations in a weak magnetic field — Numerical aspects," Phys. Rev. **174**, 758–766.

Nelson, A. R., 1974, "Anisotropic relaxation time in quantized (110) silicon inversion layers," J. Appl. Phys. **45**, 2935–2937.

Nelson, A. R., and E. Brown, 1974, "Conduction in quantized silicon inversion layers with many occupied subbands," Phys. Rev. B **9**, 1664–1668.

Nelson, D. R., 1978, "Study of melting in two dimensions," Phys. Rev. B **18**, 2318–2338.

Nelson, D. R., and B. I. Halperin, 1979, "Dislocation-mediated melting in two dimensions," Phys. Rev. B **19**, 2457–2484.

Neppl, F., J. P. Kotthaus, J. F. Koch, and Y. Shiraki, 1977, "Intersubband spectroscopy by photoconductivity and absorption in inversion layers on *p*-Si(100)," Phys. Rev. B **16**, 1519–1524.

Neppl, F., J. P. Kotthaus, and J. F. Koch, 1979, "Mechanism of intersubband resonant photoresponse," Phys. Rev. B **19**, 5240–5250.

Nérou, J. P., A. Filion, and P.-E. Girard, 1976, "Low temperature surface conductivity of GaSb," J. Phys. C **9**, 479–489.

Neugebauer, T., K. von Klitzing, G. Landwehr, and G. Dorda, 1975, "Surface quantum oscillations in (110) and (111) *n*-type silicon inversion layers," Solid State Commun. **17**, 295–300.

Neugebauer, T., K. von Klitzing, G. Landwehr, and G. Dorda, 1976, "Quantum oscillations in (110) and (111) *n*-channel MOSFETs," Surf. Sci. **58**, 261–262.

Neugebauer, T., and G. Landwehr, 1980, "Determination of the phonon modes involved in the carrier-phonon interaction in silicon inversion layers at low temperatures by nonohmic transport measurements," Phys. Rev. B **21**, 702–708.

Neugebauer, T., G. Landwehr, and K. Hess, 1978, "Negative differential resistance in (100) *n*-channel silicon inversion layers," Solid-State Electron. **21**, 143–146; Surf. Sci. **73**, 163–165 (extended abstract).

Neumark, G. F., 1968, "New model for interface charge-carrier mobility: The role of misfit dislocations," Phys. Rev. Lett. **21**, 1252–1256.

Neumark, G. F., 1969, "Misfit dislocations and interface mobility," in *International Conference on Properties and use of M.I.S. Structures, Grenoble,* edited by J. Borel (Centre d'Etudes Nucleaires, Grenoble), pp. 337–350.

Neumark, G. F., 1970, "Theory of the influence of misfit dislocations on interfacial mobility and Hall effect," Phys. Rev. B **1**, 2613–2622.

Ngai, K. L., and T. L. Reinecke, 1976, "Contributions to localization in the silicon inversion layer from states in the gap in SiO_x," Phys. Rev. Lett. **37**, 1418–1422.

Ngai, K. L., and C. T. White, 1978, "Critical comparisons between experiment and the predictions of the random pair attractive interaction model of carrier localization in Si inversion layers," Surf. Sci. **73**, 31–39.

Ngai, K. L., and C. T. White, 1981, "A model of interface states and charges at the Si-SiO_2 interface: Its predictions and comparisons with experiments," J. Appl. Phys. **52**, 320–337.

Nicholas, R. J., 1979, "Shubnikov-de Haas oscillations in *n*-channel silicon ⟨100⟩ MOSFETs in magnetic fields up to 35 T," Solid State Commun. **31**, 437–441.

Nicholas, R. J., E. Kress-Rogers, F. Kuchar, M. Pepper, J. C. Portal, and R. A. Stradling, 1980, "Electron transport in silicon inversion layers at high magnetic fields and the influence of substrate bias," Surf. Sci. **98**, 283–298.

Nicholas, R. J., and R. A. Stradling, 1976, "A time-dependent anomalous threshold in silicon MOS devices fabricated on high-resistivity subtrates," J. Phys. D **9**, L109–L113.

Nicholas, R. J., R. A. Stradling, S. Askenazy, P. Perrier, and J. C. Portal, 1978, "The analysis of thermal activation of two-dimensional Shubnikov–de Haas conductivity minima and maxima," Surf. Sci. **73**, 106–115.

Nicholas, R. J., R. A. Stradling, and R. J. Tidey, 1977, "Evidence for Anderson localisation in Landau level tails from the analysis of two-dimensional Shubnikov–de Haas conductivity minima," Solid State Commun. **23**, 341–345.

Nicholas, R. J., K. von Klitzing, and Th. Englert, 1980, "An investigation of the valley-splitting in *n*-channel silicon ⟨100⟩ inversion layers," Solid State Commun. **34**, 51–55.

Nicholas, R. J., K. von Klitzing, and R. A. Stradling, 1976, "An observation by photoconductivity of strain splitting of shallow bulk donors located near to the surface in silicon MOS devices," Solid State Commun. **20**, 77–80.

Nicollian, E. H., and J. R. Brews, 1982, *MOS Physics and Technology* (Wiley, New York).

Niederer, H. H. J. M., 1974, "Magneto oscillatory conductance in *n*-type inverted silicon surfaces," in *Proceedings of the Second International Conference on Solid Surfaces, Kyoto* [Jpn. J. Appl. Phys. Suppl. 2, Pt. 2, 339–342].

Niederer, H. H., J. M., A. P. M. Matthey, and M. J. Sparnaay, 1981a, "Temperature dependent metallic conductance above the mobility edge of a silicon inversion layer," J. Phys. C **14**, 4167–4175.

Niederer, H. H. J. M., A. P. M. Matthey, and M. J. Sparnaay, 1981b, "Thermally activated conductance of a silicon inversion layer by electrons excited above the mobility edge," J. Phys. C **14**, 4177–4184.

Nimtz, G., B. Schlicht, E. Tyssen, R. Dornhaus, and L. D. Haas, 1979, "A magneto-transport anomaly in semiconductors at low carrier densities, a Wigner condensation?" Solid State Commun. **32**, 669–671.

Ning, T. H., and C. T. Sah, 1972, "Theory of scattering of electrons in a nondegenerate-semiconductor-surface inversion layer by surface-oxide charges," Phys. Rev. B **6**, 4605–4613.

Ning, T. H., and C. T. Sah, 1974, "Effects of imhomogeneities of surface-oxide charges on the electron energy levels in a semiconductor surface-inversion layer," Phys. Rev. B **9**, 527–535.

Nishi, Y., and H. Hara, 1978, "Physics and device technology of silicon on sapphire," in *Proceedings of the 9th Conference on Solid State Devices, Tokyo, 1977* [Jpn. J. Appl. Phys. **17**, Suppl. 17-1, 27–35].

Nishina, Y., S. Tanuma, and H. W. Myron, eds., 1981, *Proceedings of the Yamada Conference IV on Physics and Chemistry of Layered Materials, Sendai, 1980* [Physica **105B**, 1–503].

Nitzan, M., Y. Grinshpan, and Y. Goldstein, 1979, "Field-effect mobility in quantized accumulation layers on ZnO surfaces," Phys. Rev. B **19**, 4107–4115.

Niu, H., and M. Takai, 1978, "Lateral photovoltaic effect in MOS structures," Jpn. J. Appl. Phys. **17**, 1873–1874.

Nkoma, J. S., 1981, "Effect of impurities on the two-dimensional electron gas polarisability," J. Phys. C **14**, 1685–1691.

Norton, P., T. Braggins, and H. Levinstein, 1973, "Impurity and lattice scattering parameters as determined from Hall and mobility analysis in *n*-type silicon," Phys. Rev. B **8**, 5632–5653.

Noti, G., 1972 "Normalization of wave functions in an MIS structure," Solid-State Electron. **15**, 723–725.

Nougier, J. P., D. Sodini, M. Rolland, D. Gasquet, and G. Lecoy, 1978, "Noise of hot carriers in the channel of *n* silicon junction gate field effect transistors," Solid-State Electron. **21**, 133–138.

Nozières, P., and D. Pines, 1958, "Correlation energy of a free electron gas," Phys. Rev. **111**, 442–454.

Oakley, R. E., and M. Pepper, 1972, "The influence of dielectric charge on the hole field-effect mobility in silicon inversion layers," Phys. Lett. A **41**, 87–88.

O'Connell, R. F., 1977, "One-dimensional hydrogenic atom in

an electric field with solid-state applications," Phys. Lett. A **60**, 481–482.
O'Connell, R. F., 1978, "Rydberg states in strong electric and magnetic fields," Phys. Rev. A **17**, 1984–1987.
O'Connell, R. F., 1981, "Intersubband-cyclotron combined resonance in a surface space-charge layer," Physica **103B**, 348–350.
O'Connell, R. F., and G. L. Wallace, 1981a, "Null Faraday rotation—A clean method for determination of relaxation times and effective masses in MIS and other systems," Solid State Commun. **38**, 429–432.
O'Connell, R. F., and G. L. Wallace, 1981b, "Faraday rotation in the Appel-Overhauser model for inversion-layer electrons in Si," Phys. Rev. B **24**, 2267–2269.
Ohkawa, F. J., 1976a, "Quasi-particle properties in surface quantized states of silicon," Surf. Sci. **58**, 326–332.
Ohkawa, F. J., 1976b, "The electronic structure of *p*-channel inversion layers of silicon (100) M.O.S.: Many-body effects on the subbands," J. Phys. Soc. Japan **41**, 122–129.
Ohkawa, F. J., 1978a, "Electric breakthrough in an inversion layer: Exactly solvable model," Solid State Commun. **26**, 69–71.
Ohkawa, F. J., 1978b, "Electric break through in *n*-channel Si inversion layer tilted from (100) surface," J. Phys. Soc. Japan **45**, 1427–1428.
Ohkawa, F. J., 1979a, "Multi-valley effective mass theory," J. Phys. Soc. Japan **46**, 736–743.
Ohkawa, F. J., 1979b, "Interference effects of Γ and X electric-break-throughs in inversion layers of Si," J. Phys. Soc. Japan **46**, 855–860.
Ohkawa, F. J., 1980, "Electric break-throughs in vicinal planes of (001) Si inversion layers," Surf. Sci. **98**, 350–357.
Ohkawa, F. J., and Y. Uemura, 1974a, "Quantized surface states of a narrow gap semiconductor," in *Proceedings of the Second International Conference on Solid Surfaces, Kyoto* [Jpn. J. Appl. Phys. Suppl. 2, Pt. 2, 355–358].
Ohkawa, F. J., and Y. Uemura, 1974b, "Quantized surface states of a narrow-gap semiconductor," J. Phys. Soc. Japan **37**, 1325–1333.
Ohkawa, F. J., and Y. Uemura, 1975, "Hartree approximation for the electronic structure of a *p*-channel inversion layer of silicon M.O.S.," Prog. Theor. Phys. Suppl. **57**, 164–175.
Ohkawa, F. J., and Y. Uemura, 1976, "Valley splitting in an *n*-channel (100) inversion layer on *p*-type silicon," Surf. Sci. **58**, 254–260.
Ohkawa, F. J., and Y. Uemura, 1977a, "Theory of valley splitting in an *n*-channel (100) inversion layer of Si. I. Formulation by extended zone effective mass theory," J. Phys. Soc. Japan **43**, 907–916.
Ohkawa, F. J., and Y. Uemura, 1977b, "Theory of valley splitting in an *n*-channel (100) inversion layer of Si. II. Electric break through," J. Phys. Soc. Japan **43**, 917–924.
Ohkawa, F. J., and Y. Uemura, 1977c, "Theory of valley splitting in an *n*-channel (100) inversion layer of Si. III. Enhancement of splittings by many-body effects," J. Phys. Soc. Japan **43**, 925–932.
Ohmura, Y., 1979, "Galvanomagnetic effect for holes and the valence band in (001) silicon on sapphire," J. Phys. Soc. Japan **47**, 145–152.
Ohta, K., 1971a, "Broadening of Landau levels in two-dimensional electron gas: Its effect on surface capacitance," Jpn. J. Appl. Phys. **10**, 850–863.
Ohta, K., 1971b, "Broadening of Landau levels in two-dimensional electron gas. II. Transverse magnetoconductance," J. Phys. Soc. Japan **31**, 1627–1638.
Ohwada, A., H. Maeda, and K. Tanaka, 1969, "Effect of the crystal orientation upon electron mobility at the Si-SiO_2 interface," Jpn. J. Appl. Phys. **8**, 629–630.
Okamoto, H., K. Muro, S. Narita, and S. Kawaji, 1980, "Far-infrared investigation of high index surfaces on silicon," Surf. Sci. **98**, 505–512.
Ol'shanetskii, B. Z., and A. V. Rzhanov, 1980, "One-dimensional periodic structure on high-index silicon surfaces," Zh. Eksp. Teor. Fiz. Pis'ma Red. **32**, 337–340 [JETP Lett. **32**, 313–315 (1980)].
Onga, S., K. Hatanaka, S. Kawaji, Y. Nishi, and Y. Yasuda, 1978, "Effect of residual stress on hole mobility of SOS MOS devices," Jpn. J. Appl. Phys. **17**, 1587–1592.
Onga, S., K. Hatanaka, S. Kawaji, and Y. Yasuda, 1977, "Influence of crystalline defects and residual stress on the electrical characteristics of SOS MOS devices," Jpn. J. Appl. Phys. **17**, 413–422.
Onga, S., W. H. Ko, K. Hatanaka, and S. Kawaji, 1980, "Electrical characteristics of depletion-type SOS MOS devices," Jpn. J. Appl. Phys. **19**, 1675–1682.
Onga, S., T. Yoshii, K. Hatanaka, and Y. Yasuda, 1976, "Effect of cystalline defects on electrical properties in silicon films on sapphire," in *Proceedings of the 7th Conference on Solid State Devices, Tokyo, 1975* [Jpn. J. Appl. Phys. **15**, Suppl. 15-1, 225–231].
Ono, Y., and U. Paulus, 1979, "Low-lying collective modes in the charge density wave state in *n*-type inversion layers of semiconductors," Z. Phys. B **34**, 11–15.
Ono, Y., D. Yoshioka, and H. Fukuyama, 1981, "Magnetoresistance of two-dimensional Anderson localized system in self-consistent treatment," J. Phys. Soc. Japan **50**, 2143–2144.
Onuki, A., 1977, "Collective modes of a two-dimensional electron fluid," J. Phys. Soc. Japan **43**, 396–405.
Oppermann, R., and F. Wegner, 1979, "Disordered systems with n orbitals per site: $1/n$ expansion," Z. Phys. B **34**, 327–348.
Orlov, L. K., and Yu. A. Romanov, 1976, "Two-photon absorption in semiconductors with a superlattice," Fiz. Tekh. Poluprovodn. **10**, 1052–1057 [Sov. Phys. — Semicond. **10**, 625–628 (1976)].
Orman, M., and N. J. M. Horing, 1974, "Inversion layer plasma waves in quantizing magnetic field," Solid State Commun. **15**, 1381–1385.
Orman, M., N. J. M. Horing, and M. L. Glasser, 1977, "Two dimensional magnetoplasma waves for adjoining media of different dielectric properties," in *Proceedings of the Seventh International Vacuum Congress and the Third International Conference on Solid Surfaces, Vienna,* edited by R. Dobrozemsky, F. Rüdenauer, F. P. Viehböck, and A. Breth (Berger, Horn, Austria), Vol. I, pp. 545–548.
Osaka, Y., 1977, "Interface states induced by amorphous SiO_2 in MOS structures," J. Phys. Soc. Japan **42**, 533–541.
Osaka, Y., 1980, "Effects of long range components of random potentials on conductivity in two dimensions," Surf. Sci. **98**, 244–249.
Osbourn, G. C., 1980, "Tunneling transmission coefficients for electrons through (100) GaAs-$Ga_{1-x}Al_xAs$-GaAs heterostructures," J. Vac. Sci. Technol. **17**, 1104–1107.
Osbourn, G. C., 1981, "Electron transmission probabilities through GaAs/strained GaAsP/GaAs(100) heterostructures," J. Vac. Sci. Technol. **19**, 592–595.
Osipov, E. B., 1978, "Changes in the electron spectrum of a

semiconductor film in a quantizing magnetic field due to the interaction with optical phonons," Fiz. Tekh. Poluprovodn. **12**, 2060–2062 [Sov. Phys. — Semicond. **12**, 1228 (1978)].
Otto, A., 1967, "Theory of plasmon excitation in thin films by electrons of non-normal incidence," Phys. Status Solidi **22**, 401–406.
Ovadyahu, Z., and Y. Imry, 1981, "Magnetoconductive effects in an effectively two-dimensional system. Weak Anderson localization," Phys. Rev. B **24**, 7439–7442.
Overhauser, A. W., 1962, "Spin density waves in an electron gas," Phys. Rev. **128**, 1437–1452.
Overhauser, A. W., 1971, "Simplified theory of electron correlations in metals," Phys. Rev. B **3**, 1888–1898.
Overhauser, A. W., 1978, "Effective-mass variation in silicon inversion layers," Phys. Rev. B **18**, 2884–2887.
Ovsyuk, N. N., and M. P. Sinyukov, 1980, "Effect of quantization on electrical reflection spectra in the surface region of a semiconductor," Zh. Eksp. Teor. Fiz. Pis'ma Red. **32**, 366–370 [JETP Lett. **32**, 342–345 (1980)].
Pals, J. A., 1972a, "A general solution of the quantization in a semiconductor surface inversion layer in the electric quantum limit," Phys. Lett. A **39**, 101–102.
Pals, J. A., 1972b, "Experimental verification of the surface quantization of an *n*-type inversion layer of silicon at 300 and 77 K," Phys. Rev. B **5**, 4208–4210.
Pals, J. A., 1972c, "Quantization effects in semiconductor inversion and accumulation layers," Philips Research Reports Suppl. 7, pp. 1–84.
Pals, J. A., 1973, "Measurements of the surface quantization in silicon *n*- and *p*-type inversion layers at temperatures above 25 K," Phys. Rev. B **7**, 754–760.
Pals, J. A., and W. J. J. A. van Heck, 1973, "Peaked structure in field-effect mobility of silicon MOS transistors at very low temperatures," Appl. Phys. Lett. **23**, 550–552.
Pandey, K. C., and J. C. Phillips, 1976, "Atomic densities of states near Si (111) surfaces," Phys. Rev. B **13**, 750–760.
Pantelides, S. T., 1977, "Recent advances in the theory of electronic structure of SiO_2," Comments Solid State Phys. **8**, 55–60.
Pantelides, S. T., 1978a, "The electronic structure of impurities and other point defects in semiconductors," Rev. Mod. Phys. **50**, 797–858.
Pantelides, S. T., ed., 1978b, *The Physics of SiO_2 and its Interfaces* (Pergamon, New York).
Pantelides, S. T., 1979, "Multiband and multivalley effective-mass theory for impurities in semiconductors," Solid State Commun. **30**, 65–70.
Pantelides, S. T., and M. Long, 1978, "Continuous-random-network models for the Si-SiO_2 interface," in *The Physics of SiO_2 and its Interfaces*, edited by S. T. Pantelides (Pergamon, New York), pp. 339–343.
Park, H. S., A. van der Ziel, R. J. J. Zijlstra, and S. T. Liu, 1981, "Discrimination between two noise models in metal-oxide-semiconductor field-effect transistors," J. Appl. Phys. **52**, 296–299.
Parrinello, M., and N. H. March, 1976, "Thermodynamics of Wigner crystallization," J. Phys. C **9**, L147–L150.
Paulus, U., 1978, "Two-valley model for studying the low temperature phases in *n*-type inversion layers of semiconductors," Z. Phys. B **30**, 165–166.
Peierls, R. E., 1935, "Quelques propriétés typiques des corps solides," Ann. Inst. Henri Poincaré **5**, 177–222.
Pepper, M., 1977a, "The Anderson transition in silicon inversion layers: The origin of the random field and the effect of substrate bias," Proc. R. Soc. London Ser. A **353**, 225–246.
Pepper, M., 1977b, "An introduction to silicon inversion layers," Contemp. Phys. **18**, 423–454.
Pepper, M., 1977c, "A metal-insulator transition in the impurity band of *n*-type GaAs induced by loss of dimension," J. Phys. C **10**, L173–L177.
Pepper, M., 1977d, "Electron and hole localization at the Si-SiO_2 interface," in *Amorphous and Liquid Semiconductors*, edited by W. E. Spear (Centre for Industrial Consultancy and Liaison, University of Edinburgh), pp. 477–486.
Pepper, M., 1977e, "The radiation hardness of the Si-SiO_2 interface and carrier localization in the inversion layer," J. Phys. C **10**, L445–L450.
Pepper, M., 1978a, "Some aspects of localization in two-dimensional systems," Surf. Sci. **73**, 40–45.
Pepper, M., 1978b, "Magnetic localization in silicon inversion layers," Philos. Mag. B **37**, 83–95.
Pepper, M., 1978c, "The metal-insulator transition in the impurity band of *n*-type GaAs induced by a magnetic field and loss of dimension," Philos. Mag. B **37**, 187–198.
Pepper, M., 1978d, "Inversion layer transport and the radiation hardness of the Si-SiO_2 interface," IEEE Trans. Nucl. Sci. NS-**25**, 1283–1287.
Pepper, M., 1978e, "The Si-SiO_2 interface and localization in the inversion layer," in *The Physics of SiO_2 and its Interfaces*, edited by S. T. Pantelides (Pergamon, New York), pp. 407–411.
Pepper, M., 1978f, "The Hall effect in impurity bands and inversion layers," Philos. Mag. B **38**, 515–526.
Pepper, M., 1978g, "The metal non-metal transition in two-dimensional systems," in *The Metal Non-metal Transition in Disordered Systems*, edited by L. R. Friedman and D. P. Tunstall (Scottish Universities Summer School in Physics, Edinburgh), pp. 285–311.
Pepper, M., 1979a, "Two dimensional impurity bands in Si and GaAs," in *Physics of Semiconductors, 1978*, edited by B. L. H. Wilson (Institute of Physics, Bristol), pp. 997–1000.
Pepper, M., 1979b, "Metal-insulator transitions induced by a magnetic field," J. Non-Cryst. Solids **32**, 161–185.
Pepper, M., 1979c, "Conductance oscillations in a two-dimensional impurity band," J. Phys. C **12**, L617–L625.
Pepper, M., 1980a, "Conductance oscillations in two-dimensional transport," Surf. Sci. **98**, 218–219.
Pepper, M., 1980b, "Ballistic injection of electrons in metal-semiconductor junctions: III. Phonon and sub-band spectroscopy of silicon inversion layers," J. Phys. C **13**, L721–L723.
Pepper, M., and N. F. Mott, 1976, "The Si-SiO_2 interface and Anderson localization in the inversion layer," in *Proceedings of the 13th International Conference on the Physics of Semiconductors, Rome*, edited by F. G. Fumi (North-Holland, Amsterdam), pp. 762–765.
Pepper, M., S. Pollitt, and C. J. Adkins, 1974a, "Anderson localisation of holes in a Si inversion layer," Phys. Lett. A **48**, 113–114.
Pepper, M., S. Pollitt, and C. J. Adkins, 1974b, "The spatial extent of localized state wavefunctions in silicon inversion layers," J. Phys. C **7**, L273–L277.
Pepper, M., S. Pollitt, C. J. Adkins, and R. E. Oakley, 1974c, "Variable-range hopping in a silicon inversion layer," Phys. Lett. A **47**, 71–72.
Pepper, M., S. Pollitt, C. J. Adkins, and R. A. Stradling, 1975, "Anderson localization in silicon inversion layers," Crit. Rev. Solid State Sci. **5**, 375–384.
Pepper, M., M. J. Uren, and R. E. Oakley, 1979, "Conduc-

tance oscillations and source-drain-limited conduction in Si MOSFET's," J. Phys. C **12**, L897—L900.

Petrov, V. A., 1978, "Possibility of formation of one- and two-dimensional periodic superstructures in thin films and on semiconductor surfaces," Fiz. Tekh. Poluprovodn. **12**, 380—382 [Sov. Phys. — Semicond. **12**, 219—220 (1978)].

Petukhov, B. V., V. L. Pokrovskii, and A. V. Chaplik, 1967, "States of electrons localized at surface charges," Fiz. Tverd. Tela (Leningrad) **9**, 70—74 [Sov. Phys. — Solid State **9**, 51—54 (1967)].

Philipp, H. R., 1979, "The infrared optical properties of SiO_2 and SiO_2 layers on silicon," J. Appl. Phys. **50**, 1053—1057.

Phillips, J. C., 1973, *Bonds and Bands in Semiconductors* (Academic, New York).

Pichard, J. L., and G. Sarma, 1981a, "Finite size scaling approach to Anderson localisation," J. Phys. C **14**, L127—L132.

Pichard, J. L., and G. Sarma, 1981b, "Finite size scaling approach to Anderson localisation: II. Quantitative analysis and new results," J. Phys. C **14**, L617—L625.

Pierret, R. F., and C. T. Sah, 1968, "An MOS-oriented investigation of effective mobility theory," Solid-State Electron. **11**, 279—290.

Pietronero, L., and S. Strässler, 1981, "Mechanism of electron-phonon scattering and resistivity in graphite intercalation compounds," Phys. Rev. B **23**, 6793—6796.

Pietronero, L., S. Strässler, and H. R. Zeller, 1979, "Nonlinear screening in layered semimetals," Solid State Commun. **30**, 399—401.

Piller, H., 1979, "Far infrared Faraday rotation in a two-dimensional electron gas," J. Vac. Sci. Technol. **16**, 2096—2100.

Pinczuk, A., H. L. Störmer, R. Dingle, J. M. Worlock, W. Wiegmann, and A. C. Gossard, 1979, "Observation of intersubband excitations in a multilayer two dimensional electron gas," Solid State Commun. **32**, 1001—1003.

Pinczuk, A., J. M. Worlock, H. L. Störmer, R. Dingle, W. Wiegmann, and A. C. Gossard, 1980a, "Inelastic light scattering spectroscopy of a multilayer two dimensional electron gas," Surf. Sci. **98**, 126—133.

Pinczuk, A., J. M. Worlock, H. L. Störmer, R. Dingle, W. Wiegmann, and A. C. Gossard, 1980b, "Intersubband spectroscopy of two-dimensional electron gases: Coulomb interactions," Solid State Commun. **36**, 43—46.

Pinczuk, A., J. M. Worlock, H. L. Störmer, R. Dingle, W. Wiegmann, and A. C. Gossard, 1980c, "Light scattering spectroscopy of two dimensional electron gas in semiconductors," *Proceedings of the 15th International Conference on the Physics of Semiconductors, Kyoto* [J. Phys. Soc. Japan **49**, Suppl. A, 1025—1028].

Pinczuk, A., J. Shah, A. C. Gossard, and W. Wiegmann, 1981a, "Light scattering by photoexcited two-dimensional electron plasma in GaAs-(AlGa)As heterostructures," Phys. Rev. Lett. **46**, 1341—1344.

Pinczuk, A., J. M. Worlock, H. L. Störmer, A. C. Gossard, and W. Wiegmann, 1981b, "Light scattering spectroscopy of electrons in GaAs-(AlGa)As heterostructures: Correlation with transport properties," J. Vac. Sci. Technol. **19**, 561—563.

Pippard, A. B., 1962, "Quantization of coupled orbits in metals," Proc. R. Soc. London Ser. A **270**, 1—13.

Platzman, P. M., and G. Beni, 1976, "Comment on plasmon linewidth experiments for electrons on a helium surface," Phys. Rev. Lett. **36**, 626—628; 1350(E).

Platzman, P. M., and H. Fukuyama, 1974, "Phase diagram of the two-dimensional electron liquid," Phys. Rev. B **10**, 3150—3158.

Platzman, P. M., and B. I. Halperin, 1978, "The effect of parallel magnetic field on interband transitions in two-dimensional systems," Phys. Rev. B **18**, 226—232.

Platzman, P. M., A. L. Simons, and N. Tzoar, 1977, "High-frequency conductivity of electrons on a helium surface," Phys. Rev. B **16**, 2023—2026.

Platzman, P. M., and N. Tzoar, 1976a, "Many-body effects in the absorption spectrum of electrons in two-dimensional systems," Surf. Sci. **58**, 289—291.

Platzman, P. M., and N. Tzoar, 1976b, "Oscillations of a two-dimensional classical plasma," Phys. Rev. B **13**, 3197—3199.

Ploog, K., A. Fischer, G. H. Döhler, and H. Künzel, 1981a, "Novel periodic doping structures in GaAs grown by molecular beam epitaxy," in *Gallium Arsenide and Related Compounds, 1980,* edited by H. W. Thim (Institute of Physics, Bristol), pp. 721—730.

Ploog, K., H. Künzel, J. Knecht, A. Fischer, and G. H. Döhler, 1981b, "Simultaneous modulation of electron and hole conductivity in a new periodic GaAs doping multilayer structure," Appl. Phys. Lett. **38**, 870—872.

Pogrebinskii, M. B., 1977, "Mutual drag of carriers in a semiconductor-insulator-semiconductor system," Fiz. Tekh. Poluprovodn. **11**, 637—644 [Sov. Phys. — Semicond. **11**, 372—376 (1977)].

Poindexter, E. H., P. J. Caplan, B. E. Deal, and R. R. Razouk, 1981, "Interface states and electron spin resonance centers in thermally oxidized (111) and (100) silicon wafers," J. Appl. Phys. **52**, 879—884.

Poirier, R., 1966, "Mobilité électronique dans une couche d'inversion à la surface d'un semi-conducteur," C. R. Acad. Sci. Ser. B **262**, 281—284.

Poirier, R., 1968, "Magnétorésistance dans une couche électronique d'inversion sur une surface (100) d'un cristal de silicium a 77°K," J. Phys. (Paris) **29**, Colloques, C2-65—C2-68.

Pollak, M., 1972, "A percolation treatment of dc hopping conduction," J. Non-Cryst. Solids **11**, 1—24.

Pollak, M., 1980, "Effect of electron-electron interactions on hopping and on delocalization," Philos. Mag. B **42**, 781—798.

Pollitt, S., 1976, "Further investigations of the spatial extent of localized-state wave functions," Commun. Phys. **1**, 207—212.

Pollitt, S., M. Pepper, and C. J. Adkins, 1976, "The Anderson transition in silicon inversion layers," Surf. Sci. **58**, 79—88.

Pollmann, J., and H. Büttner, 1975, "Upper bounds for the ground-state energy of the exciton-phonon system," Solid State Commun. **17**, 1171—1174.

Pollmann, J., and H. Büttner, 1977, "Effective Hamiltonians and binding energies of Wannier excitons in polar semiconductors," Phys. Rev. B **16**, 4480—4490.

Polyanovskii, V. M., 1980a, "Quantum oscillations in semiconductors with a superlattice in magnetic fields," Fiz. Tverd. Tela (Leningrad) **22**, 1529—1531 [Sov. Phys. — Solid State **22**, 894—895 (1980)].

Polyanovskii, V. M., 1980b, "Quantum theory of galvanomagnetic effects in superlattice semiconductors," Fiz. Tverd. Tela (Leningrad) **22**, 1975—1979 [Sov. Phys. — Solid State **22**, 1151—1154 (1980)].

Pomerantz, M., 1978, "Experimental evidence for magnetic ordering in a literally two-dimensional magnet," Solid State Commun. **27**, 1413—1416.

Pomerantz, M., 1980, "Studies of literally two-dimensional

magnets of manganese stearate," in *Phase Transitions in Surface Films,* edited by J. G. Dash and J. Ruvalds (Plenum, New York), pp. 317–346.

Portal, J. C., R. J. Nicholas, E. Kress-Roger, A. Chevy, J. Besson, J. Galibert, and P. Perrier, 1980, "Two-dimensional behaviour of electrons in bulk InSe from Shubnikov–de Haas oscillations and cyclotron resonance," in *Proceedings of the 15th International Conference on the Physics of Semiconductors, Kyoto* [J. Phys. Soc. Japan **49**, Suppl. A, 879–882].

Prange, R. E., 1969, "Electron-Rayleigh-wave interaction," Phys. Rev. **187**, 804–808.

Prange, R. E., 1981, "Quantized Hall resistance and the measurement of the fine-structure constant," Phys. Rev. B **23**, 4802–4805.

Prange, R. E., and T. -W. Nee, 1968, "Quantum spectroscopy of the low-field oscillations in the surface impedance," Phys. Rev. **168**, 779–786.

Prasad, M., 1978, "On the magnetic field dependence of resonance line width in the inversion layer," Solid State Commun. **26**, 85–86.

Prasad, M., 1979, "Quantum theory of the cyclotron resonance lineshape for a two-dimensional electron-phonon system," Phys. Lett. A **70**, 127–130.

Prasad, M., 1980, "Generalized transport method and applications," J. Phys. C **13**, 3239–3251.

Prasad, M., and S. Fujita, 1977a, "On the cyclotron resonance width of an electron impurity system in two dimensions," Solid State Commun. **21**, 1105–1106.

Prasad, M., and S. Fujita, 1977b, "Comparison between the two theories of cyclotron resonance lineshape for a two-dimensional electron-impurity system," Solid State Commun. **23**, 551–553.

Prasad, M., and S. Fujita, 1977c, "Matthiessen's rule and its variation for cyclotron resonance width in two and three dimensions," Phys. Lett. A **63**, 147–148.

Prasad, M., and S. Fujita, 1978, "Quantum theory of cyclotron resonance lineshape for an electron-impurity system in two dimensions," Physica **91A**, 1–16.

Prasad, M., T. K. Srinivas, and S. Fujita, 1977, "On the temperature dependent cyclotron resonance lineshape of inversion layer electrons in Si," Solid State Commun. **24**, 439–441; Surf. Sci. **73**, 505–508 (1978).

Prelovšek, P., 1978a, "Numerical study of the conductivity in the vicinity of mobility edges," Phys. Rev. Lett. **40**, 1596–1599.

Prelovšek, P., 1978b, "Diffusion in the Anderson model of a disordered system: A numerical study," Phys. Rev. B **18**, 3657–3664.

Prelovšek, P., 1981, "Conductor-insulator transition in the Anderson model of a disordered solid," Phys. Rev. B **23**, 1304–1319.

Preuss, E., 1971, "Field-effect of indium antimonide in a magnetic field," Surf. Sci. **24**, 515–534.

Price, P. J., 1962, "Transmission of Bloch waves through crystal interfaces," in *Proceedings of the 6th International Conference on the Physics of Semiconductors, Exeter* (Institute of Physics, London), pp. 99–103.

Price, P. J., 1973, "Transport properties of the semiconductor superlattice," IBM J. Res. Dev. **17**, 39–46.

Price, P. J., 1980, "Dielectric function of superlattice materials," in *Basic Optical Properties of Materials, Summaries of Papers,* edited by A. Feldman (U.S. Government Printing Office, Washington), NBS Special Publication 574, pp. 164–166.

Price, P. J., 1981a, "Two-dimensional electron transport in semiconductor layers. I. Phonon scattering," Ann. Phys. (N.Y.) **133**, 217–239.

Price, P. J., 1981b, "Mesostructure electronics," IEEE Trans. Electron Devices **ED-28**, 911–914.

Price, P. J., 1981c, "Two-dimensional electron transport in semiconductor layers. II. Screening," J. Vac. Sci. Technol. **19**, 599–603.

Prokop'ev, E. P., 1966, "Localized electron states on a nonideal surface of a semiconductor," Fiz. Tverd. Tela (Leningrad) **8**, 2770–2772 [Sov. Phys.—Solid State **8**, 2209–2210 (1967)].

Quinn, J. J., 1976, "Transport studies in inversion layers," in *Proceedings of the 13th International Conference on the Physics of Semiconductors, Rome,* edited by F. G. Fumi (North-Holland, Amsterdam), pp. 733–740.

Quinn, J. J., and G. Kawamoto, 1978, "Charge density waves in silicon inversion layers: Effect of four valley interaction terms," Solid State Commun. **28**, 797–801.

Quinn, J. J., G. Kawamoto, and B. D. McCombe, 1978, "Subband spectroscopy by surface channel tunneling," Surf. Sci. **73**, 190–196.

Rahman, T. S., and A. A. Maradudin, 1980, "Effect of surface roughness on the image potential," Phys. Rev. B **21**, 504–521.

Rahman, T. S., and D. L. Mills, 1980, "Electron-phonon coupling in image-potential bound states," Phys. Rev. B **21**, 1432–1444.

Rahman, T. S., D. L. Mills, and P. S. Riseborough, 1981, "Electron-phonon interactions and electron inversion layers on polar semiconductors," Phys. Rev. B **23**, 4081–4088.

Raider, S. I., and R. Flitsch, 1976, "Stoichiometry of SiO_2/Si interfacial regions. I. Ultrathin oxide films," J. Vac. Sci. Technol. **13**, 58 (abstract).

Raider, S. I., and R. Flitsch, 1978, "X-ray photoelectron spectroscopy of SiO_2-Si interfacial regions," in *The Physics of SiO_2 and its Interfaces,* edited by S. T. Pantelides (Pergamon, New York), pp. 384–388.

Rajagopal, A. K., 1977a, "Longitudinal and transverse dielectric functions of a two-dimensional electron system: Inclusion of exchange correlations," Phys. Rev. B **15**, 4264–4269.

Rajagopal, A. K., 1977b, "Itinerant electron ferromagnetism of a two-dimensional system," Solid State Commun. **21**, 483–486.

Rajagopal, A. K., and J. C. Kimball, 1977, "Correlations in a two-dimensional electron system," Phys. Rev. B **15**, 2819–2825.

Rajagopal, A. K., S. P. Singhal, M. Banerjee, and J. C. Kimball, 1978a, "Ferromganetism of two-dimensional electron systems," Surf. Sci. **73**, 365–373.

Rajagopal, A. K., S. P. Singhal, M. Banerjee, and J. C. Kimball, 1978b, "Correlations in two-dimensional electron systems. Magnetic properties," Phys. Rev. B **17**, 2262–2268.

Rakhmanov, S. Ya., 1979, "The Wigner crystal in a semiconductor film in a high magnetic field," Solid State Commun. **30**, 779–782.

Rau, A. R. P., 1977, "Phenomena exhibiting strong field mixing," Phys. Rev. A **16**, 613–617.

Rau, A. R. P., 1979, "Rydberg states in electric and magnetic fields: Near-zero-energy resonances," J. Phys. B **12**, L193–L198.

Rau, A. R. P., 1980, "Two-dimensional electron layers: A system for studying strong field mixing effects," Surf. Sci. **98**, 513–514.

Rauh, H., and R. Kümmel, 1980a, "Theory of the temperature dependence of the enhanced valley splitting in surface states of silicon MOSFETs," Surf. Sci. **98**, 370–377.

Rauh, H., and R. Kümmel, 1980b, "Critical temperatures for the observation of valley-splitting in Si-MOSFETs," Solid State Commun. **35**, 731–733.

Rauh, H., and R. Kümmel, 1980c, "Many-body enhancement of the valley splitting in Si-MOSFETs at finite temperatures: Reexamination of the 2-dimensionality of the system and critical temperatures for the valley splitting," in *Proceedings of the 15th International Conference on the Physics of Semiconductors, Kyoto* [J. Phys. Soc. Japan **49**, Suppl. A, 971–974].

Rauh, H., and R. Kümmel, 1980d, "On the two-dimensionality of many-body effects in surface quantum states of Si-MOSFETs," Z. Phys. B **39**, 219–226.

Redin, R. D., H. A. Undem, and H. H. Soonpaa, 1977, "Effects of adsorption on the electrical conductivity of thin crystals of bismuth tellurium sulfide," Surf. Sci. **69**, 702–707.

Reisinger, H., and F. Koch, 1981, "Spectroscopy of InAs subbands," Solid State Commun. **37**, 429–431.

Rendell, R. W., and S. M. Girvin, 1981, "Hall voltage dependence on inversion-layer geometry in the quantum Hall-effect regime," Phys. Rev. B **23**, 6610–6614.

Ribeiro, C. A., and J. C. Pfister, 1972, "Hall effect measurements of hole mobility in an inversion layer of a MOS structure at low temperatures," Solid State Commun. **10**, 63–69.

Rice, T. M., 1965, "The effects of electron-electron interaction on the properties of metals," Ann. Phys. (N.Y.) **31**, 100–129.

Ritchie, R. H., 1957, "Plasma losses by fast electrons in thin films," Phys. Rev. **106**, 874–881.

Roberts, G. G., and M. J. Morant, eds., 1980, *Insulating Films on Semiconductors, 1979* (Institute of Physics, Bristol).

Roberts, G. G., K. P. Pande, and W. A. Barlow, 1977, "InP-Langmuir-film M.I.S. structures," Electron. Lett. **13**, 581–583.

Roberts, G. G., K. P. Pande, and W. A. Barlow, 1978, "InP/Langmuir-film M.I.S.F.E.T.," IEE J. Solid State Electron Devices **2**, 169–175.

Roberts, O. D., 1975, "Reflectance of an array of charge conducting layers," Z. Phys. B **22**, 21–30.

Romanov, O. V., V. Ya. Uritskii, and B. F. Gruzinov, 1969, "Carrier mobility in the inversion layers on the surface of silicon," Fiz. Tekh. Poluprovodn. **3**, 1414–1416 [Sov. Phys.—Semicond. **3**, 1183–1184 (1970)].

Romanov, O. V., V. Ya. Uritskii, and A. M. Yafyasov, 1976, "Influence of ion implantation on surface transport of carriers in silicon," Fiz. Tekh. Poluprovodn. **10**, 332–337 [Sov. Phys. — Semicond. **10**, 198–201 (1976)].

Romanov, O. V., A. M. Yafyasov, and V. Ya. Uritskii, 1979, "Influence of various factors on surface charge transport in the valence band of silicon," Fiz. Tekh. Poluprovodn. **13**, 2100–2105 [Sov. Phys.—Semicond. **13**, 1228–1231].

Romanov, Yu. A., 1979, "Plasma oscillations in a superlattice subjected to a strong high-frequency electric field," Fiz. Tverd. Tela (Leningrad) **21**, 877–882 [Sov. Phys.—Solid State **21**, 513–516 (1979)].

Romanov, Yu. A., and E. V. Demidov, 1980, "Nonlinear conductivity of thin semiconductor films," Fiz. Tekh. Poluprovodn. **14**, 1526–1531 [Sov. Phys. — Semicond. **14**, 906–908 (1980)].

Rona, M., and A. Erçelebi, 1979, "Polaron model for localization in Si inversion layers," in *Physics of Semiconductors, 1978*, edited by B. L. H. Wilson (Institute of Physics, Bristol), pp. 1239–1242.

Roos, M., and H. Köhler, 1979, "Investigation of the reproducibility of electronic properties in *n*-type inverted silicon MOSFET surfaces," Phys. Status Solidi B **94**, 469–475.

Roos, M., and H. Köhler, 1980, "Valley splitting and valley degeneracy factor in *n*-type silicon (110) and (111) inversion layers," in *Proceedings of the 15th International Conference on the Physics of Semiconductors, Kyoto* [J. Phys. Soc. Japan **49**, Suppl. A, 975–978].

Roos, M., and G. Landwehr, 1978, "Shubnikov–de Haas oscillations caused by a two-dimensional leakage channel on silicon MOSFETs induced by electron irradiation," IEEE Trans. Nucl. Sci. **NS-25**, 1246–1250.

Rosenbaum, T. F., K. Andres, G. A. Thomas, and P. A. Lee, 1981, "Conductivity cusp in a disordered metal," Phys. Rev. Lett. **46**, 568–571.

Rosthal, R. A., and R. E. Prange, 1976, "Effects of finite thickness on the interacting electron gas in a surface inversion layer," Surf. Sci. **58**, 325 (abstract).

Roth, L. M., H. J. Zeiger, and T. A. Kaplan, 1966, "Generalization of the Ruderman-Kittel-Kasuya-Yosida interaction for nonspherical Fermi surfaces," Phys. Rev. **149**, 519–525.

Roy, J. B., P. K. Basu, and B. R. Nag, 1980, "Mobility of electrons in a quantized accumulation layer on ZnO limited by phonon scattering," Phys. Status Solidi B **102**, K125–K128.

Roychoudhury, D., and P. K. Basu, 1977, "Density-of-states mass for quantized accumulation layers measured from *C-V* characteristics," Solid-State Electron. **20**, 1023–1024.

Roychoudhury, D., and P. K. Basu, 1980, "Mobility of electrons in a quantized silicon inversion layer due to phonon scattering," Phys. Rev. B **22**, 6325–6329.

Rozhkov, S. S., and P. M. Tomchuk, 1977, "Current fluctuations in semiconductors in the presence of a quantizing electric field," Zh. Eksp. Teor. Fiz. **72**, 248–256 [Sov. Phys. — JETP **45**, 130–134 (1977)].

Rundgren, J., and G. Malmstrom, 1977, "Transmission and reflection of low-energy electrons at the surface barrier of a metal," J. Phys. C **10**, 4671–4687.

Rutledge, J. L., and W. E. Armstrong, 1972, "Effective surface mobility theory," Solid-State Electron. **15**, 215–219.

Rybalko, A. S., 1980, "Interaction of helium surface electrons with electromagnetic radiation," Fiz. Nizk. Temp. **6**, 141–146 [Sov. J. Low Temp. Phys. **6**, 67–69 (1980)].

Rybalko, A. S., B. N. Esel'son, and Yu. Z. Kovdrya, 1979, "Liquid-crystal phase transition in a system of surface electrons at temperatures below 0.3 K," Fiz. Nizk. Temp. **5**, 947–949 [Sov. J. Low Temp. Phys. **5**, 450–451].

Rybalko, A. S., Yu. Z. Kovdrya, and B. N. Esel'son, 1975, "Electron mobility near the surface of liquid helium at temperatures down to 0.5 °K," Zh. Eksp. Teor. Fiz. Pis'ma Red. **22**, 569–572 [JETP Lett. **22**, 280–281 (1976)].

Rytova, N. S., 1966, "Resonance absorption of electromagnetic waves in a thin film," Fiz. Tverd. Tela (Leningrad) **8**, 2672–2678 [Sov. Phys. — Solid State **8**, 2136–2140 (1967)].

Ryzhii, V. I., 1968, "Quantum oscillations of electrical conductivity of thin films in a magnetic field," Fiz. Tverd. Tela (Leningrad) **10**, 2887–2889 [Sov. Phys. — Solid State **10**, 2286–2287 (1969)].

Ryzhii, V. I., 1969, "Quantum theory of the electrical conductivity of thin semiconducting films in a strong magnetic field," Fiz. Tekh. Poluprovodn. **3**, 1704–1706 [Sov. Phys. — Semicond. **3**, 1432–1433 (1970)].

Ryzhii, V. I., 1971, "New type of conductivity oscillation in a semiconductor surface layer in a transverse quantizing magnetic field," Fiz. Tverd. Tela (Leningrad) **13**, 3139–3141

[Sov. Phys. — Solid State **13**, 2644—2645 (1972)].
Sabnis, A. G., and J. T. Clemens, 1979, "Characterization of the electron mobility in the inverted ⟨100⟩ Si surface," in *1979 International Electron Devices Meeting Technical Digest* (IEEE, Piscataway, N.J.), pp. 18—21.
Sah, C. T., 1976a, "Bulk and interface imperfections in semiconductors," Solid-State Electron. **19**, 975—990.
Sah, C. T., 1976b, "The origin of interface states and interface charges generated by ionizing radiation," IEEE Trans. Nucl. Sci. NS-**23**, 1563—1568.
Sah, C. T., J. R. Edwards, and T. H. Ning, 1972a, "Observation of mobility anisotropy of electrons on (110) silicon surfaces at low temperatures," Phys. Status Solidi A **10**, 153—160.
Sah, C. T., T. H. Ning, and L. L. Tschopp, 1972b, "The scattering of electrons by surface oxide charges and by lattice vibrations at the silicon-silicon dioxide interface," Surf. Sci. **32**, 561—575.
Sai-Halasz, G. A., 1979, "Semiconductor superlattices," in *Physics of Semiconductors, 1978,* edited by B. L. H. Wilson (Institute of Physics, Bristol), pp. 21—30.
Sai-Halasz, G. A., 1980, "Man-made semiconductor superlattices," in *New Developments in Semiconductor Physics,* edited by F. Beleznay, G. Ferenczi, and J. Giber (Lecture Notes in Physics, Vol. 122; Springer, Berlin), pp. 215—225.
Sai-Halasz, G. A., L. L. Chang, J.-M. Welter, C.-A. Chang, and L. Esaki, 1978a, "Optical absorption of $In_{1-x}Ga_xAs$-$GaSb_{1-y}As_y$ superlattices," Solid State Commun. **27**, 935—937.
Sai-Halasz, G. A., L. Esaki, and W. A. Harrison, 1978b, "InAs-GaSb superlattice energy structure and its semiconductor-semimetal transition," Phys. Rev. B **18**, 2812—2818.
Sai-Halasz, G. A., A. Pinczuk, P. Y. Yu, and L. Esaki, 1978c, "Superlattice umklapp processes in resonant Raman scattering," Surf. Sci. **73**, 232—237.
Sai-Halasz, G. A., A. Pinczuk, P. Y. Yu, and L. Esaki, 1978d, "Resonance enhanced umklapp Raman processes in GaAs-$Ga_{1-x}Al_xAs$ superlattices," Solid State Commun. **25**, 381—384.
Sai-Halasz, G. A., R. Tsu, and L. Esaki, 1977, "A new semiconductor superlattice," Appl. Phys. Lett. **30**, 651—653.
Saitoh, M., 1977, "Warm electrons on the liquid ^{4}He surface," J. Phys. Soc. Japan **42**, 201—209.
Saitoh, M., and T. Aoki, 1978a, "Theory of hot electrons on the surface of ^{4}He," Surf. Sci. **73**, 291—295.
Saitoh, M., and T. Aoki, 1978b, "Theory of hot electrons on the liquid ^{4}He surface," J. Phys. Soc. Japan **44**, 71—79.
Saitoh, M., and T. Aoki, 1980, "Cyclotron resonance of hot electrons on the surface of ^{4}He," Surf. Sci. **98**, 61—65.
Sak, J., 1972, "Theory of surface polarons," Phys. Rev. B **6**, 3981—3986.
Sakaki, H., 1980, "Scattering suppression and high-mobility effect of size-quantized electrons in ultrafine semiconductor wire structures," Jpn. J. Appl. Phys. **19**, L735—L738.
Sakaki, H., L. L. Chang, G. A. Sai-Halasz, C. A. Chang, and L. Esaki, 1978, "Two-dimensional electronic structure in InAs-GaSb superlattices," Solid State Commun. **26**, 589—592.
Sakaki, H., L. L. Chang, and L. Esaki, 1979, "Subband-structure related anisotropy in negative magnetoresistivity of semiconductor superlattices," in *Physics of Semiconductors, 1978,* edited by B. L. H. Wilson (Institute of Physics, Bristol), pp. 737—740.
Sakaki, H., K. Hoh, and T. Sugano, 1970, "Determination of interface-state density and mobility ratio in silicon surface inversion layers," IEEE Trans. Electron Devices ED-**17**, 892—896.
Sakaki, H., and T. Sugano, 1971, "Galvanomagnetic effects in silicon surface inversion layers," Jpn. J. Appl. Phys. **10**, 1016—1027.
Sakaki, H., and Sugano, T., 1972a, "Anisotropic channel conductivity of a MOS transistor on the (110) surface of silicon," in *Proceedings of the 3rd Conference on Solid State Devices, Tokyo, 1971* [J. Japan Soc. Appl. Phys. **41** Suppl., 141—149].
Sakaki, H., and Sugano, T., 1972b, "Nonlinear transport and negative differential mobility of hot electrons in silicon surface inversion layers," Ann. Rep. Eng. Res. Inst. Univ. Tokyo **31**, 121—125.
Sakaki, H., and T. Sugano, 1974, "Negative differential resistance and thermal effect in silicon MOS field-effect transistors," in *Proceedings of the 5th Conference on Solid State Devices, Tokyo, 1973* [J. Japan Soc. Appl. Phys. **43** Suppl., 314—322].
Sakaki, H., K. Wagatsuma, J. Hamasaki, and S. Saito, 1976, "Velocity-field characteristics of size-quantized electrons in thin semiconductor films having corrugated surfaces," Seisan-Kenkyu **28**, 78—80.
Sakurai, T., and T. Sugano, 1980, "Gap states of crystalline silicon and amorphous SiO_2 system," in *The Physics of MOS Insulators,* edited by G. Lucovsky, S. T. Pantelides, and F. L. Galeener (Pergamon, New York), pp. 241—245.
Salashchenko, V. N., B. N. Zvonkov, O. N. Filatov, and I. A. Karpovich, 1975, "Quantum size effect in thin films of lead telluride," Fiz. Tverd. Tela (Leningrad) **17**, 3641—3643 [Sov. Phys. — Solid State **17**, 2367—2368 (1975)].
Sander, L. M., 1975, "Electron localization at a liquid helium surface," Phys. Rev. B **11**, 4350—4354.
Sander, L. M., J. H. Rose, and H. B. Shore, 1980, "Charge density waves in two- and three-dimensional jellium," Phys. Rev. B **21**, 2739—2744.
Sanders, T. M., Jr., and G. Weinreich, 1976, "Energies of external electron surface states on liquid helium," Phys. Rev. B **13**, 4810—4814.
Sandomirskii, V. B., 1967, "Quantum size effect in a semimetal film," Zh. Eksp. Teor. Fiz. **52**, 158—166 [Sov. Phys. — JETP **25**, 101—106 (1967)].
Sardaryan, V. S., and M. M. Arakelyan, 1978, "Bound states of electrons and optical phonons under conditions of one-dimensional quantizing," Phys. Status Solidi B **85**, 459—463.
Saris, F. W., W. K. Chu, C.-A. Chang, R. Ludeke, and L. Esaki, 1980, "Ion backscattering and channeling study of InAs-GaSb superlattices," Appl. Phys. Lett. **37**, 931—933.
Sarker, S., and E. Domany, 1981, "Scaling theory of Anderson localization: A renormalization-group approach," Phys. Rev. B **23**, 6018—6036.
Sato, K., and Y. Nagaoka, 1978, "Polarization-wave instability in quasi-two-dimensional system of electrons," Solid State Commun. **26**, 299—301.
Sato, T., Y. Takeishi, and H. Hara, 1969, "Effects of crystallographic orientation on mobility, surface state density, and noise in *p*-type inversion layers on oxidized silicon surfaces," Jpn. J. Appl. Phys. **8**, 588—598.
Sato, T., Y. Takeishi, H. Hara, and Y. Okamoto, 1971a, "Mobility anisotropy of electrons in inversion layers on oxidized silicon surfaces," Phys. Rev. B **4**, 1950—1960.
Sato, T., Y. Takeishi, H. Tango, H. Ohnuma, and Y. Okamoto, 1971b, "Drift-velocity saturation of holes in Si inversion

layers," J. Phys. Soc. Japan **31**, 1846.
Satpathy, S., and M. Altarelli, 1981, "Model calculation of the optical properties of semiconductor quantum wells," Phys. Rev. B **23**, 2977–2982.
Schaber, H., and R. E. Doezema, 1979, "Magnetoreflectivity of the inversion layer on *p*-PbTe in the far infrared," Phys. Rev. B **20**, 5257–5266.
Schaber, H., R. E. Doezema, J. F. Koch, and A. Lopez-Otero, 1978, "Magnetoreflectance of surface space charge layers on PbTe," Solid State Commun. **26**, 7–10; Surf. Sci. **73**, 503–504 (extended abstract).
Schaber, H., R. E. Doezema, P. J. Stiles, and A. Lopez-Otero, 1977, "Quantum oscillations in an inversion layer on *p*-PbTe," Solid State Commun. **23**, 405–408.
Schäffler, F. and F. Koch, 1981, "Subband spectroscopy at room temperature," Solid State Commun. **37**, 365–368.
Schiff, L. I., 1955, *Quantum Mechanics,* 2nd ed. (McGraw-Hill, New York), p. 120.
Schmid, A., 1974, "On the dynamics of electrons in an impure metal," Z. Phys. **271**, 251–256.
Schneider, P. M., and W. B. Fowler, 1978, "One-electron energy bands of silicon dioxide in the ideal β-cristobalite structure," Phys. Rev. B **18**, 7122–7133.
Schoepe, W., and G. W. Rayfield, 1973, "Tunneling from electronic bubble states in liquid helium through the liquid-vapor interface," Phys. Rev. A **7**, 2111–2121.
Scholz, J., and F. Koch, 1980, "Spectroscopy of electron subbands on Ge-(111)," Solid State Commun. **34**, 249–251.
Schrieffer, J. R., 1957, "Mobility in inversion layers: Theory and experiment," in *Semiconductor Surface Physics,* edited by R. H. Kingston (University of Pennsylvania Press, Philadelphia), pp. 55–69.
Schulman, J. N., and T. C. McGill, 1977, "Band structure of AlAs-GaAs(100) superlattices," Phys. Rev. Lett. **39**, 1680–1683; **40**, 483(E) (1978).
Schulman, J. N., and T. C. McGill, 1979a, "Electronic properties of AlAs-GaAs (001) interface and superlattice," Phys. Rev. B **19**, 6341–6349.
Schulman, J. N., and T. C. McGill, 1979b, "Ideal CdTe/HgTe superlattices," J. Vac. Sci. Technol. **16**, 1513–1516.
Schulman, J. N., and T. C. McGill, 1981, "Complex band structure and superlattice electronic states," Phys. Rev. B **23**, 4149–4155.
Schulte, F. K., 1977, "Energies and Fermi levels of electrons in size-quantized metal films," Phys. Status Solidi B **79**, 149–153.
Schulte, F. K., 1979, "Theory of valley-splitting without effective-mass approximation," Solid State Commun. **32**, 483–485.
Schulte, F. K., 1980a, "Electron energies in *n*-inversion layers of Si/SiO_2 calculated without effective-mass approximation," Surf. Sci. **98**, 366–369.
Schulte, F. K., 1980b, "$K_{||}$-dependence of subband energies for Si(001) *n*-inversion layers," Solid State Commun. **35**, 65–67.
Schulz, M., 1980, "MOS interface states," in *Insulating Films on Semiconductors, 1979,* edited by G. G. Roberts and M. J. Morant (Institute of Physics, Bristol), pp. 87–96.
Schulz, M., and N. M. Johnson, 1978, "Evidence for multiphonon emission from interface states in MOS structures," Solid State Commun. **25**, 481–484.
Schulz, M., E. Klausmann, and A. Hurrle, 1975, "Correlation of surface states with impurities," Crit. Rev. Solid State Sci. **5**, 319–325.
Schulz, M., and G. Pensl, eds., 1981, *Insulating Films on Semiconductors* (Springer, Berlin).
Sernelius, B. E., and K.-F. Berggren, 1980, "Variation of the electron effective mass with ionic scattering in silicon inversion layers," Surf. Sci. **98**, 191–196.
Sesselmann, W., T. Cole, J. P. Kotthaus, R. Kellerer, H. Gesch, I. Eisele, G. Dorda, and P. Goy, 1979, "Investigation of the band structure in inversion layers on vicinal planes of (100)-Si," in *Physics of Semiconductors, 1978,* edited by B. L. H. Wilson (Institute of Physics, Bristol), pp. 1343–1346.
Sesselmann, W., and J. P. Kotthaus, 1979, "Spectroscopic determination of the energy gaps in the inversion layer bandstructure on vicinal planes of Si(001)," Solid State Commun. **31**, 193–196.
Severson, K. E., and H. H. Soonpaa, 1977, "Peaked structure in a single-crystal film," Thin Solid Films **42**, 61–67.
Sham, L. J., 1979a, "Theory of inversion layers on high-index surface of silicon," in *Physics of Semiconductors, 1978,* edited by B. L. H. Wilson (Institute of Physics, Bristol), pp. 1339–1342.
Sham, L. J., 1979b, "Quasi-two dimensional electron system at the semiconductor interface," in *Physics of Low-Dimensional Systems (Proceedings of Kyoto Summer Institute, 1979),* edited by Y. Nagaoka and S. Hikami (Publication Office, Progress of Theoretical Physics, Kyoto), pp. 195–230.
Sham, L. J., S. J. Allen, Jr., A. Kamgar, and D. C. Tsui, 1978, "Valley-valley splitting in inversion layers on a high index surface of silicon," Phys. Rev. Lett. **40**, 472–475.
Sham, L. J., and W. Kohn, 1966, "One-particle properties of an inhomogeneous interacting electron gas," Phys. Rev. **145**, 561–567.
Sham, L. J., and M. Nakayama, 1978, "Effect of interface on the effective mass approximation," Surf. Sci. **73**, 272–280.
Sham, L. J., and M. Nakayama, 1979, "Effective-mass approximation in the presence of an interface," Phys. Rev. B **20**, 734–747.
Sheka, V. I., 1964, "Electron combination resonance intensity in semiconductors with a narrow forbidden band," Fiz. Tverd. Tela (Leningrad) **6**, 3099–3106 [Sov. Phys. — Solid State **6**, 2470–2475 (1965)].
Sherman, A. V., 1981, "Dependence of the polaron binding energy and effective mass in a crystal layer on its thickness," Solid State Commun. **39**, 273–277.
Shevchenko, S. I., 1976, "Theory of superconductivity of systems with pairing of spatially separated electrons and holes," Fiz. Nizk. Temp. **2**, 505–516 [Sov. J. Low Temp. Phys. **2**, 251–257 (1976)].
Shevchenko, S. I., 1977, "Ginzburg-Landau equations and quantum coherent phenomena in systems with electron-hole pairing," Fiz. Nizk. Temp. **3**, 605–622 [Sov. J. Low Temp. Phys. **3**, 293–302 (1977)].
Shevchenko, S. I., and I. O. Kulik, 1976, "Electrodynamics of electron pairing in low-dimensionality crystals without inversion centers," Zh. Eksp. Teor. Fiz. Pis'ma Red. **23**, 171–173 [JETP Lett. **23**, 150–153 (1976)].
Shik, A. Ya., 1974, "Superlattices — periodic semiconductor structures (review)," Fiz. Tekh. Poluprovodn. **8**, 1841–1864 [Sov. Phys. — Semicond. **8**, 1195–1209 (1974)].
Shik, A. Ya., 1976, "Conductivity of inhomogeneous surface channels," Zh. Eksp. Teor. Fiz. **70**, 2211–2217 [Sov. Phys. — JETP **43**, 1154–1157 (1976)].
Shikin, V. B., 1974, "Excitation of capillary waves in helium by a Wigner lattice of surface electrons," Zh. Eksp. Teor. Fiz. Pis'ma Red. **19**, 647–650 [JETP Lett. **19**, 335–336 (1974)].
Shikin, V. B., 1975, "Collective modes of a system of electrons

on a helium surface," Zh. Eksp. Teor. Fiz. Pis'ma Red. **22**, 328–331 [JETP Lett. **22**, 154–155 (1975)].
Shikin, V. B., 1977a, "The collective-excitation spectrum of the Wigner electron crystal on a liquid-helium surface," Zh. Eksp. Teor. Fiz. **72**, 1619–1629 [Sov. Phys. — JETP **45**, 850–856 (1977)].
Shikin, V. B., 1977b, "Cyclotron resonance with surface electrons in liquid helium," Zh. Eksp. Teor. Fiz. Pis'ma Red. **25**, 425–428 [JETP Lett. **25**, 397–400 (1977)].
Shikin, V. B., 1978a, "Theory of localized electron states on the liquid helium surface," Surf. Sci. **73**, 396–410.
Shikin, V. B., 1978b, "Multielectron bubbles in liquid helium," Zh. Eksp. Teor. Fiz. Pis'ma Red. **27**, 44–47 [JETP Lett. **27**, 39–41 (1978)].
Shikin, V. B., 1978c, "Parametric excitation of electrons at the liquid helium surface in a magnetic field," J. Phys. (Paris) **39**, Colloques, C6-336–C6-337.
Shikin, V. B., 1979a, "Parametric excitation of electrons on the surface of liquid helium in a magnetic field," Zh. Eksp. Teor. Fiz. **76**, 199–211 [Sov. Phys. — JETP **49**, 102–108 (1979)].
Shikin, V. B., 1979b, "The cyclotron frequency shift for electrons localized at the surface of liquid helium," Zh. Eksp. Teor. Fiz. **77**, 717–732 [Sov. Phys. — JETP **50**, 361–369 (1979)].
Shikin, V. B., 1979c, "Some properties of two-dimensional Wigner crystal on the liquid helium surface," in *Physics of Low-Dimensional Systems (Proceedings of Kyoto Summer Institute, 1979)*, edited by Y. Nagaoka and S. Hikami (Publication Office, Progress of Theoretical Physics, Kyoto), pp. 177–193.
Shikin, V. B., and P. Leiderer, 1980, "Many-electron holes on the surface of liquid helium," Zh. Eksp. Teor. Fiz. Pis'ma Red. **32**, 439–442 [JETP Lett. **32**, 416–418 (1980)].
Shikin, V. B., and Yu. P. Monarkha, 1973, "Free electrons on the surface of liquid helium in the presence of external fields," Zh. Eksp. Teor. Fiz. **65**, 751–761 [Sov. Phys. — JETP **38**, 373–377 (1974)].
Shikin, V. B., and Yu. P. Monarkha, 1974, "On the interaction of surface electrons in liquid helium with oscillations of the vapor-liquid interface," J. Low Temp. Phys. **16**, 193–208.
Shikin, V. B., and Yu. P. Monarkha, 1975, "Surface charges in helium (a survey)," Fiz. Nizk. Temp. **1**, 957–983 [Sov. J. Low Temp. Phys. **1**, 459–472 (1975)].
Shikin, V. B., and F. I. B. Williams, 1981, "Electrons on a dielectric liquid-vapor interface. Stability in presence of normal magnetic field," J. Low Temp. Phys. **43**, 1–15.
Shinba, Y., and K. Nakamura, 1981, "Phonon-limited electron mobility in Si(100) inversion layer at low temperatures," J. Phys. Soc. Japan **50**, 114–120.
Shiraki, Y., 1977, "Photoconductivity of silicon inversion layers," J. Phys. C **10**, 4539–4544.
Shiue, C. C., and C. T. Sah, 1976, "Studies of electron screening effects on the electron mobility in silicon surface inversion layers," Surf. Sci. **58**, 153–161.
Shiue, C. C., and C. T. Sah, 1979, "New mobility-measurement technique on inverted semiconductor surfaces near the conduction threshold," Phys. Rev. B **19**, 2149–2162.
Shiue, C. C., and C. T. Sah, 1980, "Theory and experiment of electron mobility on silicon surface in weak inversion," Surf. Sci. **98**, 173.
Shklovskii, B. I., 1977, "Critical behavior of the Hall coefficient near the percolation threshold," Zh. Eksp. Teor. Fiz. **72**, 288–295 [Sov. Phys. — JETP **45**, 152–156 (1977)].
Shmelev, G. M., I. A. Chaikovskii, V. V. Pavlovich, and É. M. Épshtein, 1977a, "Electron-phonon interaction in a superlattice," Phys. Status Solidi B **80**, 697–710.
Shmelev, G. M., I. A. Chaikovskii, V. V. Pavlovich, and É. M. Épshtein, 1977b, "Plasma oscillations in a superlattice," Phys. Status Solidi B **82**, 391–395.
Shockley, W., and G. L. Pearson, 1948, "Modulation of conductance of thin films of semi-conductors by surface charges," Phys. Rev. **74**, 232–233.
Shore, H. B., E. Zaremba, J. H. Rose, and L. Sander, 1979, "Density-functional theory of Wigner crystallization," Phys. Rev. B **18**, 6506–6509.
Siggia, E. D., and P. C. Kwok, 1970, "Properties of electrons in semiconductor inversion layers with many occupied electric subbands. I. Screening and impurity scattering," Phys. Rev. B **2**, 1024–1036.
Sigmon, T. W., W. K. Chu, E. Lugujjo, and J. W. Mayer, 1974, "Stoichiometry of thin silicon oxide layers on silicon," Appl. Phys. Lett. **24**, 105–107.
Silbermann, R., and G. Landwehr, 1975, "Surface quantum oscillations in accumulation and inversion layers on tellurium," Solid State Commun. **16**, 1055–1058.
Silbermann, R., and G. Landwehr, 1976, "Quantized electrons and holes in tellurium surfaces," Surf. Sci. **58**, 252–253.
Silbermann, R., G. Landwehr, and H. Köhler, 1971, "Field effect in tellurium," Solid State Commun. **9**, 949–951.
Silbermann, R., G. Landwehr, J. C. Thuillier, and J. Bouat, 1974, "Influence of external electric fields on surface quantum oscillations in tellurium," in *Proceedings of the Second International Conference on Solid Surfaces, Kyoto* [Jpn. J. Appl. Phys. Suppl. 2, Pt. 2, 359–362].
Silin, V. P., and O. M. Tolkachev, 1979, "Cyclotron resonance of skipping electrons and determination of the electron-electron interaction in bismuth," Fiz. Tverd. Tela (Leningrad) **21**, 1300–1306 [Sov. Phys. — Solid State **21**, 753–757 (1979)].
Silversmith, D. J., 1972, "Nonuniform lateral ionic impurity distributions at Si-SiO_2 interfaces," J. Electrochem. Soc. **119**, 1589–1593.
Singh, J., and A. Madhukar, 1981, "The origin and nature of silicon band-gap states at the Si/SiO_2 interface," Appl. Phys. Lett. **38**, 884–886.
Singwi, K. S., M. P. Tosi, R. H. Land, and A. Sjölander, 1968, "Electron correlations at metallic densities," Phys. Rev. **176**, 589–599.
Sinha, S. K., ed., 1980, *Ordering in Two Dimensions* (Elsevier–North-Holland, New York).
Sjögren, L., 1980, "Collective properties of a two-dimensional classical electron liquid," J. Phys. C **13**, L841–L846.
Sjöstrand, M. E., T. Cole, and P. J. Stiles, 1976, "Low temperature saturation of the channel conductivity in silicon inversion layers," Surf. Sci. **58**, 72–78.
Sjöstrand, M. E., and P. J. Stiles, 1975, "The channel conductivity in *n*-type Si inversion layers at very low electron densities," Solid State Commun. **16**, 903–907.
Smith, J. L., and P. J. Stiles, 1972, "Electron-electron interactions continuously variable in the range $2.1 > r_s > 0.9$," Phys. Rev. Lett. **29**, 102–104.
Smith, J. L., and P. J. Stiles, 1974, "The dependence of the electron-electron enhancement of the effective mass on magnetic field," in *Low Temperature Physics-LT 13*, edited by K. D. Timmerhaus, W. J. O'Sullivan, and E. F. Hammel (Plenum, New York), Vol. 4, pp. 32–36.
Smith, R. A., 1978, *Semiconductors*, 2nd ed. (Cambridge University Press, London).

Snel, J., 1981, "The doped Si/SiO_2 interface," Solid-State Electron. **24**, 135–139.

Solomon, P. M., 1977, "On the establishment of an inversion layer in *p*- and *n*-type silicon substrates under conditions of high oxide fields," Appl. Phys. Lett. **30**, 597–598.

Solomon, P. M., and D. J. DiMaria, 1981, "Effect of forming gas anneal on Al-SiO_2 internal photoemission characteristics," J. Appl. Phys. **52**, 5867–5869.

Sommer, W. T., and D. J. Tanner, 1971, "Mobility of electrons on the surface of liquid ^{4}He," Phys. Rev. Lett. **27**, 1345–1349.

Soonpaa, H. H., 1975, "An unusual *C-V* effect," Crit. Rev. Solid State Sci. **5**, 341–343.

Soonpaa, H. H., 1976a, "Electrical conductivity in a conductor 5 atoms thick," Surf. Sci. **58**, 42–47.

Soonpaa, H. H., 1976b, "A size effect semiconductor," in *Proceedings of the 13th International Conference on the Physics of Semiconductors, Rome,* edited by F. G. Fumi (North-Holland, Amsterdam), pp. 364–367.

Soonpaa, H. H., 1978a, "Thin crystal as a 2D system," Surf. Sci. **73**, 90–95.

Soonpaa, H. H., 1978b, "Minimum metallic conductivity in a thin crystal," Solid State Commun. **27**, 877–879.

Soonpaa, H. H., 1979, "Low field magnetoconductivity in thin crystals," Solid State Commun. **31**, 493–496.

Soonpaa, H. H., 1980, "Experimental observations on thin crystals of $Bi_2(Te_{1-x}S_x)_3$ in the localization region," Surf. Sci. **98**, 220–224.

Soukoulis, C. M., and E. N. Economou, 1980, "Localization in disordered two-dimensional systems," Phys. Rev. Lett. **45**, 1590–1593.

Spasojević, Ž., V. Milanović, and D. Tjapkin, 1980, "The calculation of the carrier concentration in a symmetrical MISIM structure inversion layer," Solid State Commun. **34**, 489–492.

Spenke, E., 1955, *Elektronische Halbleiter* (Springer, Berlin), p. 282.

Springett, B. E., M. H. Cohen, and J. Jortner, 1967, "Properties of an excess electron in liquid helium: The effect of pressure on the properties of the negative ion," Phys. Rev. **159**, 183–190.

Srinivasan, G., and M. Jonson, 1975, "Dielectric screening in inversion layers," J. Phys. C **8**, L37–L40.

Stallhofer, P., J. P. Kotthaus, and G. Abstreiter, 1979, "Effects of uniaxial stress on the cyclotron resonance in inversion layers on Si(100)," Solid State Commun. **32**, 655–658.

Stallhofer, P., J. P. Kotthaus, and J. F. Koch, 1976, "Surface cyclotron resonance in Si under uniaxial stress," Solid State Commun. **20**, 519–522.

Stallhofer, P., H. Miosga, and J. P. Kotthaus, 1978, "The effect of temperature and stress on the surface cyclotron resonance in (100)Si," Surf. Sci. **73**, 340–341.

Stannard, J. E., T. A. Kennedy, and B. D. McCombe, 1976, "Properties of surface carriers at GaAs-native oxide interfaces," J. Vac. Sci. Technol. **13**, 869–872.

Stark, D., and P. Zwicknagl, 1980, "Experimental study of quantum size effects in very thin metal films," Appl. Phys. **21**, 397–406.

Stauffer, D., 1979, "Scaling theory of percolation clusters," Phys. Rep. **54**, 1–74.

Stein, J., and U. Krey, 1979, "Numerical studies on the Anderson localization problem. I. Localization edges and critical exponents," Z. Phys. B **34**, 287–296.

Stein, J., and U. Krey, 1980a, "Numerical studies on the Anderson localization problem. II. Conductivity," Z. Phys. B **37**, 13–22.

Stein, J., and U. Krey, 1980b, "On the size-dependence of the electrical conductivity for strongly disordered two-dimensional systems," Solid State Commun. **36**, 951–955.

Stern, F., 1967, "Polarizability of a two-dimensional electron gas," Phys. Rev. Lett. **18**, 546–548.

Stern, F., 1968, "Transverse Hall effect in the electric quantum limit," Phys. Rev. Lett. **21**, 1687–1690.

Stern, F., 1970a, "Iteration methods for calculating self-consistent fields in semiconductor inversion layers," J. Comput. Phys. **6**, 56–67.

Stern, F., 1970b, "Quantum and continuum results for inversion layers," in *Proceedings of the Tenth International Conference on the Physics of Semiconductors, Cambridge, Massachusetts,* edited by S. P. Keller, J. C. Hensel, and F. Stern (U. S. Atomic Energy Commission, Oak Ridge, Tennessee), pp. 451–458.

Stern F., 1972a, "Surface quantization and surface transport in semiconductor inversion and accumulation layers," J. Vac. Sci. Technol. **9**, 752–753.

Stern, F., 1972b, "Self-consistent results for *n*-type Si inversion layers," Phys. Rev. B **5**, 4891–4899.

Stern, F., 1973, "Electron exchange energy in Si inversion layers," Phys. Rev. Lett. **30**, 278–280.

Stern, F., 1974a, "Quantum properties of surface space-charge layers," Crit. Rev. Solid State Sci. **4**, 499–514.

Stern, F., 1974b, "Evidence for a mobility edge in inversion layers," Phys. Rev. B **9**, 2762–2765.

Stern, F., 1974c, "Evidence for a mobility edge in inversion layers. II," J. Vac. Sci. Technol. **11**, 962–964.

Stern, F., 1974d, "Exchange energy in inversion layers: Thickness effects," in *Proceedings of the Second International Conference on Solid Surfaces, Kyoto* [Jpn. J. Appl. Phys. Suppl. **2**, Pt. 2, 323–328].

Stern, F., 1974e, "Calculated energy levels and optical absorption in *n*-type Si accumulation layers at low temperature," Phys. Rev. Lett. **33**, 960–963.

Stern, F., 1976a, "Screening and level broadening in inversion layers with random fixed charges," Surf. Sci. **58**, 162–168.

Stern, F., 1976b, "Recent progress in electronic properties of quasi-two-dimensional systems," Surf. Sci. **58**, 333–340.

Stern, F., 1976c, "Image and exchange effects on inversion layer wave functions," Bull. Am. Phys. Soc. **21**, 343.

Stern, F., 1977, "Effect of a thin transition layer at a Si-SiO_2 interface on electron mobility and energy levels," Solid State Commun. **21**, 163–166.

Stern, F., 1978a, "Two-subband screening and transport in (001) silicon inversion layers," Surf. Sci. **73**, 197–206.

Stern, F., 1978b, "Image potential near a gradual interface between two dielectrics," Phys. Rev. B **17**, 5009–5015.

Stern, F., 1980a, "Conference Summary [Yamada Conference II on Electronic Properties of Two-Dimensional Systems (Third International Conference)]," Surf. Sci. **98**, 613–616.

Stern, F., 1980b, "Calculated temperature dependence of mobility in silicon inversion layers," Phys. Rev. Lett. **44**, 1469–1472.

Stern, F., and W. E. Howard, 1967, "Properties of semiconductor surface inversion layers in the electric quantum limit," Phys. Rev. **163**, 816–835.

Stiles, P. J., 1974a, "Properties of carriers at the Si-SiO_2 interface in MOSFET structures," J. Vac. Sci. Technol. **11**, 958–961.

Stiles, P. J., 1974b, "Electronic properties of interface carriers

at low temperatures," in *Proceedings of the Second International Conference on Solid Surfaces, Kyoto* [Jpn. J. Appl. Phys. Suppl. 2, Pt. 2, 333–338].

Stiles, P. J., 1978, "The artificial superlattice in a two-dimensional system," Surf. Sci. **73**, 252–257.

Stiles, P. J., 1979, "Transport in quasi-two-dimensional space charge layers," in *Physics of Semiconductors, 1978,* edited by B. L. H. Wilson (Institute of Physics, Bristol), pp. 41–52.

Stiles, P. J., 1980, "Quasi-two-dimensional electron systems in semiconductor space charge layers," Surf. Sci. **98**, 143–144.

Stiles, P. J., T. Cole, and A. A. Lakhani, 1977, "Evidence for a superlattice at Si-SiO_x interface," J. Vac. Sci. Technol. **14**, 969–971.

Störmer, H. L., 1980, "Modulation doping of semiconductor superlattices and interfaces," in *Proceedings of the 15th International Conference on the Physics of Semiconductors, Kyoto* [J. Phys. Soc. Japan **49**, Suppl. A, 1013–1020].

Störmer, H. L., R. Dingle, A. C. Gossard, W. Wiegmann, and R. A. Logan, 1979a, "Electronic properties of modulation-doped GaAs-$Al_xGa_{1-x}As$ superlattices," in *Physics of Semiconductors, 1978,* edited by B. L. H. Wilson (Institute of Physics, Bristol), pp. 557–560.

Störmer, H. L., R. Dingle, A. C. Gossard, W. Wiegmann, and M. D. Sturge, 1979b, "Two-dimensional electron gas at a semiconductor-semiconductor interface," Solid State Commun. **29**, 705–709.

Störmer, H. L., R. Dingle, A. C. Gossard, W. Wiegmann, and M. D. Sturge, 1979c, "Two-dimensional electron gas at differentially doped GaAs-$Al_xGa_{1-x}As$ heterojunction interface," J. Vac. Sci. Technol. **16**, 1517–1519.

Störmer, H. L., A. C. Gossard, and W. Wiegmann, 1981a, "Backside-gated modulation-doped GaAs-(AlGa)As heterojunction interface," Appl. Phys. Lett. **39**, 493–495.

Störmer, H. L., A. C. Gossard, W. Wiegmann, and K. Baldwin, 1981b, "Dependence of electron mobility in modulation-doped GaAs-(AlGa)As heterojunction interfaces on electron density and Al concentration," Appl. Phys. Lett. **39**, 912–914.

Störmer, H. L., A. Pinczuk, A. C. Gossard, and W. Wiegmann, 1981c, "Influence of undoped (AlGa)As spacer on mobility enhancement in GaAs-(AlGa)As superlattices," Appl. Phys. Lett. **38**, 691–693.

Störmer, H. L., and W. -T. Tsang, 1980, "Two-dimensional hole gas at a semiconductor heterojunction interface," Appl. Phys. Lett. **35**, 685–687.

Stradling, R. A., 1980, "The physics of space charge layers," in *Insulating Films on Semiconductors, 1979,* edited by G. G. Roberts and M. J. Morant (Institute of Physics, Bristol), pp. 1–11.

Stradling, R. A., and R. J. Tidey, 1975, "Peaked structure appearing in the field effect mobility of silicon MOS devices at temperatures above 20 K," Crit. Rev. Solid State Sci. **5**, 359–368.

Studart, N., and O. Hipólito, 1979, "Correlations and plasma oscillations of a two-dimensional classical electron system," Phys. Rev. A **19**, 1790–1795.

Studart, N., and O. Hipólito, 1980, "Electrodynamical properties of two-dimensional classical electron systems," Phys. Rev. A **22**, 2860–2865.

Sturge, M. D., A. Kamgar, and D. C. Tsui, 1978, "Time-resolved photoconductivity measurements in Si MOSFETs," Bull. Am. Phys. Soc. **23**, 326.

Sugano, T., 1974, "Electron transport in silicon surface inversion layer," in *Proceedings of the 5th Conference on Solid State Devices, Tokyo, 1973* [J. Japan Soc. Appl. Phys. **43** Suppl., 309–313].

Sugano, T., 1980, "Physical and chemical properties of Si-SiO_2 transition regions," Surf. Sci. **98**, 145–153.

Sugano, T., J. J. Chen, and T. Hamano, 1980, "Morphology of Si-SiO_2 interface," Surf. Sci. **98**, 154–166.

Sugano, T., K. Hoh, H. Sakaki, T. Iizuka, K. Hirai, K. Kuroiwa, and K. Kakemoto, 1973, "Quantum state and electron transport of silicon-silicon dioxide interface and MIS device technology," J. Faculty Engineering, Univ. Tokyo (B) **XXXII**, 155–371.

Sugano, T., H. Sakaki, and K. Hoh, 1968, "Hall mobility of electrons in silicon surface inversion layers," Jpn. J. Appl. Phys. **7**, 1131.

Sugano, T., H. Sakaki, and K. Hoh, 1970, "Effect of heat treatment on interface mobility of carriers in MOS structures," in *Proceedings of the 1st Conference on Solid State Devices, Tokyo, 1969* [J. Japan Soc. Appl. Phys. **39** Suppl., 192–202].

Suh, Y. B., 1978, "Surface magnetic properties of Bloch electron gas in opposing electric and magnetic fields at $T=0$ K," Phys. Lett. A **66**, 337–340.

Suzuki, K., and Y. Kawamoto, 1973, "The g-factors of itinerant electrons in silicon inversion layers," J. Phys. Soc. Japan **35**, 1456–1459.

Svensson, C. M., 1978, "The defect structure of the Si-SO_2 interface, a model based on trivalent silicon and its hydrogen 'compounds'," in *The Physics of SiO_2 and its Interfaces,* edited by S. T. Pantelides (Pergamon, New York), pp. 328–332.

Sze, S. M., 1969, *Physics of Semiconductor Devices* (Wiley, New York) (or 2nd ed., 1981).

Takada, Y., 1977, "Acoustic plasmons in MOS inversion layers," J. Phys. Soc. Japan **43**, 1627–1636.

Takada, Y., 1978, "Plasmon mechanism of superconductivity in two- and three-dimensional electron systems," J. Phys. Soc. Japan **45**, 786–794.

Takada, Y., 1979, "Effects of screening and neutral impurity on mobility in silicon inversion layers under uniaxial stress," J. Phys. Soc. Japan **46**, 114–122.

Takada, Y., 1980a, "Theory of cyclotron resonance in Si(100) inversion layers under [001] uniaxial stress," Surf. Sci. **98**, 442–450.

Takada, Y., 1980b, "First-principle calculation of superconductivity transition temperature of MOS inversion layers," J. Phys. Soc. Japan **49**, 1713–1721.

Takada, Y., and T. Ando, 1978, "Stress effects on electronic properties of silicon inversion layers," J. Phys. Soc. Japan **44**, 905–913.

Takada, Y., K. Arai, N. Uchimura, and Y. Uemura, 1980a, "Theory of the electronic properties of n-channel inversion layers on narrow-gap semiconductors. I. Subband structure of InSb," J. Phys. Soc. Japan **49**, 1851–1858.

Takada, Y., K. Arai, N. Uchimura, and Y. Uemura, 1980b, "Theory of the electronic properties of n-channel inversion layers on narrow-gap semiconductors," in *Proceedings of the 15th International Conference on the Physics of Semiconductors, Kyoto* [J. Phys. Soc. Japan **49**, Suppl. A, 947–950].

Takada, Y., and Y. Uemura, 1976, "Acoustic plasmon and possibility of superconductivity in MOS structures," in *Proceedings of the 13th International Conference on the Physics of Semiconductors, Rome,* edited by F. G. Fumi (North-Holland, Amsterdam), pp. 754–757.

Takada, Y., and Y. Uemura, 1977, "Subband structures of n-channel inversion layers on III-V compounds — A possibility

of the gate controlled Gunn effect," J. Phys. Soc. Japan **43**, 139–150.

Takahashi, T., 1972, "The quantization of elastic waves in Si-SiO_2 system," M. S. thesis, Department of Physics, Faculty of Science, Gakushuin University, Tokyo (unpublished).

Takeishi, Y., T. Sato, H. Maeda, and K. Hirabayashi, 1972, "Effects of surface orientation on transport properties of electrons and holes on oxidized silicon surfaces," J. Vac. Sci. Technol. **9**, 769 (abstract).

Tangena, A. G., N. F. de Rooij, and J. Middelhoek, 1978, "Sensitivity of MOS structures for contamination with H^+, Na^+, and K^+ ions," J. Appl. Phys. **49**, 5576–5583.

Tannous, C., and A. Caille, 1980, "Two-dimensional plasmon-surface phonon interaction for ionic semiconductors," Phys. Status Solidi B **97**, K77–K80.

Tansal, S., A. B. Fowler, and R. F. Cotellessa, 1969, "Anomalous magnetoconductance in silicon surfaces," Phys. Rev. **178**, 1326–1327.

Tasch, A. F., Jr., D. D. Buss, R. T. Bate, and B. H. Breazeale, 1970, "Landau levels in the inversion layer on *p*-type $Hg_{1-x}Cd_xTe$," in *Proceedings of the Tenth International Conference on the Physics of Semiconductors, Cambridge, Massachusetts,* edited by S. P. Keller, J. C. Hensel, and F. Stern (U. S. Atomic Energy Commission, Oak Ridge, Tennessee), pp. 458–463.

Tatarskii, V. V., and V. B. Shikin, 1980, "Cyclotron resonance linewidth of electrons above the surface of liquid helium," Fiz. Nizk. Temp. **6**, 1365–1370 [Sov. J. Low Temp. Phys. **6**, 665–667 (1980)].

Tavger, B. A., and Demikhovskii, V. Ya., 1968, "Quantum size effects in semiconducting and semimetallic films," Usp. Fiz. Nauk **96**, 61–86 [Sov. Phys.—Usp. **11**, 644–658 (1969)].

Taylor, B. N., and W. D. Phillips, eds., 1982, *Proceedings of the Second International Conference on Precision Measurement and Fundamental Constants, Gaithersburg, 1981* (Special Publication 617, National Bureau of Standards, Washington).

Tews, H., 1978, "Hartree calculations for *n*-inversion layers on stressed silicon surfaces," Solid State Commun. **26**, 349–352.

Theis, T. N., 1980, "Plasmons in inversion layers," Surf. Sci. **98**, 515–532.

Theis, T. N., J. P. Kotthaus, and P. J. Stiles, 1977, "Two-dimensional magnetoplasmon in the silicon inversion layer," Solid State Commun. **24**, 273–277.

Theis, T. N., J. P. Kotthaus and P. J. Stiles, 1978a, "Generation of 2D plasmon resonances at multiple wave-vectors; a test of the dispersion relation," Surf. Sci. **73**, 434–436.

Theis, T. N., J. P. Kotthaus, and P. J. Stiles, 1978b, "Wavevector dependence of the two-dimensional plasmon dispersion relationship in the (100) silicon inversion layer," Solid State Commun. **26**, 603–606.

Thompson, J. P., 1978a, "Hall effect measurements on silicon inversion layers," Phys. Lett. A **66**, 65–66.

Thompson, J. P., 1978b, "Is the Hall effect in silicon inversion layers consistent with macroscopic inhomogeneities?" Philos. Mag. B **38**, 527–533.

Thorstensen, B., T. A. Fjeldly, and J. S. Johannessen, 1977, "Field effect in Si-SiO_2 structures induced by adsorption of polar gas molecules," in *Proceedings of the Seventh International Vacuum Congress and the Third International Conference on Solid Surfaces, Vienna,* edited by R. Dobrozemsky, F. Rüdenauer, F. P. Viehböck, and A. Breth (Berger, Horn, Austria), Vol. I, pp. 575–578.

Thouless, D. J., 1974, "Electrons in disordered systems and the theory of localization," Phys. Rep. **13**, 93–142.

Thouless, D. J., 1976, "Localization by correlation and by disorder," J. Phys. (Paris) **37**, Colloques, C4-349–C4-352.

Thouless, D. J., 1977, "Maximum metallic resistance in thin wires," Phys. Rev. Lett. **39**, 1167–1169.

Thouless, D. J., 1978, "Melting of the two-dimensional Wigner lattice," J. Phys. C **11**, L189–L190.

Thouless, D. J., 1979, "Percolation and localization," in *Ill-Condensed Matter,* edited by R. Balian, R. Maynard, and G. Toulouse (North-Holland, Amsterdam), pp. 1–62.

Thouless, D. J., 1980, "The effect of inelastic electron scattering on the conductivity of very thin wires," Solid State Commun. **34**, 683–685.

Thouless, D. J., 1981, "Localisation and the two-dimensional Hall effect," J. Phys. C **14**, 3475–3480.

Thouless, D. J., and M. E. Elzain, 1978, "The two-dimensional white noise problem and localisation in an inversion layer," J. Phys. C **11**, 3425–3438.

Thouless, D. J., and S. Kirkpatrick, 1981, "Conductivity of the disordered linear chain," J. Phys. C **14**, 235–245.

Thuillier, J. C., 1975, "Surface quantization in tellurium," in *Physique sous Champs Magnétiques Intenses, Grenoble, 1974* (Colloques Internationaux No. 242, Éditions du Centre National de la Recherche Scientifique, Paris), pp. 189–193.

Thuillier, J. C., and F. Bazenet, 1979, "Properties of oxide-$Hg_{1-x}Cd_xTe$ interfaces," J. Vac. Sci. Technol. **16**, 1417 (abstract).

Tidey, R. J., and R. A. Stradling, 1974, "Peaked structure appearing in the field effect mobility of silicon MOS devices at temperatures above 20 K," J. Phys. C **7**, L356–L361.

Tidey, R. J., R. A. Stradling, and M. Pepper, 1974, "Peaked structure appearing in the field effect mobility of silicon MOS devices at liquid helium temperatures," J. Phys. C **7**, L353–L355.

Ting, C. S., 1980, "Effect of intervalley electron-electron coupling on the cyclotron resonance line shape for electrons in the Si surface inversion layers," Surf. Sci. **98**, 437–441.

Ting, C. S., and A. K. Ganguly, 1979, "Effect of the Auger-like transition on the intersubband optical absorption in Si surface inversion layers," Phys. Rev. B **20**, 4244–4250.

Ting, C. S., A. K. Ganguly, and W. Y. Lai, 1981, "Theory of cyclotron resonance for electrons in a Si surface inversion layer under a uniaxial stress," Phys. Rev. B **24**, 3371–3379.

Ting, C. S., T. K. Lee, and J. J. Quinn, 1975, "Effective mass and *g* factor of interacting electrons in the surface inversion layer of silicon," Phys. Rev. Lett. **34**, 870–874.

Ting, C. S., S. C. Ying, and J. J. Quinn, 1976, "Infrared cyclotron resonance in semiconducting surface inversion layers," Phys. Rev. Lett. **37**, 215–218.

Ting, C. S., S. C. Ying, and J. J. Quinn, 1977, "Theory of cyclotron resonance of interacting electrons in a semiconducting surface inversion layer," Phys. Rev. B **16**, 5394–5404.

Tjapkin, D., V. Milanović, and Ž. Spasojević, 1981, "The Einstein relation for two-dimensional strongly inverted layers," Phys. Status Solidi A **63**, 737–742.

Tobey, M. C., Jr., and N. Gordon, 1974, "Concerning the onset of heavy inversion in MIS devices," IEEE Trans. Electron Devices **ED-21**, 649–650.

Toda, M., 1969, "Propagation of surface charge waves in *n*-InSb MOS structure in a magnetic field," J. Phys. Soc. Japan **27**, 428–436.

Toda, M., 1970, "Nonlinear effects of surface charge waves in a *n*-InSb MOS structure in a transverse magnetic field," Jpn. J. Appl. Phys. **9**, 49–57.

Tokuda, A. R., and P. O. Lauritzen, 1974, "MOSFET thresholds at 4.2 K induced by cooling bias," IEEE Trans. Electron Devices **ED-21**, 606–607.

Toscano-Rico, A., and J. C. Pfister, 1971, "Hall effect measurements of hole mobility in an inversion layer at the Si-SiO_2 interface," Phys. Status Solidi A **5**, 209–218.

Totsuji, H., 1975, "Thermodynamic properties of surface layer of classical electrons," J. Phys. Soc. Japan **39**, 253–254.

Totsuji, H., 1976, "Theory of two-dimensional classical electron plasma," J. Phys. Soc. Japan **40**, 857–862.

Totsuji, H., 1978, "Numerical experiment on two-dimensional electron liquids. Thermodynamic properties and onset of short-range order," Phys. Rev. A **17**, 399–406.

Totsuji, H., 1979a, "Cluster expansion for two-dimensional liquids," Phys. Rev. A **19**, 889–893.

Totsuji, H., 1979b, "Lower bounds for thermodynamic quantities of two- and three-dimensional one-component plasmas," Phys. Rev. A **19**, 1712–1716.

Totsuji, H., 1979c, "Lower bounds for thermodynamic quantities of d-dimensional classical one-component plasmas with d-dimensional Coulomb interactions ($d=1$, 2, and 3)," Phys. Rev. A **19**, 2433–2439.

Totsuji, H., 1980, "Effect of electron correlation on the high-frequency conductivity of electron liquids on a liquid helium surface," Phys. Rev. B **22**, 187–190.

Totsuji, H., and H. Kakeya, 1979, "Longitudinal properties of two-dimensional classical electron liquids," Phys. Lett. A **73**, 23–25.

Totsuji, H., and H. Kakeya, 1980, "Dynamical properties of two-dimensional classical electron liquids," Phys. Rev. A **22**, 1220–1228.

Toyoda, T., D. Y. Kojima, and A. Isihara, 1978, "Correlations in a 2D electron gas," Surf. Sci. **73**, 266–268.

Tremblay, A.-M., and V. Ambegaokar, 1979, "Eigenmodes of the coupled two-dimensional Wigner-crystal–liquid-surface system and instability of a charged liquid surface," Phys. Rev. B **20**, 2190–2195.

Troyanovskii, A. M., A. P. Volodin, and M. S. Khaikin, 1979a, "Electron localization over a liquid hydrogen surface," Zh. Eksp. Teor. Fiz. Pis'ma Red. **29**, 65–68 [JETP Lett. **29**, 59–62 (1979)].

Troyanovskii, A. M., A. P. Volodin, and M. S. Khaikin, 1979b, "Electron localization over the surface of crystalline hydrogen and neon," Zh. Eksp. Teor. Fiz. Pis'ma Red. **29**, 421–425 [JETP Lett. **29**, 382–385 (1979)].

Trylski, J., 1976, "Theoretical re-examination of the effective masses as obtained from Shubnikov–de Haas oscillations," in *Proceedings of the 13th International Conference on the Physics of Semiconductors, Rome,* edited by F. G. Fumi (North-Holland, Amsterdam), p. 1153 (abstract).

Tsu, R., and G. Döhler, 1975, "Hopping conductivity in a 'superlattice'," Phys. Rev. B **12**, 680–686.

Tsu, R., and L. Esaki, 1973, "Tunneling in a finite superlattice," Appl. Phys. Lett. **22**, 562–564.

Tsu, R., and J. Janak, 1974, "Magnetic quantization in a superlattice," Phys. Rev. B **9**, 404–408.

Tsu, R., A. Koma, and L. Esaki, 1975, "Optical properties of semiconductor superlattice," J. Appl. Phys. **46**, 842–845.

Tsui, D. C., 1970a, "Observation of Landau levels in InAs by electron tunneling," Solid State Commun. **8**, 113–116.

Tsui, D. C., 1970b, "Observation of surface bound state and two-dimensional energy band by electron tunneling," Phys. Rev. Lett. **24**, 303–306.

Tsui, D. C., 1970c, "Some recent developments in semiconductor tunneling," in *Proceedings of the Tenth International Conference on the Physics of Semiconductors, Cambridge, Massachusetts,* edited by S. P. Keller, J. C. Hensel, and F. Stern (U. S. Atomic Energy Commission, Oak Ridge, Tennessee), pp. 468–477.

Tsui, D. C., 1971a, "Effect of a parallel magnetic field on surface quantization," Solid State Commun. **9**, 1789–1792.

Tsui, D. C., 1971b, "Electron-tunneling studies of a quantized surface accumulation layer," Phys. Rev. B **4**, 4438–4449.

Tsui, D. C., 1972, "Quantum effects in a semiconductor surface layer," in *Proceedings of the 11th International Conference on the Physics of Semiconductors, Warsaw* (PWN–Polish Scientific, Warsaw), Vol. 1, pp. 109–125.

Tsui, D. C., 1973, "Electron tunneling and capacitance studies of a quantized surface accumulation layer," Phys. Rev. B **8**, 2657–2669.

Tsui, D. C., 1975a, "Landau-level spectra of conduction electrons at an InAs surface," Phys. Rev. B **12**, 5739–5748.

Tsui, D. C., 1975b, "Tunneling and some electronic properties of compound semiconductors," Crit. Rev. Solid State Sci. **5**, 353–357.

Tsui, D. C., 1977, "High field magnetoconductivity of Si inversion layers," Solid State Commun. **21**, 675–678.

Tsui, D. C., 1978, "Conference summary [Second International Conference on the Electronic Properties of Two-Dimensional Systems, Berchtesgaden, 1977]," Surf. Sci. **73**, 560–564.

Tsui, D. C., and S. J. Allen, Jr., 1974, "Mott-Anderson localization in the two-dimensional band tail of Si inversion layers," Phys. Rev. Lett. **32**, 1200–1203.

Tsui, D. C., and S. J. Allen, Jr., 1975, "Localization and the minimum metallic conductivity in Si inversion layers," Phys. Rev. Lett. **34**, 1293–1295.

Tsui, D. C., and S. J. Allen, Jr., 1981, "Localization and the quantized Hall resistance in the two-dimensional electron gas," Phys. Rev. B **24**, 4082.

Tsui, D. C., S. J. Allen, Jr., R. A. Logan, A. Kamgar, and S. N. Coppersmith, 1978, "High frequency conductivity in silicon inversion layers: Drude relaxation, 2D plasmons and minigaps in a surface superlattice," Surf. Sci. **73**, 419–433.

Tsui, D. C., Th. Englert, A. Y. Cho, and A. C. Gossard, 1980, "Observation of magnetophonon resonances in a two-dimensional electronic system," Phys. Rev. Lett. **44**, 341–344.

Tsui, D. C., and E. Gornik, 1978, "Far infrared emission from Si MOSFETs on high index surfaces," Appl. Phys. Lett. **32**, 365–367.

Tsui, D. C., E. Gornik, and R. A. Logan, 1980, "Far infrared emission from plasma oscillations of Si inversion layers," Solid State Commun. **35**, 875–877.

Tsui, D. C., E. Gornik, and W. Müller, 1979, "Voltage tunable emission from Si-inversion layers," in *Physics of Semiconductors, 1978,* edited by B. L. H. Wilson (Institute of Physics, Bristol), pp. 1347–1350.

Tsui, D. C., and A. C. Gossard, 1981, "Resistance standard using quantization of the Hall resistance of GaAs-$Al_xGa_{1-x}As$ heterostructures," Appl. Phys. Lett. **38**, 550–552.

Tsui, D. C., A. C. Gossard, G. Kaminsky, and W. Wiegmann, 1981, "Transport properties of GaAs-$Al_xGa_{1-x}As$ heterojunction field-effect transistors," Appl. Phys. Lett. **39**, 712–714.

Tsui, D. C., A. Kamgar, and M. D. Sturge, 1979, "New minigaps in electron inversion layers on vicinal planes of (100) Si," in *Physics of Semiconductors, 1978,* edited by B. L. H. Wilson (Institute of Physics, Bristol), pp. 1335–1338.

Tsui, D. C. and G. Kaminsky, 1975a, "Seebeck effect in Si inversion layers," Bull. Am. Phys. Soc. **20**, 555.

Tsui, D. C., and G. Kaminsky, 1975b, "Observation of higher sub-band in *n*-type (100) Si inversion layers," Phys. Rev. Lett. **35**, 1468–1471.

Tsui, D. C., and G. Kaminsky, 1976a, "Influence of uniaxial stress on quantum effects in Si inversion layers," Surf. Sci. **58**, 187–192.

Tsui, D. C., and G. Kaminsky, 1976b, "Valley degeneracy of electrons in accumulation and inversion layers on Si (111) surfaces," Solid State Commun. **20**, 93–95.

Tsui, D. C., and G. Kaminsky, 1979, "Observation of sixfold valley degeneracy in electron inversion layers on Si (111)," Phys. Rev. Lett. **42**, 595–597.

Tsui, D. C., and G. Kaminsky, 1980, "Si inversion layers with a six-fold valley degeneracy," Surf. Sci. **98**, 400–406.

Tsui, D. C., G. Kaminsky, and P. H. Schmidt, 1974, "Tunneling study of surface quantization in *n*-PbTe," Phys. Rev. B **9**, 3524–3531.

Tsui, D. C., G. Kaminsky, and P. H. Schmidt, 1978, "Tunneling spectroscopy of PbTe surfaces," in *Physics of Narrow Gap Semiconductors,* edited by J. Rauluszkiewicz, M. Górska, and E. Kaczmarek (PWN–Polish Scientific, Warsaw), pp. 405–410.

Tsui, D. C., and R. A. Logan, 1979, "Observation of two-dimensional electrons in LPE-grown GaAs-$Al_xGa_{1-x}As$ heterojunctions," Appl. Phys. Lett. **35**, 99–101.

Tsui, D. C., H. L. Störmer, A. C. Gossard, and W. Wiegmann, 1980, "Two-dimensional electrical transport in GaAs-$Al_xGa_{1-x}As$ multilayers at high magnetic fields," Phys. Rev. B **21**, 1589–1595.

Tsui, D. C., M. D. Sturge, A. Kamgar, and S. J. Allen, Jr., 1978, "Surface band structure of electron inversion layers on vicinal planes of Si (100)," Phys. Rev. Lett. **40**, 1667–1670.

Tsukada, M., 1976a, "Wigner lattice in MOS inversion layers under strong magnetic field," J. Phys. Soc. Japan **40**, 1515–1517.

Tsukada, M., 1976b, "On the tail states of the Landau subbands in MOS structures under strong magnetic field," J. Phys. Soc. Japan **41**, 1466–1472.

Tsukada, M., 1977a, "Two-dimensional crystallization of the electrons in MOS structures induced by strong magnetic field," J. Phys. Soc. Japan **42**, 391–398.

Tsukada, M., 1977b, "Two-dimensional Wigner crystal in MOS structures under strong magnetic fields," in *Proceedings of the Seventh International Vacuum Congress and the Third International Conference on Solid Surfaces, Vienna,* edited by R. Dobrozemsky, F. Rüdenauer, F. P. Viehböck, and A. Breth (Berger, Horn, Austria), Vol. I, pp. 403–406.

Tsuzuki, T., 1981, "Electric field dependence of non-metallic conduction in a two-dimensional random system," Solid State Commun. **38**, 915–917.

Tzoar, N., 1979a, "High-frequency conductivity of a two-dimensional electron gas interacting with optical phonons," Phys. Rev. B **20**, 1306–1309.

Tzoar, N., 1979b, "The interaction of polar-optical phonons with a two-dimensional electron gas," Surf. Sci. **84**, 440–448.

Tzoar, N., and P. M. Platzman, 1979, "High-frequency conductivity of a two-dimensional two-component electron gas," Phys. Rev. B **20**, 4189–4193.

Tzoar, N., P. M. Platzman, and A. Simons, 1976, "High-frequency conductivity of electrons in two-dimensional inversion layers," Phys. Rev. Lett. **36**, 1200–1203.

Uchimura, N., and Y. Uemura, 1979a, "Hot electron effects in Landau levels of MOS inversion layers," in *Physics of Semiconductors, 1978,* edited by B. L. H. Wilson (Institute of Physics, Bristol), pp. 331–334.

Uchimura, N., and Y. Uemura, 1979b, "Hot electron effects in Landau levels of MOS inversion layers," J. Phys. Soc. Japan **47**, 1417–1425.

Uemura, Y., 1974a, "Landau levels and electronic properties of semiconductor interface," in *Proceedings of the Second International Conference on Solid Surfaces, Kyoto* [Jpn. J. Appl. Phys., Suppl. 2, Pt. 2, 17–24].

Uemura, Y., 1974b, "Quantum galvano-magnetic phenomena in M.O.S. inversion layers," in *Proceedings of the 12th International Conference on the Physics of Semiconductors, Stuttgart,* edited by M. H. Pilkuhn (Teubner, Stuttgart), pp. 665–674.

Uemura, Y., 1976, "Theoretical considerations on quantization for carriers in MOS structures," Surf. Sci. **58**, 1–16.

Uemura, Y., and Y. Matsumoto, 1971, "An analysis for anomalous galvano-magnetic effects in surface inversion layer of semiconductors," in *Proceedings of the 2nd Conference on Solid State Devices, Tokyo, 1970* [J. Japan Soc. Appl. Phys. **40**, Suppl., 205–213].

Ulinich, F. R., and N. A. Usov, 1979, "Phase diagram of a two-dimensional Wigner crystal in a magnetic field," Zh. Eksp. Teor. Fiz. **76**, 288–294 [Sov. Phys.—JETP **49**, 147–150 (1979)].

Undem, H. A., K. E. Severson, and H. H. Soonpaa, 1977, "*I-V* and magnetoconductivity measurements on a quasi-two-dimensional crystal," Solid State Commun. **23**, 695–697.

Uren, M. J., R. A. Davies, and M. Pepper, 1980, "The observation of interaction and localisation effects in a two-dimensional electron gas at low temperatures," J. Phys. C **13**, L985–L993.

Uren, M. J., R. A. Davies, M. Kaveh, and M. Pepper, 1981, "Magnetic delocalisation of a two dimensional electron gas and the quantum law of electron-electron scattering," J. Phys. C **14**, L395–L402.

Ury, I., and J. W. Holm-Kennedy, 1978, "Two-dimensional subbanding in junction field effect structures," Surf. Sci. **73**, 179–189.

van Bruggen, C. F., C. Haas, and H. W. Myron, eds., 1980, *Proceedings of the International Conference on Layered Materials and Intercalates, Nijmegen, 1979* [Physica **99B**, 1–550].

Vandamme, L. K. J., 1980, "Model for $1/f$ noise in MOS transistors biased in the linear region," Solid-State Electron. **23**, 317–323.

Van den dries, L., C. Van Haesendonck, Y. Bruynseraede, and G. Deutscher, 1981, "Two-dimensional localization in thin copper films," Phys. Rev. Lett. **46**, 565–568.

van der Ziel, J. P., R. Dingle, R. C. Miller, W. Wiegmann, and W. A. Nordland, Jr., 1975, "Laser oscillation from quantum states in very thin GaAs-$Al_{0.2}Ga_{0.8}As$ multilayer structures," Appl. Phys. Lett. **26**, 463–465.

Van Horn, H. M., 1967, "Instability and melting of the electron solid," Phys. Rev. **157**, 342–349.

Van Overstraeten, R. J., G. Declerck, and G. L. Broux, 1973, "The influence of surface potential fluctuations on the operation of the MOS transistor in weak inversion," IEEE Trans. Electron Devices **ED-20**, 1154–1158.

van Ruyven, L. J., H. J. A. Bluyssen, and F. Williams, 1979, "Effective band edges at a heterojunction interface due to quantum and grading effects," in *Physics of Semiconductors, 1978,* edited by B. L. H. Wilson (Institute of Physics, Bristol),

pp. 769–772.
Varley, R. L., and J. E. Tigner, 1979, "Velocity autocorrelation function in a strongly coupled, magnetized pure electron plasma," Phys. Rev. Lett. **43**, 1113–1116.
Vas'ko, F. T., 1979, "Spin splitting in the spectrum of two-dimensional electrons due to the surface potential," Zh. Eksp. Teor. Fiz. Pis'ma Red. **30**, 574–577 [JETP Lett. **30**, 541–544 (1979)].
Vas'ko, F. T., and N. A. Prima, 1979, "Spin splitting of the spectrum of two-dimensional electrons," Fiz. Tverd. Tela (Leningrad) **21**, 1734–1738 [Sov. Phys.—Solid State **21**, 994–996 (1979)].
Vass, E., and K. Hess, 1976, "Energy loss of warm and hot carriers in surface inversion layers of polar semiconductors," Z. Phys. B **25**, 323–325.
Velchev, N. B., V. N. Holiavko, B. V. Morozov, and E. M. Skok, 1976, "Galvanomagnetic properties of p diffusion, accumulation and inversion layers at the Si-SiO_2 interface in the low temperature range," Thin Solid Films **35**, 305–319.
Velchev, N. B., and I. S. Nachev, 1980, "Self-consistent results for n-channel silicon MOST at high magnetic fields," Surf. Sci. **98**, 308–320.
Verwey, J. F., 1980, "Mobility and trapping of ions in SiO_2," in *Insulating Films on Semiconductors, 1979,* edited by G. G. Roberts and M. J. Morant (Institute of Physics, Bristol), pp. 62–74.
Veuhoff, E., and D. Kohl, 1981, "Hall effect measurements on ZnO accumulation layers," J. Phys. C **14**, 2395–2407.
Vincett, P. S., and G. G. Roberts, 1980, "Electrical and photoelectric transport properties of Langmuir-Blodgett films and a discussion of possible device applications," Thin Solid Films **68**, 135–171.
Vinter, B., 1975a, "Correlation energy and effective mass of electrons in an inversion layer," Phys. Rev. Lett. **35**, 1044–1047.
Vinter, B., 1975b, "Effect of the electron-electron interaction on the excitation energies of an n-inversion layer on Si," Phys. Rev. Lett. **35**, 598–601.
Vinter, B., 1976, "Many-body effects in n-type Si inversion layers. I. Effects in the lowest subband," Phys. Rev. B **13**, 4447–4456.
Vinter, B., 1977, "Many-body effects in n-type Si inversion layers. II. Excitations to higher subbands," Phys. Rev. B **15**, 3947–3958.
Vinter, B., 1978, "Self-consistent calculation of impurity scattering in inversion layers," Solid State Commun. **28**, 861–863.
Vinter, B., 1979a, "Subband energies in n-channel inversion layers on (111)-Ge," Phys. Rev. B **20**, 2395–2397.
Vinter, B., 1979b, "Density-functional calculation of subband structure of Si inversion layers under stress," Solid State Commun. **32**, 651–653.
Vinter, B., 1980, "Impurity scattering in inversion layers in density functional formalisms," Surf. Sci. **98**, 197–201.
Vinter, B., and A. W. Overhauser, 1980, "Resolution of Shubnikov–de Haas paradoxes in Si inversion layers," Phys. Rev. Lett. **44**, 47–50.
Vinter, B., and F. Stern, 1976, "Many-body effects in the first excited subband of the n-inversion layer of Si," Surf. Sci. **58**, 141–145.
Viscor, P., 1979, "Comment on two-dimensional variable-range hopping conduction in group IV amorphous elemental semiconductors," Solid State Commun. **32**, 281–284.
Visscher, P. B., and L. M. Falicov, 1971, "Dielectric screening in a layered electron gas," Phys. Rev. B **3**, 2541–2547.
Vlasenko, E. V., R. A. Suris, and B. I. Fuks, 1977, "Possibility of determination of the surface mobility in a charge-transfer MIS structure," Fiz. Tekh. Poluprovodn. **11**, 1112–1117 [Sov. Phys.—Semicond. **11**, 657–660 (1977)].
Vlasenko, E. V., R. A. Suris, A. M. Filachev, and B. I. Fuks, 1980, "Surface mobility of carriers in indium antimonide," Zh. Eksp. Teor. Fiz. Pis'ma Red. **31**, 49–52 [JETP Lett. **31**, 44–47 (1980)].
Vogel, F. L., and A. Hérold, eds., 1977, *Proceedings of the Franco American Conference on Intercalation Compounds of Graphite, La Napoule* [Mater. Sci. Engin. **31**, 1–355].
Voisin, P., G. Bastard, C. E. T. Goncalvès da Silva, M. Voos, L. L. Chang, and L. Esaki, 1981, "Luminescence from InAs-GaSb superlattices," Solid State Commun. **39**, 79–82.
Voisin, P., Y. Guldner, J. P. Vieren, M. Voos, C. Benoit à la Guillaume, N. J. Kawai, L. L. Chang, and L. Esaki, 1980, "Optical studies of InAs-GaSb superlattices," in *Proceedings of the 15th International Conference on the Physics of Semiconductors, Kyoto* [J. Phys. Soc. Japan **49**, Suppl. A, 1005–1008].
Vojak, B. A., N. Holonyak, Jr., W. D. Laidig, K. Hess, J. J. Coleman, and P. D. Dapkus, 1980, "The exitonic recombination in $Al_xGa_{1-x}As$-GaAs quantum-well heterostructures," Solid State Commun. **35**, 477–481.
Voland, G., and H. Paginia, 1975, "Steps and fine structure in the drain current of MISFETs after x-irradiation under bias," Appl. Phys. **8**, 211–215.
Volkov, V. A., and T. N. Pinsker, 1976, "Size quantization and the surface states in semiconductors," Zh. Eksp. Teor. Fiz. **70**, 2268–2278 [Sov. Phys.—JETP **43**, 1183–1189 (1976)].
Volkov, V. A., and T. N. Pinsker, 1977, "Electron dispersion law in a bounded crystal," Zh. Eksp. Teor. Fiz. **72**, 1087–1096 [Sov. Phys.—JETP **45**, 568–573 (1977)].
Volkov, V. A., and T. N. Pinsker, 1979, "Boundary conditions, energy spectrum, and optical transitions of electrons in bounded narrow gap crystals," Surf. Sci. **81**, 181–192.
Volkov, V. A., and V. B. Sandomirskii, 1978, "Influence of a natural superlattice from a surface with high indices on the spectrum of 2D electrons in a multivalley semiconductor," Zh. Eksp. Teor. Fiz. Pis'ma Red. **27**, 688–692 [JETP Lett. **27**, 651–654 (1978)].
Volkov, V. A., and V. B. Sandomirskii, 1979, "On the theory of a natural (orientational) superlattice in a two-dimensional electron gas," Phys. Status Solidi B **94**, 349–352.
Vollhardt, D., and P. Wölfle, 1980a, "Anderson localization in $d \leq 2$ dimensions: A self-consistent diagrammatic theory," Phys. Rev. Lett. **45**, 842–846; 1370(E).
Vollhardt, D., and P. Wölfle, 1980b, "Diagrammatic self-consistent treatment of the Anderson localization in $d \leq 2$ dimensions," Phys. Rev. B **22**, 4666–4679.
Volodin, A. P., and V. S. Édelman, 1979, "Spectrum of electrons localized above liquid ^3He," Zh. Eksp. Teor. Fiz. Pis'ma Red. **30**, 668–671 [JETP Lett. **30**, 633–636 (1979)].
Volodin, A. P., M. S. Khaikin, and V. S. Édelman, 1976, "Surface electronic states above a helium film," Zh. Eksp. Teor. Fiz. Pis'ma Red. **23**, 524–527 [JETP Lett. **23**, 478–481 (1976)].
Volodin, A. P., M. S. Khaikin, and V. S. Édel'man, 1977, "Development of instability and bubblon production on a charged surface of liquid helium," Zh. Eksp. Teor. Fiz. Pis'ma Red. **26**, 707–711 [JETP Lett. **26**, 543–546 (1977)].
von Barth, U., and L. Hedin, 1972, "A local exchange-

correlation potential for the spin polarized case: I," J. Phys. C **5**, 1629–1642.

von Klitzing, K., 1980, "Lineshape analysis of Shubnikov–de Haas oscillations in (100) *n*-type silicon inversion layers," Surf. Sci. **98**, 390–399.

von Klitzing, K., 1981, "The fine structure constant α. A contribution of semiconductor physics to the determination of α," in *Festkörperprobleme/Advances in Solid State Physics,* edited by J. Treusch (Vieweg, Braunschweig), Vol. XXI, pp. 1–23.

von Klitzing, K., G. Dorda, and M. Pepper, 1980, "Realization of a resistance standard based on fundamental constants," Phys. Rev. Lett. **45**, 494–497.

von Klitzing, K., Th. Englert, E. Bangert, and D. Fritzsche, 1980a, "Transport properties of a two-dimensional electron gas at the surface of InP—Field effect transistors," in *Proceedings of the 15th International Conference on the Physics of Semiconductors, Kyoto* [J. Phys. Soc. Japan **49**, Suppl. A, 979–982].

von Klitzing, K., Th. Englert, and D. Fritzsche, 1980b, "Transport measurements on InP inversion metal-oxide-semiconductor transistors," J. Appl. Phys. **51**, 5893–5897.

von Klitzing, K., Th. Englert, G. Landwehr, and G. Dorda, 1977, "Surface quantum oscillations in *n*-type (100) silicon inversion layers on sapphire," Solid State Commun. **24**, 703–706.

von Klitzing, K., and G. Landwehr, 1971, "Surface quantum states in tellurium," Solid State Commun. **9**, 2201–2205.

von Klitzing, K., G. Landwehr, and G. Dorda, 1974a, "Shubnikov–de Haas oscillations in *p*-type inversion layers on *n*-type silicon," Solid State Commun. **14**, 387–393.

von Klitzing, K., G. Landwehr, and G. Dorda, 1974b, "Quantum oscillations in *p*-type inversion layers of (111) and (100) silicon field effect transistors," Solid State Commun. **15**, 489–493.

von Klitzing, K., G. Landwehr, and G. Dorda, 1974c, "Surface quantum oscillations in *p*-type channels on *n*-type silicon," in *Proceedings of the Second International Conference on Solid Surfaces, Kyoto* [Jpn. J. Appl. Phys., Suppl. 2, Pt. 2, 351–354].

von Klitzing, K., R. J. Nicholas, and R. A. Stradling, 1976, "An observation by photoconductivity of strain splitting of shallow bulk donors located near to the surface in silicon MOS devices," in *Proceedings of the 13th International Conference on the Physics of Semiconductors, Rome,* edited by F. G. Fumi (North-Holland, Amsterdam), pp. 784–787.

von Ortenberg, M., 1975, "Substrate effects on the cyclotron resonance in surface layers of silicon," Solid State Commun. **17**, 1335–1338.

von Ortenberg, M., 1980, "Optical properties of the quasi two-dimensional systems on tellurium surfaces," Surf. Sci. **98**, 481–492.

von Ortenberg, M., S. Merz, and A. Schlachetzki, 1976, "Magneto-spectroscopy of electrons in accumulation layers on gallium arsenide surfaces," in *Proceedings of the 13th International Conference on the Physics of Semiconductors, Rome,* edited by F. G. Fumi (North-Holland, Amsterdam), pp. 766–769.

von Ortenberg, M., and R. Silbermann, 1975, "Cyclotron resonance of electrons and holes in electric surface subbands of tellurium," Solid State Commun. **17**, 617–620.

von Ortenberg, M., and R. Silbermann, 1976, "Surface cyclotron resonance of accumulation and inversion layers in tellurium," Surf. Sci. **58**, 202–206.

von Ortenberg, M., and U. Steigenberger, 1977, "Submillimeter cyclotron resonance of electrons in accumulation layers on indium antimonide surfaces," J. Opt. Soc. Am. **67**, 928–931.

von Ortenberg, M., J. Tuchendler, R. Silbermann, and J. C. Thuillier, 1979, "Frequency dependence of the surface cyclotron resonance of tellurium," Phys. Rev. B **19**, 2276–2282.

von Wienskowski, J., and W. Mönch, 1974, "Surface states at clean and cesiated Ge (111) surfaces," in *Proceedings of the 12th International Conference on the Physics of Semiconductors, Stuttgart,* edited by M. H. Pilkuhn (Teubner, Stuttgart), pp. 734–738.

Voos, M., and L. Esaki, 1981, "InAs-GaSb superlattices in high magnetic fields," in *Physics in High Magnetic Fields,* edited by S. Chikazumi and M. Miura (Springer, Berlin), pp. 292–300.

Voshchenkov, A. M., and J. N. Zemel, 1974, "Admittance studies of surface quantization in (100)-oriented Si metal-oxide-semiconductor field-effect transistors," Phys. Rev. B **9**, 4410–4421; **12**, 815(E) (1975).

Voss, R. F., 1977, "$1/f$ noise in Si inversion layers: The effect of oxide charge and conduction mechanism," in *Proceedings of the Symposium on $1/f$ Fluctuations, Tokyo* (Institute of Electrical Engineers of Japan, Tokyo), pp. 132–139.

Voss, R. F., 1978, "$1/f$ noise and percolation in impurity bands in inversion layers," J. Phys. C **11**, L923–L926.

Vul, B. M., and E. I. Zavaritskaya, 1978, "Shubnikov–de Haas oscillations in the cleavage plane of a germanium bicrystal," Zh. Eksp. Teor. Fiz. Pis'ma Red. **27**, 580–583 [JETP Lett. **27**, 547–550 (1978)].

Vul, B. M., and E. I. Zavaritskaya, 1979a, "Two-dimensional electronic phenomena in germanium," in *Physics of Semiconductors, 1978,* edited by B. L. H. Wilson (Institute of Physics, Bristol), pp. 421–424.

Vul, B. M., and E. I. Zavaritskaya, 1979b, "Two-dimensional electronic phenomena in bicrystals of germanium at helium temperatures," Zh. Eksp. Teor. Fiz. **76**, 1089–1099 [Sov. Phys.—JETP **49**, 551–557 (1979)].

Vul, B. M., E. I. Zavaritskaya, Yu. A. Bashkirov, and V. M. Vinogradova, 1977, "Minimum of metallic conductivity in a two-dimensional system," Zh. Eksp. Teor. Fiz. Pis'ma Red. **25**, 204–207 [Sov. Phys.—JETP **25**, 187–189 (1977)].

Wagner, R. J., T. A. Kennedy, B. D. McCombe, and D. C. Tsui, 1976a, "Frequency dependence of cyclotron resonance in Si inversion layers in the region of activated conductivity," Surf. Sci. **58**, 207–211.

Wagner, R. J., T. A. Kennedy, B. D. McCombe, and D. C. Tsui, 1976b, "Magnetooptical studies of low-density inversion layers in Si MOSFETs," in *Proceedings of the 13th International Conference on the Physics of Semiconductors, Rome,* edited by F. G. Fumi (North-Holland, Amsterdam), pp. 770–773.

Wagner, R. J., T. A. Kennedy, B. D. McCombe, and D. C. Tsui, 1980, "Cyclotron resonance of electron inversion layers in Si (001) metal-oxide-semiconductor field-effect transistors (MOSFET's)," Phys. Rev. B **22**, 945–958.

Wagner, R. J., T. A. Kennedy, and H. H. Wieder, 1978, "Magneto-transconductance study of surface accumulation layers in InAs," in *Physics of Narrow Gap Semiconductors,* edited by J. Rauluszkiewicz, M. Górska, and E. Kaczmarek (PWN—Polish Scientific, Warsaw), pp. 427–432; Surf. Sci. **73**, 545–546 (extended abstract).

Wagner, R. J., and D. C. Tsui, 1979, "Submillimeter cyclotron resonance studies of inversion layers at low electron density," J. Magn. Magn. Mater **11**, 26–31.

Wagner, R. J., and D. C. Tsui, 1980, "Submillimeter laser cy-

clotron resonance of inversion layers at low electron densities," Surf. Sci. **98**, 256–261.

Wakabayashi, J., K. Hatanaka, and S. Kawaji, 1979, "Magnetoconductance oscillations in inversion layers in silicon on sapphire (SOS)," in *Physics of Semiconductors, 1978,* edited by B. L. H. Wilson (Institute of Physics, Bristol), pp. 1251–1254.

Wakabayashi, J., and S. Kawaji, 1978, "Hall effect in silicon MOS inversion layers under strong magnetic fields," J. Phys. Soc. Japan **44**, 1839–1849.

Wakabayashi, J., and S. Kawaji, 1980a, "Hall conductivity in *n*-type silicon inversion layers under strong magnetic fields," Surf. Sci. **98**, 299–307.

Wakabayashi, J., and S. Kawaji, 1980b, "Hall current measurement under strong magnetic fields for silicon MOS inversion layers," J. Phys. Soc. Japan **48**, 333–334.

Wang, W. I., C. E. C. Wood, and L. F. Eastman, 1981, "Extremely high electron mobilities in modulation doped GaAs-$Al_xGa_{1-x}As$ heterojunction superlattices," Electron. Lett. **17**, 36–37.

Wanner, M., and P. Leiderer, 1979, "Charge-induced ripplon softening and dimple crystallization at the interface of ^{3}He-^{4}He mixtures," Phys. Rev. Lett. **42**, 315–317.

Wannier, G. H., 1959, *Elements of Solid State Theory* (Cambridge University Press), pp. 191–193.

Washburn, H. A., and J. R. Sites, 1978, "Oscillatory transport coefficients in InAs surface layers," Surf. Sci. **73**, 537–544.

Washburn, H. A., J. R. Sites, and H. H. Wieder, 1979, "Electronic profile of *n*-InAs on semi-insulating GaAs," J. Appl. Phys. **50**, 4872–4878.

Weaire, D., and B. Kramer, 1979, "Numerical methods in the study of the Anderson transition," J. Non-Cryst. Solids **32**, 131–140.

Weaire, D., and B. Kramer, 1980, "Numerical methods for electronic properties of disordered solids," J. Non-Cryst. Solids **35/36**, 9–14.

Weaire, D., and V. Srivastava, 1977, "The Anderson localisation problem II. Some detailed numerical results," J. Phys. C **10**, 4309–4318.

Weaire, D., and A. R. Williams, 1977, "The Anderson localization problem: I. A new numerical approach," J. Phys. C **10**, 1239–1245.

Weber, W., G. Abstreiter, and J. F. Koch, 1976, "Electrons in a surface space charge layer on germanium—Shubnikov–de Haas oscillations and cyclotron resonance," Solid State Commun. **18**, 1397–1399.

Wegner, F., 1979, "The mobility edge problem: Continuous symmetry and a conjecture," Z. Phys. B **35**, 207–210.

Weimer, P. K., 1962, "The TFT—A new thin-film transistor," Proc. IRE **50**, 1462–1469.

Weinberg, Z. A., 1977, "Tunneling of electrons from Si into thermally grown SiO_2," Solid-State Electron. **20**, 11–18.

Weinberg, Z. A., W. C. Johnson, and M. A. Lampert, 1976, "High field transport in SiO_2 on silicon induced by corona charging of the unmetallized surface," J. Appl. Phys. **47**, 248–255.

Weisbuch, C., R. Dingle, A. C. Gossard, and W. Wiegmann, 1980, "Optical properties and interface disorder of GaAs-$Al_xGa_{1-x}As$ multi-quantum well structures," in *Gallium Arsenide and Related Compounds, 1980,* edited by H. W. Thim (Institute of Physics, Bristol), pp. 711–720; see also J. Vac. Sci. Technol. **17**, 1128–1129 (summary abstract).

Weisbuch, C., R. Dingle, A. C. Gossard, and W. Wiegmann, 1981a, "Optical characterization of interface disorder in GaAs-$Al_xGa_{1-x}As$ multi-quantum well structures," Solid State Commun. **38**, 709–712.

Weisbuch, C., R. C. Miller, R. Dingle, A. C. Gossard, and W. Wiegmann, 1981b, "Intrinsic radiative recombination from quantum states in GaAs-$Al_xGa_{1-x}As$ multiquantum well structures," Solid State Commun. **37**, 219–222.

Weissman, Y., 1976, "Quantum spatial distribution of a nondegenerate free charge carrier gas in semiconductors subject to high external electric fields at low temperatures," J. Phys. C **9**, 2353–2363.

Weisz, J. F., J. B. Sokoloff, and J. E. Sacco, 1979, "Impurity pinning in one, two, and three dimensions in incommensurate modulated lattices," Phys. Rev. B **20**, 4713–4720.

Werthamer, N. R., 1969, "Theory of quantum crystals," Am. J. Phys. **37**, 763–782.

Wheeler, R. G., 1976, "Far infrared photoresistive response in silicon inversion layers and electric subband spectra," Surf. Sci. **58**, 146 (abstract).

Wheeler, R. G., 1981, "Magnetoconductance and weak localization in silicon inversion layers," Phys. Rev. B **24**, 4645–4651.

Wheeler, R. G., and H. S. Goldberg, 1975, "A novel voltage tuneable infrared spectrometer-detector," IEEE Trans. Electron Devices **ED-22**, 1001–1009.

Wheeler, R. G., and R. W. Ralston, 1971, "Continuously voltage-tunable line absorption in surface quantization," Phys. Rev. Letters **27**, 925–928.

Whelam, M. V., A. H. Goemans, and L. M. C. Goosens, 1967, "Residual stresses at an oxide-silicon interface," Appl. Phys. Lett. **10**, 262–264.

White, C. T., and K. L. Ngai, 1978a, "Random attractive electron-electron interactions in two-dimensional systems," Surf. Sci. **73**, 116–120.

White, C. T., and K. L. Ngai, 1978b, "Metastabilities at the Si-SiO_x interface," in *The Physics of SiO_2 and its Interfaces,* edited by S. T. Pantelides (Pergamon, New York), pp. 412–416.

White, C. T., and K. L. Ngai, 1979, "Reconstructing states at the Si-SiO_2 interface," J. Vac. Sci. Technol. **16**, 1412–1416.

White, C. T., and K. L. Ngai, 1980, "Polaron and bipolaron states in Si-inversion layers: Possible origins and effects," Surf. Sci. **98**, 227–242.

White, S. R., and L. J. Sham, 1981, "Electronic properties of flat-band semiconductor heterostructures," Phys. Rev. Lett. **47**, 879–882.

Wieder, H. H., 1980, "The problems and prospects of compound semiconductor field-effect transistors," J. Vac. Sci. Technol. **17**, 1009–1018.

Wieder, H. H., 1981, "Materials options for field-effect transistors," J. Vac. Sci. Technol. **18**, 827–837.

Wiesinger, K., W. Beinvogl, and J. F. Koch, 1979, "IR spectroscopy of subband levels on InSb surfaces," in *Physics of Semiconductors, 1978,* edited by B. L. H. Wilson (Institute of Physics, Bristol), pp. 1215–1218.

Wigner, E., 1934, "On the interaction of electrons in metals," Phys. Rev. **46**, 1002–1011.

Wigner, E., 1938, "Effects of the electron interaction on the energy levels of electrons in metals," Trans. Faraday Soc. **34**, 678–685.

Williams, F. I. B., 1980, "Two dimensional adsorbed charges," J. Phys. (Paris) **41**, Colloques, C3-249–C3-262.

Williams, G. A., and J. Theobald, 1980, "Localized ions under the surface of liquid helium," Phys. Lett. A **77**, 255–257.

Williams, P. M., 1976, "Phase transitions and charge density

waves in the layered transition metal dichalcogenides," in *Crystallography and Crystal Chemistry of Materials with Layered Structures,* edited by F. Lévy (Reidel, Dordrecht), pp. 51–92.

Williams, R., 1974, "Image force interactions at the interface between an insulator and a semiconductor," J. Appl. Phys. **45**, 1239–1242.

Williams, R., 1977, "Properties of the silicon-SiO_2 interface," J. Vac. Sci. Technol. **14**, 1106–1111.

Williams, R., and R. S. Crandall, 1971, "Deformation of the surface of liquid helium by electrons," Phys. Lett. A **36**, 35–36.

Williams, R., and M. H. Woods, 1973, "Image forces and the behavior of mobile positive ions in silicon dioxide," Appl. Phys. Lett. **22**, 458–459.

Wilson, B. A., S. J. Allen, Jr., and D. C. Tsui, 1980, "Evidence for a collective ground state in Si inversion layers in the extreme quantum limit," Surf. Sci. **98**, 262–271; Phys. Rev. Lett. **44**, 479–482.

Witkowski, L. C., T. J. Drummond, S. A. Barnett, H. Morkoç, A. Y. Cho, and J. E. Greene, 1981a, "High mobility GaAs-$Al_xGa_{1-x}As$ single period modulation-doped heterojunctions," Electron. Lett. **17**, 126–128.

Witkowski, L. C., T. J. Drummond, C. M. Stanchak, and H. Morkoç, 1981b, "High mobilities in $Al_xGa_{1-x}As$-GaAs heterojunctions," Appl. Phys. Lett. **37**, 1033–1035.

Wu, C.-Y., and G. Thomas, 1972, "Theory of the electron mobility in inversion layers on oxidized silicon surface at room temperature," Phys. Rev. B **6**, 4581–4587.

Wu, C.-Y., and G. Thomas, 1974, "Two-dimensional electron-lattice scattering in thermally oxidized silicon surface inversion layers," Phys. Rev. B **9**, 1724–1732.

Yagi, A., and S. Kawaji, 1978, "Oxide thickness effects on electron scatterings at a thermally grown Si-SiO_2 interface," Appl. Phys. Lett. **33**, 349–350.

Yagi, A., and S. Kawaji, 1979, "Effects of nitrogen annealing on electron scatterings in Si-SiO_2 interface," Solid-State Electron. **22**, 261–263.

Yagi, A., and S. Kawaji, 1981, "Effects of tailing of density of state on the mobility of Si-MOSFETs at low temperatures—A proposal for the characterization of Si-SiO_2 interfaces," Jpn. J. Appl. Phys. **20**, 909–915.

Yagi, A., and M. Nakai, 1980, "Coulomb scattering in the band tail of *n*-channel silicon MOSFETs," Surf. Sci. **98**, 174–180.

Yagi, A., M. Namiki, K. Kusuda, and S. Kawaji, 1978, "Characterization of Si-SiO_2 interface with Cl^- ions by low temperature electron conduction measurements," Surf. Sci. **73**, 129–134.

Yamada, E., 1974, "Theory of hot electrons and saturation velocities in silicon inversion layers," in *Proceedings of the 5th Conference on Solid State Devices, Tokyo, 1973* [J. Japan Soc. Appl. Phys. **43** Suppl., 323–326].

Yoshino, S., and M. Okazaki, 1976, "Numerical study of localization in Anderson model for disordered systems," Solid State Commun. **20**, 81–83.

Yoshino, S., and M. Okazaki, 1977, "Numerical study of electron localization in Anderson model for disordered systems: Spatial extension of wavefunction," J. Phys. Soc. Japan **43**, 415–423.

Yoshino, S., and M. Okazaki, 1978, "Chain like localization in the two dimensional disordered system," Solid State Commun. **27**, 557–560.

Yoshioka, D., and H. Fukuyama, 1978, "Existence of dipole-density-wave (DDW) state in electron-hole junction systems," J. Phys. Soc. Japan **45**, 137–147; **47**, 327(E) (1979).

Yoshioka, D., and H. Fukuyama, 1979, "Charge density wave state of two-dimensional electrons in strong magnetic fields," J. Phys. Soc. Japan **47**, 394–402.

Yoshioka, D., and H. Fukuyama, 1980, "Charge density wave state of two-dimensional electrons in strong magnetic fields," Surf. Sci. **98**, 272–275.

Yoshioka, D., and H. Fukuyama, 1981a, "Two-dimensional charge density wave state in a strong magnetic field," in *Physics in High Magnetic Fields,* edited by S. Chikazumi and M. Miura (Springer, Berlin), pp. 288–291.

Yoshioka, D., and H. Fukuyama, 1981b, "Effects of higher Landau levels and valley degeneracy on charge density wave instability of two-dimensional electrons in strong magnetic fields," J. Phys. Soc. Japan **50**, 1560–1569.

Yoshioka, D., Y. Ono, and H. Fukuyama, 1981, "Self-consistent treatment of two-dimensional Anderson localization in magnetic fields," J. Phys. Soc. Japan **50**, 3419–3426; **51**, 340(E) (1982).

Young, D. R., 1980, "Electron trapping in SiO_2," in *Insulating Films on Semiconductors, 1979,* edited by G. G. Roberts and M. J. Morant (Institute of Physics, Bristol), pp. 28–39.

Zaĭužny, M., 1978, "Two-photon interband absorption in size-quantized semiconductor films," Thin Solid Films **55**, 243–252.

Zaĭužny, M., 1979a, "Light absorption in size-quantized film of a many valley semiconductor," Acta Phys. Polon. A **55**, 819–826.

Zaĭužny, M., 1979b, "On the optical orientation of free carriers in size quantized $Pb_{1-x}Sn_xTe$ films," Phys. Status Solidi B **96**, K51–K55.

Zaĭužny, M., 1981a, "On the optical transitions in size quantized films," Surf. Sci. **104**, L222–L224.

Zaĭužny, M., 1981b, "Intersubband dipole matrix elements of narrow-gap semiconductor films," Thin Solid Films **76**, 307–312.

Zaĭužny, M., 1981c, "Interband absorption in size-quantized InSb films," Thin Solid Films **81**, 161–167.

Zaĭužny, M., and M. Pilat, 1979, "Two-photon absorption in size-quantized films with tilted valleys," Thin Solid Films **61**, 99–103.

Zemel, A., and J. R. Sites, 1977, "Electronic transport near the surface of indium antimonide films," Thin Solids Films **41**, 297–305.

Zemel, J. N., 1979, "Chemically sensitive devices," Surf. Sci. **86**, 322–334.

Zemel, J. N., and M. Kaplit, 1969, "Degeneracy effects on semiconductor surfaces," Surf. Sci. **13**, 17–29.

Zener, C., 1934, "A theory of the electrical breakdown of solid dielectrics," Proc. R. Soc. London Ser. A **145**, 523–529.

Zia, R. K. P., 1973, "Electron correlation in a high density gas confined to very thin films," J. Phys. C **6**, 3121–3129.

Ziegler, K., and E. Klausmann, 1976, "Properties of the interface charge inhomogeneities in the thermally grown Si-SiO_2 structure," Appl. Phys. Lett. **28**, 678–681.

Zimmermann, J., R. Fauquembergue, M. Charef, and E. Constant, 1980, "Electron dynamics in *p*-Si MOSFET inversion channels," Electron. Lett. **16**, 664–666.

Zipfel, C. L., T. R. Brown, and C. C. Grimes, 1976a, "Spectroscopic studies of electron surface states on liquid helium," Surf. Sci. **58**, 283–288.

Zipfel, C. L., T. R. Brown, and C. C. Grimes, 1976b, "Measurement of the velocity autocorrelation time in a two-

dimensional electron liquid," Phys. Rev. Lett. **37**, 1760—1763.

Zittartz, J., and J. S. Langer, 1966, "Theory of bound states in a random potential," Phys. Rev. **148**, 741—747.

Zvonkov, B. N., N. N. Salashchenko, and O. N. Filatov, 1979, "Size quantization of the E_0 and E_1 absorption edges in InSb," Fiz. Tverd. Tela (Leningrad) **21**, 1344—1348 [Sov. Phys.—Solid State **21**, 777—779 (1979)].